

EARLY PROTEROZOIC GRANITOID MAGMATISM AND  
CRUSTAL EVOLUTION IN THE MAKKOVIK PROVINCE  
OF LABRADOR: A GEOCHEMICAL AND ISOTOPIC STUDY

CENTRE FOR NEWFOUNDLAND STUDIES

TOTAL OF 10 PAGES ONLY  
MAY BE XEROXED

(Without Author's Permission)

ANDREW KERR, B.Sc., M.Sc.





National Library  
of Canada

Bibliothèque nationale  
du Canada

Canadian Theses Service    Service des thèses canadiennes

Ottawa, Canada  
K1A 0N4

## NOTICE

The quality of this microform is heavily dependent upon the quality of the original thesis submitted for microfilming. Every effort has been made to ensure the highest quality of reproduction possible.

If pages are missing, contact the university which granted the degree.

Some pages may have indistinct print especially if the original pages were typed with a poor typewriter ribbon or if the university sent us an inferior photocopy.

Reproduction in full or in part of this microform is governed by the Canadian Copyright Act, R.S.C. 1970, c. C-30, and subsequent amendments.

## AVIS

La qualité de cette microforme dépend grandement de la qualité de la thèse soumise au microfilmage. Nous avons tout fait pour assurer une qualité supérieure de reproduction.

S'il manque des pages, veuillez communiquer avec l'université qui a conféré le grade.

La qualité d'impression de certaines pages peut laisser à désirer, surtout si les pages originales ont été dactylographiées à l'aide d'un ruban usé ou si l'université nous a fait parvenir une photocopie de qualité inférieure.

La reproduction, même partielle, de cette microforme est soumise à la Loi canadienne sur le droit d'auteur, SRC 1970, c. C-30, et ses amendements subséquents.

---

**EARLY PROTEROZOIC GRANITOID MAGMATISM AND  
CRUSTAL EVOLUTION IN THE MAKKOVIK PROVINCE OF  
LABRADOR: A GEOCHEMICAL AND ISOTOPIC STUDY**

---

by



Andrew Kerr, B.Sc, M.Sc.

A thesis submitted to the School of Graduate  
Studies in partial fulfillment of the requirements  
for the degree of Doctor of Philosophy

Department of Earth Sciences  
Memorial University of Newfoundland

June, 1989

St. John's  
Newfoundland  
CANADA





National Library  
of Canada

Bibliothèque nationale  
du Canada

Canadian Theses Service    Service des thèses canadiennes

Ottawa, Canada  
K1A 0N4

The author has granted an irrevocable non-exclusive licence allowing the National Library of Canada to reproduce, loan, distribute or sell copies of his/her thesis by any means and in any form or format, making this thesis available to interested persons.

The author retains ownership of the copyright in his/her thesis. Neither the thesis nor substantial extracts from it may be printed or otherwise reproduced without his/her permission.

L'auteur a accordé une licence irrévocable et non exclusive permettant à la Bibliothèque nationale du Canada de reproduire, prêter, distribuer ou vendre des copies de sa thèse de quelque manière et sous quelque forme que ce soit pour mettre des exemplaires de cette thèse à la disposition des personnes intéressées.

L'auteur conserve la propriété du droit d'auteur qui protège sa thèse. Ni la thèse ni des extraits substantiels de celle-ci ne doivent être imprimés ou autrement reproduits sans son autorisation.

ISBN 0-315-65315-9

### THREE PERSPECTIVES ON THE ORIGIN AND INTERPRETATION OF GRANITES

"Field studies of granites deal with end products of processes long since completed, and the most detailed mapping and study of these products may fail to give convincing evidence concerning the exact nature of the processes responsible for the relations."

From : **O.F.Tuttle and N.L.Bowen, 1958.** Origin of granite in the light of experimental studies in the system  $\text{NaAlSi}_3\text{O}_8 - \text{KAlSi}_3\text{O}_8 - \text{SiO}_2 - \text{H}_2\text{O}$ .

From the book that ended the "granite controversy", and laid the foundations for most current thought on silicic magmatism.

"The road to understanding orogenic processes, particularly in Precambrian terranes, is littered with misused discriminant diagrams and the hope of a simple link between the trace element compositions of igneous rocks and tectonic environment."

From: **C.J.Hawkesworth, M.A.Menzies and P. van Calsteren, 1986.** Geochemical and tectonic evolution of the Damara Belt, Namibia.

From a symposium on collision tectonics, organized by the Geological Society of Great Britain.

"I would certainly hope that 100 years hence, we will not be debating the origins of granites!"

From: **W.S.Fyfe, 1988.** Granites and a wet convecting ultramafic planet.

From a conference on the origin of granites, organized by the Royal Society of Edinburgh to commemorate the bicentennial of James Hutton.

### Thesis Abstract

The Lower to Middle Proterozoic Trans-Labrador Granitoid Belt in the Makkovik Structural Province is divided on the basis of field relationships and geochronology into **Makkovikian** and **Labradorian** plutonic assemblages, representing approximate time intervals of 1840 - 1720 and 1670 - 1600 Ma respectively. The Makkovikian assemblage includes both syn- and post-tectonic associations, but precise U-Pb zircon ages mostly cluster around 1800 Ma, suggesting a single main intrusive episode that transcended the later deformation associated with the Makkovikian orogeny. The Labradorian assemblage is not associated with local deformation or metamorphism, but is probably a distal effect of the ca. 1650 Ma Labradorian orogeny, prevalent south of the study area. Both assemblages are broadly correlative with volcanic sequences of similar age and geochemical affinity.

The Makkovikian assemblage is dominated by siliceous, potassic, commonly porphyritic, granites and alkali-feldspar granites, associated with subordinate monzonite to quartz syenite. High-silica granite suites are commonly fluorite-bearing. In geochemical terms, most Makkovikian granitoids are metaluminous to slightly peralkaline, Fe-enriched, and enriched in Zr, Nb, Hf, REE, Zn and fluorine. A comparative analysis suggests that they are transitional in character between Phanerozoic post-orogenic (post-collisional) assemblages and "A-type" or "within-plate" granitoid assemblages. Similarly enigmatic characteristics have been reported from Early Proterozoic granitoid batholiths elsewhere in the world.

The subordinate, bimodal, Labradorian plutonic assemblage comprises gabbro-diorite-monzonite-syenite suites, derived from mafic parental magmas, and an assortment of siliceous, generally leucocratic, granitoid rocks. Mafic rocks resemble high-K calc-alkaline or shoshonitic basalts, and their associated felsic differentiates are enriched in Rb, Cs, Th, and U, as a consequence of protracted fractionation. Other Labradorian granites (s.s.) are metaluminous to peraluminous in composition, and depleted in Zr, Nb, Hf, REE, Zn and fluorine, indicating that they had quite different sources from their Makkovikian counterparts.

The Makkovikian assemblage displays geographically systematic Nd isotopic variations. In the west, negative  $\epsilon_{\text{Nd}}^{\text{CHUR}}$  indicates ancient (probably Archean) crustal material in sources, but values are too high to permit derivation entirely from such material. These rocks probably represent mixtures of juvenile, mantle-derived, magma and older polycyclic Archean crust. In the east, positive  $\epsilon_{\text{Nd}}^{\text{CHUR}}$  indicates juvenile, Proterozoic sources, and gneissic rocks representing possible basement have depleted-mantle Nd model ages of ca. 2100 Ma. Discrete, high-silica, "A-type" granite plutons show an east-west shift in

$\epsilon_{\text{Nd}}^{\text{CHUR}}$  from +6 to -6, but retain remarkably similar ~~elemental~~ characteristics in both domains. It is concluded that magmas in the east also contained a significant crustal component, but that this component had a short crustal residence period. Nd isotopic data thus define a fundamental crustal boundary between an Archean Craton and a younger (accreted?) Proterozoic crustal province. Makkovikian magmatism accompanied and followed accretion of the younger domain, and is suggested to have resulted from emplacement of anhydrous, hot, mantle-derived mafic magmas into the lower crust, where they crystallized, assimilated and mixed with crustal rocks and melts thereof.

Labradorian rocks mostly have  $\epsilon_{\text{Nd}}^{\text{CHUR}}$  of +1 to -2, regardless of composition or location. Olivine-bearing mafic rocks, which cannot represent crustally-derived magmas, have  $\epsilon_{\text{Nd}}^{\text{CHUR}}$  of ca. +1, significantly below postulated values for concurrent depleted mantle. It is suggested that this crustal component was introduced to depleted mantle via subduction of continent-derived sediment, as suggested for modern arc magmas. However, some Labradorian granites that lack mafic parents could be derived by anatexis of Makkovikian "mixed" crust, or juvenile material underplated during Makkovikian events. Labradorian magmatism is tentatively interpreted as a distal-arc assemblage above a subduction zone that records renewal of tectonic activity following Makkovikian terrane accretion and magmatism.

The isotopic characteristics of both assemblages underline the importance of the Early Proterozoic as a period of new crustal growth. Makkovikian magmatism *reorganized* previously generated crust, and added significantly to it, particularly in the "juvenile" eastern domain. Largely *ensialic* crustal growth of this type may have been more important in a hotter, Proterozoic Earth and, in concert with ensimatic crust generation linked to subduction, may account for the high crustal growth rates deduced for this crucial period in planetary evolution.

The transitional characteristics of the Makkovikian assemblage may also be a function of greater heat flow. Recent models for "anorogenic" magmatism invoke insulation of the mantle by newly-accreted crust or aggregated megacontinents, resulting in mantle upwelling, plume activity, magmatism and (eventually) rifting. In a hotter Proterozoic Earth, the time-lag between aggregation and mantle upwelling would be shorter, and conditions now associated with "anorogenic" magmatism would prevail widely in post-orogenic environments. It is perhaps significant in this respect that worldwide Lower Proterozoic (1900 - 1700 Ma) orogenic events have recently been interpreted to record the assembly of an early Pangean-type supercontinent.

**KEY WORDS :** Labrador, Precambrian Proterozoic, Granitoids, Granite, Batholiths, Petrology, Ge chemistry, Comparative, Isotopes, Neodymium, Petrogenesis, Crustal Evolution.

### Acknowledgements

The only portion of writing a Ph.D. thesis that I can truly describe as *pleasurable* is acknowledging the many people whose support, encouragement and direct assistance enabled me to overcome periodic disillusionment and frustration, and complete this seemingly endless task.

My greatest debt is to my wife Vi, whose love, support and patient understanding, whilst our lives were disrupted by the demands of this project, continues to amaze me and remind me of my good fortune. I dedicate this tome to her, for enduring all this nonsense with such grace and good humour.

The Geological Survey Branch of the Newfoundland Department of Mines (NDM) provided the logistical and technical support that made a project of this type feasible within the framework of a government geoscience survey. I acknowledge this vital assistance, and also their constant encouragement of scientific research, discourse and innovation in all their employees. Tom Krogh's U-Pb zircon geochronology built the framework within which geochemical data were interpreted, and I thank him sincerely for his interest and assistance.

Derek Wilton initially suggested this project, and is therefore responsible also for my current position at NDM, for which he certainly deserves more than mere acknowledgement ! He offered sound advice, assistance and prompt constructive criticism throughout, and continues to do so. Brian Fryer served as chairman of my committee, and is thanked for his unusually prompt reading of earlier drafts, and valuable insight into isotope geochemistry and the black art of mass spectrometry. My external committee member, Charlie Gower (NDM), provided incisive and detailed

critical reviews of early drafts, which greatly improved the final version.

At the Geological Survey Branch, I wish also to thank Bruce Ryan (for unpublished data, samples and valuable discussion) , Dick Wardle (for the same, and proposing the project for funding), Lawson Dickson (for advice on numerous matters and cigarettes in moments of weakness), Peter Davenport (for statistical and geochemical advice), Jim Butler (for assembling Newfoundland granite data), Scott Swinden and John Tuach (for advice, and proving that it *can* be done !), and the Larry Nolan - Keith Parsons team (for assistance with SPSS-X, UNIX and other user-malevolent computer programs).

Field work for a project such as this is beyond the capabilities of any one individual. At least a dozen people gave their assistance over three field seasons. In particular, I thank senior assistants Gerry Squires (1985) and Hamish Sandeman (1986) for their friendship and enthusiasm, and two remarkable aces of the rotary wing, Alain Piche and Larry Labadie.

At Memorial University, I wish to acknowledge the assistance and friendship of Pamela King, Bill Gosse and Patricia Horan, their competent training in laboratory procedures, and Pam's assistance in building a good working relationship with *Miss Piggy*. George Jenner, Allen Nutman, Simon Jackson, Henry Longerich, Greg Dunning, Bill Davis, Craig MacDougall and Leonard MacKenzie are also thanked for advice and discussions.

Several individuals provided data for comparative studies. I wish particularly to thank John McConnell at NDM, Ingo Ermanovics and Joseph Whalen at the Geological Survey of Canada, Mike Brown at Kingston Polytechnic, London, U.K., and François Debon of the CNRS-CRPG research centre at Nancy, France, for published and unpublished information, and valuable discussion and correspondence.



## TABLE OF CONTENTS

Perspectives on the Origin and Interpretation of Granites	i
Thesis Abstract	ii
Acknowledgements	iv
TABLE OF CONTENTS	vi
LIST OF TABLES	xiv
LIST OF FIGURES	xvii
LIST OF PLATES	xxii
LIST OF ABBREVIATIONS	xxiii
<b>CHAPTER ONE : INTRODUCTION.</b>	<b>1</b>
1.1 PROJECT OVERVIEW.	1
Proterozoic Magmatism and Crustal Evolution.	1
Aims and Objectives	3
Scale Considerations.	6
1.2 GENERAL INFORMATION.	7
Location, Topography And Access.	7
Previous Work from 1800 to 1985.	8
Central Mineral Belt Granitoid Project.	9
Relevant Work Outside the Study Area.	10
1.3 TERMINOLOGY AND NOMENCLATURE.	11
Classification and Nomenclature of Plutonic Rocks.	11
Descriptive Geochemical Terminology.	13
Environments of Granitoid Magmatism.	15
Classifications Based On Source Materials.	18
Classifications Based On Tectonic Environment.	21
Investigative Methods.	22
Sample Populations.	22
Overview of Geochemical Analysis Program.	23
<b>CHAPTER 2 : GEOLOGICAL FRAMEWORK.</b>	<b>26</b>
Chapter Abstract.	26
2.1 REGIONAL GEOLOGY.	27
General Geology of Labrador.	27
Labrador as Part of A Proterozoic Supercontinent.	29
Trans-Labrador Granitoid Belt.	31
2.2 GEOLOGY OF THE MAKKOVIK PROVINCE AND ADJACENT AREAS.	34
Archean Rocks.	34
Cape Harrison Metamorphic Suite.	37
Moran Lake Group and Lower Aillik Group.	37
Upper Aillik Group.	38
Syn-Tectonic Makkovikian Plutonic Rocks.	40
Post-Tectonic Makkovikian Plutonic Rocks.	41
Labradorian Plutonic Rocks.	41
Unclassified Plutonic Rocks.	41
Bruce River Group.	42
Michael Gabbro Intrusions.	42
Granitoid Gneisses of The Grenville Province.	42
Structural and Metamorphic Patterns.	43
2.3 STRATIGRAPHIC GROUPINGS AND TERMINOLOGY.	46
General Information.	46
Intrusive Suites and Units.	46

<b>CHAPTER THREE : SYN-TECTONIC MAKKOVIKIAN PLUTONIC ROCKS. . . . .</b>	<b>49</b>
Chapter Abstract. . . . .	49
Introduction. . . . .	51
3.1 GEOLOGY AND PETROLOGY. . . . .	56
3.1.1 Long Island Quartz Monzonite. . . . .	56
3.1.2 Kennedy Mountain Intrusive Suite. . . . .	58
3.1.3 Melody Granite. . . . .	61
3.1.4 Brumwater Granite. . . . .	63
3.1.5 Pitre Lake Granite. . . . .	64
3.1.6 Manak Island Granitoid. . . . .	66
3.1.7 Deus Cape Granitoid. . . . .	67
3.1.8 Island Harbour Bay Intrusive Suite. . . . .	67
3.2 DESCRIPTIVE GEOCHEMISTRY. . . . .	70
3.2.1 General Geochemistry. . . . .	70
Summary of Numerical Data. . . . .	70
Abundance and Distribution of Rock Types. . . . .	73
3.2.2 Geochemical Trends and Contrasts. . . . .	75
Major Element Patterns. . . . .	75
Normative Compositions. . . . .	77
Trace Element Patterns. . . . .	80
Trace Element Variation and Alkali Disturbance . . . . .	85
Trace Element Ratios. . . . .	85
Rare Earth Element (REE) Patterns. . . . .	90
3.3 SUMMARY AND DISCUSSION. . . . .	92
Geological and Petrographic Associations. . . . .	92
Geochemical Associations. . . . .	93
Origin of Compositional Variations. . . . .	94
Metasomatism in the Kennedy Mountain Intrusive Suite. . . . .	96
<b>CHAPTER FOUR : POST-TECTONIC MAKKOVIKIAN PLUTONIC ROCKS. . . . .</b>	<b>98</b>
Chapter Abstract. . . . .	98
Introduction. . . . .	100
4.1 GEOLOGY AND PETROLOGY. . . . .	104
4.1.1 Numok Intrusive Suite. . . . .	104
Definition and Distribution. . . . .	104
Monzonite and Quartz Monzonite. . . . .	104
Syenite and Quartz Syenite. . . . .	108
Plagiophyric Monzodiorite and Monzonite. . . . .	110
4.1.2 Strawberry Intrusive Suite. . . . .	110
Definition and Distribution. . . . .	110
Bayhead Granite. . . . .	111
Cape Strawberry Granite and Related Rocks. . . . .	111
Dog Islands Granite. . . . .	117
Tukialik Granite. . . . .	118
4.1.3 Lanceground Intrusive Suite. . . . .	119
Definition and Distribution. . . . .	119
Lanceground Hills and Pistol Lake Granites. . . . .	119
Tarun Granite. . . . .	122
4.1.4 Big River Granite. . . . .	123

4.2 DESCRIPTIVE GEOCHEMISTRY. . . . .	126
4.2.1 General Geochemistry. . . . .	126
Summary of Numerical Data. . . . .	126
Abundance and Distribution of Rock Types. . . . .	131
4.2.2 Geochemical Trends and Contrasts. . . . .	131
Major Element Patterns. . . . .	131
Normative Compositions. . . . .	135
Trace Element Patterns. . . . .	137
Trace Element Ratios. . . . .	141
Rare Earth Element (REE) Patterns. . . . .	144
4.3 SUMMARY AND DISCUSSION. . . . .	146
Geological and Geochemical Continuity. . . . .	146
Origin of Compositional Variations. . . . .	148
Similarity of Post-Tectonic and Syn-Tectonic Makkovikian Plutonic Rocks. . . . .	151
Geochronological Relationships. . . . .	154
 CHAPTER FIVE : LABRADORIAN PLUTONIC ROCKS. . . . .	156
Chapter Abstract. . . . .	156
Introduction. . . . .	158
5.1 GEOLOGY AND PETROLOGY. . . . .	162
5.1.1 Adlavik Intrusive Suite. . . . .	162
Definition and Distribution. . . . .	162
Mafic Plutonic Rocks. . . . .	163
Diorite and Monzodiorite. . . . .	170
Geometry and Stratigraphy of the Adlavik Bay Intrusion. . . . .	172
5.1.2 Mount Benedict Intrusive Suite. . . . .	174
Definition and Distribution. . . . .	174
Gabbro and Diorite. . . . .	175
Monzonite, Syenomonzonite and Syenite. . . . .	177
Syenite, Quartz Syenite and Granite. . . . .	178
5.1.3 Monkey Hill Intrusive Suite. . . . .	178
Definition and Distribution. . . . .	178
Lithology and Field Relationships. . . . .	179
5.1.4 Witchdoctor and Burnt Lake Granites. . . . .	182
Witchdoctor Granite. . . . .	183
Burnt Lake Granite. . . . .	185
5.1.5 Otter Lake - Walker Lake Granitoid. . . . .	185
5.2 DESCRIPTIVE GEOCHEMISTRY. . . . .	189
5.2.1 General Geochemistry. . . . .	189
Summary of Numerical Data. . . . .	189
Distribution and Abundance of Rock Types. . . . .	193
5.2.2 Geochemistry of the Adlavik Intrusive Suite. . . . .	195
Subdivisions of The Suite. . . . .	195
Major Element Patterns. . . . .	200
Trace Element Patterns. . . . .	200
Rare Earth Element (REE) Patterns. . . . .	203
5.2.3 Geochemistry of Labradorian Granitoid Rocks. . . . .	204
Major Element Patterns. . . . .	204
Normative Compositions. . . . .	207
Trace Element Patterns. . . . .	207
Trace Element Ratios. . . . .	212
Rare Earth Element (REE) Patterns. . . . .	215

5.3 SUMMARY AND DISCUSSION. . . . .	218
Contrasts Between Labradorian and Makkovikian Plutonic Associations. . . . .	218
Evolution of The Adlavik Intrusive Suite. . . . .	221
Evolution of The Mount Benedict Intrusive Suite. . . . .	222
Relationship Between The Adlavik and Mount Benedict Intrusive Suites. . . . .	223
Fractional Crystallization Models. . . . .	226
Mount Benedict Suite Fractionation Model. . . . .	227
Affinities of Labradorian Mafic Magmas and Derivatives. . . . .	230
Evolution of Labradorian Siliceous Granitoid Rocks. . . . .	233
 CHAPTER SIX : UNCLASSIFIED PLUTONIC ROCKS. . . . .	236
Chapter Abstract. . . . .	236
Introduction. . . . .	237
6.1 GEOLOGY and PETROLOGY. . . . .	237
6.1.1 Freshsteak and Noarse Lake Granitoids. . . . .	237
6.1.2 Stag Bay Granitoid. . . . .	241
6.1.3 Jeanette Bay Quartz Syenite. . . . .	244
6.1.4 Thunder Mountain Syenite. . . . .	244
6.1.5 Granitoid Gneisses South of The Benedict Fault Zone. . . . .	246
6.2 DESCRIPTIVE GEOCHEMISTRY. . . . .	250
6.2.1 General Geochemistry. . . . .	250
Summary of Numerical Data. . . . .	250
Abundance and Distribution of Rock Types. . . . .	253
6.2.2 Geochemical Trends and Contrasts. . . . .	256
Major Element Patterns. . . . .	256
Trace Element Patterns. . . . .	256
Rare Earth Element (REE) Patterns. . . . .	259
6.3 SUMMARY AND DISCUSSION. . . . .	260
 CHAPTER SEVEN : MAKKOVIKIAN AND LABRADORIAN VOLCANIC ASSEMBLAGES. .	261
Chapter Abstract. . . . .	261
Introduction. . . . .	262
7.1 GEOLOGY AND PETROLOGY . . . . .	262
7.1.1 Upper Aillik Group (Type Area). . . . .	262
General Overview. . . . .	262
Concepts of Aillik Group Stratigraphy. . . . .	264
Early Upper Aillik Group. . . . .	267
General Features of The Late Upper Aillik Group. . . . .	268
Volcanic, Pyroclastic and Volcaniclastic Rocks. . . . .	268
Hypabyssal Intrusive Rocks. . . . .	271
7.1.2 Supracrustal Rocks In The Benedict Mountains (Jagged Edge Assemblage). . . . .	272
General Overview. . . . .	272
Field Relations and Lithology. . . . .	274
7.1.3 Bruce River Group. . . . .	275
General Overview. . . . .	275
Field Relations and Lithology. . . . .	276

7.2 DESCRIPTIVE GEOCHEMISTRY. . . . .	277
7.2.1. Previous Studies. . . . .	277
7.2.2. General Geochemistry. . . . .	281
Summary of Numerical Data. . . . .	281
Abundance and Distribution of Rock Types. . . . .	283
7.2.3 Geochemical Trends and Contrasts. . . . .	284
Major Element Patterns. . . . .	284
Normative Compositions. . . . .	288
Trace Element Patterns. . . . .	288
Trace Element Variation in Response to Disturbance of Major Element Compositions. . . . .	290
Trace Element Ratios. . . . .	293
Rare Earth Element (REE) Patterns. . . . .	297
7.3 SUMMARY and DISCUSSION. . . . .	297
Correspondance of Volcanic and Plutonic Assemblages. . . . .	297
Geochemical Disturbance in Upper Aillik Group Volcanic Rocks. . . . .	301
Contrasts Between Makkovikian and Labradorian Volcanic Suites. . . . .	302
CHAPTER EIGHT : ISOTOPE GEOCHEMISTRY. . . . .	304
Chapter Abstract. . . . .	304
Introduction. . . . .	306
Analytical Methods. . . . .	306
8.1 STRONTIUM ISOTOPE GEOCHEMISTRY. . . . .	307
8.1.1 Rb-Sr Geochronology. . . . .	307
Data and Methodology. . . . .	307
Constraints from Previous Rb-Sr Investigations. . . . .	307
Big River Granite. . . . .	310
Freshsteak Granitoid. . . . .	310
Stag Bay Granitoid. . . . .	312
Lanceground Intrusive Suite. . . . .	313
Strawberry Intrusive Suite. . . . .	313
Kennedy Mountain Intrusive Suite. . . . .	315
8.1.2 Regional Variations in Sr Isotope Geochemistry. . . . .	316
Sr <sub>i</sub> Variation : Isochron Studies. . . . .	316
Sr <sub>i</sub> Variation : Single-Sample Data. . . . .	319
Problems in Calculating Sr <sub>i</sub> . . . . .	319
8.2 NEODYMIUM ISOTOPIC GEOCHEMISTRY. . . . .	323
Neodymium as a Petrogenetic Tool. . . . .	323
Overview of Nd Isotope Geochemistry Database. . . . .	325
8.2.1 Sm-Nd "Geochronology". . . . .	328
Syn-Tectonic Makkovikian Plutonic Rocks. . . . .	328
Post-Tectonic Makkovikian Plutonic Rocks. . . . .	329
Labradorian Plutonic Rocks. . . . .	331
8.2.2 Regional Variations in Nd Isotope Geochemistry . . . . .	331
Data Notation and Representation. . . . .	332
Syn-Tectonic Makkovikian Plutonic Rocks. . . . .	336
Post-Tectonic Makkovikian Plutonic Rocks. . . . .	339
Makkovikian Volcanic Rocks. . . . .	340
Labradorian Plutonic and Volcanic Rocks. . . . .	341
Unclassified Plutonic Rocks. . . . .	343
Spatial Variation in $\epsilon_{Nd}$ and $T_{DM}$ . . . . .	345

8.2.3 Nd Isotopic Trends and Contrasts. . . . .	348
Major Element Patterns. . . . .	348
Trace Element Patterns. . . . .	351
Initial Ratio Trends. . . . .	351
8.3 SUMMARY AND DISCUSSION. . . . .	354
8.3.1 The Unusual Case of The Pitre Lake Granite. . . . .	354
8.3.2 Possible Sources of Makkovikian Magmas. . . . .	357
Nature of Basement In The Makkovik Province. . . . .	357
Sources of Makkovikian Magmas. . . . .	358
Crust-Mantle Mixing Models. . . . .	360
8.3.3 Possible Sources of Labradorian Magmas. . . . .	363
Continuity of Isotopic Compositions. . . . .	363
Sources Of Labradorian Magmas. . . . .	364
Mixing and Contamination Models. . . . .	365
CHAPTER NINE : A COMPARATIVE ANALYSIS. . . . .	368
Chapter Abstract. . . . .	368
Introduction. . . . .	370
Spectral Analysis of Granitoid Batholiths. . . . .	370
9.1 OVERVIEW OF COMPARATIVE GEOCHEMICAL DATA. . . . .	371
Coastal Batholith Of Peru. . . . .	373
Mesozoic Batholith Of North-Central Chile. . . . .	375
Mesozoic Batholith Of Southern California. . . . .	376
Plutonic Belts Of Afghanistan. . . . .	378
Late- and Post-Orogenic Granitoid Rocks Of Newfoundland. . . . .	380
Proterozoic Anorogenic Granites Of Northern Labrador. . . . .	383
A-type Granites of The Lachlan Fold Belt. . . . .	385
9.2 COMPARATIVE MAJOR ELEMENT GEOCHEMISTRY. . . . .	387
9.2.1 Comparative Frequency Spectra. . . . .	387
Major Element Frequency Spectra. . . . .	387
Major Element Ratio and Function Frequency Spectra. . . . .	396
9.2.2 Abundance and Distribution Of Rock Types. . . . .	399
9.2.3 Evolutionary Trends. . . . .	401
Quartz-Poor Versus Quartz-Rich Trends. . . . .	401
Major Element Differentiation Trends. . . . .	404
9.3 COMPARATIVE TRACE ELEMENT GEOCHEMISTRY. . . . .	407
9.3.1 Comparative Frequency Spectra. . . . .	407
Trace Element Frequency Spectra. . . . .	407
Trace Element Ratio Frequency Spectra. . . . .	417
9.3.2 Trace Element Discrimination Diagrams. . . . .	417
Tectonic Setting Discrimination Diagrams. . . . .	417
Discrimination Diagrams for identification of A-type Granites. . . . .	421
9.3.3 Evolutionary Trends. . . . .	424
9.4 SUMMARY AND DISCUSSION. . . . .	427
9.4.1 Evaluation of Geochemical Discrimination Methods. . . . .	427
9.4.2 Geochemical Affinity Of The Makkovikian Assemblage. . . . .	429
Major Element Characteristics. . . . .	429
Trace Element Characteristics. . . . .	430
Conclusions. . . . .	431



9.4.3 Geochemical Affinity Of The Labradorian Assemblage. . . . .	432
Major Element Characteristics. . . . .	432
Trace Element Characteristics. . . . .	432
Affinity of Labradorian Mafic and Intermediate Rocks. . . . .	433
Discussion and Conclusions. . . . .	435
<b>CHAPTER TEN : MAGMATISM AND CRUSTAL EVOLUTION IN THE MAKKOVIK PROVINCE. . . . .</b>	<b>437</b>
Chapter Abstract. . . . .	437
Introduction. . . . .	439
<b>10.1 PETROGENESIS OF MAKKOVIKIAN MAGMAS. . . . .</b>	<b>440</b>
Summary of Important Characteristics. . . . .	440
Source Materials and Source Regions. . . . .	441
Petrogenetic Model -- General Features. . . . .	443
Petrogenetic Model -- Some Special Features. . . . .	446
Implications For The Origin of "A-type" Granites. . . . .	447
Two Younger Analogues of The Makkovikian Assemblage. . . . .	448
<b>10.2 PETROGENESIS OF LABRADORIAN MAGMAS. . . . .</b>	<b>449</b>
Summary of Important Characteristics. . . . .	449
Source Materials and Source Regions. . . . .	450
Petrogenetic Models. . . . .	452
<b>10.3 PROTEROZOIC CRUSTAL EVOLUTION IN THE MAKKOVIK PROVINCE. . . . .</b>	<b>454</b>
Implications For Crustal Growth Models. . . . .	454
A Wilson-Cycle Model For The Evolution of the Makkovik Province. . . . .	457
Early Stages -- Rifting, Sedimentation and Stage 1 Crust Generation. . . . .	457
Ensisimatic Stages -- Subduction and Stage 2 Crust Generation. . . . .	458
Early Ensialic Stages -- Accretion of Juvenile Terranes and Initiation of Stage 3 Crust Generation. . . . .	459
Late Ensialic Stages -- Episodic Post-Tectonic Magmatism and Stage 3 Crust Formation. . . . .	462
Labradorian Stages -- Initiation of a New Active Margin South of the Makkovik Province. . . . .	463
Relationship of Makkovikian and Labradorian Magmatic Provinces Within the TLGB. . . . .	464
A Younger Analogue -- The Margin of Gondwanaland in Southern South America. . . . .	466
The Makkovik Province as Part of a Chelogenic Cycle. . . . .	467
Proterozoic Magmatism and Crustal Evolution : Reprise . . . . .	469
<b>10.4 FUTURE PATHS. . . . .</b>	<b>471</b>
<b>REFERENCES CITED. . . . .</b>	<b>474</b>
<b>APPENDIX A : METHODS AND PROCEDURES. . . . .</b>	<b>497</b>
<b>A1. SAMPLE COLLECTION AND PREPARATION. . . . .</b>	<b>497</b>
<b>A2. MAJOR AND TRACE ELEMENT ANALYSIS PROCEDURES. . . . .</b>	<b>498</b>
A2.1 Assessment of Geochemical Analysis Program. . . . .	498
A2.2 Department of Mines Analysis Program. . . . .	499
Laboratory Procedures. . . . .	499
Analytical Methods. . . . .	501
Precision and Detection Limits. . . . .	502
Accuracy. . . . .	504
A2.3 Memorial University Analysis Program. . . . .	504

A3. STRONTIUM ISOTOPIC ANALYSIS PROCEDURES. . . . .	506
A3.1 Laboratory Procedures. . . . .	506
A3.2 Determination of $^{87}\text{Rb}/^{86}\text{Sr}$ . . . . .	507
A3.3 Determination of $^{87}\text{Sr}/^{86}\text{Sr}$ . . . . .	507
Mass Spectrometry. . . . .	507
Precision and Accuracy. . . . .	508
A4. NEODYMIUM ISOTOPIC ANALYSIS PROCEDURES. . . . .	510
A4.1 Laboratory Procedures. . . . .	510
A4.2 Determination of $^{147}\text{Sm}/^{144}\text{Nd}$ . . . . .	511
A4.3 Determination of $^{147}\text{Sm}/^{144}\text{Nd}$ . . . . .	512
Mass Spectrometry. . . . .	512
Precision and Accuracy. . . . .	513
APPENDIX B : GEOCHEMICAL DATA LISTINGS. . . . .	515
Major and Trace Element Data. . . . .	515
ICP-MS Trace Element Data. . . . .	515
Microfiche of Geochemical Data. . . . .	516
APPENDIX C : MISCELLANEOUS INFORMATION. . . . .	517
Partition Coefficients. . . . .	517
Chondrite Normalization Values. . . . .	517
A Note on Normative Calculations. . . . .	517
APPENDIX D : SUMMARY OF U-PB GEOCHRONOLOGICAL DATA. . . . .	519
General Statement. . . . .	519
Adlavik Intrusive Suite. . . . .	519
Deus Cape Granitoid. . . . .	521
Numok Intrusive Suite. . . . .	521
Cape Strawberry Granite -- Preliminary Data. . . . .	523
Cape Strawberry Granite -- Spring 1989 Update. . . . .	523
Mount Benedict Intrusive Suite. . . . .	524
Otter Lake - Walker Lake Granitoid. . . . .	524
Monkey Hill Intrusive Suite. . . . .	527
Big River Granite. . . . .	527
Stag Bay Granitoid. . . . .	527
APPENDIX E : GEOLOGICAL AND TOPOGRAPHIC MAPS. . . . .	528

## LIST OF TABLES

### CHAPTER ONE : INTRODUCTION

Table 1.1. Geochemical groupings of trace elements. . . . .	16
---	----

### CHAPTER TWO : GEOLOGICAL FRAMEWORK

Table 2.1. Simplified geological history of the Makkovik province and adjacent areas of east-central Labrador. . . . .	39
Table 2.2. Summary of stratigraphic names employed in this thesis for plutonic rocks. . . . .	47-48

### CHAPTER THREE : SYN-TECTONIC MAKKOVIKIAN PLUTONIC ROCKS

Table 3.1. Key features of syn-tectonic Makkovikian plutonic units. . . . .	54-55
Table 3.2. Average compositions of syn-tectonic Makkovikian plutonic rocks, subdivided into principal units. . . . .	71-72

### CHAPTER FOUR : POST-TECTONIC MAKKOVIKIAN PLUTONIC ROCKS

Table 4.1. Features of post-tectonic Makkovikian plutonic units. . . . .	102-103
Table 4.2. Average compositions of post-tectonic Makkovikian plutonic rocks, subdivided into principal units. . . . .	127-128
Table 4.3. Comparison of the average compositions of selected syn- and post-tectonic Makkovikian plutonic units. . . . .	152-153

### CHAPTER FIVE : LABRADORIAN PLUTONIC ROCKS

Table 5.1. Key features of Labradorian plutonic units. . . . .	160-161
Table 5.2. Average compositions of Labradorian plutonic rocks, subdivided into principal units. . . . .	190-193
Table 5.3. Average compositions of mineralogical and textural subdivisions in the main body of the Adlavik Intrusive Suite. . . . .	196-197
Table 5.4. Comparison of the average compositions of selected Labradorian and Makkovikian granitoid plutonic units. . . . .	219-220
Table 5.5. Average compositions of Adlavik Intrusive Suite units in comparison to "appinites", and a range of modern basalt and andesite types. . . . .	231-232

### CHAPTER SIX : UNCLASSIFIED PLUTONIC ROCKS

Table 6.1. Key features of unclassified plutonic units. . . . .	238-239
Table 6.2. Average compositions of unclassified units, in comparison to selected Makkovikian and Labradorian units. . . . .	251-252

### CHAPTER SEVEN : MAKKOVIKIAN AND LABRADORIAN VOLCANIC ASSEMBLAGES

Table 7.1. Average compositions of Makkovikian and Labradorian volcanic assemblages . . . . .	279-280
Table 7.2. A comparison of average compositions of volcanic units to plutonic units of similar major element composition. . . . .	298-299

## CHAPTER EIGHT : ISOTOPE GEOCHEMISTRY

Table 8.1. Rb-Sr concentration and isotopic data used for age determinations. . . . .	308
Table 8.2. Initial Sr isotopic compositions calculated from Rb-Sr isochrons throughout the Trans-Labrador Granitoid Belt. . . . .	317
Table 8.3. Initial Sr isotopic compositions calculated from single sample measurements conducted via this study. . . . .	318
Table 8.4. An illustration of the unreliability of initial Sr isotopic compositions calculated from single samples with high Rb-Sr ratios, and the greater reliability and consistency of calculated initial Nd compositions. . . . .	322
Table 8.5. Listing of samples analyzed for Nd isotopic compositions, with descriptive comments and age information. . . . .	326-327
Table 8.6. Sm and Nd concentration and isotopic data for Makkovikian plutonic and volcanic rocks, and basement rocks at ca. 1800 Ma. . . . .	337-338
Table 8.7. Sm and Nd concentration and isotopic data for Labradorian plutonic and volcanic rocks, and basement rocks at ca. 1650 Ma. . . . .	342
Table 8.8. Two-component mixing matrices for Makkovikian magmas, showing the proportions of crustal component required to generate a specific final $\epsilon_{Nd}^{CHUR}$ value. . . . .	362
Table 8.9. Two-component mixing and contamination matrices for Labradorian magmas, showing the proportions of crustal component required to generate a specific final $\epsilon_{Nd}^{CHUR}$ value. . . . .	366

## CHAPTER NINE : A COMPARATIVE ANALYSIS

Table 9.1. Summary of databases (including TLGB data) employed in comparative geochemical studies . . . . .	372
---	-----

## APPENDIX A : METHODS AND PROCEDURES

Table A.1. Abundance levels, detection limits and estimates of precision for major and trace elements determined at, or via, the Department of Mines laboratory. . . . .	500
Table A.2. Determinations of the international standards MRG-1, SY-2 and GSP-1 by the Department of Mines laboratory. . . . .	503
Table A.3. Determinations of trace elements in SY-2 by ICP-MS analysis at Memorial University. . . . .	505
Table A.4. Duplicate determinations of $^{87}Rb/^{86}Sr$ ratios by repeated AAS analyses at the Department of Mines laboratory. . . . .	507
Table A.5. Duplicate determinations of $^{87}Sr/^{86}Sr$ ratios by thermal ionization mass spectrometry at Memorial University. . . . .	509
Table A.6. Determinations of the Sr-carbonate standard NBS-987 during the course of this project . . . . .	509
Table A.7. Comparison of $^{147}Sm/^{144}Nd$ ratios measured by high-precision ICP-MS methods and ID methods. . . . .	511
Table A.8. Duplicate determinations of $^{143}Nd/^{144}Nd$ ratios by thermal ionization mass spectrometry at Memorial University. . . . .	513

Table A.9. Determinations of the LaJolla Nd isotope standard during the course of this project. . . . .	514
--	-----

**APPENDIX B : GEOCHEMICAL DATA LISTINGS**

Microfiche of major and trace element data from the TLGB. . . . .	516
---	-----

**APPENDIX C : MISCELLANEOUS INFORMATION**

Table C.1. Mineral-melt partition coefficients employed in trace element modelling . . . . .	518
---	-----

Table C.2. Chondrite normalization values currently in use at Memorial University . . . . .	518
--	-----

## LIST OF FIGURES

### CHAPTER ONE : INTRODUCTION

- Figure 1.1. Location of the study area in Labrador and North America. . . . . 5
- Figure 1.2. Modal and normative classification of plutonic rocks. . . . . 17

### CHAPTER TWO : GEOLOGICAL FRAMEWORK

- Figure 2.1. Regional geological framework of the study area. . . . . 28
- Figure 2.2. Labrador geology in the context of a Proterozoic supercontinent including North America, Greenland and Baltic shield complexes. . . . . 30
- Figure 2.3. Simplified geological map of the Makkovik Province and adjacent areas of east-central Labrador. . . . . 35-36

### CHAPTER THREE : SYN-TECTONIC MAKKOVIKIAN PLUTONIC ROCKS

- Figure 3.1. Location and distribution of syn-tectonic Makkovikian plutonic units. . . . . 52-53
- Figure 3.2. Relative abundance of IUGS rock types calculated from normative mineralogy of syn-tectonic Makkovikian units. . . . . 74
- Figure 3.3. Variation of selected major element oxides and ratios in syn-tectonic Makkovikian plutonic rocks. . . . . 76
- Figure 3.4. AFM, CNK and QBF ternary plots for syn-tectonic Makkovikian plutonic rocks. . . . . 78
- Figure 3.5. Variation of total alkali content and N/N+K ratios in syn-tectonic Makkovikian plutonic rocks in relation to the spectrum of normal igneous compositions. . . . . 79
- Figure 3.6. Distribution of syn-tectonic Makkovikian plutonic rocks in the quaternary system (Q - Ab - An - Or). . . . . 81
- Figure 3.7. V, Rb, Th, Cs, Sr and Ba versus  $\text{SiO}_2$  for syn-tectonic Makkovikian plutonic rocks . . . . . 83
- Figure 3.8. Zr, Y, Ce, Li, Zn, and F versus  $\text{SiO}_2$  for syn-tectonic Makkovikian plutonic rocks . . . . . 84
- Figure 3.9. Variation of selected trace elements versus N/N+K ratios in granites of the Kennedy Mountain Intrusive Suite. . . . . 86
- Figure 3.10. Variation of the trace element ratios K/Rb, Rb/Sr, Ba/Sr and  $\text{La}_N/\text{Y}_N$  in syn-tectonic Makkovikian plutonic rocks in relation to reference trends for fractionation of common silicate minerals. . . . . 88-89
- Figure 3.11. Rare Earth Element (REE) patterns for syn-tectonic Makkovikian plutonic rocks. . . . . 91

### CHAPTER FOUR : POST-TECTONIC MAKKOVIKIAN PLUTONIC ROCKS

- Figure 4.1. Location and distribution of post-tectonic Makkovikian plutonic units. . . . . 101
- Figure 4.2. Relative abundance of IUGS rock types calculated from normative mineralogy of post-tectonic Makkovikian units. . . . . 130
- Figure 4.3. Variation of selected major element oxides and ratios in post-tectonic Makkovikian plutonic rocks . . . . . 132



Figure 4.4. AFM, CNK and QBF ternary plots, and $\text{SiO}_2$ -alkali plot, for post tectonic Makkovikian plutonic rocks. . . . .	134-135
Figure 4.5. Distribution of post-tectonic Makkovikian plutonic rocks in the granite quaternary system (Q - Ab - An - Or). . . .	136
Figure 4.6. V, Rb, Th, Sr, Ba and F versus $\text{SiO}_2$ for post-tectonic Makkovikian plutonic rocks. . . . .	138
Figure 4.7. Zr, Nb, Y, La, Li and Zn versus $\text{SiO}_2$ for post-tectonic Makkovikian plutonic rocks. . . . .	140
Figure 4.8. Variation of the trace element ratios K/Rb, Rb/Sr, Ba/Sr and $\text{La}_N/\text{Y}_N$ in post-tectonic Makkovikian plutonic rocks in relation to reference trends for fractionation of common silicate minerals. . . . .	142-143
Figure 4.9. Rare Earth Element (REE) patterns for post-tectonic Makkovikian plutonic rocks. . . . .	145
<b>CHAPTER FIVE : LABRADORIAN PLUTONIC ROCKS</b>	
Figure 5.1. Location and distribution of Labradorian plutonic units	159
Figure 5.2. Simplified geological map of the main body of the Adlavik Intrusive Suite at Adlavik Bay. . . . .	164
Figure 5.3. Schematic illustration of cyclic units in the mafic cumulate facies of the Adlavik Intrusive Suite . . . . .	173
Figure 5.4. Schematic, interpretative cross-section of the main body of the Adlavik Intrusive Suite. . . . .	173
Figure 5.5. Relative abundance of IUGS rock types calculated from normative mineralogy of Labradorian units. . . . .	194
Figure 5.6. Normative Di-Ol-Hy ternary projection, illustrating subdivisions of the Adlavik Intrusive Suite. . . . .	198
Figure 5.7. Spatial distribution of normative Di, Hy and Ol in the main body of the Adlavik Intrusive Suite . . . . .	199
Figure 5.8. Variation of selected major elements against MgO in the main body of the Adlavik Intrusive Suite . . . . .	201
Figure 5.9. Variation of selected trace elements against MgO in the main body of the Adlavik Intrusive Suite . . . . .	202
Figure 5.10. Rare Earth Element (REE) patterns for the Adlavik Suite	203
Figure 5.11. Variation of selected major element oxides and ratios in Labradorian granitoid plutonic rocks. . . . .	205
Figure 5.12. AFM, CNK and QBF ternary plots for Labradorian granitoid plutonic rocks. . . . .	206
Figure 5.13. Distribution of Labradorian granitoid plutonic rocks in the granite quaternary system (Q - Ab - An - Or). . . .	208
Figure 5.14. V, Rb, Th, Sr, Ba and F versus $\text{SiO}_2$ for Labradorian granitoid plutonic rocks. . . . .	210
Figure 5.15. Zr, Nb, Y, La, Li and Zn versus $\text{SiO}_2$ for Labradorian granitoid plutonic rocks. . . . .	211

Figure 5.16. Variation of the trace element ratios K/Rb, Rb/Sr, Ba/Sr and $La_N/Y_N$ in Labradorian granitoid plutonic rocks in relation to reference trends for fractionation of common silicate minerals. . . . .	213-214
Figure 5.17. Rare Earth Element (REE) patterns for Labradorian granitoid plutonic rocks. . . . .	219
Figure 5.18. Variation of selected major and trace elements against topographic elevation in the Mount Benedict Intrusive Suite. . . . .	224
Figure 5.19. Combined variation of selected major and trace elements against $SiO_2$ for the Adlavik and Mount Benedict Intrusive Suites . . . . .	225
Figure 5.20. Comparison of fractional crystallization model for the Mount Benedict Intrusive Suite with observed compositions. . . . .	228
<b>CHAPTER SIX : UNCLASSIFIED PLUTONIC ROCKS</b>	
Figure 6.1. Location and distribution of unclassified plutonic units . . . . .	238
Figure 6.2. Relative abundance of IUGS rock types calculated from normative mineralogy of unclassified units. . . . .	254
Figure 6.3. Variation of selected major element oxides and ratios in unclassified plutonic rocks. . . . .	255
Figure 6.4. V, Rb, Th, Sr, Ba and F versus $SiO_2$ for unclassified plutonic rocks. . . . .	257
Figure 6.5. Zr, Nb, Y, Ce, Li and Zn versus $SiO_2$ for unclassified plutonic rocks. . . . .	258
Figure 6.6. Rare Earth Element (REE) patterns for unclassified plutonic rocks. . . . .	259
<b>CHAPTER SEVEN : MAKKOVIKIAN AND LABRADORIAN VOLCANIC ASSEMBLAGES</b>	
Figure 7.1. Location and distribution of volcanic assemblages . . . . .	261
Figure 7.2. Relative abundance of equivalent IUGS plutonic rock types calculated from normative mineralogy of volcanic units. . . . .	282
Figure 7.3. Variation of selected major element oxides and ratios in volcanic assemblages. . . . .	285
Figure 7.4. Variation of total alkali content and N/(N+K) ratios in volcanic assemblages in relation to the spectrum of normal igneous compositions. . . . .	286
Figure 7.5. AFM and CNK ternary plots, and Alkali- $SiO_2$ plots, for volcanic assemblages. . . . .	287
Figure 7.6. Distribution of volcanic assemblages in the granite quaternary system (Q - Ab - An - Or). . . . .	289
Figure 7.7. V, Rb, U, Sr, Ba and F versus $SiO_2$ for volcanic rocks. . . . .	291
Figure 7.8. Zr, Nb, Y, Ce, Li and Zn versus $SiO_2$ for volcanic rocks . . . . .	292
Figure 7.9. Variation of selected trace elements versus N/(N+K) ratios in Upper Aillik Group volcanic rocks . . . . .	294
Figure 7.10. Variation of the trace element ratios K/Rb, Rb/Sr, Ba/Sr and $La_N/Y_N$ in volcanic assemblages. . . . .	295
Figure 7.11. Rare Earth Element (REE) patterns for volcanic rocks. . . . .	296

## CHAPTER EIGHT : ISOTOPE GEOCHEMISTRY

Figure 8.1. Rb-Sr isochron diagrams for the Big River, Stag Bay, Freshsteak and Lanceground Hills Granitoid units . . . . .	311
Figure 8.2. Composite Rb-Sr isochron diagrams for the Strawberry and Kennedy Mountain Intrusive Suites. . . . .	314
Figure 8.3. Initial Sr isotopic compositions (from isochron and single-sample data) with reference to mantle evolution. . . . .	320
Figure 8.4. Locations of samples analyzed in neodymium isotope geochemistry study. . . . .	324
Figure 8.5. Sm-Nd isochron diagrams for selected Makkovikian and Labradorian units and unit groups. . . . .	330
Figure 8.6. Schematic illustrations of the principles of Nd isotope geochemistry. . . . .	334
Figure 8.7. Histograms of $\epsilon_{Nd}^{CHUR}$ values for Makkovikian and Labradorian plutonic assemblages. . . . .	344
Figure 8.8. Spatial variation of $\epsilon_{Nd}^{CHUR}$ in the study area, showing the proposed eastern limit of Archean crust. . . . .	346
Figure 8.9. Spatial variation of $T_{DM}$ in the study area, showing the proposed eastern limit of Archean crust. . . . .	347
Figure 8.10. Correlations between initial Nd isotopic composition ( $\epsilon_{Nd}^{CHUR}$ ) and major element compositional variations. . . . .	349
Figure 8.11. Correlations between initial Nd isotopic composition ( $\epsilon_{Nd}^{CHUR}$ ) and trace element compositional variations. . . . .	350
Figure 8.12. "Initial Ratio Isochron Diagrams", showing initial $^{143}Nd/^{144}Nd$ versus $^{147}Sm/^{144}Nd$ . . . . .	352
Figure 8.13. The unusual isotopic growth of the Pitre Lake Granite, compared to the "normal" Brumwater Granite . . . . .	355

## CHAPTER 9 : A COMPARATIVE ANALYSIS

Figure 9.1. Distribution of major volcanic-arc batholiths in the Andean-Cordilleran orogenic belt, showing areas discussed here. . . . .	374
Figure 9.2. Simplified geology of the Southern California Batholith, including part of the northern Peninsular Ranges Batholith . . . . .	377
Figure 9.3. Distribution of major plutonic belts in Afghanistan, and location of principal granitoid batholiths. . . . .	379
Figure 9.4. Distribution and setting of granitoid intrusive rocks in the Newfoundland Appalachians. . . . .	381
Figure 9.5. Location and distribution of anorogenic granitoid rocks of the Flowers River Igneous Suite in Northern Labrador. . . . .	384
Figure 9.6. Comparative major element frequency spectra for the TLGB and comparative assemblages. . . . .	388-395
Figure 9.7. Frequency spectra for major elements and derived parameters in Mesozoic batholiths from Afghanistan. . . . .	397
Figure 9.8. Proportions of IUGS rock types in the TLGB assemblages and comparative assemblages, calculated from normative data. . . . .	400

Figure 9.9. Distribution of the TLGB and comparative assemblages in the Q' - ANOR diagram of Streckeisen and LeMaitre (1979). . . . .	402
Figure 9.10. Distribution of the TLGB and comparative assemblages in the quartz - albite - orthoclase ternary system. . . . .	403
Figure 9.11. AFM and CNK trends for the TLGB and comparative assemblages, calculated as mean compositions for 5% SiO <sub>2</sub> intervals . . . . .	404
Figure 9.12. Major element trends for the TLGB and comparative assemblages, expressed as mean compositions for 5% SiO <sub>2</sub> intervals . . . . .	406
Figure 9.13. Comparative trace element frequency spectra for the TLGB and comparative assemblages. . . . .	408-415
Figure 9.14. Rb - (Y + Nb) and Nb - Y discrimination diagrams for the TLGB and comparative assemblages . . . . .	418-419
Figure 9.15. Rb/Zr - Nb discrimination diagrams for the TLGB and comparative assemblages. . . . .	420
Figure 9.16. Zr - Ga/Al x 10 <sup>4</sup> and [(K <sub>2</sub> O+Na <sub>2</sub> O)/CaO] - (Zr+Y+Nb+Ce) discrimination diagrams for the TLGB and comparative assemblages. . . . .	422-423
Figure 9.17. Trace element trends for the TLGB and comparative assemblages, expressed as mean compositions for 5% SiO <sub>2</sub> intervals. . . . .	425-426
Figure 9.18. Some major and trace element characteristics of Labradorian mafic and intermediate intrusive rocks. . . . .	434
<b>CHAPTER TEN : SYNTHESSES, MODELS and CONCLUSIONS</b>	
Figure 10.1. A generalized, schematic model for the petrogenesis of Makkovikian magmas. . . . .	444
Figure 10.2. A generalized, schematic model for the petrogenesis of Labradorian magmas. . . . .	453
Figure 10.3. A speculative plate-tectonic framework for Makkovikian and Labradorian events in the study area. . . . .	460-461
Figure 10.4. A possible paleogeographic configuration of Makkovikian, Ketilidian and Labradorian magmatic provinces at ca. 1650 Ma, compared to the margin of Gondwanaland in South America. . . . .	465
<b>APPENDIX D : SUMMARY OF U-PB ZIRCON GEOCHRONOLOGICAL DATA</b>	
Figure D.1. <sup>206</sup> Pb/ <sup>238</sup> U - <sup>207</sup> Pb/ <sup>235</sup> U concordia diagram for the diorite unit of the Adlavik Intrusive Suite. . . . .	520
Figure D.2. <sup>206</sup> Pb/ <sup>238</sup> U - <sup>207</sup> Pb/ <sup>235</sup> U concordia diagram for the Deus Cape Granitoid. . . . .	520
Figure D.3. <sup>206</sup> Pb/ <sup>238</sup> U - <sup>207</sup> Pb/ <sup>235</sup> U concordia diagram for units of the Numok Intrusive Suite. . . . .	522
Figure D.4. <sup>206</sup> Pb/ <sup>238</sup> U - <sup>207</sup> Pb/ <sup>235</sup> U concordia diagram for The Cape Strawberry Granite. . . . .	522
Figure D.5. <sup>206</sup> Pb/ <sup>238</sup> U - <sup>207</sup> Pb/ <sup>235</sup> U concordia diagram for syenite of the Mount Benedict Intrusive Suite. . . . .	525
Figure D.6. <sup>206</sup> Pb/ <sup>238</sup> U - <sup>207</sup> Pb/ <sup>235</sup> U concordia diagram for the Otter Lake - Walker Lake Granitoid and Monkey Hill Granite. . . . .	525
Figure D.7. <sup>206</sup> Pb/ <sup>238</sup> U - <sup>207</sup> Pb/ <sup>235</sup> U concordia diagram for the Big River Granite and Stag Bay Granitoid. . . . .	526

## LIST OF PLATES

3.1. Features of the Long Island Quartz Monzonite. . . . .	57
3.2. Features of the Kennedy Mountain Intrusive Suite. . . . .	59
3.3. Features of the Melody Granite. . . . .	62
3.4. Features of the Brumwater Granite. . . . .	62
3.5. Features of the Pitre Lake Granite. . . . .	65
3.6. Features of the Manak Island Granitoid. . . . .	65
4.1. Features of the Numok Intrusive Suite (monzonite - quartz monzonite unit). . . . .	105
4.2. Features of the Numok Intrusive Suite (syenite - quartz syenite unit). . . . .	107
4.3. Features of the Numok Intrusive Suite (plagiophyric monzonite unit). . . . .	109
4.4. Features of the Strawberry Intrusive Suite. . . . .	112
4.5. Features of the Strawberry Intrusive Suite (continued). . . . .	116
4.6. Features of the Lanceground Intrusive Suite. . . . .	121
4.7. Features of the Big River Granite. . . . .	124
5.1. Features of the Adlavik Intrusive Suite (mafic rocks and associated rock types). . . . .	166
5.2. Features of the Adlavik Intrusive Suite (mafic rocks and associated rock types) [ continued ]. . . . .	168
5.3. Features of the Adlavik Intrusive Suite (diorite unit). . . . .	171
5.4. Features of the Mount Benedict Intrusive Suite. . . . .	176
5.5. Features of the Monkey Hill Intrusive Suite. . . . .	180
5.6. Features of the Witchdoctor and Burnt Lake Granites. . . . .	184
5.7. Features of the Otter Lake - Walker Lake Granitoid. . . . .	187
6.1. Features of the Freshsteak and Noarse Lake Granitoids. . . . .	242
6.2. Features of the Stag Bay Granitoid. . . . .	242
6.3. Features of the Jeanette Bay Quartz Syenite. . . . .	245
6.4. Features of the Thunder Mountain Syenite. . . . .	245
6.5. Features of the granitoid gneisses exposed south of the Benedict Fault zone. . . . .	247
7.1. Features of the Upper Aillik Group volcanic and hypabyssal intrusive rocks. . . . .	269
7.2. Features of the Jagged Edge assemblage volcanic and hypabyssal intrusive rocks, exposed in the Benedict Mountains . . . . .	273

### General Acronyms

TLGB - Trans-Labrador Granitoid Belt  
MUN - Memorial University of Newfoundland  
NDM - Newfoundland Department of Mines  
BRINCO or BRINEX - British Newfoundland (Exploration) Corporation  
GSC - Geological Survey of Canada  
MASH - Melting, Assimilation, Storage and Homogenization (process)  
VAG - Volcanic Arc Granite  
ORG - Ocean Ridge Granite  
WPG - Within-Plate Granite  
COLG - Collisional Granite  
MORB - Mid-Ocean Ridge Basalt

### Geochemical Acronyms

REE - Rare Earth Elements  
HFS - High Field Strength (Elements)  
LFS - Low Field Strength (Elements)  
OCC - Octahedrally Co-ordinated Cation (Elements)  
CHUR - Chondritic Undepleted (or uniform) reservoir  
DM - Depleted Mantle  
AAS - Atomic Absorption Spectrophotometry  
ICP-ES - Inductively-Coupled Plasma Emission Spectrometry  
ICP-MS - Inductively-Coupled Plasma Mass Spectrometry  
NAA - Neutron Activation Analysis  
XRF-ES - X-Ray Fluorescence (Emission Spectrometry)  
ISE - Ion-selective Electrode (analysis)

### Geochemical Parameters

FeOt (FeO\* in diagrams only) - Total iron as FeO  
 $Fe_2O_3t$  - Total iron as  $Fe_2O_3$   
 $A/C+N+K$  (alumina index) = molecular  $[Al_2O_3/(CaO+Na_2O+K_2O)]$   
 $K+N/A$  (agpaitic index) = molecular  $[(K_2O+Na_2O)/Al_2O_3]$   
 $F/F+M$  =  $FeOt / (FeOt + MgO)$   
 $N/N+K$  =  $Na_2O / (Na_2O + K_2O)$   
N (subscript, as in  $La_N$ , or  $La^*$  in some diagrams) - normalized to chondritic value

### Mineral Abbreviations (Descriptive Tables)

Px - pyroxene	Opx - orthopyroxene	Cpx - clinopyroxene	Ae - aegirine
Hb - hornblende	Act - Actinolite	Bi - biotite	Chl - chlorite
Ol - olivine	Fa - fayalite	Ep - Epidote	Sph - sphene
Zr - zircon	Ap - apatite	All - allanite	Fl - fluorite
Qz - quartz	Ms - muscovite	Plag - plagioclase	Fsp - feldspar
Fe-Ox - iron oxide		K-fsp - potash feldspar	

### Mineral Abbreviations (CIPW Normative Minerals)

Q - quartz	C - corundum	Or - orthoclase	Ab - albite
An - anorthite	Di - diopside	Hy - hypersthene	Ol - olivine
Mt - magnetite	Il - Ilmenite	Ne - nepheline	

### Measurement Units

If units are not specified in geochemical graphs or charts, it can be assumed that major element oxides and normative minerals are expressed as weight percent, and trace elements as weight parts per million (grams/Tonne).



## CHAPTER ONE

### INTRODUCTION

---

---

#### 1.1 PROJECT OVERVIEW

##### Proterozoic Magmatism and Crustal Evolution

Sir Charles Lyell (1885) established the framework for most geological thought with his *principle of uniformitarianism*. Although this concept of the present as the key to the past remains a cornerstone of our science, some of the broader applications of Lyell's doctrine are actively debated by geoscientists who study the Precambrian.

The Proterozoic Eon, extending from 2500 Ma to 570 Ma ago, is the longest segment of Earth history for which the geological record is complete. This vast period is the best vehicle for testing concepts of long-term uniformitarian (e.g. Windley, 1983), unidirectional (e.g. Dickinson, 1981) or cyclic (e.g. Sutton, 1963; Hoffman, 1989) evolution of the Earth.

There is now general agreement that mobile lithospheric plates existed throughout the Phanerozoic, and probably during the Late (i.e., post-900 Ma ago) Proterozoic (e.g. papers in Kroner, 1981 and Medaris et al., 1983). Application of plate tectonics to the earlier Proterozoic record, however, is not as widely accepted, particularly amongst geologists working in the southern hemisphere (e.g. Kroner, 1983; Etheridge et al., 1987).

Hallmarks of the Wilson Cycle of ocean creation and destruction are diverse, including thick Atlantic-type miogeoclinal sequences, and the crucial ophiolites that

attest to former oceanic crust. Such features are absent (perhaps eroded) or strongly metamorphosed in many Proterozoic orogenic belts. Reconstructions of Proterozoic tectonic cycles thus depend heavily on interpretation of orogenic igneous rocks. Volcanic sequences are present in many areas (e.g. papers in Pharoah et al., 1987), but Proterozoic magmatic assemblages are dominated by intrusive rocks, mostly of granitoid composition. These differ radically from the sodic tonalites and trondhjemites that dominate Archean terranes (e.g. Taylor and McClennan, 1985), but their relationship to modern assemblages remains equivocal.

Several Proterozoic granitoid batholiths in the northern hemisphere have been described as "Andean" or "Cordilleran" (e.g. Hoffman, 1980; Lewry et al., 1981; Nystrom, 1982). However, geochemical studies of some have proved inconclusive, and illustrate many contrasts with modern arc magmas (e.g. Fumerton et al., 1984; Halden et al., 1987). The northern hemisphere Proterozoic also contains abundant, siliceous, potassic, evolved granitoid rocks ("rapakivi granites") and associated mafic intrusions of so-called "anorogenic" setting (e.g. Emslie, 1978; Anderson, 1983). Phanerozoic analogues of these rocks exist, particularly in Africa (e.g. Kinnaird and Bowden, 1987), but they are volumetrically insignificant compared to these Proterozoic examples.

Wyborn et al.(1987), Etheridge et al.(1987) and Wyborn (1988) have drawn attention to geochemical contrasts between Proterozoic and Phanerozoic granitoid assemblages in Australia, and propose that the former are products of vertical crustal accretion processes in an intracontinental environment, and unrelated to plate-margin processes. Page (1988) points out the episodic and continent-wide nature of Proterozoic magmatism in Australia, in contrast to the

tightly focussed, linear patterns of the Phanerozoic. These authors comment also on the siliceous, potassic and evolved geochemistry of Proterozoic granitoid rocks, and their partial affinity to anorogenic suites.

The Proterozoic was a critical period for growth of the continental crust. Orogenic belts of 1900 - 1700 Ma age are abundant on a global scale, and (in the northern hemisphere at least), comprise vast tracts of "juvenile" crust separated from the mantle after 2000 Ma ago (Patchett and Arndt, 1986). It has been suggested that crustal growth rates at this time were several times greater than current global arc magma production (Reymer and Schubert, 1986). As crustal growth is synonymous with granitoid magmatism, Proterozoic batholiths are a vital key in unlocking the mechanism(s) of early crustal evolution. In particular, if such growth occurred primarily via arc magmatism (as is widely suggested), how can this be reconciled with the apparent geochemical contrasts between Proterozoic and Phanerozoic granitoid batholiths ?

Resolution of these questions is hampered by poor knowledge of Early Proterozoic granitoid assemblages. Also, many modern or Phanerozoic granitoid assemblages that supposedly define tectonic environments are themselves poorly characterized, particularly in representative geochemical terms. This thesis attempts to address some of these problems via a large-scale geochemical and isotopic study of a major Proterozoic batholith in eastern Labrador, with reference to Phanerozoic magmatic assemblages, and the role of Proterozoic magmatism in crustal evolution.

#### **Aims and Objectives**

The focus of this study is referred to as the Trans-Labrador Granitoid Belt (TLGB). The TLGB is an

enormous zone of Lower and Middle Proterozoic plutonic rocks (and their metamorphic equivalents) that extends for ca. 600 km across Labrador (Figure 1.1). The study is localized in a well-exposed portion of the TLGB in the Makkovik Structural Province (Gower and Ryan, 1986) on the Labrador Coast. The principal objectives are listed below.

1. To document the geology, petrology and geochemistry of these plutonic rocks. Some have been described previously by localized studies, but integration of petrological and geochemical data over the entire area has never been attempted. Geochronological studies using Rb-Sr (this study) and U-Pb methods (Krogh et al., in prep.) play an important role in this work, particularly in defining discrete assemblages within the TLGB, as do results from a large-scale mapping and lithogeochemical program.
2. To examine the sources of TLGB magmas via Sr and Nd isotope geochemistry, and to provide models for their petrogenesis and evolution. This is the first Nd isotopic study of granitoid rocks in Labrador. In addition to this specific objective, Nd isotope studies are relevant to the origins of granitoid magmas and Proterozoic crustal evolution, particularly in terms of crustal growth models.
3. To attempt a quantitative comparative assessment with respect to Phanerozoic assemblages developed in various tectonic settings. In particular, can the TLGB magmatic assemblages be related directly to younger suites, or are they so distinct as to require a unique, non-uniformitarian tectonic model ? If modern analogues are identifiable, what type of environment(s) or process(es) do they suggest for generation of the TLGB and similar assemblages ?

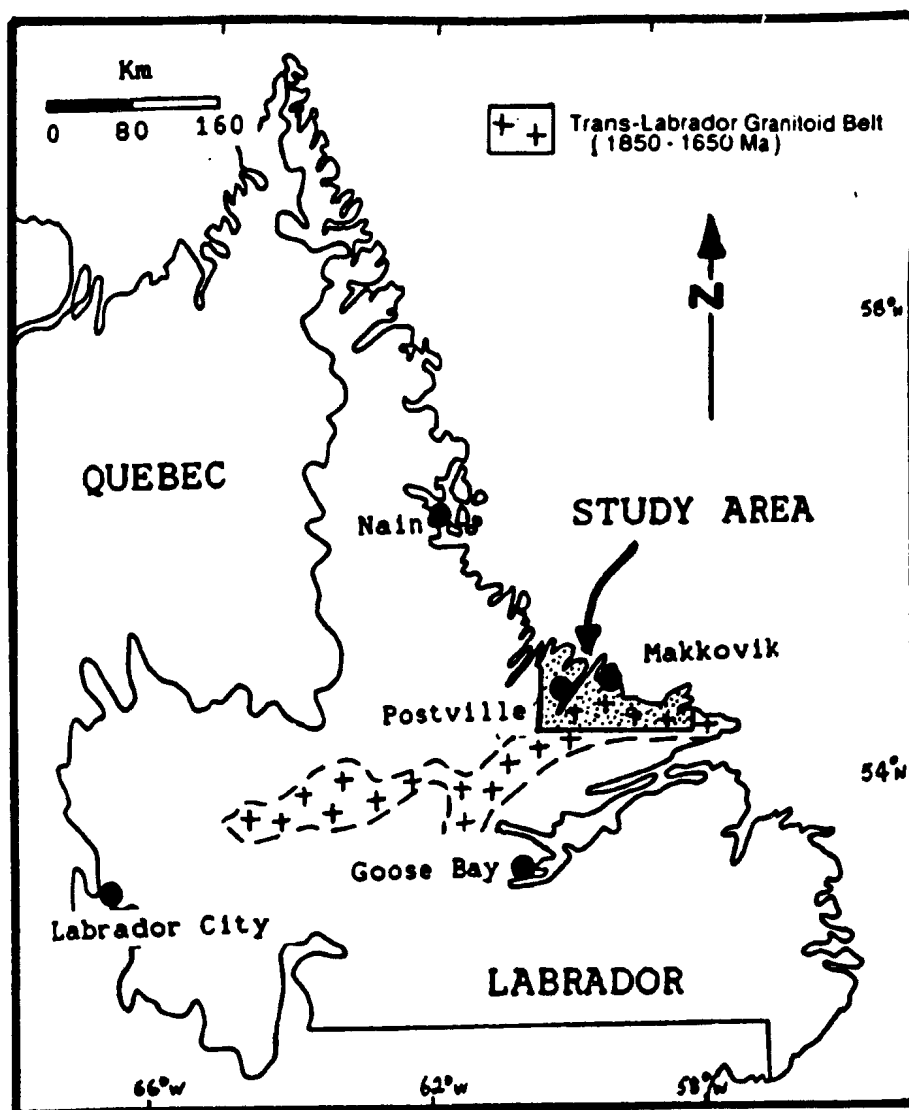


Figure 1.1. Location of the study area in Labrador, showing the approximate outline of the Trans-Labrador Granitoid Belt (TLGB).

4. To assess the role that the TLGB played in local crustal evolution and, on a wider scale, to examine implications for the role of Proterozoic magmatism in Earth history, and possible reasons for differences between these rocks and younger analogues. In particular, can such suites be accommodated in a plate-tectonic framework that is influenced by changing physical conditions (notably declining global heat production), or are non-uniformitarian tectonic models such as those of Kroner (1983) and Etheridge et al. (1987) required ?

#### Scale Considerations

This study is aimed at regional geologic problems and large-scale questions of Precambrian crustal evolution; the study area is huge, and several of the intrusive suites described herein are veritable research topics in their own right. It is impossible to deal fully with all aspects of this project within a Ph.D. dissertation. Many local details and contact relationships between units remain unresolved, and descriptions of units and their field relationships have been condensed. Some aspects of this study (e.g. specialized granites and mineral potential) are discussed elsewhere (Kerr, 1986; 1987; 1988). U-Pb geochronological data are being prepared for publication elsewhere as part of a joint project (Krogh et al., in prep.), and are only briefly summarized in Appendix D. Studies of restricted areas or time-slices in the TLGB (although undoubtedly of interest) would be uninformative in terms of the objectives above. It is important to consider the TLGB (and comparative assemblages) at the largest possible scale, and some local detail must unavoidably be sacrificed to achieve this. It is hoped that this study will establish a framework for future work.

## 1.2 GENERAL INFORMATION

### Location, Topography and Access

The study area is located approximately 150 km northeast of Goose Bay (Figure 1.1), and includes the northern half of NTS 1:250,000 sheet 13J, the eastern edge of sheet 13K, and parts of sheet 130. A rugged, well-exposed, mountainous terrain (maximum elevation 875 m above sea level) dominates eastern and northern portions of the area. The coastline is incised by several deep fiords (e.g. Makkovik Bay) and is protected from the vagaries of the Labrador Sea by numerous offshore islands. The southern and western parts of the study area consist of a variably wooded, boulder-strewn plateau that is largely obscured by glacial drift, with the exception of hilltops and watercourses. "Summer" conditions prevail from late June to late August, and are an extreme mixture of cold, damp weather and hot, humid, fly-infested periods. In Labrador, geologists are widely regarded as the only individuals foolish enough to attempt inland travel during the summer.

The communities of Makkovik and Postville (Figure 1.1) are served by Marine Atlantic coastal boat service from June to November, and by year-round scheduled ( *sensu lato* ) flights operated by Labrador Airways. The project from which this thesis evolved was operated from Makkovik, and from a dormant mineral exploration camp at Melody Lake, some 30 km south-west of Postville.

The coastline provides access to some of the northern and eastern parts of the area, but easy access to the hinterland is possible only by air. The size of the area involved in this project is such that its coverage would have been impossible without extensive helicopter support.

#### Previous Work From 1814 to 1985

Geological research on the coast of Labrador commenced with the work of Steinhauer (1814). This, and subsequent studies (e.g. Leiber, 1860; Packard, 1891; Daly, 1902), consisted largely of descriptions of coastal outcrops. The first mapping in coastal areas was conducted by the Newfoundland Geological Survey and Geological Survey of Canada (Kranck, 1939;1953; Christie et al., 1953; Douglas, 1953). 1:250,000 geological mapping, including coverage of inland areas, was completed by the Geological Survey of Canada in the 1970s (Stevenson, 1970; Taylor, 1975).

In 1954 Murray Piloski of British Newfoundland Exploration Company Ltd (BRINCO) discovered pitchblende near Makkovik. This led to a 25-year period of uranium, molybdenum and base-metal exploration by BRINCO and several joint venture partners (see Gower et al., 1982 and Ryan, 1984 for details). Most of the exploration and research work from 1955 to 1978 was related to the search for economic mineralization in uranium-bearing supracrustal sequences. Many of these studies remain confidential, but some general results were published by BRINCO geologists (e.g. Beavan, 1958; Gandhi et al., 1969; Gandhi, 1978). Uranium deposits at Kitts and Michelin were evaluated for commercial development in the late 1970s. Several more general studies with economic implications were carried out via university theses supported partly by BRINCO. These included documentation of mineralization (e.g. Gill, 1966; Barua, 1969), and also regional geological and structural syntheses (Clark, 1973,1979; Marten, 1977) in the Makkovik and Kaipokok Bay areas. The study of Marten (1977) was



particularly influential in unravelling the structural evolution of the area. A third group of thesis studies emphasized petrological and geochemical studies of uranium-bearing volcanic rocks (White, 1976; Evans, 1980).

The Newfoundland Department of Mines (NDM) started work in the area in 1976 and completed regional 1:100,000 mapping in 1980 (Bailey, 1979; Bailey et al., 1979; Ryan and Harris, 1978; Doherty, 1980; Gower, 1981). Compilation and synthesis of this information was presented by Gower et al. (1982) for the eastern half and by Bailey (1979) and Ryan (1984) for the western half of the area. These programs focused mostly on supracrustal sequences, but the areal importance of post-tectonic granitoid rocks was recognized, as was their polyphase and compositionally variable nature.

#### **Central Mineral Belt Granitoid Project**

Re-examination and sampling of a number of mineral occurrences in the study area during 1984 (Wardle, 1984; Wardle and Wilton, 1984) awakened interest in both the gold potential of the area and the possible importance of post-tectonic granitoids as hosts or progenitors to mineralization. The "Central Mineral Belt Granitoid Project" (CMBGP) was initiated to define and delimit plutonic associations and assess their potential for economic mineralization. This commenced with geochemical sampling and mapping in 1985, leading to revision of existing unit designations and definition of new regional granitoid units (Kerr, 1986). Analysis of geochemical data led to the identification and delineation of several granitoid associations considered to have some of the

characteristics of specialized granites (Kerr, 1987). The 1986 field season included follow-up mapping and sampling in these areas, and extension of regional coverage eastward into the Benedict Mountains. The petrology and geochemistry of possible specialized granitoid rocks in the area was discussed in more detail by Kerr (1988a).

The CMBGP was co-ordinated throughout its duration with related metallogenic studies by Derek Wilton and co-workers. These include thesis studies of granite-related mineral prospects (e.g. MacDougall, 1988; MacKenzie, 1988), and general assessment of the role of granitoid rocks in metallogenesis throughout the Central Mineral Belt (Wilton et al., 1986, 1987).

#### Relevant Work Outside The Study Area

Systematic mapping conducted by the NDM has led to substantial re-interpretation of geotectonic divisions within Labrador. Geological and geochronological investigations in central Labrador (Wardle et al., 1982, 1986; Nunn et al., 1985; Thomas et al., 1986) defined the geologic entity termed the Trans-Labrador Batholith, and also identified a ca. 1650 Ma old cryptic orogenic belt (Labrador Orogen) within the area occupied by the ca. 1100 Ma Grenville Province. Geologic mapping in areas adjacent to the study area (Ryan and Kay, 1982; Gower et al., 1980; Gower, 1986; Gower and Ryan, 1986; Owen et al., 1986) is also relevant to this project, and is discussed in the appropriate chapters.

### 1.3 TERMINOLOGY and NOMENCLATURE

#### Classification and Nomenclature of Plutonic Rocks

The nomenclature of plutonic rocks is based on modal proportions of quartz, alkali feldspar and plagioclase feldspar. The IUGS classification (Streckeisen, 1976; Figure 1.2a) is employed in this thesis, with substitution of the term "monzogranite" for the "3b" granite field of the IUGS scheme; the term "granite" is restricted to the "3a" granite field, although it is used *sensu lato* in some unit names. Rock names assigned in this thesis are visual estimates from cut slabs stained for K-feldspar. No point-counting of sections or slabs was attempted, as most TLGB rocks are coarse grained and/or porphyritic.

In comparative studies, an unbiased method of defining rock types is required; classification via normative mineralogy is the preferred method. Streckeisen and LeMaitre (1979) provide an empirical equivalent to the IUGS scheme using the parameters  $Q' = [ Q / (Q + Ab + An + Or) ]$  and  $ANOR [ An / (An + Or) ]$  (Figure 1.2b). The recommended normative calculation scheme is the mesonorm\* of Barth (1955), which incorporates hydrous minerals such as hornblende and biotite. This system is used widely in this thesis to provide a method of comparing and subdividing suites or assemblages. It is not used to assign unit names, but there is general agreement between names based on modal estimates and those calculated from norms.

The term "granitoid" lacks precise definition, but is generally used for all igneous plutonic rocks from diorite to alkali-feldspar granite (e.g. Strong, 1981). It includes most of the fields in Figure 1.2, with the exception of gabbro.

\* see note in caption for figure 1.2

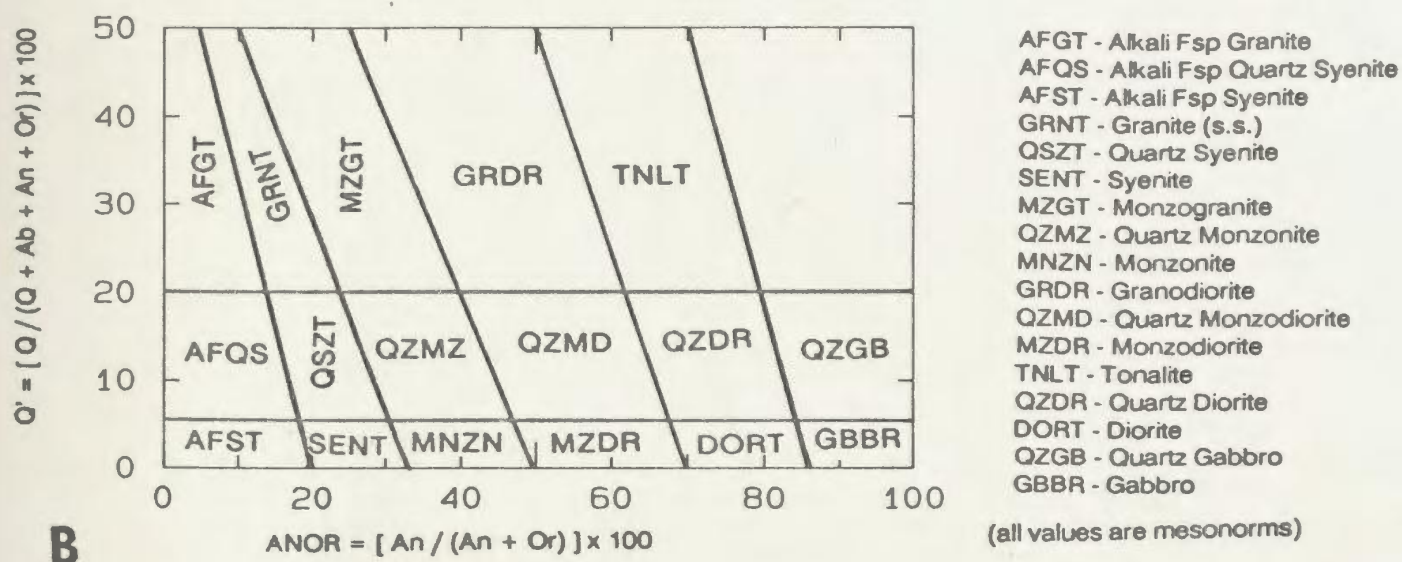
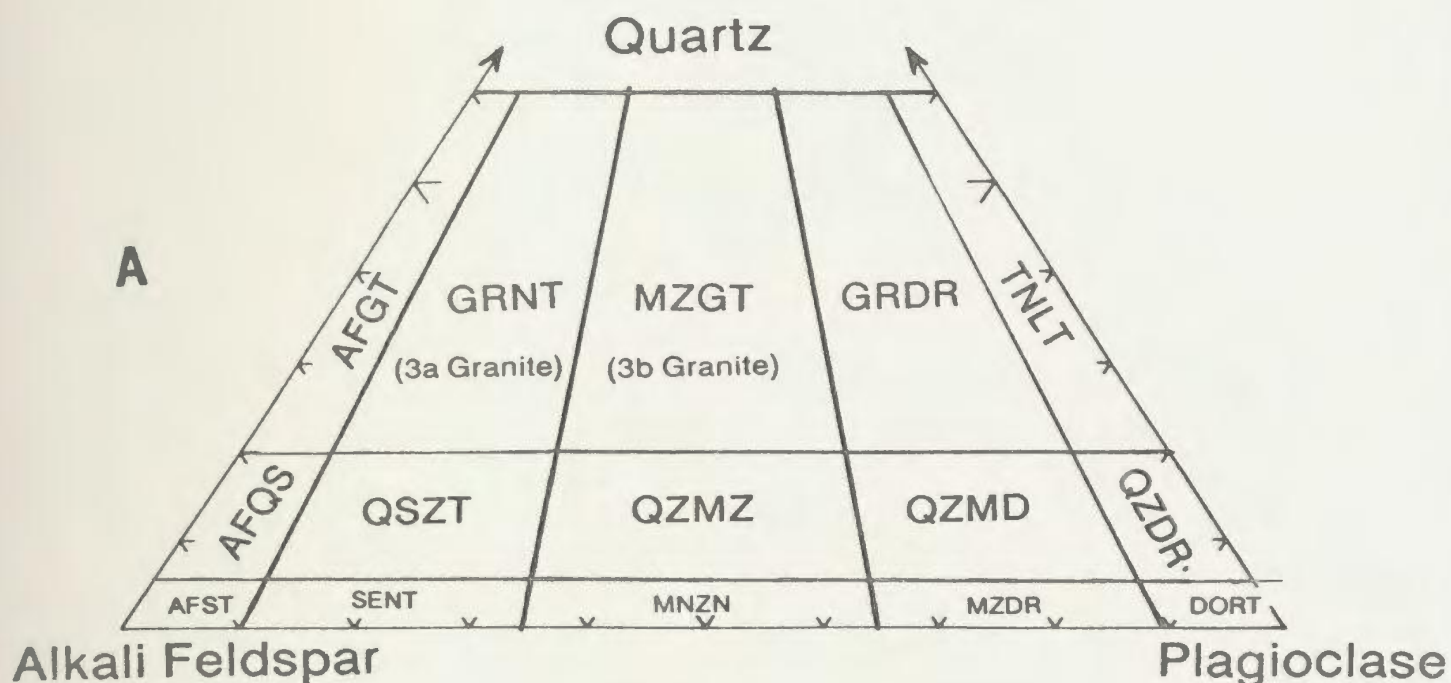


Figure 1.2. Classification and nomenclature of common plutonic rocks. (a) Modal classification of Streckeisen (1976). (b) Normative classification of Streckeisen and Lemaitre (1979).

NOTE: In practice, CIPW and Barth mesonorms yield almost identical results in the Streckeisen and LeMaitre system, as shown also by Bowden et al.(1984) for a range of rock types. For the sake of consistency with the original paper, I have employed the mesonorm.

### Descriptive Geochemical Terminology

Simple, descriptive geochemical terms outlined by Shand (1927) are used extensively in this thesis. In contrast to many other geochemical terms (see below), these have direct implications for varietal mineralogy.

The alumina index or  $A/C+N+K$  ratio [ molecular  $Al_2O_3/(CaO+Na_2O+K_2O)$  ] divides rocks into metaluminous ( $A/C+N+K < 1$ ) and peraluminous ( $A/C+N+K > 1$ ) categories. Alumina oversaturation in the latter group permits formation of aluminous phases such as muscovite, garnet and cordierite.

The agpaite index or  $K+N/A$  ratio [ molecular  $(K_2O+Na_2O)/Al_2O_3$  ] provides distinction into peralkaline ( $K+N/A > 1$ ) and subalkaline ( $K+N/A < 1$ ) categories. There is a common misconception (e.g. Bowden et al., 1984) that peralkalinity is also implied by  $A/C+N+K < 1$ ; this is not so, except in rocks with negligible CaO. Peralkaline rocks are oversaturated in  $(Na_2O+K_2O)$ , and may contain alkali-bearing mafic silicates, e.g. reibeckite and aegirine. If this property is combined with a low silica content, such rocks may contain feldspathoids such as nepheline or leucite. The term peralkaline is distinct from "alkaline", as commonly applied to mafic rocks. The latter has no precise definition, and refers only to relatively high  $(Na_2O+K_2O)$  at a given CaO or  $SiO_2$  content (see below).

Peacock (1931) introduced the alkali-lime index (ALI;  $SiO_2$  content at which  $K_2O+Na_2O$  is equal to CaO), and also the terms alkaline ( $ALI < 51\% SiO_2$ ), alkali-calcic ( $51\% < ALI < 56\% SiO_2$ ), calc-alkaline ( $56\% < ALI < 61\% SiO_2$ ) and calcic ( $ALI > 61\% SiO_2$ ). These are arbitrary

divisions, but modern petrology has endowed the terms with genetic meanings beyond their original definition. The ALI cannot be measured directly in granites with high  $(K_2O+Na_2O) / CaO$  ratios, but may be estimated by linear regression.

Two other descriptive terms employed in this thesis are the soda-potash ratio [  $N/N+K$  ;  $Na_2O/(Na_2O+K_2O)$  ] and the iron-magnesium ratio [  $F/F+M$  ;  $FeO/(FeO+MgO)$  ]. The latter uses total iron expressed as FeO (FeO). The term sodic is used where  $N/N+K > 0.5$  and potassic where  $N/N+K < 0.5$ . No descriptive labels are attached to  $F/F+M$ , which is a measure of relative iron enrichment.

Geochemical classifications developed by French researchers (e.g. La Roche, 1980; Debon and Lefort, 1982) are employed locally in this thesis. The "characteristic minerals" method of Debon and LeFort (1982) expresses oxides as cation proportions ( $\times 1000$ ), and defines the following parameters.

$Q = Si/3 - (K + Na + 2Ca/3)$  [measure of silica saturation]

$P = K - (Na + K)$

$A = Al - (K + Na + 2Ca)$  [measure of alumina saturation]

$B = Fe + Mg + Ti$

$F = 555 - (Q + B)$

These methods are hampered by the the need for sequential calculations, and by complex descriptive terminology. Conventional normative parameters or molecular ratios provide the same information in a more familiar mineralogical framework. Nevertheless, the Q-B-F ternary projection of Debon and LeFort (1982) was found to have some utility in this study.

Descriptive terminology used to subdivide trace elements into groups (Table 1.1) is adapted from Saunders et al. (1979). The new term "Octahedrally Co-ordinated Cation" (OCC) elements refers to the ability of divalent cations to substitute for  $Mg^{2+}$  and  $Fe^{2+}$  in common mafic silicate minerals. These correspond to the "compatible" trace elements of conventional terminology. The distinction is made because elements such as Ba and Sr may be compatible in granitoid magmas, yet are geochemically distinct from V, Cr, Cu and Ni.

#### **Environments of Granitoid Magmatism**

The theory of plate tectonics provides a framework for classification of present-day and recent (i.e. Mesozoic - Cenozoic) environments of granitoid magmatism. Large-scale silicic magmatism is essentially a continental phenomenon, although minor amounts of felsic volcanic rocks are associated with oceanic settings, particularly island arcs. Tectonic settings of continental granitoid magmatism are grouped loosely into three environments (e.g. Pitcher, 1983; Pearce et al., 1984).

**Volcanic Arc Magmatism** : Arcuate orogenic belts associated with subduction beneath continental margins (e.g. the Andean-Cordilleran belt) are characterized by long-lived zones of volcanism and plutonism that parallel the trench axis. The least differentiated granitoids have affinities to plutonic rocks in intra-oceanic island arcs, but most continental arcs contain compositionally extended suites dominated by metaluminous to peraluminous, sodic

Table 1.1. Descriptive terminology used for trace element associations. Classification adapted from Saunders et al.(1979), with modifications to suit granitoid rocks rather than basalts.

---

1. OCTAHEDRALLY CO-ORDINATED CATION (OCC) ELEMENTS

*Elements with divalent cations that substitute readily in the octahedral (co-ordination = 6) sites in rock-forming Mg and Fe silicates. They accumulate in crystallizing phases and therefore show COMPATIBLE behaviour.*

Sc V Cr Co Ni Cu (also MnO in most granites)

2. LOW FIELD STRENGTH (LFS) ELEMENTS

*Elements with a charge/radius ratio of  $< 0.2$ . In general, they are excluded from common silicates and accumulate in residual liquids, showing INCOMPATIBLE behaviour. This is, however, not so for Ba and Sr, which can enter feldspars. Rb may enter biotite or muscovite.*

Rb Cs U Th Pb Sr Ba

3. HIGH FIELD STRENGTH (HFS) ELEMENTS

*Elements with a charge/radius ratio of  $> 0.2$ . These commonly show INCOMPATIBLE behaviour, but are very strongly influenced by residual phases, particularly zircon, allanite, monazite, sphene and apatite. They are also widely regarded as "immobile".*

Zr Hf Nb Ta Sn W Mo (also  $\text{TiO}_2$  and  $\text{P}_2\text{O}_5$  in granites)

4. RARE EARTH ELEMENTS (REE)

*Trivalent (except Eu) elements whose behaviour is sensitive both to accessory and major phase assemblages in residual material. Y is included, although not technically a member of the rare earth (lanthanide) series.*

Y La Ce Pr Nd Sm Eu Gd Tb  
Dy Ho Er Tm Yb Lu

5. "INDETERMINATE" TRACE ELEMENTS

*Elements whose behaviour may vary widely depending on major phase assemblages in residual material and upon other chemical and physical factors.*

Li Be Ga Zn As Sb F

---



diorite, tonalite and granodiorite. These suites are commonly calcic to calc-alkaline. "Mature" oceanic island arcs include intermediate plutonic rocks that overlap extensively with continental arc suites.

**Collision Zone Magmatism** : Zones where subduction of oceanic lithosphere has ceased, but continental blocks continue to converge (e.g. the Alpine-Himalayan belt), are also characterized by large-scale granitoid magmatism. Geophysical data commonly indicate that such zones are underlain by anomalously thick continental crust, implying tectonic thickening via thrusting. Collisional zones contain a wide variety of igneous rocks, but most that accompany or follow collision are compositionally restricted monzogranite to granite. Peraluminous two-mica leucogranites are a characteristic component of many such zones. In detail, collisional orogens are tectonic collages of pre-, syn- and post-collisional magmatic environments (Debon et al., 1986; 1987a; Harris et al., 1984), and thus commonly include rocks of volcanic-arc type amongst their earliest components. Post-collisional suites associated with tensional or transcurrent tectonics may also resemble granites of the within-plate group (see below).

**Within-Plate Magmatism** : Silicic magmatism is also associated with uplift and tensional tectonics in stable cratonic areas. Examples include the modern East African Rift System, and Mesozoic granites of Nigeria and Niger (Kinnaird and Bowden, 1987). The latter were probably associated with the break-up of Gondwanaland. Continental within-plate magmatic zones contain diverse magmatic

assemblages, commonly of bimodal, alkaline-peralkaline or silica-undersaturated character. Peraluminous compositions are rare. In terms of volume, within-plate zones are insignificant compared to the huge batholiths generated in volcanic arc and collision zone environments. The term anorogenic is also commonly used for granites of this association.

*Continuity of Tectonic Environments* : The above tectonic environments do not occur in temporal or spatial isolation, but are transient situations in orogenic evolution. For example, collisional events are an unavoidable consequence of subduction. Current models for the evolution of complex belts such as the North American Cordillera (e.g. Coney et al., 1980) suggest accretion of island arcs and continental fragments against active margins. Such models imply that collisions occur repeatedly during orogenic evolution. Similarly, rifting and uplift associated with within-plate magmatism may occur in post-collisional situations (Harris et al., 1984), or in back-arc settings, distal from the locus of subduction (Brown et al., 1984). It is also important to realize that unique rock types characteristic of specific environments do not exist; there is instead a continuum of compositions.

#### Classifications Based On Source Materials

The restriction of granitoid magmatism to continental areas has led some (e.g. Chappell and White, 1974; White and Chappell, 1977) to suggest that most granitoid rocks are derived wholly from continental crust. Others contend

that they are mostly of mantle origin (e.g. Brown, 1981) or represent mixtures of crust and mantle (e.g. Didier et al., 1982). This has given rise to a veritable jungle of terminology.

***I, S, A and M-type Granites*** : A viewpoint prevalent in Australia contends that granitoid magmas "image" their sources in a simple and direct manner (e.g. Chappell and White, 1974; Chappell et al., 1988; Chappell and Stephens, 1988). Chappell and White (1974) divided granites into I-type (igneous source) and S-type (sedimentary source) categories. These terms were later redefined to denote "infracrustal" and "supracrustal" respectively (White and Chappell, 1983). S-type granites are peraluminous, and are defined by a parameter equivalent to the  $A/C+N+K$  ratio. In contrast, I-type granites are metaluminous, calcic and compositionally varied suites. The characteristics of S-type granites are supposedly inherited from sources that have passed through the surface environment.

Loiselle and Wones (1979) and Collins et al. (1982) added "A-type" (anorogenic or anhydrous) granites to the list. These are evolved, metaluminous to peralkaline rocks, considered to be anatectic derivatives of dehydrated lower crustal rocks. Pitcher (1983) introduced "M-type" (mantle) granites for calcic, plagioclase-rich intrusive rocks of oceanic areas considered to have mantle or mafic sources.

***Antipodean Viewpoints and the Restite Model*** : Many petrologists (particularly in Australia) contend that compositional variation in granites results from "unmixing" of residual source material and anatectic melt (e.g. White

and Chappell, 1976). In extreme cases, the process of total mobilization, or "remagmatization" (Chappell and Stephens, 1988) has been invoked to explain calcic or tonalitic I-type granites that are otherwise difficult to accomodate in this model. The restite model is so entrenched that other types of information, e.g. Nd and Sr isotopic data indicative of crust-mantle mixing, have been questioned on the basis of incompatibility with predictions of the model (e.g. McCulloch and Chappell, 1982). Most workers accept that "source" is indeed an important factor in magmatism, but dogmatic application of the restite hypothesis has been widely questioned (e.g. Strong, 1980; Gray, 1984; Hildreth, 1987; Wall et al., 1987).

*The Pseudo-Descriptive Viewpoint* : The restite model has not been widely accepted in Europe or North America, but its associated terminology is epidemic. I, S, A and M-type granitoids are, however, viewed as broad petrochemical groups that owe their differences to both in source characteristics and processing environment. For example, I-type granites are subdivided into Cordilleran and Caledonian subcategories developed at different stages in orogenesis (Pitcher, 1983). M-type and I-type (Cordilleran) granites are viewed as partly gradational; an implicit recognition that the latter are not wholly of crustal origin. Although this *sensu lato* usage of the source-image terminology is probably more realistic than the antipodean view, there is a tendency to view these granite types as simplistic indicators of geotectonic environments (e.g. Nystrom, 1982).

### Classifications Based On Tectonic Environment

Empirical classifications based on the trace element geochemistry of granitoid rocks from "known" tectonic settings (see above), are currently popular.

Pearce et al. (1984) coined the terms Ocean-ridge (ORG), Volcanic-Arc (VAG), Collisional (COLG) and Within-Plate (WPG) granites, and proposed distinction using trace element patterns. In general terms, these correspond to M-type, I-type, S-type and A-type granites as defined by Pitcher (1983), but there is significant overlap, particularly in "collisional" granites, which coincide partly with VAG and WPG fields. Harris et al. (1984) analyzed collisional granites in a similar fashion, and recognized four discrete types, including rocks that correspond to the VAG and WPG groups of Pearce et al. (1984). A similar study of arc-related granitoids by Brown et al. (1984) outlined a concept of "arc maturity" (i.e. age or distance from the locus of subduction). Mature (old or distal) arcs include granites similar to the COLG and WPG groups defined by Pearce et al., (1984) and Harris et al. (1984). All three studies employ essentially the same trace elements (Rb, Zr, Y, Nb, Ta) as discriminants !

It is clear that there are no simple correlations between tectonic setting and trace element geochemistry. However, this has not prevented almost universal use of such discrimination diagrams in studies of ancient granitoid rocks. In a subsequent chapter of this thesis, it is shown that examination of compositional spectra and evolutionary trends may, in combination with these methods, provide better definition of contrasting granitoid assemblages.

## Investigative Methods

The general geology of the study area is established by previous studies (Gower, 1981; Gower et al., 1982; Ryan, 1984). This project is thus a thematic mapping and sampling project, aimed largely at the plutonic rocks of the TLGB. In view of the large area (Figure 1.1), this work was accomplished mostly by a large-scale, grid-based mapping and geochemical sampling program carried out with helicopter support. Ground-based work was carried out only in well-exposed or critical parts of the area, and along the superb coastline exposures.

## Sample Populations

In total, over 1500 samples were collected and analyzed under the auspices of the the Central Mineral Belt Granitoid project. These can be divided into three groups. Regional samples were collected on a regular grid at intervals of ca. 2 km using a sample site preselected on a random basis. These provide an unbiased view of the compositional anatomy of intrusive suites and units, and are representative of the areal abundance of rock types. Follow-up samples were collected on a regular grid at intervals of ca. 1 km using random site selection methods. They were collected from selected suites defined by regional sampling, to provide assessment of mineralized or potentially specialized granitoid rocks. Geological samples were collected routinely during mapping. They represent typical examples of units, or mineralogical-textural variants thereof.

Regional and follow-up sampling methodology is based on geochemical exploration techniques (e.g. Garrett, 1983), and sampling projects in the Ackley Granite of southeastern Newfoundland (Dickson, 1983, Tuach et al., 1987). The regional population is representative of the TLGB as a whole, with no bias towards specific compositions or areas. The follow-up population, on the other hand, is strongly biased towards evolved, high-SiO<sub>2</sub> granitic compositions. It is therefore excluded from discussions relating to large-scale, regional patterns, but is retained for descriptions of specific units or suites. The geological sample population is the smallest and, although compositionally representative, is slightly biased towards coastal areas. Assessment of frequency spectra and univariate statistics indicates, however, that the characteristics of the regional population are unaffected by its inclusion. The two populations have therefore been combined for most interpretative discussions.

Geochronology samples, consisting of 20-40 Kg of fresh material, were acquired for U-Pb geochronology at selected localities (Krogh et al., in prep.), and were also used for rare earth element (REE), Sm-Nd and Rb-Sr isotopic analysis. Additional REE, Sm-Nd and Rb-Sr analyses were performed using samples selected from regional, follow-up and geological populations.

#### Overview Of Geochemical Analysis Program

Full details of analytical techniques, including estimates of precision and analyses of international standards, are presented in Appendix A. A brief overview is presented below as a convenience to the reader.

**Major Elements** : Major elements were analyzed by atomic absorption spectrometry (AAS) at the Newfoundland Department of Mines (NDM) Laboratory in St. John's. Based on 73 random duplicate analyses, the median (50th percentile) analytical precision is  $\pm 5.0$  % or better for all oxides except  $\text{Fe}_2\text{O}_3$  (6.5%).

**Trace Elements by AAS** : Li, V, Cr, Ni, Cu, Zn, Rb, Sr, Ba and Pb were determined by AAS at the NDM laboratory. Median precision for all is  $\pm 5.0$  % or better, except for Li (8.2%).

**Trace Elements by ICP-ES** : Ga, Y, Zr, Nb, La, Ce and Th were determined by inductively-coupled plasma emission spectroscopy at the NDM laboratory. Median precision for all is  $\pm 5.0$  % or better, except for Th (13.3 %). The latter is affected by determinations at or near detection limit in mafic rocks; precision for granites is considerably better.

**Trace Elements by INAA** : Sc, Cs, Sm, Yb, Hf and U were determined by instrumental neutron-activation analysis by Becquerel Ltd. and Nuclear Activation Services Ltd.(U) laboratories. Median precision is  $\pm 6.0$  % or better, except for Sc (9.5%) and Hf (12.2%).

**Other Trace Element Methods** : Fluorine (ion-selective electrode method; NDM) has median precision of  $\pm 9.4$ %. Sn (XRF, Bondar-Clegg) has poor median precision of  $\pm 66$  % ; this reflects near-detection limit levels of Sn in most samples; the method is capable of resolving anomalous data only.



*Rare-Earth Element Analyses by ICP-MS* : The rare earth element (REE) analyses presented here were determined by inductively-coupled plasma mass spectrometry (ICP-MS) at Memorial University. Precision for all elements by this method is estimated at  $\pm 5.0$  % or better (H.Longerich and S.Jackson, pers. comm., 1988).

## CHAPTER TWO

### GEOLOGICAL FRAMEWORK

---

#### Chapter Abstract

In southern and eastern Labrador, the Makkovik Province and the Grenville Province are part of a long-lived Proterozoic mobile zone that can be traced from Scandinavia to Mexico. Much of the Grenville Province in Labrador is a reworked ca. 1650 Ma old mobile belt termed the Labrador Orogen. A major, arcuate belt of granitoid rocks, termed the Trans-Labrador Granitoid Belt (TLGB), forms the northern edge of the Labrador Orogen. In the Makkovik Province, the TLGB is a composite belt including Makkovikian (ca. 1800 Ma) and Labradorian (ca. 1650 Ma) plutonic assemblages.

The oldest rocks in the study area are Archean gneisses. These form the basement to metasedimentary - mafic volcanic supracrustal sequences (Moran Lake and Lower Aillik Groups) that are at least 1860 Ma old. These rocks are overlain by a thick felsic volcanic sequence (Upper Aillik Group), deposited ca. 1860 - 1800 Ma ago. All of these rocks were affected by Makkovikian deformation ca. 1800 Ma ago.

Early Proterozoic plutonic rocks form three main associations. "Syn-tectonic" Makkovikian plutonic rocks (emplaced ca. 1840-1800 Ma ago) underwent the final episode(s) of Makkovikian deformation. "Post-tectonic" Makkovikian plutonic rocks (1800-1760 Ma) overlap in age with the syn-tectonic association, suggesting that both groups form a single magmatic pulse that transcends the Makkovikian orogeny. The plutonic rocks are dominated by quartz monzonite to granite, and are probably temporally equivalent to parts of the Upper Aillik Group. Labradorian plutonic rocks (1670-1600 Ma) are entirely post-tectonic, and consist of layered gabbro-monzonite-syenite intrusions, and quartz monzonite to granite plutons. A Labradorian volcanic sequence (Bruce River Group) occurs west of the study area. There is no evidence of Labradorian deformation in the Makkovik Province.

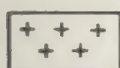
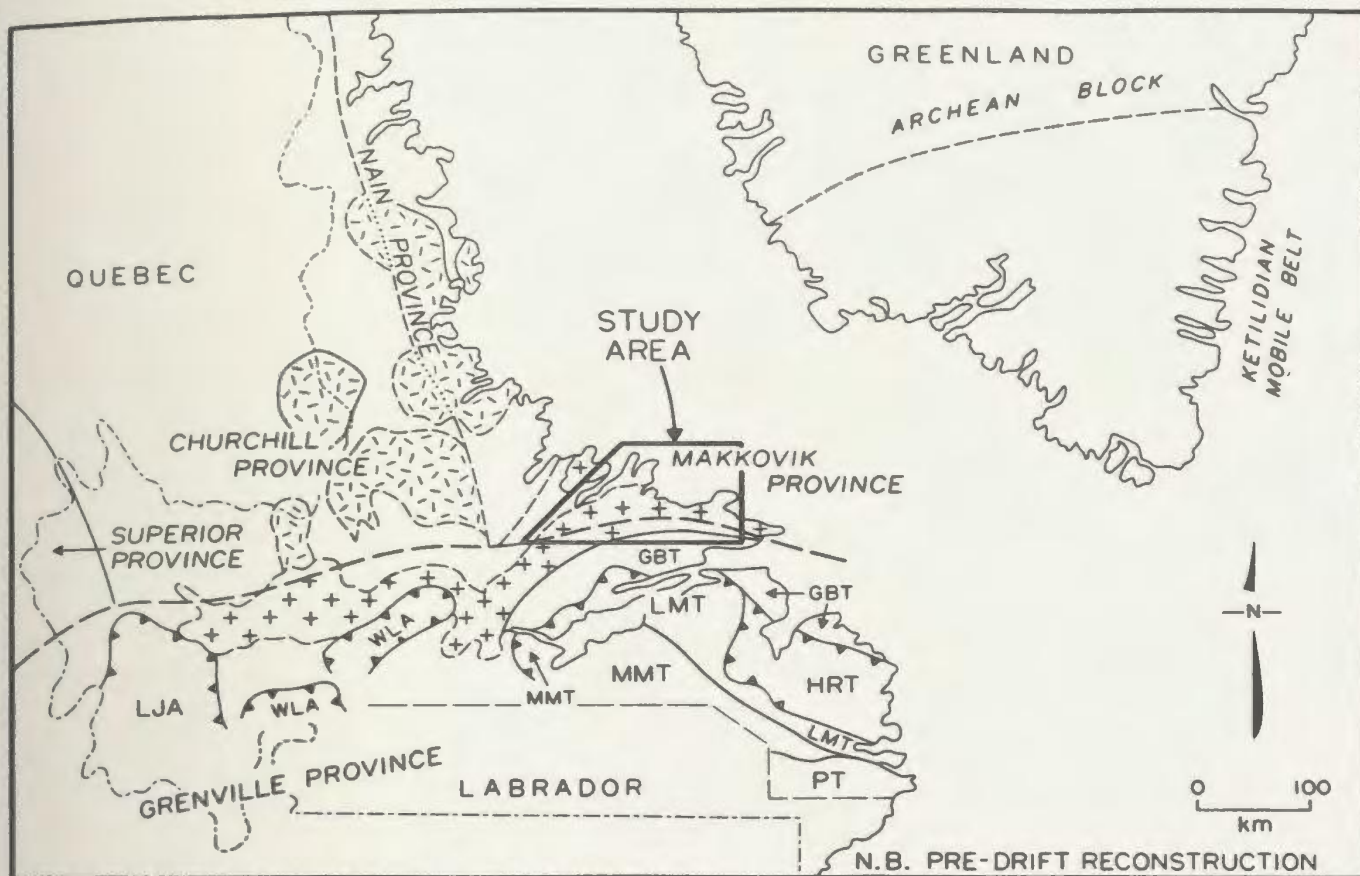
The southern part of the area was subsequently affected by Grenvillian deformation, which imposed east-trending fabrics on most of the above. A number of major east-trending Grenvillian faults divide the remainder of the area into structural blocks that expose differing crustal levels.

## 2.1 REGIONAL GEOLOGY

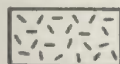
### General Geology Of Labrador

The geology of Labrador is illustrated and discussed by Greene (1974) and Nunn et al. (in prep.). Labrador is divided into five Precambrian structural provinces (Figure 2.1), based on trends and "stabilization events" defined by Rb-Sr and K-Ar age data (after Stockwell, 1972). The Nain and Superior Provinces are of Archean age (stabilized ca. 2800-2500 Ma ago), and are separated by the Proterozoic Churchill Province (stabilized ca. 1800 Ma ago). The Nain Province is part of the North Atlantic Archean Craton (Bridgwater et al., 1973), and was originally contiguous with west Greenland (Figure 2.1). The Nain Province is bounded to the southeast by the Proterozoic Makkovik Province (Gower and Ryan, 1986), which was mostly stabilized ca. 1800 Ma ago, but includes some ca. 1650 Ma old intrusive rocks.

The southern part of Labrador forms part of the Grenville Province, which was stabilized ca. 1100 Ma ago. Geochronological studies completed since 1980 (e.g. Wardle et al., 1986; Thomas et al., 1986) have shown that many gneisses in the Labrador portion of the Grenville Province were formed and/or metamorphosed ca. 1650 Ma ago. Mapping has shown that it is composed of a number of thrust-bounded terranes that were assembled into their current positions



Trans-Labrador Granitoid Belt  
(1850 - 1650 Ma)



Anorthosite-Granitoid Complexes  
(1500 - 1300 Ma)

#### LABRADORIAN HIGH-GRADE TERRANES (ca. 1650 Ma)

WLA - Wilson Lake Allochthon  
LJA - Lac Joseph Allochthon  
MMT - Mealy Mountains Terrane  
LMT - Lake Melville Terrane  
GBT - Groswater Bay Terrane  
HRT - Hawke River Terrane  
PT - Pinware Terrane

----- Provincial Border

----- Geological Boundary

--- Thrust Zone

— Terrane Boundary

----- Grenville Front Zone  
(Northern Boundary of  
Grenvillian Deformation)

Figure 2.1. Summary map showing major structural provinces in Labrador and adjacent parts of Greenland, location of the Trans-Labrador Granitoid Belt (TLGB), and locations and names of Labradorian high-grade terranes contained within the Grenville Province. Compiled from Gower and Ryan (1986), Wardle et al. (1986) and Gower et al. (1987, 1988). For descriptions of Labradorian Terranes, see these references. Dashed line in southern Labrador indicates current limit of mapping.

during or prior to the Grenvillian Orogeny. These terranes represent a structurally reworked belt of ca. 1650 Ma old crust termed the Labrador Orogen (Thomas et al., 1986), and are termed the Labradorian high-grade terranes. The interface between the high-grade terranes and older structural provinces to the north is marked by the Trans-Labrador Granitoid Belt (TLGB), discussed in detail below.

In addition to the major structural provinces discussed above, the Nain and Churchill Provinces are intruded by anorogenic gabbro-anorthosite-granite plutons of ca. 1500-1300 Ma age (e.g. Emslie, 1978).

#### Labrador as Part of a Proterozoic Supercontinent

Palaeomagnetic evidence (e.g. Piper, 1983) suggests that the shield areas of the northern hemisphere formed a single mass throughout much of the Proterozoic. Lower and Middle Proterozoic mobile belts occur all along the southern margin of this supercontinent (Figure 2.2), but are largely overprinted by the younger Grenville Province. The Makkovik Province is continuous with the Ketilidian mobile belt of Greenland (Allaart, 1976; Gower and Ryan, 1986), and (ultimately) with the Svecofennian Province of Scandinavia (Gower and Owen, 1984). Equivalents of the Labradorian high grade terranes are present in the Sveconorwegian belt (Gower and Owen, 1984). As in Labrador, the interface between these ca. 1650 Ma old terranes and older parts of Scandinavia is marked by a major belt of granitoid plutonic rocks, termed the Småland-Varmland or Trans-Scandinavian Granitoid Belt (Lindh, 1987). Gower and Owen (1984) suggested that this is equivalent to the TLGB.

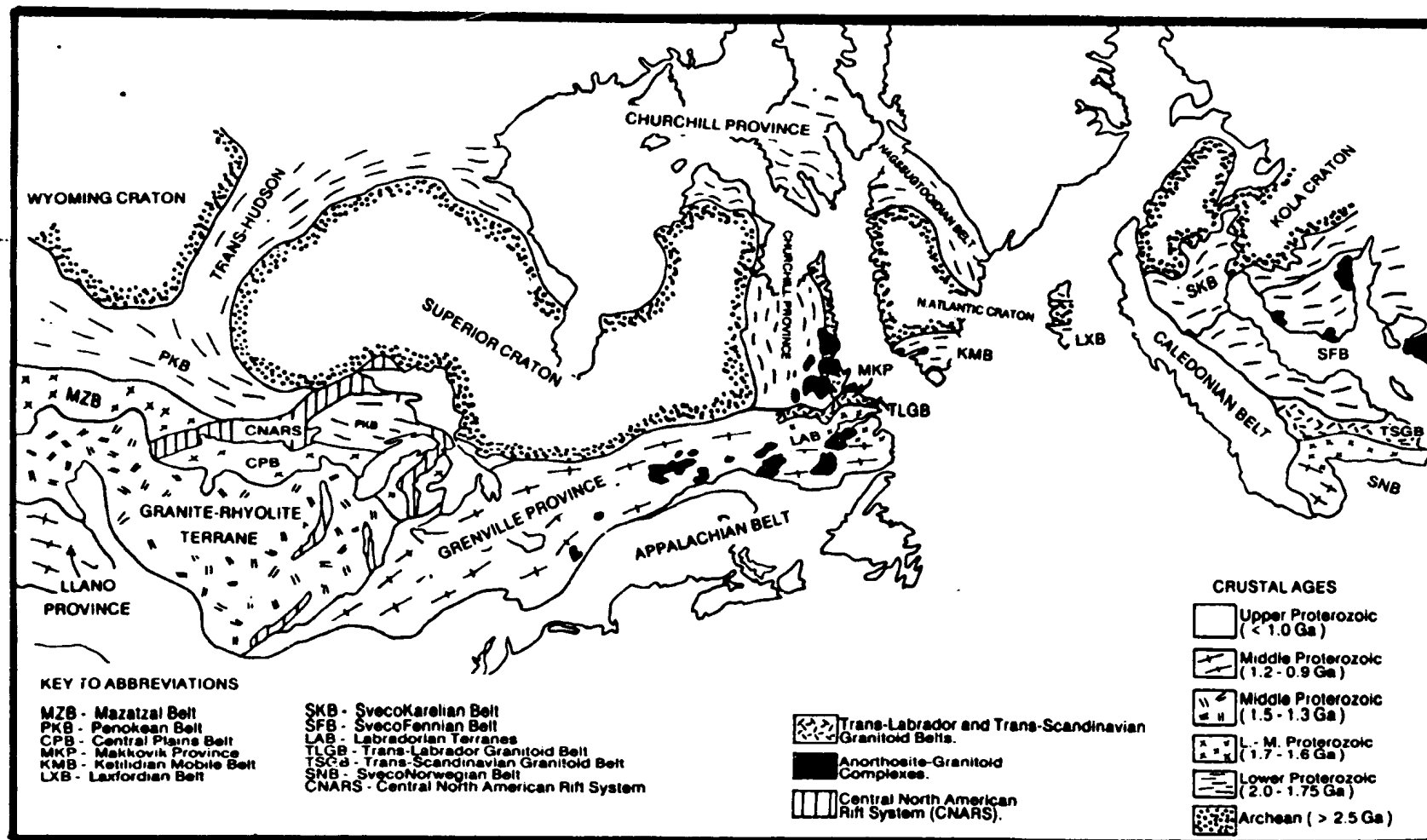


Figure 2.2. Lower and Middle Proterozoic mobile belts along the "southern" margin of a Precambrian supercontinent (Piper, 1983). Correlations are based on Gower and Owen, 1984, Thomas et al., 1985, and Gower (unpublished data). Map adapted from an original by C.F.Gower.

In the central and western United States, a number of Lower and Middle Proterozoic terranes have been recognized in the subsurface and as basement uplifts (Condie, 1981, 1982; Van Schmus and Bickford, 1981; Sims et al., 1987). These include probable equivalents of the Makkovik Province and Labrador Orogen (Thomas et al., 1985).

Post-1600 Ma rocks in the midcontinent region can also be correlated broadly with Labrador geology. The 1500 to 1300 Ma granite - rhyolite terrane (Sims et al., 1987) is probably equivalent to the anorogenic magmatism in Canada (Emslie, 1978; Anderson, 1983). The Grenville Province is largely coincident with the younger Appalachian Orogen, but emerges to form the ca. 1100 Ma old Llano Province of Texas and northeastern Mexico (Condie, 1981).

#### **Trans-Labrador Granitoid Belt**

**Definition** : The Trans-Labrador Granitoid Belt (TLGB) corresponds generally to the Trans-Labrador Batholith of Wardle et al. (1982). It was previously considered to be mostly ca. 1650 Ma in age (Gower and Owen, 1984; Wardle et al., 1986; Kerr, 1986, 1987) and, in general terms, to be part of the Labrador Orogen. Rb-Sr and U-Pb geochronology (this study; Krogh et al., in prep.) demonstrate, however, that undeformed plutonic rocks in the study area include suites of both ca. 1650 Ma and ca. 1800 Ma age. The latter are similar in age to foliated granitoid rocks that had previously been recognized as a distinct, older, assemblage (Gower and Owen, 1984; Gower and Ryan, 1986).

Trans-Labrador Granitoid Belt, as defined here, includes both foliated and undeformed Early Proterozoic plutonic rocks in the study area. The older and younger components of the belt are termed Makkovikian and

Labradorian assemblages respectively, with reference to the orogenic events with which they appear to be broadly associated (see below). The term "granitoid belt" is preferred over "batholith", as it more clearly indicates the probable composite nature of the belt.

In central and western Labrador, the TLGB is deformed and metamorphosed, and there is (as yet) no geochronological evidence of a Makkovikian component. Field relationships and geochronological data suggest that its emplacement post-dated Labradorian deformation and metamorphism (Wardle et al., 1986).

*Geological Relationships* : To the north, the TLGB is in contact with older supracrustal rocks and gneisses of the Makkovik and Churchill Provinces. In central and western Labrador (within the Grenville Province), this contact is mostly a thrust fault of probable Grenvillian age; in eastern Labrador (outside the Grenville Province), it is an intrusive contact (Wardle et al., 1986). The TLGB is bounded to the south by the Labradorian high-grade terranes; this contact is generally a thrust, and corresponds with a rapid increase in metamorphic grade and deformation state (Gower and Owen, 1984; Wardle et al., 1986). Orthogneiss assemblages, and gabbroic to granitoid intrusive rocks within the high-grade terranes, are probably equivalent to the less deformed parts of the TLGB to the north, and some yield U-Pb zircon crystallization ages of 1670 - 1630 Ma (Schärer et al., 1986; Schärer and Gower, 1988). The original width of the TLGB was probably greater than it now appears, due to shortening during later deformation.



**Plutonic Assemblages** : The TLGB in eastern Labrador is divided in this study into Makkovikian and Labradorian plutonic assemblages. These terms refer broadly to periods of time from 1860 to 1750 Ma (c.f. Gower and Ryan, 1986; see below) and 1700 to 1600 Ma (Thomas et al., 1986) respectively. The minimum age for the Makkovikian assemblage differs from the 1790 Ma limit suggested by Gower and Ryan (1986), as there is evidence that Makkovikian plutonism continued until at least 1750 Ma, and possibly beyond (Krogh et al., in prep.).

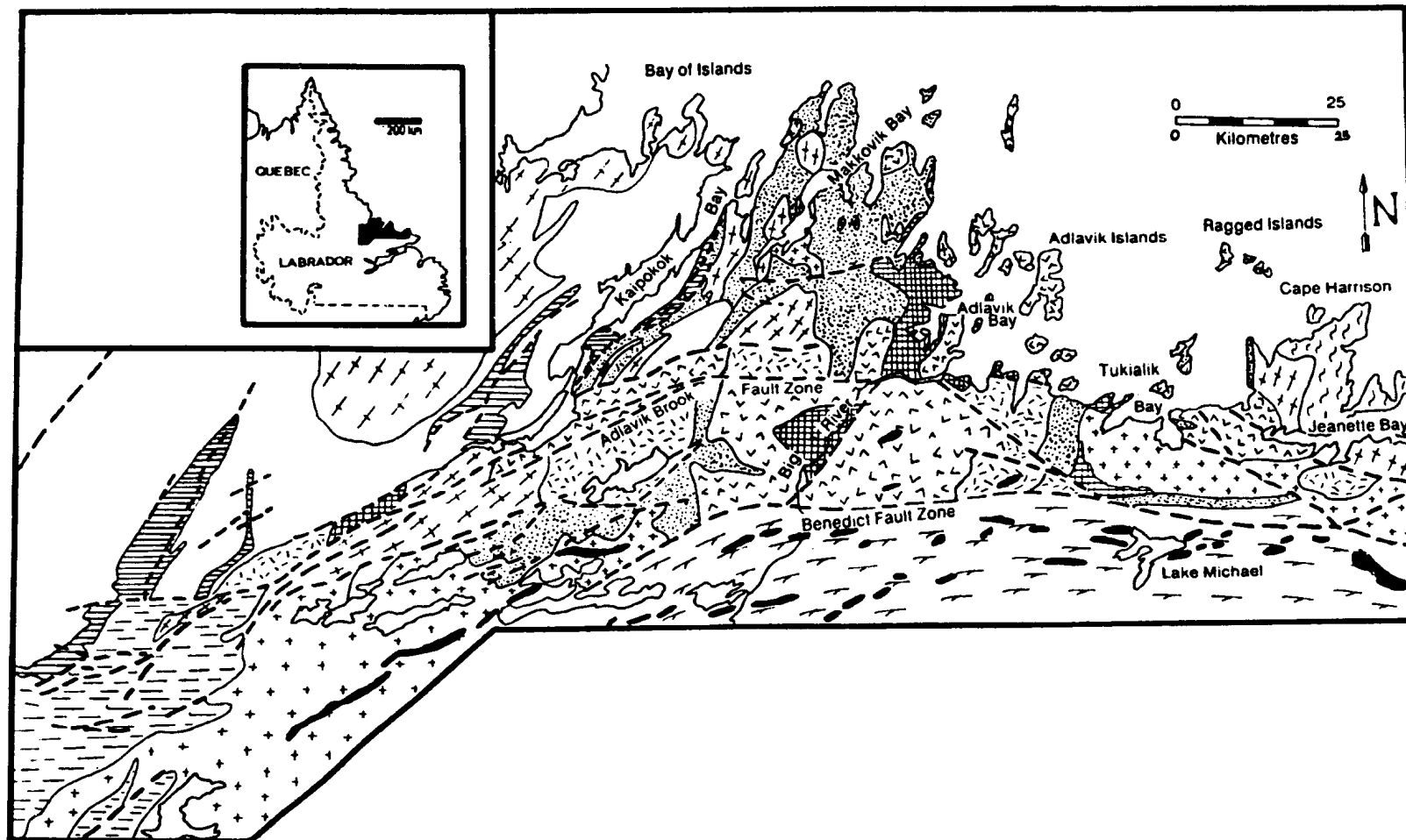
Makkovikian plutonic rocks are further subdivided into syn-tectonic and post-tectonic associations. These are compositionally similar and are regarded by the author as closely related. Rb-Sr (this study) and U-Pb (Krogh et al., in prep.) data indicate that they are also partly of similar age. The distinction is convenient for descriptive purposes, although the syn- and post-tectonic aspects may simply reflect heterogeneous Makkovikian deformation, rather than a significant difference in emplacement age.

## 2.2 GEOLOGY OF THE MAKKOVIK PROVINCE AND ADJACENT AREAS

The geological evolution of the Makkovik province is depicted in simplified form in Table 2.1. For the purposes of description, it is subdivided into several lithological packages, which are indicated on a simplified geological map (Figure 2.3).

### **Archean Rocks**

Archean gneisses are exposed in the northwest of the Makkovik Province, and in the adjacent Nain Province (Ryan et al., 1983; Korstgård and Ermanovics, 1985). They represent probable basement material for the western portion of the study area. They comprise banded quartzofeldspathic orthogneiss (possibly as old as 3100 Ma; Loveridge et al., 1987), containing lenses of older amphibolite and paragneiss. These orthogneisses are intruded by sodic granitoid rocks dated at ca. 2800 Ma (Loveridge et al., 1987), and by several generations of mafic dykes. In the Makkovik Province, all of these rocks have been affected by Lower Proterozoic orogenic events termed the Makkovikian orogeny (Gower and Ryan, 1986), and possibly also by earlier events. The degree of metamorphic and structural reworking of the Archean increases from northwest to southeast towards Kaipokok Bay (Ryan and Kay, 1982). Small areas of similar gneisses occur southeast of Kaipokok Bay, associated with the Aillik Group (see below). These are undated, but are presumed to be Archean (Gower et al., 1982).



## LEGEND

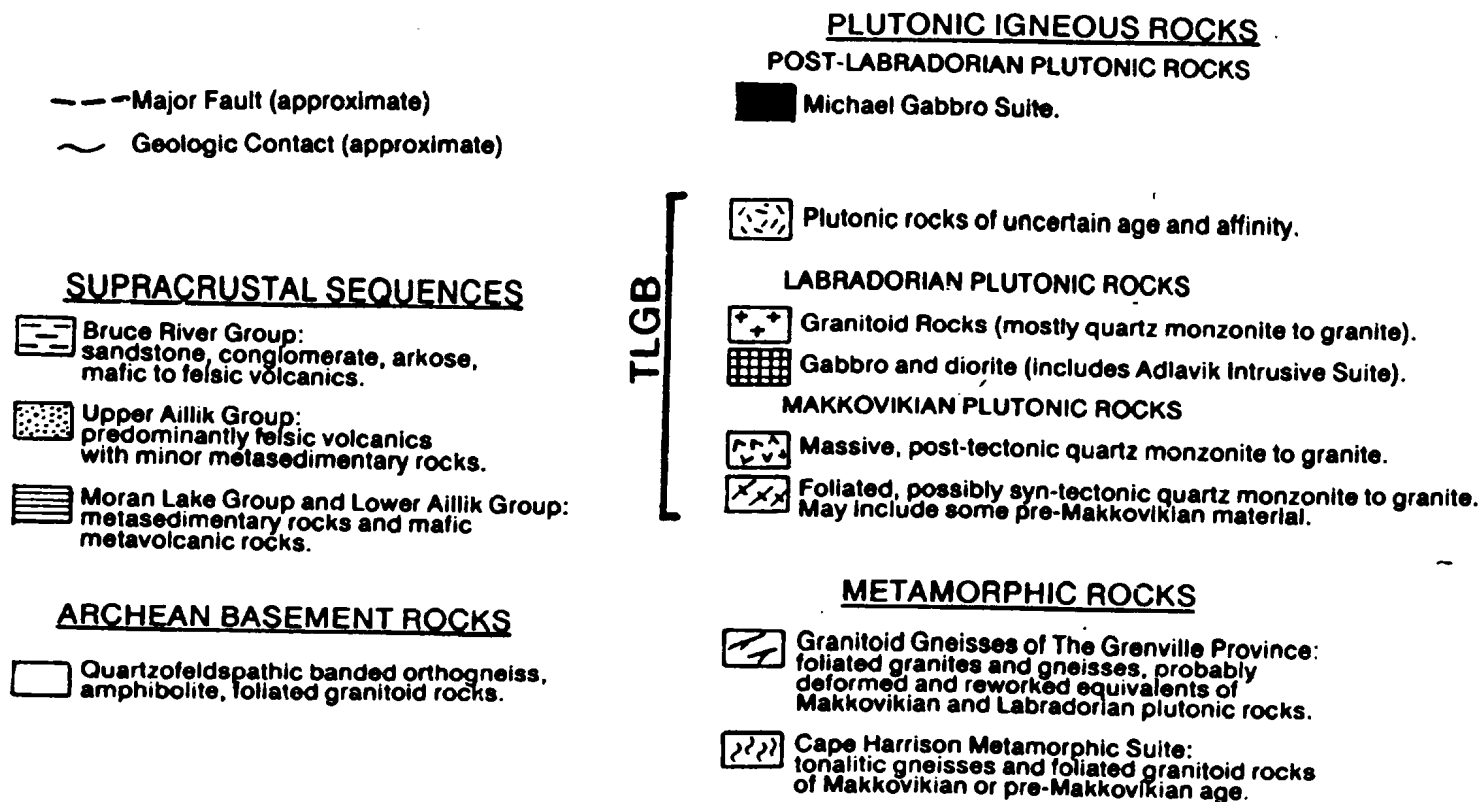


Figure 2.3. Generalized geological map of the Makkovik Province and adjacent areas of Labrador. Geology compiled from Gower (1981), Gower et al. (1982), Ryan (1984), Ryan et al. (1983) and Kerr (1986, 1987, 1988).

### Cape Harrison Metamorphic Suite

The Cape Harrison Metamorphic Suite (Gower, 1981) is the oldest recognized component in the eastern part of the study area (Figure 2.3). It consists of massive to banded orthogneiss, ranging in composition from diorite to granodiorite, with lesser amounts of foliated granodiorite and granite. In terms of field appearance, it resembles the Archean gneisses in many respects. Brooks (1983) obtained a Rb-Sr errorchron age of  $1740 \pm 85$  Ma, with a low initial ratio of 0.7034 that apparently precludes extensive crustal prehistory. Nd isotopic compositions (Chapter 9; Kerr and Fryer, in press) also indicate that the suite is unlikely to be older than 2100 Ma, and must therefore represent Proterozoic material which has undergone a period of high-grade metamorphism not recorded by adjacent Makkovikian plutonic rocks. It is thus the only candidate for pre-Makkovikian basement in the eastern part of the study area.

### Moran Lake Group and Lower Aillik Group

The Moran Lake and Lower Aillik Groups are Early Proterozoic supracrustal rocks of uncertain age that are dominated by sedimentary and mafic volcanic rocks. The Moran Lake Group (Ryan, 1984) rests unconformably upon Archean gneisses in the west of the Makkovik Province. It consists of a lower sedimentary sequence including quartzite, shale, dolostone and iron formation, overlain by mafic volcanic rocks. It has been metamorphosed to greenschist facies, and is moderately deformed.

The Lower Aillik Group (described by Gandhi, 1978; Gower et al., 1982) is exposed in a zone of intense folding

and thrusting along Kaipokok Bay and consists of arenaceous to pelitic metasedimentary rocks overlain by mafic metavolcanic rocks. It is at least 1860 Ma old, based on U-Pb ages from an overlying sequence and granitoid plutons that intrude it (see below). The contact between the Lower Aillik Group and the Archean is a mylonite zone (Marten, 1977), and a number of similar structures (interpreted as slides or thrusts) occur in higher parts of the sequence. It may have been deposited as a cover sequence upon the Archean, but no unconformity is preserved. The Lower Aillik Group was metamorphosed to amphibolite facies, and underwent several phases of folding (Marten, 1977; Gower et al., 1982).

The similarity in stratigraphy and setting of the Moran Lake and Lower Aillik Groups suggests that they are equivalent (Wardle and Bailey, 1981; Gower and Ryan, 1986).

#### Upper Aillik Group

The Upper Aillik Group (described by Gandhi, 1978 and Gower et al., 1982) consists of felsic volcanic and volcanoclastic rocks, related volcanogenic sedimentary rocks and subvolcanic intrusions. The volcanic rocks yield U-Pb zircon ages of ca. 1860 and 1807 Ma (Schärer et al., 1988), suggesting at least two episodes of volcanism. The relationship between Lower and Upper Aillik Groups is unclear; their mutual contact is a mylonite zone that may represent a modified unconformity (Marten, 1977).

The stratigraphy of the Upper Aillik Group is poorly known; in general terms, it consists of a lower sequence of sandstone, arkose, conglomerate and tuff overlain by a massive accumulation of dacitic to rhyolitic flows and

Table 2.1. Summary of the geological evolution of the Makkovik Province

TIMING	DESCRIPTION OF EVENT(S)
< 1000 Ma	Emplacement of mafic dykes of several ages, deposition of Late Proterozoic Double Mer Formation in rift or graben basins of the Lake Melville area.
1200 - 1000 Ma	GRENVILLIAN OROGENY - Thrusting and metamorphism south of Grenville Front Zone, minor effects in Makkovik Province.
1450 - 1300 Ma	Emplacement of Michael Gabbro Suite (ca. 1430 Ma). Minor gabbro to syenite intrusions in adjacent Labradorian high-grade terranes. Emplacement of anorthosite-granite intrusions in Nain and Churchill Provinces.
1670 - 1600 Ma	Emplacement of Labradorian plutonic rocks (gabbro, diorite and granitoids). Extrusion of Bruce River Group volcanic rocks and possibly some volcanic rocks in Makkovik Province. Emplacement of ca. 1.65 Ga plutonic rocks following deformation/metamorphism in adjacent high-grade terranes.
1800 - 1750 Ma	Emplacement of post-tectonic Makkovikian intrusive rocks (quartz monzonite to granite), possibly coeval with localized late deformation (see below). Extrusion of parts of the Upper Aillik Group felsic volcanic sequence.
1850 - 1800 Ma	Emplacement of syn-tectonic and late-tectonic Makkovikian plutonic rocks (quartz monzonite to granite). Some of these are similar in age to undeformed Makkovikian granitoids, suggesting that deformation may have been heterogeneous. Extrusion of parts of the Upper Aillik Group sequence.
ca. 1860 Ma	Extrusion of earliest known volcanic rocks in the Upper Aillik Group.
?	Deformation and metamorphism of Lower Aillik Group. This may postdate deposition/extrusion of earliest Upper Aillik Group.
ca. 1900 Ma	Emplacement of poorly known pre-Makkovikian granitoid rocks. May predate deposition of Moran Lake - Lower Aillik Group.
2000 - 1860 Ma	Deposition of sedimentary and volcanic rocks of the Moran Lake Group and Lower Aillik Group.
?	Migmatization of Archean basement rocks (poorly defined).
2500 - 2000 Ma	Emplacement of mafic dyke swarms into Archean gneiss complex.
2800 - 2500 Ma	Stabilization of Archean gneiss complex.

pyroclastic rocks (Gower and Ryan, 1987). The sequence is variably metamorphosed, but is generally at or below greenschist facies; some parts of the sequence show little or no evidence of deformation. Volcanic sequences in the east of the study area are included with the Upper Aillik Group in Figure 2.3 but may represent a younger sequence (see discussion in Chapter 7). The Upper Aillik Group overlaps partly in age with the TLGB Makkovikian assemblage (see below), and is regarded partly as a Makkovikian volcanic sequence (c.f. Gower and Ryan, 1987; see Chapter 7 for discussion).

#### **Syn-Tectonic Makkovikian Plutonic Rocks**

These granitoid plutons have NE or NNE-trending fabrics. They intrude the Archean gneisses, Lower Aillik Group and parts of the Upper Aillik Group, but share their general structural trends. They are therefore syn-tectonic with respect to deformation during the Makkovikian orogeny (Marten, 1977). U-Pb zircon, Rb-Sr and K-Ar ages from these rocks are mostly between 1840 and 1800 Ma (Loveridge et al., 1987; Gandhi et al., 1988; Krogh et al., in prep.). They include quartz monzonite, granodiorite and fluorite-bearing granite south of Kaipokok Bay, and a large, complex, polyphase tonalite-granite body that intrudes the Archean gneisses north of Kaipokok Bay. Gandhi et al. (1988) and Brooks (1983) report ages greater than 1900 Ma from poorly-known foliated granites to the west of the study area. The extent and significance of this earlier (pre-Makkovikian) magmatism is presently unclear.



### Post-Tectonic Makkovikian Plutonic Rocks

These are massive, unfoliated plutonic rocks that intrude the Upper Aillik Group. They comprise monzonite - quartz monzonite - syenite intrusions, and granite to alkali-feldspar granite, commonly fluorite-bearing. Rb-Sr (this study) and U-Pb (Krogh et al., in prep.) ages of ca. 1800 Ma are similar to those from some of their syn-tectonic counterparts (see above), and it is likely that both groups represent a single pulse of magmatism that transcended late Makkovikian deformation. Some members of this group may, however, be as young as ca. 1760 Ma. In the south of the area, these rocks have east-west structural trends that were imposed by the Grenvillian Orogeny.

### Labradorian Plutonic Rocks

The TLGB Labradorian assemblage consists entirely of undeformed plutonic rocks that intrude the Upper Aillik Group and Makkovikian plutonic rocks. They include layered gabbro - monzonite - syenite intrusions, regionally extensive quartz monzonite to granite, and small leucocratic granite plutons. U-Pb zircon ages (Brooks, 1983; Krogh et al., in prep.) are between 1670 and 1630 Ma, but cluster around 1650 Ma. In the south of the area, these rocks have east-west structural trends that were imposed by the Grenvillian Orogeny.

### Unclassified Plutonic Rocks

There are no field criteria for separation of post-tectonic Makkovikian and Labradorian assemblages. Several units are therefore unclassified at present. These range in composition from quartz monzonite to granite.

### Bruce River Group

The Bruce River Group (Ryan, 1984; Ryan et al., 1987) is a supracrustal sequence in the west of the area depicted in Figure 2.3, but outside the confines of the study area. It rests unconformably upon the Moran Lake Group, and has suffered only minimal (Grenvillian) deformation and metamorphism. It consists of arkose, conglomerate and sandstone, overlain by a thick (8 km) accumulation of mafic to felsic volcanic and pyroclastic rocks. U-Pb zircon dating (Schärer et al., 1988) indicates an age of ca. 1649  $\pm$  1 Ma, in contrast to previous Rb-Sr ages of ca. 1530 - 1510 Ma (Kontak, in Ryan, 1984). It is thus regarded as a volcanic sequence equivalent to the TLGB Labradorian assemblage (after Ryan, 1984; see Chapter 7 for discussion).

### Michael Gabbro Intrusions

Small bodies of mafic intrusive rocks (Michael Gabbro) are widespread in the southern part of the Makkovik Province and adjacent Grenville Province. They consist of olivine-gabbro and gabbro-norite emplaced ca. 1425 Ma (U-Pb zircon; Schärer et al., 1986), and have variably developed coronitic structures that record the effects of Grenvillian metamorphism or metamorphic conditions at the time of their emplacement (Gower, 1986).

### Granitoid Gneisses Of The Grenville Province

The Grenville Front Zone is represented in the study area by the Benedict fault system (Figure 2.3; see below). The area south of the fault is dominated by deformed

granitoid rocks and granitoid gneisses with relict porphyritic (i.e. augen) textures and cataclastic fabrics. These are associated with fine-grained, banded, mylonitic rocks. These gneisses are probably reworked equivalents of the granitoid intrusive rocks of the Makkovik Province (Gower and Owen, 1984), but Makkovikian and Labradorian components cannot be discerned. The granitoid gneisses are thus described in conjunction with unclassified plutonic rocks (see above). Deformed (variably coronitic) intrusions of the Michael Gabbro Suite (see above) are most common south of the Benedict fault system.

#### **Structural and Metamorphic Patterns**

**Structural Trends** : The structure of the study area has been discussed by Gower et al. (1982), Ryan (1984), Clark (1973, 1979) and Marten (1977). It is dominated by two major structural trends (Figure 2.3). The older trend has a NE or NNE orientation, and is typified by the fold and thrust belt along Kaipokok Bay. This trend is present also in syn-tectonic Makkovikian plutonic rocks. It represents structures developed during the Makkovikian orogeny at or before ca. 1800 Ma ago (Gower and Ryan, 1986). Major faults associated with this trend include slide and thrust zones in the Lower Aillik Group (Marten, 1977).

The second trend is of broadly east-west orientation, and is probably related to the Grenvillian Orogeny at ca. 1100 Ma. The NE to NNE "Makkovikian trend" and the E to ENE "Grenvillian trend" are distinct in the east and north of the area, but their discrimination becomes more difficult in the south-west, where both trends converge into a general NE direction (Figure 2.3). There is no evidence of Labradorian (ca. 1650 Ma) deformation in the study area.

The Grenvillian trend is most strongly developed south of the Benedict fault system, but several fault zones in the Makkovik Province share its general orientation.

**Major Faults** : A number of major east-trending faults divide the area into structural blocks. The most important is the Benedict fault system, which is the locus of the Grenville Front Zone (Gower et al., 1980). This is probably a high-angle reverse or thrust fault (Gower, 1981; Owen et al., 1986). The subparallel Adlavik Brook fault system (Gower et al., 1982) has a transcurrent displacement of ca. 20-30 km. This fault marks the northern limit of recognisable Grenvillian deformation. The area between these two fault systems is characterized by local, strongly foliated to cataclastic, zones subparallel to the major faults. It is dominated by areally extensive "regional" granitoid units (Kerr, 1987). North of the Adlavik Brook fault system, the Upper Aillik Group is areally dominant, and TLGB plutonic rocks occur as discrete, isolated bodies. The distribution and characteristics of these plutonic rocks suggest that the upper surface of the TLGB is close to the erosion surface in this area.

Contrasts across the Benedict and Adlavik Brook fault systems are interpreted to reflect differences in crustal levels imposed by reverse faulting and thrusting during the Grenvillian Orogeny (Gower and Ryan, 1986; Kerr, 1987; Owen et al., 1988), which exposed progressively deeper levels of the crust in the south.

**Metamorphism** : Metamorphic events correspond to development of Makkovikian and Grenvillian structural trends. Makkovikian metamorphism affected the Archean

gneisses, Aillik Group and syn-tectonic Makkovikian plutonic rocks. In the Lower Aillik Group, upper amphibolite facies conditions were attained, and pelitic rocks were partially melted. The Upper Aillik Group ranges from greenschist to lower amphibolite facies, with a regional decrease in grade from northwest to southeast (Gower et al., 1982). Foliated granitoid rocks are variably recrystallized, but most retain relict igneous mineral assemblages, suggesting that their emplacement post-dated the peak of metamorphism. Grenvillian metamorphism is prevalent south of the Adlavik Brook fault zone, and is manifested by recrystallization, strain, and variable retrogression of igneous mineral assemblages in all components of the TLGB. These effects become stronger within the Grenville Province, but relict igneous textures are locally visible well to the south of the Benedict fault system.

Contact metamorphic effects associated with plutonic rocks of the TLGB appear minor; this is probably a function of the unreactive quartzofeldspathic compositions of the Upper Aillik Group felsic volcanic rocks that form the dominant country rocks. In areas adjacent to plutonic rocks, these are commonly saccharoidal in texture, suggesting static, thermal recrystallization of quartz and feldspar.

### 2.3 STRATIGRAPHIC GROUPINGS AND TERMINOLOGY

#### General Information

Makkovikian and Labradorian plutonic assemblages are each divided into a number of units and intrusive suites. New names are proposed for some of these divisions (Table 2.2). This terminology is introduced here to familiarize the reader prior to definition and description of these associations in subsequent chapters. Locations of units and divisions in Table 2.2 are shown on the 1:250,000 geological map (enclosure) and in summary location maps at the start of the relevant descriptive chapters.

#### Intrusive Suites and Units

The term "intrusive suite" is used in two senses. Firstly, it is used to group geographically discrete units that are closely similar in petrology and geochemistry. These geographically discrete units have generally been given individual names. Secondly, it is used to group units of differing composition that are spatially and genetically related. In the latter case, individual units are generally not named. This corresponds with conventional use and with suggestions made by Salvador (1987) and Bateman (1988) for the International Subcommittee on Stratigraphic Conventions. In descriptions of units and suites in subsequent chapters, the qualifier "intrusive" is sometimes omitted for the sake of brevity.

Intrusive Suite		Unit(s)	(best data)	Comments
ASSEMBLAGE  LABRADORIAN	not named	Otter Lake - Walker Lake Granitoid (name after Ryan, 1984)	1647 +/- 2 Ma (U-Pb zircon) (Krogh et al., in prep.) 1550 +/- 55 Ma (Rb-Sr WR) (Kontak, in Ryan, 1984)	Regionally extensive unit ranging in composition from quartz monzonite to granite.
	Monkey Hill* Intrusive Suite	Monkey Hill Granite* Little Monkey Hill Granite* Duck Island Granite* Bent's Cove Granite* Round Pond Granite Kidlaluit Granite*	Monkey Hill Granite : 1640 +/- 10 Ma (U-Pb zircon) (Krogh et al., in prep.)  Round Pond Granite : 1620 +/- 60 Ma (K-Ar biotite) (Wanless et al., 1970)	Consists of a number of small, epizonal plutons comprising fine-grained leucogranite. Little Monkey Hill Granite Cuts gabbro and diorite of Adlavik Intrusive Suite.
	not named	Burnt Lake Granite  Witchdoctor Granite*	1548 +/- 90 Ma (Rb-Sr WR) (MacKenzie and Wilton, 1988)  1632 +/- 9 Ma (U-Pb zircon) (Brooks, 1983)	Leucocratic granite units, probably two phases of the same body. Locally similar to Monkey Hill Intrusive Suite granites.
	Mount Benedict* Intrusive Suite	(units not named) Gabbro to diorite unit Monzonite to syenite unit Syenite to granite unit	1650 +/- 10 Ma (U-Pb zircon) (Krogh et al., in prep.)  1625 +/- 50 Ma (Rb-Sr, w.r.) (Brooks, 1983)	Layered assemblage, diorite and gabbro at base, evolved syenite at the top. Gabbro and diorite are very similar to Adlavik Intrusive Suite.
	Adlavik Intrusive Suite	(units not named) Diorite to Monzonite unit Gabbro and leucogabbro unit	1649 +/- 1 Ma (U-Pb zircon) (Krogh et al., in prep.)	Polyphase layered mafic intrusion, evolving to diorite and monzonite. Parts of suite resemble Mount Benedict Suite.
ASSEMBLAGE  MAKOVIKIAN  POST-TECTONIC ASSOCIATION	not named	Big River Granite*	1798 +/- 28 Ma (Rb-Sr WR) (this study)	Regionally extensive granite unit with mantled-fsp texture.
	Strawberry* Intrusive Suite	Bayhead Granite* Cape Strawberry Granite October Harbour Granite Dog Islands Granite* Tukialik Granite*	Preliminary Data (discordant): 1800 to 1760 Ma (U-Pb zircon) (Krogh et al., in prep.) 1694 +/- 56 Ma (Rb-Sr WR) (this study)	Array of epizonal plutons of closely similar, coarse grained biotite granite, commonly K-fsp porphyritic, and fluorite-bearing.
	Lanceground * Intrusive Suite	Lanceground Hills Granite* Pistol Lake Granite Tarun Granite*	Lanceground Hills Granite : 1692 +/- 32 Ma (Rb-Sr WR) (this study) [Age is considered disturbed]	Coarse grained, locally hyper- solvus, quartz syenite to granite plutons, with abundant zircon, allanite, fluorite.
	Numok* Intrusive Suite	(units not named) Monzonite to quartz monzonite Syenite to quartz syenite	1801 +/- 2 Ma (U-Pb zircon) (Krogh et al., in prep.)	Coarse grained monzonite to quartz syenite. Some syenitic rocks resemble Lanceground Intrusive Suite.

MAKKOVIKIAN SYN-TECTONIC	ASSEMBLAGE	not named	Long Island Quartz Monzonite (after Gower et al., 1982)	1802 $\pm$ 13 / -7 Ma (U-Pb zircon) (Gandhi et al., 1988)	Foliated, melanocratic quartz monzonite.
	ASSOCIATION	not named	Melody Granite*	age unknown	Strongly foliated granite
		not named	Brumwater Granite Pitre Lake Granite Manak Island Granitoid*	ages unknown, but foliation suggests > 1800 Ma for all.	Small, leucocratic granitoid units.
		not named	Deus Cape Granitoid*	1837 $\pm$ 6 / -4 Ma (U-Pb zircon) (Krogh et al., in prep.)	Part of a regionally extensive unit exposed east of study area.
		Kennedy Mountain* Intrusive Suite	Kennedy Mountain Granite* Narrows Granite* Cross Lake Granite* Other (not named)	1778 $\pm$ 98 Ma (Rb-Sr WR) (this study) [age considered disturbed]	Coarse grained, foliated, K-fsp porphyritic granite, commonly fluorite-bearing.
		Island Harbour Bay Intrusive Suite (after Ryan et al., 1983)	(units not named)	1805 $\pm$ 5 Ma (U-Pb zircon) (Loveridge et al., 1987) (coarse-grained granite only)	Complex, polyphase tonalite to granite intrusion emplaced into Archean gneiss complex.
UNCLASSIFIED PLUTONIC ROCKS		not named	Freshsteak Lake Granitoid* Noarse Lake Granitoid*	Freshsteak Granitoid : 1798 $\pm$ 48 Ma (Rb-Sr WR) (this study)	Closely similar melanocratic quartz monzonite to monzogranite. probably Makkovikian age.
		not named	Stag Bay Granitoid*	1714 $\pm$ 44 Ma (Rb-Sr WR) (this study)	Affinity uncertain.
		not named	Thunder Mountain Syenite* Jeanette Bay Quartz Syenite*	undated	Small, massive syenitic bodies of uncertain affinity.
		not named	Granitoid gneisses South of Benedict Fault Zone	undated	Probably represents deformed equivalents of both Makkovikian and Labradorian assemblages.

Table 2.2. Summary of stratigraphic terminology employed in this thesis.  
New names are indicated by (\*).



## CHAPTER THREE

### SYN-TECTONIC MAKKOVIKIAN PLUTONIC ROCKS

---

---

#### Chapter Abstract

Syn-tectonic Makkovikian plutonic rocks have regionally developed north or northeast-trending foliations that indicate imposition of at least some Makkovikian deformation upon them. U-Pb zircon ages indicate emplacement between 1840 and 1800 Ma ago. They are divisible into two principal associations on both geological and geochemical grounds.

The first (areally dominant) association is formed by the Long Island Quartz Monzonite, granites of the Kennedy Mountain Intrusive Suite, and the Melody Granite. The first two are homogeneous, regional units that show sharp, intrusive contacts with their country rocks, and appear to have source regions well below the present level of exposure. They range in composition from quartz monzonite to alkali-feldspar granite, are commonly plagioclase and/or K-feldspar porphyritic, and show increasing biotite/hornblende ratios with differentiation. Leucocratic (alaskitic) granites of the Kennedy Mountain Suite are hornblende-free and fluorite-bearing. In geochemical terms, this association is metaluminous to weakly peralkaline, and shows enrichment in fluorine, Zr, Y and REE. Trace element trends are consistent with evolution via plagioclase  $\pm$  K-feldspar fractionation. High HFS and REE contents indicate a source enriched in these elements, and also reflect the role of fluorine in retarding crystallization of accessory minerals. The Kennedy Mountain Suite has undergone local alkali-metasomatism. This is correlated with similar geochemical disturbance reported from felsic volcanic rocks of the Upper Aillik Group, which may be partly equivalent to these plutons. This disturbance has affected LFS trace element patterns, but had little effect on HFS elements and REE. The Melody Granite resembles the Kennedy Mountain Suite in most respects, but displays more intense deformation and hematization.

In contrast, two small intrusions near Kaipokok Bay (Brunwater and Pitre Lake Granites) appear to have been derived by anatectic melting of local country rocks at or slightly below the present level of exposure. Their contacts are diffuse, and

they contain abundant gneissic and metasedimentary xenoliths respectively. They are variably peraluminous in composition, and have low levels of Zr and REE that suggest residual hornblende, zircon or sphene in their source regions. The Pitre Lake Granite shows LREE depletion suggesting residual monazite or allanite in its source, and F and Li enrichment suggesting muscovite breakdown. The Manak Island Granitoid is geochemically similar to the Brumwater Granite, and may have had a similar origin.

A large, composite plutonic body to the north of the study area (Island Harbour Bay Intrusive Suite) appears to contain elements of both settings, as it has a partially migmatitic exterior, but a homogeneous core. It also contains tonalitic and trondhjemitic rocks, that are atypical of intrusions within the study area. Such compositions appear to preclude complete derivation by anatexis of older sialic crust, although such material may have contributed partly to the magmas.

In summary, although anatexis of local country rocks was important in the Kaipokok Bay area, where metamorphic grade is highest, major syn-tectonic Makkovikian plutons mostly came from deeper sources and evolved by fractional crystallization. The character of this magmatism in the study area is granitic, with only minor quartz monzonite to granodiorite.

## Introduction

Syn-tectonic Makkovikian plutonic rocks are those that have north to northeast-trending foliations similar in orientation to structural trends within the Aillik Group. They have thus experienced at least the latest period(s) of Makkovikian deformation. The label "syn-tectonic" is therefore applied to these rocks. It is recognized, however, that the contrast in deformation state between these rocks and their "post-tectonic" Makkovikian counterparts (Chapter 4) may reflect heterogenous deformation, rather than significant age differences between them.

Syn-tectonic Makkovikian plutonic rocks are mostly located in the north-west of the study area (Figure 3.1). The most areally extensive units are the Long Island Quartz Monzonite, Kennedy Mountain Intrusive Suite and Melody Granite. Two units in the Kaipokok Bay area (Brumwater and Pitre Lake Granites) are of limited extent, but show critical field relationships with deformed Archean gneisses and supracrustal rocks. Foliated granites also occur locally in the east of the study area (Deus Cape and Manak Island Granitoids).

The largest single member of this association is the Island Harbour Bay Intrusive Suite (Ryan et al., 1983), which intrudes Archean rocks north of Kaipokok Bay, and is outside the study area. Key field and petrographic characteristics of all units (excluding the Island Harbour Bay Suite) are summarized in Table 3.1.

.

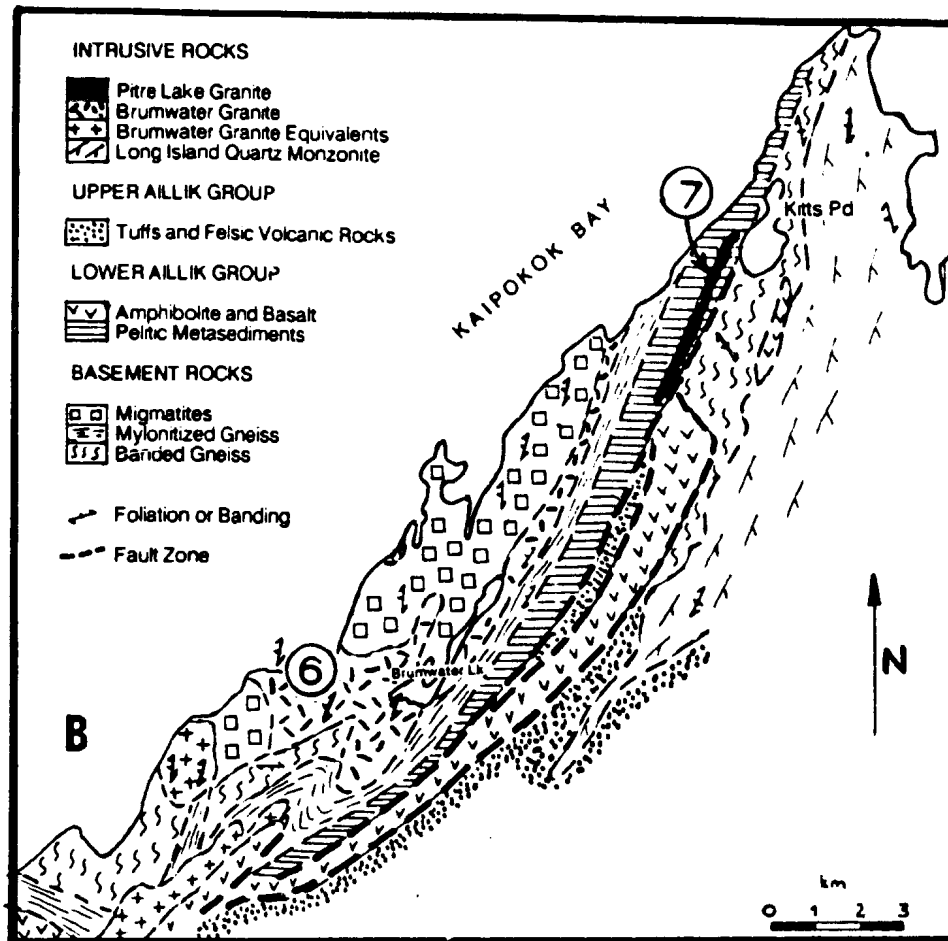


Figure 3.1 (INSET). Geology of part of the eastern side of Kaipokok Bay, showing the location and setting of the Brumwater and Pitre Lake Granites. After Marten (1977) and Gower et al. (1982).

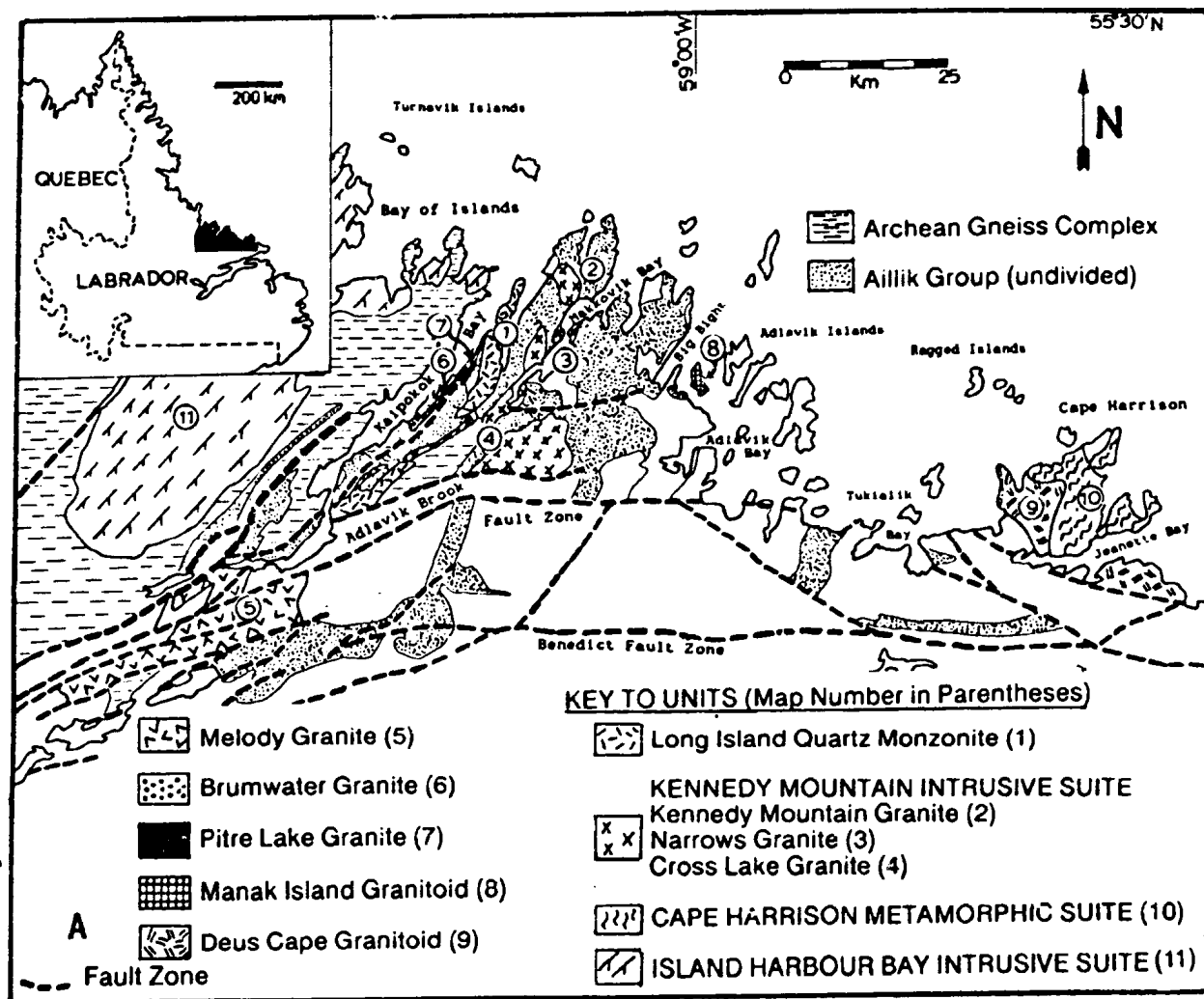


Figure 3.1. Summary map illustrating the distribution and extent of syn-tectonic Makkovikian plutonic rocks. Inset is an enlargement of the east side of Kaipokok Bay, and illustrates location and setting of Brumwater and Pitre Lake units. Geology in inset after Marten (1977) and Gower et al. (1982).

Table 3.1. Key features of syn-tectonic Makkovikian plutonic rocks.

Map Unit	Suite/Unit/Age	General Characteristics	Textural Characteristics
10	Long Island Quartz Monzonite 1832 +/- 58 [K/Ar biotite] 1802 +/- 13/-7 [U-Pb zircon] (Gandhi et al., 1969; 1988)	Grey, melanocratic, foliated Hb-Bi quartz-monzonite to monzogranite. Fabric is strongly developed in marginal portions; core is less deformed. Contains deformed xenoliths of dioritic material.	Fine to medium grained, porphyritic with plagioclase phenocrysts up to 1 cm diameter. Fabric defined by Hb-Bi aggregates, flattened phenocrysts and inclusions. Schlieric to banded near margin.
11	KENNEDY MOUNTAIN INTRUSIVE SUITE [ including ] 11.1 Kennedy Mountain Granite 11.2 Marrows Granite 11.3 Cross Lake Granite 11.4 Unnamed minor bodies 1531 +/- 38 [K-Ar biotite] 1778 +/- 98 Ma (Rb-Sr WR) [ ages are not reliable ]	Pink to white or buff, foliated, variably porphyritic, Hb-Bi monzogranite, granite and alkali-feldspar granite. Generally leucocratic, locally alaskitic. NE-trending fabric is obvious in porphyritic / melanocratic types, but diffuse in leucogranites. Locally K-fsp depleted, possibly albitized. Widespread fluorite, particularly in leucocratic variants.	Commonly medium to coarse-grained, with K-fsp and lesser plagioclase phenocrysts, variably augened by fabric. Fabric defined by Hb-Bi-Sph aggregates and/or augen texture. Equigranular, leucocratic variants may appear massive. Unit is generally inclusion-free. pegmatite veining widespread.
12	Melody Granite (? 1910 +/- 10 Ma (U-Pb zircon) ?) (Gandhi et al., 1988) See text for discussion; depends on a rather uncertain correlation	Pink to brick-red, variably porphyritic, strongly foliated, leucocratic granite and alkali-feldspar granite.	Coarse grained, porphyritic to porphyroclastic, with "augen" textures, locally mylonitic. Textural variants are defined by variations in mafic content.
13	Brunwater Granite > 1794 +/- 2 [U-Pb monazite] (Scharer et al., 1988)	Grey to pale pink, foliated to lineated, equigranular, leucocratic biotite-granodiorite and monzogranite.	Medium to coarse-grained, locally porphyritic. Contains gneissic inclusions, locally nebulitic. Fabric defined by Bi aggregates and pegmatitic seams.
14	Pitre Lake Granite (Description partly after Marten, 1977)	White to pale pink or buff, equigranular, foliated Bi-Kfs leucogranite forming tabular body within metasedimentary rocks of Lower Aillik Group.	Medium-grained and homogeneous. locally displays ghost layering that defines fold structures. Concordant pegmatite and quartzose segregations.
15	Manak Island Granitoid > 1801 +/- 2 Ma [ U-Pb z ] [based on age from Munok Suite] (Krogh et al., in prep.)	White to pale grey, foliated, locally porphyritic, leucocratic Bi-granodiorite to monzogranite.	Medium to coarse-grained and homogeneous; inclusion-free.
16	Deus Cape Granitoid 1837 +/- 4 Ma [U-Pb zircon] (Krogh et al., in prep.)	Grey to pink, porphyritic to megacrystic, foliated Hb-Bi granodiorite.	Commonly K-fsp porphyritic, locally seriate-textured.

Table 3.1 (continued)

Ke; Field Relationships	Mineralogy	Petrography
Cuts early (D1,D2) structures in Aillik Group and Archean, but has S3 fabric. Intruded by Duck Island Granite of Monkey Hill Intrusive Suite.	Qz (10-20%) Mi (30-40%) Plag (An30; 30-40%) Bb-Bi (10-25% total) Sph Fe Oxide (1-2%) Accessory Zr, Ap, All	Groundmass Qz-Fsp recrystallized. Plag phenocrysts variably saussuritized, recrystallized and zoned. Bb and Bi present in subequal amounts, recrystallized to aggregates, with Sph, Ep, Chl.
Intrudes supracrustal rocks of Upper Aillik Group, and truncates bedding and early (S1,S2) fabrics. Kennedy Mountain Granite and Narrows Granite are cut by Monkey Hill Granite.	Qz (15-35%) Mi (25-60%) Plag (An20-30; 10-50%) Bb-Bi (1-15% total, normally < 5%) Sph (1-3%) Fl (0-2%) Abundant Accessory Zr, Ap, All	Variably recrystallized, but K-fsp phenocrysts preserved with local interstitial quartz. Mi is patch-perthite, with local Na-plag rims. Bb/Bi ratios variable; leucocratic variants are Bb-free. Recrystallization is very strong in fine-grained variants, which are saccharoidal. K-fsp depleted types dominated by Na-plag + Qz.
Contact relations unknown. Unit is bounded by inferred faults and unexposed zones.	Qz (15-40%) Mi (30-65%) Plag (An20-30; 20-40%) Bi-Chl-Ep-Sph (2-7% total) Bb (relict) Accessory All, rare Zr, Fl	Extensively recrystallized and mylonitized. Qz, Mi, Plag form ribbons or granular aggregates. Mafic minerals reduced to Chl-Ep-Sph aggregates, with relict Bi +/- Bb. Mi phenocrysts hematized.
Unit intrudes refoliated Archean gneisses with S1/S2 fabric. Fabric in granite considered to be D3 feature. Gradational relationship with migmatitic Archean gneisses.	Qz (15-30%) Mi (25-40%) Plag (An25; 25-40%) Bi (2-7%), rare Muscovite Accessory All, Zr.	Recrystallized, fabric defined by orientation of Bi aggregates.
Truncates S1 or S2 fabrics in Lower Aillik Group, but contains foliation parallel to layering. Contains inclusions of pelitic sediments similar to host rocks.	Qz (20-30%) Mi (30-60%) Plag (An20-30; 20-30%) Ms-Bi (5-10% total, Ms > Bi) Accessory Fl, Mn?	Recrystallized extensively. Fabric defined by alignment of Bi-Ms aggregates and faint layering.
Probably forms a screen between younger units. Unit is intruded by Gabbro of Adlavik Intrusive Suite, probably also by Wumok Intrusive Suite.	Qz (15-20%) Mi (20-40%) Plag (An25-35; 40-60%) Bi (5%) Accessory Sph, Ap. Rare Zr, All.	All components recrystallized to polygonal aggregates. Scattered Mi phenocrysts are preserved.
Lacks polydeformed character of adjacent Cape Harrison Metamorphic Complex.		

### 3.1 GEOLOGY and PETROLOGY

#### 3.1.1 Long Island Quartz Monzonite

This unit forms an elongate body in the Kaipokok Bay area (Figure 3.1), and was originally termed the "Long Island gneiss" (Gandhi et al., 1969). It is rarely gneissic, and subsequent workers used the term "Long Island Quartz Monzonite" (Gower et al., 1982; Kerr, 1986). Definition and boundaries of the unit remain unchanged from those of Gandhi et al. (1969) and Gower et al. (1982). The unit consists of medium-grained, melanocratic, foliated, hornblende-biotite quartz monzonite, granodiorite and (rare) monzogranite (Table 3.1; Plate 3.1). It is characteristically plagioclase-porphyritic, containing small (1 cm) equant phenocrysts.

A penetrative fabric is strongly developed around its margins, but parts of the interior appear massive. Marten (1977) stated that the unit truncates early ( $S_1$  and  $S_2$ ) fabrics in surrounding Archean and Aillik Group units, and considered the foliation to be a relatively late ( $D_3$ ) feature. In the area around Mark's Bight, the unit is disrupted and net-veined by the Duck Island Granite of the Monkey Hill Intrusive Suite (see Chapter 5).

The unit is recrystallized, but igneous textures (e.g. zoned plagioclase phenocrysts) are variably preserved. In the more strongly deformed variants, hornblende and biotite are retrogressed to biotite - chlorite - epidote - sphene aggregates.

The Long Island Quartz Monzonite has been dated at  $1832 \pm 58$  Ma by K-Ar whole-rock methods (Gandhi et al., 1969) and at  $1802 \pm 13/-7$  Ma by U-Pb zircon methods (Gandhi et al., 1988). The latter sample also yielded a U-Pb sphene (titanite) age of  $1746 \pm 2$  Ma, which provides a minimum age for deformation and metamorphism.



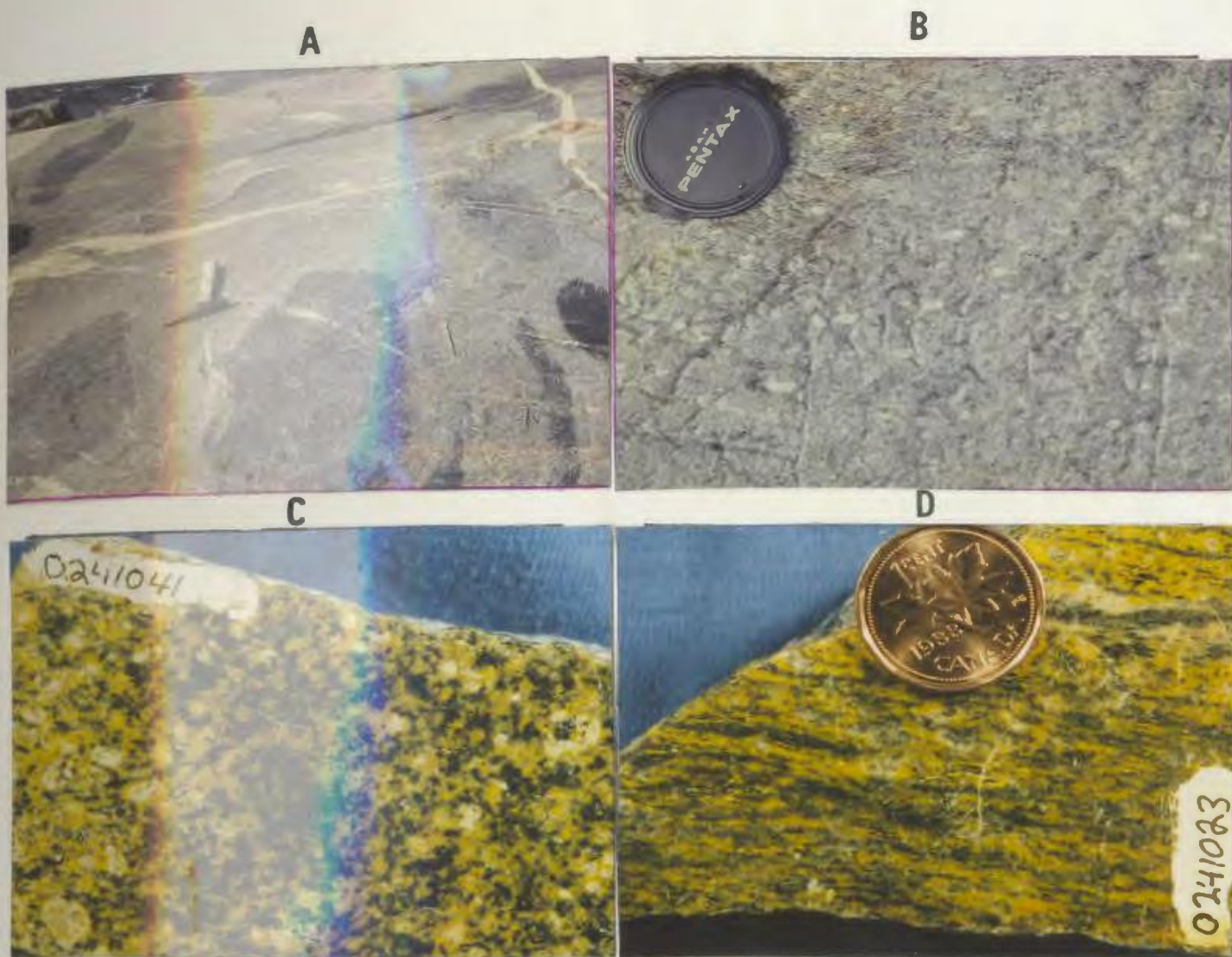


Plate 3.1. Features of the Long Island Quartz Monzonite. (a) Dioritic inclusions (deformed) in grey quartz monzonite, Mark's Bight. (b) Typical weathered surface with plagioclase phenocrysts, Mark's Bight. (c) Massive quartz monzonite from centre of body (phenocrysts ca. 0.5 cm diameter). (d) Strongly deformed variant from eastern margin of body. All slabs stained to turn K-feldspar yellow.

### 3.1.2 Kennedy Mountain Intrusive Suite

This is a new name introduced for several discrete bodies of similar foliated granitoid rocks in the Makkovik Bay area (Figure 3.1). These include units 17a and 17c of Gower et al. (1982), and foliated granitoid rocks outlined by Kerr (1986, 1987). The type area (Kennedy Mountain Granite) corresponds to the Kennedy's Cove "gneiss" of Clark (1973), but is rarely gneissic. The suite is dominated by foliated, variably K-feldspar porphyritic, monzogranite, granite and alkali-feldspar granite, commonly containing accessory fluorite (Table 3.1; Plate 3.2). The unit is not dated reliably. Gandhi et al. (1969) obtained a K-Ar (mixed hornblende and biotite) age of  $1531 \pm 38$  Ma, which is probably anomalously young. A composite Rb-Sr isochron (Chapter 8) suggests an age of  $1778 \pm 98$  Ma, but this is not considered reliable. No U-Pb data are available as of writing.

**Field Relationships** : The Kennedy Mountain Granite and Narrows Granite intrude the Upper Aillik Group, but are cut by the Labradorian Monkey Hill Granite (Chapter 5). Units assigned to the suite contain a single NE-trending foliation; by analogy with the Long Island unit, this is interpreted to be a  $D_3$  feature resulting from Late Makkovikian deformation, and implies a similar minimum age of 1800 Ma. Foliations are most obvious in relatively melanocratic, porphyritic variants, whereas equigranular and leucocratic variants commonly appear massive and unfoliated. However, all are recrystallized and display fabrics in thin section; in leucocratic variants, orientations are defined by elongation of quartz and feldspar. Coarse grained, fluorite and/or pyrite-bearing



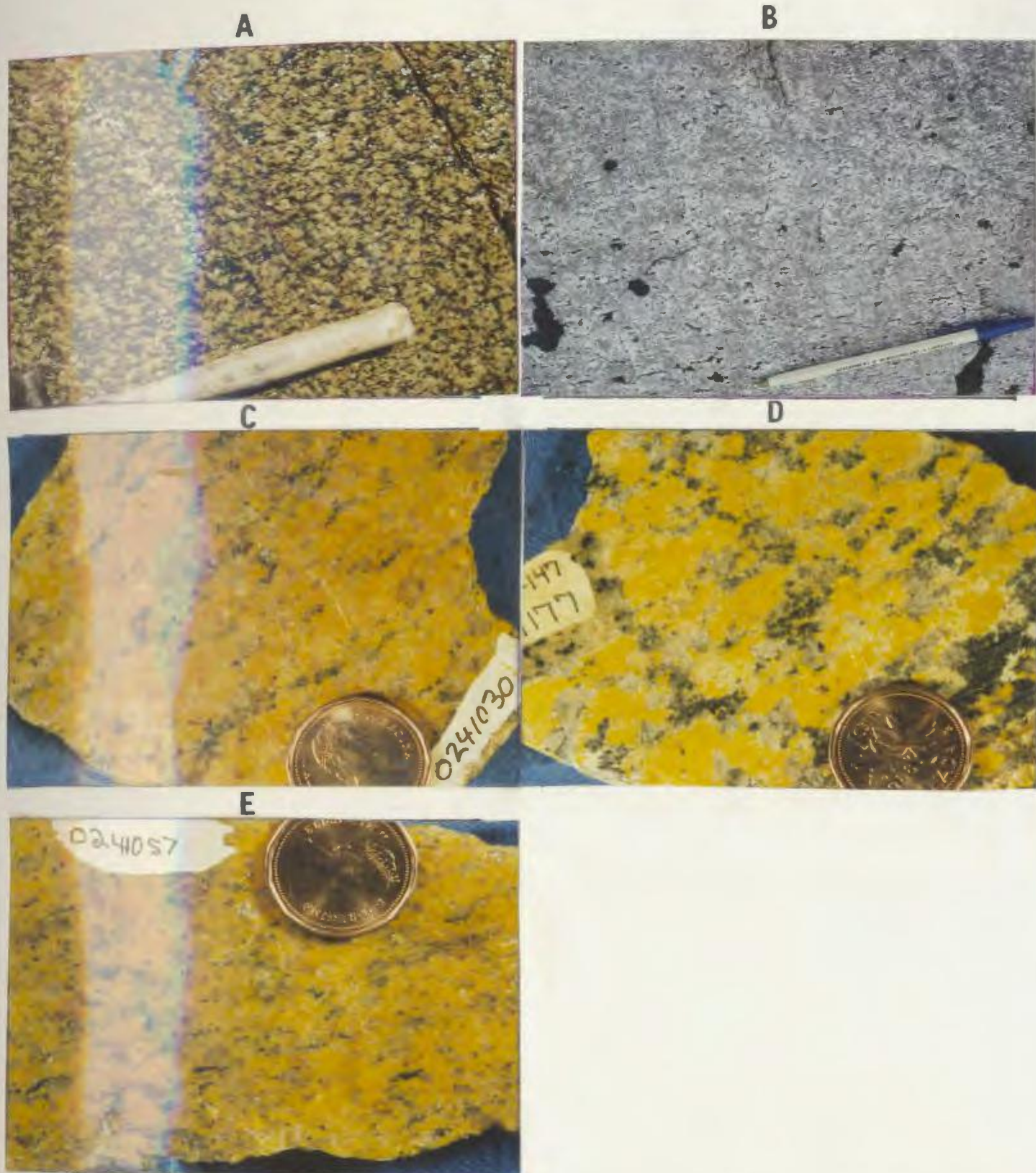


Plate 3.2. Features of the Kennedy Mountain Intrusive Suite. (a) Coarse-grained monzogranite (Narrows Granite, Makkovik Bay). (b) Fine-grained alaskitic variant of the Cross Lake Granite; the superb glacial polish is a reflection of the pervasive recrystallization, which reduces the natural tendency of granite to disaggregate. (c) Fluorite-bearing leucogranite (Kennedy Mountain Granite, Makkovik Bay), foliation is parallel to slab label. (d) Coarse-grained biotite-hornblende granite (Narrows Granite), section cut normal to foliation. (e) Fine-grained potassic leucogranite (Cross Lake Granite). All slabs stained to turn K-feldspar yellow.

pegmatite veins (locally containing amazonite, a green variety of K-feldspar) intrude many outcrops, particularly in the Cross Lake Granite. Xenoliths of country rocks are rare except adjacent to contacts; cognate xenoliths (normally darker than their host) occur locally. The Cross Lake Granite appears to be more leucocratic than other units of the suite, and is locally alaskitic (i.e., a fine-grained rock consisting essentially of quartz and alkali-feldspar; Johannsen, 1920).

**Petrography** : Most examples contain both hornblende and biotite, but leucocratic variants are hornblende-poor or hornblende-free. Purple fluorite is widespread (particularly in leucocratic rocks), and forms coarse patches along foliation planes. Sphene is also prominent in many hand samples. In thin section, most examples are recrystallized, but original igneous textures (K-feldspar phenocrysts and, more rarely, interstitial quartz) are variably preserved. Mafic minerals and sphene form aggregates, associated with prominent and abundant zircon, allanite, apatite and fluorite crystals. Chlorite and/or epidote are locally important as alteration products of hornblende and biotite.

Anomalous rock types consisting almost entirely of sodic plagioclase ( $< \text{An}_{15}$ ) and quartz are present locally within all units of the Kennedy Mountain Suite. These are considered to be Na-metasomatized, rather than original, compositions (see 3.2 and 3.3). Rare albite rims or patches on K-feldspar phenocrysts in "normal" variants form the only petrographic evidence for this process; the anomalously sodic rocks are thoroughly recrystallized.

.

### 3.1.3 Melody Granite

The new name Melody Granite is introduced for an elongate unit of strongly foliated granitoid rocks in the western part of the study area (Figure 3.1). The unit is dominated by pink to brick-red, K-feldspar-rich granite and alkali-feldspar granite (Table 3.1; Plate 3.3). It corresponds to parts of unit 14 of Bailey (1979) and parts of unit 27 of Gower et al. (1982).

**Field Relations** : The contact relations of the Melody Granite are unknown, as most of its boundaries correspond with inferred fault zones or unexposed areas. It has a widely developed cataclastic to protomylonitic fabric and commonly shows augen texture. There are two textural variants, defined by variation in total mafic mineral content. The melanocratic variants commonly show more obvious relict porphyritic textures, but leucocratic variants are also strongly K-feldspar porphyritic where weakly deformed. The distribution of these two variants corresponds generally to units 23 and 24 of Ryan (1984), described as granite and granodiorite respectively

**Petrography** : In thin section, the Melody Granite is strongly recrystallized. It displays a granular texture, and many examples contain quartz and feldspar ribbons, oriented parallel to microcrystalline mylonitic zones. The mafic mineral assemblage varies with intensity of deformation and metamorphism; weakly-deformed samples contain aggregates of fine-grained green-brown biotite and local relict hornblende, whereas strongly deformed variants contain only sphene - chlorite - epidote aggregates along foliation planes.



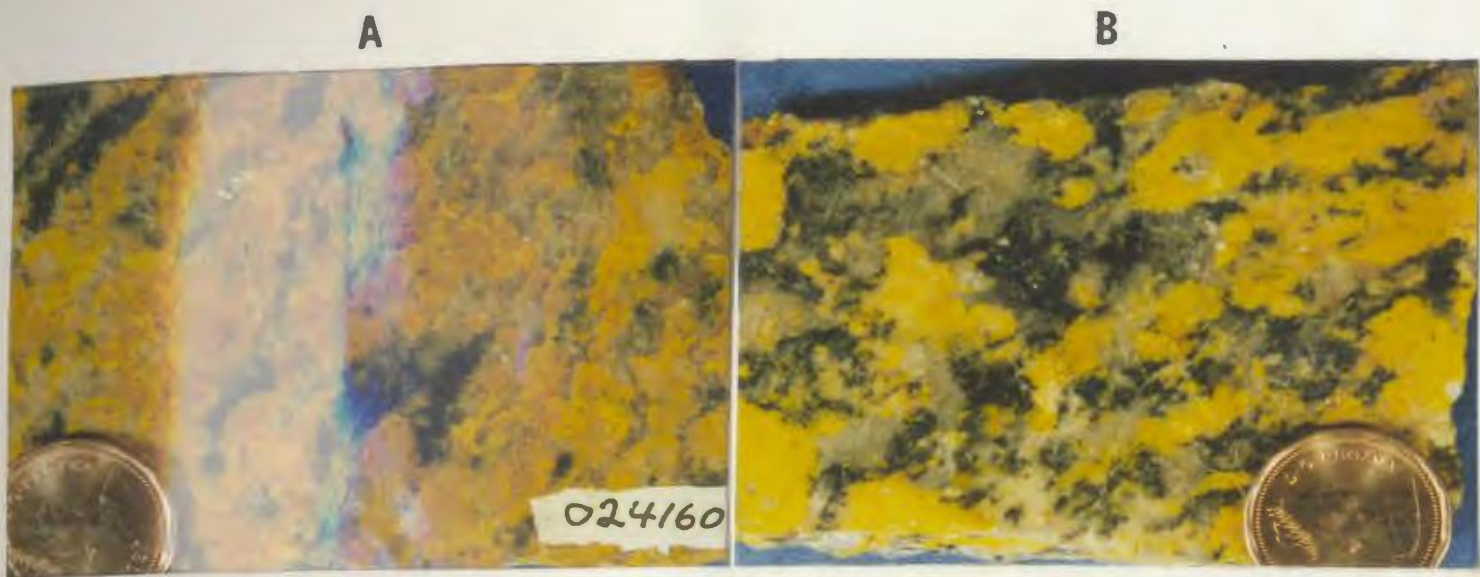


Plate 3.3. Features of the Melody Granite. (a) Strongly deformed granitoid with ribbon quartz and cataclastic texture, but with relict K-feldspar phenocrysts. (b) Weakly deformed, porphyritic, melanocratic variant. All slabs stained to turn K-feldspar yellow.

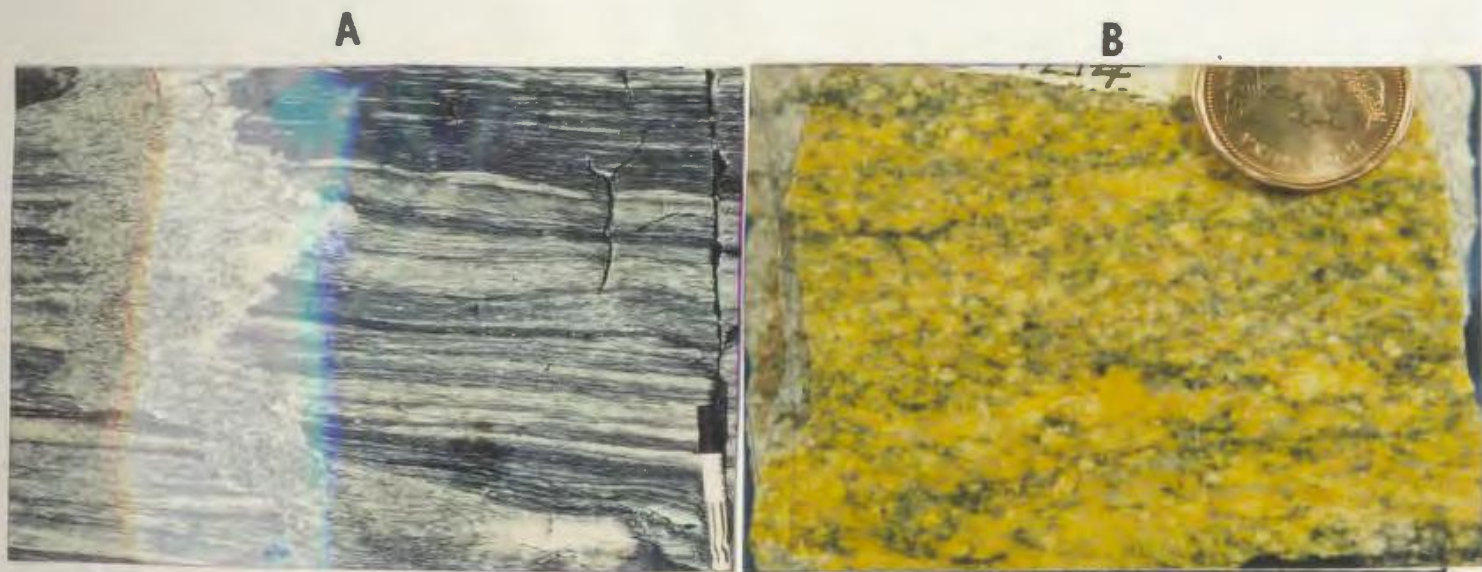


Plate 3.4. Features of the Brumwater Granite. (a) Vein of grey granite cutting refoliated Archean gneiss, Kaipokok Bay area. Note that vein truncates banding, but is affected by later deformation, and shares the same general fabric. (b) Typical stained slab, showing heterogeneous and slightly banded appearance of many examples.

**Age Uncertainty** : The Melody Granite is undated. Ryan (1984) mapped it as continuous with his unit 23, based on compilation of unpublished BRINCO descriptions. Ryan's unit 23 has yielded an age of  $1910 \pm 10$  Ma about 50 km west of the study area (Gandhi et al., 1988). This result may indicate a pre- Makkovikian age for the Melody Granite; however, the correlation is based purely on general lithology, and the author has not examined the sample of Gandhi et al. (1988). For the purposes of the current discussion, therefore, the Melody Granite is regarded as a syr-tectonic Makkovikian intrusion, although this may be subject to revision.

#### 3.1.4 Brumwater granite

The Brumwater granite (Marten, 1977) is a small, tabular body that intrudes reworked Archean basement rocks southeast of Kaipokok Bay (Figure 3.1, inset). It was defined and mapped by Marten (1977), and visited briefly during this project. It consists of grey to pink, foliated, leucocratic, biotite- granodiorite and monzogranite (Table 3.1; Plate 3.4). Marten (1977) describes similar rock types from other parts of the Archean inlier along Kaipokok Bay, which he correlated with the Brumwater Granite (Figure 3.1, inset).

**Field Relationships and Age** : Marten (1977) described a gradational relationship between this unit and adjacent migmatized Archean gneisses, and suggested that it may be an anatectic derivative of them. Enclaves of gneissic material are locally present, and a "ghost layering" is present in some outcrops. The granite truncates layering in refoliated Archean gneisses that is considered to be a  $D_2$

structure, and foliation in the granite is thus considered to be a  $D_3$  feature (Marten, 1977). Its relationship to deformation is therefore analogous to the Long Island Quartz Monzonite (see above). The foliation is defined by biotite aggregates and concordant pegmatitic and quartzose seams. An augen texture is locally developed.

Schärer et al. (1988) obtained a U-Pb monazite age of  $1794 \pm 2$  Ma from a biotite leucogranite that cuts migmatites correlated with the Brumwater granite; this provides a lower limit on the age of the unit. An attempt to date the granite itself failed due to a highly discordant, U-rich zircon population (U. Schärer, pers. comm. to R.J. Wardle).

#### 3.1.5 Pitre Lake Granite

The Pitre Lake granite, defined and mapped by Marten (1977), is a thin, tabular, subconcordant body that is confined to metasedimentary rocks of the Lower Aillik Group in the Kitts Pond area (Figure 3.1, inset). It was visited only briefly during this study. The unit consists of medium-grained, equigranular biotite-muscovite granite (Table 3.1; Plate 3.5).

The granite truncates the foliation in the host metasediments (a composite  $D_1/D_2$  structure; Marten, 1977), but contains a weak to moderate foliation subparallel to or slightly oblique to its contacts. Marten (1977) considered this to be a  $D_3$  feature, and suggested that the unit was a syn- $D_3$  intrusion.

Metasedimentary xenoliths similar to the pelitic to psammitic country rocks are common, and amphibolite inclusions occur locally. Folding defined by "ghost layering" may indicate a more complex structural history than other foliated granitoids. However, this layering



A



B



Plate 3.5. Features of the Pitre Lake Granite. (a) Part of a concordant metasedimentary inclusion (centre) within the granite, which is the white material to left and right. (b) Complexly folded "ghost" layering, possibly inherited from the metasedimentary protolith.

A



B



Plate 3.6. Features of the Manak Island Granitoid. (a) and (b) Typical stained slabs of weakly foliated, leucocratic monzogranite. Foliation is not obvious in slabs, but is easily recognized on outcrop surfaces (no photo available).

could be an inherited feature if the granite was derived by anatexis of its host rocks, which show similarly intricate folding in nearby outcrops. No geochronological data are available from the unit.

#### **3.1.6 Manak Island Granitoid**

This unit is located near Adlavik Bay (Figure 3.1), and was previously grouped with the Cape Strawberry Granite by Doherty (1980) and Gower et al. (1982). It is lithologically distinct from the latter in all respects and has a N-trending foliation. It consists of white to grey, foliated granodiorite and monzogranite (Table 3.1; Plate 3.6). The unit resembles the more homogeneous variants of the Brumwater Granite (see above), but is generally free of xenoliths and ghost layering.

The unit forms a narrow zone between gabbro and diorite of the Adlavik Intrusive Suite (see Chapter 5) and adjacent monzonite and quartz monzonite of the Numok Intrusive Suite (see Chapter 4). These surrounding units are massive and undeformed, and the Manak Island unit probably represents a screen between younger intrusions. It is intruded by gabbro and diorite of the Adlavik Suite on the adjacent mainland, but contacts with the Numok Suite and the Upper Aillik Group at the southern end of Manak Island have not been observed.

In thin section, the unit is variably recrystallized to a polygonal mosaic, although scattered microcline and (locally) zoned plagioclase phenocrysts are preserved. It contains only minor amounts of sphene, apatite, zircon and allanite.

No geochronological data are available from the unit, but undeformed rocks of the adjacent Numok Suite have given a U-Pb zircon age of  $1801 \pm 2$  Ma. (Krogh et al., in

prep.). If differences in deformation state indicate differences in age, this provides a lower limit for the age of the Manak Island Granitoid.

#### 3.1.7 Deus Cape Granitoid

This unit occurs in the extreme east of the study area, adjacent to the Cape Harrison Metamorphic Suite (Gower, 1981). It has been visited only in a few localities during this project. The unit consists of coarse grained, pink to grey, foliated, K-feldspar megacrystic to seriate granodiorite (Table 3.1; details partly from Gower, 1981).

Contact relations are unknown, but the unit displays a single NNE-trending foliation, and contrasts with the adjacent polydeformed migmatitic rocks of the Cape Harrison Suite (Gower, 1981). This contrast suggests that it occupies a time slot between the Cape Harrison Metamorphic Suite and undeformed Makkovikian plutonic rocks. Krogh et al. (in prep) report a U-Pb zircon age of  $1837 \pm 6/-4$  Ma from this unit, which provides a minimum age for the Cape Harrison Metamorphic Suite, which is the only candidate for "basement" in the east of the area.

#### 3.1.8 Island Harbour Bay Intrusive Suite

The Island Harbour Bay Intrusive Suite (Ryan et al., 1983) lies outside the study area, but, as the largest single Makkovikian plutonic body, merits some discussion. The following outline is taken from Ermanovics et al. (1982), Ryan et al. (1983) and I. Ermanovics (pers. comm., 1988).

The suite includes a wide variety of rock types that display complex field relationships. Ryan et al. (1983) divided it into a grey tonalite to granodiorite, and a

homogeneous pink granite. The former is more abundant and forms the outer part of the intrusion; it is compositionally varied, inclusion-rich and polyphase. Ryan et al.(1983) distinguished diorite, quartz diorite, K-feldspar megacrystic granodiorite, and leucocratic granite, all of which show mutually intrusive relationships suggesting synchronous emplacement. The central granite unit lacks this complexity, and is commonly inclusion-free. It consists of pink to grey, feldspar porphyritic, locally megacrystic, biotite granite, locally containing interstitial fluorite. All of the above phases are intruded by pegmatite and aplite dykes.

The contact between outermost tonalite-granodiorite and Archean gneisses is described by Ryan et al.(1983) as a complex lit-par-lit migmatite zone, where foliations in the granitoid rocks are parallel to those in the gneisses. Early foliated granitoid dykes are cut by later undeformed phases, indicating syn- to post-tectonic emplacement. Foliations in the outer parts of the intrusion are locally cataclastic to mylonitic, and have concentric structural trends (Ryan et al., 1983). Rafts of Archean gneiss within this marginal zone display the strong "straightened" layering associated with early Makkovikian deformation (Ryan and Kay, 1982). The central portion of the body, in particular the granite unit, is massive to weakly foliated, and appears post-tectonic.

The Island Harbour Bay Intrusive Suite has been dated by a variety of methods. U-Pb zircon data from the dominant grey granodiorite (Loveridge et al, 1988) suggests an age of  $1805 \pm 5$  Ma, similar to that of the Long Island Quartz Monzonite. This agrees well with Rb-Sr ages of  $1805 \pm 42$  for the granite unit, and  $1843 \pm 90$  Ma and  $1794 \pm 71$  Ma for the tonalite-granodiorite unit (Grant et al., 1983). An

U-Pb zircon age of  $1973 \pm 15$  Ma (Brooks, 1982) from the tonalite unit is enigmatic. It may reflect inheritance, but there is no evidence of inclusions in outcrop (B.Ryan pers.comm., 1988), and no cores are reported from the zircons. I.Ermanovics (pers. comm., 1988) considers the ca. 1800 Ma ages from the granite unit to be minimum ages only, and states that the tonalitic rocks may be somewhat older. As will be shown later, these tonalitic and trondhjemitic compositions are not typical of the Makkovikian plutonic assemblage in the study area.

### 3.2. DESCRIPTIVE GEOCHEMISTRY

Syn-tectonic Makkovikian plutonic rocks are represented by 186 samples; 121 of these are from "regional" samples collected on a 2 km grid spacing. The remainder are follow-up samples (mostly from the Kennedy Mountain Suite), and a small number of geological samples from all units (see Chapter 1 for explanation of sample populations). No samples were collected from the Island Harbour Bay Intrusive Suite; this is represented by 20 unpublished analyses supplied by B.Ryan (pers. comm., 1987).

#### 3.2.1 General Geochemistry

##### Summary of Numerical Data

Average major, trace and partial CIPW normative compositions of syn-tectonic Makkovikian plutonic rocks are listed in Table 3.2. The Long Island Quartz Monzonite and tonalite to granodiorite of the Island Harbour Bay Intrusive Suite are silica-poor (63-65%  $\text{SiO}_2$ ) compared to all other units (72-75%  $\text{SiO}_2$ ). The four component units of the Kennedy Mountain Intrusive Suite have similar major and trace element compositions, as do the two geographic subdivisions of the Long Island Quartz Monzonite. The Melody Granite is broadly similar in composition to granites of the Kennedy Mountain Suite.

The remaining units show similar major element compositions but distinct trace element patterns. The Pitre Lake Granite is characterized by high Rb, F and Li relative

Table 3.2 . Average compositions of syn-tectonic Makkovikian plutonic rocks, subdivided by principal units.

UNIT	10.1		10.2		11.1		11.2		11.3		11.4		12.0	
n1	14		9		19		18		74		5		31	
n2	5				8		1		16		1		19	
(Wt%)	Mean	S.D.	Mean	S.D.	Mean	S.D.	Mean	S.D.	Mean	S.D.	Mean	S.D.	Mean	S.D.
SiO <sub>2</sub>	63.22	1.27	65.46	7.11	75.05	1.37	71.05	2.73	74.49	2.63	69.35	4.36	72.27	3.26
TiO <sub>2</sub>	0.88	0.06	0.69	0.34	0.28	0.24	0.42	0.15	0.23	0.13	0.51	0.22	0.35	0.21
Al <sub>2</sub> O <sub>3</sub>	15.79	0.23	15.84	2.42	12.31	0.48	13.71	0.82	12.32	1.01	14.45	1.55	13.50	1.10
Fe <sub>2</sub> O <sub>3</sub>	1.81	0.38	1.95	1.18	1.32	0.41	1.39	0.72	1.27	0.75	1.11	0.55	0.97	0.68
FeO	3.09	0.75	1.90	0.59	0.91	0.32	1.69	0.83	1.28	1.26	2.05	0.59	1.74	1.12
MnO	0.10	0.01	0.07	0.03	0.04	0.01	0.07	0.03	0.06	0.03	0.07	0.02	0.04	0.02
MgO	1.26	0.44	0.99	0.63	0.13	0.04	0.38	0.22	0.12	0.20	0.58	0.44	0.41	0.37
CaO	2.97	0.49	2.71	1.82	0.51	0.27	1.25	0.42	0.76	0.59	1.64	0.76	1.18	0.72
Na <sub>2</sub> O	4.28	0.26	4.28	0.31	4.61	1.16	4.30	0.92	4.34	1.13	3.99	0.43	3.80	0.76
K <sub>2</sub> O	4.77	0.51	4.50	0.31	4.14	1.82	4.84	1.15	4.19	1.56	5.25	0.49	4.59	0.99
P <sub>2</sub> O <sub>5</sub>	0.26	0.03	0.25	0.20	0.03	0.01	0.09	0.04	0.03	0.04	0.11	0.07	0.09	0.07
LOI	0.63	0.24	0.72	0.34	0.36	0.13	0.42	0.19	0.47	0.23	0.41	0.03	0.70	0.34
TOTAL	99.16		99.36		99.67		99.60		99.55		99.53		99.63	
(ppm) Trace Elements														
Li	23.6	4.6	19.9	15.8	15.2	10.2	25.6	15.5	10.4	7.0	27.2	8.1	18.1	13.5
F	873.2	214.7	809.8	499.5	661.5	544.7	936.1	315.2	1092.4	982.5	1145.8	484.2	613.7	481.2
Sc	9.6	1.7			1.5	0.6	0.8	0.0	1.1	0.7	4.4	0.0	2.9	1.6
V	76.3	19.2	49.0	31.8	12.7	6.2	21.4	8.6	12.3	10.5	45.6	21.5	24.3	17.7
Cr	5.6	3.6	3.2	1.4	4.3	4.0	3.6	1.9	5.3	4.0	3.2	2.2	3.7	3.5
Ni	2.7	1.9	1.2	0.4	1.4	1.1	1.3	0.7	1.3	1.3	1.6	0.9	1.7	1.5
Cu	9.3	3.9	5.2	2.0	2.5	0.8	5.2	4.3	3.6	3.9	6.2	4.1	7.3	15.1
Zn	74.0	8.8	61.8	17.9	65.8	29.7	73.7	24.7	87.3	61.8	60.6	19.2	45.0	27.9
Ga	18.4	1.2	14.4	4.4	16.5	7.1	14.5	5.7	17.3	7.7	18	2.0	18.3	2.2
Rb	127.9	24.4	118.0	29.2	129.7	62.1	163.0	49.3	127.9	67.4	185	42.0	122.0	36.0
Sr	327.2	40.5	348.8	274.2	31.8	9.4	103.9	55.2	51.6	78.5	137.2	86.1	106.8	89.9
Y	36.5	2.0	32.3	7.0	52.5	14.2	55.1	15.5	82.8	31.3	45.8	9.4	45.2	17.8
Zr	227.9	66.6	250.1	107.2	409.5	126.5	356.7	119.6	401.4	156.2	237.6	54.2	361.9	162.9
Nb	14.1	1.1	13.2	3.7	19.9	4.1	23.9	6.4	32.0	15.1	19.6	5.0	20.6	5.6
Mo	4.3	0.5	5.4	3.2	3.4	2.3	4.4	2.1	3.4	1.5	4.6	1.1	3.4	1.0
Sn	1.0	0.0			3.5	2.0	7.0	0.0	3.4	2.9	5	0.0	4.4	3.7
Cs	1.3	1.2			0.7	0.5	0.5	0.0	0.6	0.4	0.5	0.0	2.2	1.4
Ba	1424.3	120.6	1243.6	449.1	152.6	77.4	717.6	315.9	390.0	439.9	846	390.9	827.6	481.8
La	53.6	4.9	44.9	16.4	62.8	28.4	73.1	22.7	85.0	39.1	57.2	9.7	85.2	38.2
Ce	103.0	6.2	89.3	26.9	130.9	52.7	143.1	40.3	177.2	73.2	117.2	18.8	171.4	66.8
Sm	9.2	0.8			10.5	2.0	13.0	0.0	13.7	3.8	11	0.0	13.8	5.0
Yb	2.5	0.0			4.2	2.4	10.0	0.0	8.9	3.0	7	0.0	5.2	2.5
Hf	8.0	1.2			12.8	3.5	12.0	0.0	12.2	3.5	12	0.0	10.8	4.1
Pb	15.5	3.8	18.6	4.3	17.7	6.6	24.9	4.5	18.1	11.9	22.6	2.3	14.1	7.5
Th	9.5	2.7	8.1	9.6	10.7	7.7	19.2	6.8	15.9	10.3	23.8	12.0	12.1	6.1
U	4.9	0.8	3.3	1.0	3.7	2.5	6.3	2.9	4.5	2.9	7.16	2.8	3.7	2.0
(Wt%) Partial CIPW norms														
Q	12.07	1.68	17.31	11.38	31.61	2.89	24.31	5.12	31.64	5.41	21.40	8.76	29.06	5.53
C	0.00	0.00	0.09	0.15	0.03	0.07	0.01	0.03	0.01	0.07	0.02	0.05	0.38	0.46
Or	28.59	3.02	26.91	1.83	24.63	10.87	28.84	6.85	24.96	9.31	31.32	3.06	27.43	5.87
Ab	36.73	2.08	35.85	1.28	39.17	9.84	36.67	7.84	36.86	9.30	34.09	3.77	32.48	6.48
An	9.97	1.50	10.61	5.54	0.66	0.47	3.82	1.88	1.84	1.97	5.98	2.69	5.24	3.02
Di	3.05	1.23	1.34	2.07	0.84	0.63	1.53	1.07	1.08	1.21	1.42	0.99	0.20	0.45
Hy	4.62	1.78	2.31	1.72	0.26	0.39	1.81	1.51	0.94	2.08	2.89	1.12	2.94	2.30
Ol	0.00	0.00	0.39	0.78	0.00	0.00	0.00	0.00	0.00	0.00	0.00	0.00	0.00	0.00
Ht	2.67	0.56	2.63	1.35	1.64	0.57	1.69	0.90	1.57	0.80	1.62	0.81	1.25	0.74
Il	1.69	0.13	1.34	0.66	0.53	0.45	0.77	0.31	0.44	0.24	0.98	0.42	0.67	0.41

KEY TO UNITS (KMIS - Kennedy Mountain Intrusive Suite)

10.1 -- Long Island Quartz Monzonite (main body) 10.2 -- Long Island Quartz Monzonite (other)

11.1 -- (KMIS) Kennedy Mountain Granite 11.2 -- (KMIS) Narrows Granite

11.3 -- (KMIS) Cross Lake Granite 11.4 -- (KMIS) other units

12.0 -- Melody Granite

n1 -- number of analyses for all elements except those listed below.

n2 -- number of analyses for Sc, Sn, Cs, Sm, Yb and Hf.

Table 3.2 (continued)

UNIT	13.0		14.0		15.0		16.0		18.1		18.2	
n1	4		4		6		2		15		5	
n2												
(Wt%)	Mean	S.D.	Mean	S.D.	Mean	S.D.	Mean	S.D.	Mean	S.D.	Mean	S.D.
SiO <sub>2</sub>	72.73	1.26	76.18	0.38	70.13	0.69	75.68	4.42	66.13	6.51	73.38	1.52
TiO <sub>2</sub>	0.16	0.09	0.05	0.02	0.31	0.03	0.17	0.10	0.52	0.36	0.20	0.05
Al <sub>2</sub> O <sub>3</sub>	14.66	0.44	12.87	0.23	15.83	0.40	12.64	1.94	16.44	1.40	14.52	0.73
Fe <sub>2</sub> O <sub>3</sub>	0.64	0.44	0.36	0.24	1.06	0.26	1.03	0.28	1.19	0.97	0.30	0.15
FeO	0.66	0.29	0.43	0.25	0.90	0.19	0.54	0.20	2.26	1.46	0.96	0.11
MnO	0.03	0.01	0.03	0.01	0.04	0.01	0.04	0.01	0.05	0.04	0.03	0.01
MgO	0.65	0.27	0.02	0.01	0.54	0.03	0.31	0.23	1.41	1.36	0.38	0.23
CaO	0.99	0.03	0.47	0.17	1.78	0.21	0.63	0.11	3.48	1.94	0.97	0.61
Na <sub>2</sub> O	5.06	0.93	4.31	0.26	4.89	0.19	3.36	1.08	4.61	0.50	4.03	0.28
K <sub>2</sub> O	3.34	1.46	4.32	0.24	3.93	0.14	4.79	0.08	2.52	1.08	4.08	1.16
P <sub>2</sub> O <sub>5</sub>	0.06	0.02	0.02	0.01	0.12	0.01	0.03	0.03	0.19	0.19	0.04	0.01
LOI	0.93	0.29	0.62	0.04	0.42	0.16	0.67	0.11	0.98	0.42	0.78	0.02
TOTAL	99.91		99.66		99.95		99.86		99.78		99.67	
(ppm)												
Li	11.5	1.7	162.5	98.0	22.5	6.1	12.0	0.0				
F	187.5	68.4	2660.5	746.6	411.3	133.9	230.0	14.1				
Sc												
V	21.5	8.5	13.0	2.4	29.0	4.9	14.0	7.1	55.7	48.4	28.0	24.1
Cr	7.5	5.7	4.5	1.7	2.5	0.8	1.0	0.0	15.0	37.5	5.0	0.0
Ni	3.0	2.7	1.5	0.6	1.5	0.5	1.5	0.7				
Cu	3.5	1.3	2.0	1.2	4.5	1.2	8.5	5.0				
Zn	29.3	3.9	61.3	23.9	43.2	10.2	54.0	4.2				
Ga	6.8	1.7	16.5	7.2	13.2	2.9	16.5	2.1	21.5	2.6	19.6	3.4
Rb	96.5	41.0	411.5	163.4	79.3	24.9	164.5	37.5	70.7	24.8	257.0	166.0
Sr	273.5	47.5	7.8	2.2	596.3	75.3	48.0	25.5	540.2	290.5	173.0	177.8
Y	5.8	1.7	125.0	32.8	8.5	1.2	41.5	21.9	10.9	7.1	45.0	51.3
Zr	88.0	38.0	114.3	23.1	162.0	26.1	256.0	53.7	163.3	76.4	110.0	19.1
Nb	2.0	0.0	36.5	11.6	5.0	1.3	23.5	0.7	8.3	5.7	20.8	18.6
Mo	2.0	0.0	2.0	0.0	2.0	0.9	3.5	0.7				
Sn												
Cs												
Ba	912.5	446.6	42.0	38.2	1560.0	174.4	209.5	171.8	774.4	330.4	674.0	592.0
La	13.8	4.6	12.3	4.3	26.0	5.3	49.0	2.8	29.2	11.0	22.6	5.2
Ce	19.0	11.6	32.5	9.9	46.0	8.7	103.0	5.7	50.3	17.0	36.4	8.6
Sm												
Yb												
Hf												
Pb	12.5	7.9	61.5	1.3	11.3	2.8	5	14.8				
Th	1.8	1.0	23.3	18.2	4.8	2.9	7.8		6.3	4.1	24.0	19.2
U	1.7	0.5	8.6	8.2	1.8	0.4	2.8					
(Wt%)												
Q	27.56	2.39	33.68	0.70	22.02	1.87	36.33	11.44	19.78	8.28	31.50	5.77
C	0.98	0.48	0.30	0.23	0.40	0.24	0.86	0.05	0.51	0.46	1.80	1.73
Or	19.88	8.64	25.77	1.40	23.32	0.82	28.50	0.57	15.08	6.46	24.39	6.87
Ab	43.23	8.08	36.77	2.22	41.55	1.66	28.67	9.27	39.48	4.30	34.42	2.37
An	4.84	0.26	2.24	0.90	8.59	1.06	2.99	0.40	15.51	7.54	4.75	3.13
Di	0.00	0.00	0.00	0.00	0.00	0.00	0.00	0.00	0.84	1.89	0.00	0.00
Hx	2.12	0.72	0.60	0.40	1.78	0.43	0.77	0.59	5.52	4.53	2.22	0.45
Ol	0.00	0.00	0.00	0.00	0.00	0.00	0.00	0.00	0.07	0.26	0.00	0.00
Pl	0.94	0.64	0.38	0.14	1.40	0.32	1.37	0.38	1.75	1.43	0.44	0.21
Il	0.31	0.17	0.10	0.03	0.58	0.07	0.33	0.19	0.99	0.70	0.38	0.11

KEY TO UNITS (IBBIS -- Island Harbour Bay Intrusive Suite)

13.0 -- Brunwater Granite

14.0 -- Pitre Lake Granite

15.0 -- Manak Island Granitoid

16.0 -- Deus Cape Granitoid

18.1 -- IBBIS (tonalite-granodiorite)

18.2 -- IBBIS (granite)

n1 -- number of analyses for all elements except those listed below.

n2 -- number of analyses for Sc, Sn, Cs, Sm, Yb and Hf.



to all other units. The Manak Island and Brumwater units are similar, but the former shows higher Ba and Sr, consistent with a lower  $\text{SiO}_2$  content. These units, and the granites from the Island Harbour Bay Suite, are distinguished by low Zr, Y, Nb, La and Ce compared to the Long Island and Kennedy Mountain units. The mean composition for the Deus Cape Granitoid (2 samples only) is probably not representative of the unit.

#### **Abundance and Distribution of Rock Types**

IUGS rock types were calculated from normative data (after Streckeisen and LeMaitre, 1979, see Chapter 1) for regional and geological sample populations. This provides an unbiased method of comparing compositional spectra. Relative abundances (Figure 3.2) indicate that this association is dominated by granite (s.s.) and alkali-feldspar granite, with lesser amounts of quartz monzonite, quartz syenite and monzogranite.

The Long Island unit contains most of the quartz monzonite to monzogranite, whereas the Kennedy Mountain Intrusive Suite and Melody Granite are dominated by granite and alkali-feldspar granite. Minor units (not figured) are also dominated by granite (s.s.), except for the Manak Island unit, which is a monzogranite. No analysis has been attempted for the Island Harbour Bay Suite (data are insufficient), but a major-element study by Ermanovics (pers. comm., 1988) suggests a wide range of compositions, including significant tonalite - trondhjemite (see also Ryan et al., 1983)

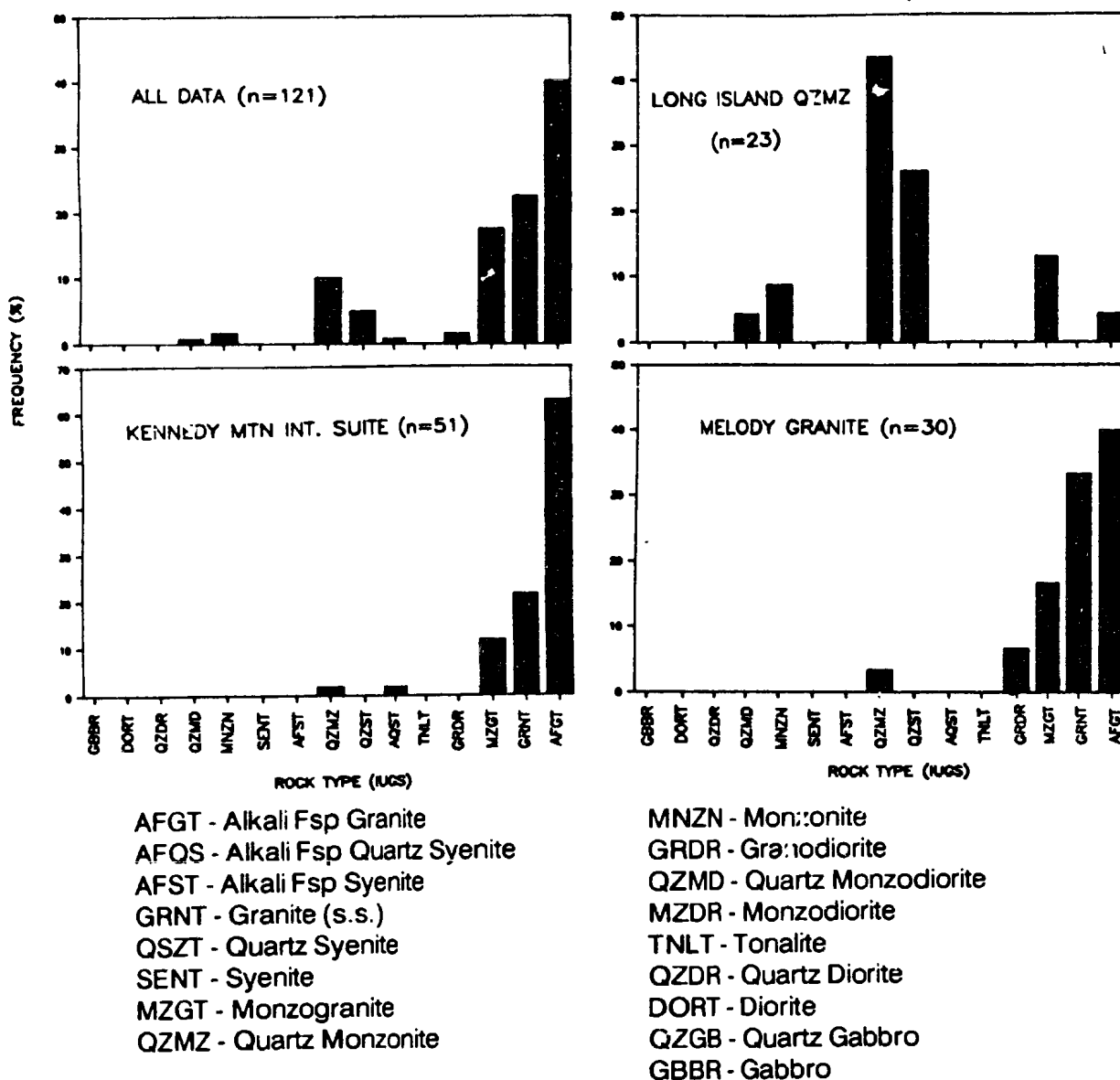


Figure 3.2 . Relative abundance of IUGS rock types calculated from normative mineralogy using the method of Streckeisen and LeMaitre (1979). Note that this is based on Barth mesonorms, not the CIPW norms listed in Table 3.2. Abundances are not given for minor units, due to small numbers of samples.

### 3.2.2 Geochemical Trends and Contrasts

Syn-tectonic Makkovikian plutonic rocks are subdivided into three groups (A,B and C) represented by separate columns of diagrams in Figures 3.3 to 3.11. This method is intended to reduce "clutter", and no genetic links are implied by these groupings.

#### **Major Element Patterns**

Major element variations show expected patterns. All elements (except  $\text{Na}_2\text{O}$  and  $\text{K}_2\text{O}$ ) are negatively correlated with  $\text{SiO}_2$  (e.g.  $\text{TiO}_2$  and  $\text{FeO}$ ; Figure 3.3), and do not discriminate between units. Within the Kennedy Mountain Suite, the Kennedy Mountain and Cross Lake Granites show the most evolved, high- $\text{SiO}_2$  compositions. The Melody Granite coincides with the Kennedy Mountain Intrusive Suite.  $\text{Na}_2\text{O}$  (Figure 3.3) and  $\text{K}_2\text{O}$  (not shown) display little systematic variation and exhibit considerable scatter above 70%  $\text{SiO}_2$  in the Kennedy Mountain Suite.

Agpaitic Index [ $\text{K+N/A}$ ] and Alumina Index [ $\text{A/C+N+K}$ ] (see Chapter 1 for details) distributions provide better unit discrimination.  $\text{K+N/A}$  defines two subparallel trends (Figure 3.3; dotted line defines boundary). The "upper trend" includes the Long Island Quartz Monzonite and Kennedy Mountain Intrusive Suite, and terminates in a dense grouping at 75-78%  $\text{SiO}_2$  that includes some peralkaline compositions ( $\text{K+N/A} > 1.0$ ). The "lower trend" is defined by the Melody, Manak Island, Brumwater and P'tre Lake units, and by parts of the Island Harbour Bay Suite; this terminates at  $\text{K+N/A}$  values below 0.94.  $\text{A/C+N+K}$  values (Figure 3.3) indicate that the "lower trend" units are

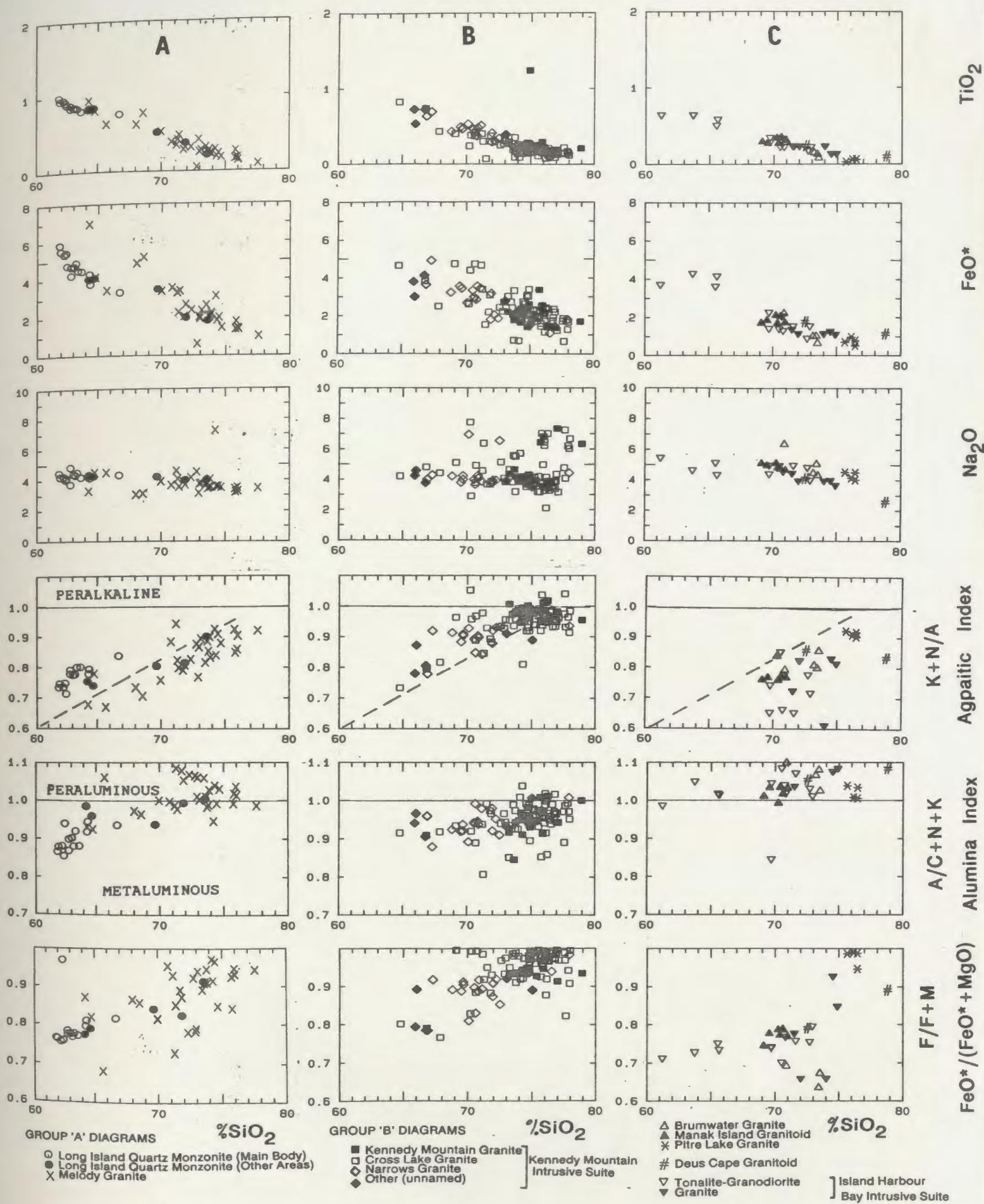


Figure 3.3 . Variation of selected major elements and derived ratios in syn-tectonic Makkovikian plutonic units. See text for discussion.

largely peraluminous ( $A/C+N+K > 1.0$ ), whereas the "upper trend" is metaluminous. These two contrasting groups are referred to below as the metaluminous-peralkaline and peraluminous associations respectively.  $F/F+M$  ratios (Figure 3.3) indicate that the former association shows Fe-enrichment relative to most members of the peraluminous association. Note also that the latter are not "S-type" granites in the sense of Chappell and White (1974), which are defined as having  $A/C+N+K \geq 1.1$ .

Ternary AFM [ $(Na_2O+K_2O) - FeO - MgO$ ] and CNK [ $Na_2O - K_2O - CaO$ ] projections (Figure 3.4) show a superficial "calc-alkaline" trend for all units. Linear regression of all data suggests that the alkali-lime index (i.e.  $SiO_2$  value at which  $Na_2O+K_2O = CaO$ ) is ca. 57%; in the original definition of such terms (Peacock, 1931) this association is alkali-calcic. The Q-B-F ternary projection of Debon and LeFort (Figure 3.4) suggests an affinity to subalkaline or alkaline-oversaturated (their terminology), rather than calc-alkaline suites.

The CNK projection (Figure 3.4) indicates alkali disturbance (mostly Na-enrichment) in granites of the Kennedy Mountain Intrusive Suite. Variation of  $N/N+K$  [ $Na_2O/(Na_2O+K_2O)$ ] ratios and total alkali content (Figure 3.5; c.f. Hughes, 1973) indicate that disturbed compositions lie outside the normal igneous spectrum, suggesting post-crystallization alteration (see later discussion). Total alkali content is unaffected by alkali disturbance (Figure 3.5).

### Normative Compositions

All units of the peraluminous association are corundum-normative (Table 3.2). Variations in the Q - Ab - An - Or quaternary system (Figure 3.6) indicate that the

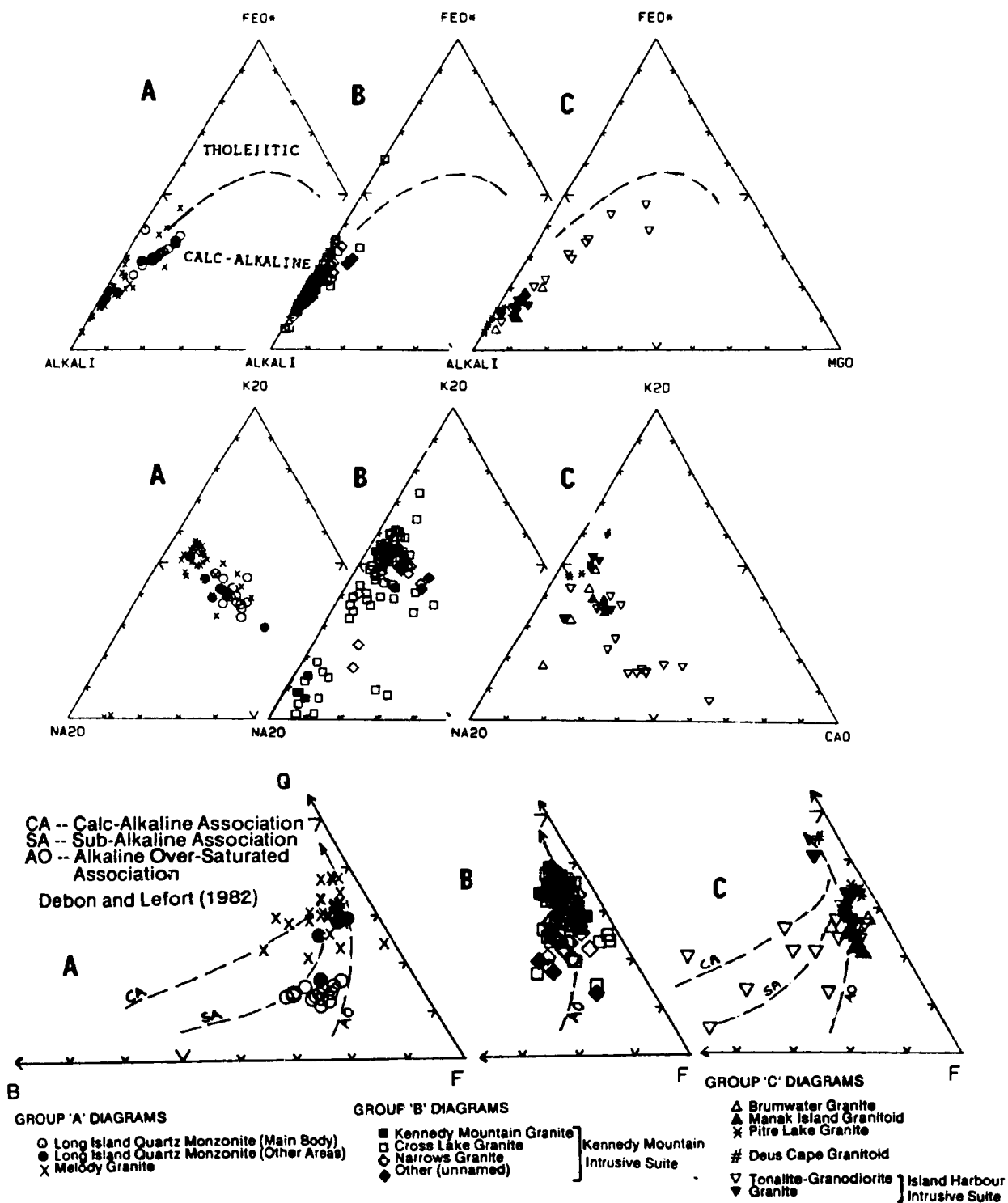


Figure 3.4 . AFM, CNK and QBF ternary projections for syn-tectonic Makkovikian plutonic units. See text for discussion.

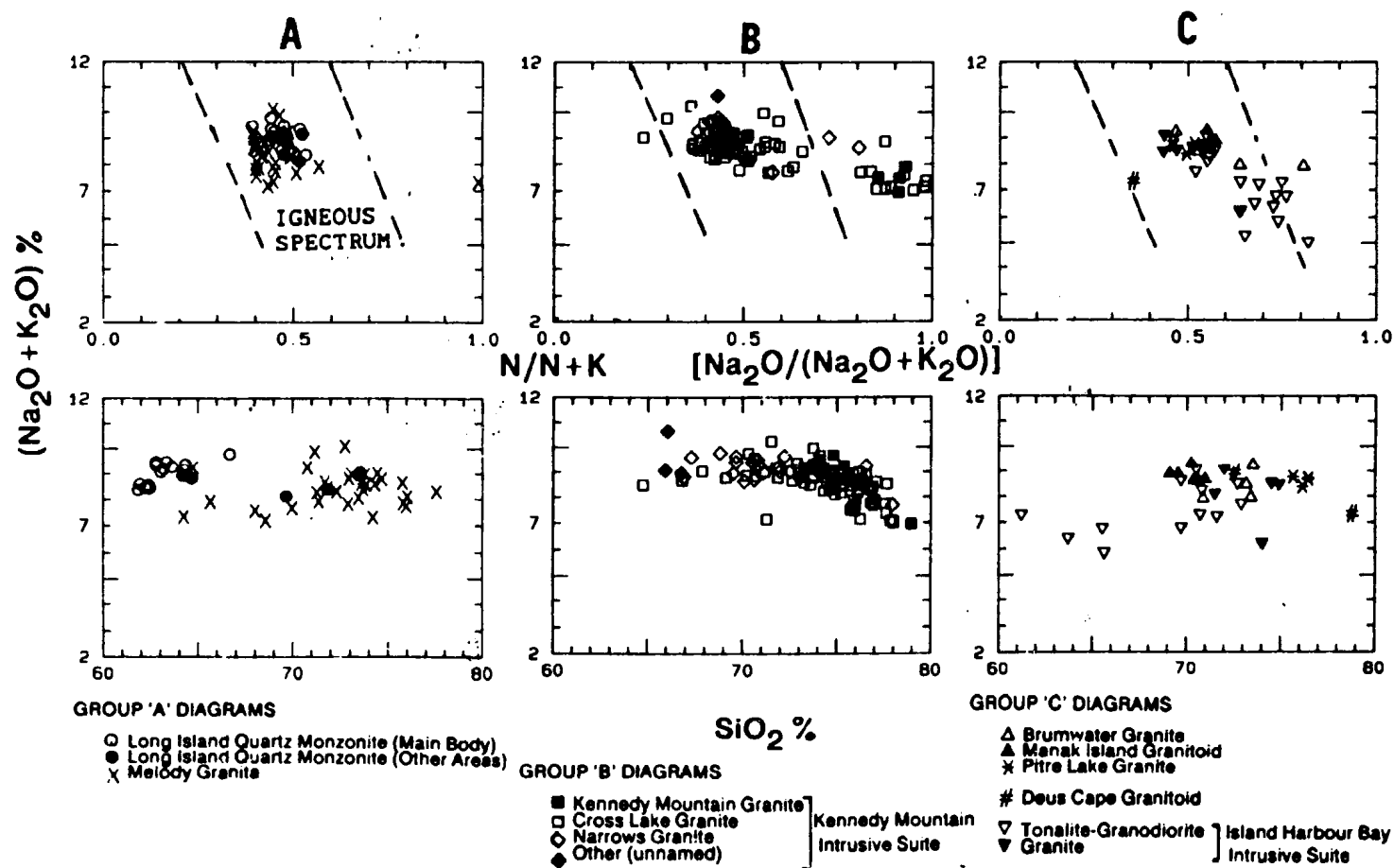


Figure 3.5. Distribution of alkali elements and N/N+K ratios in relation to the igneous spectrum (after Hughes, 1973). The SiO<sub>2</sub>-total alkali plot demonstrates the constancy of (Na<sub>2</sub>O+K<sub>2</sub>O) in altered and unaltered variants.

Kennedy Mountain Suite and Melody Granite contain less than 10% normative anorthite, and lie close to the ternary eutectic minima for bulk compositions with appropriate Ab/An ratios (James and Hamilton, 1969). Granite units of the peraluminous association are displaced from this location towards the Ab corner, but still lie in the general area of ternary minima for the granite system. The Long Island Quartz Monzonite lies close to the plagioclase - K-feldspar cotectic lines of James and Hamilton (1969) for An-poor compositions. Note the anomalously calcic composition of tonalites and granodiorites from the Island Harbour Bay Suite compared to all other units.

#### **Trace Element Patterns**

Trace element patterns are discussed in terms of element groupings defined in Chapter 1, adapted from Saunders et al. (1979).

##### ***Octahedrally Co-ordinated Cation (OCC) Elements :***

These "compatible" trace elements show strong inverse correlation with  $\text{SiO}_2$  (e.g. V, Figure 3.7). Only the Long Island Quartz Monzonite has significant enrichment, consistent with its lower  $\text{SiO}_2$  content compared to other units.

***Low Field Strength (LFS) Elements :*** Incompatible (e.g. Rb, Th, Cs) and compatible (e.g. Ba, Sr) LFS elements show antithetic behaviour (Figure 3.7). Ba and Sr are inversely correlated with  $\text{SiO}_2$ , particularly above 70%  $\text{SiO}_2$ . The Manak Island and Brumwater units, and parts of the Island Harbour Bay Suite, are characterized by high Ba and Sr for their  $\text{SiO}_2$  content. Extreme depletion in both elements is shown by high-silica rocks of the Kennedy Mountain Suite, and also by the Pitre Lake Granite.



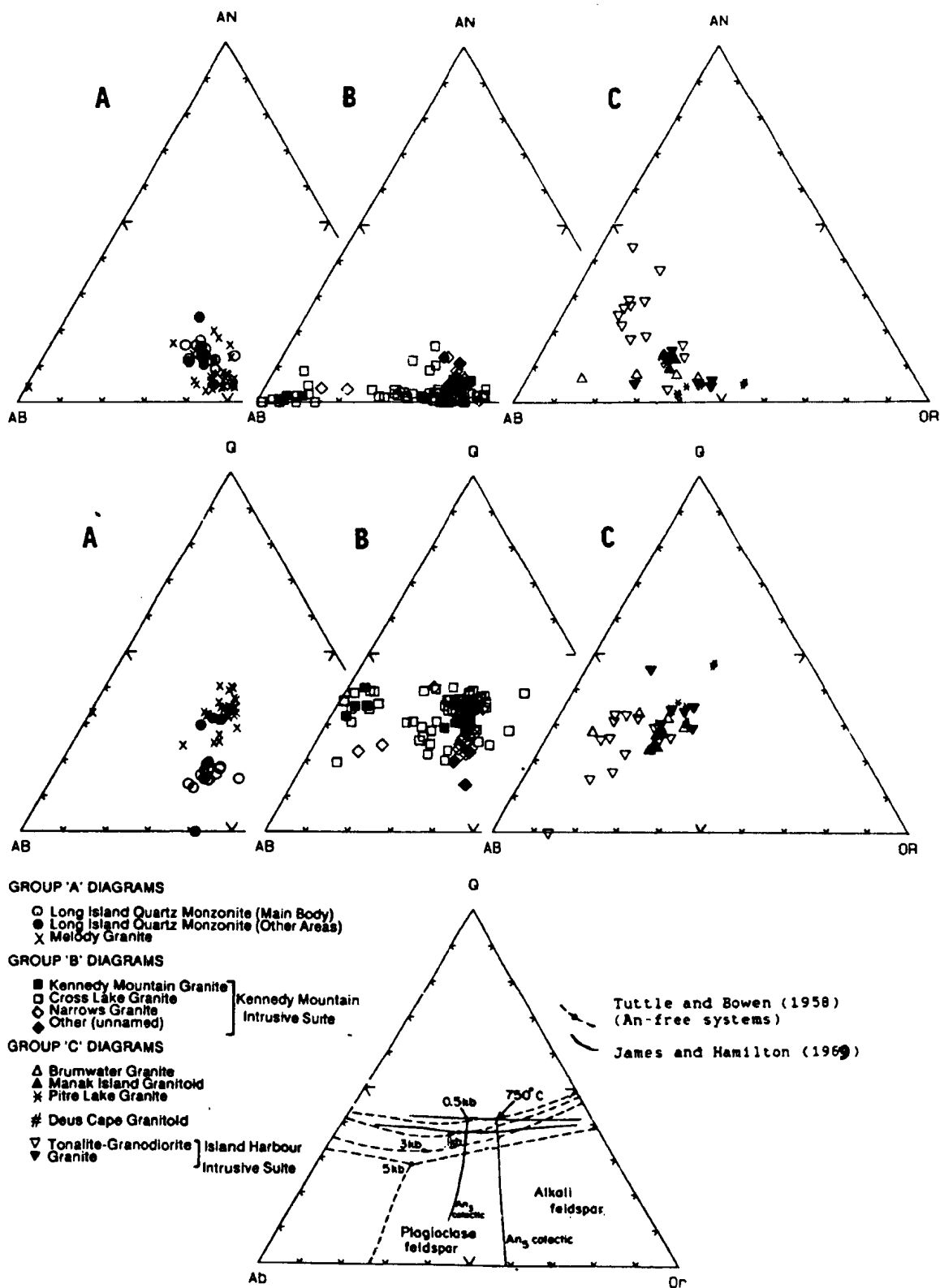


Figure 3.6. Variation of syn-tectonic Makkovikian plutonic units in the quartz - albite - anorthite - orthoclase quaternary system. All norms are CIPW. See text for discussion.

Rb and Th (Figure 3.7) lack good correlation with  $\text{SiO}_2$ . Weak positive trends exist below 70%  $\text{SiO}_2$ , but data are scattered in high-silica granites, particularly in the Kennedy Mountain Intrusive Suite. Partial data for Cs (Figure 3.7) suggest that the Melody Granite is enriched relative to all other units for which data are available. The Pitre Lake granite has very high Rb; 2 samples have over 400 ppm Rb and are excluded from the figure. Some of the granites from the Island Harbour Bay Suite have Rb and Th contents similar to the Pitre Lake granite.

**High Field Strength (HFS) Elements** : Zr (Figure 3.8) and also Nb and Hf (not figured) are enriched in the Kennedy Mountain Intrusive Suite relative to most other units, and are disorganized above 70%  $\text{SiO}_2$ . The Melody Granite is partly coincident with the Kennedy Mountain Suite for these elements, but shows generally lower Zr. Most other members of the peraluminous association are depleted in Zr. The Pitre Lake shows an unusual combination of Nb enrichment and Zr depletion, which is also shown by some granites of the Island Harbour Bay Suite.

**Rare Earth Elements (REE)** : Variation patterns for Ce and Y (Figure 3.8) resemble those for Zr and Nb respectively. The Island Harbour Bay Suite, Manak Island, and Brumwater units are characterized by low REE abundances relative to the Kennedy Mountain Suite. The Pitre Lake Granite shows Y enrichment and Ce depletion. Partial data for Sm and La resemble Ce; partial data for Yb resemble Y.

**Indeterminate Trace Elements** : Li is strongly enriched in the muscovite-bearing Pitre Lake Granite (two samples contain over 150 ppm Li), but is low in most other

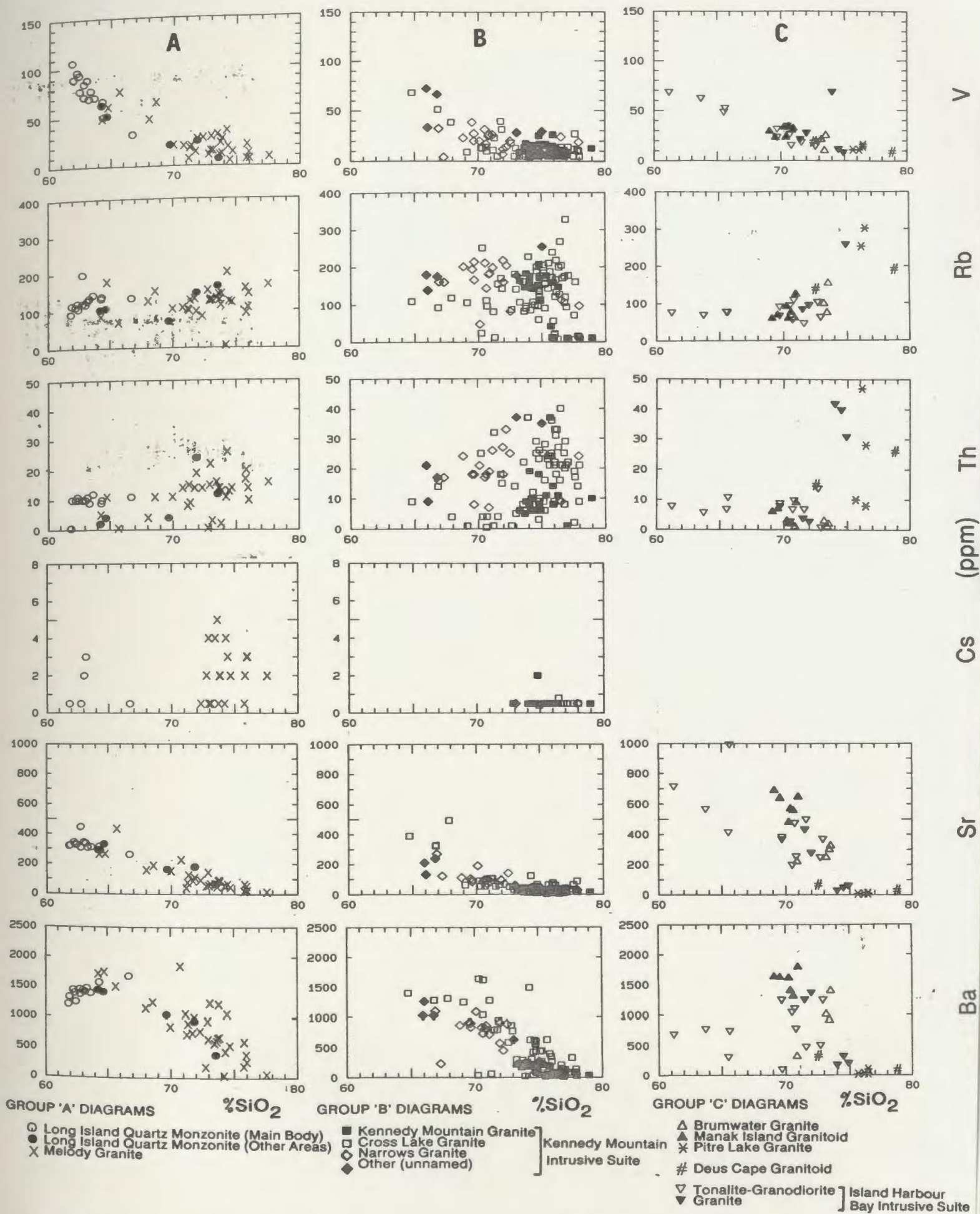


Figure 3.7. V, Rb, Th, Cs, Sr and Ba versus  $\text{SiO}_2$  in syn-tectonic Makkovikian plutonic units. See text for discussion.

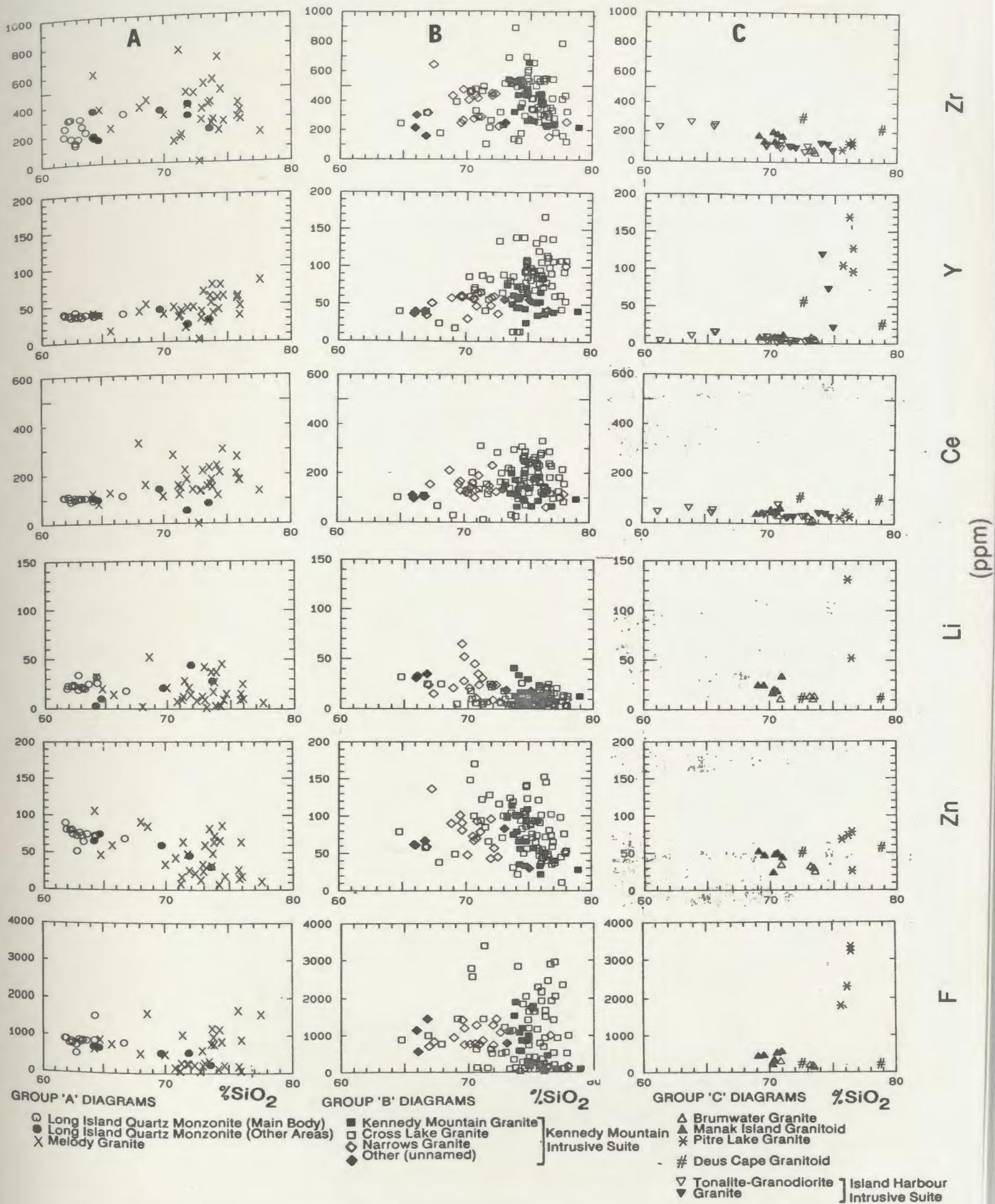


Figure 3.8 . Zr, Y, Ce, Li, Zn and F versus  $\text{SiO}_2$  in syn-tectonic Makkovikian plutonic units. See text for discussion.

units. The Kennedy Mountain Intrusive Suite shows variable Zn and F enrichment at high  $\text{SiO}_2$  contents, and is locally strongly F-enriched (up to 4000 ppm). Granitoids of the peraluminous association are low in F, except for the Pitre Lake Granite.

#### Trace Element Variation and Alkali Disturbance

Correlation between trace element behaviour and alkali disturbance in the Kennedy Mountain Suite was assessed by using  $\text{N}/(\text{N}+\text{K})$  as the X-axis variable (Figure 3.9). For LFS trace elements (e.g. Rb, U, Ba and Sr, possibly also Li), disturbed Na-rich compositions show depletion, but there is little systematic variation of HFS elements, REE, Zn and F. This indicates that any metasomatic processes affected feldspars and micas, and had minimal effect on accessory or mafic phases. In conjunction with constant total alkali contents, it suggests cation-exchange as a possible mechanism (c.f. White and Martin, 1980). It also indicates that the enhanced levels of fluorine, HFS elements and REE that characterize the Kennedy Mountain Suite are primary features of the parent magmas, not a consequence of hydrothermal activity (see later discussion).

#### Trace Element Ratios

Trace element ratios provide a method of assessing fractionation history, as evolution paths resulting from fractional crystallization should define lines or smooth curves in log-log plots (e.g. McCarthy and Hasty, 1976). Reference paths for common silicates, using crystal-liquid partition coefficients from Arth (1976) and Hanson (1978) are illustrated in the key to figure 3.10.



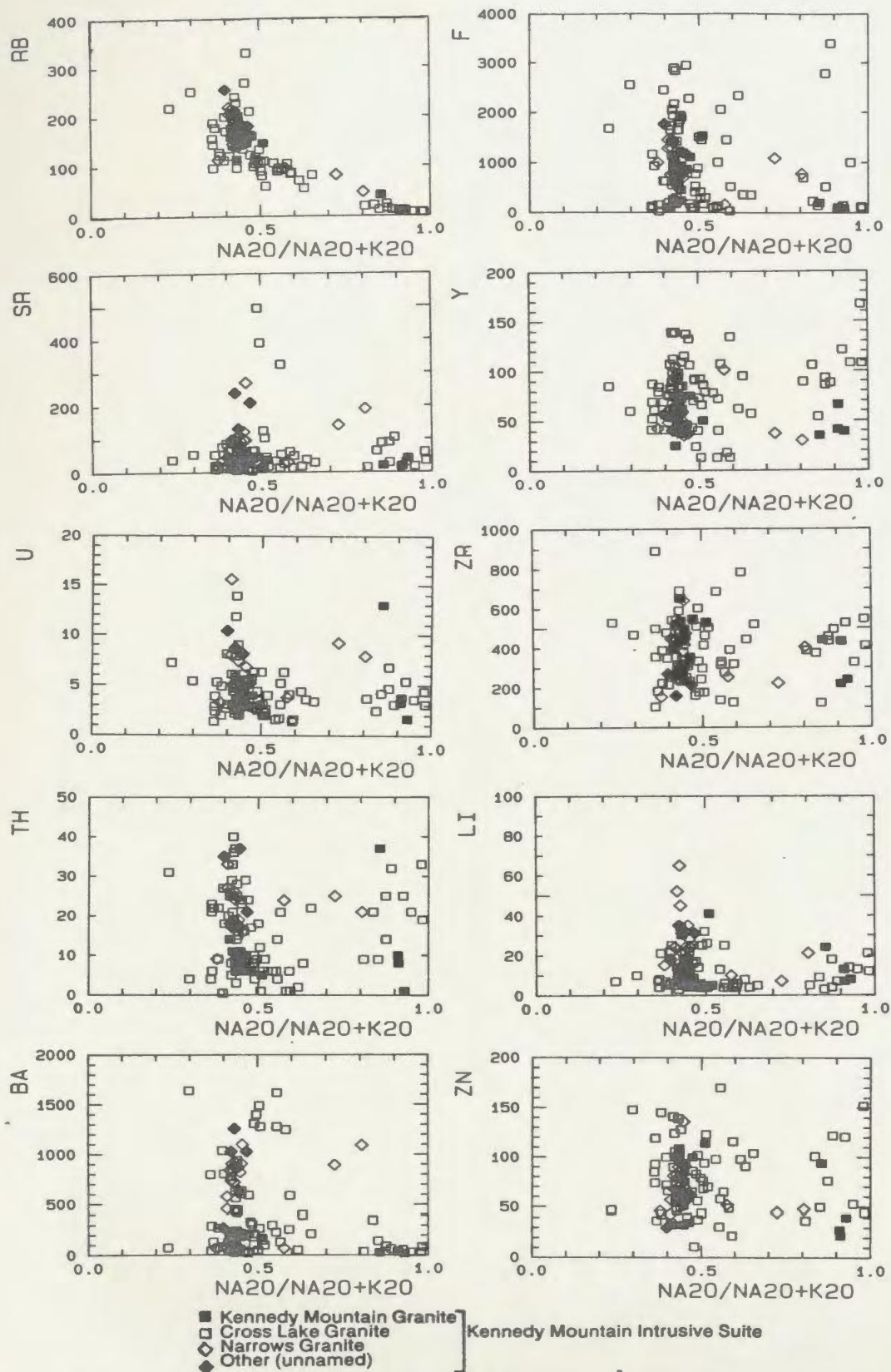


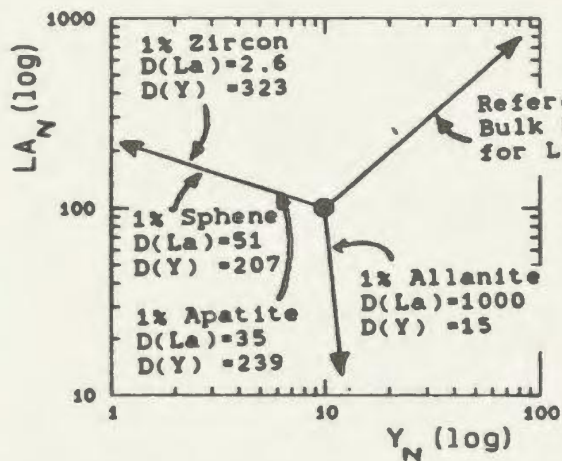
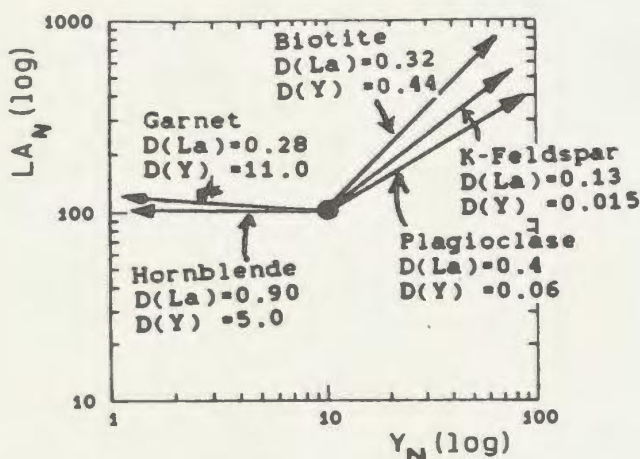
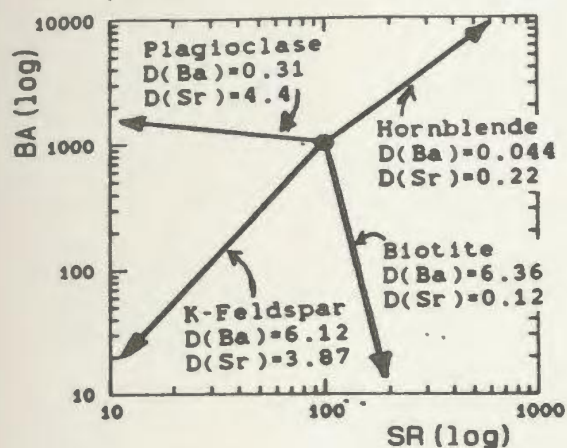
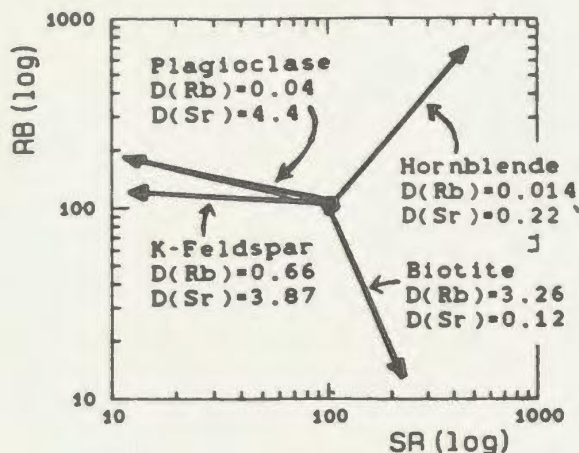
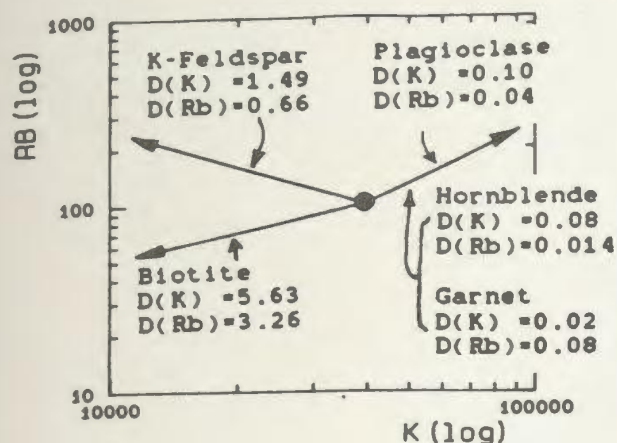
Figure 3.9 . Variation of selected trace elements against  $\text{N}/\text{N}+\text{K}$  [ $\text{Na}_2\text{O} / (\text{Na}_2\text{O}+\text{K}_2\text{O})$ ] in the Kennedy Mountain Intrusive Suite.

K/Rb ratios show minimal variation (Figure 3.10) from 500 to 200; only the Pitre Lake Granite, parts of the Island Harbour Bay Suite and a few granites from the Kennedy Mountain Suite show ratios below 200. The general trend is towards lower K/Rb with increasing  $\text{SiO}_2$ . The Kennedy Mountain Suite includes a disturbed population depleted in both K and Rb (note the different X-axis scale for the group B diagram).

Rb/Sr ratios vary widely (Figure 3.10). The Long Island unit, Kennedy Mountain Suite (note disturbed population) and Melody Granite have flat-lying trends suggesting moderate Rb enrichment, consistent with feldspar fractionation.

Ba/Sr ratios are broadly similar (1 - 30) for all units (Figure 3.10). The metaluminous-peralkaline association and Melody Granite have curvilinear trends indicating progressive Ba and Sr depletion, and increasing depletion of Ba relative to Sr. The remaining members of the peraluminous association show higher Ba and Sr, and define a shallower depletion trend. The steep, curved trends are consistent with significant effects from K-feldspar or biotite fractionation.

Variation in  $\text{La}_N/\text{Y}_N$  ratios (subscript indicates normalization to chondrite) indicates REE fractionation, as Y mimics the heavy rare-earth element (HREE) Yb. It also provides a fingerprint for effects caused by accessory phases (see key to Figure 3.10 for details). The metaluminous-peralkaline association is tightly clustered and positively correlated, with a range in  $\text{La}_N/\text{Y}_N$  from 20 to 80. A similar distribution is shown by the Melody Granite. La and Y are correlated weakly with  $\text{SiO}_2$  (Figure 3.8; La is similar to Ce), but strong enrichment expected



Idealized fractionation trends for Rayleigh fractionation (i.e. perfect separation of crystals and liquid). The  $LA_N/Y_N$  trends for accessory phases show the effects of only 1% of each phase upon a reference trend where bulk partition coefficients for the remaining 99% of the fractionate are 0.1 for both La and Y. The latter approximates a "normal" path for fractionation of common silicates. Partition coefficient data from compilations by Arth (1976) and Hanson (1978) for most minerals, and from Gromet and Silver (1983) for allanite and sphene.



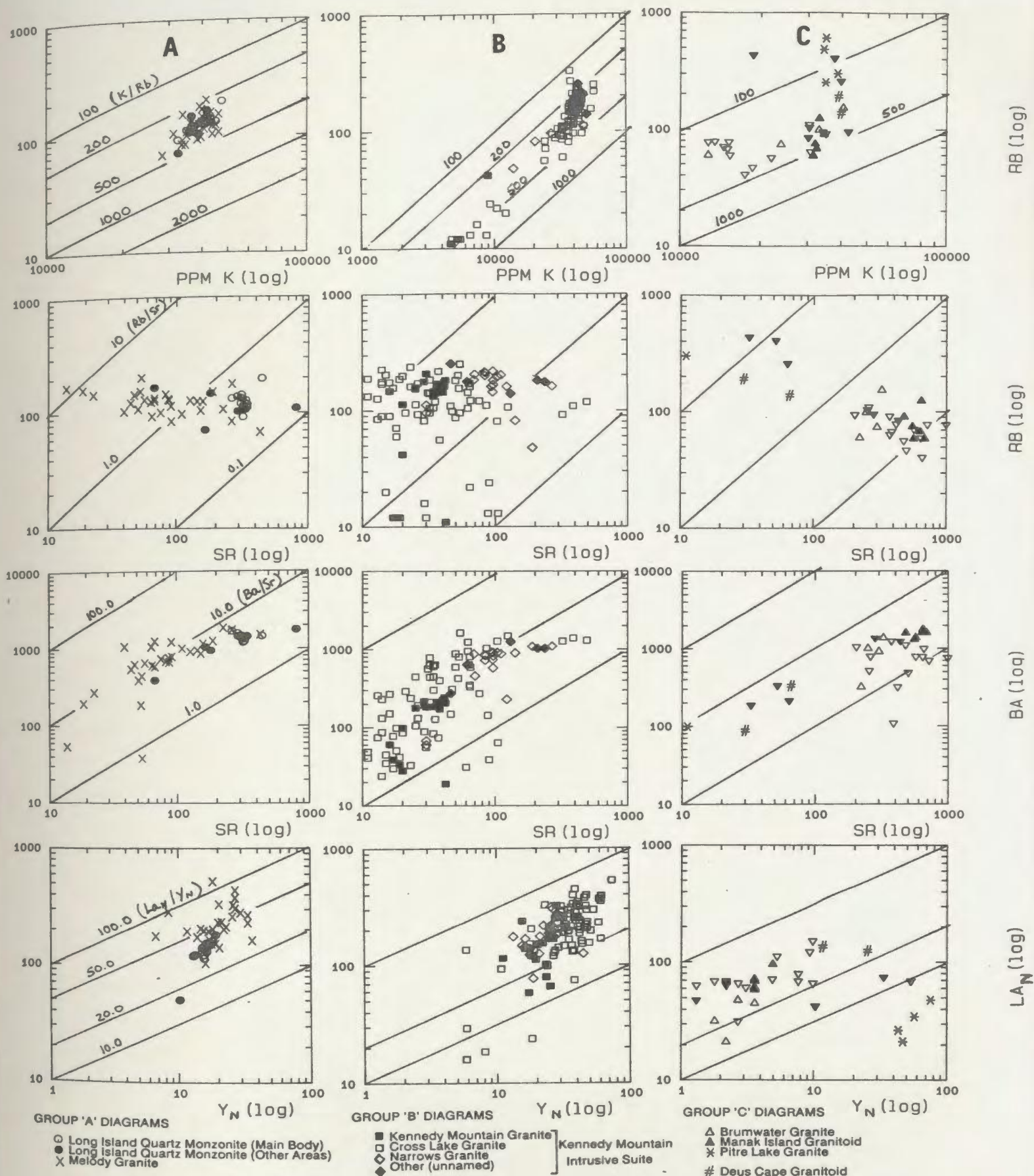


Figure 3.10 . Variation in the trace element ratios K/Rb, Rb/Sr, Ba/Sr and  $La_N/Y_N$  in syn-tectonic Makkovikian plutonic units. See opposite for reference fractional crystallization trends.

from feldspar fractionation is not obvious. There is, however, no evidence for the Y depletion that should accompany significant fractionation of sphene, zircon or apatite, or La depletion caused by allanite or monazite.

Remaining granitoids of the peraluminous association show low La and Y, but greater variation of  $La_N/Y_N$ . Their trends are consistent with effects from "removal" of accessory phases; in the case of the Pitre Lake Granite, this must have been a LREE-rich phase such as allanite or monazite. As discussed subsequently (3.3), this may be a function of residual material, rather than fractional crystallization.

#### Rare-Earth Element (REE) Patterns

Representative samples have been analyzed for the full REE spectrum (Figure 3.11; data listed in Appendix B). The Kennedy Mountain Suite granites have fractionated LREE patterns (200-300 x chondrite), strong negative Eu anomalies, and HREE patterns that vary from flat to steep. Deepening of the Eu anomaly is associated with increasing HREE fractionation. The least fractionated patterns resemble the Long Island REE pattern. The Eu anomaly indicates plagioclase and/or K-feldspar fractionation (see also Figure 3.10); HREE fractionation is probably a function of sphene and zircon extraction in the most fractionated rocks. The Melody Granite REE pattern resembles typical Kennedy Mountain Suite examples.

REE patterns for the Manak Island and Brumwater Granitoids are remarkably similar; they are steep, and lack negative Eu anomalies. A similar profile is shown by the tonalite-granodiorite unit of the Island Harbour Bay Suite. The Pitre Lake Granite has an unusual flat REE pattern with a strong negative Eu anomaly.

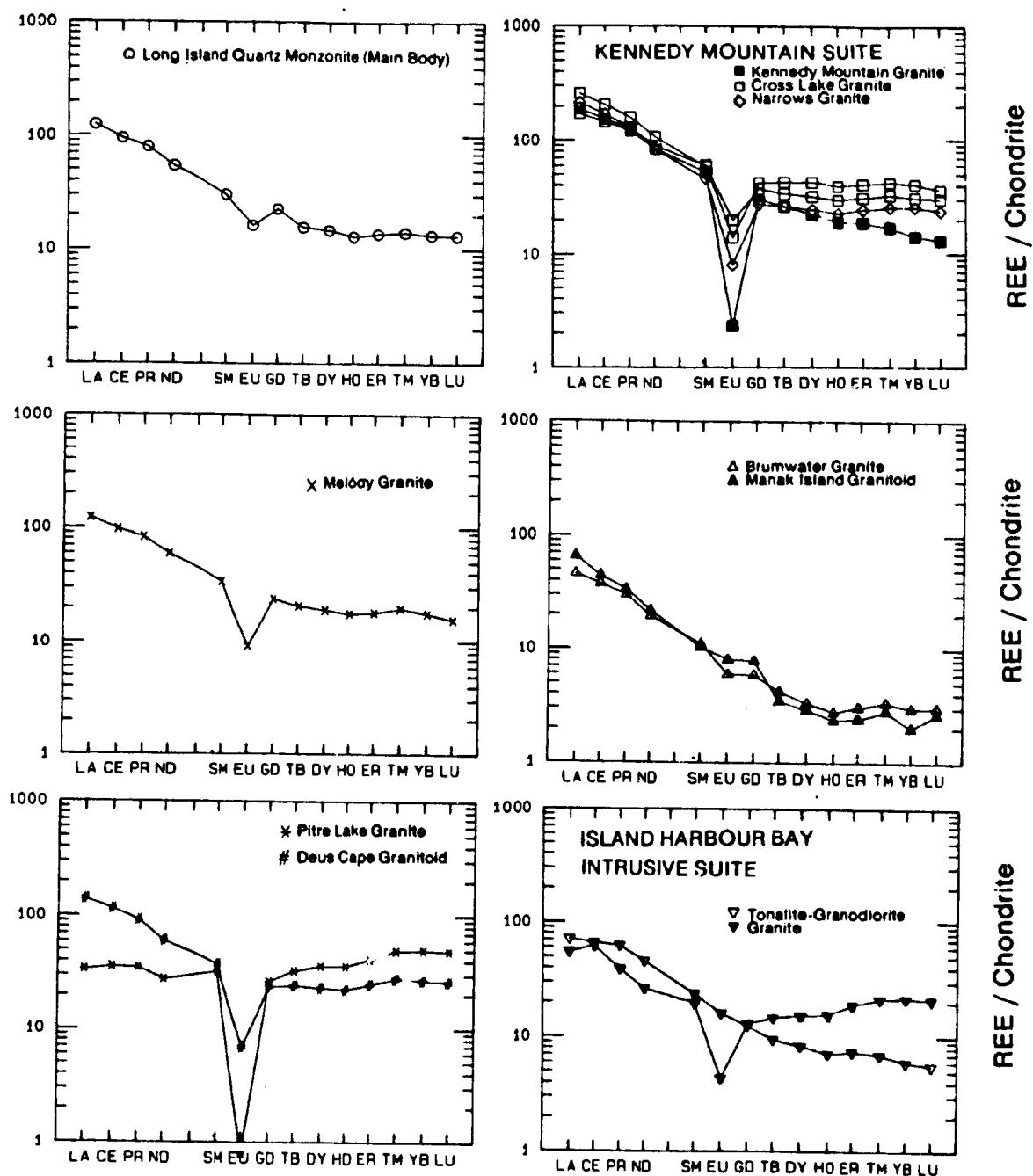


Figure 3.11 . Rare Earth element (REE) patterns for representative syn-Makkovikian plutonic rocks. Values are normalized to chondritic values (listed in Appendix C).

### 3.3 SUMMARY AND DISCUSSION

#### Geological and Petrographic Associations

Syn-tectonic Makkovikian plutonic rocks can be divided into two groups based on their field and petrographic characteristics.

The Long Island Quartz Monzonite, Kennedy Mountain Intrusive Suite and Melody Granite are regionally extensive, homogeneous units. They are xenolith-poor; inclusions, where present, commonly appear to be cognate, darker-coloured phases. There is no evidence of anatectic melting in their country rocks, suggesting that they were derived from well below the current level of exposure. The Long Island and Kennedy Mountain Suite units are both dominated by hornblende - biotite granitoids, with hornblende-poor leucocratic variants. Whatever the ultimate sources of these intrusions, they were not derived from their country rocks at the present level of exposure.

A totally different environment is represented by small foliated granitoid units of the Kaipokok Bay area (Brumwater and Pitre Lake Granites). These units are confined to specific units in the basement complex or Lower Aillik Group, and, although intrusive, have contacts that are regionally concordant to layering and/or stratigraphy. Both the Pitre Lake and Brumwater Granite locally appear gradational with surrounding rocks (Marten, 1977), and contain abundant metasedimentary and gneissic xenoliths respectively. There is evidence of migmatization in the country rocks, and Marten (1977) suggested that the Brumwater Granite was gradational with migmatitic Archean gneiss. The composition and setting of the Pitre Lake unit

suggests derivation by anatexis of local metasedimentary rocks. Both units were apparently derived by melting of their country rocks at (or slightly below) the present level of exposure. They are the only rocks in the study area for which such a relationship can be demonstrated. It is interesting to speculate also that the Manak Island Granitoid, which is compositionally similar to the Brumwater Granite (note, for example, their coincident REE patterns) is a product of the same process in the east of the area. This unit, however, is not obviously xenolith-rich.

The Island Harbour Bay Intrusive Suite was not examined directly in this study, but apparently has elements of both settings (Ryan et al., 1983; I. Ermanovics, pers. comm., 1988). The outer portion is rich in gneissic xenoliths, and has a migmatitic contact with surrounding gneisses. In contrast, the inner portions of the body are massive and relatively xenolith-free. The presence of dioritic and tonalitic rocks, however, indicates that the suite cannot be entirely of anatectic origin, as such rocks are impossible to derive by partial melting of the Archean gneisses, which have a bulk composition approximating tonalite or granodiorite (Korstgård and Ermanovics, 1985).

#### Geochemical Associations

Syn-tectonic Makkovikian plutonic rocks are also divisible into two associations on geochemical grounds. These partially correspond to those outlined above.

The Long Island Quartz Monzonite and Kennedy Mountain Intrusive Suite define a metaluminous-peralkaline association that shows Fe-enrichment and sporadic peralkaline compositions in the latter. They define smooth,

continuous, major and trace element trends, that terminate with evolved high-silica granites of the Kennedy Mountain Suite. They are regarded here as genetically related, possibly as a magma sequence derived by fractionation of a single parent. This association is characterized by distinct enrichment in fluorine, Zn, HFS elements and REE.

In contrast, remaining syn-tectonic granitoid units define a mostly peraluminous association. Peralkaline rocks are absent, and F/F+M ratios are lower at a given  $\text{SiO}_2$  content, except for the Melody Granite (see below). These show (as a group) significantly lower F, Zn, HFS element and REE abundances, indicating a quite different origin (or source material). The Pitre Lake Granite has a distinct mineralogy and geochemistry (high Li, Rb, Th, low LREE) consistent with field evidence for a metasedimentary source. The Melody Granite is enigmatic; it is variably peraluminous, but in most other respects (including trace element geochemistry), it is akin to metaluminous - peralkaline granites of the Kennedy Mountain Suite, and probably has a similar origin.

#### Origin of Compositional Variations

***Metaluminous - Peralkaline Association*** : This association is characterized by geochemical trends that are explicable either by fractional crystallization or unmixing of anatectic residue (e.g. White and Chappell, 1977; Wall et al., 1987). In the case of the Kennedy Mountain Suite, alkali metasomatism has superimposed scatter on LFS element trends (see below). In the granite quaternary system, this association evolves from the plagioclase volume to the plagioclase - K-feldspar cotectic, and then terminates close to the eutectic minimum (Figure 3.6). Such characteristics favour control by crystal fractionation, also indicated by the porphyritic nature of many rocks.

Trends for Ba, Sr, K and Rb (Figure 3.10) are close to those predicted by idealized fractionation of plagioclase ( $\pm$  mafics) in the Long Island unit, and plagioclase  $\pm$  K-feldspar in the Kennedy Mountain Suite (also the Melody Granite). Curvature of the Ba-Sr trend probably reflects a greater proportion of K-feldspar fractionation at high  $\text{SiO}_2$  contents. This interpretation is consistent with observed phenocryst assemblages in these rocks. It is also consistent with the prominent negative Eu anomalies in REE patterns. There is some evidence of accessory mineral fractionation in the most evolved rocks. Late crystallization of accessories, and resultant HFS and REE enrichment, is a common feature of F-enriched granitoids with high K+N/A ratios, and probably reflects retention of these elements in the melt as alkali-fluoride or alkali-zirconosilicate complexes (Collins et al., 1982; Linthout, 1984; Whalen et al., 1987).

**Peraluminous Association** : Field evidence for local anatectic derivation of the Brumwater and Pitre Lake Granites implies that partial melting had greater influence on geochemistry than any subsequent fractional crystallization (c.f. White and Chappell, 1977). The Brumwater Granite has unusually high Sr and low Rb for an anatectic melt; this probably reflects incorporation of plagioclase-bearing restite. Such material is also required to explain the absence of a negative Eu anomaly (Figure 3.11). The low HFS element and REE abundances in all peraluminous units (except Melody Granite) indicate that sphene and zircon were "removed" early in crystallization; it is likely that this reflects their stability in anatectic residuum. Low Y in most of these units may indicate similar residual hornblende. Large, euhedral

sphene crystals in some Island Harbour Suite granitoids (B.Ryan, pers. comm., 1988) suggests fractional crystallization in this particular case. Strong La depletion and Y enrichment in the Pitre Lake Granite probably indicates an allanite or monazite-bearing residuum. (c.f. Mittlefeldt and Miller, 1983).

### **Metasomatism in The Kennedy Mountain Intrusive Suite**

High-silica granitoids of the Kennedy Mountain Intrusive Suite include a population that has N/N+K ratios beyond the normal range of magmatic rocks. There is no systematic geographic variation in N/N+K; these ultrasodic samples appear to be dispersed randomly through areas of "normal" composition.

It is suggested that this reflects deuteric or hydrothermal albitization related to late-magmatic or post-crystallization processes. Similar alkali metasomatism has been documented in felsic volcanic rocks of the Upper Aillik Group by White and Martin (1980) and Evans (1980), and in this study (see Chapter 7). White and Martin (1980) suggested that the Upper Aillik Group alteration is analogous to fenitization, a process commonly associated with alkaline magmas. They also recognized K-metasomatism, which they interpreted to occur at a lower temperature than the predominant albitization. The alteration in the Kennedy Mountain Suite is interpreted here to record the same event that affected the Upper Aillik Group; this is consistent with the inferred age of the former (> 1800 Ma) and measured ages for the latter (1860 - 1810 Ma). The predominance of Na-metasomatism is consistent with a deeper level, plutonic environment (c.f. White and Martin, 1980).



Since the Kennedy Mountain Suite granites cut the Upper Aillik Group, this metasomatism and alteration must have been post-volcanic in timing. There are, however, no firm constraints on the time interval between volcanism, granitoid intrusion and alteration, and they may have followed each other rapidly. As will be shown later (Chapter 7), there are strong geochemical similarities between the Kennedy Mountain Suite and Upper Aillik Group felsic volcanic rocks, that suggest partial equivalence.

White and Martin (1980) suggested that trace element variations, particularly U, Th, Pb, Zr and F, could be linked to the degree and type of alteration in the Upper Aillik Group. In contrast, this study suggests little coherent variation, except for some LFS trace elements and Li, which are variably depleted in metasomatized granites. The data of White and Martin (1980), however, included mineralized samples which had suffered silica loss in association with albitization and K-metasomatism. None of the granite samples in this study display such extreme alteration, and silica levels remain relatively constant with alteration (e.g. Figures 3.5; 3.6).

## CHAPTER FOUR

# POST-TECTONIC MAKKOVIKIAN PLUTONIC ROCKS

---

---

### Chapter Abstract

Post-tectonic Makkovikian plutonic rocks are generally undeformed, except in the south of the area, where they have generally east-trending (Grenvillian) foliations. U-Pb zircon and Rb-Sr ages indicate that most were emplaced ca. 1800 Ma ago, although some may be 1760 Ma old or younger. They are divisible into a monzonite to quartz syenite association, and three suites of siliceous rocks dominated by granite and alkali-feldspar granite.

The Numok Intrusive Suite ranges from plagioclase-porphyritic monzonite to hypersolvus, alkali-feldspar quartz syenite. These rocks are biotite and hornblende-bearing, with variable amounts of clinopyroxene. The syenitic rocks locally contain fayalite.  $\text{SiO}_2$  contents are moderate (58-66%), but all members of the suite are alkali-rich and potassic. Trace element patterns are characterized by HFS element and REE enrichment. LFS elements (e.g. Rb) approach abundance levels typical of high- $\text{SiO}_2$  units. Geochemical trends suggest that the Numok Suite evolved by fractional crystallization of plagioclase and K-feldspar ( $\pm$  mafic minerals). The parent magmas must have been at least as mafic as monzonite to generate the observed compositional range.

The Strawberry Intrusive Suite comprises several discrete plutons consisting of closely similar fluorite-bearing, K-feldspar porphyritic, subsolvus, biotite granite and alkali-feldspar granite. Sodic amphibole (reibeckite or arfvedsonite) occurs locally in some of these. The plutons were emplaced at shallow depths, and probably had low viscosities and solidus temperatures as a consequence of their fluorine enrichment. They show direct evidence of biotite ( $\pm$  hornblende) and accessory mineral (zircon, allanite) fractionation in the form of cumulate mafic mineral layers. The close similarity of five plutons over a lateral distance of 125 km indicates identical sources and/or processes. The Lanceground Intrusive Suite comprises three plutons of K-feldspar porphyritic, variably hypersolvus, biotite-hornblende quartz syenite and alkali-feldspar granite. These locally contain fayalite, reibeckite and aegirine-augite, and locally resemble syenites of

the Numok Intrusive Suite. The Big River Granite is a regional unit of K-feldspar porphyritic, subsolvus, biotite-hornblende granite and alkali-feldspar granite that has mantled-feldspar phenocrysts with plagioclase interiors (pseudorapakivi texture).

In geochemical terms, all siliceous granitoid suites are closely similar, and resemble the Numok Suite. They are metaluminous to weakly peralkaline, potassic and Fe-enriched ( $F/F+M > 0.85$ ). The more evolved members lie close to the ternary minimum in the Q - Ab - Or - An system. All are characterized by enrichment in fluorine, HFS elements (e.g. Zr, Nb and Hf), REE (Y, La, Ce, Sm), depletion in Ba and Sr, and moderate enrichment in incompatible LFS elements (Rb, U and Th). Trace element patterns vary in detail; for example, the Lanceground Suite has the greatest HFS and REE enrichment, whereas the Strawberry suite is richest in fluorine. The Big River Granite is generally less evolved and more variable in composition than the smaller plutons that constitute the Strawberry and Lanceground Suites.

Geochemical trends indicate that all evolved primarily by fractionation of plagioclase and K-feldspar ( $\pm$  mafic minerals). Hypersolvus suites show little or no evidence of plagioclase extraction, and K-feldspar fractionation dominated the later stages in the subsolvus suites. In the Strawberry Intrusive Suite, geochemical variation caused by liquid-state processes (e.g. thermogravitational diffusion, convective fractionation) has been superimposed on trends generated by crystal-liquid processes. Some fractionation of accessory phases and biotite also occurred in this suite.

These suites collectively have a strong affinity to the syn-tectonic metaluminous-peralkaline association described in Chapter 3. This is most evident for the F-enriched granites, which resemble the syn-tectonic Kennedy Mountain Intrusive Suite in both geochemical and petrological terms, if the effects of deformation in the latter are disregarded. A close temporal relationship between syn- and post-tectonic Makkovikian plutonic associations is indicated by geochronological data, which cluster around 1800 Ma in both. The consanguineous and partly contemporaneous nature of these associations suggests that they represent a single episode of magmatism that transcended Makkovikian deformation, which may also have been inhomogeneous in its effects. There are, however, no obvious post-tectonic equivalents of the syn-tectonic Makkovikian peraluminous association described in Chapter 3.

## Introduction

This association comprises largely undeformed plutonic rocks. There are few field criteria to separate these from similarly undeformed Labradorian plutonic rocks (Chapter 5) and this association is presently defined mostly by geochronological data. As discussed previously (Chapter 2, Chapter 3), "post-tectonic" is a label of convenience; it does not necessarily mean that they are significantly younger than the "syn-tectonic" Makkovikian association; in fact, U-Pb geochronological data (Krogh et al., in prep., see below) suggest a close similarity in age. The term also does not imply a universal absence of foliations; in the south of the area, these rocks locally display evidence of deformation. However, the predominance of east-trending fabrics (parallel to the Grenville Front Zone) in such areas suggests that these represent Grenvillian, rather than Makkovikian, deformation. Post-tectonic Makkovikian plutonic rocks are divided into four main associations (Figure 4.1; Table 4.1).

The Numok Intrusive Suite ranges in composition from monzodiorite to quartz syenite, but is dominated by quartz monzonite. The Strawberry Intrusive Suite includes several plutons of distinctive fluorite-bearing granite. The Lanceground Intrusive Suite consists of three quartz syenite to granite plutons that locally show hypersolvus characteristics. The Big River Granite is an extensive body of porphyritic granite that shows distinctive mantled feldspar ("pseudorapakivi") textures.

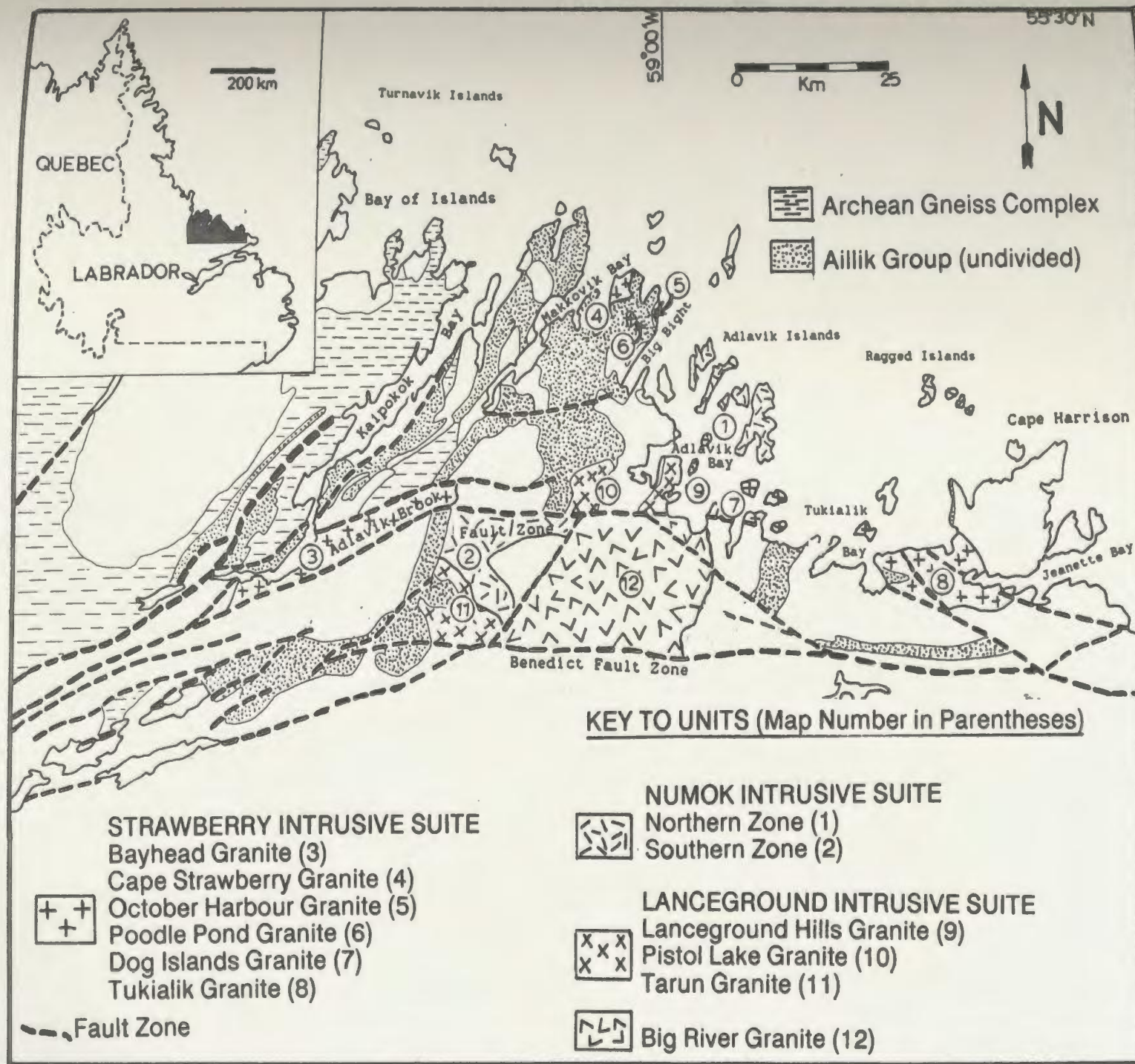


Figure 4.1. Summary map illustrating the distribution and extent of post-tectonic Makkovikian plutonic units.

Table 4.1. Key features of post-tectonic Makkovikian plutonic units.

Map Unit	Suite/Unit/Age	General Characteristics	Textural Characteristics
<b>NUMOK INTRUSIVE SUITE</b>			
20.1 20.2	Monzonite - Quartz Monzonite 1801 +/- 2 Ma [ U-Pb Zircon ] (Krogh et al., in prep.)	Homogeneous, white, grey or pink, variably porphyritic, massive Hb-Bi (+/- Px) monzonite, quartz monzonite and lesser syenite. Undeformed and massive in all areas except at the western margin of the northern zone near Adlaviik Bay. K-feldspar +/- plagioclase phenocrysts, K-fsp more abundant.	Coarse grained, commonly porphyritic, with phenocrysts of K-fsp and Plag, up to 2 cm in diameter. Hb and Bi form euhedral crystals, up to 5-10 mm in length. Interstitial material is mostly Qtz and K-fsp. Inclusions of gabbro and diorite occur locally, particularly near Adlaviik Bay, but the unit is mostly inclusion-poor.
21.1 21.2	Syenite and Quartz Syenite 1801 +/- 2 Ma [ U-Pb Zircon ]	Homogeneous, grey-green to brown, K-fsp porphyritic, Cpx-Hb-Bi (+/- Fa) syenite, alkali-fsp syenite, Qtz-syenite and granite. Locally hypersolvus. Massive in north; locally deformed in south. Displays intense surface weathering to yellow-brown gravel. Blue quartz occurs in silicic rocks.	Commonly coarse to very coarse grained, with euhedral to ovoidal phenocrysts of coarse perthitic K-fsp. Locally fine-grained syenite. Mafic minerals and quartz are interstitial. Generally inclusion-poor. East-trending fabrics common in southern zone (Grenvillian?).
22.2	Plagiophytic Monzonite	Grey to brown, plag-porphyritic Px-Hb monodiorite and monzonite. Forms a mappable unit only in southern zone, but similar rocks occur locally in the northern zone.	Coarse to very coarse grained, with large, rounded to subhedral plag phenocrysts. Mafic minerals, Qtz and K-fsp are interstitial to locally oikocrystic. Unit locally has a cumulate texture, but is not layered.
<b>STRAWBERRY INTRUSIVE SUITE</b>			
23.0 24.1	Bayhead Granite 1570 +/- 50 Ma [ K-Ar Bi ] (Wanless et al., 1970) Cape Strawberry Granite ca. 1760 Ma [ U-Pb Zircon ] (Krogh et al., in prep.) 1565 +/- 50 Ma [ K-Ar Bi ] 1600 +/- 34 Ma [ K-Ar Bi ] (Wanless et al., 1970) 1694 +/- 56 Ma [ Rb-Sr WR, composite ] (this study)	All units (except Poodie Pond) consist dominantly of massive, homogeneous, white, pink, orange or brick-red, K-feldspar-porphyritic biotite granite, quartz syenite and alkali-fsp granite, commonly with conspicuous purple fluorite. Fine-grained phases (including Qtz-Fsp porphyry) are present locally in most units, and dominate the Poodie Pond Granite. The Bayhead granite is the most melanocratic, and the Tukialik granite is the most potassic. Cape Strawberry Granite is the most variable texturally.	Commonly coarse to very coarse grained or pegmatitic in texture. Fine-grained microlitic rocks occur as marginal phases and minor bodies. Related Qtz-Fsp porphyry and pegmatite dykes and veins cut adjacent units. Commonly porphyritic or megacrystic. K-feldspar phenocrysts up to 3 cm in diameter. Dog Islands Granite is locally Qtz-porphyritic. Xenolith-rich only in contact zones. Tuffisite veinlets and breccia zones, with Pl-Bi rich matrix, cut xenoliths and coarse-grained granite. Distinctive mafic mineral layering, with trough-bedded "cumulate" geometry.
24.3 24.2 25.0 26.0	Poodie Pond Granite October Harbour Granite Dog Islands Granite Tukialik Granite		
<b>LANCEGROUND INTRUSIVE SUITE</b>			
27.0 28.0 29.0	Lanceground Hills Granite 1692 +/- 32 Ma [ Rb-Sr WR ] (this study, age probably disturbed) Pistol Lake Granite Tarum Granite	All units consist dominantly of homogeneous, pink to buff or brown, K-fsp porphyritic, quartz syenite granite and alkali-fsp granite. Lanceground Hills and Pistol Lake Granites are massive and undeformed in most places; Tarum granite is variably foliated and recrystallized. Locally similar to syenite unit of the Numok Intrusive Suite.	Medium to coarse grained, commonly K-feldspar porphyritic, with euhedral phenocrysts of coarse perthitic K-fsp (Bi), with relict simple twinning (originally Or?). Many examples lack plagioclase and are hypersolvus granites. Rounded mafic clots occur locally, but inclusions are uncommon.
30.1 30.2	Big River Granite 1798 +/- 28 Ma [ Rb-Sr WR ] (this study) (equigranular phase)	White, pink and brick-red, K-fsp porphyritic Bi-Hb granite and alkali-feldspar granite, lesser quartz monzonite to quartz syenite. An equigranular variant (30.2) occurs on a mappable scale in the south-east and northwest of the body. The southern part of the unit has variably developed augen texture and cataclastic fabric (Grenvillian).	Commonly coarse to very coarse-grained, with K-fsp phenocrysts up to 5 cm in size. Distinctive pseudorapakivi texture (K-fsp rims on Plag cores) is developed widely. Texture locally varies to seriate. Unmantled Plag phenocrysts occur locally, and small K-fsp phenocrysts lack plagioclase cores. Foliations in south defined by K-fsp augen / mafic aggregates.

Table 4.1 (continued)

Key Field Relationships	Mineralogy	Petrography
Western boundary of northern zone is a complex agmatite, including blocks of gabbro and diorite. This zone has a variably developed N-trending foliation (see text). Relationship with syenite unit is gradational in the northern zone. On Adlavik Islands, unit is cut by Qtz-Fsp porphyry dykes correlated with adjacent Dog Islands Granite.	Qtz (5-20%) Ni (30-50%) Plag (An30-40; 30-50%) Hb + Bi (5-25% total, subequal) Cpx (relict, < 5%) Accessory Sph, Zr, Ap, Fe-Ox Rare All, Pl	Well-preserved Igneous textures and interstitial quartz crystals. K-fsp (Ni) phenocrysts are variably perthitic, and larger than coexisting Plag phenocrysts. Plag phenocrysts locally have K-feldspar rims. Mafic minerals form subhedral to euhedral crystals / aggregates. Hb locally contains relict Cpx cores.
Relationship to Aillik Group is unknown, but probably intrusive. Contact with quartz monzonite unit appears gradational in the northern zone, but they are separated by plagiophytic monzonite in southern zone (unit 22).	Qtz (0-15%), K-fsp (40-80%) Plag (5-30%, excluding perthite) (free Plag locally absent) Cpx + Hb + Bi (5-25% total) - (Cpx + Bi > Hb) Fayalitic Olivine (relict, < 5%) Some variants lack Hb. Accessory Zr, Ap, Sph. (Zr prominent)	Igneous textures well-preserved in northern zone, variable recrystallization in southern zone. Perthitic K-fsp phenocrysts have relict simple twinning (originally Or?) Cpx is green, Fe-rich variety. Bi is red in color, also Fe-rich. Olivine strongly altered to Fe-Oxide.
Relationships with other units of Mumok Suite unknown. Probably a mafic end-member of the monzonite-quartz monzonite unit, which it locally resembles.	Qtz (0-10%) Ni (15-40%) Plag (An35-50; 30-70%) Cpx + Bi + Hb (10-25% total) (Cpx > Bi > Hb, except if altered) Cpx (rare < 5%) Accessory Ap, Sph, Fe-Ox.	Igneous textures are well-preserved. Plag phenocrysts are locally zoned. Mafic minerals in fresh variants are Cpx and lesser Bi. In more altered variants, Plag is strongly saussuritized and mafics are retrogressed to Act-Ep-Sph aggregates.
Cape Strawberry Granite intrudes Upper Aillik Group, but fine-grained granite is difficult to distinguish from country rocks. Contacts range from clean, sharp and intrusive, to hybrid zones of interaction with and alteration of country rocks. Qtz-fsp porphyry dykes correlated with Dog Islands granite cut Qtz-monzonite of Mumok Intrusive Suite. Cape Strawberry Granite is associated with stockwork Mo-Py mineralization. Dog Island Granite hosts disseminated Cu-Pb mineralization. Cu-Mo and Pb-Zn vein mineralization in Aillik Group country rocks near to granites.	Qtz (20-45%) Ni (40-70%) Plag (An15-25; 10-35%) Bi +/- Chl (1-6%) (Bi altered to Chl) Hb (relict, altd to Bi) rare blue sodic amphibole Accessory Zr, Sph, All, Pl  Dog Islands Granite includes a syenitic phase that locally contains a green relict Cpx, possibly Ae-augite. Fine-grained phases of Cape Strawberry Granite contain poikilitic blue amphibole.	Igneous textures well-preserved. K-fsp (Ni) is variably hematized, coarse patch perthite. Plagioclase normally occurs in groundmass only, but forms local phenocrysts in Bayhead Granite. Qtz is anhedral to interstitial. Red-brown biotite is variably altered to chlorite and Fe-Ox along cleavage traces. In strongly hematized rocks, Bi is totally chloritized. Blue-green Hb occurs locally as a relict phase, altered to Bi. Pl is present interstitially, in mafic aggregates, and tiny veinlets. "Cumulate" layers contain euhedral Bi, Hb, Zr, All.
Dykes correlated with Lanceground Hills Granite cut agmatitic western contact zone of Mumok Intrusive Suite. Pistol Lake Granite intrudes Upper Aillik Group, and is cut by gabbro (possibly Adlavik Suite?) Farun Granite is fault-bounded, and lies topographically below Qtz-Fsp porphyry at White Bear Mountain, that is grouped with Upper Aillik Group.	Qtz (5-35%) Ni (50-80%) Plag (An10-25; 0-25%, excl. perthite) Bi (red, Fe-rich) + Hb (0-10% total) Cpx (relict, < 2%, Ae-augite?) Rare blue sodic amphibole. Fayalitic olivine (rare, altd to Fe-Ox) Accessory Zr, All, Pl, Sph Biotite typically red variety Amorphous Fe-Ox clots are probably after olivine.	Igneous textures well-preserved in north, recrystallized in south. Plagioclase phenocrysts are rare. Quartz shows interstitial habit. Hb and Bi interstitial, locally poikilitic. Hb crystals locally show relict pale green Cpx cores. Fluorite interstitial, associated with mafic minerals. Euhedral zircons up to 4 mm length.
Contact relations unknown. Western boundary of unit is a major fault escarpment along Big River. Southern boundary is formed by Benedict Fault system. Eastern boundary is difficult to define. Foliated grey granitoids near eastern edge are atypical, and may be a screen of older material. Granitoid gneisses south of Benedict fault zone may be deformed equivalents.	Qtz (20-35%) Ni (40-70%) Plagioclase (An20-35; 10-40%) Hb + Bi (2-10% total, Hb > Bi) (Hb is blue-green in colour) Cpx (relict, < 2%, Ae-augite?) Accessory Sph, All, Ep, Zr Rare Pl, disseminated Py. Equigranular variants have similar mineralogy, but are richer in quartz and biotite, poorer in Hb.	Igneous textures are best preserved in northern part of unit. Composite phenocrysts are Ni-perthite with zoned, saussuritized, plag cores. Quartz has variably interstitial habit. Ni and Plag both occur in groundmass. Hb and Bi form clots, associated with Fe-Ox and accessory minerals. Foliated and cataclastic variants show retrogression of mafic minerals to Chl, Ep and Sph.

#### **4.1 GEOLOGY AND PETROLOGY**

Key field and petrographic characteristics of post-tectonic Makkovikian plutonic rocks are summarized in Table 4.1.

##### **4.1.1 Numok Intrusive Suite**

###### **Definition and Distribution**

This is a new name introduced for monzonite, quartz monzonite, syenite and quartz syenite exposed in two areas referred to below as the northern and southern zones (Figure 4.1). These rocks were previously grouped with the Adlavik Intrusive Suite by Kerr (1986, 1987), because they resemble some of its more differentiated variants. U-Pb geochronological data, however, indicate that this interpretation is incorrect (see below). The northern and southern zones of the Numok Suite are interpreted as disrupted halves of an originally continuous pluton. Three compositional units (not named) are defined within the suite, and are described below in order of abundance.

###### **Monzonite and Quartz Monzonite**

In the northern zone, this unit corresponds broadly with Unit 23 of Gower et al. (1982); in the southern zone, it is a new subdivision of their Unit 26. The unit is dominated by homogeneous, coarse grained biotite-hornblende monzonite, quartz monzonite and (locally) syenite (Table 4.1; Plate 4.1).

In the northern zone, on the Adlavik Islands, this unit appears to be gradational with syenite and quartz syenite.



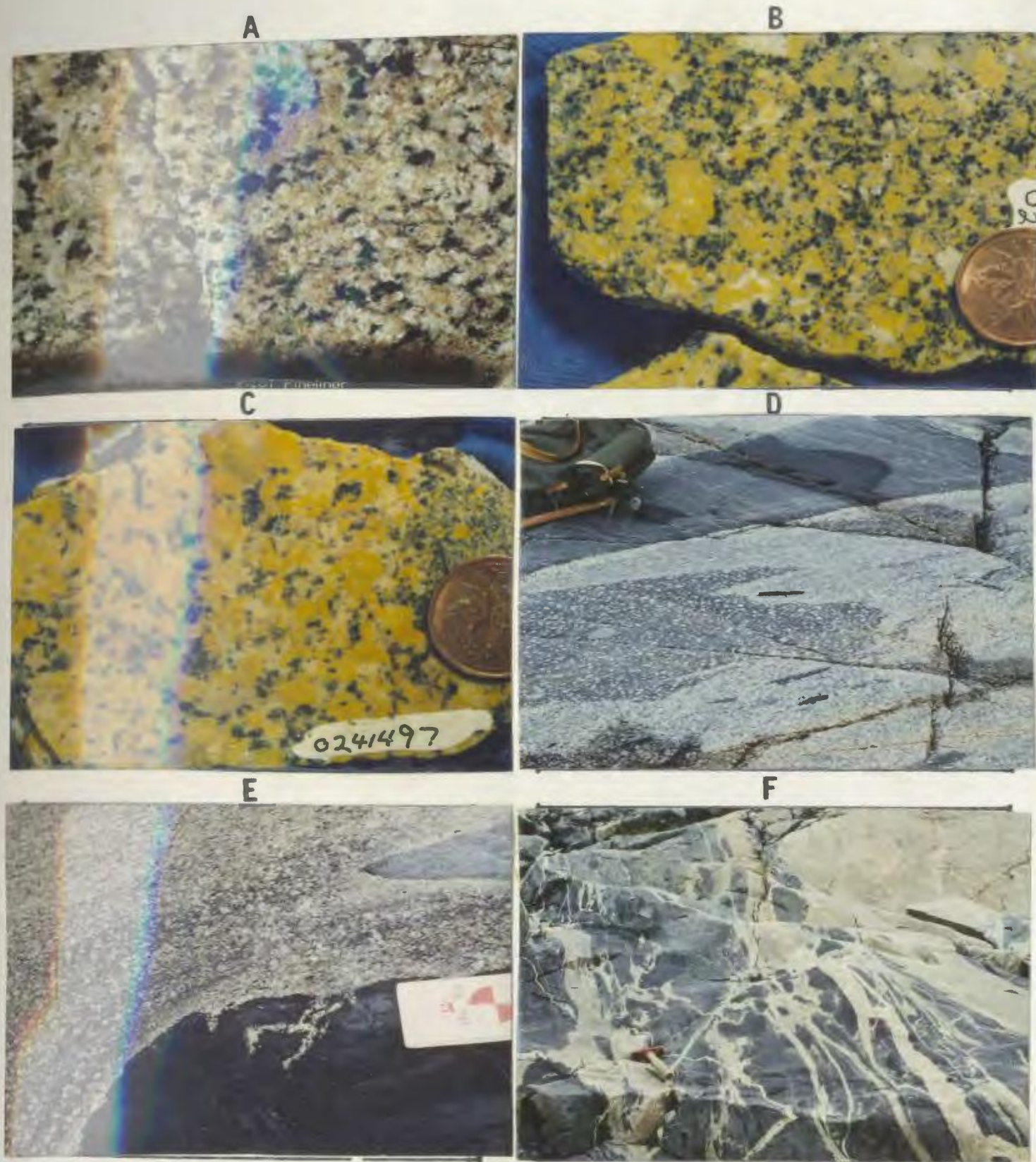


Plate 4.1. Features of the Numok Intrusive Suite (monzonite - quartz monzonite unit). (a) Typical homogeneous quartz monzonite, Long Tickle Island. (b) Porphyritic variant, same area. (c) Typical example with part of cognate xenolith, Big River Area. (d) Undeformed agmatitic border zone, north side of Adlavik Bay. (e) Flow fabric around mafic xenolith in agmatite. (f) Foliated agmatite cut by later fine-grained granitoid material, south side of Adlavik Bay. Slabs are stained for K-feldspar.

The western boundary of the unit in the north consists of a complex agmatite zone up to 1 km wide, exposed near the mouth of Adlavik Bay. The northern part of this zone comprises grey-brown quartz monzonite containing numerous stoped blocks of diabase, gabbro, leucogabbro and porphyritic diorite, some of which display cumulate layering. A fabric around some of the larger inclusions is probably a flow feature, as the inclusions themselves are undeformed. On the south shore of Adlavik Bay, less than 1 kilometre along strike, the same agmatite has a north-trending foliation, present also in the mafic inclusions, which are here transformed to amphibolite. This complex zone was previously interpreted in terms of forcible emplacement of quartz monzonite into gabbro and diorite of the adjacent Adlavik Intrusive Suite (Gower, 1981; Gower et al., 1982; Kerr, 1986). However, U-Pb ages from the agmatite neosome at Adlavik Bay indicate crystallization at  $1801 \pm 2$  Ma (Krogh et al., in prep.), indicating that the mafic inclusions are older than 1800 Ma, and are hence unrelated to the nearby Adlavik Suite, dated at  $1649 \pm 1$  Ma (Krogh et al., in prep). The fabric in the deformed part of the zone may result from syn-emplacement deformation at the original margin of the Numok Suite, or it may be associated with emplacement of the adjacent Adlavik Intrusive Suite. As it affects both paleosome and neosome in the agmatite, it must be younger than 1801 Ma. It is clearly of local extent only, as it dies out quickly to the north.

Excluding this complex western margin, the unit is undeformed and homogeneous in both northern and southern zones, generally inclusion-poor (although it contains sporadic gabbroic blocks) and consistent in both mineralogy and texture (Table 4.1 for details; Plate 4.1).



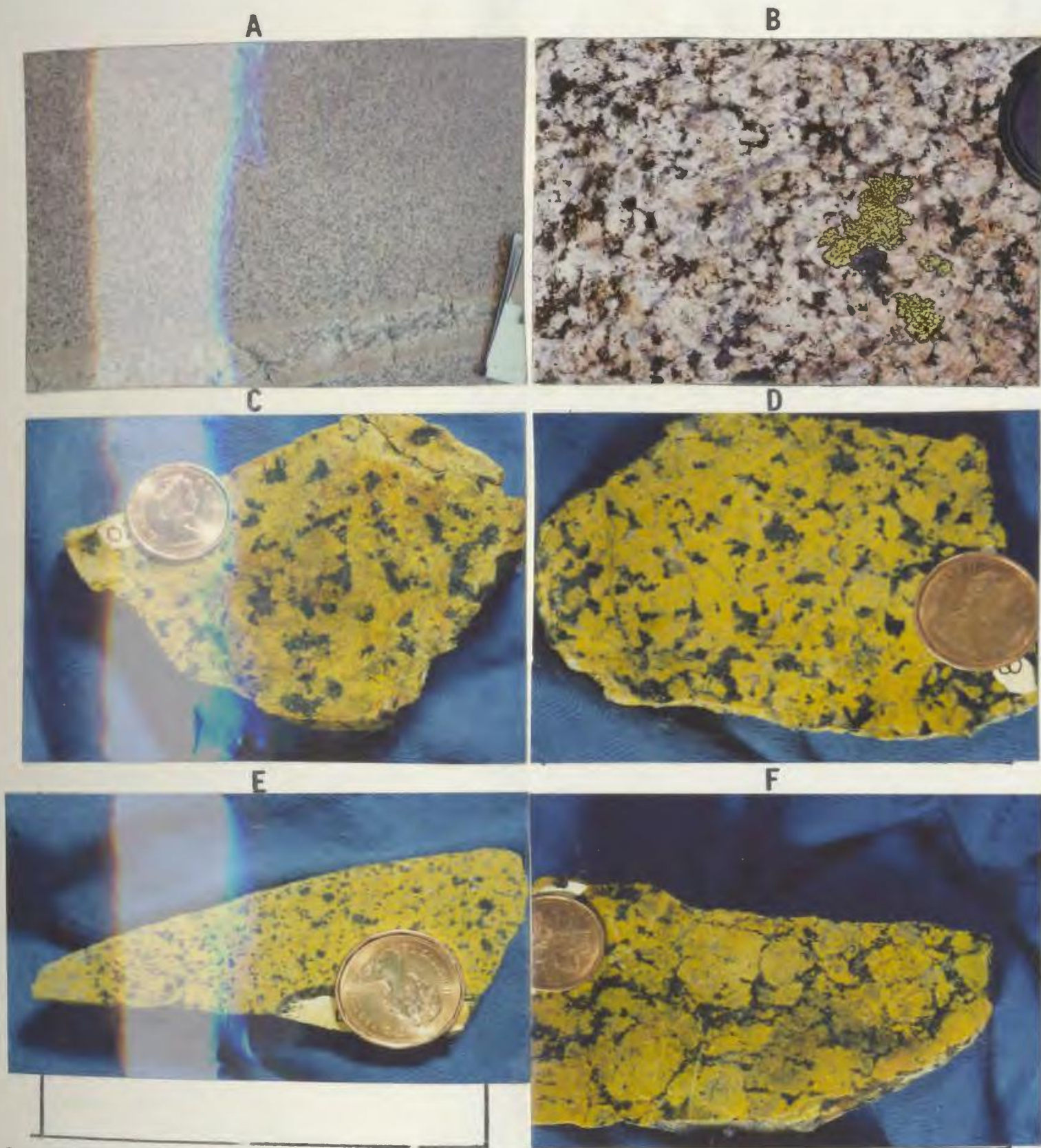


Plate 4.2. Features of the Numok Intrusive Suite (syenite - quartz syenite unit. (a) Homogeneous syenite, Dunn Island. (b). Coarse-grained quartz syenite, north of White Bear Mountain. (c) Hypersolvus, K-feldspar-porphyritic, fayalite-pyroxene syenite, Cape Kitchener. (d) Quartz syenite, Kikkertavak Island. (e) Fine-grained phase in same general area. (f) Coarse-grained syenite with ovoidal phenocrysts and weak deformation, north of White Bear Mountain. Slabs are stained for K-feldspar.

### Syenite and Quartz Syenite

This unit occurs on the outer Adlavik islands, but is most extensively exposed in the southern zone. In the north, it corresponds generally with Unit 31 of Gower et al. (1982), and in the south, with the Tarun Syenite of Gandhi et al. (1989) and Gower et al. (1982; Unit 26c). Similar rocks occur on the Ragged Islands (Gower, 1981), suggesting that it may also be regionally extensive in the north. It is dominated by pink, brown or grey-green, coarse grained, K-feldspar porphyritic, pyroxene - biotite - hornblende syenite, quartz syenite and alkali-feldspar syenite with interstitial quartz and mafic phases (Table 4.1; Plate 4.2). Intense weathering to a yellow-brown gravel is characteristic in many areas, particularly on the Adlavik Islands. The southern zone displays variable recrystallization and deformation, particularly close to the Adlavik Brook fault zone. Massive syenite from Kikkertavak (Numok) Island has given a concordant U-Pb zircon age of  $1801 \pm 2$  Ma (Krogh et al., in prep.).

Distinctive petrographic features include a green, locally pleochroic, Fe-rich clinopyroxene and red-brown biotite. Pyroxene is commonly mantled by variable amounts of hornblende. Variably retrogressed fayalitic olivine occurs locally, surrounded by clots of amorphous iron oxide and hydroxide ("iddingsite"). Patches of this material in other samples are probably pseudomorphs after fayalite. The intense weathering is probably related to the former presence of fayalite; similar effects are present in fayalite-bearing rapakivi granites elsewhere in Labrador (Hill, 1982; Ryan, pers.comm., 1988).



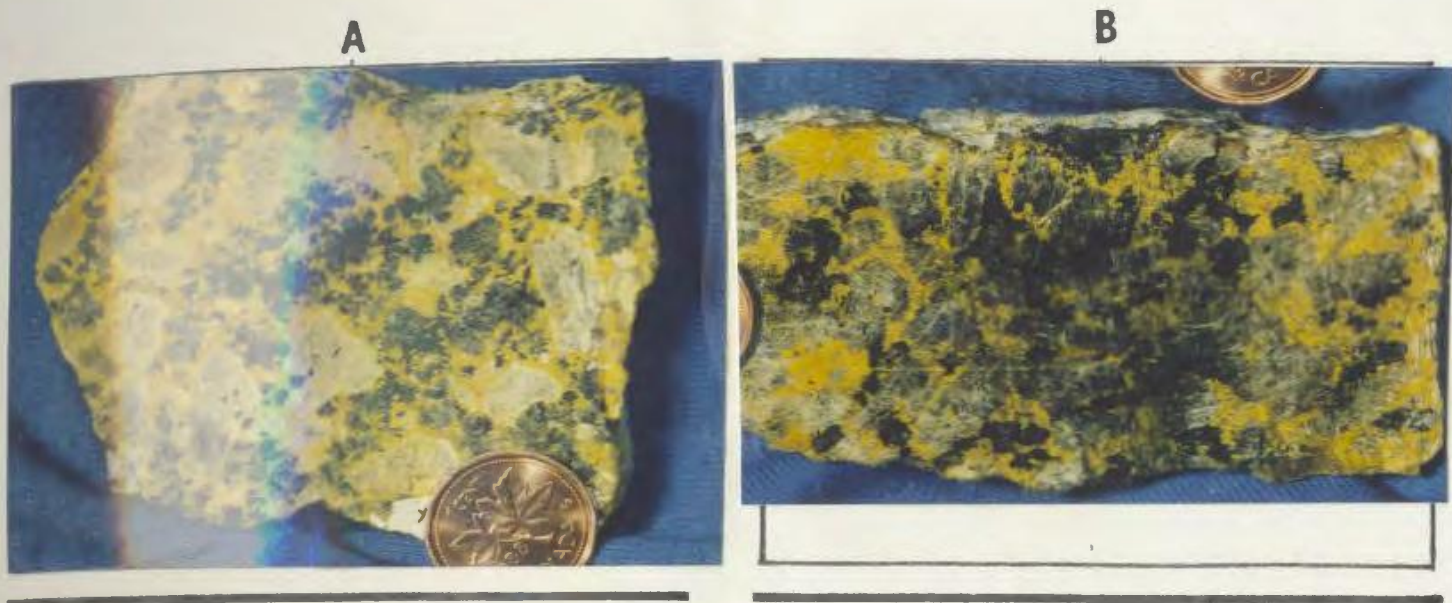


Plate 4.3. Features of the Numok Intrusive Suite (plagiophyric monzonite unit). (a) Monzonite with zoned, ovoidal, plagioclase phenocrysts and interstitial pyroxene-amphibole. (b) Plagioclase-rich variant (cumulate ?), with oikocrystic mafic minerals. Both samples from area west of Big River. Slabs are stained for K-feldspar.

### **Plagiophyric Monzodiorite and Monzonite**

This unit is sandwiched between the quartz monzonite and quartz syenite units in the southern zone. It consists of distinctive, plagioclase - porphyritic, pyroxene-hornblende monzodiorite and monzonite (Table 4.1; Plate 4.3).

Textures in many samples are of "cumulate" aspect, and mafic minerals commonly show an oikocrystic habit. Fresh variants are augite ( $\pm$  hypersthene) - biotite monzonites with minor amphibole, but altered variants dominated by saussuritized plagioclase and fine-grained actinolite are more common. The unit is probably a mafic variant of the monzonite to quartz monzonite unit, which is locally plagioclase-porphyritic. The rounded, zoned plagioclase phenocrysts impart a distinctive texture.

#### **4.1.2 Strawberry Intrusive Suite**

##### **Definition and Distribution**

Strawberry Intrusive Suite is a new name proposed for several discrete plutons scattered over an east-west distance of 125 km (Figure 4.1). All show very similar characteristics, and they are considered to be equivalent. Each pluton is dominated by coarse grained, homogeneous, white, pink or red, K-feldspar porphyritic to megacrystic, biotite granite, commonly with accessory fluorite (Table 4.1; Plates 4.4 and 4.5). The granites from the type area (Cape Strawberry) are described in most detail below.

### **Bayhead Granite**

This is a new subdivision of Unit 27 of Gower et al. (1982). Its southern boundary is formed by the Adlavi Brook fault zone, and its northern boundary by an inferred fault. Contact relations are thus unknown. No displaced equivalent of the Bayhead Granite has been recognized south of the Adlavi Brook fault zone, suggesting that it was either restricted to the north side or perhaps that the (presumably upthrown) block to the south represents a level of the crust below its emplacement level. K-Ar data from this unit (Wanless et al., 1970) gave an age of  $1570 \pm 50$  Ma. On the basis of correlation with the Cape Strawberry Granite, it is considered here to be ca. 1760 Ma old (see later discussion).

The Bayhead Granite is the least differentiated pluton in the Strawberry Suite; it is relatively melanocratic (up to 10% total mafic minerals), locally plagioclase-porphyritic, and commonly contains minor relict amphibole. Most of the unit is homogeneous, although it includes a few gabbroic blocks up to 10 m in diameter. Faint mafic mineral layering is present locally (see below for discussion).

### **Cape Strawberry Granite and Related Rocks**

**General Information** : These form the type locality for the Strawberry Intrusive Suite. The Cape Strawberry and October Harbour Granites correspond to part of Unit 29 of Gower et al. (1982), and the Poodle Pond granite was formerly included in their unit 28a. The Cape Strawberry Granite is dominated by pink or red porphyritic granite, associated with subordinate fine-grained material; the October Harbour Granite tends to be white in color. The



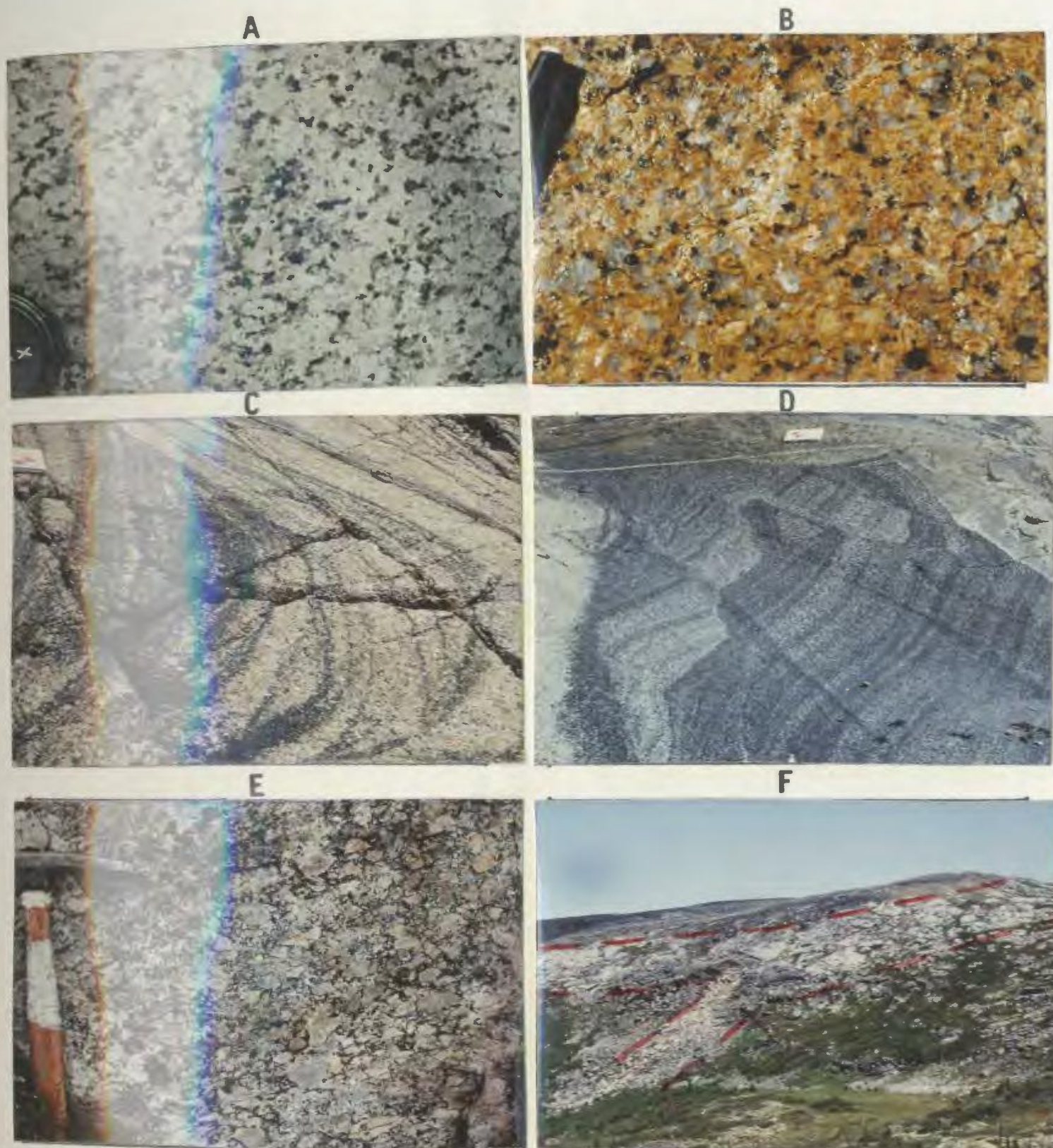


Plate 4.4. Features of the Strawberry Intrusive Suite (see also Plate 4.5). (a) Pale pink, coarse-grained Bayhead granite, Makkovik Lake area. (b) Orange-red, slightly quartz-porphyrific, hematized Dog Island granite, Iron Island (typical also of Cape Strawberry Granite). (c) Trough-bedded, cumulate, mafic mineral layering, near Cape Strawberry. (d) Rhythmically layered granite block, Ford's Bight. (e) "Tuffisite" breccia, near southern contact of Cape Strawberry Granite. (f) Sill of fine-grained, white-weathering granite, with feeder dyke, near Poodle Pond. Sill has a thickness of 30 - 50 m, and intrudes Upper Aillik Group (grey in photo).



Poodle Pond Granite consists of two or more sill-like bodies of medium grained equigranular granite. Single and multiphase aplite, granite and pegmatite dykes and sheets cut the Upper Aillik Group throughout the area around Cape Strawberry. Many are fluorite-bearing, and they are considered to be minor intrusions related to the Strawberry Suite. Some pegmatites near Ford's Bight host molybdenite mineralization (Gower et al., 1982; Wilton and Wardle, 1987).

**Geochronology** : U-Pb zircon data from the Cape Strawberry Granite (Krogh et al., in prep.) are discordant due to Pb loss, but indicate an age of 1800-1760 Ma. The uncertainty is a function of a lack of fractions near concordia; if a 1000 Ma (Grenvillian) lower intercept is assumed (this is shown by other discordant U-Pb zircon data from the study area), the age could be ca. 1800 Ma, whereas a regression of the data points alone suggests ca.  $1760 \pm 15$  Ma. In the remainder of this thesis, the latter age has been employed. A second sample, collected from a zone containing low-U cumulus zircon (see below) is currently being analyzed in an attempt to better resolve this uncertainty\*.

---

\* **NOTE** : When the final copy of this thesis was almost ready for submission, U-Pb data from the second sample became available (Krogh et al., in prep.). The data are concordant at  $1719 \pm 3$  Ma, some 40 Ma younger than the ca. 1760 Ma age used herein. This makes little difference to initial Nd calculations (Chapter 8) and tables and text have not been amended. The Strawberry Suite is still viewed as a post-tectonic Makkovikian association, but it is obvious that the younger limit of the "Makkovikian" time slot must be now be further revised.

Wanless et al. (1970) report K-Ar ages of  $1565 \pm 50$  and  $1600 \pm 34$  from the Cape Strawberry Granite. A composite Rb-Sr isochron from plutons of the suite (this study; Chapter 8) yields an age of  $1694 \pm 56$  Ma, but shows evidence of disturbance (i.e. unreasonably low initial Sr isotope ratio).

**Field Relationships :** Contact zones range from clean, sharp boundaries to zones of interaction and hybridization where the Upper Aillik Group country rocks appear strongly altered. The contacts of the Cape Strawberry granite are steep where exposed on the coast, but the southern contact is more complex, and several enclaves of country rock occur adjacent to it. These are interpreted as roof pendants, and the contact probably dips gently southward.

Xenolith-rich zones near contacts contain fragments of fine-grained granite, Aillik Group metavolcanic rocks, and "hybrid" rock types. Brecciated zones with a biotite-rich matrix are present in xenoliths and in outcrops close to contacts. Alteration, bleaching and pyritization of adjacent country rocks are evident adjacent to contacts. Irregular silicified zones, aplites and pegmatites crosscut the contacts. These features suggest volatile exsolution and hydrothermal activity, which in turn suggest a high level of emplacement. Amphibolites in country rocks at the margin of the October Harbour Granite contain calcite - diopside - andradite  $\pm$  fluorite skarnoid patches, and the margin of the granite itself contains a pale green-brown (andradite?) garnet that is probably a xenocrystic phase derived from this material.

**Compositional and Textural Variation :** Granites of the Cape Strawberry area display the greatest textural variation in the Suite. Fine grained, locally miarolitic,

equigranular variants occur locally around contacts, crosscut contacts, and form the Poodle Pond Granite. A distinctive fine to medium grained grey phase is present in the northeast part of the Cape Strawberry body, and occurs as xenoliths in the coarse facies, suggesting that it is an early component. Locally, this shows a diffuse foliation and ghostly inclusion textures suggesting that it could be an altered Upper Aillik Group porphyry, but in other areas it appears massive and resembles a fine-grained version of the granite. It also has a distinctive mineralogy (see below).

The Cape Strawberry Granite contains distinctive mafic mineral accumulations with a trough-bedded, locally cross-bedded, geometry indicative of cumulate processes. It also contains a single large (10x10 m) block of rhythmically layered granitoid. The presence of such features suggests a low viscosity during crystallization of the granite, probably due to its high fluorine content (see later discussion).

**Petrographic Features :** Biotite in the Cape Strawberry Granite is almost invariably altered to chlorite along cleavage traces. In strongly hematitic variants, chlorite is the only mafic silicate. Fluorite is prominent, and accessory phases such as allanite, apatite, zircon and sphene are obvious and abundant.

Fine-grained pink phases of the Cape Strawberry granite have a similar mineralogy to the dominant coarse-grained phase, but are commonly miarolitic and/or graphic in texture. The distinctive grey phase described above contains poikilitic crystals of deep blue reibeckite or arfvedsonite amphibole, and displays some evidence of recrystallization. "Cumulate" mafic mineral layers consist

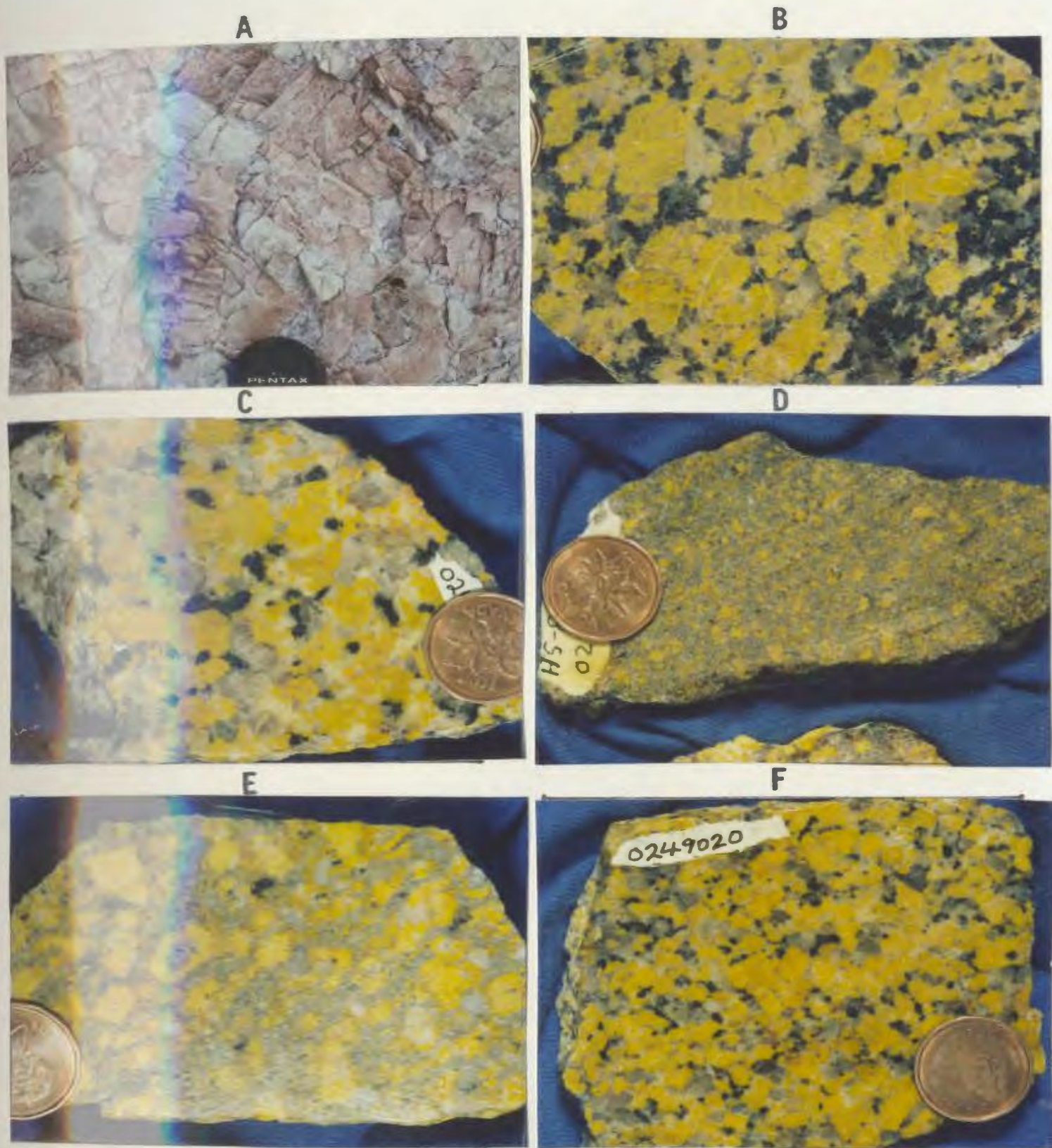


Plate 4.5. Features of the Strawberry Intrusive Suite (see also Plate 4.4). (a) Molbdenite-bearing pegmatite, Ford's Bight. (b) Melanocratic variant of the Bayhead Granite, south of Kaipokok Bay. (c) Typical Cape Strawberry Granite. (d) Fine-grained, reibeckite-bearing, grey phase of Cape Strawberry Granite. (e) Quartz-feldspar porphyry associated with Dog Islands Granite, note oscillatory feldspar zoning. (f) Medium-grained, variably porphyritic Tukialik Granite. Slabs stained for K-feldspar.

of euhedral biotite and hornblende crystals, associated with euhedral sphene, allanite and zircon. They indicate at least local fractionation of biotite and accessory minerals.

#### Dog Islands Granite

The name Dog Islands Granite is introduced for granites on Dog Island, Iron Island, Burnt Island, and the adjacent mainland (Figure 4.1), corresponding to Units 17 and 18 of Gower (1981). Fluorite-bearing quartz-feldspar porphyry dykes that resemble the granite cut quartz monzonite of the Numok Intrusive Suite on nearby islands. This suggests a maximum age of ca. 1800 Ma; correlation with the Cape Strawberry Granite suggests an age of ca. 1760 Ma. The Dog Islands Granite is almost identical to the type area, but is more homogeneous, and locally quartz-porphyritic (Plate 4.5). Mafic mineral layering occurs at the western end of Iron Island (see also Gower, 1981), and is interpreted here as a cumulus feature. A syenite to quartz syenite variant present in the east of Dog Island and on Burnt Island (corresponding partly to unit 18 of Gower, 1981) locally contains distinctive blue poikilitic amphibole (reibekite or arfvedsonite). A pleochroic, green, clinopyroxene (probably aegirine-augite) is present in one sample. Other mafic phases include green hornblende and biotite, associated with fluorite, zoned allanite and euhedral zircon. The mineralogy is very similar to the fine-grained, marginal, grey phase of the Cape Strawberry Granite (see above).

Feldspar and quartz-feldspar porphyry dykes assigned to the Dog Islands granite are mineralogically similar to the coarse phase. Quartz phenocrysts show rounded and resorbed



outlines. K-feldspar phenocrysts locally contain cores of saussuritized plagioclase and, in one instance, alternating rings of K-feldspar and plagioclase indicate oscillatory growth. Chloritized biotite, fluorite, magnetite and sphene form interstitial clots.

#### **Tukialik Granite**

Tukialik Granite is a new name introduced for rocks exposed on Bear Island and in the eastern Benedict Mountains, corresponding to Unit 23 of Gower (1981). It consists dominantly of coarse grained biotite granites similar to those described above.

The unit is in contact with monzonite and syenite of the Mount Benedict Intrusive Suite (see Chapter 5) along its southern boundary; this contact is interpreted to be the continuation of the Adlavik Brook fault zone in the west. The nature of the southern contact in the east is unknown. To the west, the Tukialik Granite may be continuous with the Dog Islands Granite. Bailey (field notes, 1979) suggested that the granite was gradational with metavolcanic rocks east of Tukialik Bay; however, this enclave is locally cut by veins of pink granite.

In comparison to other members of the Strawberry Suite, the Tukialik Granite is richer in K-feldspar, slightly finer-grained, and locally equigranular. Blue quartz is prominent in many samples. A quartz-feldspar porphyry variant occurs locally on Bear Island and resembles similar rock types grouped with the Dog Islands granite. Alteration of biotite to chlorite appears less intense than in the Cape Strawberry or Dog Islands Granites.

#### 4.4.3 Lanceground Intrusive Suite

##### **Definition and Distribution**

Lanceground Intrusive Suite is a new name introduced for three discrete plutons; two of these are located near Adlaviik Bay, and the third is adjacent to the Adlaviik Brook Fault zone (Figure 4.1). All three show similar characteristics, but the most southerly has been affected by Grenvillian deformation and metamorphism. There appears to be a spatial association between these granites and the Numok Intrusive Suite, although a case could also be made for a spatial link to the Adlaviik Intrusive Suite. A Rb-Sr isochron from the Lanceground Hills Granite (Chapter 8) suggests an ambiguous age of  $1692 \pm 32$  Ma, but is probably disturbed, as it has a very low initial ratio. U-Pb zircon geochronology is in progress as of thesis submission. The Lanceground Suite shows a strong geochemical affinity to other known members of the post-tectonic Makkovikian association (see section 4.2).

##### **Lanceground Hills and Pistol Lake Granites**

The Lanceground Hills Granite corresponds to part of unit 26c of Gower et al.(1982), and the Pistol Lake Granite to part of their unit 28a (Monkey Hill Granite). The two units are, however, closely similar, and both consist dominantly of coarse grained, K-feldspar porphyritic, locally hypersolvus, biotite-hornblende syenite, quartz syenite, granite and alkali-feldspar granite (Table 4.1; Plate 4.6).

**Field Relations :** Contact zones of the Lanceground Hills Granite coincide with the agmatite zone at the

western margin of the Numok Intrusive Suite. A dyke of brown-weathering, hypersolvus, quartz syenite (typical of the suite) cuts the foliated agmatite, indicating that emplacement of the granite post-dated the leucosome (dated at ca. 1800 Ma, see above) and also deformation (unconstrained). The relationship between the Lanceground Hills Granite and adjacent gabbro-diorite of the Adlavik Intrusive Suite is unknown. The Pistol Lake Granite is in contact with the Upper Aillik Group for 10 km, but most of the contact is obscured by drift. The granite intrudes the Aillik Group in two localities, and is locally intruded by biotite-bearing gabbro that resembles parts of the Adlavik Suite.

Both units are generally fresh and massive, although the western part of the Lanceground Hills granite locally displays a moderate northeast to east-trending foliation. Syenitic variants resemble equivalent rocks of the Numok Suite (see above), and parts of the Lanceground Hills Granite show the same intense weathering to yellow gravel.

**Petrographic Characteristics :** Both units include rocks that show hypersolvus characteristics, and virtually all contain euhedral to rounded phenocrysts of very coarse microcline-perthite, locally displaying relict simple twinning suggesting original orthoclase or sanidine crystals. Free plagioclase (where present) is confined to the groundmass, although it locally forms isolated phenocrysts mantled by K-feldspar.

Red-brown biotite is the most common mafic mineral, and in relatively melanocratic variants, is accompanied by variably poikilitic blue-green hornblende. A few samples also contain small amounts of an intense blue arfvedsonite or reibeckite amphibole. A green, pleochroic clinopyroxene



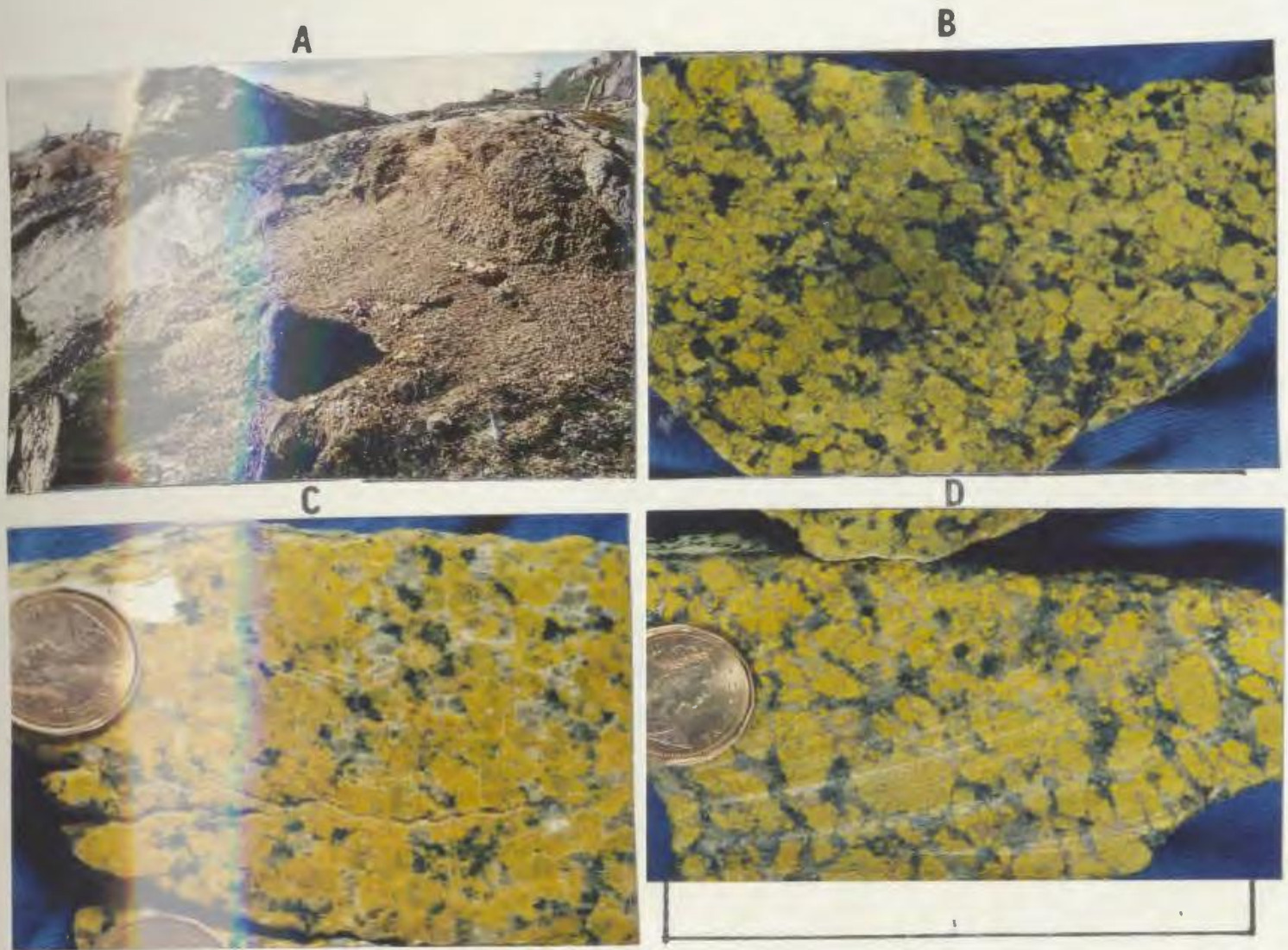


Plate 4.6. Features of the Lanceground Intrusive Suite. (a) Intense weathering of the Lanceground Hills Granite, near Adlaviik Bay, probably indicating the former presence of fayalite. (b) Hypersolvus syenite, Adlaviik Bay. Note coarse perthite, and similarity to Numok Suite syenites (Plate 4.2). (c) Alkali-feldspar quartz syenite of the Pistol Lake Granite, south of Bernard Lake. (d) Coarse-grained, deformed alkali-feldspar granite from the Tarun Granite, near White Bear Mountain. Slabs stained for K-feldspar.

that locally occurs as relict grains within hornblende is probably aegirine-augite. Amorphous iron-oxide - hydroxide clots locally contain relict fayalitic olivine. Minor phases include prominent interstitial fluorite, prominent allanite (intergrown with mafic silicates), apatite, sphene, and euhedral zircon crystals up to 2 mm in length.

### Tarun Granite

The Tarun Granite is located near the Benedict fault zone, and around White Bear Mountain. It corresponds to part of Unit 26c of Gower et al (1982). Original igneous textures and mineralogy have been obliterated by recrystallization in many samples. Well-preserved examples are pink or buff, coarse grained, K-feldspar porphyritic granites that resemble those from the type area; there is also a strong geochemical similarity (see 4.2).

Contact relationships of the Tarun Granite are poorly known. The northern limit is difficult to place as there is little contrast between the granite and syenite-quartz syenite of the Numok Suite. The most likely position coincides with the projected trace of a fault indicated by Gower et al.(1982); alternatively, the two might be gradational.

The Tarun granite is spatially associated with quartz-feldspar porphyry (assigned to the Upper Aillik Group; see Chapter 7) that forms the main peak of White Bear Mountain. The northern contact of the porphyry unit (from Gower et al., 1982) is approximately coincident with the 1200-1400 feet (400-475 m) contour interval, and follows the topography. It is suggested that this contact has a shallow inclination, and that the Tarun granite is

•

continuous beneath the peak. The nature of the granite - porphyry contact is unknown, but there is a strong compositional similarity between them (Chapter 7) that may indicate a genetic link.

#### 4.1.4 Big River Granite

This is a new name proposed for an extensive granitoid unit in the southeast of the study area (Figure 4.1). It corresponds to unit 26b and part of unit 23 of Gower et al. (1982). It is dominated by pink to red or white, coarse grained, K-feldspar porphyritic, leucocratic, hornblende-biotite granite and alkali-feldspar granite, locally ranging in composition to quartz monzonite and quartz syenite (Table 4.1; Plate 4.7). Textural variants include a dominant porphyritic granitoid, and a subordinate equigranular phase. The former is characterized by mantled plagioclase phenocrysts with K-feldspar rims for which the term "pseudorapakivi texture" is used here (classical rapakivi or "wiborgite" textures consist of albite on orthoclase; e.g. Vorma, 1976).

**Field Relationships** : The western boundary of the unit coincides with an inferred fault zone that links the Benedict and Adlavik Brook fault zones, marked by a prominent linear escarpment. The southern boundary corresponds with the Benedict Fault system. The nature of the poorly-exposed eastern boundary is unclear; a foliated grey dioritic granitoid in this area is atypical of most of the unit, and may represent a screen of older material between it and adjacent units.



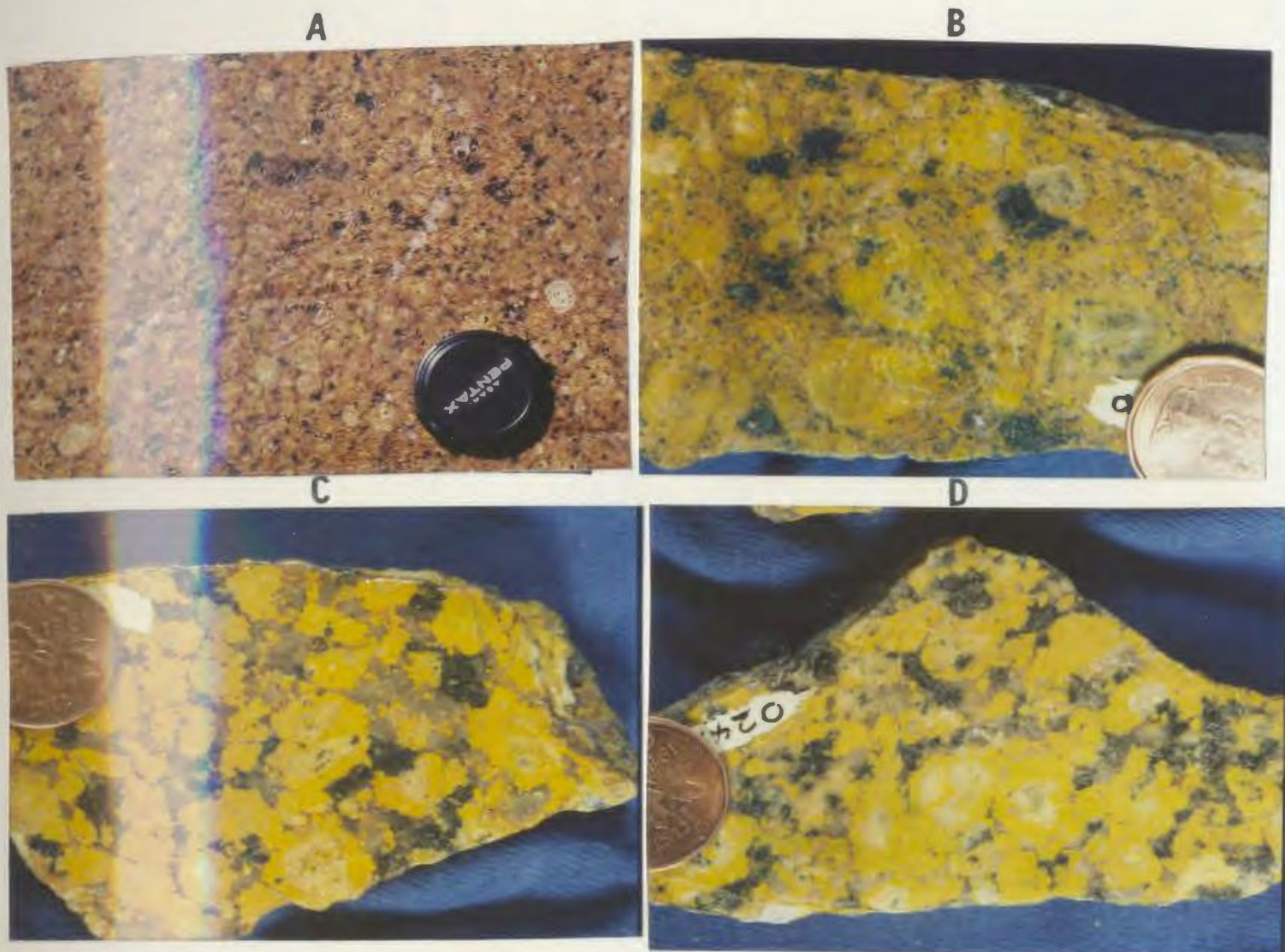


Plate 4.7. Features of the Big River Granite. (a) Red-weathering pseudorapakivi granite, south of the estuary of Big River, note ovoidal phenocrysts. (b) Fine-grained, porphyritic phase, with feldspar zoning partly defined by mafic inclusion trails, near Big River. (c) and (d) Typical coarse-grained pseudorapakivi granites, from the escarpment east of Big River Valley. Slabs stained for K-feldspar.

*Geochronology* : A Rb-Sr isochron from the dominant porphyritic granite (Chapter 8) yields an age of  $1798 \pm 28$  Ma, and shows no evidence of disturbance.

*Lithology and Petrography* : Pseudorapakivi texture is variably developed, but is present in at least vestigial form in most porphyritic variants. Massive, undeformed variants dominate the northern part of the unit, but variably foliated and/or cataclastic rocks occur in the south. Foliations have a general east-west trend, but are locally variable. The transition from foliated to massive granite appears to be gradational, and the cataclastic rocks probably form local zones of high strain parallel to the Benedict Fault zone. Medium-grained equigranular variants occur mostly in the southeast and northwest of the unit. They are more siliceous than the porphyritic phase and have a higher biotite/hornblende ratio.

Hornblende in this unit is a deep green or blue-green variety. Pale green, locally faintly pleochroic clinopyroxene (possibly aegirine-augite) is present rarely as a relict phase, altered to amphibole and/or biotite. Gower (1981) also reports reibeckite in two such samples from the unit, but this mineral does not appear to be widespread in the unit. Sphene is a prominent minor phase (up to 1% in some samples), and is commonly euhedral. Other accessory phases are prominent, but not as abundant as in the Strawberry and Lanceground Suites. Composite phenocrysts commonly have zoned, variably saussuritized plagioclase cores, surrounded by perthitic microcline. In most cases, there is a single mantle only; oscillating zones of plagioclase and K-feldspar are very rare.

## 4.2 DESCRIPTIVE GEOCHEMISTRY

Post-tectonic Makkovikian plutonic rocks are represented by 460 samples; 264 of these are regional samples collected on a 2 km random grid spacing. The remainder include 114 follow-up samples, collected from granites of the Strawberry and Lanceground Intrusive Suites, and 82 geological samples distributed approximately equally amongst all units. Characteristics of and usage of sample populations are explained in Chapter 1.

### 4.2.1 General Geochemistry

#### Summary of Numerical Data

Average major element, trace element and partial CIPW normative compositions of post-tectonic Makkovikian units are listed in Table 4.2. The Numok Intrusive Suite is characterized by lower  $\text{SiO}_2$  (60-65%) than other units, and is discussed separately from remaining units, which are referred to below collectively as "siliceous granitoids".

**Numok Intrusive Suite :** The plagiophyric monzodiorite and monzonite unit has the least differentiated composition. There are significant compositional differences between the quartz monzonite unit in northern and southern zones; in the south it has lower  $\text{SiO}_2$ , and is closer in composition to the plagiophyric monzonite unit than to the syenite unit. In contrast, the quartz monzonite and quartz syenite units of the northern zone are similar in composition, although the latter is richer in  $\text{K}_2\text{O}$ .

Table 4.2 . Average compositions of post-tectonic Makkovikian plutonic rocks, subdivided by principal units.

UNIT	20.1		20.2		21.1		21.2		22.2		23.0		24.1		24.2	
n1	42		15		18		22		10		57		42		7	
n2	10		2		4		2		3		35		38		6	
(Wt%)	Mean	S.D.	Mean	S.D.	Mean	S.D.	Mean	S.D.	Mean	S.D.	Mean	S.D.	Mean	S.D.	Mean	S.D.
SiO <sub>2</sub>	64.98	4.21	59.64	4.32	64.31	5.04	66.73	2.80	57.60	2.33	69.78	5.20	72.85	3.56	70.59	3.83
TiO <sub>2</sub>	0.73	0.35	0.83	0.23	0.72	0.40	0.54	0.17	0.91	0.21	0.43	0.35	0.21	0.11	0.26	0.09
Al <sub>2</sub> O <sub>3</sub>	15.62	1.28	17.76	1.70	15.35	1.41	14.79	1.00	17.87	0.77	13.94	1.27	12.99	1.42	14.54	1.71
Fe <sub>2</sub> O <sub>3</sub>	1.43	0.67	2.00	0.82	1.40	0.74	1.47	0.47	2.10	0.39	1.05	0.75	1.14	0.80	1.14	0.59
FeO	3.22	1.24	3.60	0.99	4.07	2.14	3.24	1.36	4.45	1.02	2.37	1.47	1.34	0.82	1.37	0.56
MnO	0.13	0.06	0.10	0.03	0.17	0.09	0.13	0.05	0.11	0.02	0.07	0.05	0.06	0.06	0.07	0.06
MgO	0.72	0.54	1.71	1.20	0.49	0.43	0.31	0.14	2.35	0.62	0.51	0.61	0.29	0.62	0.28	0.14
CaO	2.05	0.92	3.78	1.68	1.90	0.88	1.61	0.54	5.02	1.09	1.49	1.08	0.96	1.33	0.95	0.21
Na <sub>2</sub> O	4.68	0.53	4.45	0.29	4.56	0.77	4.46	0.37	4.44	0.73	3.95	0.71	4.16	1.26	4.18	0.57
K <sub>2</sub> O	5.35	0.77	4.92	1.40	5.93	0.86	5.68	0.47	4.01	0.57	5.07	1.04	4.92	1.15	5.76	1.16
P <sub>2</sub> O <sub>5</sub>	0.21	0.17	0.27	0.11	0.20	0.19	0.10	0.06	0.32	0.08	0.10	0.11	0.03	0.03	0.07	0.04
LOI	0.50	0.21	0.65	0.48	0.49	0.27	0.42	0.19	0.76	0.42	0.59	0.19	0.62	0.35	0.56	0.12
TOTAL	99.62		99.71		99.59		99.48		99.94		99.35		99.57		99.77	
(ppm) Trace Elements																
Li	20.0	12.3	22.1	7.1	14.7	9.8	11.3	5.5	18.5	4.9	22.5	18.7	29.7	26.2	20.6	6.5
P	732.0	404.6	1125.7	468.1	465.6	312.3	390.1	228.4	696.9	370.5	922.9	723.5	1669.0	942.8	893.9	558.7
Sc	10.5	3.5	10.5	0.7	14.9	7.1	7.0	0.6	10.8	3.9	4.6	4.3	1.6	1.5	3.9	1.8
V	33.5	25.2	78.2	49.7	20.1	11.9	15.4	8.0	103.6	29.7	28.9	30.4	22.2	47.7	14.4	9.1
Cr	3.1	3.9	10.9	16.0	2.0	1.2	4.8	3.5	22.1	9.1	4.7	4.8	5.8	7.4	8.4	12.7
Ni	1.3	0.5	6.1	8.8	1.0	0.0	1.2	1.1	11.8	4.1	2.1	3.5	2.6	6.6	1.9	1.6
Cu	6.7	3.6	20.5	15.5	7.5	4.5	5.3	1.7	34.6	9.1	4.6	4.1	13.2	51.2	5.3	3.6
Zn	93.5	26.2	79.1	20.7	107.9	42.4	120.7	46.0	79.4	13.7	74.0	38.8	84.7	70.5	115.7	149.5
Ga	20.2	3.6	20.7	2.3	20.8	2.6	22.5	10.0	19.7	2.3	17.4	7.0	17.1	7.3	18.4	6.1
Rb	102.4	42.3	141.3	53.4	94.8	55.9	126.8	53.0	109.5	31.2	151.7	63.6	181.7	64.0	170.3	33.3
Sr	204.8	132.2	453.9	201.0	114.9	75.1	102.1	79.0	512.1	103.2	119.4	110.4	66.5	67.0	113.6	73.5
Y	39.6	12.9	38.8	14.2	33.4	15.5	73.6	24.2	34.0	4.5	57.1	37.3	66.8	48.2	46.7	6.6
Zr	460.1	260.2	564.6	233.9	577.8	446.6	951.0	328.7	352.6	236.5	467.8	399.5	447.2	314.1	454.6	166.0
Nb	18.0	7.2	20.3	9.8	15.3	5.3	27.3	8.5	15.7	3.6	25.7	13.2	30.8	36.3	21.4	2.2
Mo	3.9	1.1	4.3	0.8	2.9	0.9	3.9	1.3	4.1	1.0	4.3	1.8	3.9	2.2	3.3	1.4
Sn	2.4	2.5	3.0	2.8	1.5	1.0	1.0	0.0	2.3	1.5	4.0	2.9	5.3	3.3	3.7	3.0
Cs	1.9	2.3	1.3	1.1	0.9	0.8	0.5	0.0	1.5	0.9	1.2	1.1	1.1	0.7	1.4	1.1
Ba	1134.0	804.3	1063.9	311.6	743.2	656.5	832.2	427.6	860.3	166.7	706.4	479.6	327.7	266.4	504.0	220.6
La	73.4	46.3	56.2	17.2	60.9	28.6	93.4	24.3	53.8	6.5	101.5	108.0	78.0	43.8	105.3	46.9
Ce	144.2	87.0	117.7	39.5	115.9	56.8	196.8	52.6	104.5	18.0	198.5	199.2	161.7	81.5	196.3	83.1
Sm	11.5	4.8	15.0	1.4	11.5	1.3	17.5	6.4	8.8	0.7	13.1	7.3	12.9	6.7	14.2	4.5
Yb	3.3	1.7	4.3	2.5	2.5	0.0	8.0	0.0	2.5	0.0	5.3	2.2	8.2	5.5	5.3	2.2
Hf	8.7	5.5	15.0	1.4	11.5	7.1	17.0	2.8	7.7	1.2	11.0	6.5	13.6	8.1	13.3	4.0
Pb	16.3	6.9	15.5	6.3	14.5	6.8	17.1	7.4	13.2	3.7	23.6	7.9	22.5	9.8	26.9	9.5
Th	6.7	6.9	11.5	14.5	1.8	2.5	8.4	7.2	7.4	4.4	17.0	16.4	27.0	31.3	14.0	8.1
U	3.2	1.9	3.1	1.5	1.8	1.5	3.1	1.4	3.6	1.6	4.5	3.8	8.0	11.3	4.7	1.0
(Wt%) Partial CIPW norms																
Q	11.33	8.12	4.70	4.67	7.14	9.46	14.40	6.02	2.40	2.11	23.06	9.88	27.54	8.62	21.90	10.29
C	0.00	0.00	0.09	0.35	0.03	0.09	0.00	0.00	0.00	0.00	0.16	0.28	0.04	0.11	0.18	0.21
Or	31.90	4.54	31.03	5.07	31.19	7.99	33.84	2.79	23.86	3.36	30.30	6.19	29.36	6.81	34.26	6.93
Ab	39.95	4.43	37.96	2.52	42.45	8.60	38.11	3.11	37.68	5.85	33.79	6.08	35.17	10.88	35.25	4.03
An	5.84	3.12	12.89	5.84	6.97	5.74	3.58	1.81	17.11	3.99	5.00	2.93	2.33	1.66	3.46	1.57
Di	2.86	1.57	2.84	1.39	3.62	2.71	3.41	1.78	5.12	1.70	1.65	2.36	1.57	4.86	0.40	0.85
Hx	4.14	2.01	4.91	2.50	3.22	2.54	3.22	1.61	7.03	3.99	3.39	2.15	1.48	1.39	1.80	0.98
Ol	0.01	0.08	0.80	2.09	1.21	2.72	0.00	0.00	1.12	2.37	0.02	0.13	0.00	0.03	0.00	0.00
Wt	2.09	0.97	2.72	0.94	2.15	0.94	1.96	0.62	3.06	0.58	1.51	1.04	1.25	0.90	1.66	0.87
Il	1.40	0.68	1.56	0.44	1.38	0.66	1.04	0.32	1.73	0.40	0.83	0.64	0.41	0.22	0.50	0.17

KEY TO UNITS (NIS - Mumok Intrusive Suite, SIS - Strawberry Intrusive Suite)

- 20.1 -- (NIS) Monzonite to Quartz Monzonite (Northern Zone)
- 20.2 -- (NIS) Monzonite to Quartz Monzonite (Southern Zone)
- 21.1 -- (NIS) Syenite to Quartz Syenite (Northern Zone)
- 21.2 -- (NIS) Syenite to Quartz Syenite (Southern Zone)
- 22.2 -- (NIS) Plagiophytic Monzodiorite and Monzonite
- 23.0 -- (SIS) Bayhead Granite
- 24.1 -- (SIS) Cape Strawberry Granite
- 24.2 -- (SIS) October Harbour Granite

n1 -- number of analyses for all elements except those listed below

n2 -- number of analyses for Sc, Sn, Cs, Sm, Yb and Hf

Table 4.2 (continued).

UNIT	24.3		25.0		26.0		27.0		28.0		29.0		30.1		30.2	
n1	4		33		50		22		19		41		64		15	
n2	3		31		29		20		15		31		13		0	
(Wt)	Mean	S.D.	Mean	S.D.	Mean	S.D.	Mean	S.D.	Mean	S.D.	Mean	S.D.	Mean	S.D.	Mean	S.D.
SiO <sub>2</sub>	74.58	0.83	70.80	5.02	71.99	4.15	72.50	2.01	70.12	3.39	72.84	2.75	69.00	5.09	74.81	1.47
TiO <sub>2</sub>	0.14	0.04	0.32	0.36	0.28	0.15	0.26	0.07	0.44	0.32	0.30	0.11	0.44	0.21	0.16	0.08
Al <sub>2</sub> O <sub>3</sub>	13.14	1.39	13.91	1.40	13.64	1.76	13.16	0.77	13.76	1.72	12.99	1.34	14.75	1.77	13.09	0.65
Fe <sub>2</sub> O <sub>3</sub>	1.43	1.28	0.95	0.94	1.00	0.51	1.10	0.50	1.65	0.74	1.07	0.39	1.25	0.57	0.78	0.18
FeO	0.34	0.23	1.92	2.37	1.20	0.80	1.30	0.56	1.79	1.35	1.35	0.68	1.72	0.93	0.49	0.26
MnO	0.03	0.01	0.06	0.08	0.05	0.04	0.05	0.02	0.09	0.05	0.06	0.03	0.07	0.04	0.04	0.02
MgO	0.11	0.06	0.26	0.36	0.31	0.27	0.17	0.21	0.23	0.15	0.17	0.15	0.59	0.91	0.13	0.11
CaO	0.51	0.34	1.06	0.81	0.95	0.73	0.77	0.38	1.14	0.60	0.82	0.42	1.56	1.25	0.53	0.30
Na <sub>2</sub> O	3.52	0.50	4.08	0.48	4.11	0.68	3.95	0.43	4.09	0.68	3.92	0.66	4.21	0.72	4.59	0.84
K <sub>2</sub> O	5.76	0.60	5.41	1.25	5.15	0.69	5.58	0.41	5.46	1.57	5.42	0.67	5.25	0.92	4.47	1.18
P <sub>2</sub> O <sub>5</sub>	0.01	0.01	0.07	0.11	0.06	0.08	0.04	0.03	0.07	0.07	0.04	0.02	0.11	0.07	0.03	0.03
LOI	1.44	1.97	0.62	0.18	0.79	0.26	0.56	0.11	0.56	0.30	0.50	0.18	0.61	0.31	0.49	0.12
TOTAL	101.01		99.46		99.53		99.44		99.40		99.48		99.56		99.61	
(ppm)																
Li	11.0	6.5	31.2	30.3	22.7	23.3	15.6	7.2	10.3	4.9	14.6	15.2	15.4	6.1	12.1	6.0
P	623.5	1106	1868.1	1455	1592.0	1256	1804.5	1069	941.4	879.6	1084.7	763.1	590.7	387.9	1105.4	533.5
Sc	0.6	0.2	4.0	6.6	2.5	1.6	2.5	1.7	7.0	10.2	3.2	1.7	2.4	0.9		
V	19.3	1.7	18.8	11.1	21.2	13.3	10.6	8.9	13.3	6.9	13.8	7.4	24.1	17.7	10.1	5.8
Cr	5.5	2.7	1.9	1.2	6.3	7.8	3.3	2.3	4.1	2.8	3.8	3.3	4.8	14.9	4.7	7.0
Ni	2.0	1.4	1.1	0.4	2.3	2.8	1.3	0.9	1.1	0.3	1.8	2.4	2.2	8.0	4.1	7.5
Cu	5.8	3.9	16.1	72.9	6.5	5.4	5.7	3.5	9.0	18.1	4.7	3.5	7.0	6.5	3.1	1.6
Zn	60.0	52.2	82.0	107.1	61.7	48.7	87.9	53.6	106.1	67.2	82.8	59.0	63.6	42.5	17.3	14.8
Ga	8.3	2.5	22.1	8.1	12.1	6.5	27.1	9.2	26.0	10.6	16.2	7.3	16.1	4.9	11.1	4.5
Rb	169.0	34.1	200.6	73.6	198.8	52.6	186.5	29.2	168.1	35.9	167.1	52.5	123.8	53.3	144.6	42.5
Sr	151.5	84.9	94.5	64.5	139.8	190.9	54.6	57.8	71.3	69.9	60.0	68.8	179.3	154.7	81.3	110.0
Y	37.3	21.2	60.2	65.3	41.4	23.3	69.6	36.3	77.6	36.8	75.5	29.3	44.8	17.7	32.4	10.3
Zr	325.5	246.4	573.5	803.3	465.9	637.0	776.0	707.5	691.7	330.0	560.7	280.9	409.4	213.0	195.9	50.0
Nb	18.0	6.5	26.7	18.3	22.2	8.7	28.6	10.9	30.4	13.8	29.2	10.1	18.4	7.3	22.3	6.2
Mo	2.8	0.5	6.3	18.4	3.6	2.6	5.1	2.9	4.8	2.8	3.6	1.5	3.7	1.2	3.4	1.5
Sn	3.3	0.6	10.0	20.4	5.1	2.7	3.7	2.3	4.1	2.7	4.2	2.8	2.7	2.7		
Cs	1.1	0.5	0.7	0.5	1.7	1.5	1.1	0.7	1.1	0.6	1.1	0.7	0.7	0.6		
Ba	396.0	247.0	448.2	192.2	456.4	360.0	274.5	222.0	440.0	311.4	308.1	244.0	762.3	465.6	227.7	272.3
La	29.8	29.1	137.6	214.3	65.3	40.5	147.6	73.6	133.0	82.1	104.7	36.4	67.2	29.8	45.9	26.1
Ce	76.5	63.7	249.1	367.9	134.7	80.6	293.2	145.2	270.3	155.0	211.9	71.6	134.6	59.2	93.6	47.7
Sm	8.1	5.4	16.1	18.7	10.3	4.6	21.5	10.0	25.8	13.1	18.0	6.6	10.4	3.9		
Yb	4.8	2.3	7.1	6.9	6.0	2.5	7.8	4.7	10.5	5.7	8.5	2.9	4.2	2.0		
Hf	9.8	6.2	17.1	25.1	12.1	6.2	20.1	13.4	22.6	11.0	16.8	7.0	10.1	3.0		
Pb	26.8	3.6	113.6	500.5	18.8	10.2	23.6	11.0	25.0	18.9	24.7	12.0	19.4	11.5	10.1	4.6
Th	6.8	1.7	20.7	22.8	12.8	9.3	16.4	7.4	14.3	7.0	22.3	7.3	13.0	10.2	13.1	6.5
U	3.0	0.7	5.4	3.3	5.3	2.8	5.2	2.0	4.1	1.6	6.3	2.4	4.2	2.7	5.9	2.0
(Wt)																
Q	30.86	4.00	23.27	8.74	26.17	8.48	26.46	4.40	23.17	10.42	27.49	7.01	20.30	10.05	30.06	2.46
C	0.19	0.16	0.06	0.12	0.16	0.28	0.03	0.09	0.35	1.45	0.01	0.05	0.07	0.15	0.02	0.07
Or	34.17	3.56	31.23	3.82	30.83	4.12	33.33	2.43	32.53	9.25	32.33	3.97	31.35	5.43	26.65	7.01
Ab	29.87	4.30	35.21	3.75	35.09	5.63	33.64	3.65	34.66	5.96	33.46	5.51	35.93	6.02	39.13	7.19
An	2.53	1.82	3.63	1.93	3.21	3.18	1.70	1.58	2.26	1.88	1.84	1.57	5.69	4.27	1.88	1.67
Di	0.00	0.00	1.18	2.03	0.88	1.38	1.51	1.34	1.98	1.71	1.50	1.17	1.28	1.80	0.40	0.24
By	0.36	0.26	2.34	3.54	1.35	1.17	0.85	0.89	1.16	1.50	0.92	0.89	2.16	1.22	0.29	0.52
Ol	0.00	0.00	0.07	0.38	0.06	0.39	0.00	0.00	0.00	0.00	0.00	0.00	0.22	1.78	0.00	0.00
Wt	0.71	0.52	1.40	1.40	1.35	0.73	1.53	0.77	2.03	1.00	1.50	0.57	1.74	0.84	0.97	0.34
Il	0.21	0.04	0.64	0.73	0.53	0.28	0.50	0.14	0.85	0.62	0.57	0.20	0.84	0.41	0.31	0.16

KEY TO UNITS (LIS - Lanceground Intrusive Suite. SIS - Strawberry Intrusive Suite.)

24.3 (SIS) Poodle Pond Granite

25.0 (SIS) Dog Islands Granite

26.0 (SIS) Tukialik Granite

27.0 (LIS) Lanceground Hills Granite

28.0 (LIS) Pistol Lake Granite

29.0 (LIS) Tarun Granite

30.1 Big River Granite (porphyritic phase)

30.2 Big River Granite (equigranular phase)

n1 -- number of analyses for all elements except those listed below

n2 -- number of analyses for Sc, Sn, Cs, Sb, Yb and Hf



Trace element patterns are also similar, except for lower F, Sr and Ba in the syenite unit. This similarity is consistent with apparent gradational contacts between them in this area.

*Siliceous Granitoid Units* : Contrasts in geochemistry amongst these units are subtle. The Lanceground Intrusive Suite has slightly higher mean  $K_2O$ , and lower mean  $Al_2O_3$  and MgO than other granitoid units. The Bayhead granite has the least evolved and most variable major element composition in the Strawberry Suite; the Cape Strawberry and Poodle Pond Granites have the most evolved compositions. In the Lanceground Suite, the Pistol Lake Granite has the least evolved composition.

Trace element patterns in the Strawberry and Lanceground Intrusive Suites are similar, but there are small but consistent differences between them. Fluorine contents tend to be higher in the Strawberry Suite, as do Li, Sr and Ba. The Lanceground Suite shows generally higher levels of Zr, La, Ce, Y and other REE. Note that the high Pb content of the Dog Islands granite is a reflection of a single anomalous sample; if this is excluded, it is similar to other members of the suite.

The Big River Granite is similar to all of the above in major element composition, but has higher Ba and Sr, and lower F, Zn, Rb, Nb, La, Ce, Th and Y contents. Trace element abundances in the main phase of the Big River Granite are similar to those of the Numok Intrusive Suite although the latter has a much less evolved major element composition. The equigranular phase of the Big River Granite is more siliceous than the main phase, and has lower Ba and Sr, but shows similar levels for most other trace elements.

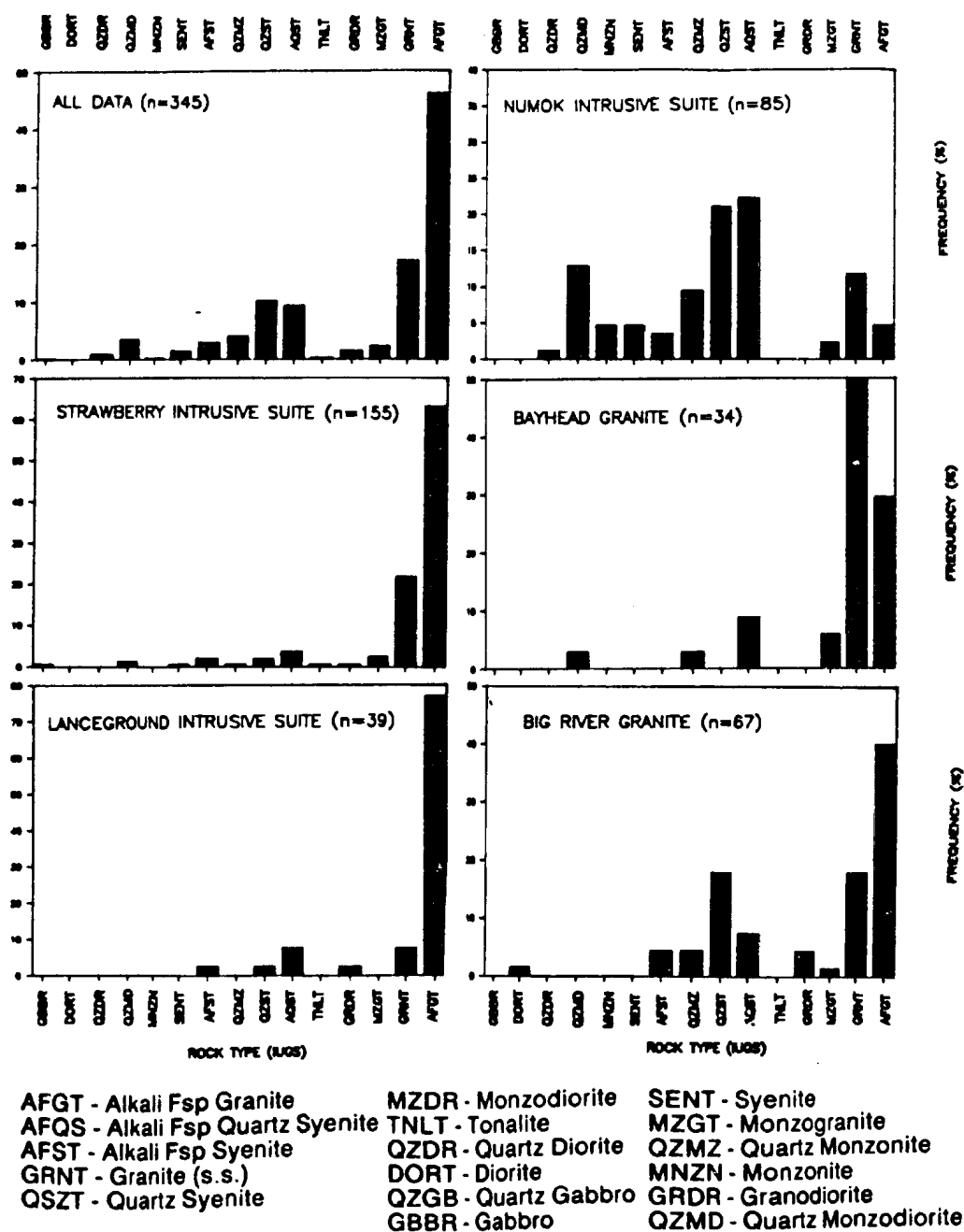


Figure 4.2 . Relative abundance of IUGS rock types calculated from normative mineralogy using the method of Streckeisen and LeMaitre (1979). Note that this is based on Barth mesonorms, not the CIPW norms listed in Table 4.2. Regional and geological sample populations only.

## Abundance and Distribution of Rock Types

Relative abundances of IUGS rock types calculated from normative data (regional and geological samples only, after Streckeisen and LeMaitre, 1979) show that post-tectonic Makkovikian rocks are dominated by alkali-feldspar granite and granite, with lesser quartz monzonite and quartz syenite (Figure 4.2). The general distribution resembles that of their syn-tectonic counterparts (Figure 3.2, p.74). The Numok Intrusive Suite is dominated by quartz monzonite, quartz syenite and alkali-feldspar quartz syenite. Siliceous granitoid units are dominated by alkali-feldspar granite and lesser granite (s.s). Alkali-feldspar granite is most abundant in the Lanceground Suite (ca. 80% of total). Within the Strawberry Suite, only the Bayhead Granite is dominated by granite (s.s); all other units are dominated by alkali-feldspar granite (up to 60% of total).

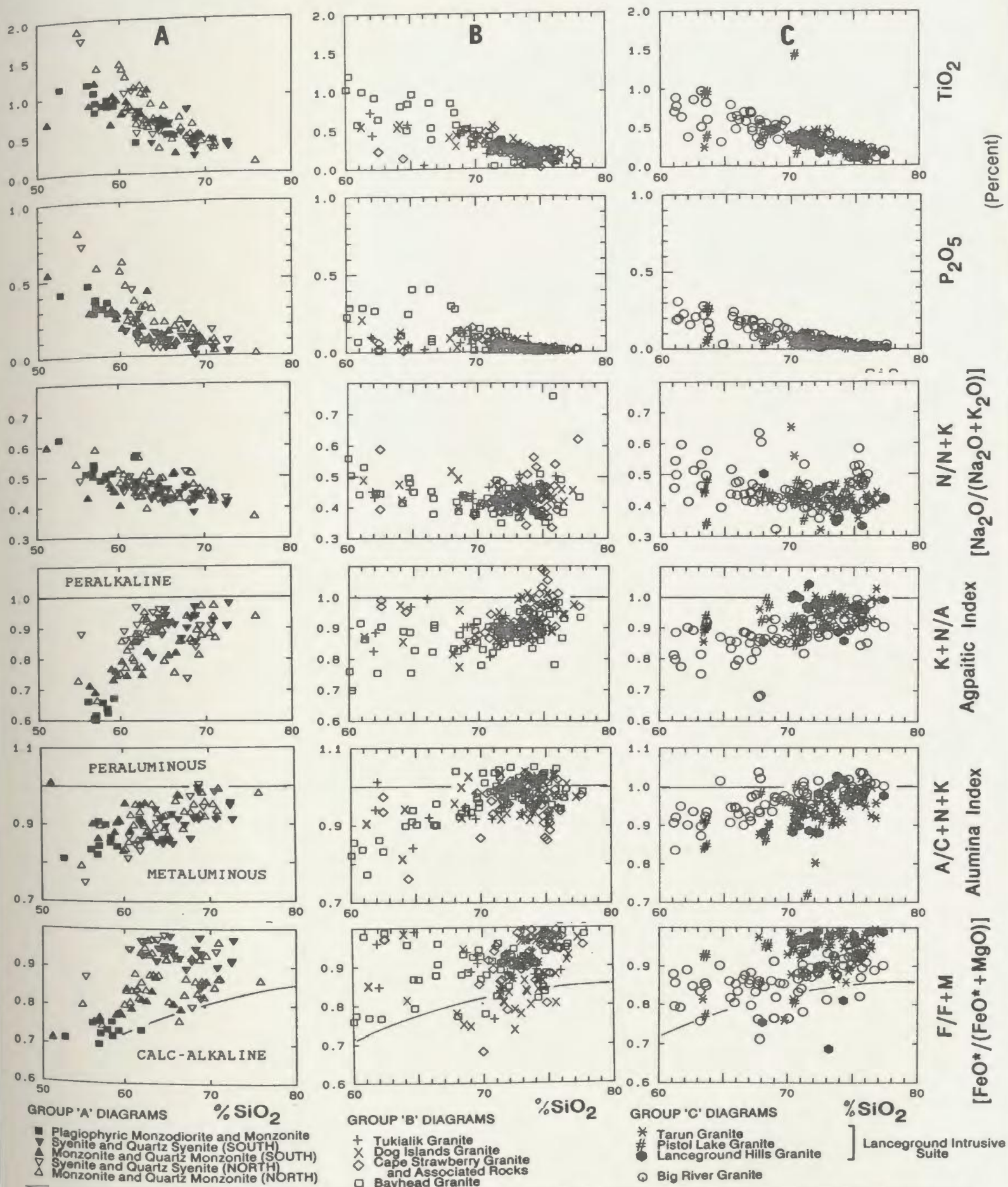
### 4.2.2 Geochemical Trends and Contrasts

Post-tectonic Makkovikian plutonic rocks are divided into three groups (A, B and C), represented by separate columns of diagrams in Figures 4.3 to 4.10. These subdivisions are intended primarily to reduce "clutter"; they do not necessarily imply genetic links between units.

Note that variation diagrams using  $\text{SiO}_2$  as the X-axis employ a different horizontal scale for the Numok Suite, as it has a greater  $\text{SiO}_2$  range. Y-axis scales are constant for all figure groups.

### Major Element Patterns

Major element trends against  $\text{SiO}_2$  show expected patterns, and do not discriminate between units well. The



Numok Suite is dominated by rocks with  $< 65\%$   $\text{SiO}_2$ ; these have the highest levels of other major elements except  $\text{Na}_2\text{O}$  and  $\text{K}_2\text{O}$  (see Table 4.2). Amongst the siliceous granitoid rocks, the Big River Granite and Bayhead Granite show the greatest range of major element compositions. Other units within the Strawberry Suite, and the Lanceground Suite, have restricted  $\text{SiO}_2$  ranges (70-77%).

$\text{TiO}_2$  and  $\text{P}_2\text{O}_5$  (Figure 4.3) define separate trends for the northern and southern zones of the Numok Suite that coalesce at ca. 65% silica; the northern zone is enriched in both.  $\text{N/N+K}$  [ $\text{Na}_2\text{O}/(\text{Na}_2\text{O} + \text{K}_2\text{O})$ ] ratios (Figure 4.3) show a pronounced negative trend against  $\text{SiO}_2$  in the Numok Suite, indicating relative enrichment of  $\text{K}_2\text{O}$  with differentiation, but are approximately constant in other units.  $\text{N/N+K}$  is almost invariably  $\leq 0.5$  above 70%  $\text{SiO}_2$ , except in a few Na-enriched samples from the Strawberry Intrusive Suite.

$\text{K+N/A}$  (agpaitic index) values are generally  $> 0.95$ , and both the Strawberry and Lanceground Suites are locally peralkaline.  $\text{A/C+N+K}$  ratios increase smoothly with  $\text{SiO}_2$  (reflecting decreasing Ca for the most part), and parts of the Strawberry Suite (notably the Bayhead Granite) are weakly peraluminous. No units are dominated by peraluminous rocks. All units show high  $\text{F/F+M}$  (generally  $\geq 0.85$ ), with the exception of parts of the Numok Suite. They lie above the calc-alkaline field indicated by Anderson (1983), and are akin to his "anorogenic" association.

Ternary AFM and CNK projections (Figure 4.4) demonstrate a superficial calc-alkaline trend for all units. Note the alkali-rich nature of even the silica-deficient rocks in the Numok Intrusive Suite. Alkali-lime indices ( $\text{SiO}_2$  content at which  $\text{Na}_2\text{O} + \text{K}_2\text{O} = \text{CaO}$ ) are difficult to calculate, as very few samples have  $\text{CaO} > (\text{Na}_2\text{O} + \text{K}_2\text{O})$ . Linear regression of all

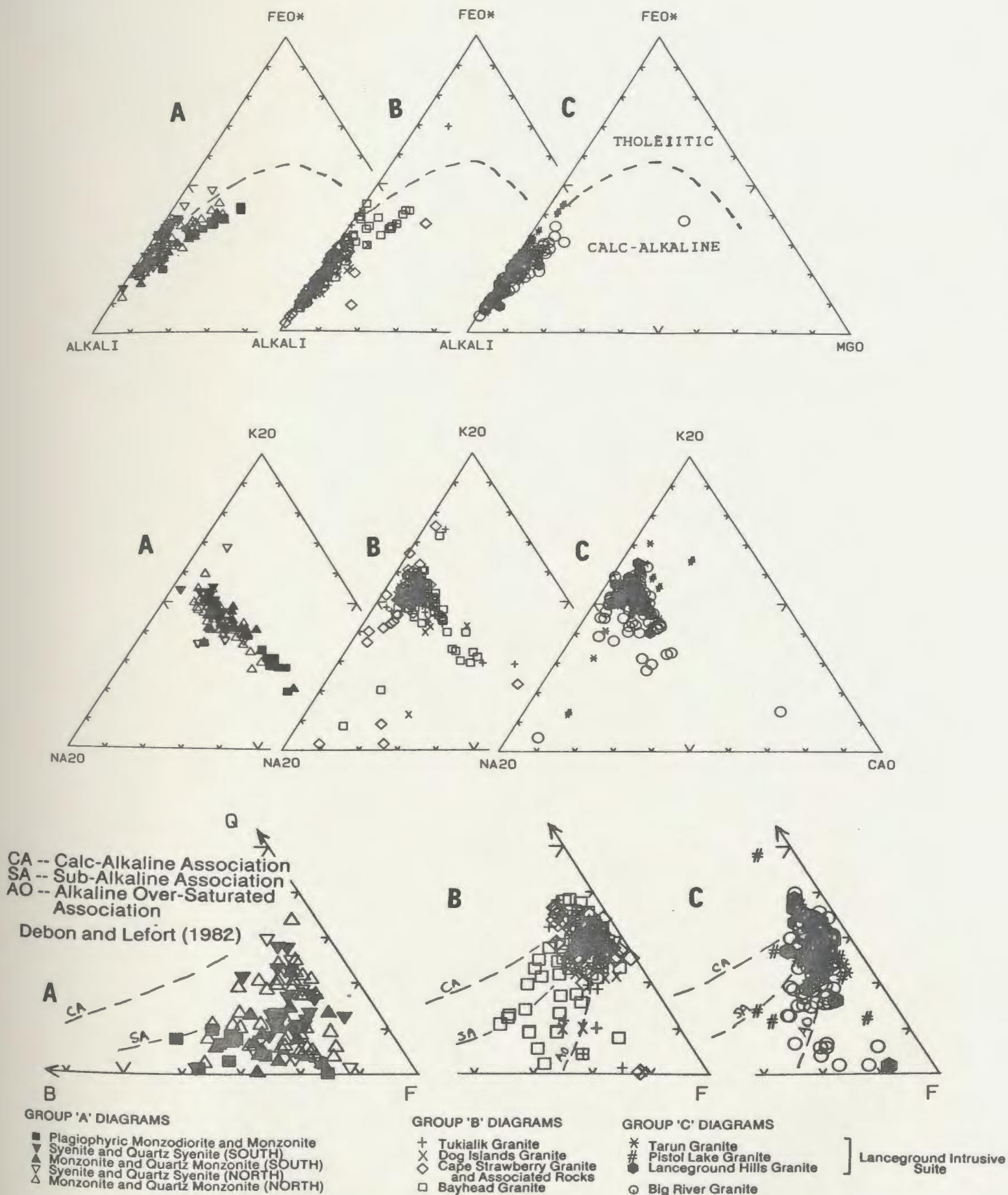


Figure 4.4. AFM, CNK and QBF projections for post-tectonic Makkovikian plutonic units. See text for discussion.



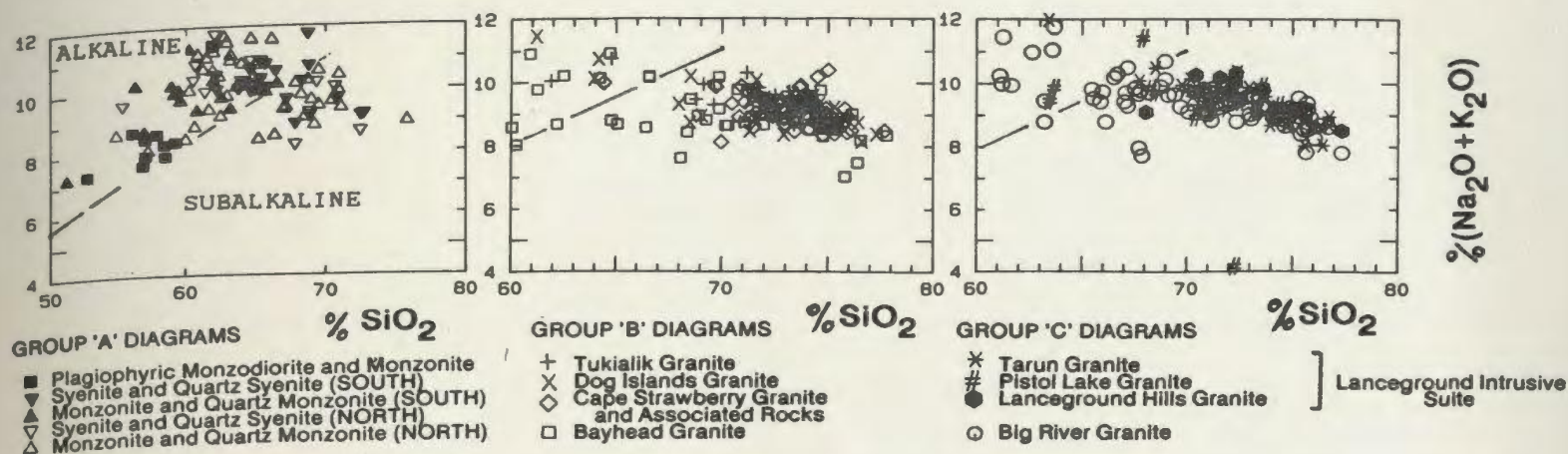


Figure 4.4 (continued). (Na<sub>2</sub>O+K<sub>2</sub>O) - SiO<sub>2</sub> projection for post-tectonic Makkovikian plutonic units. Alkaline and subalkaline fields from Irvine and Baragar (1971).

post-tectonic Makkovikian data suggests a value of ca. 55 % SiO<sub>2</sub>, i.e. alkali-calcic in the terminology of Peacock (1931). The CNK diagram also illustrates minor alkali disturbance in the Strawberry Suite.

The Q-B-F ternary projection (Figure 4.4) of Debon and Lefort (1982) indicates an affinity to their "alkaline-oversaturated" association, rather than typical calc-alkaline suites. In the (Na<sub>2</sub>O+K<sub>2</sub>O)-SiO<sub>2</sub> plot (Figure 4.4), many of the Numok Intrusive Suite rocks fall in the alkaline field of Irvine and Baragar (1971).

### Normative Compositions

No units contain significant normative corundum (Table 4.2). In the quartz - albite - anorthite - orthoclase quaternary system (Figure 4.5), only the Numok Suite contains significant anorthite. The total proportion of normative An in the quaternary system is ≤ 5% for virtually all of the siliceous granitoid units.

In the Q-Ab-Or projection, granites of the Strawberry and Lanceground Suites are clustered tightly around the

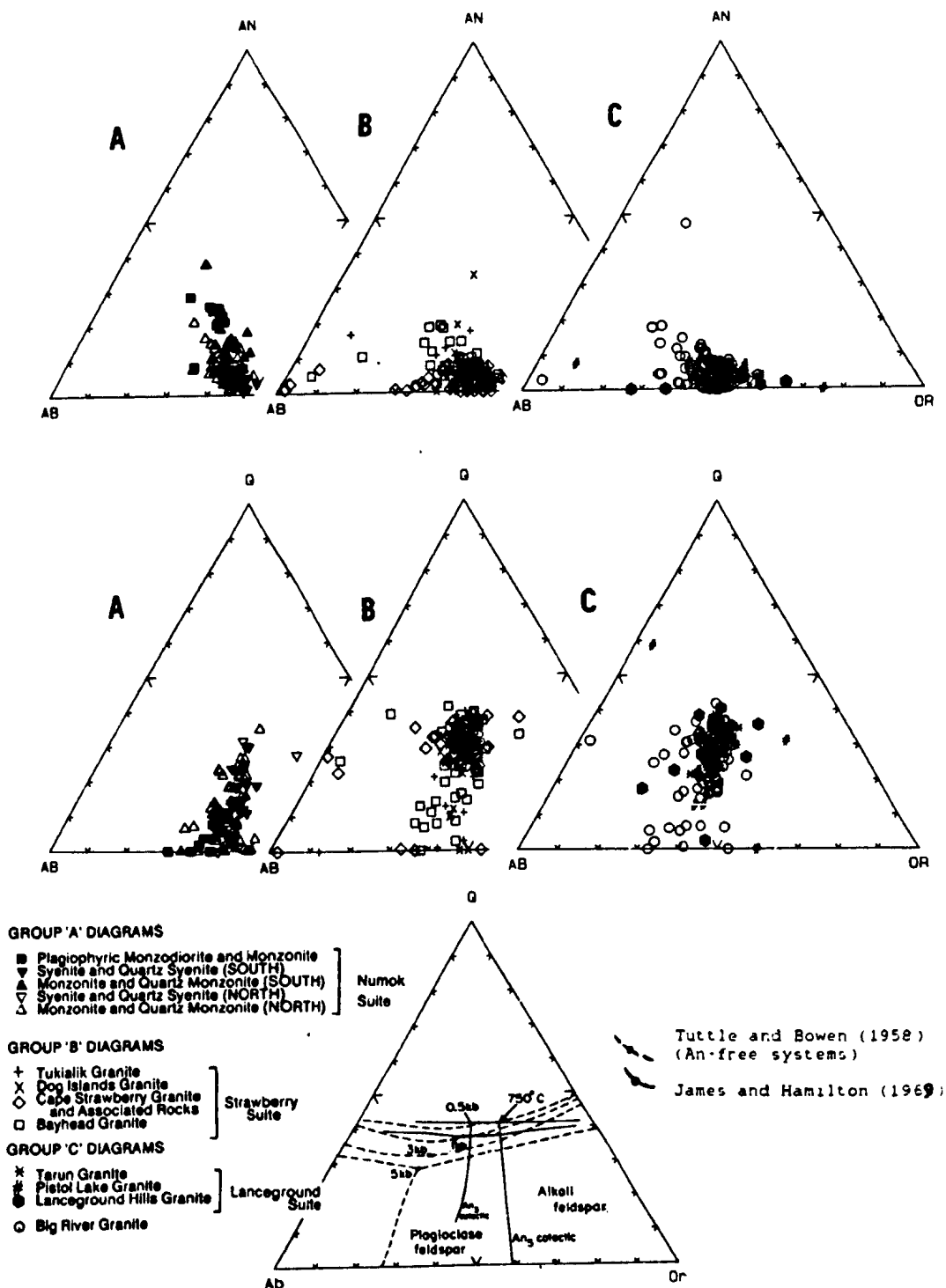


Figure 4.5. Variation of post-tectonic Makkovikian plutonic rocks in the quartz - albite - anorthite - orthoclase quaternary system. All norms are CIPW. See text for discussion.



ternary minimum for appropriate Ab/An ratios (James and Hamilton, 1969). The Numok Suite defines a smooth trend from quartz-free monzodiorites to granites that are close to minimum melt compositions. This trend is coincident with plagioclase - K-feldspar cotectic lines derived experimentally by (James and Hamilton, 1969; Figure 4.5), but these are not strictly applicable to the least evolved rocks of the Numok Suite, which contain 7-20% An (relative to quaternary system). The less differentiated members of the Bayhead and Big River Granites cluster around this same trend.

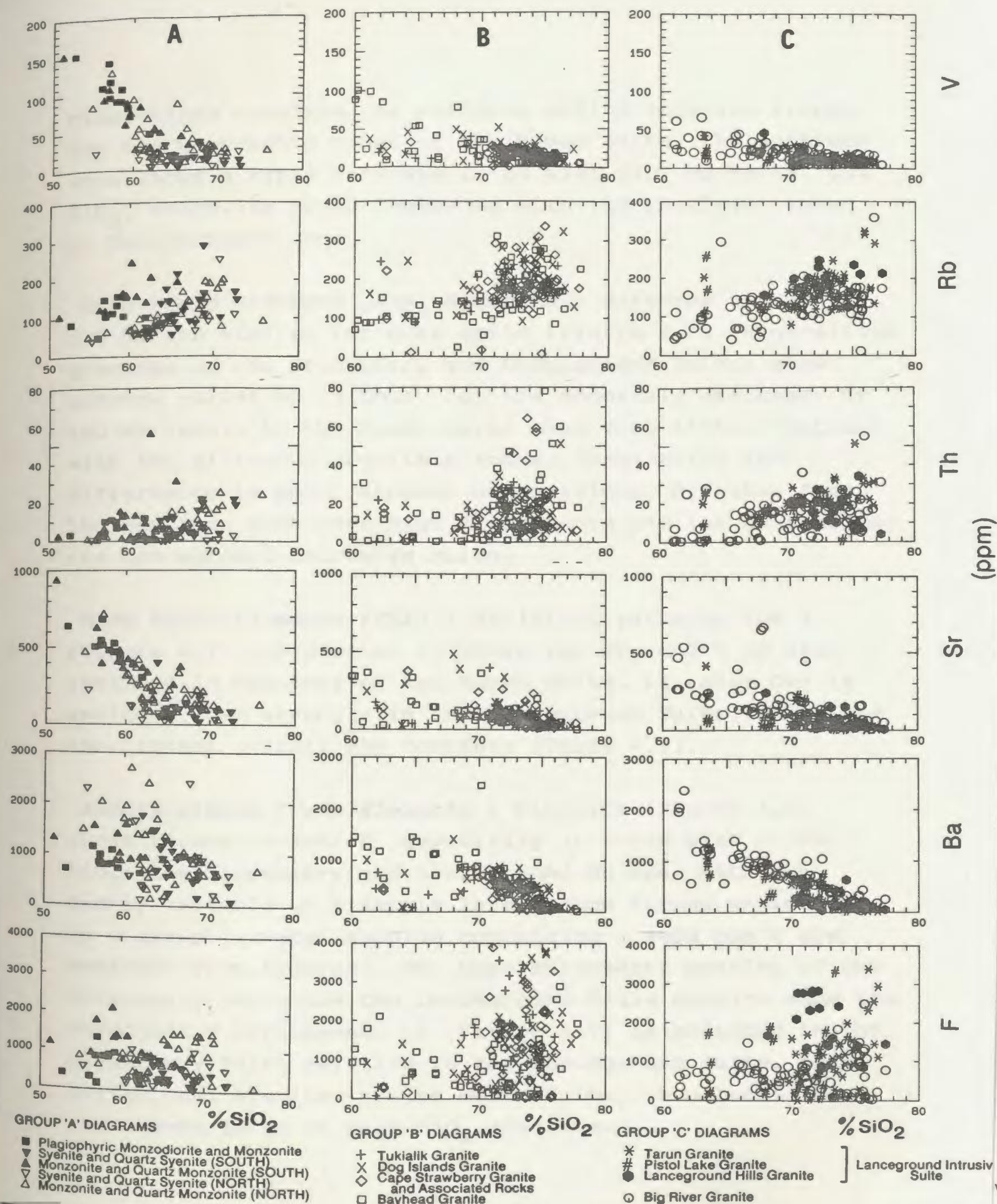
#### Trace Element Patterns

*Octahedrally Co-ordinated Cation (OCC) Elements* : V, Cr, Cu, Ni, and Sc all show strong inverse correlation with  $\text{SiO}_2$  (e.g. V, Figure 4.6). These elements do not discriminate between units.

*Low Field Strength (LFS) Elements* : Incompatible LFS elements (e.g. Rb and Th, Figure 4.6) provide little distinction between units. Rb defines two trends in the Numok Intrusive Suite; many rocks with  $< 65\%$   $\text{SiO}_2$  in the southern zone show Rb contents similar to those of siliceous granitoid units.

Rb and Th are enriched in Strawberry Suite granites, and are scattered above ca.  $70\%$   $\text{SiO}_2$ . Similar disorganized variation is shown by U and Pb (not figured).

Sr and Ba show inverse trends against  $\text{SiO}_2$  (Figure 4.6), and resemble patterns for compatible OCC trace elements. Sr is highest in parts of the Numok Intrusive Suite, particularly the southern area, where the plagiophyric monzonite unit is probably partly a



plagioclase cumulate. Ba patterns define separate trends for the geographic zones of the Numok Suite. The northern zone shows a rapid decrease in Ba with  $\text{SiO}_2$  up to ca. 65%  $\text{SiO}_2$ , where its trend coalesces with the shallower trend of the southern zone.

**High Field Strength (HFS) Elements** : Patterns for Zr and Nb are similar for most units (Figure 4.7). High-silica granites of the Strawberry and Lanceground Suites show extreme variation in both, but are generally enriched. Zr and Nb levels in the Numok Suite show very little contrast with the siliceous granitoid rocks, considering the differences in major element compositions. Syenites from the southern zone have high Zr contents similar to those of the Lanceground Intrusive Suite.

**Rare Earth Elements (REE)** : Variation patterns for Y (Figure 4.7) are similar to those for Zr, and Y is also enriched in syenites of the Numok Suite. La (also Ce) is enriched most strongly in the Lanceground Suite, which has the highest overall REE contents (Table 4.2).

**Indeterminate Trace Elements** : Fluorine (Figure 4.6) shows strong variation, especially in rocks with > 70%  $\text{SiO}_2$ . The Strawberry and Lanceground Suites, although highly variable at a sample level, show strong enrichment as a group (several samples containing > 4000 ppm F are excluded from figures). The Cape Strawberry granite of the Strawberry Suite and the Lanceground Hills Granite show the strongest F enrichment. Li (Figure 4.7) is enriched in the Strawberry Suite relative to the Lanceground Suite. Both suites, and syenites of the Numok Suite, show local enrichment in Zn at high  $\text{SiO}_2$  contents.



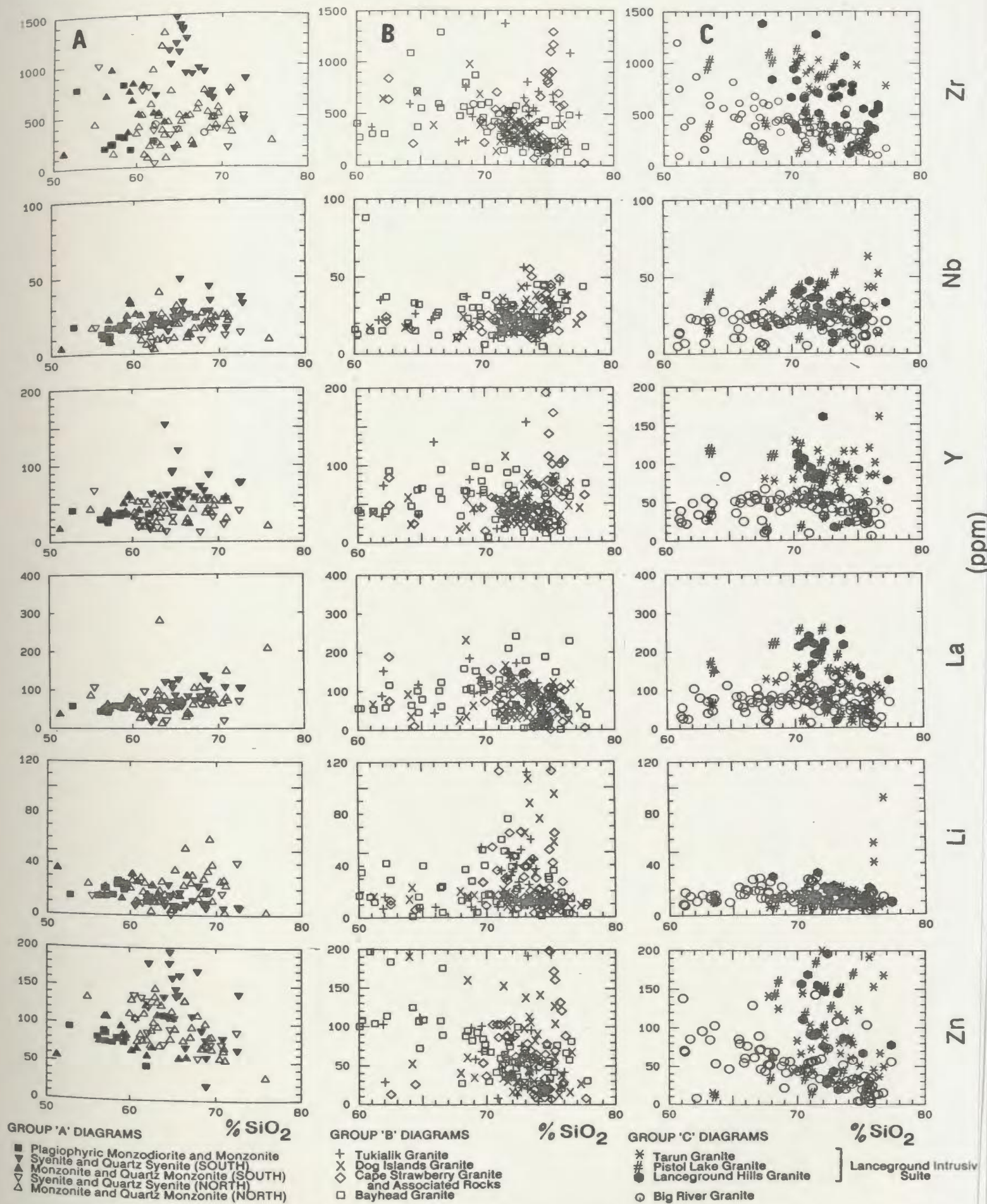


Figure 4.7. Zr, Nb, Y, La, Li, Zn and F versus  $\text{SiO}_2$  in post-tectonic Makkovikian plutonic units. See text for discussion.

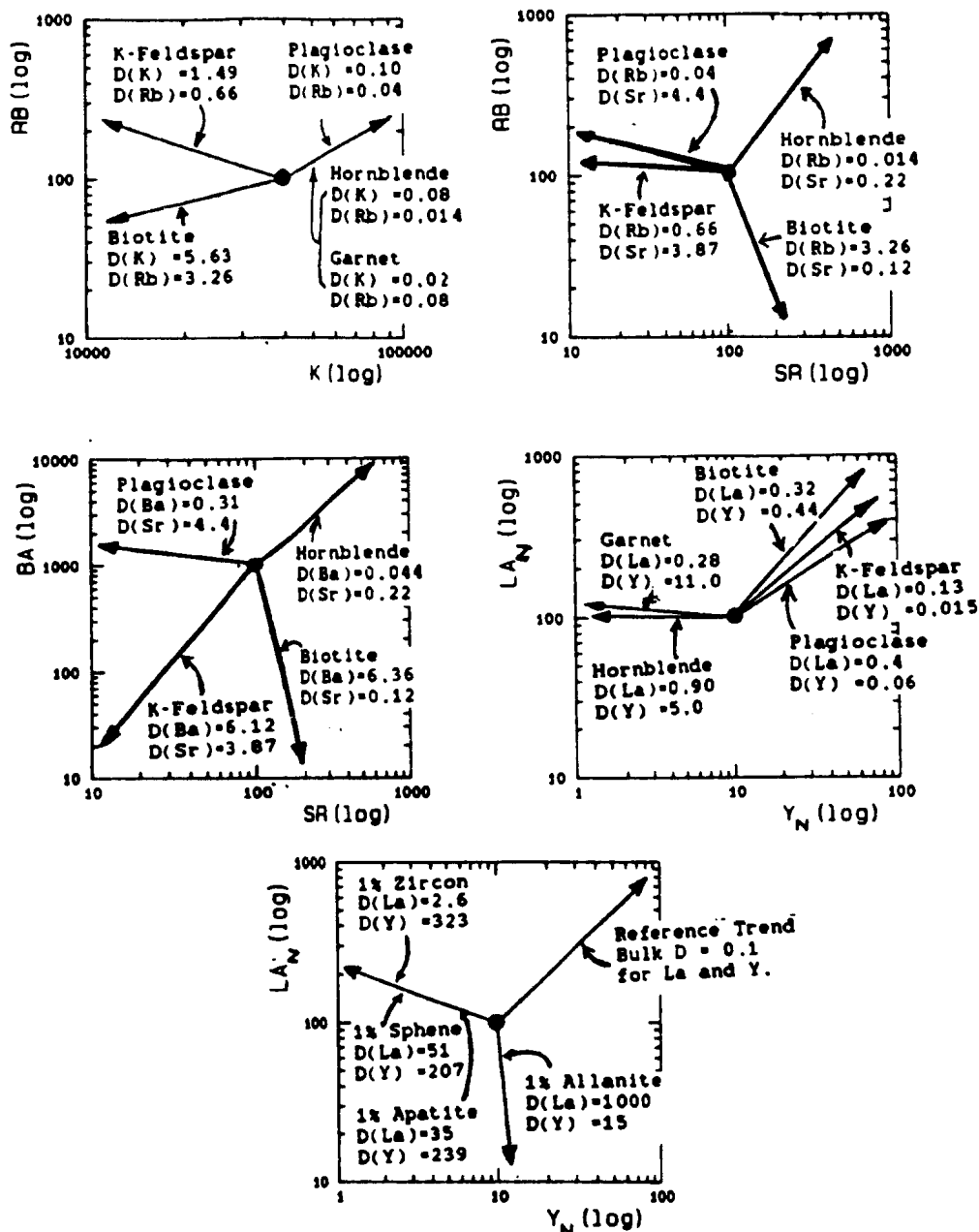
### Trace Element Ratios

K/Rb ratios (Figure 4.8) range from ca. 1000 in the northern area of the Numok Intrusive Suite to less than 150 in granites of the Strawberry Suite. The southern zone of the Numok Suite shows lower K/Rb than the northern zone.

Rb/Sr ratios range from 0.1 to 10.0 (Figure 4.8) and define flat-lying to slightly negative trends for all units.

Ba/Sr ratios (Figure 4.8) vary from 10.0 to 1.0, and define linear or curvilinear positive trends. The Numok Suite has two distinct trends; the southern zone trend is initially flat-lying (i.e. constant Ba, increasing Ba/Sr) whereas the northern zone has essentially constant Ba/Sr throughout. The Strawberry Intrusive Suite has a well-defined curved trend, where Ba/Sr initially increases to ca. 10.0, but decreases to  $< 1.0$  in the most  $\text{SiO}_2$ -rich rocks. The Big River Granite shows a similar curved trend, but the Lanceground Intrusive Suite shows essentially constant Ba/Sr.

In comparison to reference trends for fractionation of common minerals (Figure 4.8, inset), these trends are consistent with fractionation of plagioclase and/or K-feldspar. The contrasting trends in the Numok Suite imply that plagioclase extraction was initially more important in the southern zone. The curved Ba/Sr trend of the Strawberry Intrusive Suite suggests an increase in the relative proportion of K-feldspar extracted (assuming that partition coefficients for both minerals remained constant). It is closely similar to the trend for the syn-tectonic Kennedy Mountain Intrusive Suite (Figure 3.10, p.89). The constant Ba/Sr trend of the Lanceground Intrusive Suite implies little or no plagioclase fractionation, consistent with its variably hypersolvus character.



Idealized fractionation trends for Rayleigh fractionation (i.e. perfect separation of crystals and liquid). The  $LA_N/Y_N$  trends for accessory phases show the effects of only 1% of each phase upon a reference trend where bulk partition coefficients for the remaining 99% of the fractionate are 0.1 for both La and Y. The latter approximates a "normal" path for fractionation of common silicates. Partition coefficient data from compilations by Arth (1976) and Hanson (1978) for most minerals, and from Gromet and Silver (1983) for allanite and sphene.

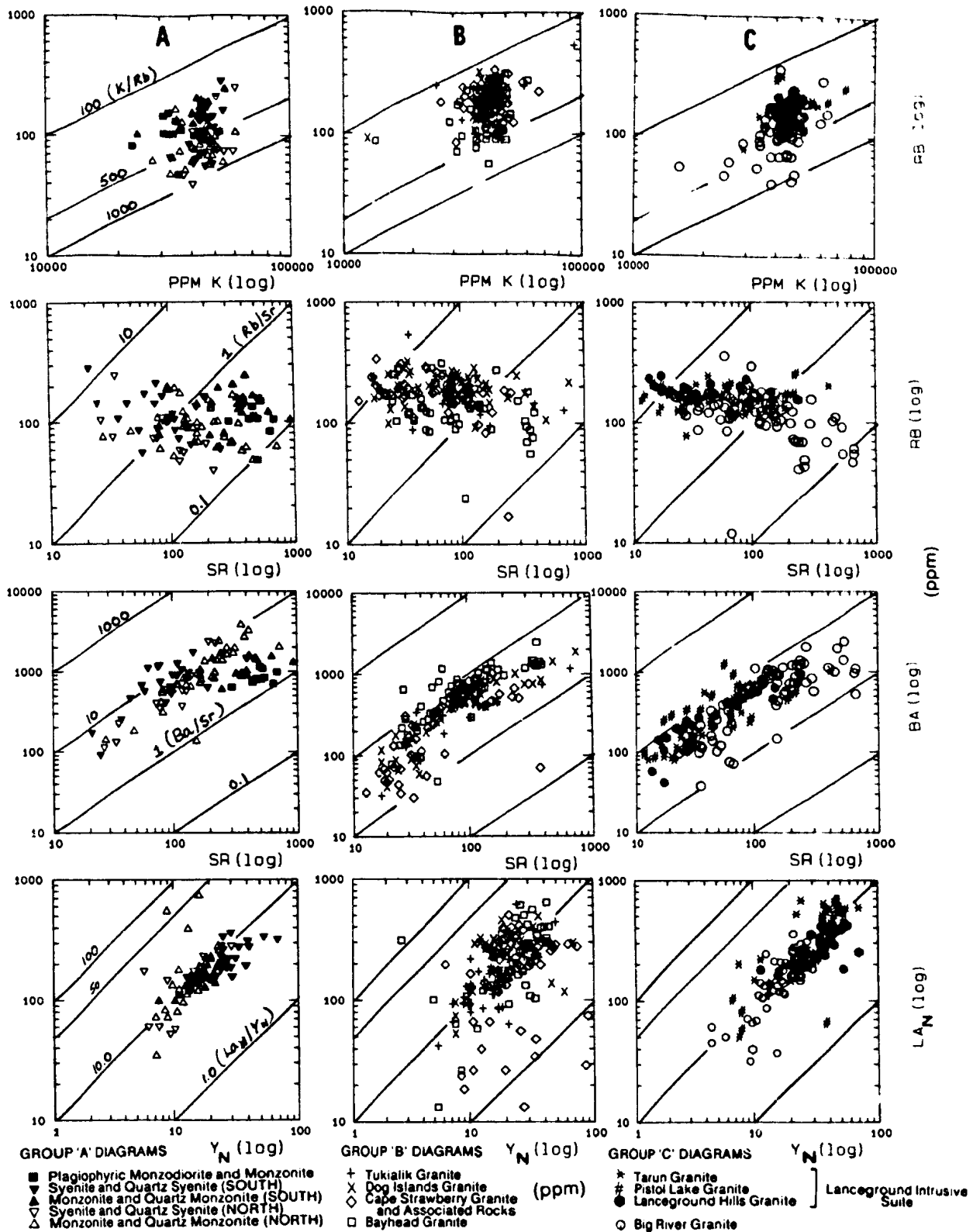


Figure 4.8 . Variation in the trace element ratios K/Rb, Rb/Sr, Ba/Sr and  $La_N/Y_N$  in post-tectonic Makkovikian plutonic rocks. See opposite for reference fractional crystallization trends.

$\text{La}_N/\text{Y}_N$  ratios (both elements normalized to chondritic values) are remarkably consistent during evolution of the Numok Intrusive Suite and Lanceground Suite ( $\text{La}_N/\text{Y}_N$  ca. 10). Increases in both with  $\text{SiO}_2$  (Figure 4.7) argue against significant extraction of accessory phases. The Strawberry Suite shows a similar range of values, but is locally anomalous ( $\text{La}_N/\text{Y}_N < 10$ , or even  $< 1$ ). This is consistent with local fractionation of LREE-enriched phases such as allanite, which occurs in "cumulate" mafic mineral layers in some of these granites.

#### Rare Earth Element (REE) Patterns

REE patterns are similar for all post-tectonic Makkovikian units (Figure 4.9; data in Appendix B). The Numok Intrusive Suite shows the least fractionated REE pattern, but absolute REE abundances approach those shown by siliceous granitoid units. A monzonite from the northern zone shows a small negative Eu anomaly, but syenites from both zones appear to lack Eu anomalies. This is puzzling in view of evidence for feldspar fractionation outlined by Ba-Sr-Rb behaviour (Figure 4.8), but it is not yet clear if this absence is a general feature of syenites in the suite. K-feldspar was probably the dominant fractionating phase in these rocks, but should also generate a negative Eu anomaly (e.g. Hanson, 1978).

Strawberry Intrusive Suite granites show identical REE patterns that are characterized by steep LREE profiles, coupled with negative Eu anomalies and flat to slightly fractionated HREE patterns. These are closely similar to REE patterns from the syn-tectonic Kennedy Mountain Intrusive Suite (Figure 3.11, p.91). Patterns for the Lanceground Intrusive Suite are identical in shape to both,



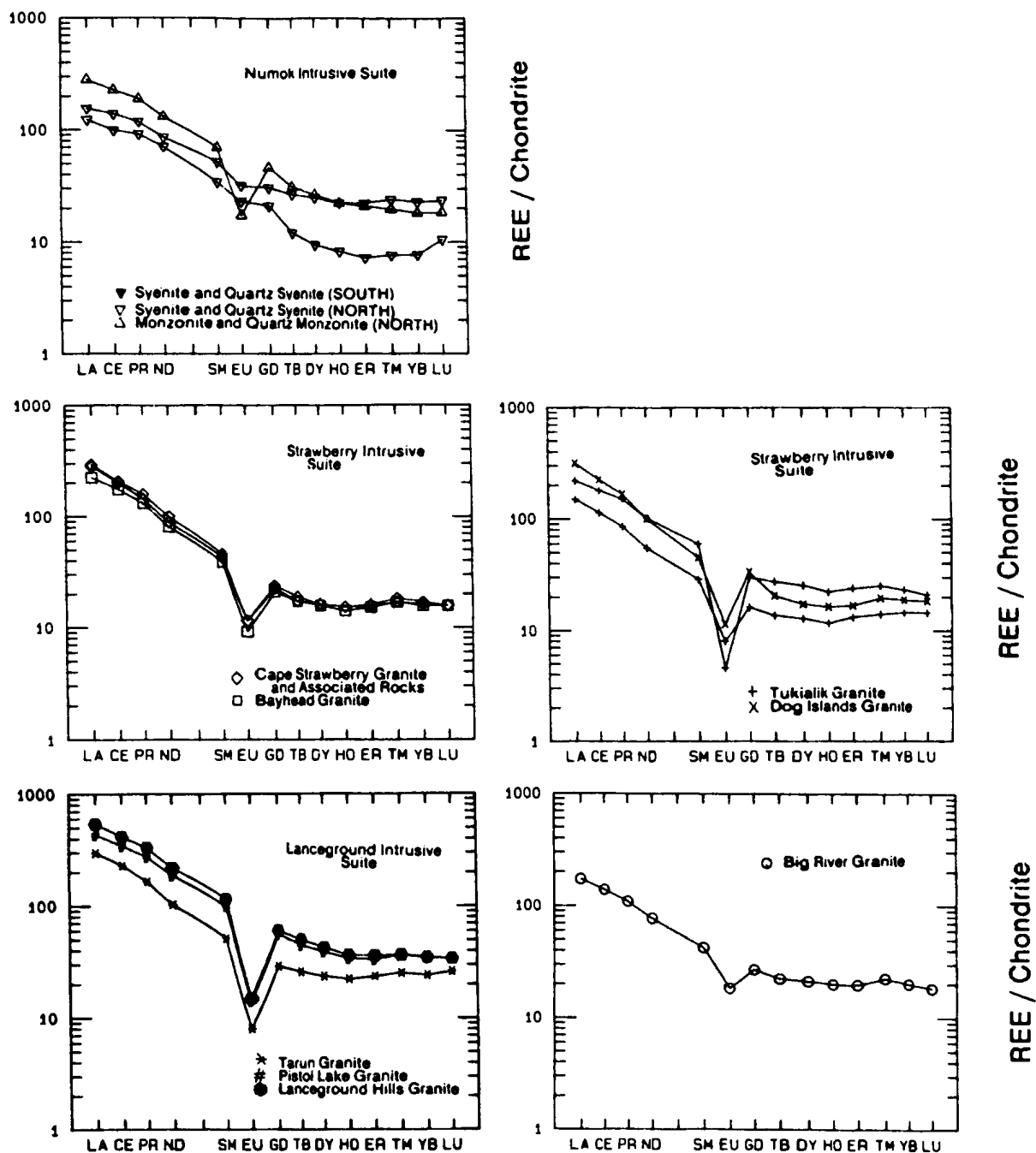


Figure 4.9 . Rare Earth element (REE) patterns for representative post-tectonic Makkovikian plutonic rocks. Values are normalized to chondritic values (listed in Appendix C).

but show higher overall REE abundances (up to 800 x chondrite). The Big River Granite shows an unremarkable pattern that resembles both of the above in general terms, but has a smaller Eu anomaly.

#### 4.3 SUMMARY AND DISCUSSION

##### **Geological and Geochemical Continuity**

All post-tectonic Makkovikian units described here are of regional extent in the sense that they outcrop over hundreds of square kilometres, or occur as discrete, closely similar bodies dispersed over wide areas. Those that retain contacts with country rocks show intrusive relationships, and there is no sign of extensive migmatization around them. They are generally homogeneous, and contain xenoliths only in their marginal zones. They are clearly discordant magma bodies that have risen from depths well below the current level of exposure.

A generalized distinction can be made between the Numok Intrusive Suite and siliceous granitoid rocks. The former is dominated by quartz-poor rock types (monzonite to quartz syenite) that are associated (in the south) with plagiophyric monzodiorite and monzonite of probable cumulate origin. Mafic inclusions in the agmatitic border zone of the quartz monzonite unit (in the north) also suggest a general association with mafic magmas.

Siliceous granitoid units, in contrast, are dominated by quartz-rich, K-feldspar porphyritic, commonly fluorite-bearing, biotite or biotite-hornblende granite and alkali-feldspar granite. Although textural and mineralogical differences allow suites and units to be defined amongst these rocks, the similarities between them far outweigh any differences.

The separation between the Numok Suite and these rocks is not, however, absolute; the most differentiated variants of the former include granites and alkali-feldspar granites, and some Numok Suite quartz syenites resemble the Lanceground Intrusive Suite. A possible link between them is suggested by local relict fayalite in both; this is an uncommon phase, reported mostly from granites of anorogenic or "rapakivi" associations (e.g. Anderson, 1983).

Siliceous granitoid rocks also have some features in common. For example all units locally contain minor blue sodic amphibole and/or relict aegirine-augite, and a small proportion of peralkaline rocks; such features are also common in anorogenic granitoid assemblages.

Trace element geochemistry further emphasizes the continuity of the post-tectonic assemblage. The Numok Intrusive Suite is distinct in terms of major element patterns (i.e. less siliceous, yet obviously alkali-rich), and also for some compatible OCC and LFS trace elements. However, it has REE, LFS and HFS element contents similar to siliceous granitoid units. The latter have very coherent trace element patterns. There are some absolute distinctions, e.g. higher F in the Strawberry Suite, and higher Zr, Y and REE in the Lanceground Suite, but there is an overwhelming similarity between all these rocks.

This geochemical continuity is also geographically continuous; the various units of the Strawberry Intrusive Suite show closely similar characteristics over large distances (125 km). Such continuity implies a close similarity in petrogenetic processes and source materials or magmas across this distance, and indicates that a single model is required for all these granites. It is particularly significant in interpretation of Nd isotopic

data from these rocks (Chapter 8). Similar arguments apply to the Lanceground Suite, although the geographic area represented by these rocks is somewhat smaller.

#### **Origin of Compositional Variations**

**Numok Intrusive Suite :** Trace element data (notably Rb, Sr and Ba) indicate that compositional evolution reflects feldspar ( $\pm$  mafic mineral) fractionation, and that there were differences in the fractionation histories of northern and southern zones. In the southern zone, extraction of plagioclase was initially prevalent; the subsequent Ba depletion indicates increasing removal of K-feldspar. In the northern zone, K-feldspar fractionated throughout evolution, and both feldspars were removed in relatively constant proportions. This is consistent with the presence of the plagiophyric monzonite (which is probably a plagioclase cumulate) in the southern zone. The differences between northern and southern zones suggest that each represents a different level or magma batch within the Numok magma chamber. The identity and composition of the parental magma is uncertain, as the least evolved rocks (plagiophyric monzonites) are not liquid compositions. To produce the observed compositional range, it must have been at least as mafic as monzonite, assuming that the plagiophyric unit is a crystal accumulation.

**Strawberry Intrusive Suite :** Rb, Sr and Ba data indicate that evolution of these magmas was dominated initially by plagioclase fractionation but that K-feldspar quickly became dominant. This is consistent with the presence of plagioclase phenocrysts in the least differentiated rocks (e.g. Bayhead Granite).

Euhedral accessory minerals in mafic mineral layers in some of these granites imply that fractionation of such phases became important at high  $\text{SiO}_2$  contents but, as most granites are enriched in HFS elements and REE, this must have been a late phenomenon. Fine-grained granites of the Poodle Pond area, which are interpreted as high-level sills linked to subsurface Cape Strawberry Granite, show depletion of LREE and Fluorine relative to normal levels in the suite (Table 4.2). Such features are compatible with extraction of biotite and allanite ( $\pm$  amphibole) in the latter stages of evolution. The presence of cumulus textures implies a low viscosity during crystallization. Tuffisite breccias and miarolitic cavities indicate that the Cape Strawberry Granite attained high emplacement levels and exsolved volatiles, which also implies a low solidus temperature.

The high F content of the suite (as there is evidence of volatile loss, this is probably an underestimate of the actual F content at the time of emplacement) provides an explanation for these features, as fluorine reduces viscosity and solidus temperatures in experimental melts (e.g. Dingwell, 1988).

Kerr (1988) has shown that the Cape Strawberry Granite shows well-developed compositional variation, independent of obvious petrographic contrasts, that is related to distance from its southern contact.  $\text{SiO}_2$ , U, Rb, Th and Pb increase towards this contact, and Ba, Sr and Li are depleted. HFS and RE elements show contradictory behaviour; they are depleted towards some areas of the contact, but enriched in others. Zonation patterns of this type resemble those reported from rhyolitic ash-flow tuffs (e.g. Hildreth, 1979, 1981) and also from high-silica granites (e.g., Tuach et al., 1986). Although fractional crystallization,

particularly involving accessory phases, can account for such patterns (e.g. Michael, 1983), in-situ geochemical gradients of this type may also reflect liquid-state processes such as thermogravitational diffusion or convective fractionation (e.g., Hildreth, 1981; Rice, 1981; MacDonald and Smith, 1988). Dingwell (1988) pointed out that F-enrichment may promote the operation of such processes, by a direct increase in diffusion rates, and also by increasing the longevity of magmatic systems via solidus depression. Processes of this nature may have modified and disturbed trace element patterns produced by fractionation. Strong variation in a range of trace elements above ca. 70% SiO<sub>2</sub> (Figures 4.6; 4.8) is probably a result of these effects.

***Lanceground Intrusive Suite*** : The Lanceground Intrusive Suite is locally a hypersolvus granite. Such characteristics imply relatively dry magma and high levels of emplacement. Geochemical variation is largely a result of K-feldspar fractionation, as the Ba/Sr trend is very close to the ideal Rayleigh fractionation trend for this mineral (Figure 4.8). Mineralogical similarities (e.g. fayalitic olivine, local hypersolvus character) suggest a genetic link between the Lanceground Suite and syenitic rocks of the Numok Suite. HFS element and REE enrichment, and Sr depletion, is qualitatively consistent with derivation by fractionation of the Numok Suite, which shows similar tendencies at a lower SiO<sub>2</sub> content.

***Big River Granite*** : Evolution of the Big River Granite appears to have been generally similar to that of the Strawberry Intrusive Suite, i.e. initial plagioclase-dominated fractionation, followed by increasing removal of K-feldspar.

Pseudorapakivi textures are consistent with this interpretation, but provide an interesting problem in themselves. Classical rapakivi textures are commonly interpreted to result either from intersection of the liquidus and feldspar solvus due to high vapor pressure (Tuttle and Bowen, 1958), or from expansion of the plagioclase field in the granite system due to vapor pressure reduction (Stewart, 1959). Both readily explain mantling of K-feldspar by plagioclase, but do not provide a simple explanation for reverse textures, which apparently require contraction of the plagioclase stability field. The best explanation is that crystallization of the Big River Granite took place close to the plagioclase-alkali feldspar cotectic, where a small change in physical conditions would produce the required effect. This is supported by the proximity of the Big River data to the cotectic lines determined by James and Hamilton (1969) (Figure 4.5).

#### Similarity of Post-Tectonic and Syn-Tectonic Makkovikian Associations

There are many similarities between post-tectonic Makkovikian plutonic rocks and some of the syn-tectonic associations described in Chapter 3. This is most obvious in the case of the syn-tectonic metaluminous-peralkaline association comprising the Long Island quartz monzonite and Kennedy Mountain Intrusive Suite. In contrast, there are no presently recognized post-tectonic equivalents of the syn-tectonic peraluminous association.

Table 4.3 lists average major element, trace element and partial CIPW normative compositions for several syn- and post-tectonic suites. There is a good correspondence between the granites of the Strawberry and Kennedy Mountain

Table 4.3 . Comparison of average compositions for selected syn-tectonic and post-tectonic Makkovikian plutonic units.

UNIT	10		20		21		11 (all)		11 (unaltd)	
n1	15		57		40		108		97	
n2	5		12		6		22		23	
(Wt%)	Mean	S.D.	Mean	S.D.	Mean	S.D.	Mean	S.D.	Mean	S.D.
SiO <sub>2</sub>	63.32	1.27	62.31	4.27	65.52	3.92	73.74	3.09	73.58	2.98
TiO <sub>2</sub>	0.88	0.06	0.78	0.29	0.63	0.29	0.28	0.18	0.29	0.19
Al <sub>2</sub> O <sub>3</sub>	15.81	0.24	16.69	1.49	15.07	1.21	12.65	1.13	12.67	1.15
Fe <sub>2</sub> O <sub>3</sub>	1.79	0.37	1.72	0.75	1.44	0.61	1.29	0.67	1.24	0.70
FeO	3.06	0.73	3.41	1.12	3.66	1.75	1.34	1.13	1.39	1.17
MnO	0.10	0.01	0.12	0.05	0.15	0.07	0.06	0.03	0.06	0.02
MgO	1.25	0.42	1.22	0.87	0.40	0.29	0.19	0.24	0.19	0.25
CaO	2.95	0.48	2.92	1.30	1.76	0.71	0.84	0.61	0.82	0.56
Na <sub>2</sub> O	4.27	0.25	4.57	0.41	4.51	0.57	4.40	1.08	4.00	0.48
K <sub>2</sub> O	4.75	0.49	5.14	1.09	5.81	0.67	4.29	1.56	4.85	0.64
P <sub>2</sub> O <sub>5</sub>	0.26	0.03	0.24	0.14	0.15	0.13	0.05	0.05	0.05	0.05
LOI	0.63	0.23	0.58	0.35	0.46	0.23	0.45	0.21	0.45	0.22
TOTAL	99.07		99.67	0.00	99.54		99.58		99.57	
(ppm)	Trace Elements									
Li	22.7	5.7	21.0	9.7	13.0	7.6	14.6	11.3	14.9	11.7
F	860.5	212.7	928.9	436.3	427.8	270.3	1014.0	847.4	1029.9	803.8
Sc	9.6	1.7	10.5	2.1	11.0	3.8	1.3	0.9	1.4	0.9
V	74.6	19.6	55.9	37.5	17.7	10.0	15.6	12.7	15.9	13.4
Cr	5.5	3.5	7.0	9.9	3.4	2.4	5.0	3.8	4.7	3.8
Ni	2.6	1.9	3.7	4.7	1.1	0.5	1.4	1.2	1.3	1.2
Cu	9.1	3.8	13.6	9.5	6.4	3.1	3.8	3.8	3.9	3.9
Zn	74.1	8.5	86.3	23.4	114.3	44.2	81.8	53.3	77.1	29.9
Ca	18.3	1.2	20.5	2.9	21.6	6.3	16.6	7.3	16.5	6.8
Rb	126.4	24.2	121.9	47.9	110.8	54.5	134.6	64.9	153.5	47.1
Sr	327.6	39.0	329.4	166.6	108.5	77.0	62.0	75.6	60.8	77.5
Y	36.5	1.9	39.2	13.6	53.5	19.9	72.2	30.5	70.9	28.9
Zr	236.6	83.2	486.3	255.9	794.8	411.2	388.7	146.8	387.0	151.8
Nb	14.2	1.1	19.1	8.5	21.3	6.9	28.3	13.8	27.9	14.0
Mo	4.3	0.5	4.1	1.0	3.4	1.1	3.6	1.8	3.7	1.9
Sn	1.0	0.0	2.7	2.7	1.3	0.5	3.3	2.1	3.5	2.5
Cs	1.3	1.2	1.6	1.7	0.7	0.4	0.7	0.4	0.6	0.4
Ba	1424.0	116.2	1099.0	558.0	787.7	542.1	433.8	433.5	453.1	411.7
La	53.3	4.9	64.8	31.7	77.2	26.4	78.9	35.2	76.6	33.3
Ce	102.7	6.1	131.0	63.2	156.4	54.7	163.1	66.9	158.7	65.7
Sm	9.2	0.8	13.3	3.1	14.5	3.8	12.4	3.7	12.6	3.5
Yb	2.5	0.0	3.8	2.1	5.3	0.0	7.2	3.6	7.7	3.2
Hf	8.0	1.2	11.9	3.5	14.3	5.0	12.2	3.4	12.1	3.1
Pb	15.9	3.9	15.9	6.6	15.8	7.1	19.3	10.6	20.3	10.4
Th	9.2	3.0	9.1	10.7	5.1	4.8	15.7	9.7	15.2	9.6
U	4.8	0.9	3.1	1.7	2.4	1.4	4.8	2.9	4.7	3.0
(wt%)	CIPW norm (partial)									
Q	12.25	1.76	8.02	6.40	10.77	7.74	29.87	6.15	29.80	6.01
C	0.00	0.00	0.05	0.18	0.02	0.05	0.01	0.06	0.02	0.06
Or	28.50	2.93	31.47	4.81	32.52	5.39	25.57	9.35	28.89	3.89
Ab	36.71	2.01	38.96	3.48	40.28	5.85	37.39	8.96	34.11	4.02
An	10.08	1.50	9.37	4.48	5.28	3.78	2.16	2.24	2.30	2.27
Di	2.88	1.35	2.85	1.48	3.52	2.25	1.15	1.07	1.08	0.87
By	4.65	1.72	4.53	2.26	3.22	2.08	1.08	1.93	1.22	2.00
Ol	0.00	0.00	0.41	1.09	0.61	1.36	0.00	0.00	0.00	0.00
Wt	2.64	0.55	2.41	0.96	2.06	0.78	1.63	0.78	1.58	0.75
Il	1.69	0.12	1.48	0.56	1.21	0.49	0.54	0.34	0.54	0.36

KEY TO UNITS (NIS - Mumok Intrusive Suite, KNIS - Kennedy Mountain Suite)  
 10 -- Long Island Quartz Monzonite (all data)  
 20 -- Mumok Intrusive Suite (Monzonite to Quartz Monzonite)  
 21 -- Mumok Intrusive Suite (Syenite to Quartz Syenite)  
 11 (all data) - (KNIS) All data including albitized rocks  
 11 (unaltd) - (KNIS) Excluding rocks with W/M+K < 0.3 or > 0.65  
 n1 -- Number of analyses for all elements except those listed below  
 n2 -- Number of analyses for Sc, Sn, Cs, Sm, Yb and Hf



Table 4.3 (continued).

UNIT	23-26		24		27-29		30	
n1	197		55		82		79	
n2	142		47		66		13	
(Wt%)	Mean	S.D.	Mean	S.D.	Mean	S.D.	Mean	S.D.
SiO <sub>2</sub>	71.29	4.71	72.81	3.56	72.12	2.93	70.11	5.15
TiO <sub>2</sub>	0.31	0.27	0.21	0.11	0.32	0.19	0.39	0.72
Al <sub>2</sub> O <sub>3</sub>	13.68	1.55	13.20	1.50	13.22	1.34	14.43	1.74
Fe <sub>2</sub> O <sub>3</sub>	1.05	0.74	1.14	0.80	1.21	0.57	1.16	0.55
FeO	1.68	1.47	1.23	0.81	1.44	0.87	1.49	0.97
MnO	0.06	0.06	0.05	0.05	0.06	0.04	0.06	0.04
MgO	0.36	0.50	0.27	0.55	0.18	0.17	0.50	0.84
CaO	1.14	1.04	0.91	1.17	0.88	0.47	1.36	1.20
Na <sub>2</sub> O	4.09	0.86	4.21	1.26	3.97	0.61	4.28	0.75
K <sub>2</sub> O	5.12	1.10	4.97	1.33	5.47	0.90	5.11	1.01
P <sub>2</sub> O <sub>5</sub>	0.07	0.09	0.04	0.03	0.04	0.04	0.10	0.08
LOI	0.67	0.37	0.67	0.60	0.53	0.20	0.58	0.29
TOTAL	99.52		99.71		99.44		99.57	

(ppm)								
Li	25.0	23.5	26.5	23.8	13.9	11.7	14.8	6.2
F	1420.0	1141	1541.1	1021	1244.6	935.7	688.5	462.5
Sc	3.1	4.1	1.9	1.7	3.8	5.3	2.4	0.9
V	23.3	29.2	20.4	41.9	12.8	7.7	21.5	17.1
Cr	5.1	6.5	6.3	7.9	3.7	2.9	4.8	13.7
Ni	2.2	3.9	2.6	5.8	1.5	1.8	2.6	7.9
Cu	9.3	38.4	11.3	44.8	6.0	9.2	6.3	6.1
Zn	75.1	69.6	84.3	82.3	89.6	59.6	54.8	42.8
Ga	16.9	8.6	17.6	10.2	21.4	10.0	15.2	5.2
Rb	178.4	65.0	176.1	62.1	172.5	44.1	127.8	51.8
Sr	111.7	130.2	77.5	71.8	61.2	65.8	160.7	151.6
Y	55.4	43.8	64.3	46.9	74.4	32.8	42.5	17.2
Zr	491.5	558.5	471.5	418.2	675.7	439.3	368.8	210.3
Nb	26.0	21.0	29.9	33.4	29.3	11.1	19.1	7.2
Mo	4.3	7.7	3.7	2.0	4.3	2.3	3.7	1.2
Sn	5.8	9.9	5.0	3.2	4.0	2.6	2.7	2.7
Cs	1.2	1.0	1.1	0.7	1.1	0.7	0.7	0.6
Ba	501.9	382.6	344.9	264.0	329.6	260.1	660.8	482.6
La	90.7	111.7	75.4	46.8	122.8	62.6	63.1	30.2
Ce	178.7	197.0	156.9	84.8	247.2	121.1	126.8	59.2
Sm	13.1	10.4	12.8	6.4	20.8	9.8	10.4	3.9
Yb	6.6	4.7	7.6	5.1	8.8	4.3	4.2	2.0
Hf	13.3	13.3	13.3	7.5	19.1	10.3	10.1	3.0
Pb	37.3	205.3	23.3	9.6	24.5	13.5	17.6	11.2
Tb	18.3	20.5	23.4	28.3	18.9	8.0	13.0	9.6
U	5.8	7.0	8.0	11.9	5.5	2.3	4.5	2.6

(wt%)								
Q	24.90	9.23	27.17	8.65	26.22	7.51	22.16	9.88
C	0.12	0.23	0.07	0.14	0.10	0.70	0.06	0.14
Or	30.38	5.96	29.63	7.92	32.64	5.34	30.45	6.00
Ab	34.90	7.35	35.58	10.85	33.79	5.15	36.54	6.34
An	3.66	2.94	2.43	1.67	1.90	1.64	4.97	4.19
Di	1.28	2.82	1.25	4.29	1.62	1.35	1.11	1.66
By	2.15	2.26	1.39	1.32	0.96	1.05	1.81	1.34
Ol	0.03	0.26	0.00	0.02	0.00	0.00	0.18	1.60
Mt	1.38	1.00	1.25	0.88	1.63	0.77	1.60	0.82
Il	0.61	0.52	0.39	0.22	0.62	0.36	0.74	0.43

KEY TO UNITS (SIS - Strawberry Suite, LIS - Lanceground Suite)  
 23-26 -- Strawberry Intrusive Suite (all data)  
 24 -- Cape Strawberry Granite and Related Rocks  
 27-29 -- Lanceground Intrusive Suite (all data)  
 30 -- Big River Granite (all data)

n1 -- Number of analyses for all elements except those listed below  
 n2 -- Number of analyses for Sc, Sn, Cs, Sm, Yb and Hf

Intrusive Suites, especially when altered granites with  $N/N+K < 0.3$  or  $> 0.65$  are excluded from the latter. This complements their obvious similarity in texture and mineralogy, if the effects of deformation are disregarded. However, alkali disturbance is not present to the same extent in the Strawberry Suite, although there are signs of some minor effects (e.g. Figure 4.4). The Long Island Quartz Monzonite and Numok Intrusive have similar major element compositions, but dissimilar trace element patterns (Table 4.3).

#### Geochronological Relationships

The geochemical continuity discussed above is consistent with closely similar U-Pb and Rb-Sr ages obtained from the Island Harbour Bay Intrusive Suite, Long Island Quartz Monzonite, the Numok Intrusive Suite and the Big River Granite, all of which fall in the interval  $1800 \pm 15$  Ma (Loveridge et al., 1987; Gandhi et al., 1988; Krogh et al., in prep). Data from the Strawberry Intrusive Suite are more difficult to assess; these rocks may be somewhat younger at ca. 1760 Ma. These geochronological and geochemical data indicate that "syn-tectonic" and "post-tectonic" Makkovikian associations are (at least in part) manifestations of the same event. They are regarded by the author as closely related, and, in subsequent chapters (e.g. Chapter 9), are treated as a single assemblage.

They may collectively represent a single pulse of magmatism that transcended a very short-lived deformational event -- i.e., the age difference between "syn-tectonic" and "post-tectonic" suites is real, but below isotopic resolution. A second possibility is that late Makkovikian

deformation at ca. 1800 Ma may have been heterogeneous in nature. As discussed recently by Paterson and Tobisch (1988), the response of plutons to deformation is highly variable, and the use of foliations to date them may be misleading. As neither deformation or intrusion are instantaneous events, the distinction between these two alternatives is largely semantic.

## CHAPTER FIVE

# LABRADORIAN PLUTONIC ROCKS

---

### Chapter Abstract

Labradorian plutonic rocks are undeformed suites for which geochronology and/or field relationships indicate ages between 1670 and 1600 Ma. There is no evidence of Labradorian deformation that preceded or accompanied their emplacement in the study area, but deformation and metamorphism of this age is widespread in high-grade terranes to the south. Labradorian units in the southwest of the area have variably-developed east-trending foliations, that are presumed to record Grenvillian deformation. The Labradorian assemblage is characterized by two contrasting groups of rocks that were derived respectively from mafic parental magmas and more siliceous granitoid magmas.

The Adlavik Intrusive Suite (ca. 1650 Ma) is a mafic to intermediate association that forms a complex, multiphase, layered intrusion and a number of isolated bodies. These mafic rocks are compositionally and texturally diverse, and include ultramafic rocks (originally pyroxenites), layered mafic cumulate rocks, plagioclase-cumulate leucogabbro, diabase and pegmatitic gabbro. These are associated with lesser amounts of diorite and monzodiorite. Field relationships are exceedingly complex, and suggest multiple batches of mafic magma, including both gabbroic and gabbro-noritic compositions. Cumulate textures are widespread. An original pyroxene ( $\pm$  olivine) -bearing mineralogy was variably transformed to an amphibole-bearing assemblage, probably via late-magmatic or deuteritic volatile build-up during crystallization. The gabbro is moderately  $K_2O$ -rich, and shows major and trace element affinity to "Shoshonitic" basalts, and possibly to "appinitic" gabbro suites associated with some Phanerozoic granites.

The Mount Benedict Intrusive Suite (ca. 1650 Ma) ranges in composition from gabbro and diorite to alkali-feldspar granite, but is dominated by hornblende-biotite monzonite, syenite and quartz syenite. The suite is crudely layered, with evolved compositions at high elevations. The least evolved rocks are locally olivine-bearing plagioclase cumulates that resemble the Adlavik Suite. Variably preserved plagioclase phenocrysts in all members of the suite imply significant fractionation of this mineral. Well-defined geochemical trends within the suite are

consistent with derivation from a mafic to intermediate parent by sequential fractionation of mafic minerals, plagioclase and K-feldspar. Strong incompatible element enrichment is consistent with this extended fractionation history, and trace element modelling confirms that Adlavik Suite mafic magmas are a possible parent composition. The Adlavik and Mount Benedict Suites are thus regarded as closely related, complementary associations.

The Monkey Hill Intrusive Suite (ca. 1640 Ma) comprises several small, closely similar, epizonal, biotite-leucogranite plutons that probably represent cupolas connected to a larger body at depth. These are slightly peraluminous, and depleted in fluorine, HFS elements and REE. Two plutons that belong to the suite are associated with endocontact Mo and exocontact Mo-Cu ( $\pm$  Pb-Zn) mineralization, and show strong depletion in a range of trace elements. The latter is probably due to hydrothermal activity associated with mineralization. Two ca. 1630 Ma old granitoid plutons in the southwest of the area (Witchdoctor and Burnt Lake Granites) have closely similar petrographic and geochemical features, contain minor muscovite and garnet, and are also associated with Mo mineralization. These show evidence of Grenvillian deformation, as they lie close to the Benedict Fault zone.

The Otter Lake - Walker Lake Granitoid (ca. 1650 Ma) is a regionally extensive, variably deformed, porphyritic granitoid suite ranging from biotite-hornblende quartz monzonite to biotite granite. It has a mildly peraluminous composition, and is generally poor in fluorine, HFS elements and REE.

As a group, Labradorian siliceous granitoid units differ from their Makkovikian counterparts in their lack of transitional peralkaline behaviour, general peraluminous affinity and lack of fluorine, HFS element and REE enrichment. Such features probably reflect different source materials and/or generative processes for the two groups of granitoid rocks, rather than different fractionation histories or hydrothermal effects in epizonal plutons.

## Introduction

This association comprises post-Makkovikian, largely undeformed, post-tectonic plutonic rocks for which geochronological data and/or field relationships suggest ages between 1670 and 1600 Ma. As discussed previously (Chapter 4), "post-tectonic" does not imply a universal absence of deformation, as some units in the south have east-trending foliations of probable Grenvillian age. There is no evidence of Labradorian deformation in the study area. The term "anorogenic", however, is not appropriate for these plutons, as there is clear evidence for Labradorian deformation and metamorphism in high-grade terranes to the south (e.g. Wardle et al., 1986). Labradorian plutonism may thus be temporally related to orogenesis, but the study area apparently lay outside the zone affected directly by metamorphism and deformation.

Labradorian plutonic rocks are divided into five main associations. The Adlavik Intrusive Suite consists of layered gabbro, leucogabbro and diorite. The Mount Benedict Intrusive Suite includes minor diorite and gabbro of similar aspect, but is dominated by monzonite to quartz syenite. The Monkey Hill Intrusive Suite comprises a number of small, leucocratic, epizonal granite plutons. The Witchdoctor and Burnt Lake Granites are similar leucocratic granites. The Otter Lake - Walker Lake Granitoid is a regionally extensive porphyritic quartz monzonite to granite unit. The latter two associations have been affected by Grenvillian deformation.

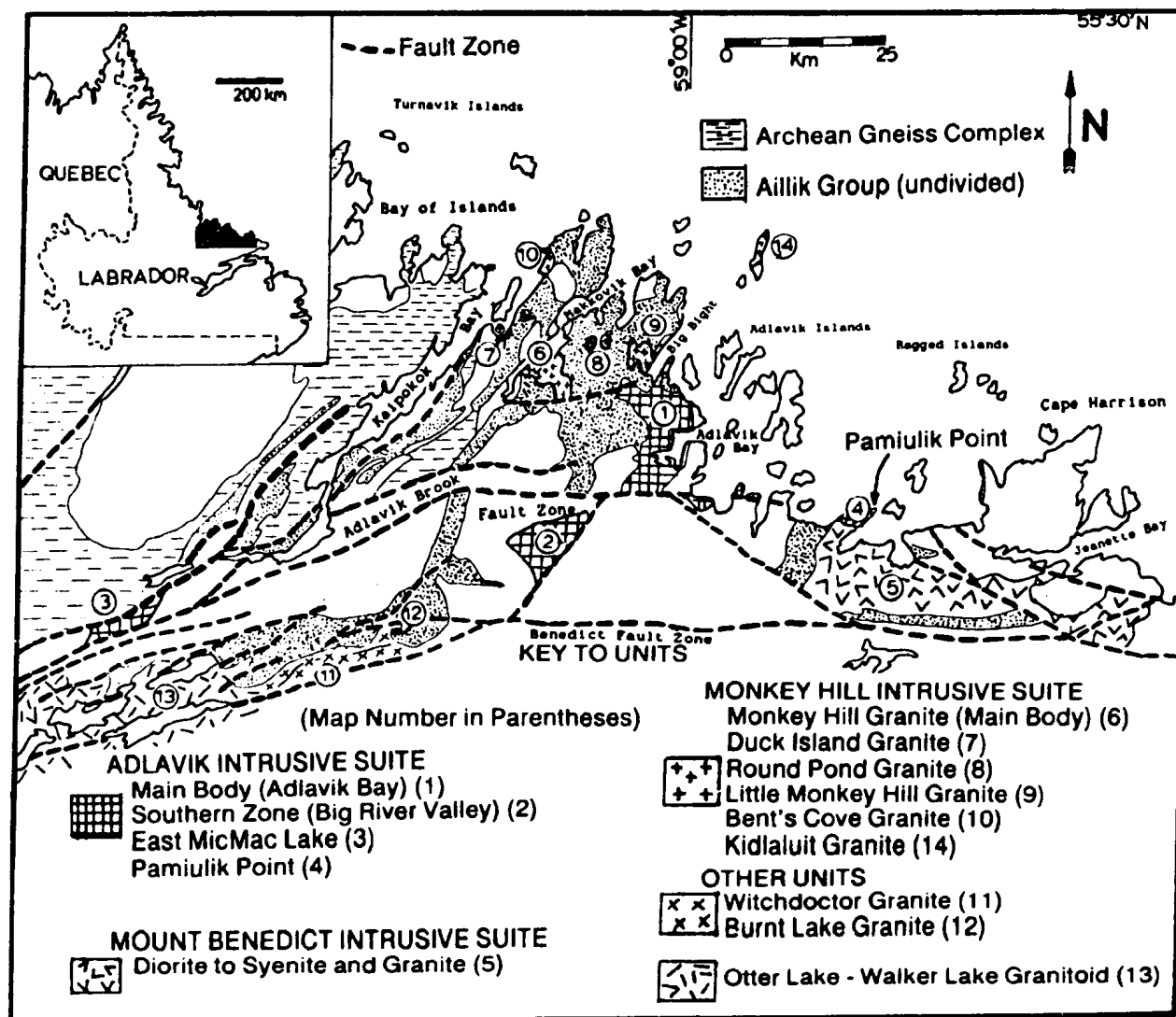


Figure 5.1. Summary map illustrating the distribution and extent of Labradorian plutonic units.

Table 5.1. Key features of Labradorian plutonic units.

Map Unit	Suite/Unit/Age	General Characteristics	Textural Characteristics
ADLAVIK INTRUSIVE SUITE			
40.1 40.2 40.3 40.4	Gabbro, Gabbro-norite and Leucogabbro	Texturally variable, layered assemblage of ultramafic rocks, gabbro, gabbro-norite, plagioclase cumulate leucogabbro, and diorite. All of the above are cut by agmatitic composite diabase (commonly net-veined) and by coarse pegmatitic gabbro.	Dominantly coarse-grained to very coarse-grained. Cumulate layering is variably developed. Mafic cumulates occur at the base and/or margin of the intrusion, and also occur sporadically within the dominant plagioclase cumulate facies.
41.1 41.2 41.3 41.4	Diorite and Monzodiorite  1649 +/- 1 Ma [ U-Pb zircon ] (Krogh et al., in prep.)	Homogeneous, grey to yellow-brown, massive, locally plagioclase-porphyritic Px-Bb or Bb-diorite, monzodiorite to (locally) monzonite and syenite.	Generally coarse-grained and homogeneous. Locally displays wispy mafic mineral layering, and thin mafic cumulate zones. Contains xenoliths of gabbro, leucogabbro and mafic cumulate.
MOUNT BENEDICT INTRUSIVE SUITE			
42.0	Diorite and Monzodiorite [possibly including Gabbroic Rocks]	Massive, grey to black-and-white, plagioclase-porphyritic leucogabbro, diorite and monzodiorite. Shows a strong resemblance to parts of the Adlavik Intrusive Suite (see above).	Coarse to very coarse-grained, with large (5 cm) Plag megacrysts, ranging in shape from euhedral to rounded. Mafic minerals show interstitial to oikocrystic habit. Interstitial granophyric material.
43.0	Monzonite, Syenite and Quartz Syenite	Ranges from a grey to brown or buff Plag-porphyritic monzonite (similar to above) to pink or buff syenite and quartz syenite. Relict, mantled plagioclase xtals give "speckled-eggshell" texture.	Medium to coarse-grained, massive, ranges from porphyritic to seriate and (locally) equigranular. Interstitial Qz + K-fsp, local K-feldspar phenocrysts. Mafic minerals form euhedral or subhedral aggregates.
44.0	Syenite, Quartz Syenite, Granite and alkali-feldspar Granite 1625 +/- 50 Ma (Rb-Sr WR) (Brooks, 1982) 1650 +/- 10 Ma (U-Pb zircon) (Krogh et al., in prep.)	Dominated by homogeneous, pink, grey and buff-white, locally porphyritic syenite to alkali-fsp granite. Plag-porphyritic variants resemble the above, but with small vestigial plagioclase phenocrysts only.	Generally fine to medium-grained, massive and K-feldspar porphyritic. Fine-grained equigranular rock types and quartz-feldspar porphyry occur locally. Rapid local grain size variations.
MONKEY HILL INTRUSIVE SUITE			
45.1 45.2 45.3 45.4 45.5 45.6	Monkey Hill Granite 1640 +/- 10 Ma (U-Pb zircon) (Krogh et al., in prep.) Round Pond Granite 1620 +/- 60 [ K-Ar Bi ] (Wanless et al., 1970) [ For other plutons, see Figure 5.1 ]	All plutons are dominated by grey to buff or pink, locally slightly porphyritic, homogeneous, leucocratic biotite-chlorite monzogranite, granite and (locally) alkali-fsp granite. Also includes graphic leucogranite and Qz-Fsp porphyry.	Generally fine to medium grained. Small, euhedral plagioclase crystals impart a "porphyritic" texture. Mineralized plutons are locally microplitic and/or pegmatitic. Inclusions are rare, except near contacts. Tuffisite breccias suggest volatile exsolution and high level emplacement.
46.0	Witchdoctor Granite 1632 +/- 9 [ U-Pb Zr ] 1595 +/- 34 [ Rb-Sr WR ] (Brooks, 1982, 1983)	Homogeneous, leucocratic, white to pink, Bi-Hs granite to alkali-fsp granite located close to Benedict fault zone.	Generally medium to coarse-grained. Mostly equigranular, but locally K-feldspar porphyritic. Foliation defined by ribboned quartz.
47.0	Burnt Lake Granite 1548 +/- 90 [ Rb-Sr WR ] (MacKenzie and Wilton, 1988)	Dominated by homogeneous, white, pale grey to pink, leucocratic to alaskitic monzogranite and granite. Parts of the unit resemble fine-grained Witchdoctor Granite.	Generally fine to medium-grained, equigranular to locally porphyritic. Variably foliated, but invariably has a "sugary" appearance due to recrystallization; locally it is similar to metavolcanic country rocks.
48.0	Otter Lake - Walker Lake Granitoid 1647 +/- 2 Ma (U-Pb zircon) (Krogh et al., in prep.)	Dominated by compositionally variable grey to pink or green-white, two-feldspar porphyritic, biotite-hornblende quartz monzonite, granodiorite, monzogranite and granite. Melanocratic dioritic variants occur locally.	Generally medium to coarse-grained, massive, porphyritic to seriate in texture. K-feldspar phenocrysts are larger (3-5 cm) than coexisting Plag. Mafic minerals are interstitial, or form rounded clots. Unit locally has east-trending foliation.



Table 5.1 (continued).

Key Field Relationships	Mineralogy	Petrography
Gabbro cuts Upper Aillik Group, but is cut by monzogranite of Monkey Hill Intrusive Suite. Gabbro appears to be gradational with the diorite and monzodiorite (see below), but locally it includes angular diorite xenoliths. Gabbro appears to occur both above and below the diorite unit.	Plagioclase (An40-80; 30-75 %) Cpx (augite, 10-50%) Opx (Gabbronorite only, 5-20%) Hb (green or brown, 5-50%) Bi (red-brown, 5-20%) Qz + K-fsp (interstitial, 0-7%) Olivine (minor, 5-20% in Gabbronorite) Accessory Ap, Fe-Ox.	Complete range from fresh, well-preserved examples to altered rocks dominated by saussuritized Plag and secondary Actinolite - epidote. Hb commonly forms rims on Cpx, suggesting late (deuteric?) origin. Qz and K-fsp (where present) form interstitial granophyric material.
Appears gradational with gabbros at Adlavik Bay, yet contains gabbro xenoliths. Cut by net-veined mafic dykes and veins identical to those in gabbroic unit.	Plagioclase (An40-50; 40-65%) Qz (0-8%, interstitial with K-fsp) K-fsp (5-25%, locally abundant) Cpx + Hb + Bi (10-20% total) Opx (0-10%, in Plag and Cpx-rich variants.) Accessory Ap, Zr, Fe-Ox	Continuum from fresh Px-Bi bearing diorite to Hb-diorite to variably altered Plag-Act-Ep assemblages. Primary Hb in some variants, elsewhere Hb forms rims on Cpx. Qz and K-fsp are interstitial (trapped liquid?).
Appears to be gradational with dominant monzonite and syenite unit (see below). Interpreted to form lowermost (and/or marginal) facies of the Suite.	Qz (0-2%, interstitial habit) K-fsp (Ml, 5-20%, interstitial) Plag (An40-60; 50-80%, sauss.) Cpx +/- Opx (5-20% total) Hb + Bi (0-10% total) Olivine (0-10%, mostly relict) Accessory Ap, Fe-Ox.	Most examples contain serpentine-Fe-Ox patches, probably pseudomorphs after olivine. Altered variants contain saussuritized Plag and Act-Ep-Sph-Chl aggregates.
Mafic and felsic end-members are similar to other units in Suite; relationship is probably gradational. This unit gives way to syenite and granite at high elevations.	Qz (0-10%, interstitial habit) Plagioclase (2 types, 30-60%) K-fsp (Ml, locally phenocrysts) Hb + Bi (5-15% total) Cpx (0-5%, commonly relict) Accessory Sph, Zr, All, Fl.	Clear igneous textures. Plag forms zoned phenocrysts rimmed by fresh Plag and/or K-feldspar. Cpx occurs in mafic variants, rimmed by Hb. Most K-fsp (+/- Qz) interstitial. Sphene locally forms cores to Hb.
Least differentiated examples are similar to the dominant monzonite to syenite unit. Mostly restricted to high elevations, but occurs sporadically in other units. Relationship gradational?	Qz (5-15%, up to 30% locally) K-fsp (50-80%) Plag (10-35%) Bi + Hb (3-8% total, Bi > Hb) Accessory Sph, Zr, Fl	Qz and K-fsp form graphic intergrowths with interstitial habit. Ml phenocrysts have relict simple twinning. Local plagioclase phenocrysts are embayed and resorbed. Hb locally shows poikilitic habit.
Monkey Hill Granite intrudes the Upper Aillik Group and Kennedy Mountain Suite. Duck Island Granite intrudes the Long Island Quartz Monzonite. Little Monkey Hill Granite cuts Adlavik Intrusive Suite.	Qz (20-35%, interstitial habit) Plag (An15-25; 30-50%) K-fsp (Ml, 30-50%) Bi + Chl (0-4% combined) Epidote (primary?) Ms (minor) Gnt (Kidlaluit granite only)	Igneous textures well preserved. K-fsp is mostly a groundmass phase; in equigranular variants it forms graphic intergrowths with quartz. Bi is pervasively altered to Chl; many rocks contain only Chl.
Contacts are not exposed. This unit is mineralogically and compositionally akin to the Burnt Lake Granite (see below).	Qz (25-40%) K-fsp (Ml, 40-70%) Plag (An20, 10-25%) Bi + Ms (1 - 5% total, Bi > Ms) Hb (relict) Gnt (minor, < 1%) Chl, Ep, Sph, All	Foliation defined by aggregates of Bi + Ms, Bi altered to Chl. Pink garnet is rare; commonly broken and cracked. Epidote intergrown with Hb + Bi.
Intrudes felsic volcanic rocks of the Upper Aillik Group, but locally appears gradational. Mineralogically and compositionally similar to the Witchdoctor Granite.	Qz (20-40%) K-fsp (Ml, 25-45%) Plag (20-50%) Bi + Ms (0-5% total, Bi > Ms) Accessory All, Gnt (rare), Sph.	Variably recrystallized; relict porphyritic textures preserved. Ms is intergrown with Bi, and also occurs as very fine-grained (secondary?) material.
Intrudes felsic volcanic and meta-sedimentary rocks of Upper Aillik Group. Granites correlated with this unit intrude Bruce River Group. In fault contact with Melody Granite and Archean gneisses.	Qz (15-30%) K-fsp (Ml, 30-50%) Plag (An25-40, 25-50%) Bi + Hb (3-8%, Bi > Hb) Cpx (rare, relict) Abundant Sph (up to 2%) Accessory All, Zr, Ap	Igneous textures generally well-preserved. Qz is interstitial. Ml phenocrysts are fine perthite, with local rims of sodic Plag. Plag phenocrysts have zoned, saussuritized centres. Biotite has green colour. Sphene very prominent; euhedral or interstitial habit.

## 5.1 GEOLOGY AND PETROLOGY

Locations and extent of principal Labradorian plutonic units are indicated in Figure 5.1. Key field and petrographic characteristics are summarized in table 5.1.

### 5.1.1 Adlavik Intrusive Suite

#### Definition and Distribution

This suite includes layered gabbroic and dioritic rocks exposed at Adlavik Bay and Big River valley, and also as a number of isolated bodies, of which the most important is at Pamiulik Point (Figure 5.1). The type locality at Adlavik Bay is referred to below as the "main body".

The main body was defined initially by Gandhi et al. (1969) and Stevenson (1970), and termed "Adlavik Complex", which was later modified to Adlavik Intrusive Suite by Gower (1981). A U-Pb zircon date of 1649  $\pm$  1 Ma was obtained from a potassic monzodiorite at Adlavik Bay (Krogh et al., in prep.). Gower et al. (1982) summarize previous K-Ar dates (Gandhi et al., 1969; Wanless et al., 1970) from minor intrusions possibly related to the suite; these range from 1660 to 1540 Ma. A postulated link to the rocks now termed Numok Intrusive Suite (Kerr, 1986) has since been disproved by ca. 1800 Ma U-Pb zircon ages from the latter (see Chapter 4).

The main body is a very complex, layered, multi-component intrusion that could easily form an extended Ph.D. topic by itself. The scale of mapping and sampling in this regional project is inadequate to resolve all of the problems inherent in its geometry and stratigraphy, and the following account is undoubtedly an oversimplification.

## **Mafic Plutonic Rocks**

These correspond to unit 13 of Gower (1981) and unit 22a of Gower et al. (1982), and exhibit great variety in composition and texture. Clark (1973) mapped the northern fringe of the main body, and outlined five subunits or "facies". These have been revised and augmented during this project (Kerr, 1987b; Figure 5.2), and are used as a framework for description. The following descriptions apply mostly to the main body; other areas of the suite are dominated by melagabbro and leucogabbro facies. Plates 5.1 and 5.2 illustrate various field characteristics of mafic rocks within the Adlavik Intrusive Suite.

***Marginal Gabbro and Diabase*** : This is best exposed in the Big Bight area (Figure 5.2), but occurs locally around the western edge of the main body, where it forms a thin (usually < 5 m) discontinuous margin against the Upper Aillik Group country rocks. It is a fine to medium-grained, equigranular, grey rock with variably diabasic texture. In the Big Bight area it contains primary acicular hornblende and is closer to diorite in composition. In parts of the mafic cumulate facies, it occurs as rounded xenoliths or pillows in coarse gabbro. These agmatites probably record disruption of a chilled margin by later magma, also suggested by Gower (1981) for a similar texture at Pamiulik Point.

***Mafic Cumulate Facies*** : This corresponds partly to the rhythmic layered facies of Clark (1973). It is well-exposed at Big Bight, where it forms the base or side of the intrusion. It is also present locally within the dominant leucogabbro facies and the diorite unit. Rhythmic layering,

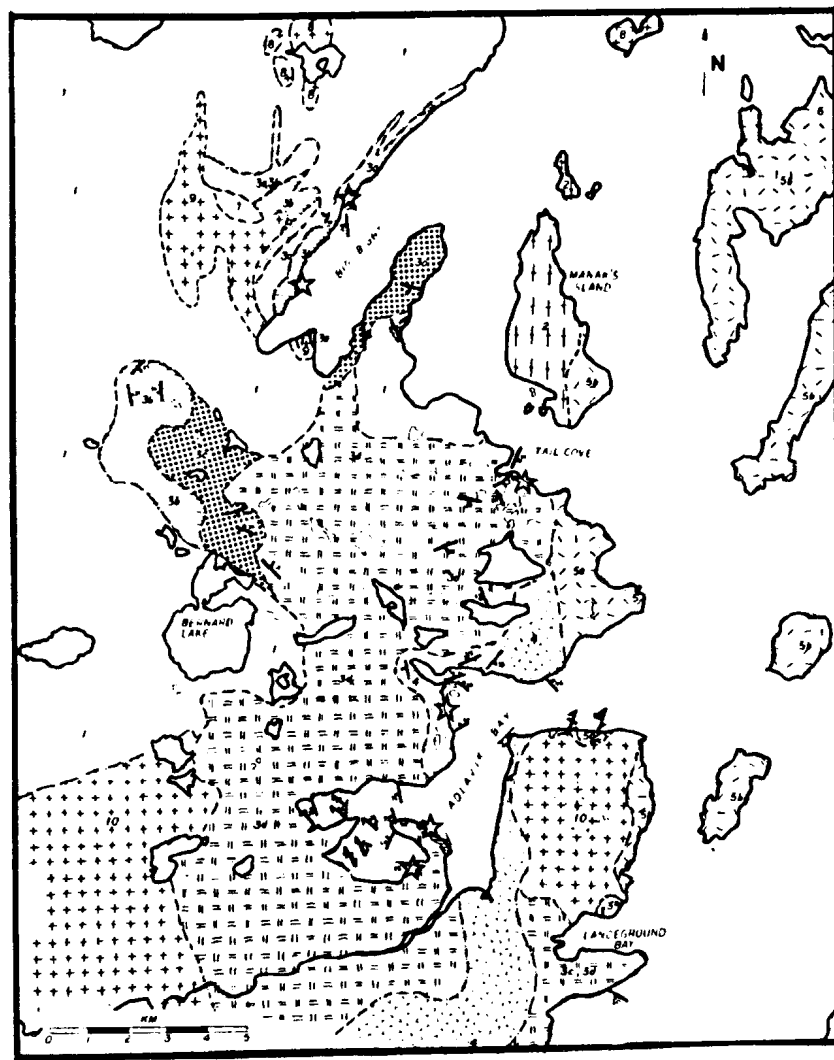


Figure 5.2. Simplified geological map of the main body of the Adlaviik Intrusive Suite. Partly after Clark (1973), Gower et al.(1982) and Kerr (1988b).

#### LABRADORIAN PLUTONIC ROCKS

- 9 Monkey Hill Intrusive Suite  
(Little Monkey Hill Granite)

#### ADLAVIK INTRUSIVE SUITE

- 4 Diorite and Monzodiorite
- 3 (d) Leucogabbro Facies  
3 (c) Melagabbro Facies  
3 (b) Mafic Cumulate Facies  
3 (a) Marginal Gabbro and Diorite

#### POST-TECTONIC MAKKOVIKIAN PLUTONIC ROCKS

- 7 Big River Granite
- 8 Strawberry Intrusive Suite  
(Poodle Pond Granite)
- 10 Lanceground Intrusive Suite
- 5 (a) Numok Intrusive Suite (Agmatitic Border)  
(b) Numok Intrusive Suite (Monzonite - Quartz Monzonite)
- 6 Numok Intrusive Suite (Syenite - Quartz Syenite)

#### SYN-TECTONIC MAKKOVIKIAN PLUTONIC ROCKS

- 2 Manak Island Granitoid

#### SUPRACRUSTAL ROCKS

- 1 Upper Aillik Group (Undivided)

#### SYMBOLS

- Geological contact (approximate, inferred)
- Igneous layering or foliation
- Penetrative foliation
- Fault (Inferred)
- ★ Location of pegmatitic gabbro-diorite material containing minor sulphide

graded bedding, and cross-bedding are well developed in these rocks. At Big Bight, they form at least two irregular cyclic units (Figure 5.3). Each cycle commences with coarse-grained ultramafic rocks, dominated by amphibole and biotite, but with a relict pyroxenite mineralogy. These are interlayered with and overlain by layered gabbro and gabbronorite, where hornblende crystals with a "stubby" habit (after pyroxene ?), containing augitic cores, define rhythmic layering and graded bedding. The upper portion of each cycle consists of very coarse-grained amphibole-bearing "pegmatites" (pegmatite facies; see below) that also occur as irregular, diffuse, veins and pods that disrupt the underlying cumulates.

**Melagabbro Facies** : The mafic cumulate facies is overlain in the Big Bight area by massive, dark grey to black, coarse-grained, melanocratic rocks (termed "massive diabase facies" by Clark, 1973, but not generally diabasic), which in turn grade upward into the dominant leucogabbro facies. The melagabbro generally contains less than 50% plagioclase; it is locally a gabbronorite, but in most areas mafic phases have been transformed to amphibole (see below). It is locally strongly epidotized around networks of fractures or veinlets.

**Leucogabbro Facies** : This areally dominant facies is a grey to white or purple-brown, coarse to very coarse-grained, leucogabbro or leucogabbronorite. It is distinguished from the melagabbro by a higher plagioclase content (up to 70%), but the two are gradational. It contains interstitial (locally oikocrystic) mafic minerals and locally has a magmatic foliation defined by plagioclase alignment. Diffuse mafic mineral accumulations and thin zones of rhythmic layering provide evidence of cumulus

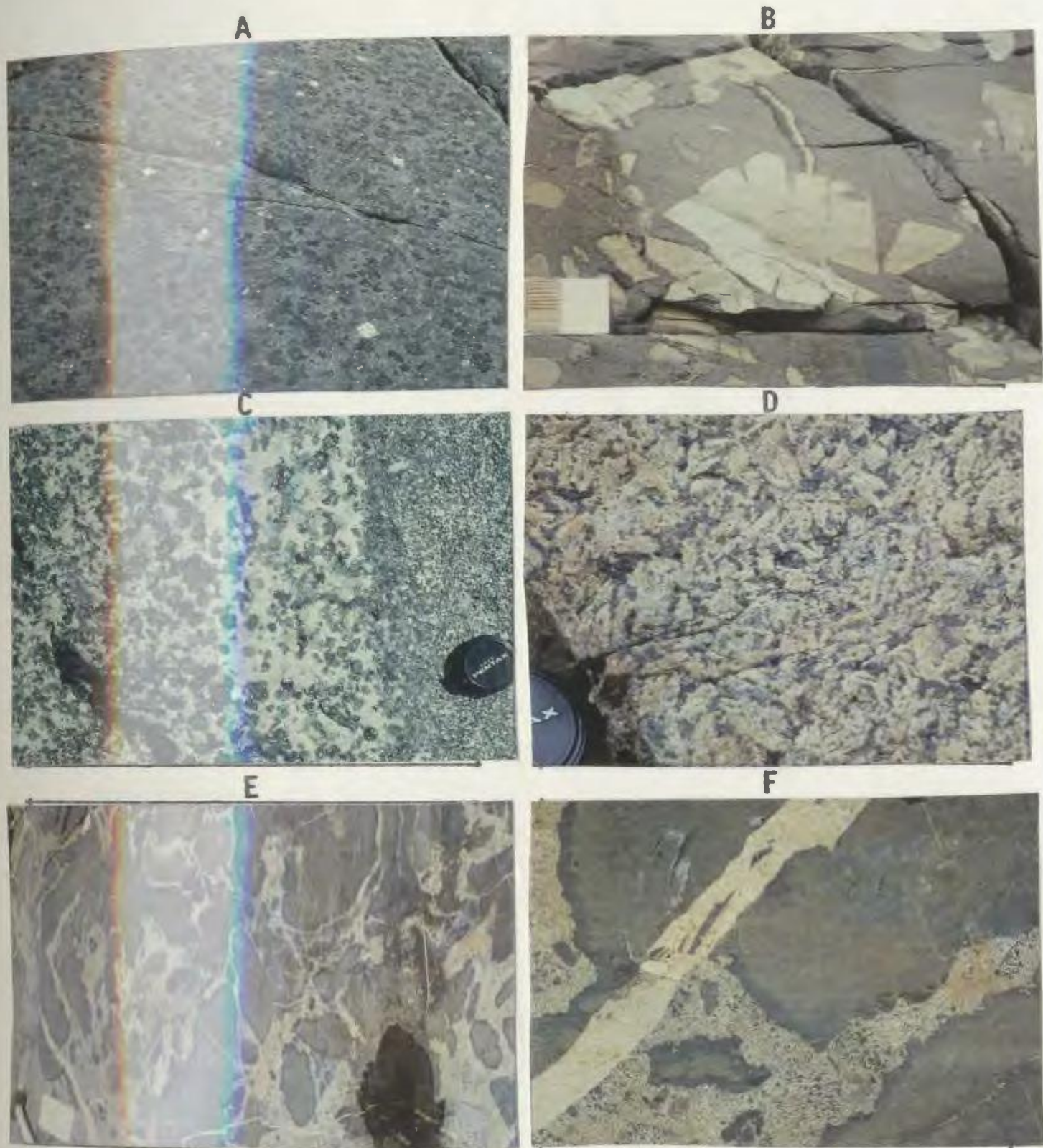


Plate 5.1. Features of mafic rocks in the Adlavik Intrusive Suite (see also Plate 5.2). (a) Mafic cumulate with amphibole megacrysts up to 5 cm diameter, containing augite cores, Pamiulik Point area. (b) Stopped blocks of diorite in melanocratic gabbro, Adlavik Bay. (c) Graded bedding in mafic cumulate, Big Bight, tops to right of photo. (d) Coarse "diabasic" texture, probably a plagioclase cumulate, coastline south of Manak Bay. (e) Composite diabase body intruding leucogabbro facies, Adlavik Bay. Note chilled margins on diabase lozenges. (f) Detail from same locality, white vein is about 5 cm wide. Note disruption of chilled margins by grey, intermediate material.



processes, and it is viewed as a plagioclase cumulate. Leucogabbro is restricted to the northern margin and inner part of Adlavik Bay, but many samples retain only relict primary mineralogy (see below), and it is therefore difficult to assess the original extent of orthopyroxene and olivine-bearing rocks.

This facies is homogeneous, except for locally voluminous cross-cutting composite diabase and gabbroic pegmatite (see below). In one locality it includes angular, stoped blocks that resemble the diorite unit (described below).

**Gabbroic Pegmatite Facies :** This consists of coarse-grained, generally quartz-free, gabbroic and dioritic "pegmatite", containing acicular hornblende (locally as unusual hollow crystals), and variable amounts of K-feldspar. It is associated with the mafic cumulate facies (see above), and occurs as sporadic masses (rarely more than 400 m<sup>2</sup>) that intrude all the above and the diorite unit. In the mafic cumulate facies, it is probably a local volatile-rich residual magma formed by crystallization of the underlying cumulates. It is suggested that it forms a late phase formed by the operation of similar processes on an intrusion-wide scale.

**Composite Diabase Facies :** Fine to medium-grained diabase forms numerous outcrop-scale dykes, veins and irregular masses that intrude and disrupt mafic and diorite units. These have a chaotic internal structure, where diabase is intruded and disrupted by grey, intermediate material that appears to originate in the local wall rocks. Chilled margins are present around individual diabase "pillows", but these are cut and net-veined by this intermediate material. Preferred orientation of diabase

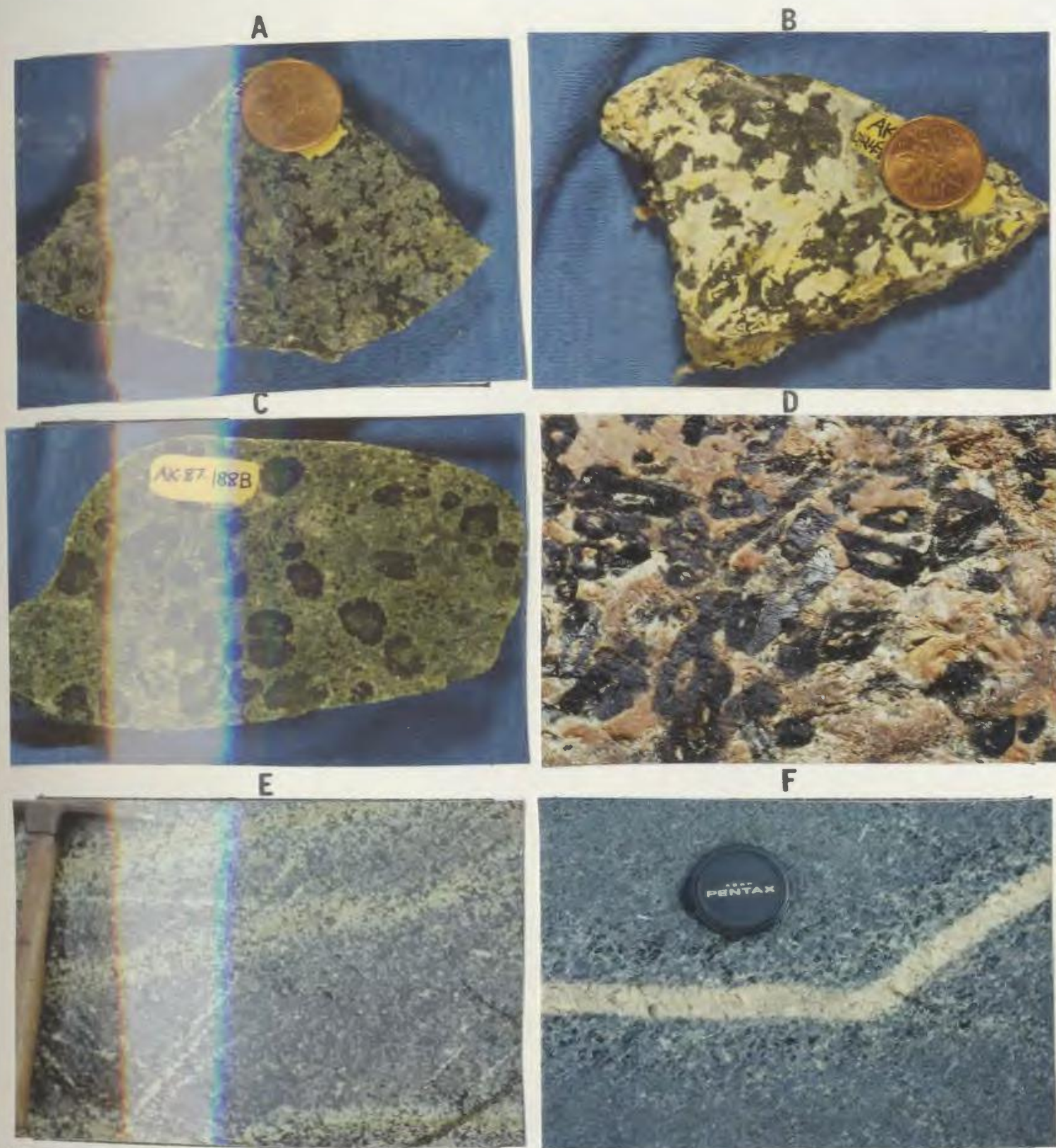


Plate 5.2. Features of mafic rocks in the Adlavik Intrusive Suite (see also Plate 5.1). (a) and (b) Typical plagioclase-cumulate leucogabbro samples. (c) Amphibole phenocrysts (after pyroxene) in a fine-grained variant from Big Bight, note cores (altered aügite). (d) Amphibole-bearing pegmatite, with unusual, hollow hornblende crystals up to 2 cm diameter (cross-section), Adlavik Bay. (e) Pervasive zones of epidotization in melagabbro facies, Big Bight. (f) Amphibolitization of gabbro around thin felsic veinlet, Jacques Island. Slabs stained for K-feldspar.



lozenges in some areas suggests that these were zones of flow, and they are interpreted as conduits through which mafic magma batches ascended to higher parts of the intrusion. They were probably emplaced into hot, partly consolidated cumulates that contained residual liquid capable of mobilization and interaction with ascending mafic magma. Their presence in the diorite unit indicates that multiple batches of mafic magma were emplaced at Adlavik Bay, and that diorite is not the youngest component.

**Petrographic Features :** Mafic rocks of the Adlavik Intrusive Suite range from fresh variants where plagioclase, pyroxene and biotite are the dominant minerals to altered variants dominated by hornblende, saussuritized plagioclase and actinolite. Samples that lie between these extremes commonly contain hornblende as mantles on pyroxene crystals, suggesting that it is a late primary phase or a deuteric alteration product. In hydrated variants, clinopyroxene ( $\pm$  orthopyroxene) occurs only locally as relict cores in hornblende. Red biotite is present in hornblende-free rocks, and is probably part of the primary assemblage.

This mineralogical continuum is interpreted to reflect variations in the water content of the magma during crystallization (c.f. Clark, 1973). Although some pyroxene-free rocks (especially gabbroic pegmatites and parts of the diorite unit, see below) contain euhedral, primary hornblende, it is suggested that most were modified extensively by late-magmatic or deuteric effects. In some areas, amphibolitization is concentrated around fractures or thin felsic veinlets, indicating that at least some transformation was post-crystallization.

Fresh gabbronorite variants contain variable amounts of pleochroic hypersthene, and fresh to locally relict olivine, commonly mantled by orthopyroxene aggregates. Olivine does not occur widely in orthopyroxene-free rocks, but many are olivine-normative (see 5.2.2).

Ultramafic rocks, and associated mafic cumulates, contain large (up to 10 cm) megacrysts or crystal aggregates of amphibole with cores of clinopyroxene. They contain abundant pale (Mg-rich?) biotite (possibly phlogopite), and were probably originally biotite-pyroxenites.

#### Diorite and Monzodiorite

The most extensive area of this unit is in the main body (Figure 5.2), but similar rocks occur at Pamiulik Point and East Micmac Lake. It is more homogeneous than the mafic component of the Adlavik Suite, but locally resembles the most leucocratic gabbroic variants. The dominant rock type is a pale brown to pink or yellow-weathering, coarse-grained, equigranular to plagioclase porphyritic, pyroxene - hornblende - biotite or two-pyroxene diorite, quartz diorite or monzodiorite (Table 5.1; Plate 5.3).

At Adlavik Bay, the diorite appears to be gradational with adjacent plagioclase cumulates. However, it also includes angular xenoliths of gabbro and mafic cumulate indicating that it is younger than some of the mafic rocks.

Discontinuous mafic mineral layers, primary foliations defined by plagioclase alignment, and thin (< 10 m) zones of mafic cumulates occur locally. The unit is cut by the composite diabase facies, and zones of coarse amphibole-feldspar pegmatite; the latter also occurs as isolated patches within coarse diorite that probably represent local volatile-rich pockets.

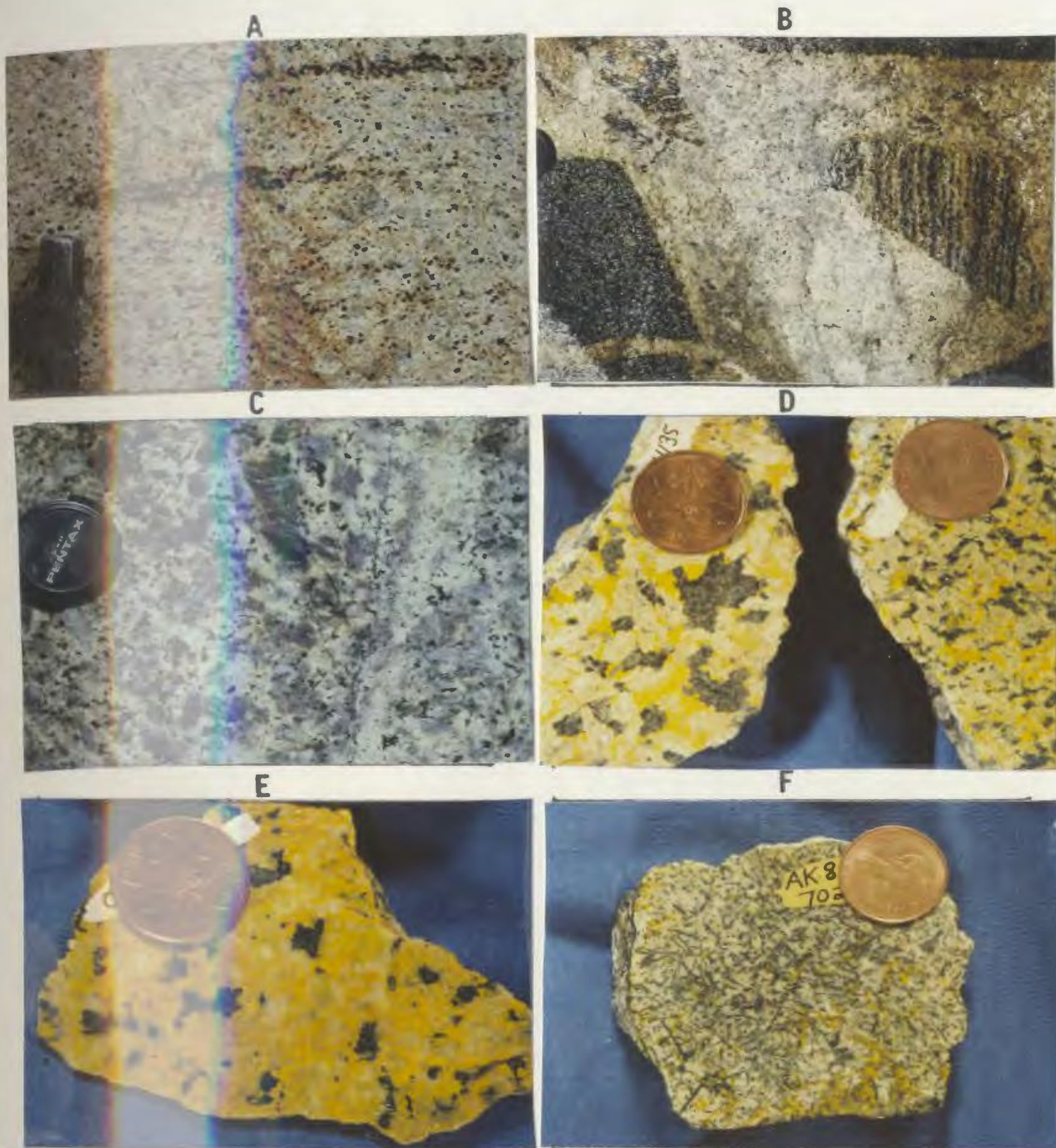


Plate 5.3. Features of the dioritic unit in the Adlavik Intrusive Suite. (a) Typical homogeneous diorite, with wispy mafic mineral layers suggesting cumulus processes, Adlavik Bay. (b) Xenoliths of leucogabbro and cumulate-layered gabbro (layered xenolith about 20 cm diameter) in diorite, Adlavik Bay. (c) Coarse-grained, plagioclase-rich variant, probably a plagioclase cumulate, Adlavik Bay. (d) Typical examples of diorite unit, Adlavik Bay, note interstitial K-feldspar. (e) Monzonitic to syenitic variant of unit. (f) Fine-grained, marginal, diorite with acicular hornblende, Big Bight area. Slabs stained for K-feldspar

As in the mafic rocks, there is a continuum from near-anhydrous variants to rocks which lack pyroxene and contain euhedral, probably magmatic hornblende. Red-brown biotite is present in most examples, and its presence appears independent of amphibole content. K-feldspar and quartz are interstitial and late. A few plagioclase-rich diorites contain both hypersthene and augite, suggesting a possible link to gabbro-noritic variants of the mafic sequence.

#### Geometry and Stratigraphy of The Adlavik Bay Layered Intrusion

There are wide variations in primary layering attitudes within single outcrops around Adlavik Bay. Reconstruction of the geometry and stratigraphy of the intrusion is thus very difficult. There is also no guarantee that layering represents the same reference orientation in all locations, or that all components were originally conformable; in fact, field relationships suggest that there are probably also internal intrusive contacts.

Layering attitudes around Adlavik Bay indicate, however, that the diorite unit is at least partly overlain by mafic rocks (assuming that their mutual contact is parallel to layering in both). A possible interpretation (Figure 5.4) is that the diorite is associated with a lower, gabbro-noritic sequence that is overlain (perhaps "unconformably") by gabbro and leucogabbro. Contrasts in normative mineralogy (see 5.2.2) also indicate that there are spatially discrete gabbro-norite and gabbro sequences. It must be stressed this is only one of a number of possible interpretations, and that space does not permit discussion of all. The composite diabase facies is



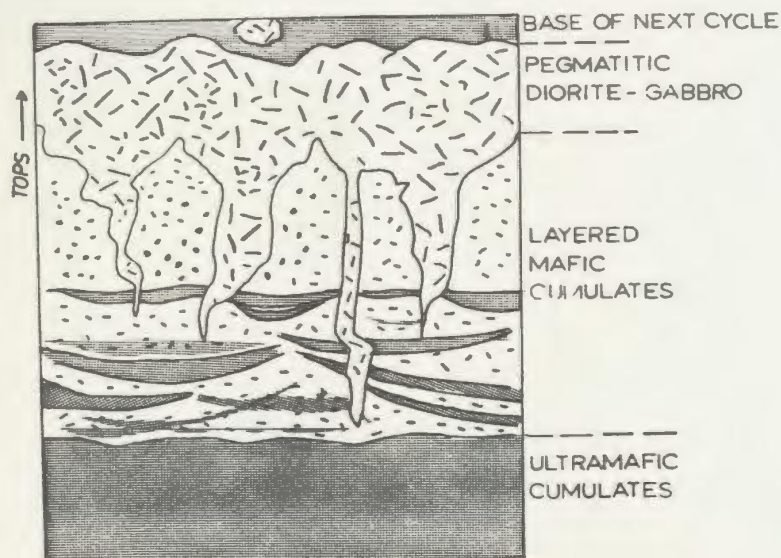


Figure 5.3. Schematic illustration of cyclic units in the Mafic Cumulate Facies in the Big Bight area, at the northern margin of the main Adlaviik Bay intrusion.

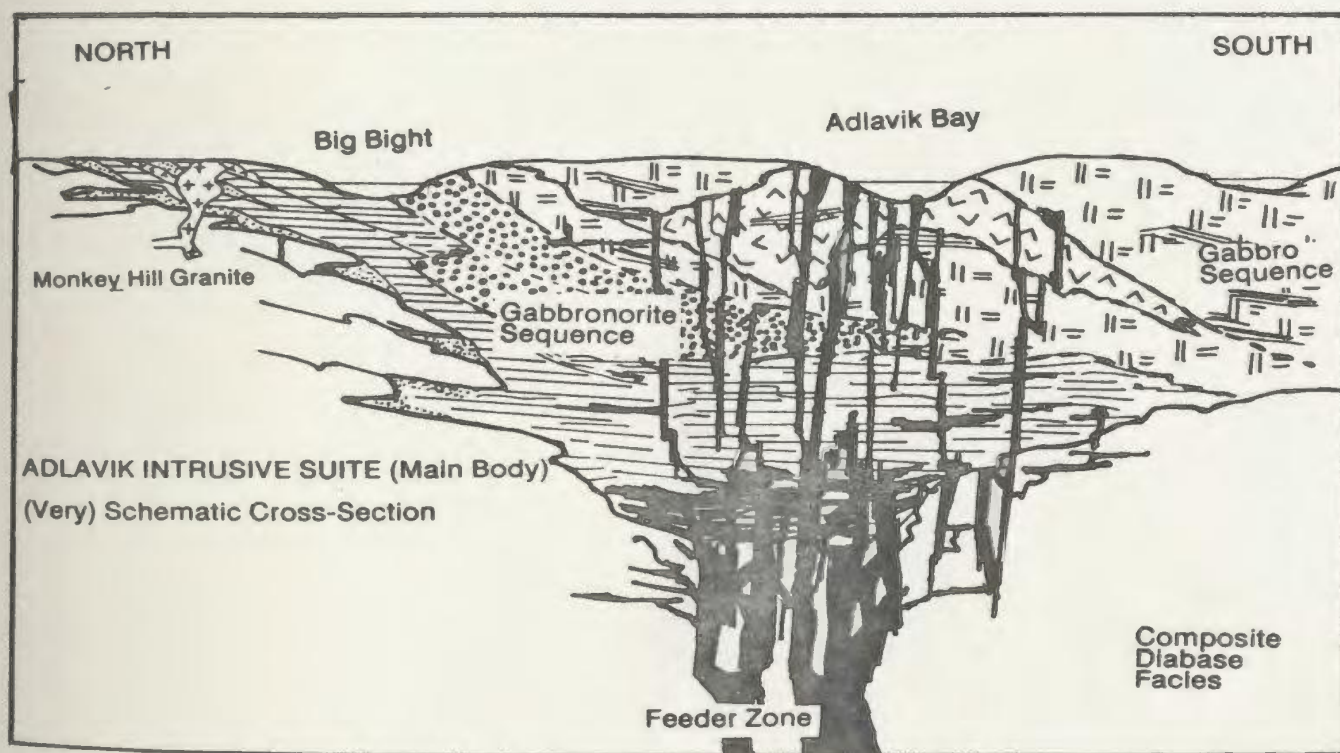


Figure 5.4. Schematic, interpretative cross-section of the main body of the Adlaviik Intrusive Suite. See text for discussion.

(Legend as for Figure 5.2)

interpreted as the feeder system for higher parts of the intrusion, and the pegmatite facies as residuum from the crystallization of individual batches of magma.

#### 5.1.2 Mount Benedict Intrusive Suite

##### Definition and Distribution

Mount Benedict Intrusive Suite is a new name introduced for compositionally varied rocks exposed in the Benedict Mountains (Figure 5.1). The term is not synonymous with "Benedict Mountains Intrusive Suite", introduced by Gower (1981) as a general label for intrusive rocks throughout this area. It is recommended that this older term be abandoned, as it includes both Makkovikian and Labradorian plutonic rocks, which cannot be directly related. The three units of the Mount Benedict Intrusive Suite correspond generally to textural variants described by Gower (1981) in his unit 21. They form a continuum from diorite and monzodiorite through monzonite and syenite to granite (s.s.) (Table 5.1; Plate 5.4). The overlap between them suggests that they are closely related and probably mutually gradational.

The southern boundary of the Mount Benedict Suite is marked by a narrow belt of strongly deformed felsic volcanic rocks that is probably bounded by faults associated with the Benedict Fault system. In the east, it is bounded by the Tukialik granite of the Strawberry Intrusive Suite, which it is presumed to intrude. The map pattern suggests dextral displacement across a fault cutting through the suite, which is here interpreted as the continuation of the Adlavik Brook Fault zone. The nature of the western contact with the volcanic rocks east of Stag Bay is unknown.

**Geochronology** : Brooks (1982) obtained a Rb-Sr whole rock isochron suggesting an age of  $1625 \pm 50$  Ma for syenite at Mount Benedict, but alluded to possible disturbance. U-Pb zircon data from a nearby locality (Krogh et al., in prep.) are slightly discordant, and indicate an age of  $1645 \pm 10$  Ma, or a maximum age of 1668 Ma assuming a 1000 Ma lower intercept. The Mount Benedict and Adlavik Suites are thus of essentially the same age.

#### **Gabbro and Diorite**

Gabbro and diorite are restricted mostly to the southwestern edge of the suite, but occur sporadically within the other two units. An area of mafic cumulate, melagabbro and monzodiorite exposed at Pamiulik Point (grouped here as Adlavik Intrusive Suite) may also be part of this unit. Gower (1981, pers.comm., 1988) states that there is no obvious structural break between these rocks and syenite to the south. As discussed subsequently (5.3), the similarity between the least evolved rocks of the Mount Benedict Suite and parts of the Adlavik Suite suggests a genetic link between them.

The unit consists of plagioclase-porphyritic pyroxene ( $\pm$  olivine) - bearing gabbro, leucogabbro and diorite, locally transitional to monzonite. Plagioclase alignment, and the oikocrystic habits of mafic minerals, indicate a cumulate origin. Several samples contain equant serpentine-iron oxide clots with cores of fresh olivine. Fresh examples contain pleochroic hypersthene, and a purple to brown titanite with prominent exsolution lamellae (probably an inverted pigeonite). Red-brown biotite is also common. Altered variants consist of saussuritized





Plate 5.4. Features of the Mount Benedict Intrusive Suite. A continuum of compositions from plagioclase cumulate (a), through diorite (b), monzonite - syenomonzonite (c), syenite (d) to quartz syenite (e). Note persistence of vestigial plagioclase phenocrysts in all but (e). (f) A combination of textures, with plagioclase crystals entrained in syenite. All samples from Mount Benedict - Jeanette Bay area. Slabs stained for K-feldspar.



plagioclase, hornblende and actinolite ( $\pm$  epidote, sphene). This unit has many petrographic similarities to gabbro and diorite of the Adlavik Intrusive Suite.

#### **Monzonite, Syenomonzonite and Syenite**

This unit forms a compositional and textural continuum from plagioclase-porphyritic, pyroxene monzodiorite to coarse-grained, biotite-hornblende syenite containing only minor plagioclase (Table 5.1; Plate 5.4). The dominant rock type is a grey to buff, seriate to porphyritic, monzonite, quartz monzonite or syenomonzonite (i.e. potassic monzonite). It is commonly plagioclase-porphyritic, although the contrast in grain size between groundmass and phenocrysts is slight. The groundmass consists of a medium-grained aggregate of quartz, K-feldspar and mafic silicates. Gower (1981) termed this "speckled-eggshell texture", and suggested that the plagioclase phenocrysts had been resorbed by the magma. In some samples, plagioclase phenocrysts have K-feldspar rims, and resemble pseudorapakivi feldspars such as those in the Big River Granite (see Chapter 4). Speckled-eggshell texture is present throughout the unit, but is developed most widely in monzonite and syenomonzonite; syenitic rocks contain only scattered vestigial plagioclase phenocrysts.

Plagioclase phenocrysts are zoned and saussuritized, whereas groundmass material forms clear laths. Interstitial quartz, or graphic quartz - K-feldspar micropegmatite, is commonly present. Relict clinopyroxene occurs in the cores of euhedral hornblende crystals in mafic variants. Locally, hornblende crystals have sphene cores, suggesting "early" crystallization of the latter.

### **Syenite, Quartz Syenite and Granite**

This unit is prevalent on the higher peaks of the Benedict Mountains, and is best exposed around Mount Benedict. It also occurs sporadically within the dominant monzonite-syenite. Partial restriction to higher elevations suggests that it may be a roof facies (Gower, 1981) or, alternatively, the uppermost portion of a compositionally layered body. The latter interpretation is supported by systematic geochemical changes with elevation (see 5.3).

It is dominated by homogeneous, pink, grey or buff colored, locally porphyritic, fine to medium-grained, leucocratic, syenite, quartz syenite or granite. Potash feldspar is a common phenocryst phase, but vestigial plagioclase phenocrysts and speckled-eggshell texture are present locally. In one location, it contains large (2 cm), embayed plagioclase crystals that appear to have been entrained in syenitic magma. The unit locally grades into a feldspar or quartz-feldspar porphyry of subvolcanic aspect, suggesting a high level of emplacement.

Graphic quartz-microcline intergrowth textures in the groundmass, and coarse perthite phenocrysts, suggest epizonal characteristics. Biotite is the dominant mafic phase, forming subhedral single crystals or aggregates with associated (usually relict) hornblende. Accessory minerals (sphene and zircon) are prominent, and fluorite occurs as interstitial material and discordant veinlets.

#### **5.1.3 Monkey Hill Intrusive Suite**

##### **Definition and Distribution**

Monkey Hill Intrusive Suite (Kerr, 1988) is a new name proposed for several discrete, small, epizonal plutons

located in the Kaipokok Bay - Makkovik Bay area (Figure 5.1). The type locality (referred to below as the "main body" is at Monkey Hill, near Makkovik. All of these plutons intrude the Upper Aillik Group, and all consist of similar fine-grained, leucocratic monzogranite and granite (Table 5.1; Plate 5.5). They are probably small stocks or cupolas connected to a larger body at depth. In a discussion of potential specialized granitoids, Kerr (1988) included the similar Witchdoctor and Burnt Lake granites (see below) with this suite. In view of the distance between these units and the type locality, and some differences in petrography, these are here treated separately. The Monkey Hill Intrusive Suite corresponds to parts of Units 28a and 28b of Gower et al. (1982).

**Geochronology** : Wanless et al. (1970) obtained a K-Ar age of  $1625 \pm 60$  Ma from the Round Pond Granite. A Rb-Sr isochron of  $1520 \pm 35$  Ma from this body (Wilton and MacDougall, pers. comm., 1988) is probably disturbed by hydrothermal activity related to mineralization. U-Pb zircon data from the main body (Krogh et al., in prep.) are discordant, but suggest an imprecise age of ca.  $1640 \pm 10$  Ma. They are colinear with zircon data from other Labradorian plutonic rocks, suggesting that all are of broadly similar age.

#### **Lithology and Field Relationships**

**Field Relationships** : The Monkey Hill Granite is a small ( $< 50 \text{ km}^2$ ) pluton that intrudes the Upper Aillik Group and foliated granitoid rocks of the Kennedy Mountain Intrusive Suite. The Duck Island Granite is a small stock or cupola restricted to a small islet in Mark's Bight;



Plate 5.5. Features of the Monkey Hill Intrusive Suite. (a) Two phases of the Monkey Hill Granite; the dominant pink granite cuts a darker, grey-brown phase, Gull Island, Makkovik Bay. (b) Vein correlated with Little Monkey Hill Granite cutting gabbro of the Adlavik Intrusive Suite, Big Bight (large gabbro block about 30 cm across). (c) Tuffisite breccia, with clasts of miarolitic granite and biotite-chlorite matrix, Makkovik Bay. (d) and (e) Typical Monkey Hill Granites, from the main body. (f) Molybdenite-bearing, slightly pegmatitic phase of the Duck Island Granite, Duck Island.

however, numerous veins and sheets of similar material intrude the Long Island Quartz Monzonite within a 2 km radius of the island. The Round Pond Granite (described by MacDougall and Wilton, 1987, and MacDougall, 1988), consists of two small bodies that intrude the Upper Aillik Group, and are associated with hydrothermal alteration and mineralization. The Little Monkey Hill Granite forms a prominent peak about 12 km east of the main body, and intrudes the Upper Aillik Group; dykes and veins associated with this body also cut mafic rocks of the Adlavik Intrusive Suite. The Bent's Cove Granite intrudes metasedimentary rocks of the Upper Aillik Group. The Kidlaluit Granite occupies most of Kidlaluit Island, and includes large blocks of coarse gabbro that resemble those of the Adlavik Suite. Contacts of all bodies are sharp, intrusive interfaces characterized by stoping and net-veining of the country rocks. The relationship with the Adlavik Suite gabbro suggests that the Monkey Hill Intrusive Suite is younger than ca. 1650 Ma.

***Lithology and Petrology*** : All members of the Suite are dominated by grey to buff or pink, fine to medium grained, faintly porphyritic, leucocratic monzogranite, granite and (locally) alkali-feldspar granite (Table 5.1; Plate 5.5). They are homogeneous, and lack inclusions except near contacts. The Duck Island and Round Pond Granites, and parts of the Kidlaluit Granite, are locally pegmatitic and/or miarolitic. The main body at Monkey Hill contains xenoliths of a darker-coloured phase on Gull Island, but is otherwise remarkably homogeneous over 900 m of vertical relief. At the northern end of Kidlaluit Island, an earlier grey phase is cut by the dominant pinkish granite. "Tuffisite" breccias consisting of granite

clasts in a biotite-rich matrix are locally exposed around Makkovik Bay, and suggest exsolution of dissolved volatiles. Shallow emplacement is also suggested by the local occurrence of a very fine-grained feldspar porphyry of subvolcanic appearance in the main body, Bent's Cove Granite, and associated with the Duck Island Granite.

The circular-shaped body northeast of the Duck Island granite consists of graphic micropegmatite that forms a network of sheets and veins intruding the Upper Aillik Group. Although petrographically atypical of the suite, it is grouped with it on the basis of proximity to three other members.

***Petrographic Characteristics*** : Plagioclase forms small (up to 5mm), euhedral to subhedral laths that appear to have crystallized early and, although similar in size to other grains, impart a "porphyritic" or "speckled" appearance. They have saussuritized cores, and are locally zoned. Quartz is interstitial or graphically intergrown with microcline. Green or green-brown biotite forms dispersed crystals or aggregates, and is altered to chlorite along cleavage traces. In many samples, chlorite is the dominant mafic mineral. Epidote is common in chlorite-bearing variants, and locally displays an interstitial habit suggesting that it may have been a primary magmatic phase. Garnet has been observed only at the northern end of the Kidlalluit Granite.

#### **5.1.4 Witchdoctor and Burnt Lake Granites**

The Witchdoctor and Burnt Lake Granites occur in the southwest of the study area, between the Benedict Fault zone and an area of Upper Aillik Group volcanic rocks.

The two units are similar in many respects, and the Burnt Lake Granite is interpreted as a fine-grained marginal or roof phase of the Witchdoctor Granite.

#### Witchdoctor Granite

This is poorly exposed, and its contact relationships are unknown. It corresponds to Unit 26e of Gower et al. (1982), and to part of the "Walker Lake Granite" of BRINCO geologists, which also included parts of the Otter Lake - Walker Lake Granitoid (see below). It was previously described as hornblende monzonite and granodiorite (Bailey, 1979; Gower et al., 1982), but this description largely reflects its supposed correlation with the quite different granitoid rocks to the west. Brooks (1983) dated this unit at  $1595 \pm 34$  Ma (Rb-Sr, whole rock) and  $1632 \pm 9$  Ma (U-Pb, zircon). It is dominated by pink to white, medium to coarse grained, variably foliated, leucocratic biotite and biotite - muscovite monzogranite to alkali-feldspar granite (Table 5.1; Plate 5.6). Most examples are homogeneous and equigranular, but recrystallization and deformation are widespread, and local east-trending fabrics are present.

Quartz is extensively recrystallized and forms elongate ribbon-like aggregates, although it locally retains a vestigial interstitial habit. Green-brown biotite is intergrown with lesser amounts of muscovite, forming aggregates parallel to foliations. Relict hornblende occurs locally in muscovite-poor variants, and chlorite occurs locally as an alteration product of biotite. Pale pink garnet is a minor constituent of several samples.



A



B



C



D



E

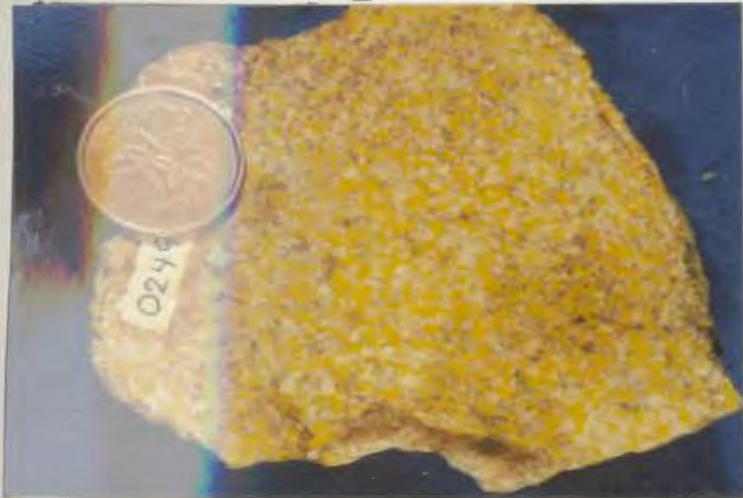


Plate 5.6. Features of the Witchdoctor and Burnt Lake Granites. (a) and (b) Typical examples of the Witchdoctor granite, showing variable recrystallization and deformation, Witchdoctor Lake area. (c) and (d) Foliated and unfoliated Burnt Lake Granites, Burnt Lake area. (e) Mirolitic Burnt Lake granite, adjacent to Burnt Lake moybdenite showing. Slabs stained for K-feldspar.



### **Burnt Lake Granite**

The Burnt Lake Granite is dominated by white to pale grey or pink, fine to medium grained, equigranular, leucocratic monzogranite, granite and (locally ) alkali feldspar granite (Table 5.1; Plate 5.6).

Failey (1979) described its contacts with the Upper Ailik Group as gradational, a reflection of the similarity between fine-grained granite and sugary, recrystallized rhyolite. However, MacKenzie and Wilton (1987) described sharp intrusive contacts from several localities. Rb-Sr data presented by MacKenzie and Wilton (1988) give a  $1548 \pm 90$  Ma errorchron, which they suggested to be disturbed by Grenvillian events. This could, however, also be interpreted as a reflection of post-crystallization hydrothermal activity (c.f. Walraven et al., 1986). Disseminated Mo mineralization is present in the contact zone of the granite, and it has also been linked to uranium - base metal mineralization in adjacent country rocks (MacKenzie and Wilton, 1987).

Most samples are recrystallized, and original igneous textures, except for relict microcline phenocrysts, are not readily discerned. Muscovite occurs both as intergrowths with biotite flakes of a similar size range, and as fine-grained fibrous aggregates of secondary appearance. It is absent in the more melanocratic variants. Minor garnet is present locally, but is less common than in the Witchdoctor Granite.

#### **5.1.5 Otter Lake - Walker Lake Granitoid**

This is a regionally extensive granitoid unit in the southwest of the study area (Figure 5.1), which extends for 50-75 km beyond the western edge. It corresponds to unit 32

of Ryan (1984), which he grouped with spatially associated muscovite-biotite granites (Crooked River Granite) to form the Nipishish Lake Intrusive Suite. The Crooked River Granite does not outcrop within the study area. Descriptions below apply only to quartz monzonite, monzogranite and granite within the study area.

Kontak (in Ryan, 1984) obtained a Rb-Sr errorchron suggesting an age of  $1550 \pm 55$  Ma from granite at Walker Lake. This is similar to ages from the Witchdoctor and Burnt Lake Granites, and is probably disturbed. U-Pb zircon data (Krogh et al., in prep.) are concordant at  $1647 \pm 2$  Ma. Ryan (1984) describes an intrusive contact between granodiorite assigned to this unit and metasedimentary rocks of the Upper Aillik Group in the Walker Lake area. The contact with the syn-tectonic Makkovikian Melody Granite corresponds with an inferred fault zone.

The Otter Lake - Walker Lake Granite is dominated by grey to pink or green-white, medium to coarse grained, porphyritic to seriate quartz monzonite, granodiorite and monzogranite (Table 5.1; Plate 5.7). Melanocratic dioritic variants occur locally. Both K-feldspar and plagioclase phenocrysts are present; in most examples the former are larger, up to 3-5 cm in size. Characteristic features include pale green, saussuritized plagioclase, and blue-grey interstitial quartz, both noted also by Ryan (1984).

Recrystallization is most intense in the south and close to inferred faults; many samples in the north are undeformed and retain good igneous textures. Microcline phenocrysts are finely perthitic and locally have rims of sodic plagioclase. Plagioclase phenocrysts display normal zonation, and contain saussuritized centers. Green or green-brown biotite is the dominant mafic silicate,

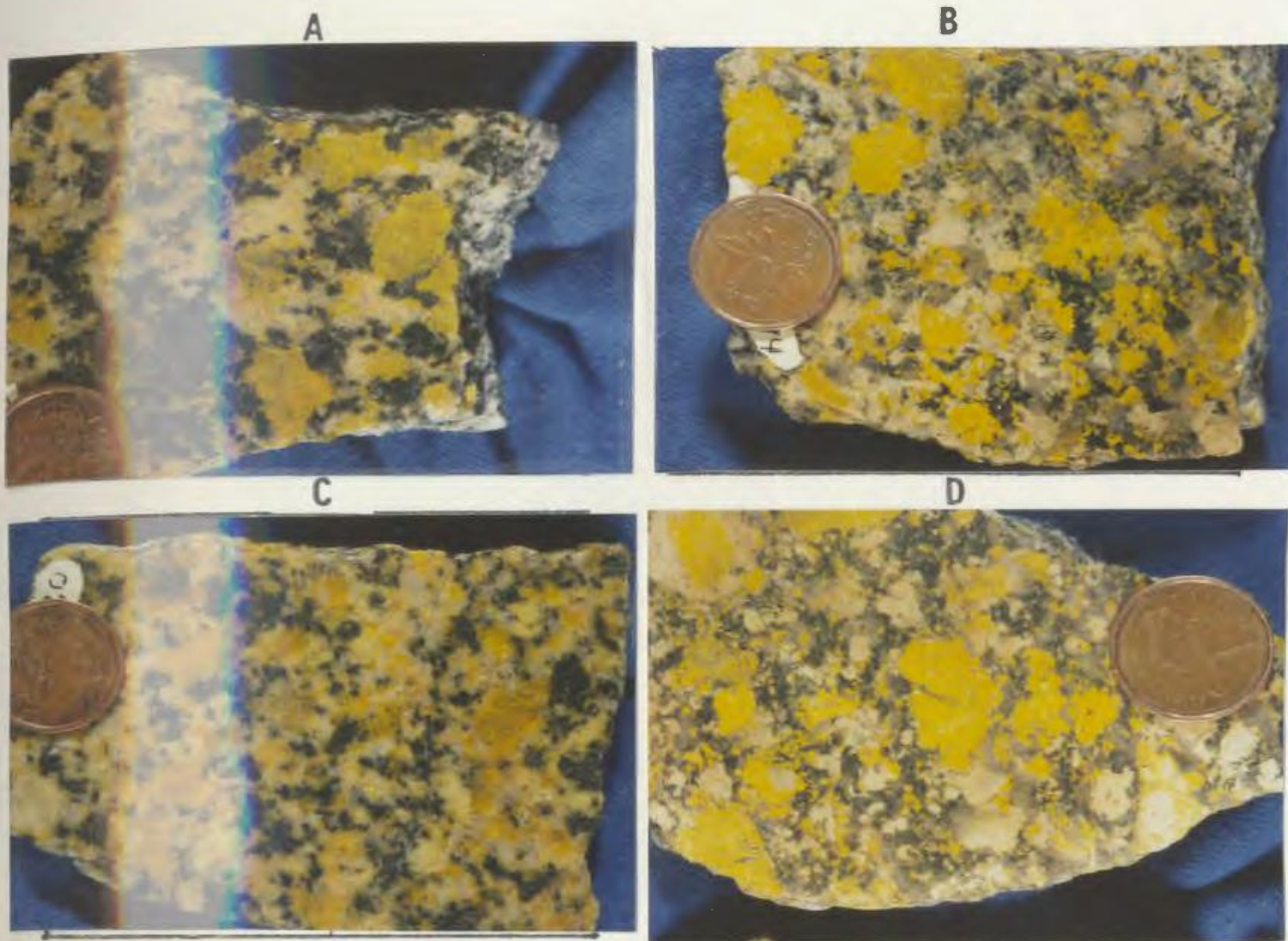


Plate 5.7. Features of the Otter Lake - Walker Lake Granitoid. (a) to (d) Typical quartz monzonite to monzogranite samples, showing variable recrystallization and deformation, but with well-preserved igneous textures. All samples from the Walker Lake area. Slabs stained for K-feldspar.

associated with lesser green hornblende. Relict clinopyroxene, altered to hornblende, is present rarely. Sphene is abundant in most samples, and locally occurs in amounts comparable to hornblende or biotite. It forms euhedral or subhedral crystals up to 3 mm in size, and in places displays a clear interstitial habit. Epidote and/or chlorite are important as alteration products of plagioclase, and are the dominant mafic silicates in the most strongly deformed samples.

## 5.2 DESCRIPTIVE GEOCHEMISTRY

Labradorian plutonic rocks are represented by 429 samples; 247 of these are regional samples collected on a 2 km random grid spacing. The remainder include 99 follow-up samples (from the Monkey Hill, Adlaviik and Mount Benedict Intrusive Suites), and 83 geological samples distributed amongst all units.

### 5.2.1 General Geochemistry

#### Summary of Numerical Data

Average compositions of principal Labradorian plutonic units are listed in Table 5.2. Four main groupings are apparent.

The Adlaviik Intrusive Suite is dominated by  $\text{SiO}_2$ -poor (< 60%) rocks, and has the highest levels of CaO, MgO, FeO and  $\text{TiO}_2$  and compatible OCC trace elements. Geographic divisions of the suite have similar mean compositions, except for the relatively siliceous gabbro at East Micmac Lake.

The Mount Benedict Intrusive Suite is dominated by rocks with 60 to 70%  $\text{SiO}_2$ . It is strongly enriched in Rb, Cs, U, Th, F and Zr compared to all other Labradorian units; enrichment is generally strongest in the syenite to granite unit. The least differentiated unit is similar in mean composition to diorite of the Adlaviik Suite.

The Monkey Hill Intrusive Suite consists of high-silica (72-75%  $\text{SiO}_2$ ) granites that have low levels of CaO, FeO and MgO. However, trace element patterns are relatively

Table 5.2 . Average compositions of Labradorian plutonic units, subdivided by principal units.

UNIT	40.1		40.2		40.3		40.4		41.1		41.2		41.3	
n1	85		17		2		11		12		6		3	
n2	15		1		0		0		2		2		1	
(Wt%)	Mean	S.D.	Mean	S.D.	Mean	S.D.	Mean	S.D.	Mean	S.D.	Mean	S.D.	Mean	S.D.
SiO <sub>2</sub>	49.94	4.57	48.03	1.82	55.55	0.35	49.77	3.34	58.21	3.21	56.46	2.79	58.43	1.33
TiO <sub>2</sub>	0.94	0.44	1.03	0.32	0.60	0.01	1.15	0.46	0.82	0.31	0.86	0.21	0.80	0.12
Al <sub>2</sub> O <sub>3</sub>	15.80	3.98	14.81	3.23	16.24	1.49	15.79	2.61	17.86	1.26	18.61	1.08	17.44	0.67
Fe <sub>2</sub> O <sub>3</sub>	3.05	1.48	3.65	1.11	1.90	0.00	2.61	0.81	1.93	0.76	2.13	0.40	1.91	0.28
FeO	6.15	1.77	6.82	0.80	5.41	1.03	6.65	1.25	3.85	1.43	4.49	1.46	5.15	0.02
MnO	0.16	0.04	0.18	0.03	0.12	0.03	0.17	0.03	0.13	0.03	0.12	0.03	0.11	0.01
MgO	7.62	5.32	8.42	3.08	5.45	0.76	7.42	5.16	2.26	1.57	2.35	1.13	2.94	0.26
CaO	9.67	3.04	10.45	1.92	7.07	0.59	8.11	2.00	4.60	1.99	5.71	1.57	4.88	0.80
Na <sub>2</sub> O	3.08	1.20	2.63	0.91	3.67	0.44	3.36	1.12	5.38	1.02	4.35	0.50	3.84	0.03
K <sub>2</sub> O	1.47	0.92	1.51	0.48	2.05	0.25	2.17	1.07	3.40	0.97	3.39	1.31	3.42	0.26
P <sub>2</sub> O <sub>5</sub>	0.34	0.39	0.29	0.17	0.25	0.00	0.41	0.43	0.30	0.15	0.38	0.12	0.31	0.14
LOI	1.38	0.79	1.61	0.56	1.31	0.35	1.45	0.84	0.75	0.31	0.94	0.31	1.19	1.16
TOTAL	99.60		99.43		99.62		99.06		99.49		99.79		100.42	
(ppm) Trace Elements														
Li	21.7	9.2	21.7	6.4	18.5	2.1	31.0	9.9	20.6	7.8	20.0	4.0	22.3	2.5
F	732.6	1120	873.5	393.0	385.0	62.2	654.4	317.9	804.8	340.9	913.3	353.4	716.7	127.2
Sc	32.3	16.2	32.9						15.0	0.0	16.9	9.8	12.0	
V	203.5	110.6	223.8	68.0	172.0	36.8	183.2	56.2	79.3	67.7	117.0	41.9	97.7	66.7
Cr	275.8	444.3	288.1	276.5	171.5	46.0	338.9	463.7	29.7	34.4	19.2	13.6	23.7	2.1
Ni	78.2	128.4	57.2	41.4	45.5	6.4	98.3	150.9	11.0	12.0	8.3	5.4	15.3	0.6
Cu	50.7	41.0	48.9	23.2	88.5	37.5	50.0	35.1	18.8	14.4	33.0	18.4	18.0	11.3
Zn	96.7	40.1	97.4	22.0	75.5	3.5	100.9	22.7	75.7	19.6	83.8	10.2	71.0	13.2
Ga	20.5	6.1	19.9	3.6	20.5	0.7	18.9	5.2	16.3	5.6	21.7	1.4	17.7	0.6
Rb	41.6	29.9	44.1	18.0	42.5	0.7	56.6	31.5	73.8	23.5	83.5	26.8	91.7	6.7
Sr	760.5	297.8	661.5	382.2	804.0	234.8	677.5	182.0	687.0	225.6	612.3	125.0	615.0	150.7
Y	19.2	10.5	23.2	6.5	11.0	4.2	19.3	9.7	21.3	6.9	33.5	9.3	17.0	1.7
Zr	73.1	64.4	115.4	79.9	87.5	1.0	116.3	87.5	99.3	58.5	351.0	159.1	116.0	12.3
Nb	3.6	4.2	3.9	4.2	2.0	0.0	3.4	2.7	10.2	3.5	13.2	6.6	5.0	0.0
Mo	3.4	1.1	5.7	8.6	3.0	0.0	4.0	2.5	3.1	0.7	4.2	2.1	3.3	0.6
Sn	1.0	0.0	1.0						1.0	0.0	1.5	0.7	1.0	
Cs	1.1	1.7	0.5						1.3	1.1	2.0	0.0	0.5	
Ba	597.9	338.3	504.5	227.8	983.5	79.9	940.1	839.7	1734.6	1297	902.8	209.2	855.0	113.5
La	22.5	14.6	28.8	18.6	30.5	2.1	28.6	15.6	34.8	9.8	47.2	9.5	28.7	5.1
Ce	48.0	30.2	55.7	39.9	55.5	3.5	54.4	32.4	61.1	23.5	96.5	29.6	58.0	8.0
Sm	5.4	2.2	8.1						6.5	0.5	7.1	0.3	5.4	
Yb	2.5	0.0	2.5						2.5	0.0	2.5	0.0	2.5	
Hf	2.3	2.0	1.0						3.0	0.0	3.5	0.7	3.0	
Pb	5.2	7.0	1.9	1.7	8.5	0.7	3.8	3.8	9.4	4.2	10.7	4.3	7.0	5.2
Th	2.2	2.9	1.3	1.3	1.5	0.7	1.7	1.9	3.1	3.8	7.0	4.3	12.3	9.0
U	1.0	0.9	1.1	0.8	0.9	0.1	1.2	1.0	1.8	1.3	3.2	1.3	1.8	0.1
(Wt%) Partial CIPW Norms														
Q	0.81	2.64	0.00	0.00	2.82	0.80	0.05	0.00	1.60	2.92	2.57	3.67	6.68	
C	0.03	0.19	0.00	0.00	0.00	0.00	0.00	0.00	0.00	0.00	0.00	0.00	0.57	
Or	8.80	5.50	9.09	2.90	12.31	1.48	13.06	0.18	20.32	5.84	20.24	7.84	20.34	
Ab	24.81	10.83	20.09	7.20	31.56	3.88	27.11	2.46	45.78	8.57	37.13	4.27	32.71	
An	25.29	9.12	24.67	5.39	22.12	2.98	22.08	0.25	14.73	5.61	21.48	6.27	18.85	
Ne	0.89	1.35	1.42	1.84	0.00	0.00	1.08	0.00	0.14	0.35	0.02	0.05	0.00	
Di	17.21	12.49	21.39	10.65	9.98	4.68	13.48	0.86	5.51	4.30	4.17	2.82	3.19	
Hy	5.20	6.01	4.15	6.40	16.63	1.49	2.59	0.47	5.10	4.25	7.27	4.79	12.60	
Ol	9.70	10.15	11.02	3.55	0.00	0.00	13.38	2.26	1.69	2.73	1.42	2.69	0.00	
Mt	4.50	2.21	5.40	1.65	2.80	0.01	3.87	0.13	2.83	1.11	3.12	0.58	2.79	
Il	1.82	0.86	2.00	0.63	1.15	0.02	2.23	0.03	1.57	0.61	1.66	0.39	1.53	

KEY TO UNITS (AIS - Adiravik Intrusive Suite)

40.1 (AIS) Gabbro-Gabbro-norite (Type Area)      41.1 (AIS) Diorite (Type Area)  
 40.2 (AIS) Gabbro-Gabbro-norite (Southern Area)      41.2 (AIS) Diorite (Southern Area)  
 40.3 (AIS) Gabbro-Gabbro-norite (East Wicmac)      41.3 (AIS) Diorite (East Wicmac)  
 40.4 (AIS) Gabbro-Gabbro-norite (Eastern Area)

n1 -- Number of analyses for all elements except those listed below.

n2 -- Number of analyses for Sc, Sn, Cs, Sm, Yb and Hf.

Table 5.2 (continued).

UNIT	42.0		43.0		44.0		46.0		47.0		48.0	
n1	17		53		67		17		17		49	
n2	1		22		39		12		17		11	
(Wt%)	Mean	S.D.	Mean	S.D.	Mean	S.D.	Mean	S.D.	Mean	S.D.	Mean	S.D.
SiO <sub>2</sub>	55.52	3.22	64.46	4.46	70.69	3.31	73.78	3.33	72.71	3.11	68.54	4.42
TiO <sub>2</sub>	0.97	0.20	0.61	0.24	0.30	0.18	0.15	0.15	0.16	0.07	0.44	0.20
Al <sub>2</sub> O <sub>3</sub>	18.23	1.64	16.03	0.93	14.39	1.06	13.77	1.22	14.18	1.74	14.98	1.62
Fe <sub>2</sub> O <sub>3</sub>	1.99	0.49	1.40	0.66	0.97	0.40	0.65	0.59	0.57	0.25	1.20	0.61
FeO	4.43	1.16	2.53	1.12	1.09	0.66	0.63	0.26	0.60	0.36	1.87	1.01
MnO	0.13	0.03	0.09	0.03	0.05	0.02	0.04	0.01	0.03	0.01	0.06	0.03
MgO	2.79	1.89	1.12	0.97	0.38	0.27	0.15	0.12	0.21	0.14	0.86	0.54
CaO	5.52	1.54	2.37	1.52	0.97	0.49	0.75	0.41	0.80	0.30	2.04	1.02
Na <sub>2</sub> O	4.37	0.44	4.51	0.36	4.28	0.43	4.13	0.40	4.40	1.53	3.89	0.55
K <sub>2</sub> O	3.61	0.95	5.41	0.93	5.58	0.51	5.04	0.64	4.93	1.07	4.70	0.62
P <sub>2</sub> O <sub>5</sub>	0.42	0.24	0.19	0.17	0.05	0.06	0.02	0.03	0.03	0.02	0.15	0.09
LOI	1.26	0.56	0.84	0.23	0.75	0.11	0.45	0.14	0.54	0.10	0.77	0.24
TOTAL	99.24		99.56		99.50		99.56		99.16		99.50	
(ppm)												
Li	32.7	12.4	31.0	10.4	25.3	11.0	14.3	13.6	27.2	23.1	25.7	12.5
P	975.1	365.5	1298.0	410.7	1240.5	617.4	137.9	97.7	217.5	130.7	679.1	257.1
Sc	6.7		5.8	2.1	2.9	1.7	2.3	1.4	1.6	1.0	6.8	2.4
V	107.9	39.5	50.6	40.9	23.1	13.1	13.1	5.7	16.3	7.7	44.6	30.2
Cr	42.3	81.7	14.5	16.6	6.5	3.8	3.8	4.9	3.2	2.3	6.5	7.0
Ni	20.7	43.2	4.3	5.3	1.9	1.7	1.8	2.3	1.5	1.9	2.1	3.0
Cu	56.9	40.0	18.9	16.9	10.1	8.8	3.4	2.6	4.2	4.6	9.1	18.7
Zn	92.1	25.5	60.3	19.1	39.9	14.0	25.1	8.2	32.5	12.1	46.9	21.4
Ga	19.4	4.5	11.3	4.7	8.6	2.1	11.5	7.1	11.9	4.1	12.8	4.1
Rb	130.0	46.4	233.2	81.8	315.3	81.3	169.5	49.6	212.8	78.4	140.5	38.7
Sr	766.5	216.7	308.9	191.0	126.8	108.3	75.4	83.5	98.8	67.7	277.7	154.8
Y	24.7	6.8	30.3	8.7	27.8	7.6	23.7	27.5	27.1	6.2	28.2	10.2
Zr	236.0	190.9	408.0	190.7	345.0	140.0	198.5	232.5	172.7	82.7	240.0	83.8
Nb	10.7	5.0	21.2	8.1	29.0	8.6	16.9	16.4	25.1	8.0	13.6	4.4
Mo	4.7	3.5	4.7	1.5	4.3	2.7	3.4	0.9	52.8	202.1	3.2	1.2
Sn	14.0		6.1	4.2	7.2	4.2	1.8	1.1	2.8	2.5	3.9	3.3
Cs	6.4		10.7	5.3	9.0	4.3	1.8	1.2	2.0	1.4	4.1	1.8
Ba	1115.7	409.1	742.8	360.6	381.9	352.6	515.1	912.7	522.9	328.7	961.5	542.3
La	44.0	10.5	50.7	13.1	56.3	22.9	28.0	25.9	34.3	17.6	50.6	14.8
Ce	89.9	22.5	108.3	30.3	114.0	43.7	60.9	55.4	65.9	33.2	100.1	28.5
Sm	10.1		8.2	1.7	6.9	1.7	3.9	1.4	4.4	2.2	9.3	3.0
Yb	4.5		4.1	1.0	4.5	0.9	2.5	0.0	3.0	0.7	2.5	0.0
Hf	20.0		12.2	3.0	9.9	3.1	5.0	1.0	6.0	1.6	12.5	21.1
Pb	12.5	4.6	17.8	6.1	23.4	8.0	22.2	5.8	31.4	14.0	16.8	8.1
Th	7.8	5.5	21.6	13.6	37.5	13.8	18.0	7.7	20.3	10.8	14.8	7.3
U	3.3	1.7	6.8	3.2	10.4	4.4	5.6	4.0	9.3	5.2	4.0	2.4
(Wt%)												
Q	1.10	1.85	10.94	6.32	22.13	7.27	27.10	9.76	26.52	9.82	22.14	8.29
C	0.00	0.00	0.02	0.10	0.12	0.24	0.25	0.20	0.26	0.23	0.26	0.36
Or	21.71	5.63	32.33	5.51	33.36	3.06	30.05	3.80	29.51	6.44	28.14	3.71
Ab	37.43	3.77	38.63	3.09	36.65	3.68	35.25	3.46	37.53	12.63	33.29	4.70
An	19.86	5.90	7.58	4.35	3.30	1.78	3.49	1.66	3.73	1.66	8.95	4.23
Me	0.13	0.35	0.00	0.00	0.00	0.00	0.00	0.00	0.11	0.47	0.00	0.00
Di	4.71	2.44	2.60	2.33	0.79	0.82	0.14	0.41	0.18	0.42	0.49	0.74
Hy	7.01	4.62	3.90	2.08	1.41	1.11	0.82	0.56	0.92	0.69	3.77	2.10
Ol	2.18	3.19	0.25	1.80	0.00	0.00	0.00	0.00	0.00	0.00	0.00	0.00
Wt	2.95	0.73	2.03	0.96	1.36	0.59	0.85	0.54	0.79	0.38	1.76	0.90
Il	1.89	0.39	1.17	0.47	0.58	0.34	0.28	0.28	0.31	0.14	0.85	0.38

KEY TO UNITS (NBIS - Mount Benedict Intrusive Suite)

42 (NBIS) Gabbro to Monzoniorite  
 43 (NBIS) Monzonite, Syenomonzonite, Syenite  
 44 (NBIS) Syenite, Quartz Syenite, Granite  
 46.0 -- Witchdoctor Granite  
 47.0 -- Burnt Lake Granite  
 48.0 -- Otter Lake - Walker Lake Granitoid

n1 -- Number of analyses for all elements except those listed below.

n2 -- Number of analyses for Sc, Sn, Cs, Sm, Yb and Hf.

Table 5.2 (continued).

UNIT	45.1		45.2		45.3		45.4		45.5		45.6	
n1	33		4		8		13		3		6	
n2	29		2		6		10		3		5	
(Wt%)	Mean	S.D.	Mean	S.D.	Mean	S.D.	Mean	S.D.	Mean	S.D.	Mean	S.D.
SiO <sub>2</sub>	72.97	5.86	75.69	1.69	72.49	2.89	74.62	2.44	72.77	3.16	74.05	0.68
TiO <sub>2</sub>	0.14	0.14	0.04	0.01	0.14	0.12	0.12	0.07	0.18	0.09	0.18	0.04
Al <sub>2</sub> O <sub>3</sub>	13.39	1.48	12.75	0.21	13.82	1.11	13.47	0.84	14.38	0.94	13.59	0.13
Fe <sub>2</sub> O <sub>3</sub>	1.57	4.65	0.42	0.07	0.78	0.78	0.55	0.23	0.59	0.62	0.66	0.28
FeO	0.88	2.23	0.12	0.08	0.58	0.47	0.49	0.52	0.90	0.40	0.84	0.23
MnO	0.06	0.04	0.01	0.00	0.04	0.02	0.04	0.02	0.04	0.03	0.04	0.01
MgO	0.21	0.22	0.06	0.02	0.15	0.13	0.26	0.37	0.26	0.20	0.35	0.28
CaO	0.75	0.54	0.38	0.10	0.84	0.29	0.80	0.36	1.01	0.42	0.86	0.16
Na <sub>2</sub> O	4.23	0.85	4.34	0.28	4.78	2.50	4.24	0.25	4.13	0.25	3.84	0.65
K <sub>2</sub> O	4.69	1.23	4.33	0.44	4.59	1.89	4.58	0.37	4.99	0.27	4.98	1.18
P <sub>2</sub> O <sub>5</sub>	0.03	0.04	0.01	0.00	0.04	0.03	0.03	0.04	0.06	0.04	0.04	0.01
LOI	0.63	0.20	0.50	0.11	0.72	0.44	0.54	0.33	0.47	0.19	0.43	0.13
TOTAL	99.55		98.65		98.97		99.74		99.78		99.86	
(ppm)												
Li	24.1	14.6	5.5	1.0	13.1	5.4	15.0	5.6	16.7	3.5	32.8	15.8
F	685.2	463.3	258.3	201.4	199.4	194.1	369.5	295.0	119.3	109.6	780.2	502.0
Sc	1.3	0.8	0.3	0.0	1.9	1.2	0.7	0.3	1.6	0.9	2.5	0.9
V	17.7	24.9	12.0	5.3	20.1	7.1	14.8	11.1	22.0	7.2	19.3	8.2
Cr	3.7	2.4	2.0	0.8	1.8	1.0	7.9	13.6	1.0	0.0	3.7	4.4
Ni	1.2	0.7	1.0	0.0	1.0	0.0	2.3	2.8	1.0	0.0	1.0	0.0
Cu	11.1	25.2	11.8	7.4	15.9	28.7	5.4	6.7	3.3	2.3	3.0	3.2
Zn	42.5	40.3	9.0	3.2	24.3	13.0	29.5	13.9	35.7	4.7	40.5	12.5
Ga	12.8	8.6	11.3	2.6	11.3	4.7	9.7	3.3	13.7	1.2	13.0	4.7
Rb	201.1	77.7	184.8	38.9	119.5	51.2	160.1	31.7	102.0	11.5	229.3	44.1
Sr	156.2	294.4	29.0	16.8	130.1	101.9	145.6	79.7	176.7	110.0	95.2	20.1
Y	34.5	30.1	11.5	1.3	20.3	11.9	20.5	7.4	12.0	2.7	25.0	7.4
Zr	178.1	111.4	100.3	31.9	155.3	80.7	116.0	53.8	123.3	14.5	219.0	48.1
Nb	19.6	10.4	17.0	9.7	13.3	2.7	15.1	4.6	8.7	3.8	20.7	2.2
Mo	146.1	826.9	2.3	1.0	129.1	356.7	1.9	0.5	2.3	0.6	1.8	1.0
Sn	3.0	2.2	1.0	0.0	1.8	1.6	2.4	2.1	1.0	0.0	5.4	2.6
Cs	3.0	2.5	0.5	0.0	1.0	0.8	1.6	1.3	0.5	0.0	2.4	1.2
Ba	343.9	263.8	47.0	21.4	589.0	339.6	292.6	387.7	892.0	549.1	424.8	160.8
La	22.8	21.5	3.8	3.5	24.9	22.9	16.2	9.5	14.7	10.3	37.3	22.2
Ce	49.8	47.7	4.0	4.8	46.1	38.6	30.9	18.5	30.3	13.6	79.0	37.2
Sm	5.1	4.9	1.0	0.4	5.1	2.7	2.5	0.9	2.7	0.6	5.3	2.2
Yb	5.0	4.7	2.5	0.0	3.3	1.8	2.6	0.2	2.5	0.0	2.9	0.6
Hf	6.0	3.2	3.0	0.0	5.5	2.7	4.0	0.8	4.0	1.0	8.3	2.8
Pb	23.5	9.6	13.0	5.4	19.4	8.3	22.6	7.5	15.7	6.4	29.8	11.2
Th	14.5	9.2	7.0	2.9	13.3	8.2	13.2	7.5	3.3	4.0	20.2	3.9
U	6.8	6.4	5.0	2.7	4.2	2.2	4.5	2.2	2.3	1.1	9.6	4.7
(Wt%)												
Q	28.74	5.32	33.60	1.86	25.39	9.02	30.50	4.64	26.87	4.34	30.17	8.78
C	0.23	0.24	0.27	0.23	0.22	0.25	0.23	0.25	0.40	0.35	0.37	0.17
Or	27.62	7.13	26.04	2.64	26.01	11.37	27.27	2.19	29.69	1.47	29.56	16.89
Ab	36.50	7.10	37.45	2.64	42.22	19.80	36.13	2.16	35.18	2.32	32.66	14.46
An	3.14	1.77	1.85	0.49	2.82	1.72	3.62	1.43	4.91	2.00	4.17	1.73
Ne	0.00	0.00	0.00	0.00	0.00	0.00	0.00	0.00	0.00	0.00	0.00	0.00
Di	0.26	0.66	0.00	0.00	0.65	1.69	0.19	0.34	0.00	0.00	0.01	0.66
Hy	0.75	0.87	0.16	0.06	0.81	0.77	0.96	1.45	1.60	0.87	1.64	0.40
Ol	0.00	0.00	0.00	0.00	0.00	0.00	0.00	0.00	0.00	0.00	0.00	0.00
Wt	2.09	7.19	0.30	0.25	0.35	0.39	0.66	0.40	0.87	0.91	0.97	0.12
Il	0.27	0.27	0.08	0.01	0.28	0.24	0.23	0.14	0.34	0.17	0.34	0.20

KEY TO UNITS (MHIS - Monkey Hill Intrusive Suite)

45.1 (MHIS) Monkey Hill Granite  
 45.2 (MHIS) Round Pond Granite  
 45.3 (MHIS) Duck Island Granite  
 45.4 (MHIS) Little Monkey Hill Granite  
 45.5 (MHIS) Bent's Cove Granite  
 45.6 (MHIS) Kidlaluit Granite

n1 -- Number of analyses for all elements except those listed below.

n2 -- Number of analyses for Sc, Sn, Cs, Sm, Yb and Hf.



unevolved; Rb, Cs, U and Th abundances are moderate and F, Zr, La and Ce are depleted relative to most other units. Note that high mean Mo values for some plutons reflect mineralized samples, and are not typical of the units as a whole. Individual plutons are otherwise similar, except for the Round Pond Granite, which shows strong depletion of Zn, Sr, Y, Zr, Ba, La, Ce, Pb and Th. The Witchdoctor and Burnt Lake Granites are similar in composition to granites of the Monkey Hill Suite.

The Otter Lake - Walker Lake unit has unremarkable major and trace element characteristics, and shows no striking enrichment or depletion patterns.

#### **Abundance and Distribution of Rock Types**

IUGS rock types were calculated from normative data after Streckeisen and LeMaitre (1979). Labradorian plutonic rocks include a higher proportion of low-SiO<sub>2</sub> rock types than the Makkovikian assemblage, and are obviously bimodal (Figure 5.5). The Adlavik Intrusive Suite is dominated by gabbro, with lesser diorite to monzonite. The Mount Benedict Intrusive Suite overlaps this range, but is dominated by quartz monzonite to quartz syenite. The Monkey Hill Intrusive Suite and Witchdoctor - Burnt Lake Granites are dominated by granite and alkali-feldspar granite. The Otter Lake - Walker Lake granite is dominated by monzogranite and granite. Mafic or intermediate rock types are essentially absent from the latter three associations, termed "siliceous granitoid units" in subsequent discussions.

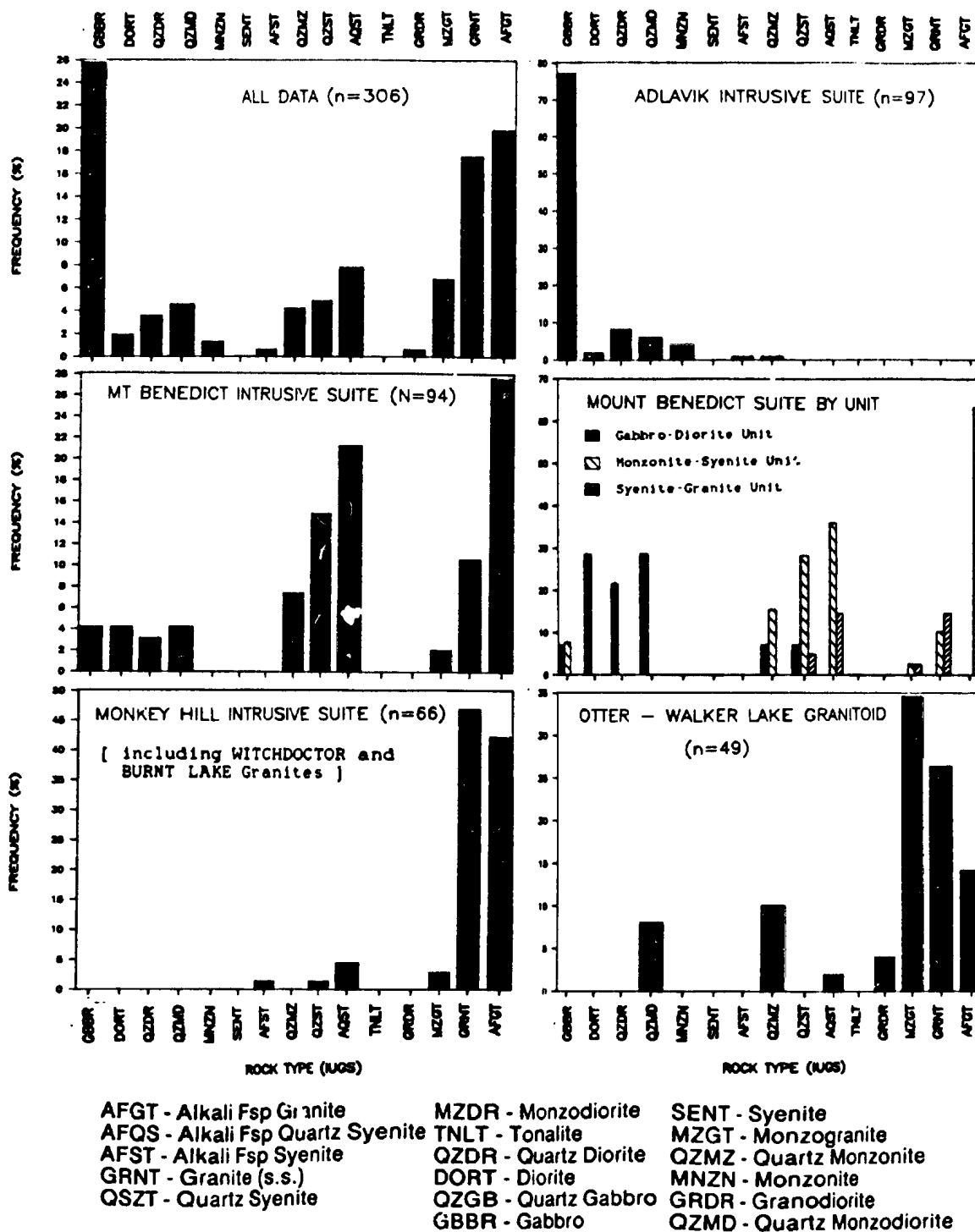


Figure 5.5. Relative abundance of IUGS rock types calculated from normative mineralogy using the method of Streckeisen and LeMaitre (1979). Note that this is based on Barth mesonorms, not the CIPW norms listed in Table 5.2. Regional and geological sample populations.

### 5.2.2 Geochemistry of The Adlavik Intrusive Suite

This discussion is based mostly on geochemical data from the main body at Adlavik Bay. Average compositions of textural and mineralogical facies from this area are listed in Table 5.3; the criteria used for subdivision are outlined below.

#### Subdivisions of The Suite

In addition to subdivision by facies, as outlined in 5.1.1, Table 5.3 incorporates a second-order grouping based on the relative abundance of normative diopside (Di), hypersthene (Hy) and olivine (Ol).

Rocks with well-preserved anhydrous mineral assemblages include both gabbronorite and gabbro variants, which appear to be discrete spatially. However, the widespread late magmatic and/or secondary hydrous mineral assemblages make it difficult to assess primary mineralogy in all areas via petrography.

A Di-Ol-Hy ternary projection (Figure 5.6) illustrates contrasting Hy-normative and Hy-free groups. Both contain variable normative Ol, but most of the Ol-free rocks are also Hy-normative. The diorite unit is also dominantly Hy-normative.

Examination of fresh samples suggests that there is good correspondence between normative and modal hypersthene; the CIPW norms therefore provide a method of classifying altered and hydrated samples, and those for which no petrographic data are available.

The distribution of Hy-normative and Hy-free variants is geographically systematic (Figure 5.7). The leucogabbro facies is predominantly Hy-free, whereas the melagabbro

Table 5.3 . Average compositions of textural and mineralogical subdivisions in the main body of the Adlavik Intrusive Suite.

KEY	1.0		2.1		2.2		2.3		3.1		3.2	
n1	7		7		2		2		4		7	
n2	1		2		0		1		0		1	
(wt%)	Mean	S.D.	Mean	S.D.	Mean	S.D.	Mean	S.D.	Mean	S.D.	Mean	S.D.
SiO <sub>2</sub>	45.07	2.62	46.39	4.29	53.35	1.48	52.08	0.46	48.78	4.19	50.24	2.18
TiO <sub>2</sub>	0.86	0.56	0.88	0.50	1.00	0.26	0.82	0.08	0.73	0.19	1.04	0.18
Al <sub>2</sub> O <sub>3</sub>	10.46	3.01	13.97	1.64	16.08	1.91	14.64	3.43	21.23	4.34	19.69	1.51
Fe <sub>2</sub> O <sub>3</sub>	4.08	1.82	4.41	3.07	3.06	0.15	2.36	0.43	3.12	1.44	3.79	0.78
FeO	6.92	1.30	6.57	2.41	5.87	1.82	7.46	1.20	4.30	1.99	5.13	0.98
MnO	0.17	0.01	0.17	0.02	0.19	0.06	0.19	0.01	0.11	0.04	0.13	0.03
MgO	17.03	8.09	8.91	1.35	5.13	1.45	8.24	4.18	4.05	2.40	3.68	1.08
CaO	8.93	2.56	13.96	2.01	7.31	0.18	7.36	0.30	10.36	2.60	9.00	1.00
Na <sub>2</sub> O	1.88	0.71	1.89	0.94	3.58	0.77	3.32	1.23	3.49	1.26	3.68	0.24
K <sub>2</sub> O	1.35	0.51	0.77	0.69	2.07	0.33	1.92	0.47	1.74	1.09	1.28	0.54
P <sub>2</sub> O <sub>5</sub>	0.49	0.79	0.09	0.10	0.39	0.25	0.22	0.04	0.37	0.27	0.80	0.46
LOI	2.62	1.64	1.49	0.45	1.56	0.37	1.06	0.98	2.01	0.80	1.13	0.62
TOTAL	99.86		99.50		99.59		99.67		100.29		99.59	
(ppm)	Trace Elements											
Li	26.9	11.6	20.7	4.7	25.5	2.1	20.0	4.2	33.5	23.6	20.4	3.7
F	638.3	324.5	305.9	325.4	804.0	189.5	765.5	27.6	600.5	484.5	1881.4	3570
Sc	25.7		48.8	0.8			23.0				19.0	
V	232.7	158.7	323.9	243.4	216.0	33.9	167.0	15.6	213.5	190.9	201.7	64.4
Cr	1014.0	665.7	140.1	193.7	96.5	123.7	113.0	62.2	78.3	127.9	24.3	19.7
Ni	348.4	277.7	45.1	27.6	26.5	29.0	55.0	19.8	19.0	17.5	13.3	11.2
Cu	52.9	39.2	88.6	49.6	63.5	30.4	28.5	2.1	37.0	29.4	26.4	9.9
Zn	94.6	32.3	100.6	40.7	132.0	41.0	168.5	94.1	71.3	29.9	98.3	16.0
Ga	19.0	8.2	21.6	10.6	19.5	0.7	18.0	7.1	21.3	2.2	25.1	3.3
Rb	41.6	49.9	18.6	7.9	71.0	19.8	61.5	16.3	64.0	45.0	28.4	15.1
Sr	495.6	231.2	730.4	114.9	682.5	202.9	516.0	63.6	1030.5	122.1	981.4	93.0
Y	13.4	11.1	15.3	4.3	25.0	9.9	24.0	2.8	13.3	5.3	20.6	6.4
Zr	38.6	7.7	39.6	20.2	116.0	32.5	104.0	15.6	53.0	52.0	65.4	43.0
Nb	2.9	2.0	1.4	1.7	3.5	0.7	1.0	1.4	5.3	6.7	2.3	2.9
Mo	2.9	0.9	3.9	2.8	3.5	0.7	3.5	0.7	3.8	0.5	3.6	0.5
Sn	1.0		1.0	0.0			1.0				1.0	
Cs	7.0		0.5	0.0			0.9				0.5	
Ba	419.7	98.8	281.7	144.6	831.0	267.3	578.5	161.9	594.8	293.8	647.9	195.6
La	18.4	17.3	8.6	7.5	30.5	10.6	26.5	6.4	22.8	14.4	25.9	9.4
Ce	42.0	45.2	30.7	11.9	58.5	10.6	46.5	7.8	45.8	33.4	57.4	21.5
Sm	3.5		4.4	0.4			5.0				5.6	
Yb	2.5		2.5	0.0			2.5				2.5	
Hf	1.0		1.0	0.0			3.1				3.0	
Pb	2.0	1.7	1.7	1.3	18.5	17.7	11.0	11.3	3.5	3.1	4.1	3.3
Th	2.6	1.5	1.4	1.1	1.0	0.0	1.0	0.0	5.4	4.8	4.2	3.1
U	0.6	0.3	0.5	0.4	2.7	0.9	0.8	0.3	1.3	1.7	0.8	0.4
(Wt%)	Partial CIPW Norm											
Q	0.00	0.00	0.00	0.00	1.81	1.12	0.00	0.00	0.00	0.00	0.98	1.26
C	0.00	0.00	0.00	0.00	0.00	0.00	0.00	0.00	0.13	0.25	0.24	0.64
Or	8.20	3.08	4.65	4.13	12.47	1.92	11.46	2.74	10.44	6.47	7.67	3.32
Ab	13.59	6.00	13.63	7.09	30.82	6.55	28.52	10.80	25.36	9.60	31.54	2.03
An	16.46	6.43	27.88	7.79	22.13	0.74	19.66	5.48	37.45	15.96	33.25	5.69
Ne	1.47	2.01	1.44	1.64	0.00	0.00	0.00	0.00	2.53	1.41	0.00	0.00
Di	20.47	6.65	33.88	6.95	10.26	0.13	13.14	2.66	10.14	11.34	5.00	3.24
Hy	1.89	2.57	0.17	0.33	15.11	6.60	12.09	11.56	0.00	0.00	11.15	3.38
Ol	28.75	15.59	9.83	4.15	0.00	0.00	9.55	0.08	6.98	2.37	0.45	1.09
Mt	6.08	2.73	6.52	4.56	4.51	0.23	3.46	0.67	4.55	2.12	5.58	1.14
Il	1.67	1.07	1.70	0.98	1.93	0.51	1.58	0.18	1.40	0.37	2.00	0.35

KEY TO ANALYSES

- 1.0 -- Ultramafic Rocks  
 2.1 -- Mafic Cumulate Facies (Cpx +/- Ol)  
 2.2 -- Mafic Cumulate Facies (Cpx + Opx)  
 2.3 -- Mafic Cumulate Facies (Cpx + Opx + Ol)  
 3.1 -- Melanocratic Gabbro Facies (Cpx +/- Ol)  
 3.2 -- Melanocratic Gabbro Facies (Cpx + Opx)

n1 -- Number of analyses for all elements except those below  
 n2 -- Number of analyses for Sc, Sn, Cs, Sm, Yb and Hf

Table 5.3 (continued)

KEY	4.1		4.2		4.3		5.0		7.0	
n1	26		8		10		14		7	
n2	5		0		2		2		1	
(Wt%)	Mean	S.D.	Mean	S.D.	Mean	S.D.	Mean	S.D.	Mean	S.D.
SiO <sub>2</sub>	47.64	2.86	54.07	2.17	51.49	1.69	57.90	3.01	53.42	5.46
TiO <sub>2</sub>	1.01	0.55	0.86	0.20	0.81	0.18	0.81	0.30	1.16	0.72
Al <sub>2</sub> O <sub>3</sub>	14.59	3.93	18.88	2.76	16.36	3.89	17.85	1.28	15.07	2.46
Fe <sub>2</sub> O <sub>3</sub>	2.88	1.35	2.41	0.75	2.38	0.56	1.94	0.72	2.98	1.42
FeO	6.98	1.56	4.88	1.47	6.09	0.81	4.01	1.45	6.04	2.14
MnO	0.18	0.04	0.13	0.04	0.15	0.04	0.13	0.03	0.17	0.03
MgO	9.22	4.68	3.62	1.46	7.45	4.94	2.46	1.55	6.07	3.54
CaO	11.57	2.80	7.50	1.48	8.82	1.30	4.83	1.92	7.31	2.60
Na <sub>2</sub> O	2.59	1.29	4.20	0.46	3.40	1.09	5.27	1.02	3.60	1.07
K <sub>2</sub> O	0.99	0.70	1.86	0.62	1.44	0.57	3.31	0.93	2.28	0.86
P <sub>2</sub> O <sub>5</sub>	0.30	0.37	0.27	0.08	0.17	0.10	0.31	0.15	0.41	0.40
LOI	1.49	0.51	0.77	0.39	0.97	0.36	0.77	0.34	1.21	0.39
TOTAL	99.44		99.45		99.53		99.59		99.72	
(ppm)										
Li	17.8	7.3	20.4	5.5	20.3	4.8	19.2	7.0	26.0	8.1
F	516.2	404.1	547.8	196.6	583.7	452.0	840.2	394.4	1286.0	896.0
Sc	43.0	19.0			21.9	6.9	15.0	0.0	20.0	
V	202.6	82.3	156.3	57.0	185.6	35.0	91.8	68.0	171.0	60.4
Cr	345.2	440.8	47.3	36.5	365.8	563.4	29.4	33.1	234.9	253.8
Mi	83.3	85.2	16.8	9.1	88.1	104.5	10.9	11.3	58.1	44.3
Cu	72.3	49.1	22.8	15.9	41.2	28.6	23.0	16.2	33.0	24.0
Zn	87.9	44.6	88.0	22.6	88.6	20.8	77.4	18.8	129.1	51.2
Ga	18.5	6.1	22.4	2.7	20.2	3.1	16.6	5.1	22.3	6.1
Rb	28.0	22.1	49.1	19.1	41.4	19.9	75.8	23.2	64.1	29.1
Sr	774.6	381.5	927.5	202.3	738.1	295.3	711.8	202.7	610.1	243.3
Y	17.8	10.3	18.1	4.6	16.8	5.5	20.7	4.6	37.3	17.2
Zr	52.3	43.0	83.4	39.4	69.4	47.0	95.9	50.6	179.0	102.8
Nb	2.3	3.1	5.1	2.9	3.7	3.1	10.0	3.4	8.9	6.4
Mo	3.0	0.5	3.8	0.5	3.6	1.7	2.9	0.8	3.6	0.8
Sn	1.0	0.0			1.0	0.0	1.0	0.0	1.0	
Cs	0.5	0.0			0.5	0.0	1.3	1.1	2.0	
Ba	542.2	455.0	776.4	215.4	593.4	276.9	1554.1	1251	824.0	483.5
La	17.5	13.9	27.5	7.0	20.8	11.0	33.4	8.2	38.3	16.5
Ce	40.3	31.3	51.1	14.1	39.3	18.8	58.6	20.7	81.6	34.9
Sm	4.5	2.5			7.0	1.5	6.5	0.5	6.2	
Yb	2.5	0.0			2.5	0.0	2.5	0.0	2.5	
Hf	1.5	0.9			2.0	1.4	3.0	0.0	5.0	
Pb	2.5	3.4	5.8	3.5	9.3	14.0	9.7	4.6	8.9	5.7
Th	1.3	0.9	1.7	2.6	0.8	0.3	3.0	3.3	5.2	4.5
U	0.5	0.5	1.5	1.0	0.9	0.6	2.0	1.3	1.9	1.1
(Wt%)										
Q	0.36	1.83	1.13	1.07	0.00	0.00	1.31	1.64	2.19	4.02
C	0.00	0.00	0.00	0.00	0.00	0.00	0.00	0.00	0.00	0.00
Or	5.94	4.23	11.09	3.72	8.62	3.45	19.79	5.61	13.63	5.06
Ab	19.29	10.55	35.94	3.99	29.08	9.30	44.86	8.61	30.82	9.13
An	25.76	7.97	27.56	8.91	25.46	6.67	15.42	5.94	18.51	5.92
Ne	1.65	1.29	0.00	0.00	0.00	0.00	0.12	0.33	0.00	0.00
Di	24.95	13.43	7.05	3.78	14.57	8.25	5.84	4.05	12.59	10.01
By	0.40	2.01	10.84	4.18	8.07	3.07	6.06	4.82	9.64	4.21
Ol	14.59	7.34	0.49	1.34	8.64	6.09	1.45	2.58	4.90	4.63
Nt	4.26	2.02	3.54	1.10	3.49	0.82	2.85	1.06	4.39	2.12
Il	1.97	1.07	1.65	0.38	1.56	0.34	1.55	0.58	2.23	1.41

KEY TO ANALYSES

- 4.1 -- Plagioclase Cumulate Facies (Cpx +/- Ol)      5.0 -- Diorite Unit (mostly Cpx + Opx)  
 4.2 -- Plagioclase Cumulate Facies (Cpx + Opx)      7.0 -- Marginal Gabbro and Diorite  
 4.3 -- Plagioclase Cumulate Facies (Cpx + Opx + Ol)

n1 -- Number of analyses for all elements except those below  
 n2 -- Number of analyses for Sc, Sn, Cs, Sm, Yb and Hf

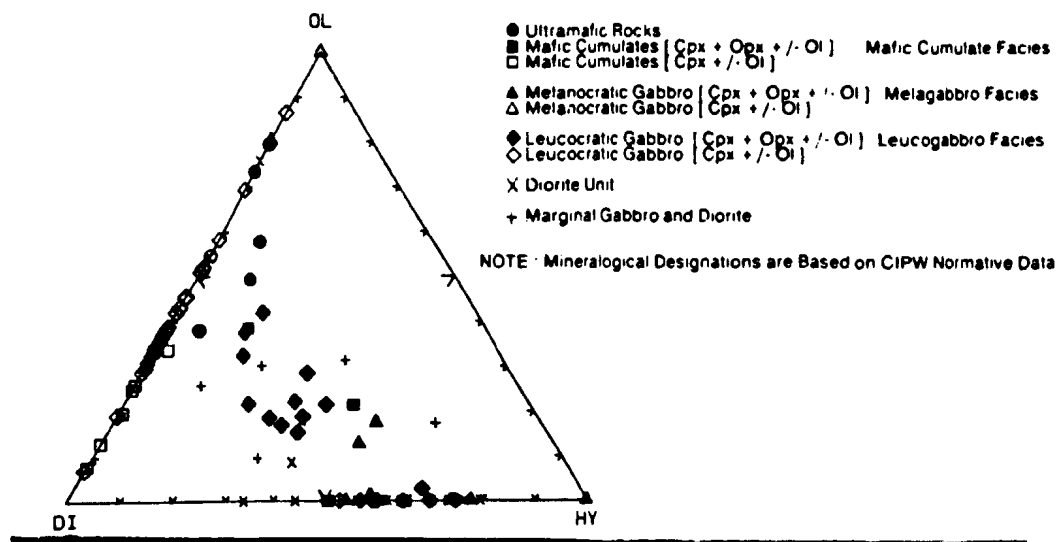


Figure 5.6. Normative olivine - diopside - hypersthene projection, showing the division of the Adlavik Intrusive Suite into hypersthene-normative and hypersthene-free components.

facies is Hy-normative. The mafic cumulate facies contains both types. As expected, there are major element geochemical contrasts between Hy-normative and Hy-free rocks, and also some trace element differences (Table 5.3).

It is suggested on this basis that the intrusion be divided into gabbronorite and gabbro sequences. The former includes the mafic cumulate facies, melagabbro facies and part of the leucogabbro facies, and is probably associated with the Hy-normative diorite unit. The gabbro sequence includes most of the leucogabbro facies, and is considered to represent stratigraphically higher parts of the complex (see cross section, Figure 5.4). The gabbronorite sequence includes Hy-free mafic cumulate rocks, but the gabbro sequence is only rarely Hy-normative.

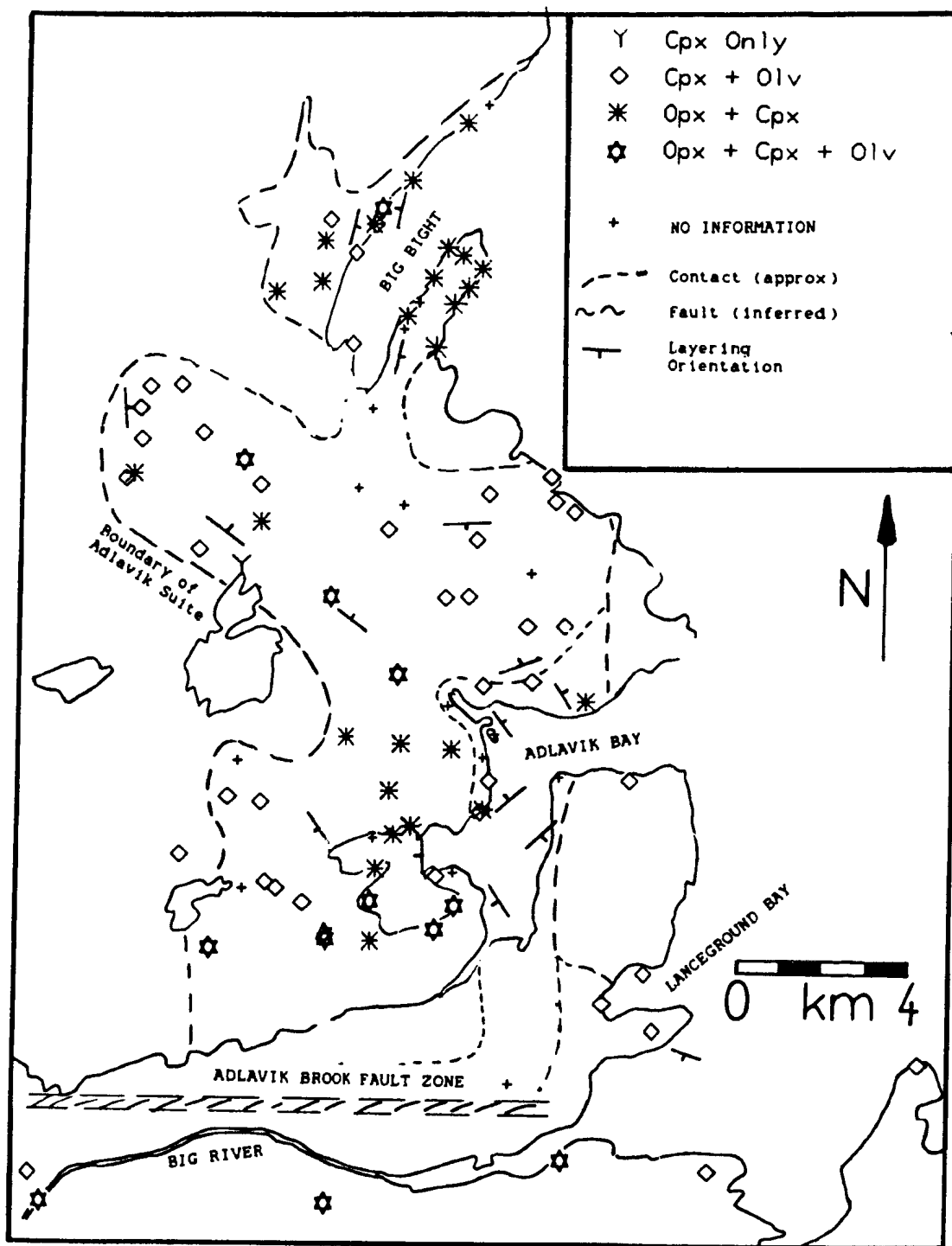


Figure 5.7. Spatial variation of normative mineralogy in the main body of the Adlavik Intrusive Suite, illustrating distribution of gabbro norite and gabbro sequences.



### Major Element Patterns

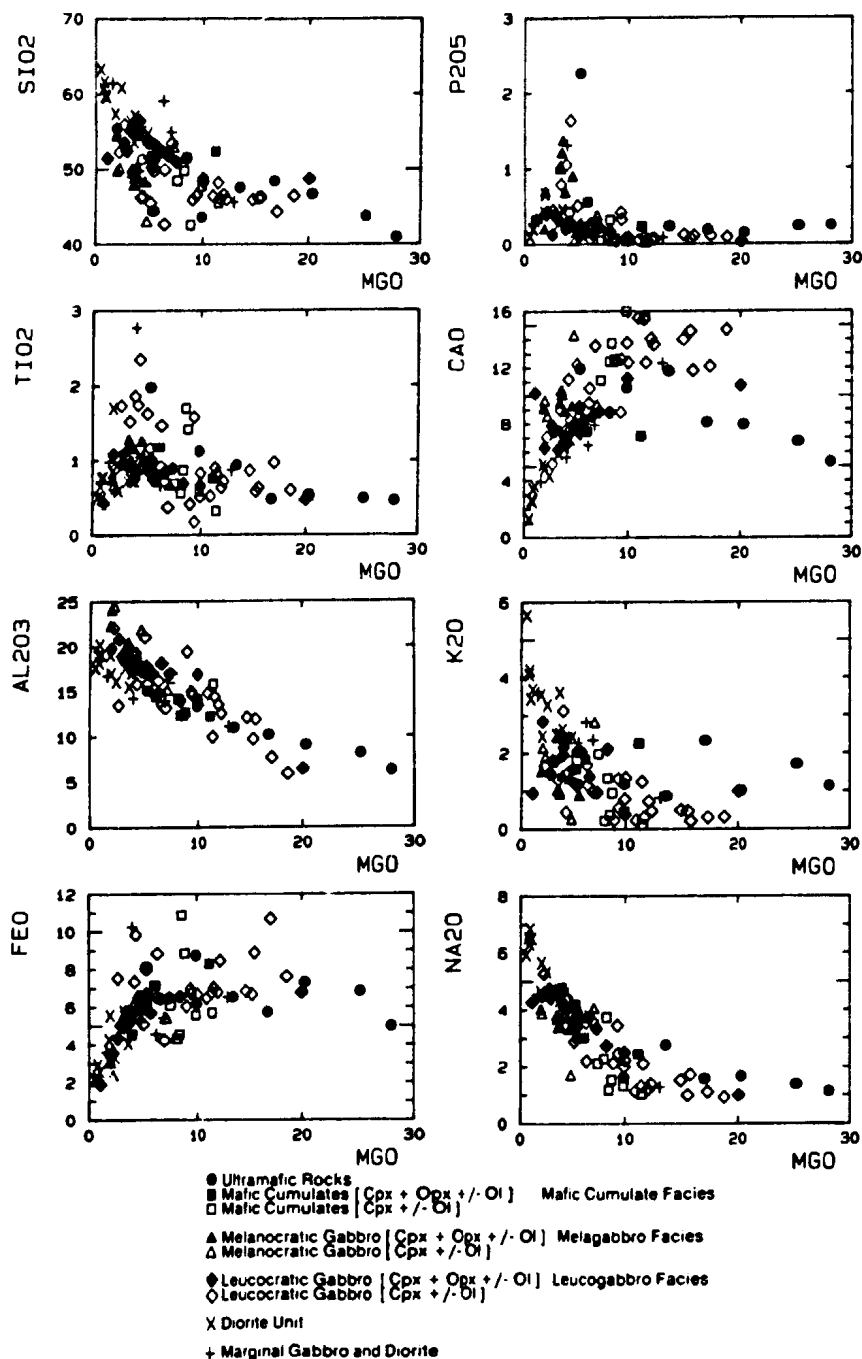
Major element variation is assessed using MgO as a differentiation index (Figure 5.8). The clearest distinction between gabbronorite and gabbro sequences is shown by  $\text{TiO}_2$ , which is strongly enriched in the latter below 10% MgO. The gabbronorite sequence has convex-upward CaO and FeO trends, and lower CaO and FeO than the gabbro sequence above 10% MgO. It also shows higher  $\text{SiO}_2$  and  $\text{K}_2\text{O}$  (see also Table 5.3), but there is considerable overlap between the two. Samples from fine-grained marginal rocks have varied compositions, and clearly do not represent any one homogeneous "parental" composition.

### Trace Element Patterns

Trace elements show predictable trends for mafic magmas (Figure 5.9), and there are few systematic differences between gabbronorite and gabbro sequences.

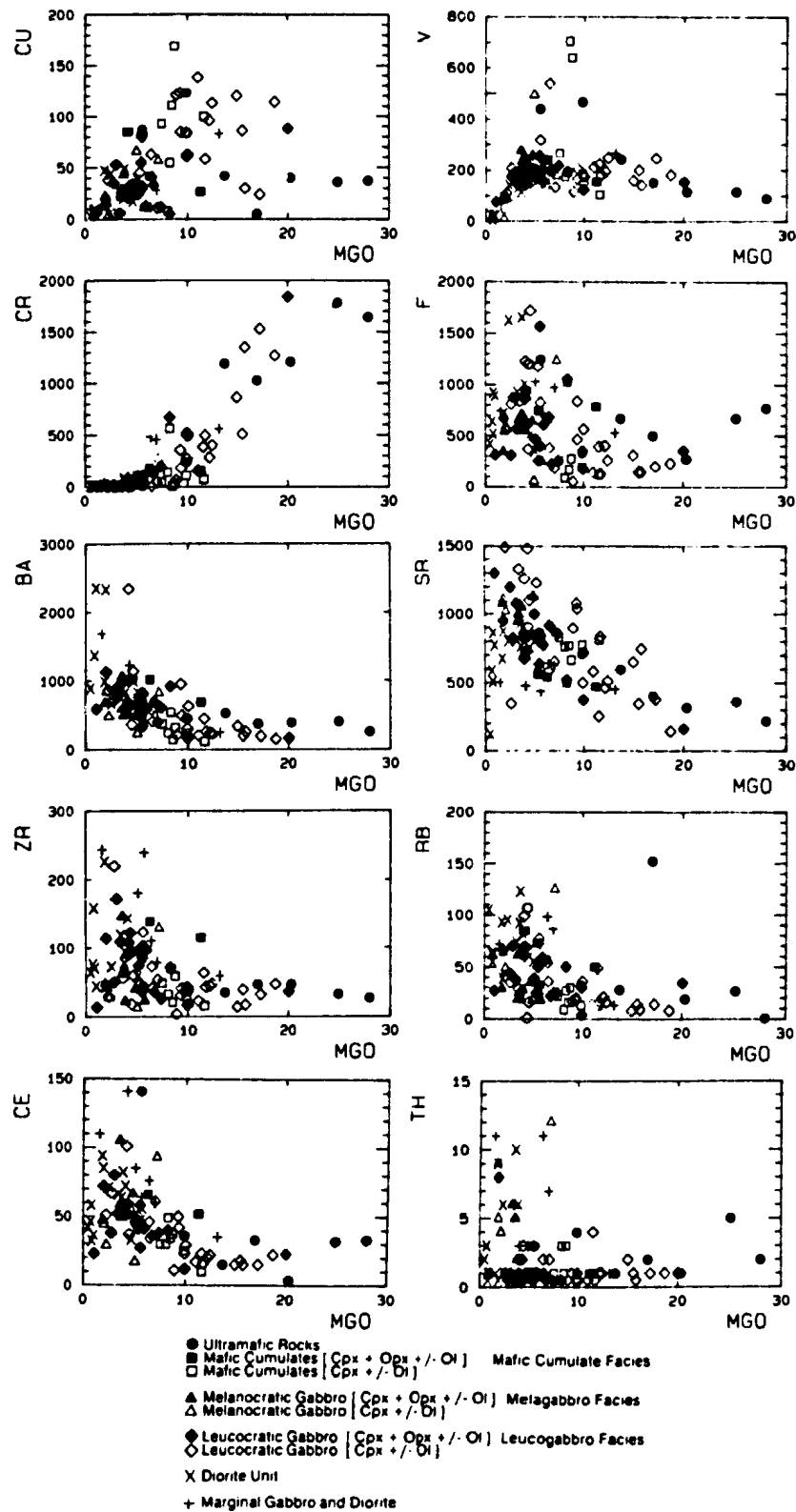
Compatible OCC trace elements (e.g. Cr, V, Cu; Figure 5.9) are positively correlated with MgO. High Cu contents characterize parts of the gabbro sequence. V shows minimal variation from 30% to 5% MgO, and possibly increases slightly down to this point. It is, however, depleted very rapidly below 5% MgO, and in the diorite unit.

LFS and HFS elements, and REE, increase with decreasing MgO, and, except for Sr, are highest in the diorite unit. Sr enrichment is most apparent in the gabbro sequence, reflecting the presence of plagioclase cumulates. The dioritic unit shows lower Sr than either the gabbronorite or gabbro sequence, but is closer to the former. Ba is incompatible throughout, and is strongly enriched in some samples from the diorite unit, which



NOTE Mineralogical Designations are Based on CIPW Normative Data.

Figure 5.8. Variation of selected major elements and derived ratios against MgO in the main body of the Adlavik Intrusive Suite. See text for discussion.



NOTE: Mineralogical Designations are Based on CIPW Normative Data

Figure 5.9. Variation of selected trace elements against MgO in the main body of the Adlavik Intrusive Suite. See text for discussion.

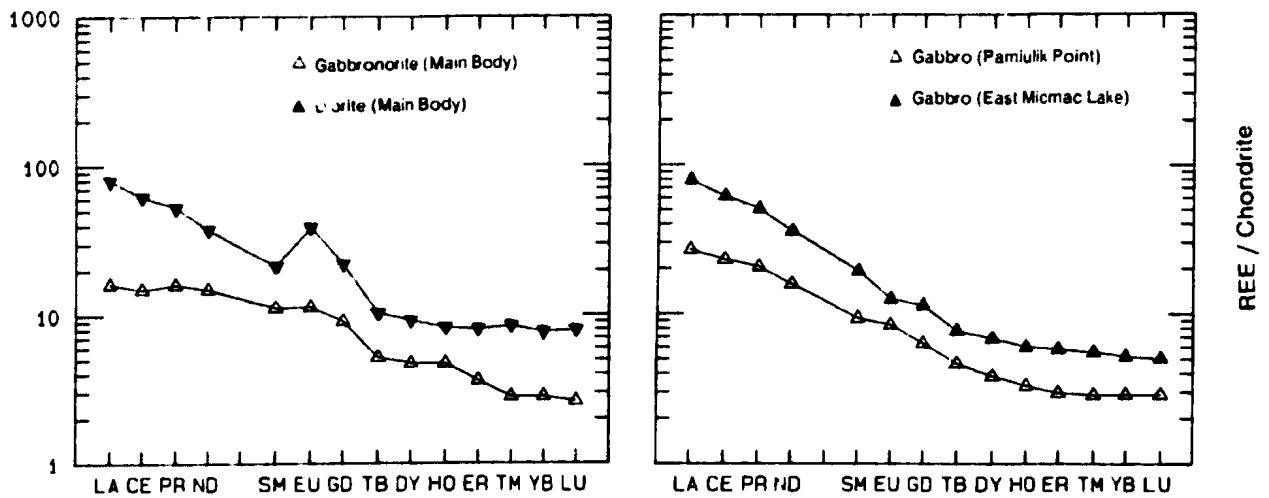


Figure 5.10. Rare Earth Element (REE) patterns for samples from the Adlavik Intrusive Suite. Normalized to chondritic values.

locally has over 4000 ppm Ba. All of these trends are broadly consistent with evolution by fractional crystallization of mafic minerals (olivine, pyroxenes), followed by plagioclase fractionation.

#### Rare Earth Element (REE) Patterns

REE analyses are available for four samples (Figure 5.10), of which two are from the main body. The mafic sample is a melanocratic olivine-bearing gabbronorite, and shows no Eu anomaly. A small positive Eu anomaly is present in the diorite sample, suggesting that it is a feldspar cumulate, but the overall shape of the pattern is similar to the gabbro. Melanocratic gabbro from Pamiulik Point is almost identical to the main body, but the sample from the East Micmac Lake body is REE - enriched, consistent with its higher  $\text{SiO}_2$  content (see also Table 5.2).

### 5.2.3 Geochemistry of Labradorian Granitoid Rocks

Labradorian granitoid rocks are divided into three groups (A, B and C) to reduce clutter in variation diagrams. Diagrams that use  $\text{SiO}_2$  as the X-axis employ a wider horizontal scale for the Mount Benedict Suite (Group A). This group of rocks is probably genetically related to the Adlavik Suite (see later discussion), but it is convenient to describe it in conjunction with siliceous granitoid units.

#### **Major Element Patterns**

Major elements follow predictable behaviour patterns (Figure 5.11), and all oxides except  $\text{Na}_2\text{O}$  and  $\text{K}_2\text{O}$  are negatively correlated with  $\text{SiO}_2$ . The Mount Benedict Intrusive Suite has, predictably, the greatest range of major element compositions, and the Monkey Hill Intrusive Suite the narrowest range. The Mount Benedict Suite has smooth, well-defined trends for all major elements from the least (diorite) to most differentiated (syenite to granite) units. Some (e.g.  $\text{CaO}$ ,  $\text{Na}_2\text{O}$ ) are curvilinear, and show inflections at a  $\text{SiO}_2$  content of ca. 62%. N/N+K ratio patterns indicate minor disturbance of alkali elements in leucocratic granites of the Monkey Hill Intrusive Suite.

K+N/A (agpaitic index) patterns indicate that there are no Labradorian peralkaline rocks. A/C+N+K (alumina index) patterns indicate that the Monkey Hill Intrusive Suite and Witchdoctor - Burnt Lake Granites are mostly peraluminous, and that the Otter Lake - Walker Lake granitoid is peraluminous above 70%  $\text{SiO}_2$ . A few high- $\text{SiO}_2$  rocks from the Mount Benedict Suite are also peraluminous.

Ternary AFM and CNK projections (Figure 5.12) are useless for unit discrimination. In the QBF ternary

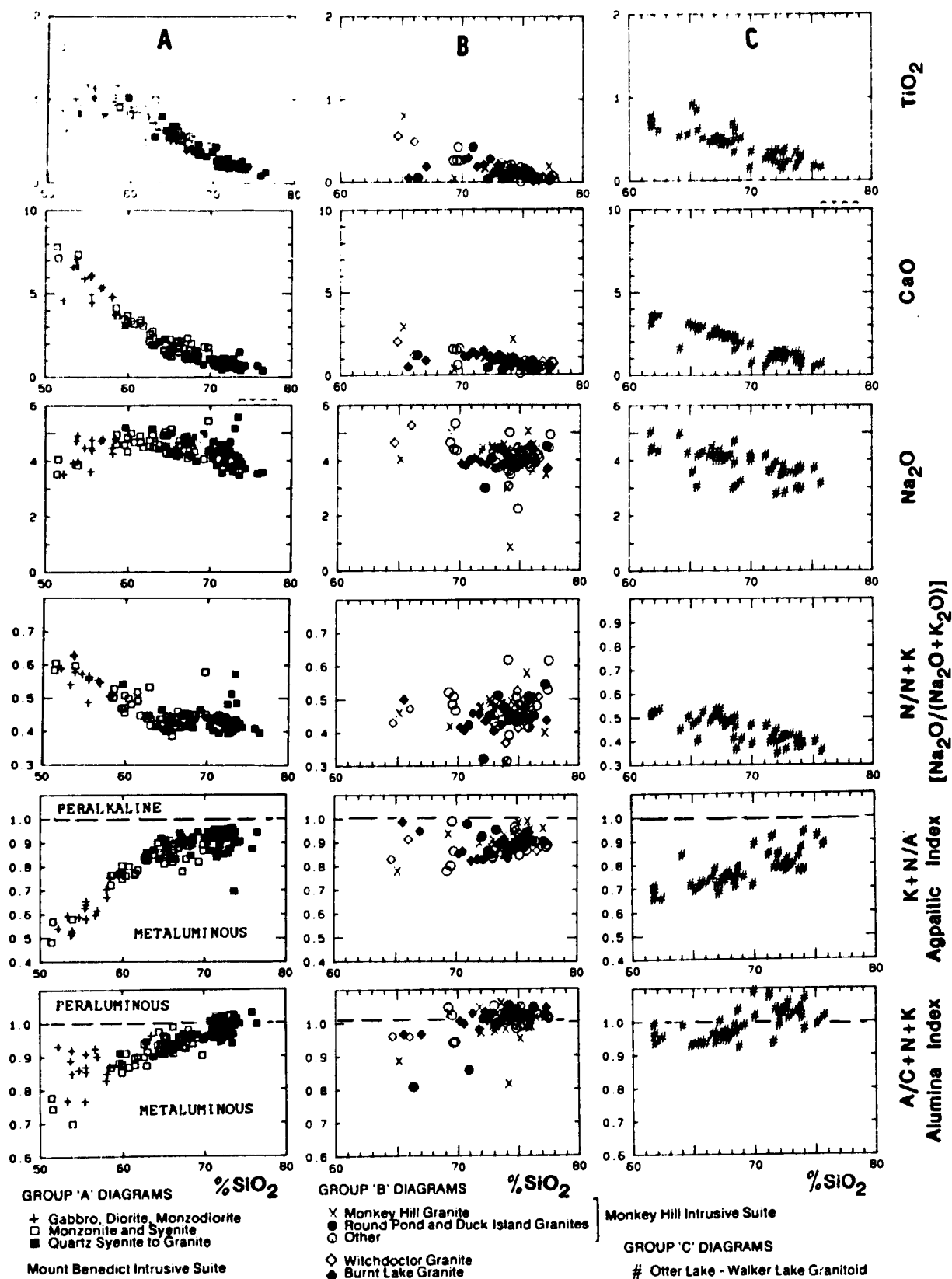


Figure 5.11. Variation of selected major elements and derived ratios Labradorian granitoid plutonic rocks. See text for discussion.

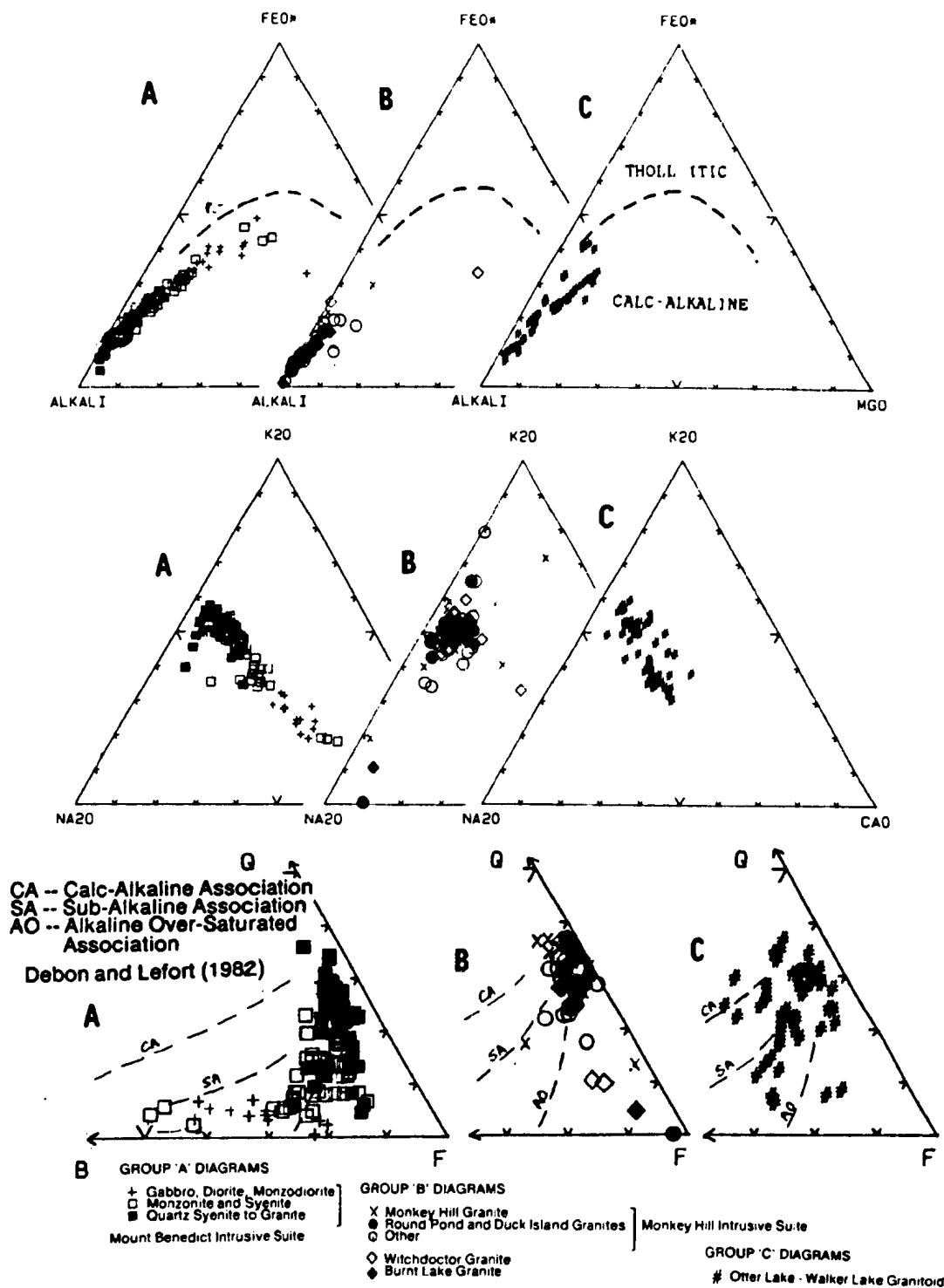


Figure 5.12. AFM, CNK and QBF projections for Labradorian granitoid plutonic units. See text for discussion.



projection (Figure 5.12) of Debon and Lefort (1982), the Mount Benedict Suite approximates to their alkaline-oversaturated association, rather than to typical calc-alkaline associations.

#### **Normative Compositions**

In the Quartz - Albite - Anorthite - Orthoclase quaternary system, only parts of the Mount Benedict Intrusive Suite contain > 20 % anorthite component. In the Q-Ab-Or projection (Figure 5.13), this suite has a well-defined trend that partly corresponds to the location of plagioclase - K-feldspar cotectic lines for high Ab/An ratios (James and Hamilton, 1969), and terminates in the ternary minimum area. In detail, there is an inflection in this trend corresponding to the ca. 62%  $\text{SiO}_2$  inflection noted above; the least evolved part of the suite lies within the plagioclase field. Granites of the Monkey Hill Intrusive Suite, Witchdoctor Granite and Burnt Lake Granite are also clustered around the ternary minimum, although some samples are scattered towards the albite corner (reflecting alkali-disturbance).

#### **Trace Element Patterns**

**Octahedrally Co-ordinated Cation (OCC) Elements** : V, Cu, Cr, Ni and Sc all show similar, uninformative inverse trends against  $\text{SiO}_2$  (e.g. V; Figure 5.14). High levels of these elements are observed only in parts of the Mount Benedict Intrusive Suite.

**Low Field Strength (LFS) Elements** : Incompatible LFS trace elements (e.g. Rb, Th; Figure 5.14) are positively correlated with  $\text{SiO}_2$ , and discriminate the Mount Benedict

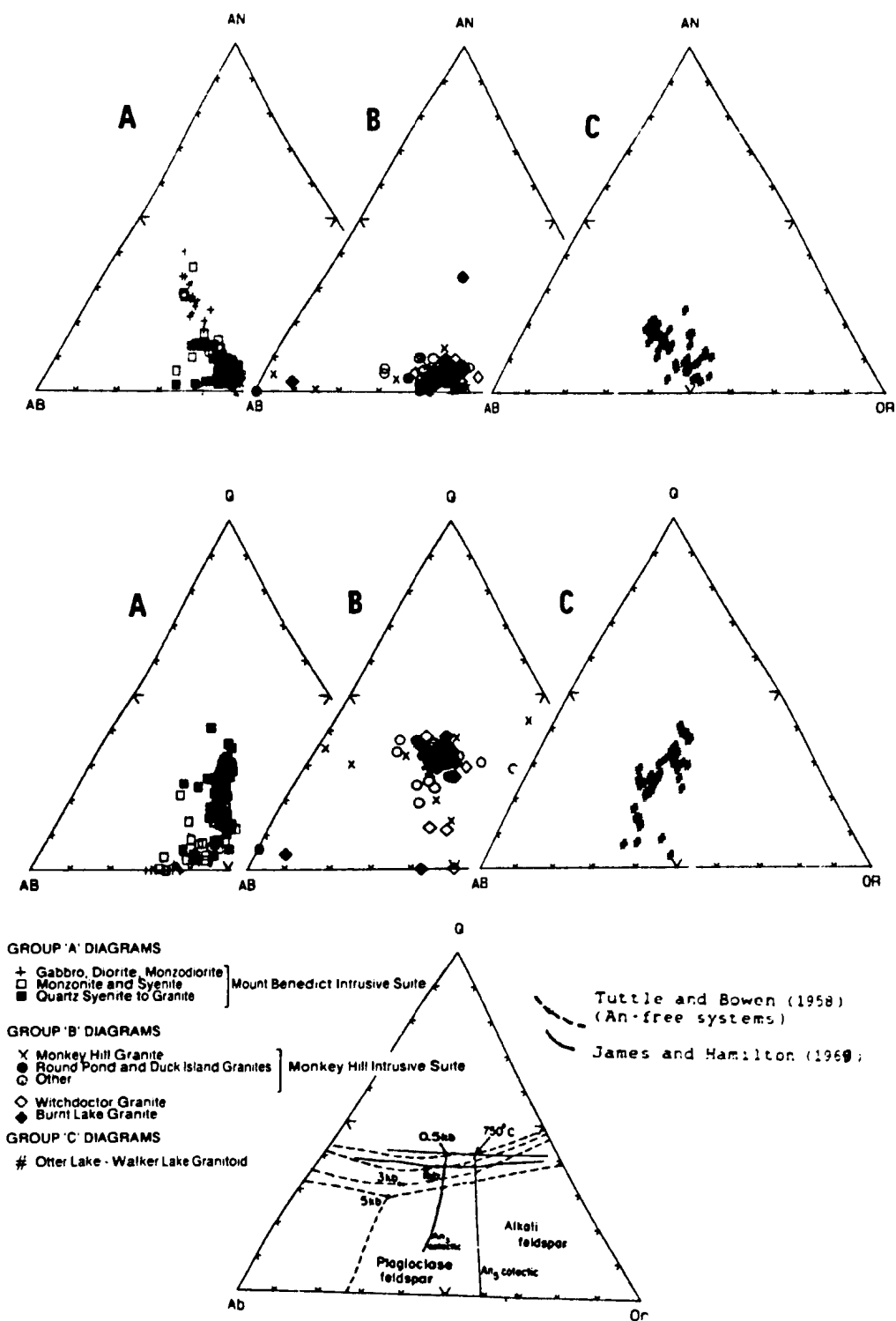


Figure 5.13. Variation of Labradorian granitoid plutonic rocks in the Quartz - Albite - Anorthite - Orthoclase quaternary system. All norms are CIPW. See text for discussion.

Suite from all other Labradorian units. This suite is enriched in Rb and Th (also Cs, Sn, U; not figured) at all  $\text{SiO}_2$  levels.

Sr and Ba show generally inverse trends against  $\text{SiO}_2$ . There is an inflection in the Ba trend for the Mount Benedict Suite at ca. 62%  $\text{SiO}_2$ ; up to this point, Ba remains constant or increases slightly. The Monkey Hill Intrusive Suite and similar granites show rapid depletion of Ba with increasing  $\text{SiO}_2$ .

**High-Field Strength (HFS) Elements** : Zr and Nb (Figure 5.15) have convex-upward trends with inflection points at ca. 67%  $\text{SiO}_2$  in the Mount Benedict Suite. At higher  $\text{SiO}_2$  contents, both are rapidly depleted. High Zr in the 60-67%  $\text{SiO}_2$  range distinguishes this suite from other Labradorian units, which mostly contain less than 300 ppm Zr, and have constant or decreasing Zr with increasing  $\text{SiO}_2$ .

**Rare-Earth Elements (REE)** : Y and Ce (Figure 5.15) have subhorizontal trends in the Mount Benedict Suite, and are depleted above 67%  $\text{SiO}_2$ . Absolute REE levels are similar for all Labradorian granitoid rocks, unlike Zr patterns.

**Indeterminate Trace Elements** : The Mount Benedict Suite is enriched in fluorine (Figure 5.14) relative to all other Labradorian units (except parts of the Adlavik Suite; Table 5.3). The convex-upward F- $\text{SiO}_2$  trend in the Mount Benedict Suite is remarkably similar to the Zr trend, and shows the same inflection at ca. 67%  $\text{SiO}_2$ . Li (Figure 5.15) does not discriminate between units, and has a scattered distribution in the Monkey Hill Suite and similar

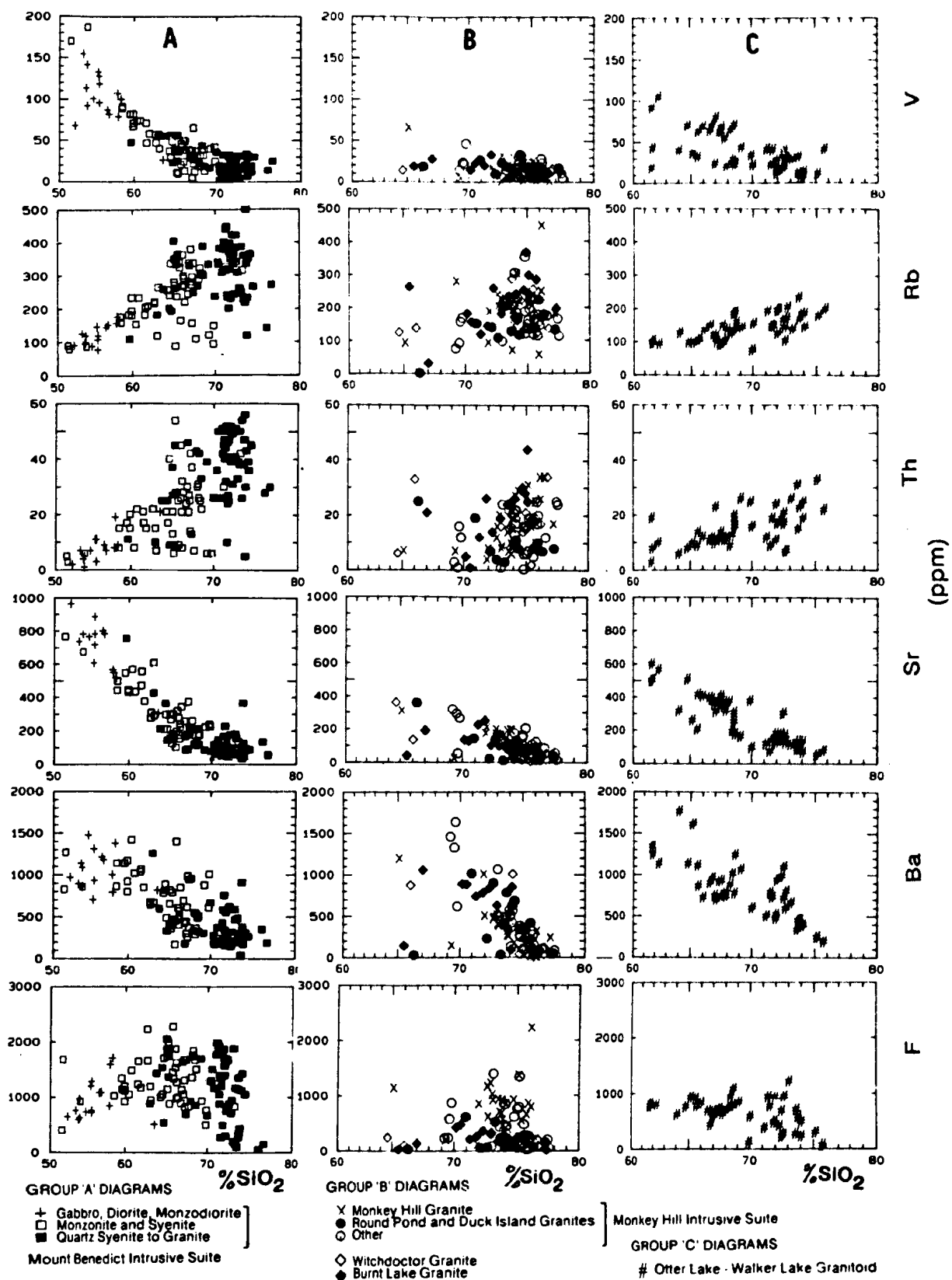


Figure 5.14. V, Rb, Th, Sr, Ba and F versus  $\text{SiO}_2$  for Labradorian granitoid plutonic rocks. See text for discussion.

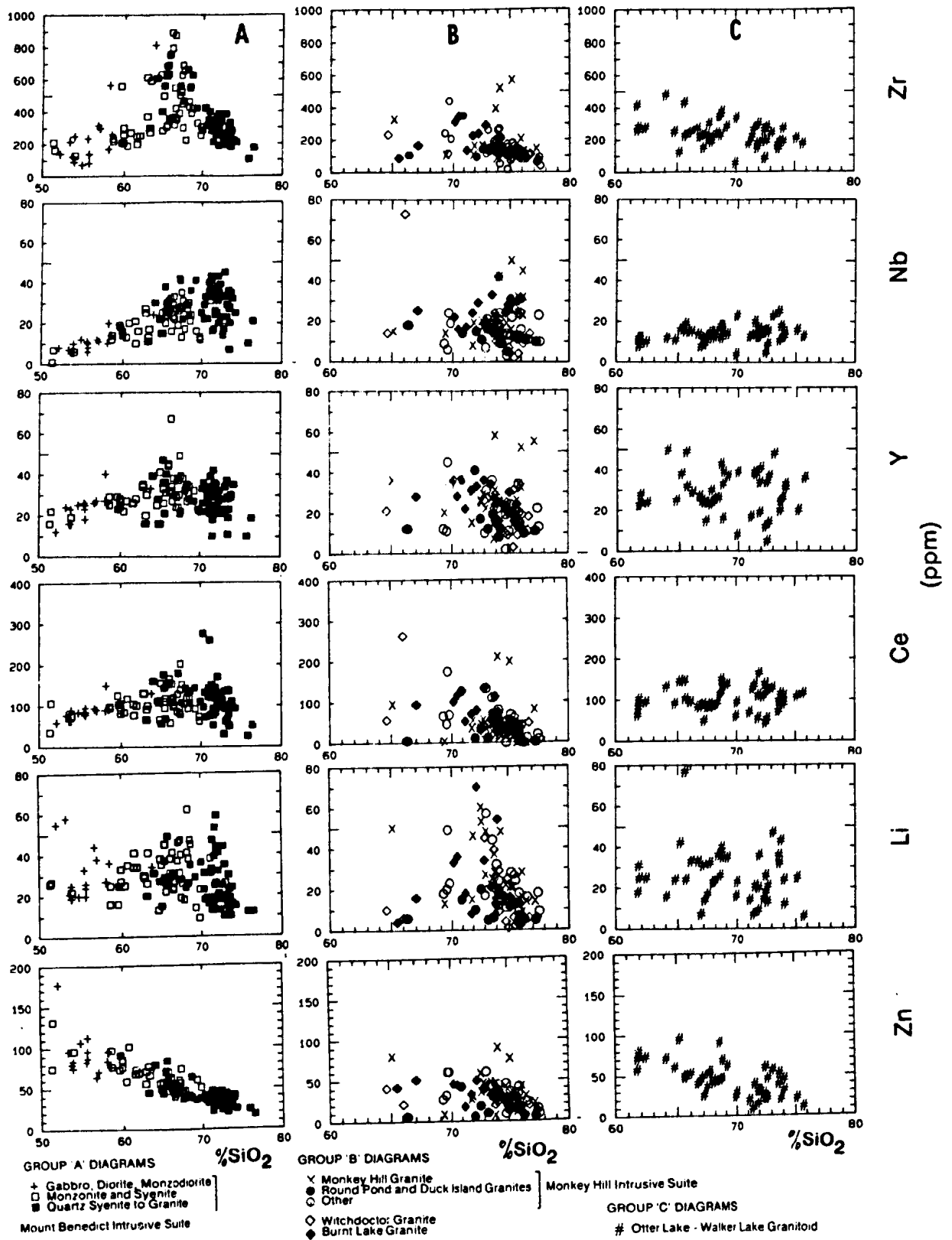


Figure 5.15. Zr, Nb, Y, Ce, Li and F versus SiO<sub>2</sub> for Labradorian granitoid plutonic rocks. See text for discussion.

granites. Zn (Figure 5.15) shows trends that resemble those of OCC trace elements in all units, and there is no Zn enrichment at high  $\text{SiO}_2$  values.

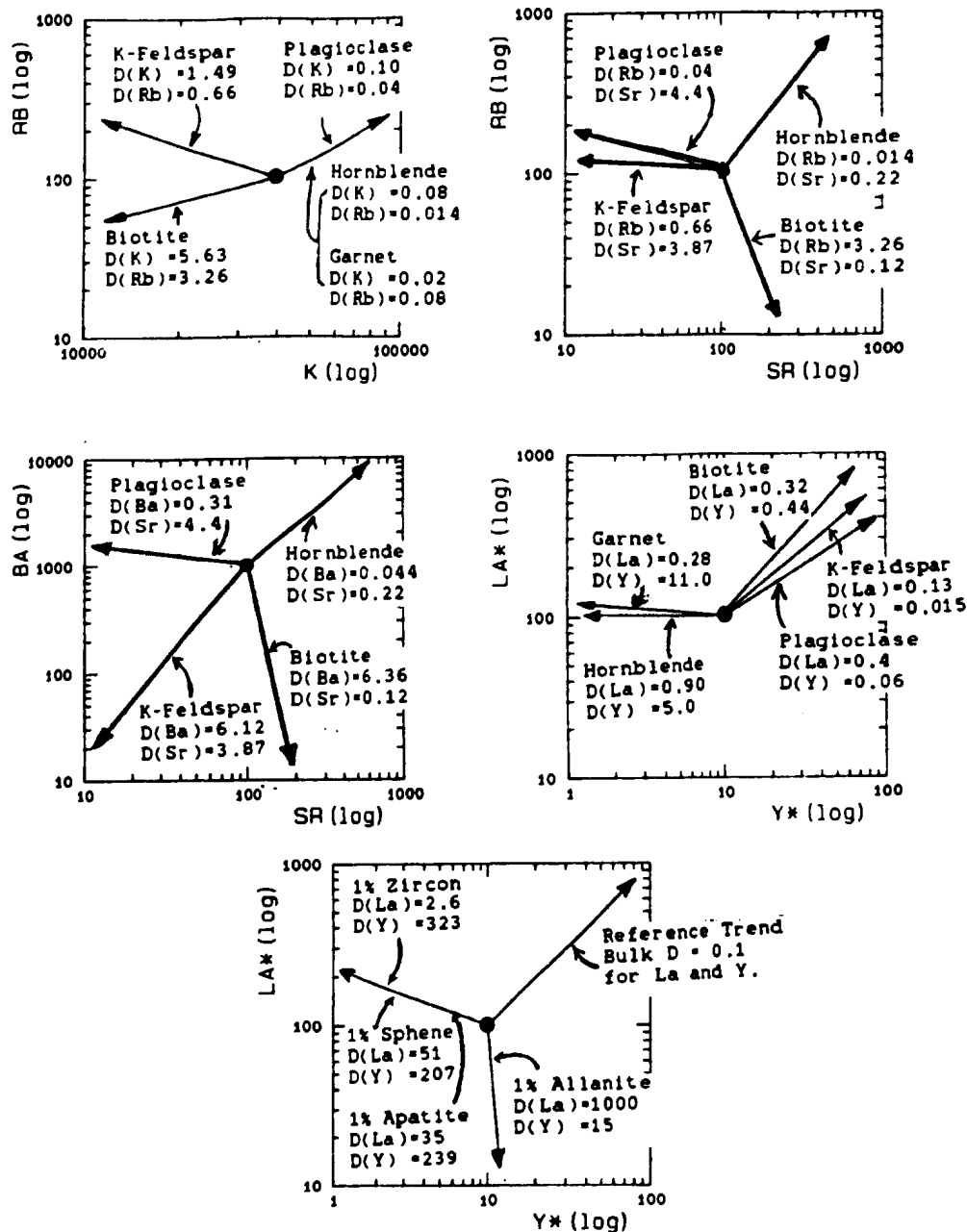
#### Trace Element Ratios

K/Rb decreases systematically throughout differentiation in the Mount Benedict Intrusive Suite (Figure 5.16). Variation of K and Rb appears to be partly decoupled in the Monkey Hill Intrusive Suite, which has constant K but variable Rb.

Rb/Sr ratios are similar for all units, but trends are subtly different (Figure 5.16). The Mount Benedict Suite has a well-defined curved trend characterized by initially strong Rb enrichment. All other units have flat or slightly inverse Rb/Sr trends that lack curvature.

The Mount Benedict Suite has a well-defined Ba-Sr trend (Figure 5.16), that is inflected at ca. 500 ppm Sr, corresponding to ca. 62%  $\text{SiO}_2$  (Figure 5.14). The monzonite-syenite and syenite-granite units show essentially constant Ba/Sr, and depletion of both elements. The Monkey Hill Suite and similar granites show scattered Ba and Sr distributions. The Otter Lake - Walker Lake trend is similar in orientation to that of the Mount Benedict Suite.

Compared to idealized trends for Rayleigh-type fractionation of common silicates (Figure 5.16, inset), the Rb/Sr trend for the Mount Benedict Suite indicates the influence of plagioclase fractionation ( $\pm$  mafic phases at high Sr contents). The Ba/Sr trend indicates that K-feldspar was also fractionated in more differentiated rocks. This is consistent with the presence of plagioclase and K-feldspar phenocrysts. The inflection point at ca. 62%



Idealized fractionation trends for Rayleigh fractionation (i.e. perfect separation of crystals and liquid). The  $La_N/Y_N$  trends for accessory phases show the effects of only 1% of each phase upon a reference trend where bulk partition coefficients for the remaining 99% of the fractionate are 0.1 for both La and Y. The latter approximates a "normal" path for fractionation of common silicates. Partition coefficient data from compilations by Arth (1976) and Hanson (1978) for most minerals, and from Gromet and Silver (1983) for allanite and sphene.

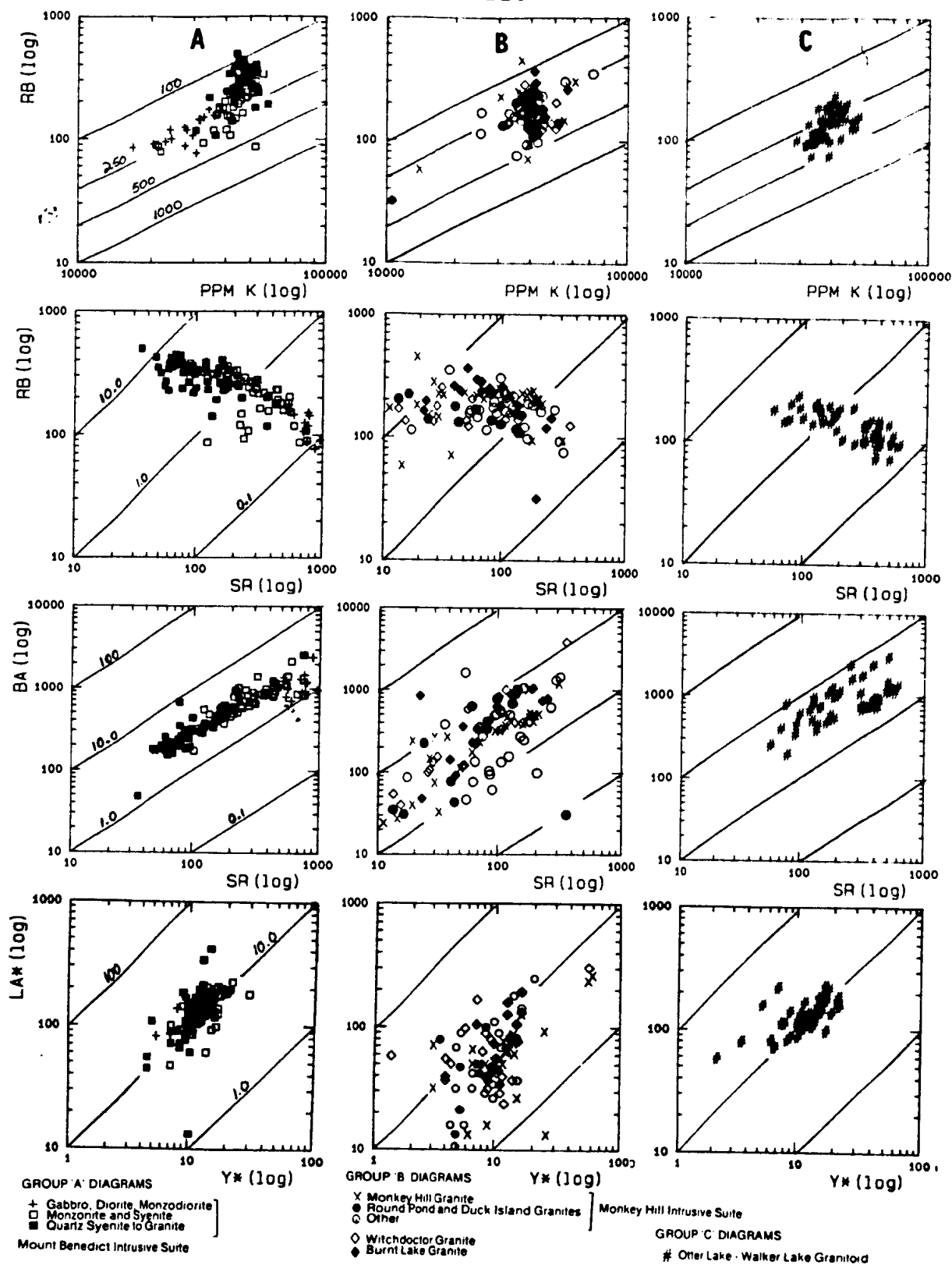


Figure 5.16. Variation in the trace element ratios K/Rb, Rb/Sr, Ba/Sr and  $La_N/Y_N$  in Labradorian granitoid plutonic rocks. See opposite for reference fractional crystallization trends.



SiO<sub>2</sub> noted above probably records the onset of significant K-feldspar fractionation. The trends for the Otter Lake - Walker Lake granitoid similarly indicate fractionation of both feldspars, consistent with the observed phenocryst assemblages.

La<sub>N</sub>/Y<sub>N</sub> (chondrite normalized) ratios (Figure 5.16) are relatively constant at 10-20 in the Mount Benedict Intrusive Suite, and there is little absolute difference between the three units. La and Y abundances are scattered in the Monkey Hill Intrusive Suite; the pattern suggests La (thus LREE) depletion.

#### Rare Earth Element (REE) Patterns

Three samples from contrasting units of the Mount Benedict Suite have similar REE patterns and abundances (Figure 5.17). The least evolved pattern resembles the Adlavik Intrusive Suite REE pattern (Figure 5.10). A strong Eu anomaly in the more evolved rocks indicates feldspar fractionation.

Granites of the Monkey Hill Intrusive Suite have varied REE patterns (Figure 5.18). The main body and Little Monkey Hill Granite have low total REE (< 100 x chondrite) and modest negative Eu anomalies. Excluding Eu, they are most depleted in Dy and Ho, and have dish-shaped patterns. The Round Pond Granite has strong LREE and MREE depletion, and inverse HREE fractionation. MacDougall (1988), in a detailed study of the Round Pond area, reported that this depletion intensifies with increasing SiO<sub>2</sub>. He suggested that the REE were lost to a hydrothermal fluid. As these granites have low total REE, even minimal extraction of allanite or monazite (in which REE are stoichiometric components) would have drastic effects, as effective

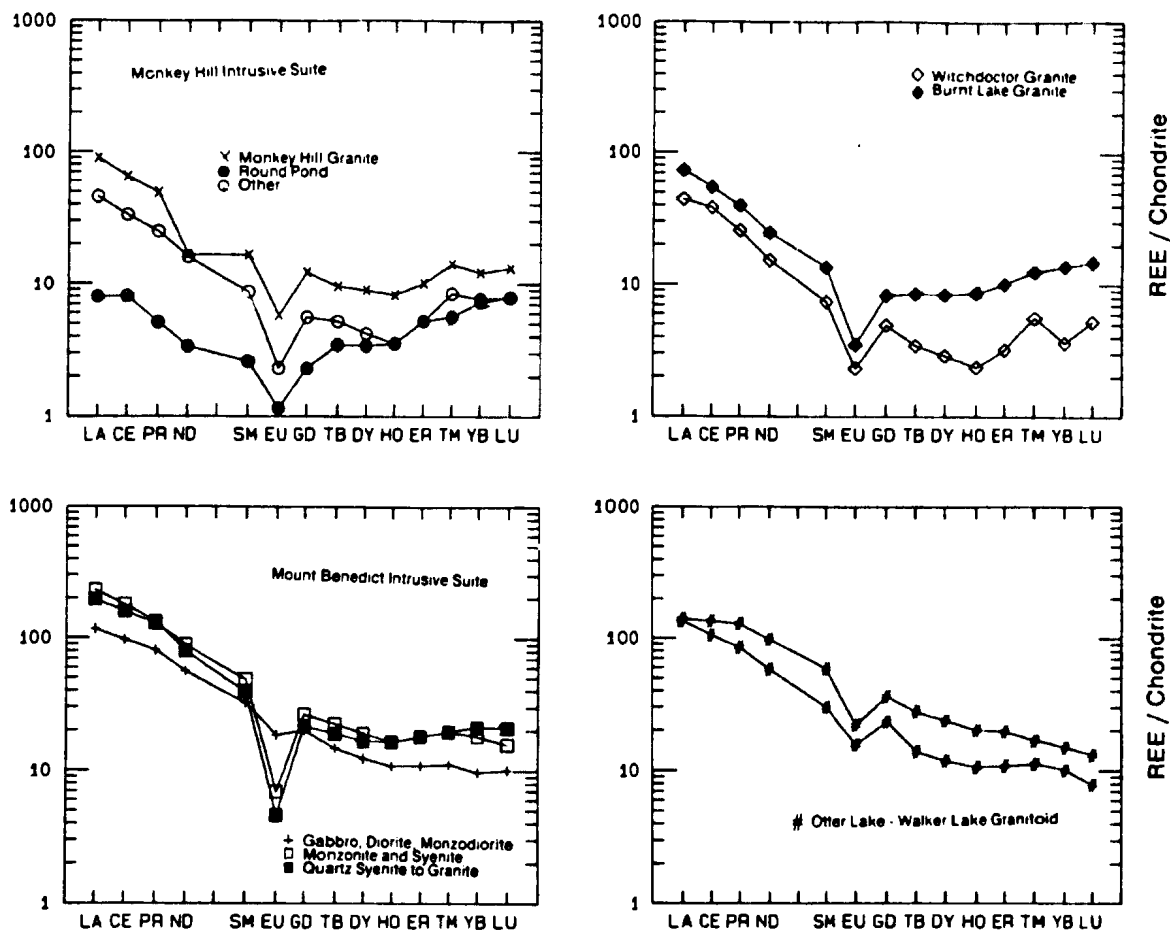


Figure 5.17 . Rare Earth element (REE) patterns for representative Labradorian granitoid plutonic rocks. Values are normalized to chondritic values (listed in Appendix C).

partition coefficients are inversely proportional to liquid concentrations (e.g. Miller and Mittlefehldt, 1982; Gromet and Silver, 1983). Depletion is, however, not confined to the REE (Table 5.2), and normal igneous processes cannot account readily for the overall trace element pattern of the Round Pond Granite. The Witchdoctor and Burnt Lake granites have closely similar REE patterns; the former has the same "valley" at Dy and Ho. This feature indicates compatible behaviour of some HREE, which may indicate effects from hornblende or (more likely) garnet as a liquidus or residual phase; It is most obvious in the slightly garnetiferous Witchdoctor Granite. The affinity of Zircon or sphene for HREE (e.g. Arth, 1976; Watson, 1982; Gromet and Silver, 1983) suggests that these minerals might also contribute to such a pattern. The Otter Lake - Walker Lake Granitoid has unremarkable REE patterns, consistent with its wide range of other totally unremarkable features.

### 5.3 SUMMARY AND DISCUSSION

#### **Contrasts Between Labradorian and Makkovikian Plutonic Associations**

Labradorian plutonic rocks differ from their Makkovikian counterparts in several respects. Firstly, the Makkovikian assemblage does not include layered mafic intrusions such as the Adlavik Intrusive Suite, although such rocks might be present below the present level of exposure (there are, for example, mafic inclusions in the border zone of the Numok Suite). Secondly, Labradorian granitoid rocks do not evolve to the marginal peralkaline compositions typical of syn- and post-tectonic Makkovikian granites (Chapters 3 and 4). They are instead mostly of slightly peraluminous character, especially above 70%  $\text{SiO}_2$ .

These contrasts are summarized in Table 5.4, which lists mean compositions for units of similar  $\text{SiO}_2$  content in both assemblages. At a given  $\text{SiO}_2$  value, Labradorian intrusions are poorer in fluorine, HFS (e.g. Zr, Nb, Hf) elements and REE (e.g. La, Ce, Sm, Yb). They show no sign of Zn enrichment at higher  $\text{SiO}_2$  contents. LFS element abundances are similar in both assemblages, except for the Mount Benedict Suite, which is enriched relative to all other units of equivalent or higher  $\text{SiO}_2$ . This suite also has F and Zr contents (particularly at 62-67%  $\text{SiO}_2$ ) that approach those of some Makkovikian units, but is depleted at higher  $\text{SiO}_2$  contents.

It must be stressed that, in spite of these differences, Makkovikian and Labradorian plutonic rocks exhibit extensive geochemical overlap. It is therefore difficult to classify single samples or small sample suites on the basis of geochemistry alone.

Table 5.4. Comparison of average compositions for selected syn-tectonic and post-tectonic Makkovikian plutonic suites, and Labradorian units of similar SiO<sub>2</sub> content.

UNIT	10		20		21		42-44		11		23-26	
n1	15		57		40		137		97		197	
n2	5		12		6		62		23		142	
(wt%)	Mean	S.D.	Mean	S.D.	Mean	S.D.	Mean	S.D.	Mean	S.D.	Mean	S.D.
SiO <sub>2</sub>	63.32	1.27	62.31	4.27	65.52	3.92	66.40	6.28	73.58	2.98	71.29	4.71
TiO <sub>2</sub>	0.88	0.06	0.78	0.29	0.63	0.29	0.50	0.31	0.29	0.19	0.31	0.27
Al <sub>2</sub> O <sub>3</sub>	15.81	0.24	16.69	1.49	15.07	1.21	15.50	1.69	12.67	1.15	13.68	1.55
Fe <sub>2</sub> O <sub>3</sub>	1.79	0.37	1.72	0.75	1.44	0.61	1.27	0.62	1.24	0.70	1.05	0.74
FeO	3.06	0.73	3.41	1.12	3.66	1.75	2.07	1.45	1.39	1.17	1.68	1.47
MnO	0.10	0.01	0.12	0.05	0.15	0.07	0.07	0.04	0.06	0.02	0.06	0.06
MgO	1.25	0.42	1.22	0.87	0.40	0.29	0.96	1.19	0.19	0.25	0.36	0.50
CaO	2.95	0.48	2.92	1.30	1.76	0.71	2.08	1.84	0.82	0.56	1.14	1.04
Na <sub>2</sub> O	4.27	0.25	4.57	0.41	4.51	0.57	4.38	0.42	4.00	0.48	4.09	0.86
K <sub>2</sub> O	4.75	0.49	5.14	1.09	5.81	0.67	5.27	0.98	4.85	0.64	5.12	1.10
P <sub>2</sub> O <sub>5</sub>	0.26	0.03	0.24	0.14	0.15	0.13	0.15	0.18	0.05	0.05	0.07	0.09
LOI	0.63	0.23	0.58	0.35	0.46	0.23	0.85	0.30	0.45	0.22	0.67	0.37
TOTAL	99.07		99.67	0.00	99.54		99.49		99.57		99.52	

(ppm) Trace Elements

Li	22.7	5.7	21.0	9.7	13.0	7.6	28.5	11.3	14.9	11.7	25.0	23.5
F	860.5	212.7	928.9	436.3	427.8	270.3	1229.8	524.6	1029.9	803.8	1420.0	1141
Sc	9.6	1.7	10.5	2.1	11.0	3.8	4.0	2.3	1.4	0.9	3.1	4.1
V	74.6	19.6	55.9	37.5	17.7	10.0	44.3	40.6	15.9	13.4	23.3	29.2
Cr	5.5	3.5	7.0	9.9	3.4	2.4	14.0	32.0	4.7	3.8	5.1	6.5
Ni	2.6	1.9	3.7	4.7	1.1	0.5	5.1	16.3	1.3	1.2	2.2	3.9
Cu	9.1	3.8	13.6	9.5	6.4	3.1	19.3	23.5	3.9	3.9	9.3	38.4
Zn	74.1	8.5	86.3	23.4	114.3	44.2	54.3	24.6	77.1	29.9	75.1	69.6
Ga	18.3	1.2	20.5	2.9	21.6	6.3	11.0	5.0	16.5	6.8	16.9	8.6
Rb	126.4	24.2	121.9	47.9	110.8	54.5	260.5	99.6	153.5	47.1	178.4	65.0
Sr	327.6	39.0	329.4	166.6	108.5	77.0	276.6	258.1	60.8	77.5	111.7	130.2
Y	36.5	1.9	39.2	13.6	53.5	19.9	28.3	8.1	70.9	28.9	55.4	43.8
Zr	236.6	83.2	486.3	255.9	794.8	411.2	356.3	174.2	387.0	151.8	491.5	558.5
Nb	14.2	1.1	19.1	8.5	21.3	6.9	23.7	10.1	27.9	14.0	26.0	21.0
Mo	4.3	0.5	4.1	1.0	3.4	1.1	4.5	2.4	3.7	1.9	4.3	7.7
Sn	1.0	0.0	2.7	2.7	1.3	0.5	6.9	4.3	3.5	2.5	5.8	9.9
Cs	1.3	1.2	1.0	1.7	0.7	0.4	9.6	4.7	0.6	0.4	1.2	1.0
Ba	1424.0	116.2	1099.0	558.0	787.7	542.1	612.5	440.7	453.1	411.7	501.9	382.6
La	53.3	4.9	64.8	31.7	77.2	26.4	52.6	18.7	76.6	33.3	90.7	111.7
Ce	102.7	6.1	131.0	63.2	156.4	54.7	108.8	37.3	158.7	65.7	178.7	197.0
Sm	9.2	0.8	13.3	3.1	14.5	3.8	7.4	1.8	12.6	3.5	13.1	10.4
Yb	2.5	0.0	3.8	2.1	5.3	0.0	4.4	0.9	7.7	3.2	6.6	4.7
Hf	8.0	1.2	11.9	3.5	14.3	5.0	10.8	3.4	12.1	3.1	13.3	13.3
Pb	15.9	3.9	15.9	6.6	15.8	7.1	19.9	7.9	20.3	10.4	37.3	205.3
Th	9.2	3.0	9.1	10.7	5.1	4.8	27.7	16.7	15.2	9.6	18.3	20.5
U	4.8	0.9	3.1	1.7	2.4	1.4	8.1	4.4	4.7	3.0	5.8	7.0

(wt%) partial CIPW norms

Q	12.25	1.76	8.02	6.40	10.77	7.74	15.19	9.84	29.80	6.01	24.90	9.23
C	0.00	0.00	0.05	0.18	0.02	0.05	0.07	0.19	0.02	0.06	0.12	0.23
Or	28.50	2.93	31.47	4.81	32.52	5.39	31.52	5.81	28.89	3.89	30.38	5.96
Ab	36.71	2.01	38.96	3.48	40.28	5.85	37.51	3.57	34.11	4.02	34.90	7.35
An	10.08	1.50	9.37	4.48	5.28	3.78	7.01	6.36	2.30	2.27	3.66	2.94
Di	2.88	1.35	2.85	1.48	3.52	2.25	1.98	2.21	1.08	0.87	1.28	2.82
Hy	4.65	1.72	4.53	2.26	3.22	2.08	3.07	2.89	1.22	2.00	2.15	2.26
Ol	0.00	0.00	0.41	1.09	0.61	1.36	0.37	1.71	0.00	0.00	0.03	0.26
Nt	2.64	0.55	2.41	0.96	2.06	0.78	1.81	0.93	1.58	0.75	1.38	1.00
Il	1.69	0.12	1.48	0.56	1.21	0.49	0.97	0.60	0.54	0.36	0.61	0.52

KEY TO UNITS (STM - syn-tect Makkovikian; PTN - post-tect Makkovikian; L - Labradorian)

- 10 -- Long Island Quartz Monzonite (all data) [STM]
- 20 -- Munk Intrusive Suite (Monzonite to Quartz Monzonite) [PTN]
- 21 -- Munk Intrusive Suite (Syenite to Quartz Syenite) [PTN]
- 42-44 -- Mount Benedict Intrusive Suite (all data) [L]
- 11 - Kennedy Mountain Intrusive Suite (all data, unaltered) [STM]
- 23-26 -- Strawberry Intrusive Suite (all data) [PTN]

n1 -- Number of analyses for all elements except those listed below  
n2 -- Number of analyses for Sc, Sn, Cs, Sm, Yb and Hf

Table 5.4 (continued)

UNIT	27-29		13-0		45		46-47		30		48	
n1	82		4		70		34		79		49	
n2	66				57		29		13		11	
(wt%)	Mean	S.D.	Mean	S.D.	Mean	S.D.	Mean	S.D.	Mean	S.D.	Mean	S.D.
SiO <sub>2</sub>	72.12	2.93	72.73	1.26	73.50	4.42	73.24	3.22	70.11	5.15	68.54	4.42
TiO <sub>2</sub>	0.32	0.19	0.16	0.09	0.14	0.12	0.15	0.11	0.39	0.22	0.44	0.20
Al <sub>2</sub> O <sub>3</sub>	13.22	1.34	14.66	0.44	13.49	1.18	13.98	1.49	14.43	1.74	14.98	1.62
Fe <sub>2</sub> O <sub>3</sub>	1.21	0.57	0.64	0.44	1.08	3.23	0.61	0.45	1.16	0.55	1.20	0.61
FeO	1.44	0.87	0.66	0.29	0.70	1.56	0.62	0.31	1.49	0.97	1.87	1.01
MnO	0.06	0.04	0.03	0.01	0.05	0.04	0.04	0.01	0.06	0.04	0.06	0.03
MgO	0.18	0.17	0.65	0.27	0.21	0.24	0.18	0.13	0.50	0.84	0.86	0.54
CaO	0.88	0.47	0.99	0.03	0.76	0.44	0.78	0.36	1.36	1.20	2.04	1.02
Na <sub>2</sub> O	3.97	0.61	5.06	0.93	4.26	1.07	4.27	1.11	4.28	0.75	3.89	0.55
K <sub>2</sub> O	5.47	0.90	3.34	1.46	4.72	1.22	4.98	0.87	5.11	1.01	4.70	0.62
P <sub>2</sub> O <sub>5</sub>	0.04	0.04	0.06	0.02	0.03	0.03	0.02	0.03	0.10	0.08	0.15	0.09
LOI	0.53	0.20	0.93	0.29	0.58	0.27	0.50	0.13	0.58	0.29	0.77	0.24
TOTAL	99.44		99.91		99.48		99.37		99.57		99.50	
(ppm)												
Li	13.9	11.7	11.5	1.7	20.5	13.6	20.7	19.8	14.8	6.2	25.7	12.5
F	1244.6	935.7	187.5	68.4	511.7	436.6	177.7	120.6	688.5	462.5	679.1	257.1
Sc	3.8	5.3			1.4	1.2	1.9	1.2	2.4	0.9	6.8	2.4
V	12.8	7.7	21.5	8.5	17.4	18.1	14.6	6.8	21.5	17.1	44.6	30.2
Cr	3.7	2.9	7.5	5.7	4.0	6.4	3.5	3.8	4.8	13.7	6.5	7.0
Ni	1.5	1.8	3.0	2.7	1.4	1.3	1.7	2.1	2.6	7.9	2.1	3.0
Cu	6.0	9.2	3.5	1.3	9.2	20.2	3.8	3.7	6.3	6.1	9.1	18.7
Zn	89.6	59.6	29.3	3.9	34.9	30.5	28.8	10.9	54.8	42.8	46.9	21.4
Ga	21.4	10.0	6.8	1.7	12.0	6.6	11.7	5.8	15.2	5.2	12.8	4.1
Rb	172.5	44.1	96.5	41.0	181.7	71.7	191.1	68.2	127.8	51.8	140.5	38.7
Sr	61.2	65.8	273.5	47.5	134.5	210.4	87.1	75.8	160.7	151.6	277.7	154.8
Y	74.4	32.8	5.8	1.7	26.5	23.0	25.3	20.2	42.5	17.2	28.2	10.2
Zr	675.7	439.3	88.0	38.0	160.1	99.3	185.6	172.3	368.8	210.3	240.0	83.8
Nb	29.3	11.1	2.0	0.0	17.2	8.5	20.8	13.6	19.1	7.2	13.6	4.4
Mo	4.3	2.3	2.0	0.0	84.5	578.7	28.1	142.9	3.7	1.2	3.2	1.2
Sn	4.0	2.6			2.9	2.3	2.4	2.1	2.7	2.7	3.9	3.3
Cs	1.1	0.7			2.2	2.1	1.9	1.3	0.7	0.6	4.1	1.8
Ba	329.6	260.1	912.5	446.6	391.2	360.5	519.0	675.5	660.8	482.6	961.5	542.3
La	122.8	62.6	13.8	4.6	22.1	21.4	30.9	22.3	63.1	30.2	50.6	14.8
Ce	247.2	121.1	19.0	11.6	45.4	43.8	63.2	45.7	126.8	59.2	100.1	28.5
Sm	20.8	9.8			4.4	4.0	4.2	1.9	10.4	3.9	9.3	3.0
Yb	8.8	4.3			3.9	3.6	2.8	0.6	4.2	2.0	2.5	0.0
Hf	19.1	10.3			5.6	3.0	5.6	1.5	10.1	3.0	12.5	21.1
Pb	24.5	13.5	12.5	7.9	22.6	9.2	26.8	11.5	17.6	11.2	16.8	8.1
Th	18.9	8.0	1.8	1.0	13.6	8.5	19.1	9.2	13.0	9.6	14.8	7.3
U	5.5	2.3	1.7	0.5	6.0	5.1	7.4	5.0	4.5	2.6	4.0	2.4
(vtt)												
O	26.22	7.51	27.56	2.39	28.99	5.57	26.82	9.65	22.16	9.88	22.14	8.29
C	0.10	0.70	0.98	0.48	0.25	0.24	0.26	0.21	0.06	0.14	0.26	0.36
Or	32.64	5.34	19.88	8.64	27.82	7.14	29.78	5.21	30.45	6.00	28.14	3.71
Ab	33.79	5.15	43.23	8.08	36.63	8.56	36.39	9.20	36.54	6.34	33.29	4.70
An	1.90	1.64	4.84	0.26	3.22	1.70	3.61	1.64	4.97	4.19	8.95	4.23
Di	1.62	1.35	0.00	0.00	0.25	0.72	0.16	0.41	1.11	1.66	0.49	0.74
Hx	0.96	1.05	2.12	0.72	0.86	0.99	0.87	0.62	1.81	1.34	3.77	2.10
Ol	0.00	0.00	0.00	0.00	0.00	0.00	0.00	0.00	0.18	1.60	0.00	0.00
Wt	1.63	0.77	0.94	0.64	1.29	4.96	0.82	0.46	1.60	0.82	1.76	0.90
Il	0.62	0.36	0.31	0.17	0.26	0.22	0.30	0.22	0.74	0.43	0.85	0.38

KEY TO UNITS (STN - syn-tect Makkovikian; PTN - post-tect Makkovikian; L - Labradorian)  
 27-29 -- Lanceground Intrusive Suite (all data) [PTN]  
 13 -- Brunwater Granite [STN]  
 45 -- Monkey Hill Intrusive Suite (all data) [L]  
 46-47 -- Witchdoctor and Burnt Lake Granites (all data) [L]  
 30 -- Big River Granite (all data) [PTN]  
 48 -- Otter Lake - Walker Lake Granitoid (all data) [L]

n1 -- Number of analyses for all elements except those listed below  
 n2 -- Number of analyses for Sc, Sn, Cs, Sm, Yb and Hf

### Evolution of The Adlavik Intrusive Suite

The Adlavik Intrusive Suite is a multiphase mafic intrusion that evolved via crystal accumulation processes. Field relationships within the main body indicate at least two (and probably many more) pulses of mafic magmatism, and it likely represents the proverbial "periodically refilled, periodically tapped, continuously evolving magma chamber" (words of O'Hara, 1977).

Although reconstruction is difficult, normative mineralogical variations (Figure 5.7) indicate that higher levels are dominated by gabbro ( $\pm$  olivine), that is poorer in  $\text{SiO}_2$ ,  $\text{K}_2\text{O}$  and incompatible elements than a lower gabbro-norite ( $\pm$  olivine) sequence. This suggests that the parental magma(s) were derived from a fractionating magma chamber at much deeper levels (the general similarity of trace element patterns in all argues against two radically different sources). The gabbro-norite sequence may have been derived from the upper, fractionated, portion of such a body, whereas the overlying gabbro sequence originated at deeper, less fractionated levels.

Once emplaced, the Adlavik Suite magmas evolved by fractionation of olivine and pyroxenes, and a later plagioclase-dominated assemblage. Residual liquids were in some cases trapped within cumulate zones (bounded by viscosity or density contrasts?), where they crystallized to form the pegmatite facies. Some residual magmas migrated on an intrusion-wide scale to form the more potassic members of the diorite unit, but much of this is probably a plagioclase cumulate with variable amounts of trapped liquid. Volatile concentration and circulation as a consequence of crystallization (and perhaps ascent) led to widespread transformation of earlier pyroxenes, and crystallization of primary hornblende from more fractionated liquids.

### Evolution of The Mount Benedict Intrusive Suite

Geochemical trends in the Mount Benedict Suite are readily interpreted in terms of fractional crystallization, and provide constraints for numerical modelling (see below).

Rb/Sr and Ba/Sr trends (Figure 5.17) indicate that plagioclase, K-feldspar and mafic minerals were the dominant liquidus phases, consistent with the observed phenocryst assemblages. Plagioclase phenocrysts occur in all but the most evolved rocks, and accumulated in the diorite unit. Initial strong Rb enrichment (Figure 5.7) is characteristic of plagioclase ( $\pm$  mafic mineral) fractionation, as is the antithetic behaviour of Ba and Sr. Both features predominate below 62%  $\text{SiO}_2$  (Figure 5.15). The inflection of Ba trends at this point indicates the onset of K-feldspar crystallization; constant Ba/Sr during subsequent evolution suggests that both feldspars continued to crystallize in roughly constant proportions (assuming that distribution coefficients remained constant). The inflection at ca. 62%  $\text{SiO}_2$  also marks the point at which the evolving liquid reached the plagioclase - alkali-feldspar cotectic line (Figure 5.13).

The convex-upward Zr- $\text{SiO}_2$  trend (Figure 5.16) defines the appearance of a Zr-rich phase (probably zircon) at ca. 67%  $\text{SiO}_2$ . The close correspondence between Zr and F trends suggests that Zr solubility may have been reduced by loss of fluorine from the magma, or that both were affected by a third factor, perhaps an increase in melt polymerization. The generally flat REE and Y trends indicate that these elements were buffered at an earlier stage, probably by accessory phases such as sphene, which locally cores hornblende. Depletion in Th and REE (Figures



5.15, 5.16) at the highest  $\text{SiO}_2$  contents may indicate the effects of allanite fractionation (c.f. Michael, 1982; Miller and Mittlefehldt, 1982).

#### Relationship Between The Adlavik and Mount Benedict Intrusive Suites

The Adlavik and Mount Benedict Intrusive Suites are viewed here as complementary associations, i.e., the mafic and plagioclase cumulates of the Adlavik Suite represent material removed from a mafic parental magma to produce the more evolved rocks of the Mount Benedict Suite. The diorite unit in the Mount Benedict Suite includes plagioclase cumulates that resemble leucogabbro and diorite of the Adlavik Suite. Their presence at the margins of the suite, and at low topographic elevations suggests a crude layering or zonation, and suggests that mafic rocks may occur below the present level of exposure. The mafic rocks at Pamiulik Point, although grouped above with the Adlavik Suite, possibly represent some of this material.

There are indications that the Mount Benedict Intrusive Suite is a crudely layered body. In the field, this is suggested by the preferred occurrence of the most evolved syenite and granite at high elevations. Compositional layering or zonation is also indicated by geochemical variation with elevation (Figure 5.18). Chemical - elevation correlations are far from perfect, but the most evolved compositions are dominant at higher altitudes.

The Adlavik and Mount Benedict Suites also define smooth and continuous geochemical trends against  $\text{SiO}_2$  (Figure 5.19), with some scatter at low  $\text{SiO}_2$  values that reflects the presence of cumulate rocks. The strong incompatible element enrichment in the evolved rocks of the

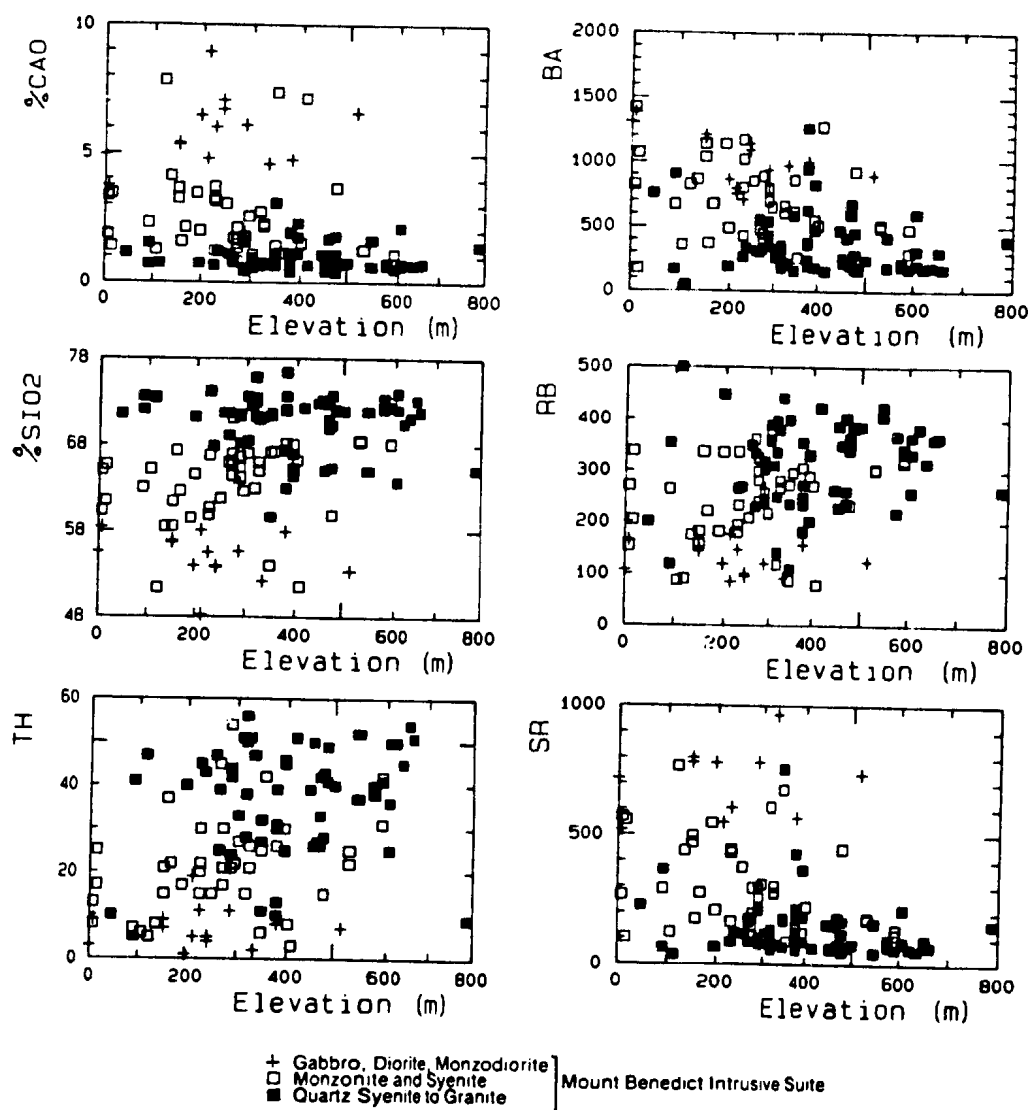


Figure 5.18. Variation of selected major and trace elements against elevation (metres above sea level) in the Mount Benedict Intrusive Suite, illustrating the dominance of evolved compositions at high elevations.

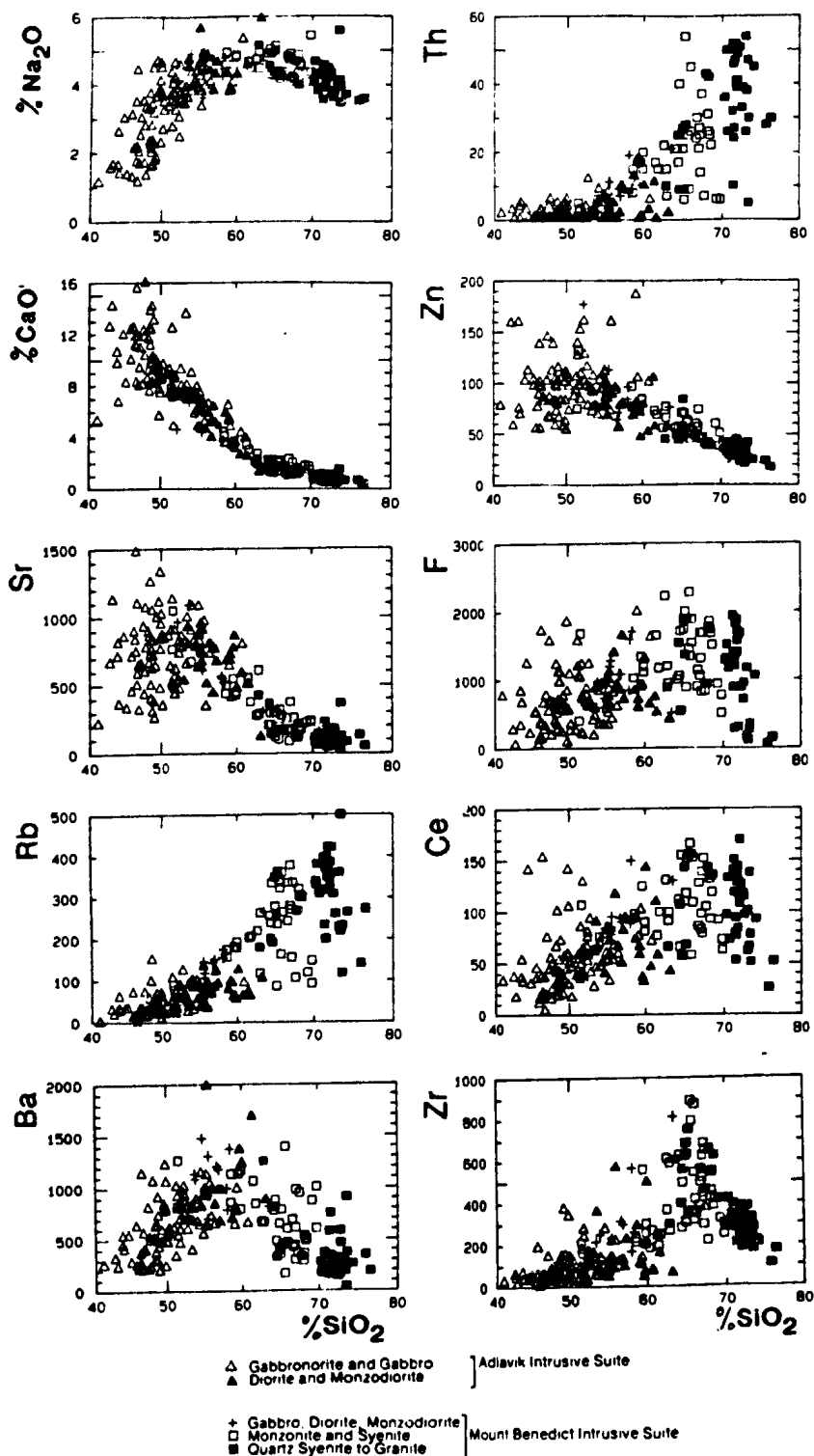


Figure 5.19. Variation of selected major and trace elements against  $SiO_2$  in the Adlavik and Mount Benedict Intrusive Suites, illustrating their geochemical continuity.

Mount Benedict Suite is consistent with extended fractionation of a mafic parent magma, for which the most logical candidate is the contemporaneous Adlavik Suite.

#### Fractional Crystallization Models

The above hypothesis was tested with a numerical crystallization model using Adlavik Suite mafic rocks as a theoretical parent magma for the Mount Benedict Suite.

Mineral/melt partition coefficients ( $K_D$ 's) used in the model are mostly mean values measured by Villemant et al. (1981) from a compositionally varied volcanic suite of alkali-basalt parentage.  $K_D$ 's for orthopyroxene and amphibole, and values for V and Y in all minerals, are from a compilation of basalt-related studies by Jenner (1984). A hypothetical composite "accessory" was awarded an arbitrary  $K_D$  value of 100 for elements considered to be concentrated in these minerals at various stages. All  $K_D$  values employed are listed in Appendix C. The model was constructed for U, Th, La, Y, Rb, Zr, Ba, Sr, V, Cr, Ni and Ti; these elements provide a spectrum of trace element behaviour.

Calculations were performed using the Rayleigh fractionation equation (e.g. Arth, 1976; Hanson, 1978), which assumes perfect instantaneous removal of solid from equilibrium. The term  $F_L$  is used below to denote the fraction of liquid remaining at each step. An incremental equilibrium crystallization model (c.f. McCarthy and Hasty, 1976) was also tested, but, unless increments are unrealistically large ( $> 0.2$ ), differs minimally from the Rayleigh model. Model compositions are represented using spider-type charts normalized to the model parental magma

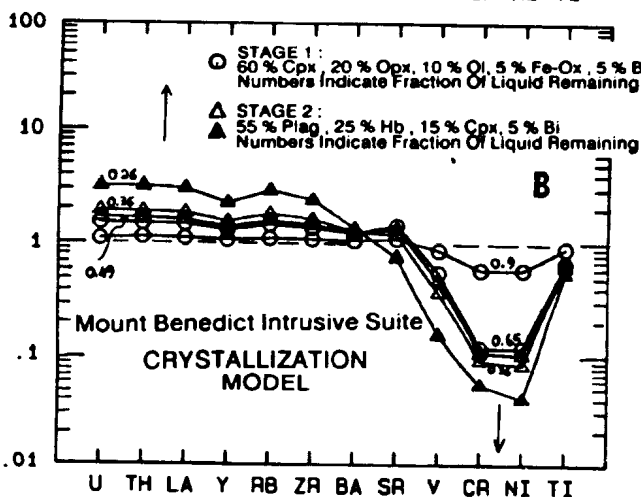
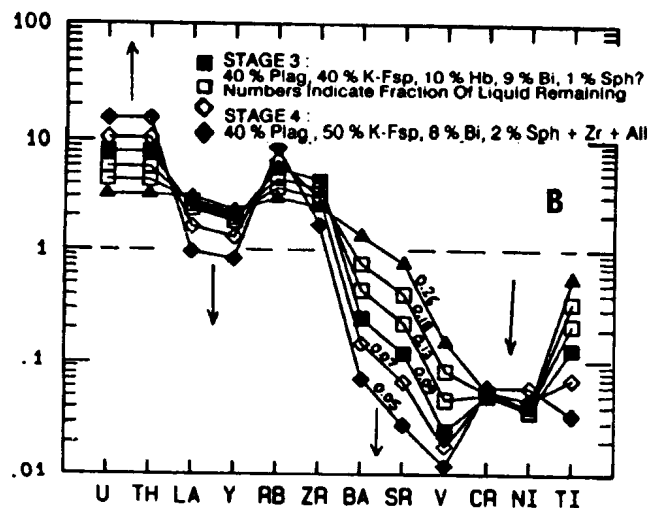
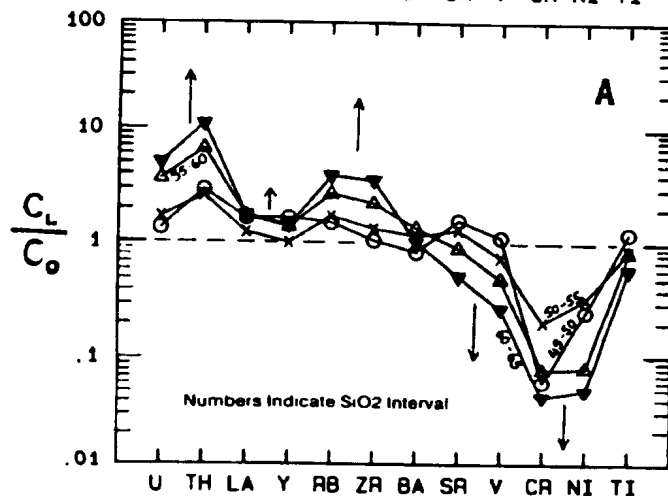
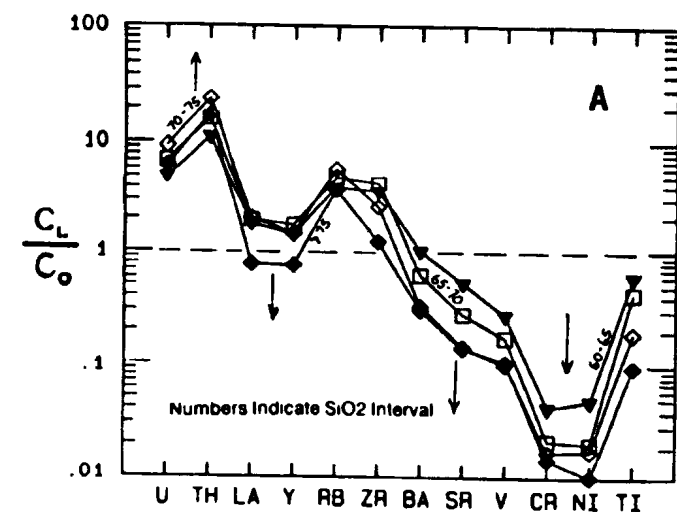
composition (Figure 5.20b). The observed compositions were summarized by calculation of arithmetic means for 5% SiO<sub>2</sub> intervals, and displayed in the same manner (Figure 5.20a).

#### Mount Benedict Suite Fractionation Model

**Starting Materials** : The average composition of Adlavik Suite mafic rocks in the east of the area (Table 3.2, partially listed in Figure 5.20) was taken as a parental magma. The mean major element composition (excluding K<sub>2</sub>O; see below) approximates average basalt (from LeMaitre, 1976), suggesting that deviations due to mafic or plagioclase cumulates are cancelled in the mean. Note that for U and Th, poor precision at low levels (Appendix A) causes some uncertainty in the "parent" composition, which is propagated throughout the model.

**Description of Model** : Stage 1 is dominated by removal of mafic minerals (60% clinopyroxene, 20% orthopyroxene, 10% olivine, 5% oxide and 5% biotite). At  $F_L=0.65$ , the model corresponds well to the observed composition at ca. 55% SiO<sub>2</sub> (except for Th). It is unlikely that this phase assemblage remained constant, but modest variations in the proportions of Cpx, Opx and Ol do not affect the results significantly. Oxide fractionation is required to deplete V and Cr.

Stage 2 assemblages consist of 55% plagioclase, 25% hornblende, 15% clinopyroxene and 5% biotite. Crystallization until  $F_L = 0.26$  creates a model composition that approximates the observed composition at 60-65% SiO<sub>2</sub>, corresponding to the dominant monzonite to syenite unit. Key features for this interval are constant Ba, slight Sr depletion, and enrichment in Rb and Zr.



# MOUNT BENEDICT SUITE PARENTAL COMPOSITION

SiO <sub>2</sub>	49.77
U	1.2
Th	1.7
La	28.6
Y	19.3
Rb	56.6
Zr	116.3
Ba	940.1
Sr	677.0
V	183.2
Cr	338.9
Ni	98.3
TiO <sub>2</sub>	1.15

Figure 5.20. Comparison of observed geochemical evolution in the Mount Benedict Intrusive Suite (A) and the results of a four-stage fractional crystallization model (B). See text for details of model and discussion.

Observed Th enrichment is greater than predicted, and La and Y are stabilized at ca. 2 x parent. The former may reflect uncertainties in the U and Th contents of the assumed parent (see above). If the discrepancy between observed and model compositions is real, an alternative explanation is enrichment of U and Th by assimilation of sialic material (see later discussion, also Chapter 8). La and Y behaviour probably reflects the precipitation of sphene, not included in the model up to this point.

Stages 3 and 4 produce the most evolved rocks by crystallization along the plagioclase - K-feldspar cotectic. The liquidus assemblage includes these minerals, plus minor hornblende, biotite and accessory minerals (Figure 5.20). At  $F_L=0.1$ , the model fits observed compositions for ca. 70%  $\text{SiO}_2$ . Buffering of La and Y, and Ti depletion, is maintained by sphene, and zircon crystallization initiates Zr depletion in the most evolved liquids, which correspond to model compositions at  $F_L=0.05$  (except for the persistent Th problem !). The observed Ba and Sr depletion is less than predicted; however, this is easily explained via retention of feldspars in the by now viscous high-silica liquid.

**Feasibility of The Model** : The model fits the petrographic and geochemical features of both suites, and the proportion of crystallization required appears reasonable. The largest crystallization interval corresponds to the areally dominant complementary association of plagioclase- cumulate leucogabbro and diorite (Adlavik Suite) and plagioclase- porphyritic monzonite and syenite (Mount Benedict Suite). The restricted extent of the most evolved rocks is consistent with a highly fractionated residual magma from a mafic source. The characteristic "speckled-eggshell" texture

probably results from transportation of cumulus plagioclase by convection currents (c.f. Marsh, 1988), which carried them to regions where they were out of equilibrium, and reacted with the liquid or were mantled by K-feldspar. Crystallization at shallow depths along a cotectic phase boundary also allows periodic fluctuations in the liquidus assemblage due to changes in vapour pressure.

Discrepancies for U and Th may, as explained above, be a function of poor estimates for parental compositions. There is, however, independent Nd isotopic evidence for minor crustal assimilation in the Mount Benedict Suite (Chapter 8). Such a process, in combination with crystal fractionation, would further reduce the proportion of crystallization required to generate the most evolved liquids (c.f. DePaolo, 1981a), and thus increases the feasibility of the model.

#### **Affinities Of Labradorian Mafic Magmas and Derivatives**

Clark (1973) described the Adlavik Intrusive Suite as a water-rich basaltic magma of "appinitic" affinity. Appinites are small, compositionally varied, mafic to intermediate, subvolcanic, volatile-rich intrusions described from the British Caledonides (e.g. Pitcher and Berger, 1972; Wright and Bowes, 1979; Fowler, 1988). They are characterized by large amphibole crystals; in this respect, the pegmatite facies has an "appinitic" texture. Wright and Bowes (1979) describe rock types and textures from Scotland that are broadly analogous to those described above from the Adlavik Suite. However, such features are not necessarily characteristic, as Mullan and Bussell (1977) report analogous features from hydrous mafic intrusions associated with Mesozoic arc batholiths in Peru and Mexico.



Table 5.5. Comparison of average compositions for the Adlavik Intrusive Suite, Scottish "appinites" (Wright and Bowes, 1979; Fowler, 1988), and modern basalt and andesite types (Condie, 1981b).

UNIT	40		41		A1		A2		A3		A4		A5	
n1	117		22		n=19		n=8		n=12		n=4		n=5	
n2	16		5											
(Wt%)	Mean	S.D.	Mean	S.D.	Mean	S.D.	Mean	S.D.	Mean	S.D.	Mean	S.D.	Mean	S.D.
SiO <sub>2</sub>	49.74	4.19	57.64	2.89	48.31	3.66	57.76	1.92	52.41	4.46	49.21	1.80	58.41	3.68
TiO <sub>2</sub>	0.96	0.43	0.84	0.26	0.97	0.29	0.63	0.12	1.12	0.46	1.32	0.32	0.86	0.34
Al <sub>2</sub> O <sub>3</sub>	15.72	3.73	18.10	1.21	12.71	1.74	16.65	1.9	16.02	2.5	12.52	1.03	15.62	1.93
Fe <sub>2</sub> O <sub>3</sub>	3.05	1.39	1.99	0.59	2.6	0.98	1.79	0.75	3.43	1.03	7.39	0.72	4.84	1.16
FeO	6.29	1.61	4.17	1.36	6.63	1.18	3.33	1.37	5.89	1.58				
MnO	0.16	0.04	0.12	0.03	0.13	0.03	0.07	0.02	0.15	0.03	0.15	0.01	0.09	0.02
MgO	7.67	4.93	2.36	1.29	11.6	2.46	4.24	2.36	6.16	3.02	7.37	1.14	3.10	1.97
CaO	9.59	2.83	4.95	1.72	8.4	1.79	4.11	1.33	6.66	1.37	9.61	1.22	4.71	2.04
Na <sub>2</sub> O	3.05	1.15	4.87	0.99	2.44	0.7	3.76	0.61	2.8	1.06	3.49	0.32	4.35	0.93
K <sub>2</sub> O	1.54	0.89	3.42	0.96	2.13	0.67	4.31	1.56	1.84	0.72	3.72	0.52	5.34	0.61
P <sub>2</sub> O <sub>5</sub>	0.34	0.36	0.33	0.14	0.25	0.13	0.26	0.09	0.26	0.17	1.68	0.80	0.64	0.37
LOI	1.42	0.76	0.90	0.51	3.96	0.86	2.51	0.88	3.75	0.98	2.76	1.05	1.55	0.78
TOTAL	99.52		99.67		100.15		99.9		99.89		99.20		99.51	
(ppm) Trace Elements														
Li	22.4	9.2	20.9	6.1	10	5	10	7						
P	732.6	973.4	836.4	316.4										
Sc	32.4	15.7	15.2	5.3	43	16	10	7	26	14				
V	202.6	100.0	91.7	59.5	223	63	227	273	269	163	156.3	22.9	86.8	40.1
Cr	280.0	415.7	24.9	26.5	453	179	83	73	151	140	296.5	45.0	113.4	111.3
Mn	76.5	119.4	10.5	9.5	160	90	49	96	67	110	81.3	36.9	34.8	19.4
Cu	50.6	38.0	22.8	15.6	107	73	82	48	63	60				
Zn	96.5	36.0	76.9	16.3	93	24	66	21	94	17	110.0	15.0	70.4	18.1
Ga	20.2	5.6	18.0	4.8	11	3	14	2	21	3				
Rb	43.0	28.4	81.6	25.5	44	18	131	49	50	33				
Sr	739.7	299.0	667.3	192.4	833	291	1055	433	474	199	2278.5	206.5	2211.2	98.8
Y	19.5	10.0	24.0	9.1	16	4	13	4						
Zr	82.9	70.1	175.6	143.3	87	26	227	96	185	77	341.5	104.1	359.2	73.0
Nb	3.6	4.0	10.4	4.8	8	8	9	5	14	6				
Mo	3.8	3.5	3.4	1.3										
Sn	1.0	0.0	1.2	0.4										
Cs	1.0	1.6	1.4	0.8										
Ba	622.4	406.6	1399.4	1042	899	372	1120	153	480	687	2536.0	644.1	2471.6	420.4
La	23.3	15.3	37.7	10.8	43	24	61	33			190.0	7.2	154.2	12.7
Ce	49.3	31.6	71.3	27.9	37	7	87	218	24	22	416.8	36.2	300.0	39.7
Sm	5.6	2.2	6.5	0.8							21.8	2.4	11.8	2.0
Yb	2.5	0.0	2.5	0.0										
Hf	2.2	2.0	3.2	0.4										
Pb	4.6	6.3	9.5	4.2	15	6	23	9	16	2				
Th	2.0	2.6	5.5	5.5	5	2	9	3	16	24				
U	1.0	0.9	2.2	1.3										

KEY TO ANALYSES:

- 40 -- Adlavik Intrusive Suite Mafic Rocks (all data)
- 41 -- Adlavik Intrusive Suite Diorites (all data)
- A1 -- "Appinite" Gabbro, Ballachulish Area (Wright and Bowes, 1979)
- A2 -- "Appinite" Diorite, Ballachulish Area (Wright and Bowes, 1979)
- A3 -- "Appinite", Loch Lomond Area (Wright and Bowes, 1979)
- A4 -- "Appinites" with < 52% SiO<sub>2</sub>, Ach'uaire Area (Fowler, 1988)
- A5 -- "Appinites" with > 52% SiO<sub>2</sub>, Ach'uaire Area (Fowler, 1988)

n1 -- Number of Analyses for all elements except those listed below  
n2 -- Number of analyses for Sc, Sn, Cs, Sm, Yb and Hf

Table 5.5 (continued)

UNIT	MORB	IAB	CAB	CFB	IASB	CASB	IAA	CAA	IASA
n1					n=42	n=21			n=22
n2									
(Wt%)	Mean	Mean	Mean	Mean	Mean	Mean	Mean	Mean	Mean
SiO <sub>2</sub>	49.80	51.10	50.20	50.30	50.62	51.41	57.30	59.50	55.46
TiO <sub>2</sub>	1.50	0.83	1.00	2.20	0.83	0.83	0.58	0.70	0.93
Al <sub>2</sub> O <sub>3</sub>	16.00	16.10	17.70	14.30	16.01	15.73	17.40	17.20	16.75
Fe <sub>2</sub> O <sub>3</sub>	2.00	3.00	3.90	3.50	4.11	4.54	2.50	2.50	2.55
FeO	7.50	7.30	6.30	9.30	4.55	3.60	2.70	5.00	4.01
MnO					0.17	0.11			0.10
MgO	7.50	5.10	5.40	5.90	6.24	5.98	3.50	3.40	4.81
CaO	11.20	10.80	9.80	9.70	9.26	6.96	8.70	7.00	6.71
Na <sub>2</sub> O	2.80	2.00	2.70	2.50	2.93	3.12	2.60	3.70	2.94
K <sub>2</sub> O	0.14	0.30	0.90	0.80	2.74	3.86	0.70	1.60	3.66
P <sub>2</sub> O <sub>5</sub>					0.44	0.61			0.60
LOI									
TOTAL									
(ppm)									
Li									
P									
Sc					25				26
V					290				218
Cr	300	50	50	100	156		40	55	141
Ni	100	20	50	100	50		15	18	53
Cu	70	80	80	100	159		50	30	115
Zn	75	80	80	90			60	80	
Ga									
Rb	1	5	10	30	59		10	30	63
Sr	135	225	300	350	943		200	385	956
Y	30	20	23	30	16		23	20	18
Zr	100	60	100	200	67		90	110	121
Nb									
Mo									
Sn									
Cs									
Ba	11	60	100	200	683		100	270	567
La	3.5	3.9	9.2	27			3	12	
Ce	12	7	25	140			6.8	25	
Sm	3.9	2.2	3.8	8.2			2.5	3	
Yb	3	2	2.5	2.5			2.7	1.9	
Hf									
Pb									
Th									
U									

KEY TO AVERAGE ANALYSES:

MORB - Mid Ocean Ridge Basalts (compiled by Condie, 1981b)  
 IAB - Island Arc Basalts (compiled by Condie, 1981b)  
 CAB - Calc-Alkaline (continental arc) Basalts (compiled by Condie, 1981b)  
 CFB - Continental Flood Basalts (compiled by Condie, 1981b)  
 IASB - Island Arc Shoshonitic Basalts (compiled by Morrison, 1980)  
 CASB - Continental Arc Shoshonitic Basalts (compiled by Morrison, 1980)  
 IAA - Island Arc Andesites (compiled by Condie, 1981b)  
 CAA - Calc-Alkaline (continental arc) Andesites (compiled by Condie, 1981b)  
 IASA - Island Arc Shoshonitic Andesites (compiled by Morrison, 1980)

NOTE : Condie (1981b) does not list sources or numbers of analyses for his compilation.

Table 5.5 lists mean compositions for the Adlavik Suite, appinites from Scotland (Wright and Bowes, 1979; Fowler, 1988), and average modern basalt and andesite types (compiled by Condie, 1981b, and Morrison, 1980). The mafic rocks of the Adlavik Suite are richer in  $K_2O$  than all common modern basalt types, but are less potassic than shoshonitic basalts. The high Cr, Rb, Sr and Ba content of the Adlavik Suite, however, corresponds well to shoshonites. The latter are potassic basalts and andesites that occur in "mature" (i.e. long-lived or distal to trench axis) portions of island-arc or continental volcanic arcs (e.g. Morrison, 1980).

Scottish appinites analyzed by Fowler (1988) have much greater enrichment in  $K_2O$ , Rb, La, Ce, Sr, Ba and Zr than typical Adlavik Suite gabbro or diorite. There is, however, a reasonable correspondence to appinites analyzed by Wright and Bowes (1979), although the Adlavik Suite has lower  $K_2O$ .

Fowler (1988) has proposed that Scottish appinites are plutonic equivalents of shoshonitic magmas. The Adlavik Suite is closer in composition to shoshonite than any other basalt type, and thus probably also represents a "shoshonitic pluton" in general terms. Morrison (1980) points out that there is complete gradation between high-K calc-alkaline volcanic rocks and shoshonites. The Adlavik Suite is obviously at the other end of the spectrum from the compositionally extreme appinites of Fowler (1988).

#### **Evolution of Labradorian Siliceous Granitoid Rocks**

Labradorian siliceous granitoid units are a metaluminous to peraluminous association that has low levels of fluorine, HFS elements and REE. In these

respects, they resemble some of the minor syn-tectonic Makkovikian granitoids, e.g. the Brumwater and Manak Island units (Chapter 3), but are distinct from most other Makkovikian units (Table 5.4).

**Monkey Hill Intrusive Suite and Similar Rocks** : The Monkey Hill suite shows great scatter in LFS element abundances over a narrow range of major element compositions. Intense depletion of a wide range of elements is shown by the mineralized Round Pond Granite (Table 5.2, see also MacDougall, 1988). MacDougall (1988) suggests that this is a function of hydrothermal alteration associated with mineralization; the scatter of data for unmineralized plutons (e.g. the main body) suggests that it may have affected these to a lesser extent.

Several characteristics of this suite are enigmatic. It attained fairly high levels in the crust, as demonstrated by associated tuffisite breccias and mineralized veins. MacDougall (1988) argued that these magmas were F-enriched, but that volatiles were mostly lost to hydrothermal fluids (c.f. Bailey, 1977). The regional geochemistry of the Monkey Hill Suite suggests that this is unlikely, as unmineralized plutons show similarly low F contents. Also, experimental studies indicate that F is preferentially associated with the silicate magma, and is not strongly partitioned into fluids (Dingwell, 1988). For example, the Cape Strawberry Granite (also associated with volatile loss and mineralization), locally retained up to 5000 ppm fluorine.

Low REE and HFS element levels in these granites probably indicate early crystallization of accessory minerals or presence of such phases in the source regions of partial melting. Hydrothermal depletion of REE was

suggested by MacDougall (1988) for the Round Pond Granite, and linked to high REE contents in associated veins. However, as in the case of fluorine, there is little evidence of REE enrichment in any Monkey Hill Suite granites. It is more likely that these granitoid magmas had low F, HFS element and REE abundances throughout evolution, and not simply as a consequence of late hydrothermal activity and mineralization. This suggests in turn radically different origins from the metaluminous - peralkaline Makkovikian granitoid magmas.

*Otter Lake - Walker Lake Granitoid* : This unit lacks the LFS element scatter evident in the Monkey Hill Suite, and trace element trends are consistent with removal of both plagioclase and K-feldspar, as indicated by phenocrysts of both. Low HFS and REE values may indicate early stabilization and removal of sphene and/or zircon. However, interstitial sphene (5.1.5) argues against early removal of this particular phase. Lack of HFS and REE enrichment in these rocks may, as outlined above, therefore reflect low levels of these elements from the outset, as a function of the source(s) and generative process(es).

## CHAPTER SIX

### UNCLASSIFIED PLUTONIC ROCKS

---

#### Chapter Abstract

Unclassified plutonic rocks comprise four largely undeformed units within the Makkovik Province, and an extensive belt of strongly foliated granitoid gneisses within the Grenville Province, south of the Benedict Fault zone.

The Freshsteak and Noarse Lake Granitoids are lithologically similar, hornblende-biotite quartz monzonite to monzogranite units that probably represent an originally continuous pluton that was disrupted by dextral movements along the Adlavi Brook fault zone. They both show petrographic and geochemical similarities to the syn-tectonic Makkovikian Long Island Quartz Monzonite.

The Stag Bay Granitoid is a compositionally variable, porphyritic to megacrystic, biotite-hornblende granodiorite to granite unit. In terms of field appearance and petrography, it resembles the Labradorian Otter Lake - Walker Lake Granitoid.

The Jeanette Bay Quartz Syenite and Thunder Mountain Syenite are minor units that show no obvious similarity to other Makkovikian or Labradorian units and, in geochemical terms, could belong to either assemblage. The former was previously grouped with the Mount Benedict Intrusive Suite, but it shows much less incompatible element enrichment.

Granitoid gneisses predominate south of the Benedict Fault system, and probably represent reworked equivalents of TLGB granitoids in the north. The Benedict Fault is a composite zone of intense deformation and mylonitization that dips steeply to the south. The gneisses form a composite unit, representing a range of protolith compositions in variable states of deformation. Locally, they appear to be strongly deformed equivalents of rocks that occur immediately to the north of the fault zone. Fine-grained, variably banded, muscovite-bearing granitoid gneisses that occur south of the fault only are probably strongly mylonitized rock types. The bulk major element compositional spectrum of the gneisses resembles that of the Makkovikian assemblage, but transitional peralkaline compositions are absent.

A Rb-Sr isochron obtained late in this study indicates a Makkovikian age of  $1798 \pm 48$  Ma for the Freshsteak Granitoid. Preliminary (discordant) U-Pb zircon data (Krogh et al., in prep.) suggest that the Stag Bay Granitoid is probably also of Makkovikian age.

## Introduction

This association comprises four largely undeformed units within the Makkovik Province, and a large area of granitoid gneisses within the Grenville Province south of the Benedict Fault zone. In the case of one unit (Freshsteak Granitoid), Rb-Sr isotopic data acquired late in thesis preparation indicate a Makkovikian age of ca. 1800 Ma. Locations and boundaries of unclassified units are indicated in Figure 6.1. Key field and petrographic features of these units are summarized in Table 6.1.

### 6.1 GEOLOGY and PETROLOGY

#### 6.1.1 Freshsteak and Noarse Lake Granitoids

These two units are closely similar in lithology, and are interpreted to be portions of an originally continuous pluton, that has been displaced dextrally by the Adlavik Brook fault zone (Figure 6.1). The northern area (Freshsteak Granitoid) is a new subdivision of unit 27 (undivided granitoid rocks) of Gower et al.(1982). The southern area (Noarse Lake Granitoid) is broadly equivalent to Unit 13 of Bailey (1979), grouped also by Gower et al.(1982) in their unit 27. Both areas are dominated by brown to grey medium-grained, plagioclase porphyritic, melanocratic quartz monzonite, granodiorite and monzogranite (Table 6.1; Plate 6.1).

The full areal extent of the Noarse Lake Granitoid is unclear, as a large area to its east is obscured by glacial drift. Matching plutonic units and the Upper Aillik Group

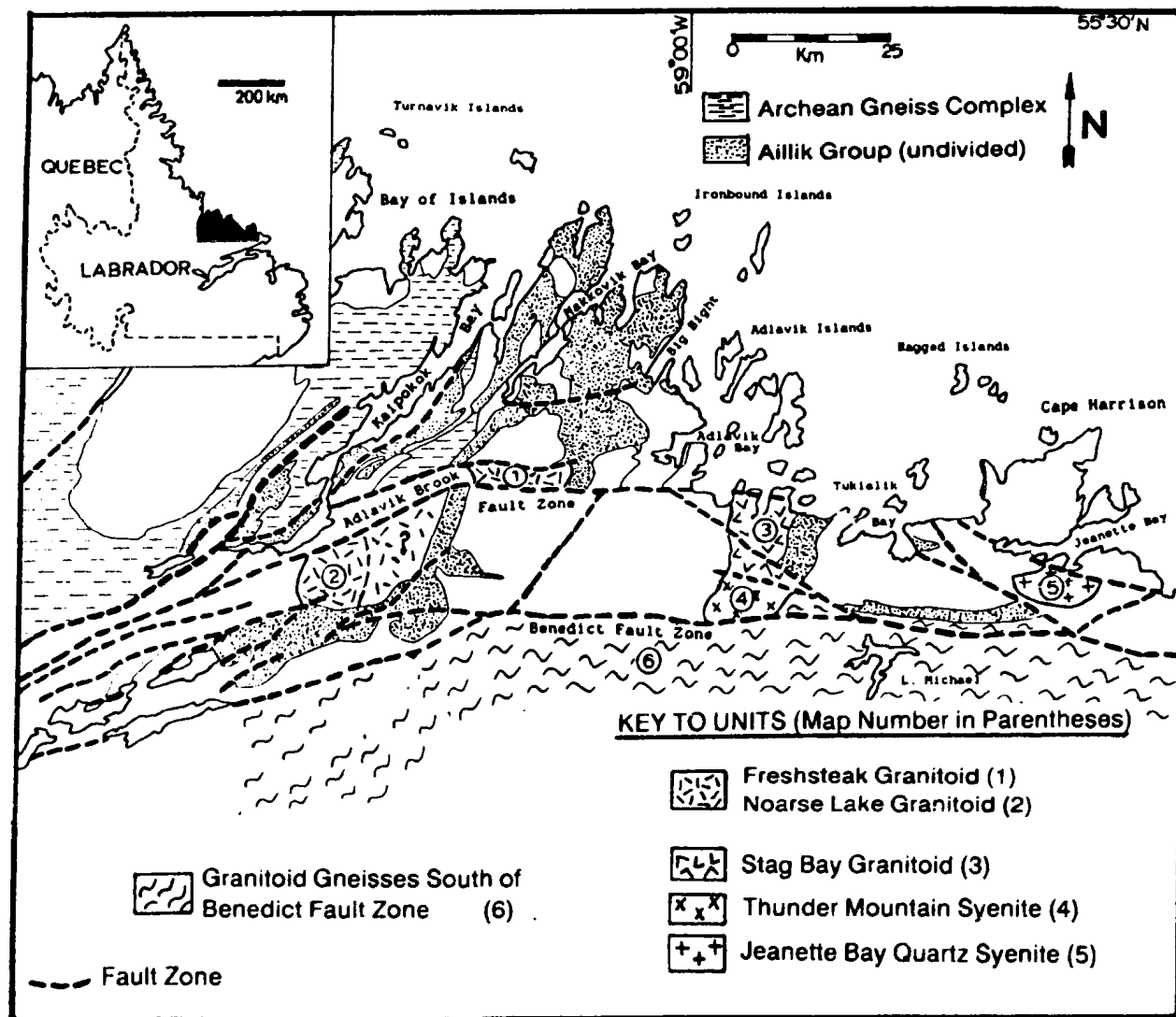


Figure 6.1. Summary map illustrating the distribution and extent of unclassified plutonic units.



Table 6.1. Key features of unclassified plutonic units.

Map Unit	Suite/Unit Age	General Characteristics	Textural Characteristics
60.0	Freshsteak Granitoid 1798 +/- 48 Ma [ Rb-Sr WR ] (this study)	Grey to green or brown, variably Plag-porphyritic, melanocratic quartz monzonite, granodiorite and monzogranite. Generally massive but slightly recrystallized, and locally foliated.	Generally medium-grained, with small, equant Plag phenocrysts up to 1 cm diameter. Locally K-feldspar porphyritic. Local foliations are defined by alignment of mafic silicates. Interstitial quartz in massive variants. Interstitial Quartz - K-feldspar graphic intergrowths in places.
61.0	Moarse Lake Granitoid	Similar to the least deformed variants of Long Island Quartz Monzonite.	
62.0	Stag Bay Granitoid 1712 +/- 24 Ma [ Rb-Sr WR ] (this study)	Grey to pink or buff, porphyritic to seriate granodiorite, monzogranite, granite and local alkali-feldspar granite. Northern part of unit is generally massive; locally foliated or sheared in the south.	Generally medium to coarse grained, commonly with phenocrysts of both Plag and K-fsp; K-fsp phenocrysts up to 5 cm diameter. Texture locally seriate or megacrystic. Groundmass equigranular to seriate. Cataclastic variants in the south are locally augen-textured.
63.0	Jeanette Bay Quartz Syenite	Pink to grey, variably K-fsp porphyritic, homogeneous quartz syenite and granite. Generally massive, but locally has sheared appearance.	Generally coarse-grained, with phenocrysts of K-fsp and Plag in most samples (K-fsp > Plag). Locally shows pseudorapakivi textures, rarely true rapakivi textures.
64.0	Thunder Mountain Syenite	Grey to buff or pink, K-feldspar porphyritic, monzonite, syenite, quartz syenite to local granite. Commonly shows interstitial blue quartz. Very fresh and massive.	Coarse to very coarse grained, with large (up to 5 cm) K-fsp phenocrysts. Smaller Plag phenocrysts occur locally. Slightly recrystallized, but not foliated.
66.0	Granitoid Gneisses South of the Benedict Fault Zone	Highly variable assemblage of foliated granitoid rocks, granitoid gneisses, and banded, mylonitic rocks. The most common rock types are augen gneisses with cataclastic textures, probably derivatives of K-fsp porphyritic or megacrystic granites.	Commonly medium to coarse grained, strongly foliated rocks. K-fsp and lesser Plag augen form deformed phenocrysts; relict pseudorapakivi textures occur locally in area south of Big River Granite. Fine-grained, banded variants have grey and pink layers, but do not appear migmatized.

Table 6.1 (continued).

Key Field Relationships	Mineralogy	Petrography
<p>Contact relations with surrounding units unknown. Presumed to intrude adjacent foliated syn-tectonic Makkovikian granitoids. Unit is disrupted by Adlavik Brook Fault zone.</p> <p>Freshsteak and Moarse Lake bodies are probably displaced portions of a single pluton.</p>	<p>Quartz (10-30%, generally &lt; 20%)</p> <p>K-fsp (Mi, perthitic, 30-50%)</p> <p>Plag (An25-40; 30-50%)</p> <p>Hb + Bi (5-20% total, subequal)</p> <p>Cpx (relict)</p> <p>Accessory Sph, Ap, lesser Zr, All</p>	<p>Igneous textures generally well-preserved. Plag phenocrysts zoned and have saussuritized cores with clear sodic rims. Graphic Qt - K-fsp intergrowths occur locally, Qt is commonly interstitial. Relict Cpx rimmed by Hb. Hb locally poikilitic.</p>
<p>Contact relations mostly unknown. Northern part of unit is cut by Feldspar-porphyry dyke that resembles the Dog Island Granite.</p> <p>Southern part of unit is cut by several faults and mylonitic zones.</p>	<p>Quartz (15-35%)</p> <p>K-fsp (Mi, 25-65%)</p> <p>Plag (saussuritized, 15-50%)</p> <p>Hb (0-5%)</p> <p>Bi (green, 5-10%)</p> <p>Accessory Sph, Ap, Zr, All</p> <p>Ep + Chl in foliated variants</p>	<p>Quartz variably strained, locally interstitial. Plag phenocrysts are subhedral, strongly saussuritized and commonly zoned. Mi is coarse patch perthite. Bi (+/- Hb) forms aggregates or clots, with variable Sph + Ep.</p>
<p>Contact relationships unknown. Previously considered to be related to syenites of Mount Benedict Suite, which adjoin it. However, geochemical data suggests that it is distinct.</p>	<p>Quartz (10-20%)</p> <p>K-Fsp (Mi, 50-70%)</p> <p>Plag (10-30%)</p> <p>Hb + Bi (5-15%, subequal)</p> <p>Cpx (relict)</p> <p>Accessory Sph, All, Zr</p> <p>Ep + Chl (secondary)</p>	<p>Cores of Plag phenocrysts are saussuritized, locally zoned. Groundmass consists of Plag + K-fsp + Qt. In many samples, mafic minerals are altered to Ep + Chl.</p>
<p>Northern and southern contacts are inferred fault zones, other contact relations unknown.</p>	<p>Quartz (interstitial, 10-20%)</p> <p>K-fsp (Mi, 50-75%)</p> <p>Plag (&gt; An30, 5-30%)</p> <p>Hb + Bi (5-12% total, Hb &gt; Bi)</p> <p>Cpx (relict)</p> <p>Accessory Sph, Ap, Zr.</p>	<p>Quartz slightly recrystallized. Mi phenocrysts have relict simple twinning, originally orthoclase? Cpx is locally green, resembles Ae-augite, but unit is not peralkaline.</p>
<p>Northern boundary is Benedict Fault zone, a 1 km wide zone of intense deformation, local mylonitization. Several East-trending structures in the granitoid gneisses are defined by mylonitic zones. Fine-grained, banded gneisses are interpreted as mylonitized granitoids.</p>	<p>Generally leucocratic, with 80-95% total Qt + Fsp. Mineral proportions variable; most are K-fsp rich siliceous granitoids, but syenitic gneisses occur locally.</p> <p>Most common mafic minerals are green Hb and brown Bi, present as fine-grained aggregates defining foliations. Cpx very rare, Chl +/- Ms present locally. Gnt very rare.</p>	<p>Very strong recrystallization, with Qt + Fsp forming polygonal or (more commonly) blastomylonitic to ribboned aggregates. Augen locally preserve perthitic texture, but commonly polygonal aggregates. Microcrystalline mylonitic zones parallel to foliation, and wrapping around Fsp augen.</p>

after removal of dextral displacement along the Adlaviik Brook fault zone suggests that the Noarse Lake granitoid may underly much of this unexposed zone. Contact relationships of both units are unknown. A Rb-Sr isochron from the Freshsteak Granitoid indicates an age of  $1798 \pm 48$  Ma (Chapter 8), suggesting that this is a Makkovikian intrusion of probable post-tectonic affinity \*.

Both units are predominantly medium-grained and melanocratic, and contain small plagioclase phenocrysts (up to 1 cm diameter), commonly with zoned and/or saussuritized cores. Groundmass quartz and feldspar is variably recrystallized, but graphic quartz/K-feldspar intergrowths or angular interstitial quartz grains are preserved in many areas. Slight foliations, of variable orientation, are present close to the trace of the Adlaviik Brook fault zone; the Noarse Lake body shows generally more intense recrystallization than the Freshsteak Granitoid.

Field appearance and petrographic characteristics of these units are similar to massive and weakly deformed examples of the Long Island Quartz Monzonite. The Rb-Sr age obtained for the Freshsteak unit (Chapter 8) is similar to K-Ar and U-Pb ages from the Long Island unit (Gandhi et al., 1969; 1988).

#### 6.1.2 Stag Bay Granitoid

This unit corresponds to Unit 19 of Gower (1981), and to a portion of Unit 26 of Gower et al. (1982). Gower (1981) grouped the unit with megacrystic granodiorite

---

\* NOTE : Preliminary Rb-Sr data were inconclusive, and additional data did not become available until after text and illustrations for Chapter 4 were finalized. The descriptive material on this unit has thus been retained in this chapter.

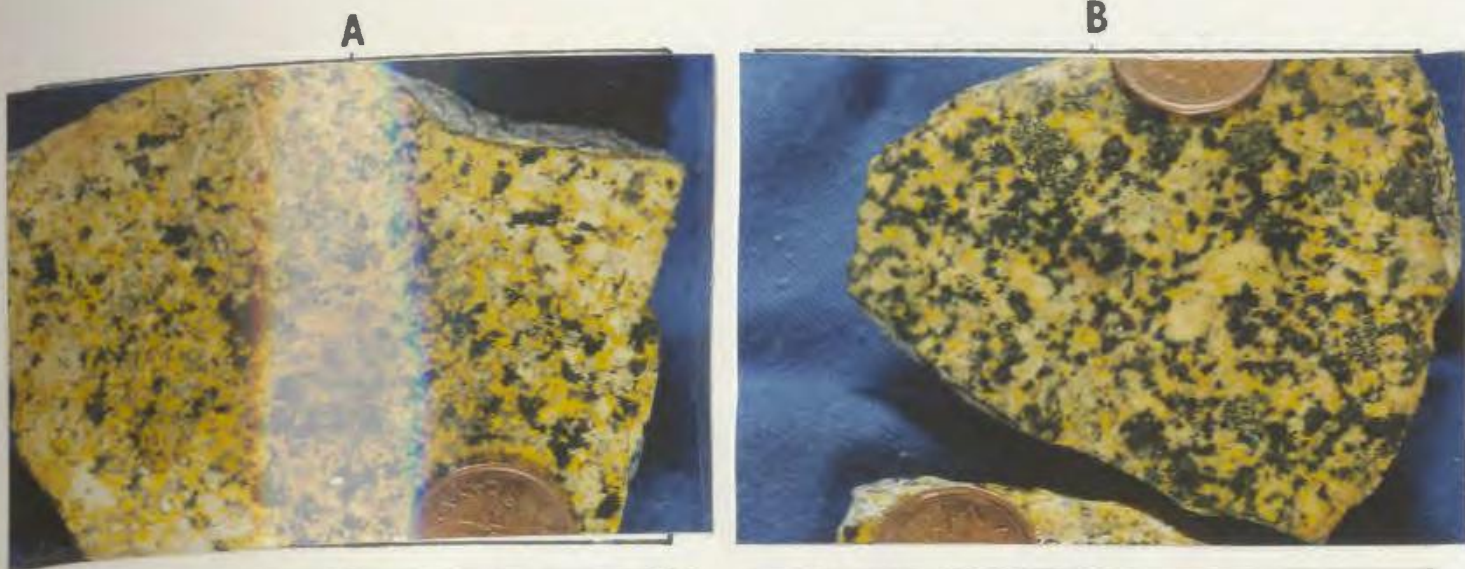


Plate 6.1. Features of the Freshsteak and Noarse Lake Granitoids. (a) Freshsteak Granitoid. (b) Noarse Lake Granitoid. Note that these units are locally more foliated and recrystallized than these slabs. Slabs stained for K-feldspar.



Plate 6.2. Features of the Stag Bay Granitoid. (a) and (b) Typical porphyritic granodiorite to monzogranite, Stag Bay. Note weak foliation in (b). Note that this unit is variable in composition and texture. Slabs stained for K-feldspar.

exposed near Deus Cape, and with similar megacrystic granitoids east of the study area. The unit includes a variety of rock types, the most abundant of which is a seriate to two-feldspar porphyritic granodiorite, monzogranite or granite (Table 6.1; Plate 6.2; see also description of Gower, 1981).

Contact relationships of the unit are unknown. At Stag Bay, it is cut by a feldspar-porphyry dyke which may be related to the nearby Dog Islands Granite, but might also be associated with nearby subvolcanic porphyry units assigned to the Upper Aillik Group (Jagged Edge assemblage; Chapter 7). Rb-Sr data (5 point only) yielded an ambiguous  $1714 \pm 44$  Ma isochron (Chapter 8). U-Pb zircon dating is in progress.\*.

K-feldspar and plagioclase are commonly both present as phenocryst phases; the former are generally larger, ranging up to 5 cm in size. In the north the unit is generally massive, but the southern part is locally foliated and/or cataclastic in texture. This area is cut by several faults that link the Adlavik Brook and Benedict fault zones, and foliation directions are highly variable. Gower (1981) indicates N-trending foliations in two areas near the coast that were not visited during this study. Of the units described in preceding chapters, this unit shows the closest resemblance to the Otter Lake - Walker Lake Granitoid, which is also two-feldspar porphyritic in most areas. The distance between the units suggests, however, that a direct connection is unlikely.

---

\* NOTE : Preliminary U-Pb zircon data (Krogh et al., in prep.) are slightly discordant, but appear colinear with other post-tectonic Makkovikian units, and indicate a similar age of 1790 - 1805 Ma. The Stag Bay unit is therefore almost certainly a Makkovikian intrusion.

#### 6.1.3 Jeanette Bay Quartz Syenite

This small body is located in the Benedict Mountains south of Jeanette Bay. It corresponds to unit 22 of Gower (1981), and was considered by him to be related to the rocks here termed Mount Benedict Intrusive Suite (unit 21 of Gower, 1981). However, it mostly lacks the distinctive textural characteristics of these rocks, and is geochemically distinct (see 6.2). It is dominated by pink to grey, coarse-grained, variably K-feldspar porphyritic quartz syenite to granite (Table 6.1; Plate 6.3). Contact relationships are unknown. It is commonly massive, but locally appears slightly foliated and/or sheared. Microcline is the most common phenocryst phase. Plagioclase cores in sporadic pseudorapakivi phenocrysts are commonly zoned and saussuritized. In many samples, the mafic mineral assemblage has been retrogressed to chlorite - epidote - sphene aggregates. The groundmass is plagioclase-rich compared to the K-feldspar and quartz groundmass typical of the adjacent Mount Benedict Suite, a contrast previously noted by Gower (1981). In general, it appears more recrystallized than the normally pristine rocks of the Mount Benedict Intrusive Suite.

#### 6.1.4 Thunder Mountain Syenite

This small body occurs southwest of Stag Bay, between the Benedict fault system and another northwest-trending fault mapped by Gower (1981). It is equivalent to a portion of unit 26 of Gower et al. (1982). It consists mostly of coarse grained, massive, K-feldspar porphyritic, hornblende monzonite, syenite, quartz syenite and granite (Table 6.1; Plate 6.4). It is in (inferred) fault contact



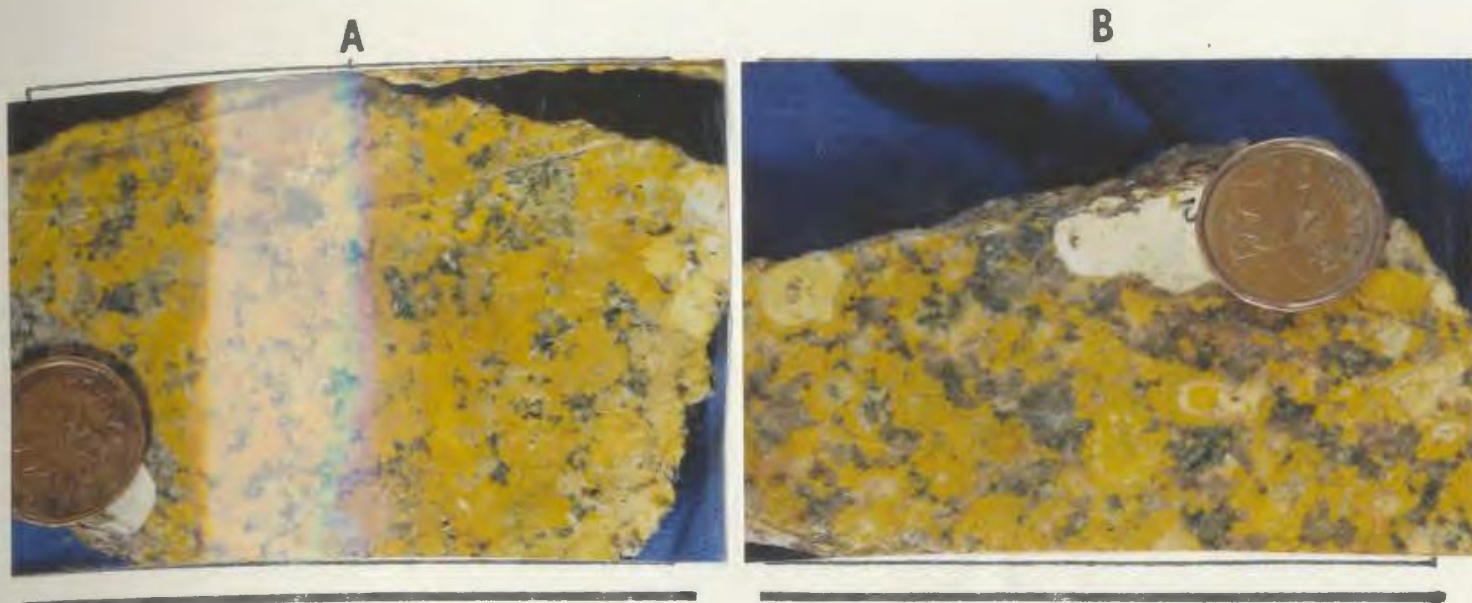


Plate 6.3. Features of the Jeanette Bay Quartz Syenite. (a) and (b) Typical examples. Slabs stained for K-feldspar.

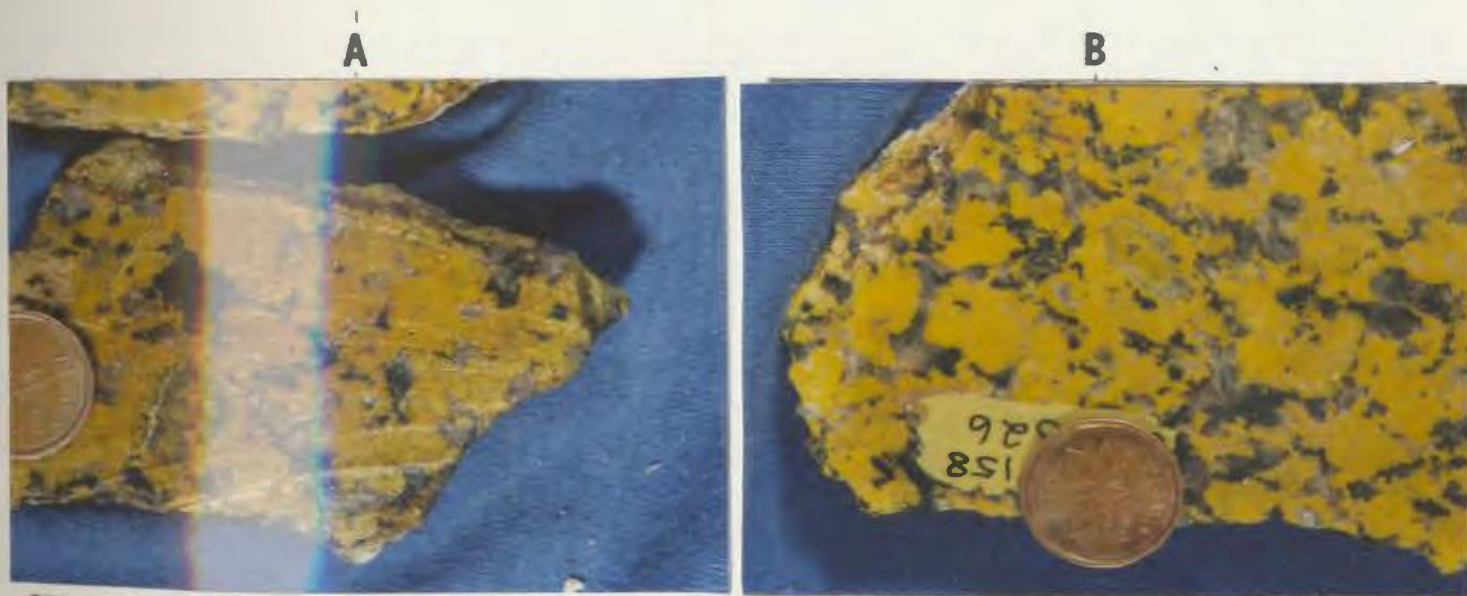


Plate 6.4. Features of the Thunder Mountain Syenite. (a) and (b) Typical examples. Slabs stained for K-feldspar.

with the Stag Bay Granitoid and part of the Mount Benedict Intrusive Suite to the north, and with granitoid gneisses of the Grenville Province to the south. Eastern and western contact relations are unknown. In most areas, it is massive and undeformed, and is characterized by distinctive interstitial blue quartz grains. Large (up to 5 cm diameter) microcline phenocrysts have both simple and polysynthetic twinning, possibly indicating original orthoclase phenocrysts. Zoned plagioclase phenocrysts are locally present. Green clinopyroxene is a local relict phase, and is altered to hornblende and a red-brown phase. The pyroxene resembles aegirine-augite, but is generally non-pleochroic.

#### 6.1.5 Granitoid Gneisses South Of The Benedict Fault Zone

**General Characteristics** : South of the Benedict fault zone (Figure 6.1), all units exhibit moderate to intense east-trending foliations attributed to Grenvillian deformation, and many are gneissic or banded in texture. These rocks have not been studied in detail in this project, and are thus grouped as a single map unit. This composite unit clearly consists of a variety of rock types in highly variable states of deformation. All areas south of the Benedict Fault zone are poorly exposed (excluding river courses), and the most prominent outcrops are invariably Michael Gabbro intrusions. Characteristics and relationships of different granitoid gneiss variants in this part of the Grenville Province are thus poorly known.

**Field Relations and Lithology** : The northern boundary of the gneissic terrane is the Benedict Fault zone itself, although some areas north of the generally accepted



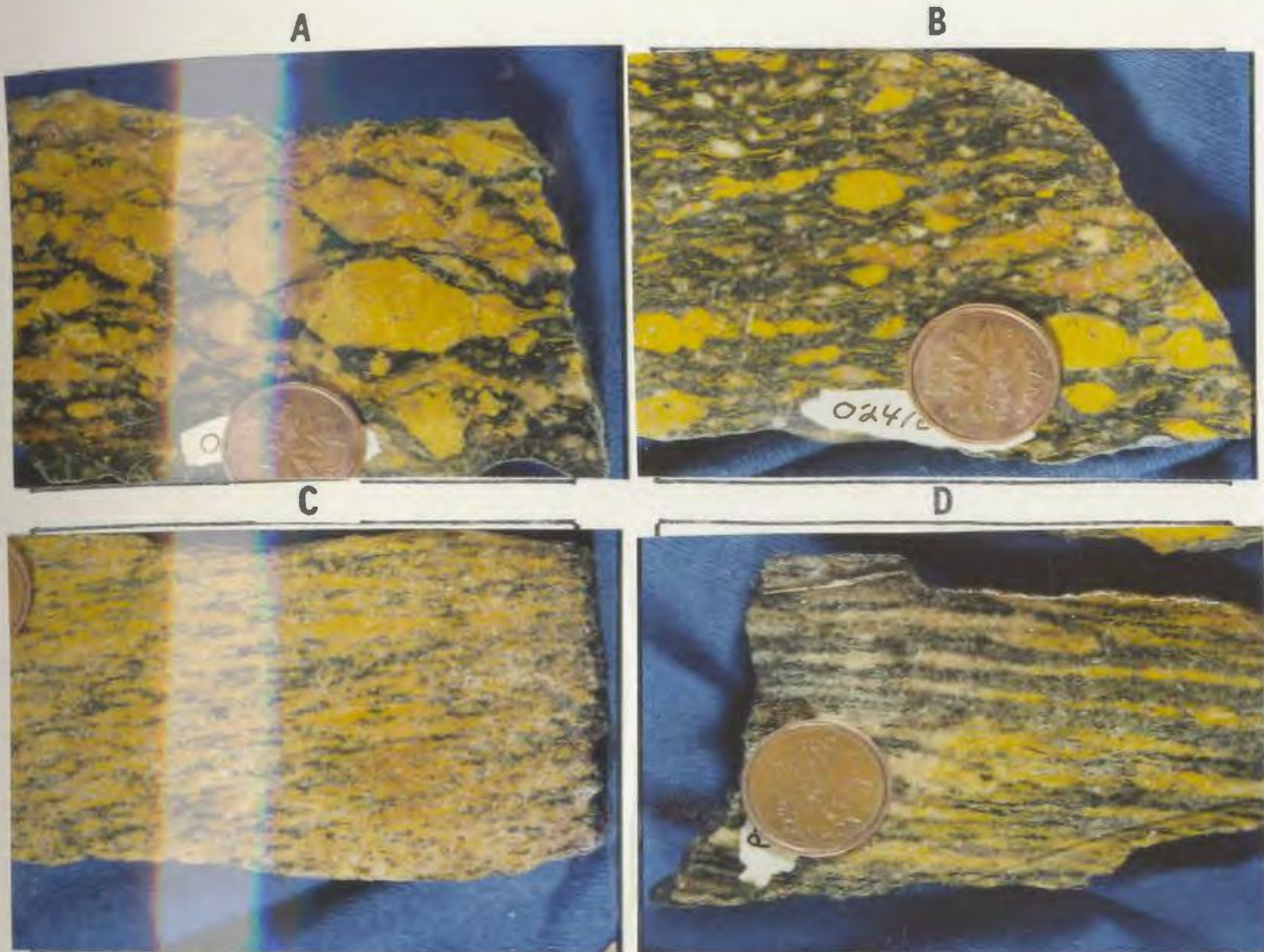


Plate 6.5. Features of the granitoid gneisses exposed south of the Benedict fault zone. (a) to (d) Typical examples, showing development of augen textures, and banded, mylonitic appearance resulting from ultradeformation. Slabs stained for K-feldspar.

position of this fault exhibit deformation of equivalent intensity, and are included in the gneiss unit (Figure 6.1). The Benedict fault is a composite zone that cannot be represented adequately by a single line on a map. In the west of the study area, it is described by Bailey (1979) as a broad zone of mylonitization displaying a subvertical lineation. The zone is well exposed in Big River, where it is a composite feature consisting of a broad zone of intense deformation (up to 1 km in width) within which occur a number of individual mylonite zones, dipping at  $40-70^{\circ}$  S, with steeply plunging lineations upon foliation surfaces. In the Benedict Mountains, Gower (1981) described it as a south-dipping reverse fault displaying evidence also of dextral motion. The contrast in deformation state across the fault is extreme in this area, and it appears to be a narrower, more tightly focussed structure than in the west (see below).

South of the main fault zone, a number of discontinuous cataclastic and mylonitic zones occur within the granitoid gneisses. Fine-grained, strongly foliated granitoid gneisses form concordant layers within coarser foliated granitoids; these may be original textural variants, but more likely represent mylonitic zones developed on a hand-sample or outcrop scale. On a regional scale, these are interpreted to have an anastomosing pattern, similar to that seen in many hand specimens that have relict porphyritic textures (Plate 6.5).

The granitoid gneisses appear (at least locally) to resemble adjacent rock types north of the Benedict Fault zone. For example, in the area south of the Big River Granite, they comprise pink or buff, coarse grained, cataclastic to mylonitic, augen-textured rocks that have a composition approximating biotite-hornblende granite or

alkali-feldspar granite. Vestiges of pseudorapakivi texture are present in the least deformed examples, and they contain blue-green hornblende typical of the Big River Granite. A similar relationship was noted by Gower (1981) in the eastern Benedict Mountains, where megacrystic granitoids and augen gneisses occur north and south of the fault respectively. South of the main Benedict Mountains massif, the contrast in deformation state across the fault is extreme, and occurs principally across faults that bound a narrow metavolcanic enclave (Figure 6.2). The rocks south of the fault zone in this area comprise a heterogeneous mixture of two contrasting rock types. Coarse-grained biotite-hornblende augen granitoids display relict K-feldspar porphyritic textures, and characteristically contain blue-green hornblende. The mafic assemblage is variably retrogressed to sphene and epidote. These rocks are interspersed with fine to medium grained, equigranular to locally banded, leucocratic, granitoid gneisses containing minor biotite and muscovite. These two variants do not necessarily represent discrete rock types; Gower (1981) suggests that they may represent variable deformation and metamorphism of a common protolith, although the presence of muscovite implies some compositional contrasts. Gower (1981) distinguished a strongly deformed augen gneiss of monzonitic to syenitic composition close to the fault zone, and also two areas of supracrustal rocks, which he considered to be of volcaniclastic origin.

## 6.2 DESCRIPTIVE GEOCHEMISTRY

Unclassified plutonic rocks are represented by 221 samples, of which 211 are regional samples collected on a 2km grid spacing. Over 60% of this population represents the granitoid gneiss unit.

### 6.2.1 General Geochemistry

#### Summary of Numerical Data

Table 6.2 lists mean compositions of unclassified plutonic units, and also mean compositions of selected Makkovikian and Labradorian plutonic units that have similar  $\text{SiO}_2$  contents.

Mean compositions of the Freshsteak and Noarse Lake units are similar, supporting their interpretation as disrupted components of an originally continuous pluton. However, the Noarse Lake unit has a lower mean silica content, and a slightly less evolved trace element pattern. Both units are similar in composition to the Long Island Quartz Monzonite. The Thunder Mountain Syenite has a similar  $\text{SiO}_2$  content to these rocks, but is poorer in  $\text{TiO}_2$  and  $\text{P}_2\text{O}_5$ .

The Stag Bay and Jeanette Bay units have similar  $\text{SiO}_2$  contents (ca. 68%), but are otherwise dissimilar. The latter is richer in  $\text{K}_2\text{O}$  and Rb, and depleted in Sr relative to Stag Bay. However, the Jeanette Bay unit has lower levels of Rb, U, and Th than rocks of comparable  $\text{SiO}_2$  content in the Mount Benedict Intrusive Suite. Note

Table 6.2 . Average compositions of unclassified plutonic rocks, subdivided by principal units, and Makkovikian and Labradorian units of similar SiO<sub>2</sub> content.

UNIT	60		61		62		63		64		66	
n1	17		10		21		12		13		146	
n2	4		1		1		0		0		0	
(Wt%)	Mean	S.D.	Mean	S.D.	Mean	S.D.	Mean	S.D.	Mean	S.D.	Mean	S.D.
SiO <sub>2</sub>	63.66	5.47	60.44	4.30	68.31	4.68	67.93	4.62	64.37	8.04	68.75	5.54
TiO <sub>2</sub>	0.87	0.39	1.05	0.35	0.36	0.12	0.47	0.19	0.55	0.29	0.48	0.35
Al <sub>2</sub> O <sub>3</sub>	15.48	1.57	16.28	0.67	15.52	1.47	14.99	1.58	16.44	2.21	14.57	1.61
Fe <sub>2</sub> O <sub>3</sub>	2.26	0.67	2.12	0.74	1.19	0.83	1.31	0.62	1.41	0.71	1.21	0.63
FeO	3.34	1.33	4.46	1.54	1.52	0.69	1.48	0.71	2.51	1.72	2.03	1.38
MnO	0.12	0.04	0.14	0.04	0.06	0.02	0.06	0.02	0.09	0.05	0.07	0.04
MgO	1.37	0.91	1.88	0.99	0.77	0.52	0.64	0.33	1.86	3.16	0.72	0.70
CaO	3.19	1.62	3.98	1.43	2.20	1.40	1.79	0.96	3.14	2.89	1.81	1.20
Na <sub>2</sub> O	4.29	0.41	4.44	0.34	4.51	0.43	4.18	0.42	4.49	0.95	4.14	0.50
K <sub>2</sub> O	4.19	1.08	3.88	1.16	4.17	0.93	5.35	0.83	4.14	1.76	4.85	0.98
P <sub>2</sub> O <sub>5</sub>	0.30	0.20	0.32	0.10	0.12	0.08	0.12	0.06	0.15	0.09	0.15	0.14
LOI	0.58	0.26	0.53	0.28	0.80	0.32	1.00	0.55	0.46	0.17	0.55	0.20
TOTAL	99.65		99.52		99.53		99.32		99.61		99.33	
(ppm)	Trace Elements											
Li	21.6	8.5	56.7	44.5	18.2	4.3	15.0	3.8	14.4	4.2	19.8	9.4
F	728.3	258.0	999.1	671.9	741.2	612.2	700.5	349.7	703.8	591.2	649.7	413.7
Sc	9.0	4.7	3.9		2.6							
V	66.9	47.0	93.2	52.6	28.3	26.8	32.7	11.5	42.9	47.8	31.2	27.4
Cr	6.9	6.7	10.1	6.6	4.1	2.4	7.5	3.5	30.3	74.6	9.2	29.6
Ni	2.5	2.5	4.1	2.3	2.4	1.7	2.3	2.2	13.6	32.2	2.7	7.5
Cu	11.7	7.2	10.8	5.0	45.9	175.0	13.3	11.3	8.9	10.1	12.9	54.5
Zn	102.9	27.5	102.8	34.6	49.3	17.2	59.8	32.0	70.3	26.8	66.2	36.7
Ga	21.5	3.1	21.9	3.6	14.1	5.6	9.5	3.4	12.9	6.9	12.3	5.8
Rb	109.1	36.7	118.3	61.8	104.7	44.8	162.9	50.6	69.5	55.7	112.6	44.7
Sr	359.9	184.7	410.4	138.2	474.5	267.3	232.8	129.0	462.0	326.8	253.4	188.7
Y	49.6	22.0	35.4	6.9	24.6	19.5	31.5	9.5	22.9	16.1	32.1	14.9
Zr	307.1	156.4	221.9	103.8	254.4	149.6	322.0	126.8	340.3	455.6	338.6	162.0
Nb	16.4	7.3	10.7	3.6	12.9	9.7	15.9	5.2	11.7	10.8	15.3	7.1
Mo	4.2	1.2	4.4	1.6	3.0	1.9	5.3	5.7	3.3	1.0	3.8	2.1
Sn	2.3	1.5	1.0		2.0							
Cs	1.9	1.0	5.0		2.0							
Ba	1368.4	545.3	1906.0	685.8	987.8	406.4	819.0	189.7	1512.1	1628	907.3	637.2
La	68.5	29.4	43.5	8.0	44.9	35.8	48.6	22.5	36.2	28.6	43.8	27.4
Ce	128.4	58.8	82.9	15.4	90.1	74.8	93.6	38.7	74.9	62.2	89.6	52.4
Sm	14.0	4.1	4.3		4.6							
Yb	4.8	2.7	2.5		2.5							
Hf	11.5	3.4	5.0		13.0							
Pb	15.3	3.6	13.8	4.7	17.3	19.8	23.8	9.7	12.2	8.0	18.6	42.4
Th	5.0	5.9	2.9	2.6	10.4	17.1	13.3	7.9	4.5	8.5	7.8	7.8
U	3.2	1.6	2.8	1.0	4.3	3.4	4.0	1.1	1.5	1.9	3.6	2.6
(Wt%)	Partial CIPW norm											
Q	14.00	8.06	8.04	6.31	19.44	8.14	19.24	9.00	13.37	11.05	20.55	10.35
C	0.00	0.00	0.00	0.00	0.21	0.26	0.03	0.06	0.10	0.20	0.08	0.16
Or	24.96	6.38	23.13	6.89	24.95	5.55	32.18	5.19	24.65	10.43	28.97	5.84
Ab	36.58	3.45	37.94	2.90	38.61	3.78	35.07	2.52	38.22	8.01	35.53	4.22
An	10.74	5.53	13.16	3.92	9.36	4.97	6.35	3.53	12.33	11.13	6.72	4.24
Di	3.04	1.64	4.28	2.44	1.02	2.17	1.50	1.73	2.32	3.10	1.41	1.62
Hx	5.03	3.06	7.62	2.80	2.58	1.28	1.90	1.44	3.56	2.13	3.21	2.76
Ol	0.00	0.00	0.00	0.00	0.15	0.70	0.00	0.00	1.95	4.96	0.02	0.19
Mt	3.31	1.00	3.11	1.07	1.75	1.20	1.89	0.87	2.07	1.05	1.76	0.93
Il	1.66	0.75	2.01	0.66	0.69	0.24	0.91	0.36	1.06	0.55	0.94	0.67

KEY TO UNITS:

- 60 -- Freshsteak Granitoid      63 -- Jeanette Bay quartz syenite  
61 -- Moarse Lake Granitoid    64 -- Thunder Mountain Syenite  
62 -- Stag Bay Granitoid        66 -- Granitoid Gneisses south of Benedict Fault

n1 -- Number of analyses for all elements except those listed below

n2 -- Number of analyses for Sc, Sn, Cs, Sm, Yb and Hf

Table 6.2 (continued).

UNIT	10		20		43		44		48		30	
n1	15		57		53		67		49		79	
n2	5		12		22		39		11		13	
(Wt%)	Mean	S.D.	Mean	S.D.	Mean	S.D.	Mean	S.D.	Mean	S.D.	Mean	S.D.
SiO <sub>2</sub>	63.32	1.27	62.31	4.27	64.46	4.46	70.69	3.31	68.54	4.42	70.11	5.15
TiO <sub>2</sub>	0.88	0.06	0.78	0.29	0.61	0.24	0.30	0.18	0.44	0.20	0.39	0.22
Al <sub>2</sub> O <sub>3</sub>	15.81	0.24	16.69	1.49	16.03	0.93	14.39	1.06	14.98	1.62	14.43	1.74
Fe <sub>2</sub> O <sub>3</sub>	1.79	0.37	1.72	0.75	1.40	0.66	0.97	0.40	1.20	0.61	1.16	0.55
FeO	3.06	0.73	3.41	1.12	2.53	1.12	1.09	0.66	1.87	1.01	1.49	0.97
MnO	0.10	0.01	0.12	0.05	0.09	0.03	0.05	0.02	0.06	0.03	0.06	0.04
MgO	1.25	0.42	1.22	0.87	1.12	0.97	0.38	0.27	0.86	0.54	0.50	0.84
CaO	2.95	0.48	2.92	1.30	2.37	1.52	0.97	0.49	2.04	1.02	1.36	1.20
Na <sub>2</sub> O	4.27	0.25	4.57	0.41	4.51	0.36	4.28	0.43	3.89	0.55	4.28	0.75
K <sub>2</sub> O	4.75	0.49	5.14	1.09	5.41	0.93	5.58	0.51	4.70	0.62	5.11	1.01
P <sub>2</sub> O <sub>5</sub>	0.26	0.03	0.24	0.14	0.19	0.17	0.05	0.06	0.15	0.09	0.10	0.08
LOI	0.63	0.23	0.58	0.35	0.84	0.23	0.75	0.11	0.77	0.24	0.58	0.29
TOTAL	99.07		99.67		99.56		99.50		99.50		99.57	
(ppm)												
Li	22.7	5.7	21.0	9.7	31.0	10.4	25.3	11.0	25.7	12.5	14.8	6.2
F	860.5	212.7	928.9	436.3	1298.0	410.7	1240.5	617.4	679.1	257.1	688.5	462.5
Sc	9.6	1.7	10.5	2.1	5.8	2.1	2.9	1.7	6.8	2.4	2.4	0.9
V	74.6	19.6	55.9	37.5	50.6	40.9	23.1	13.1	44.6	30.2	21.5	17.1
Cr	5.5	3.5	7.0	9.9	14.5	16.6	6.5	3.8	6.5	7.0	4.8	13.7
Ni	2.6	1.9	3.7	4.7	4.3	5.3	1.9	1.7	2.1	3.0	2.6	7.9
Cu	9.1	3.8	13.6	9.5	18.9	16.9	10.1	8.8	9.1	18.7	6.3	6.1
Zn	74.1	8.5	86.3	23.4	60.3	19.1	39.9	14.0	46.9	21.4	54.8	42.8
Ga	18.3	1.2	20.5	2.9	11.3	4.7	8.6	2.1	12.8	4.1	15.2	5.2
Rb	126.4	24.2	121.9	47.9	233.2	81.8	315.3	81.3	140.5	38.7	127.8	51.8
Sr	327.6	39.0	329.4	166.6	308.9	191.0	126.8	108.3	277.7	154.8	160.7	151.6
Y	36.5	1.9	39.2	13.6	30.3	8.7	27.8	7.6	28.2	10.2	42.5	17.2
Zr	236.6	83.2	486.3	255.9	408.0	190.7	345.0	140.0	240.0	83.8	368.8	210.3
Nb	14.2	1.1	19.1	8.5	21.2	8.1	29.0	8.6	13.6	4.4	19.1	7.2
Mo	4.3	0.5	4.1	1.0	4.7	1.5	4.3	2.7	3.2	1.2	3.7	1.2
Sn	1.0	0.0	2.7	2.7	6.1	4.2	7.2	4.2	3.9	3.3	2.7	2.7
Cs	1.3	1.2	1.6	1.7	10.7	5.3	9.0	4.3	4.1	1.8	0.7	0.6
Ba	1424.0	116.2	1099.0	558.0	742.8	360.6	381.9	352.6	961.5	542.3	660.8	482.6
La	53.3	4.9	64.8	31.7	50.7	13.1	56.3	22.9	50.6	14.8	63.1	30.2
Ce	102.7	6.1	131.0	63.2	108.3	30.3	114.0	43.7	100.1	28.5	126.8	59.2
Sm	9.2	0.8	13.3	3.1	8.2	1.7	6.9	1.7	9.3	3.0	10.4	3.9
Yb	2.5	0.0	3.8	2.1	4.1	1.0	4.5	0.9	2.5	0.0	4.2	2.0
Hf	8.0	1.2	11.9	3.5	12.2	3.0	9.9	3.1	12.5	21.1	10.1	3.0
Pb	15.9	3.9	15.9	6.6	17.8	6.1	23.4	8.0	16.8	8.1	17.6	11.2
Th	9.2	3.0	9.1	10.7	21.6	13.6	37.5	13.8	14.8	7.3	13.0	9.6
U	4.8	0.9	3.1	1.7	6.8	3.2	10.4	4.4	4.0	2.4	4.5	2.6
(Wt%)												
Q	12.25	1.76	8.02	6.40	10.94	6.32	22.13	7.27	22.14	8.29	22.16	9.88
C	0.00	0.00	0.05	0.18	0.02	0.10	0.12	0.24	0.26	0.36	0.06	0.14
Or	28.50	2.93	31.47	4.81	32.33	5.51	33.36	3.06	28.14	3.71	30.45	6.00
Ab	36.71	2.01	38.96	3.48	38.63	3.09	36.65	3.68	33.29	4.70	36.54	6.34
An	10.08	1.50	9.37	4.48	7.58	4.35	3.30	1.78	8.95	4.23	4.97	4.19
Di	2.88	1.35	2.85	1.48	2.60	2.33	0.79	0.82	0.43	0.74	1.11	1.66
Hy	4.65	1.72	4.53	2.26	3.90	2.08	1.41	1.11	3.77	2.10	1.81	1.34
Ol	0.00	0.00	0.41	1.09	0.25	1.80	0.00	0.00	0.00	0.00	0.18	1.60
Mt	2.64	0.55	2.41	0.96	2.03	0.96	1.36	0.59	1.76	0.90	1.60	0.82
Il	1.69	0.12	1.48	0.56	1.17	0.47	0.58	0.34	0.85	0.38	0.74	0.43

KEY TO UNITS (NIS - Mumok Intrusive Suite MBIS - Mount Benedict Intrusive Suite)  
 10 -- Long Island Quartz Monzonite 48 -- Otter Lake - Walker Lake Granitoid  
 20 -- (NIS) monzonite to quartz monzonite 30 -- Big River Granite  
 43 -- (MBIS) monzonite to syenite  
 44 -- (MBIS) syenite to granite

n1 -- Number of analyses for all elements except those listed below  
 n2 -- Number of analyses for Sc, Sn, Cs, Sm, Yb and Hf

that the high Cu content of the Stag Bay unit is a function of a single anomalous sample that has over 600 ppm Cu, and is not representative of the unit as a whole.

The mean major element composition of the granitoid gneiss unit is similar to means for either Makkovikian and Labradorian plutonic assemblages. In view of the varied lithology, this average cannot be considered representative of this composite unit.

#### **Abundance and Distribution of Rock Types**

Relative proportions of IUGS rock types were calculated from normative data after Streckeisen and LeMaitre (1979), and are shown in Figure 6.2.

The Freshsteak and Noarse Lake units are generally similar, but the Noarse Lake unit contains a higher proportion of diorite and monzodiorite. The Stag Bay unit is dominated by monzogranite with subordinate granite, and the Jeanette Bay unit by granite, rather than quartz syenite. The Thunder Mountain unit is of variable composition, but is mostly quartz-poor (i.e. quartz diorite to alkali-feldspar quartz syenite).

The large sample population for granitoid gneisses has a bimodal pattern, dominated by granite to alkali-feldspar granite, but with a smaller peak at quartz monzonite to quartz syenite. This pattern resembles that shown by syn- and post-tectonic Makkovikian plutonic associations (Chapters 3 and 4).

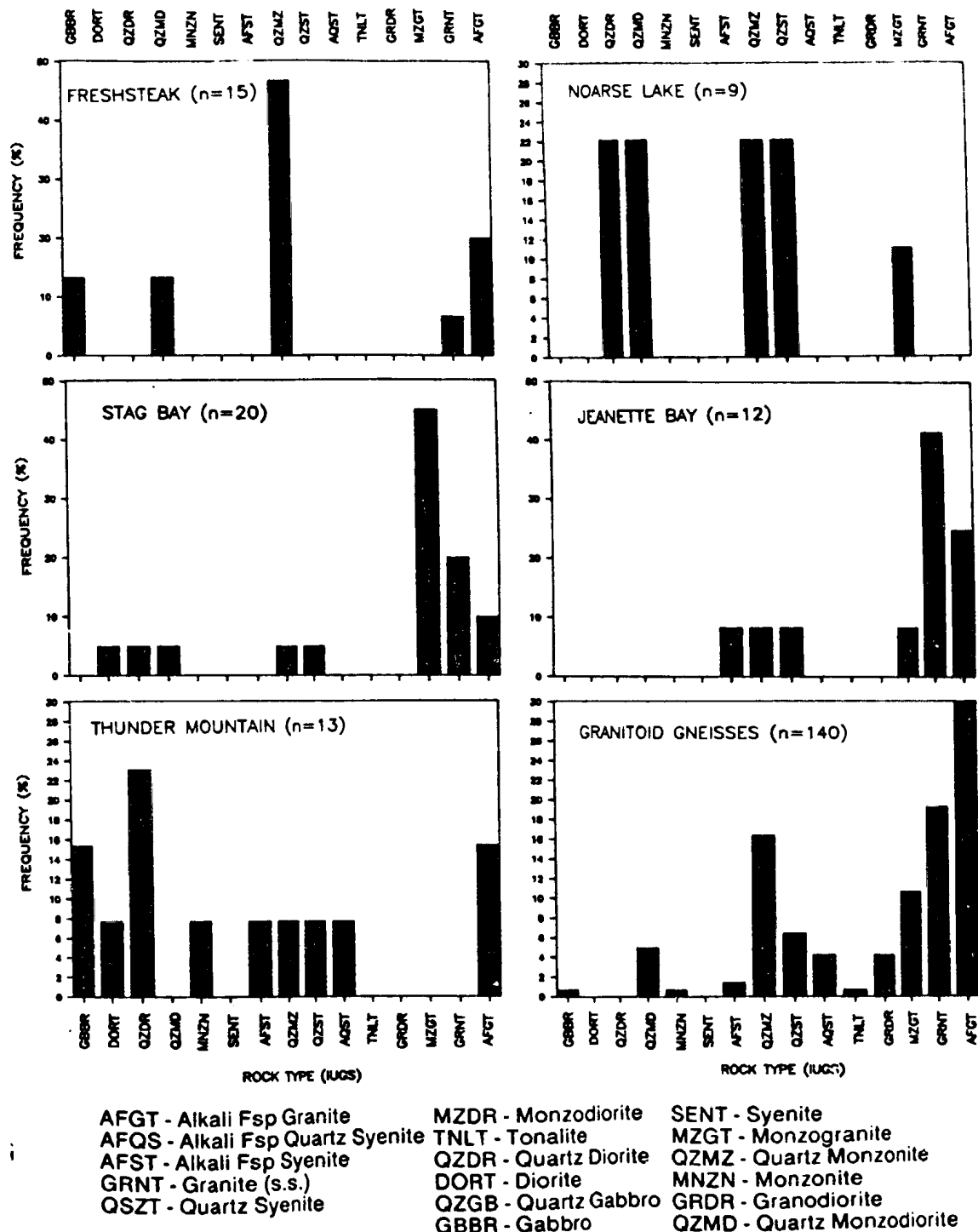


Figure 6.2 Relative abundance of IUGS rock types calculated from normative mineralogy after Streckeisen and LeMaitre (1979). Note that this is based on Barth mesonorms, not the CIPW norms listed in Table 6.2. Regional sample populations only.



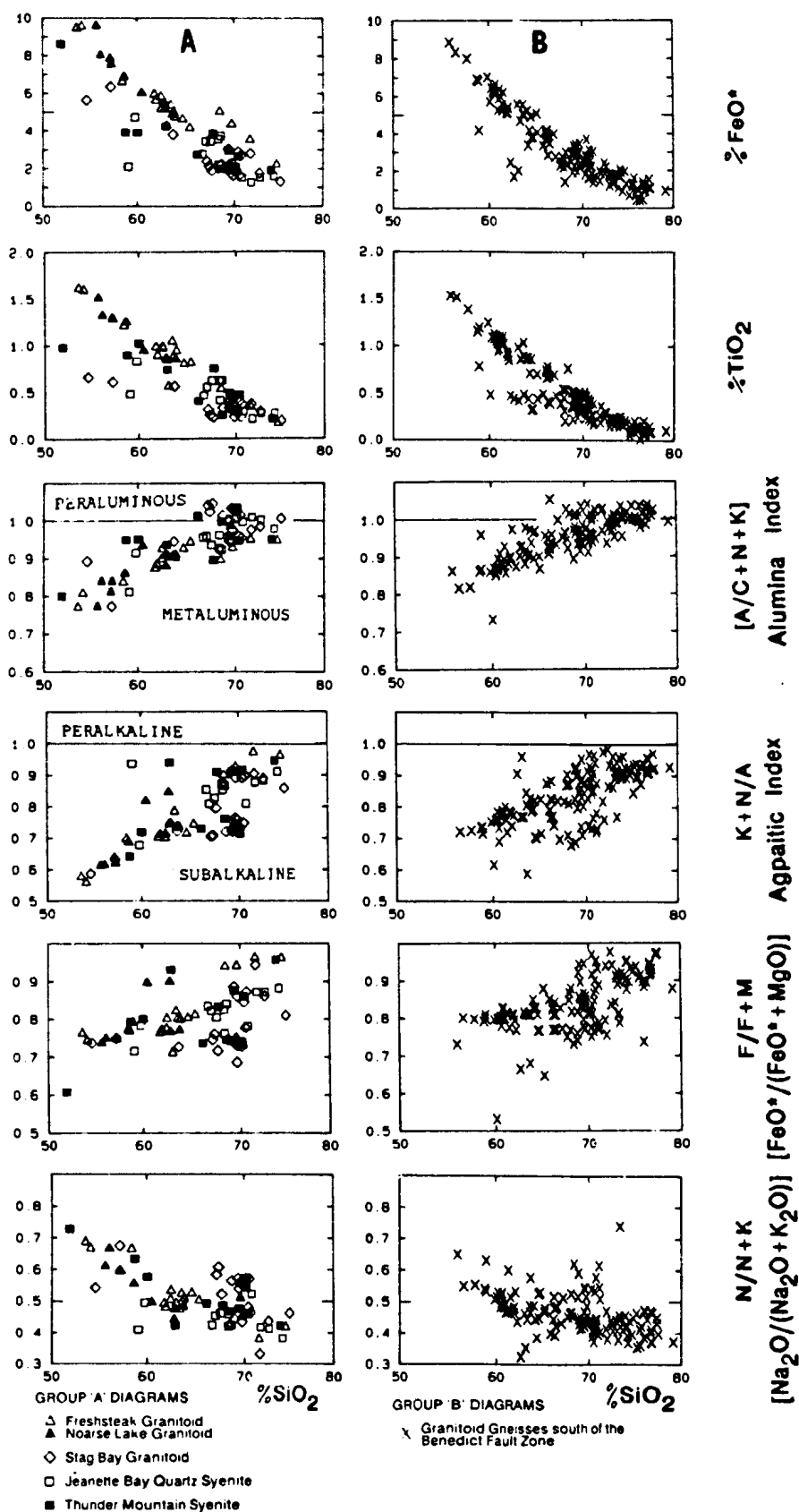


Figure 6.3. Variation of selected major elements and derived ratios in unclassified plutonic units. See text for discussion.

### 6.2.2 Geochemical Trends and Contrasts

#### Major Element Patterns

Major element patterns (Figure 6.3) follow expected trends and offer poor unit discrimination. High  $\text{TiO}_2$  (also  $\text{P}_2\text{O}_5$ ; not figured) contents below 65%  $\text{SiO}_2$  (Figure 6.3) characterize the Freshsteak and Noarse Lake units. This feature is also shown by the petrographically similar Long Island Quartz Monzonite (Table 6.2; Figure 3.3, p.76)

All units show  $\text{K+N/A}$  (agpaitic index) values below 1.0.  $\text{A/C+N+K}$  indices are greater than 1.0 in part of the Stag Bay unit, and also in a few samples from Thunder Mountain and Jeanette Bay (Figure 6.3). All other units are wholly metaluminous. Parts of the Stag Bay unit have high ( $> 0.5$ )  $\text{N/N+K}$  ratios and low  $\text{F/F+M}$  ( $< 0.8$ ) ratios above 60%  $\text{SiO}_2$ , compared to other units.

Major element patterns for the granitoid gneiss unit are similar to the overall pattern shown by discrete unclassified units (Figure 6.3). It includes no peralkaline compositions, but contains some peraluminous rocks.

#### Trace Element Patterns

Compatible OCC trace elements (e.g. V, Figure 6.4) do not discriminate between units. Rb and Th (Figure 6.4) are highest in the Jeanette Bay and Stag Bay units, consistent with their generally higher  $\text{SiO}_2$ . Sr, Ba and F (Figure 6.4) are scattered, but high Sr contents partly distinguish the Stag Bay unit. Zr, Y, Nb and Ce (Figure 6.5) provide no distinction between units, although there is some Y enrichment in the Freshsteak unit. Zn (Figure 6.5) is

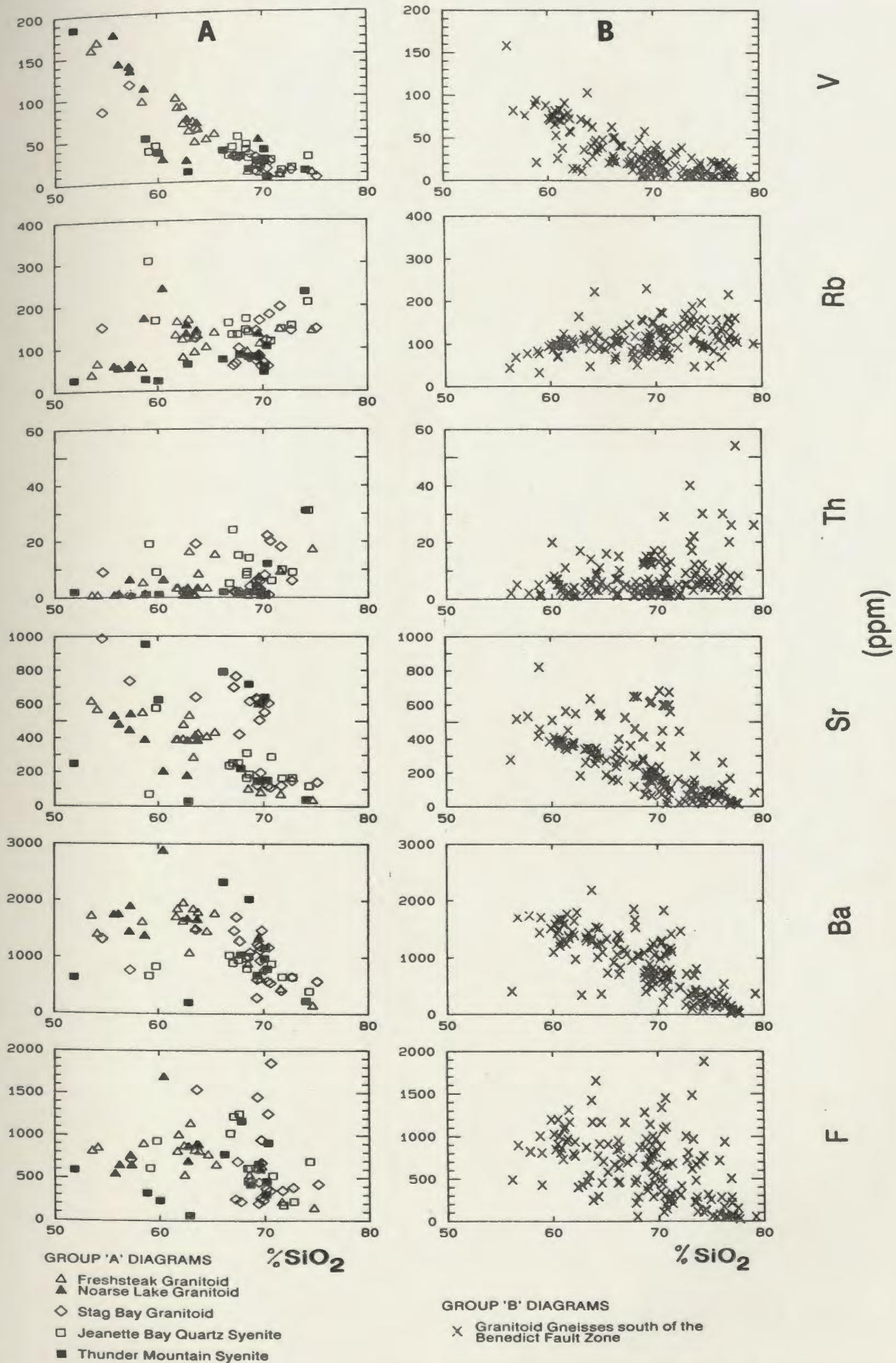


Figure 6.4. V, Rb, Th, Sr, Ba and F versus SiO<sub>2</sub> for unclassified plutonic units. See text for discussion.

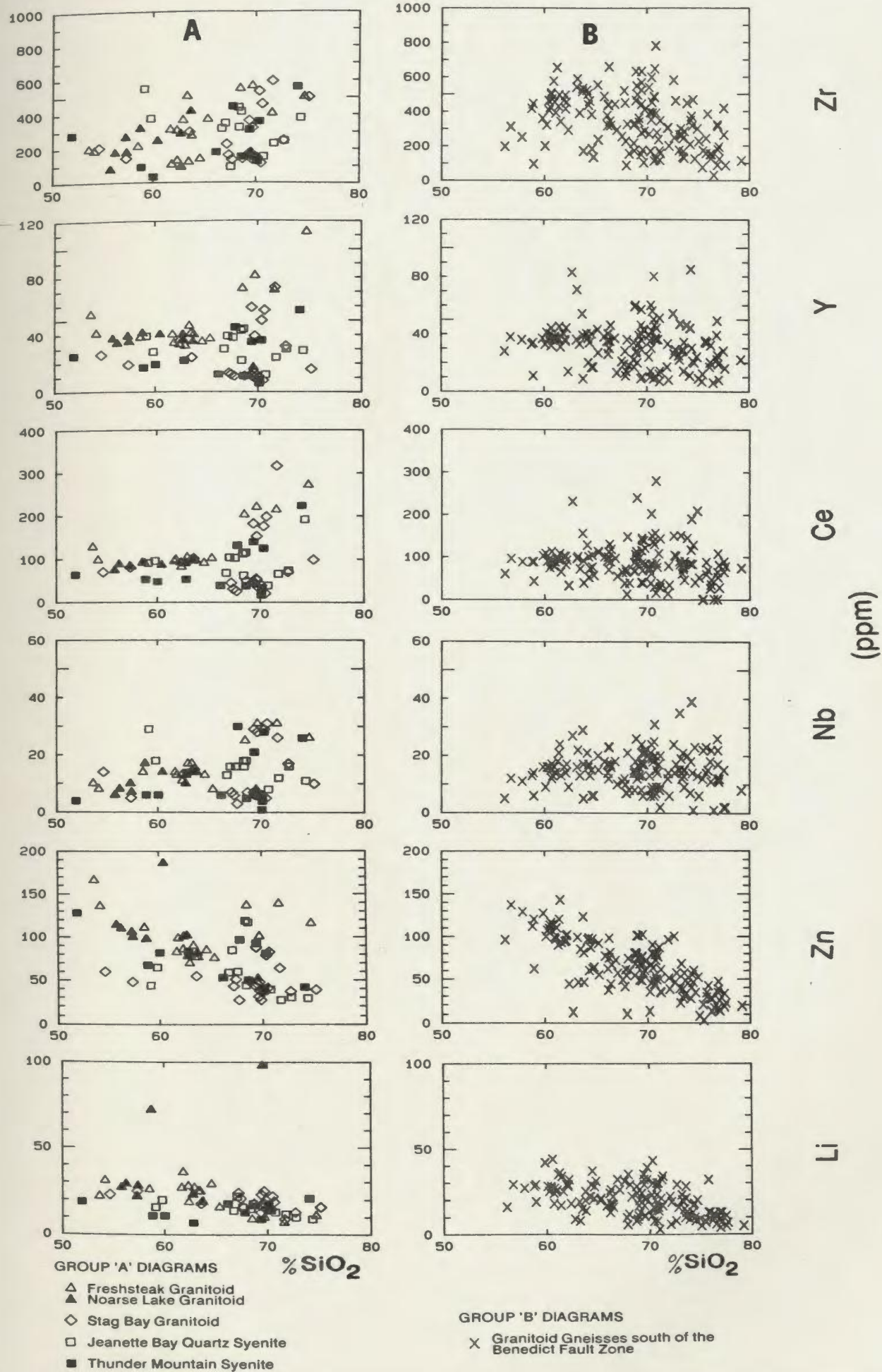


Figure 6.5. Zr, Nb, Y, Ce, Li and Zn versus SiO<sub>2</sub> for unclassified plutonic units. See text for discussion.

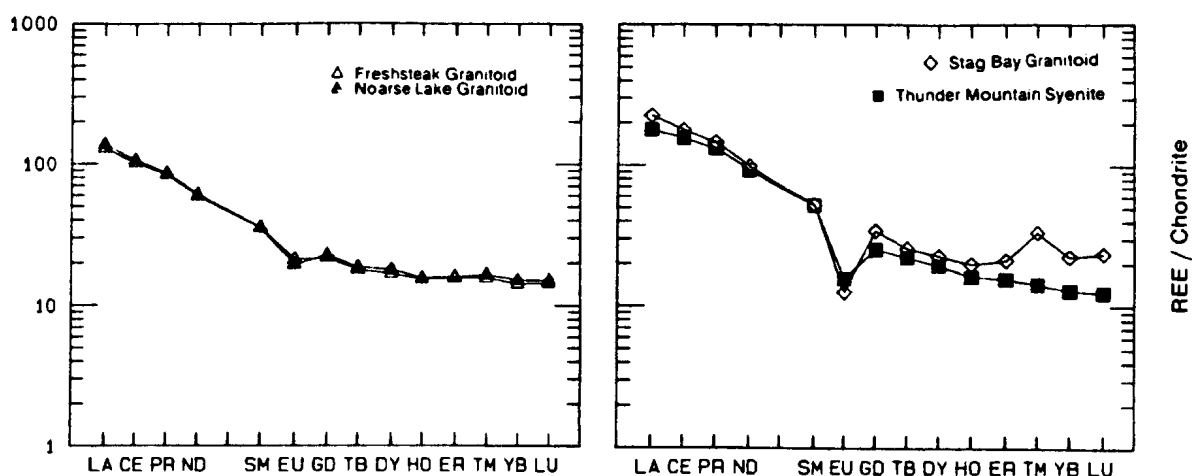


Figure 6.7. Rare Earth element (REE) patterns for representative unclassified plutonic rocks. Values are normalized to chondritic values (listed in Appendix C).

locally enriched in the Freshsteak and Noarse Lake units above 70%  $\text{SiO}_2$ , and Li is enriched in some biotite-rich rocks from the Noarse Lake unit.

The granitoid gneiss unit shows a similar range of trace element variation. Scattered distributions for LFS trace elements such as Th, Rb, Ba and Sr may in part reflect element mobility during Grenvillian metamorphism, rather than primary magmatic trends.

#### Rare Earth Element (REE) Patterns

Two samples from the Freshsteak and Noarse Lake units have identical REE patterns (Figure 6.6). The Thunder Mountain pattern is similar, but shows a larger negative Eu anomaly. The Stag Bay unit has a dish-shaped MREE pattern, similar to patterns observed in some Labradorian granitoids (e.g. Figure 5.17, p.216). No data are available for the granitoid gneiss unit.

### 6.3 SUMMARY and DISCUSSION

Geochemical contrasts between unclassified plutonic units are subtle, and they cannot be classified as Makkovikian or Labradorian on this basis alone. The fluorine, HFS element and REE contents of these units fall into the middle ground shared by both assemblages.

The Freshsteak and Noarse Lake units are, however, petrographically and geochemically similar to the Makkovikian Long Island quartz monzonite, particularly with respect to their  $\text{TiO}_2$  and  $\text{P}_2\text{O}_5$  enrichment. A general correlation between them is consistent with the Rb-Sr age ( $1798 \pm 48$  Ma) obtained from the Freshsteak Granitoid, which indicate a Makkovikian age (details in Chapter 8).

Remaining unclassified units cannot be assigned with confidence. The partially peraluminous composition of the Stag Bay unit resembles that of some Labradorian granitoids, and differs from compositions of typical Makkovikian granitoids. The Jeanette Bay unit shows lower incompatible element abundances than rocks of equivalent composition in the adjacent Mount Benedict Intrusive Suite, and is probably unrelated to them. The Thunder Mountain Syenite is broadly similar to the Freshsteak and Noarse Lake units in major and trace element composition, but different in texture.

The granitoid gneiss unit overlaps in composition with both Makkovikian and Labradorian plutonic assemblages, but the distribution of rock types within it resembles the former more closely. However, it lacks the marginally peralkaline compositions typical of the Makkovikian assemblage, and shows no extreme fluorine, HFS element and REE enrichment. There is no firm basis for correlating it with either Makkovikian or Labradorian associations alone, and it probably includes reworked equivalents of both.



## CHAPTER SEVEN

# MAKKOVIKIAN AND LABRADORIAN VOLCANIC ASSEMBLAGES

---

### Chapter Abstract

The most extensive volcanic assemblage in the study area is the Upper Aillik Group, a complex Makkovikian sequence that includes at least two components of ca. 1860 and ca. 1810 Ma age. Geochemical studies of these rocks are hampered by widespread alkali-metasomatism, which appears to be a regional feature of this assemblage. In geochemical terms, unaltered variants are closely similar to Makkovikian high-silica granites such as the Kennedy Mountain, Strawberry and Lanceground Intrusive Suites, but do not show fluorine enrichment. They do, however, display borderline-peralkaline affinity, HFS element enrichment, and REE enrichment typical of most Makkovikian plutonic assemblages. Hypabyssal intrusive rocks within the Upper Aillik Group show the closest resemblance, and also display local fluorine enrichment. Alkali-metasomatism is closely similar to analogous patterns recognized in the syn-tectonic Kennedy Mountain Intrusive Suite.

It is suggested here that the Upper Aillik Group is a two-stage sequence comprising broad equivalents of syn- and post-tectonic Makkovikian plutonic rocks. This is consistent with geochronological data from both groups, which overlap in part. However, ca. 1860 Ma volcanic rocks predate most of the syn-tectonic plutons, and younger post-tectonic granites such as the Strawberry Intrusive Suite may be significantly younger than 1800 Ma.

The Bruce River Group (described by Ryan, 1984) includes a Labradorian bimodal (felsic > mafic) volcanic sequence. Although similar to the Upper Aillik Group in terms of major element chemistry (particularly in felsic compositions), this sequence evolves to peraluminous compositions, and has lower HFS element and REE abundances. On the basis of map patterns, it appears to contain a higher proportion of basaltic and basaltic andesite compositions than the Upper Aillik Group. Such features are consistent with the mafic compositions observed in the Labradorian plutonic assemblage, and with subtle geochemical contrasts noted between Makkovikian and Labradorian plutonic assemblages.

Volcanic sequences in the Benedict Mountains (here termed Jagged Edge assemblage) have previously been grouped with the Upper Aillik Group. In geochemical terms, however, they resemble the Labradorian Bruce River Group, and may be a younger sequence. However, they are geochemically distinct from local Labradorian plutonic rocks of the Mount Benedict Intrusive Suite.

## Introduction

Volcanic and metavolcanic assemblages were not examined in detail during this project, but are an important component of Proterozoic magmatism in the study area. This chapter is mostly concerned with their possible relationship to plutonic associations described in preceding chapters. Descriptions are based partly on previous work (Bailey, 1979; Evans, 1980; Gower et al., 1982) and partly on the author's more limited observations in selected areas.

The most extensive volcanic assemblage is the Makkovikian Upper Aillik Group, which is dominated by rocks of felsic composition, with minor mafic metavolcanic rocks. The Bruce River Group, exposed beyond the western boundary of the study area, includes a thick sequence of mafic and felsic volcanic rocks, and is of Labradorian age. Volcanic rocks also form several discontinuous belts in the Benedict Mountains, which have previously been correlated with the Upper Aillik Group. The term "Jagged Edge assemblage" is used below as a label of convenience for these, although it is recognized that they may actually be part of the Upper Aillik Group sequence.

## 7.1 GEOLOGY and PETROLOGY

### 7.1.1 Upper Aillik Group (Type Area Only)

#### General Overview

The Upper Aillik Group has the dubious distinction of being the most studied yet least understood Proterozoic



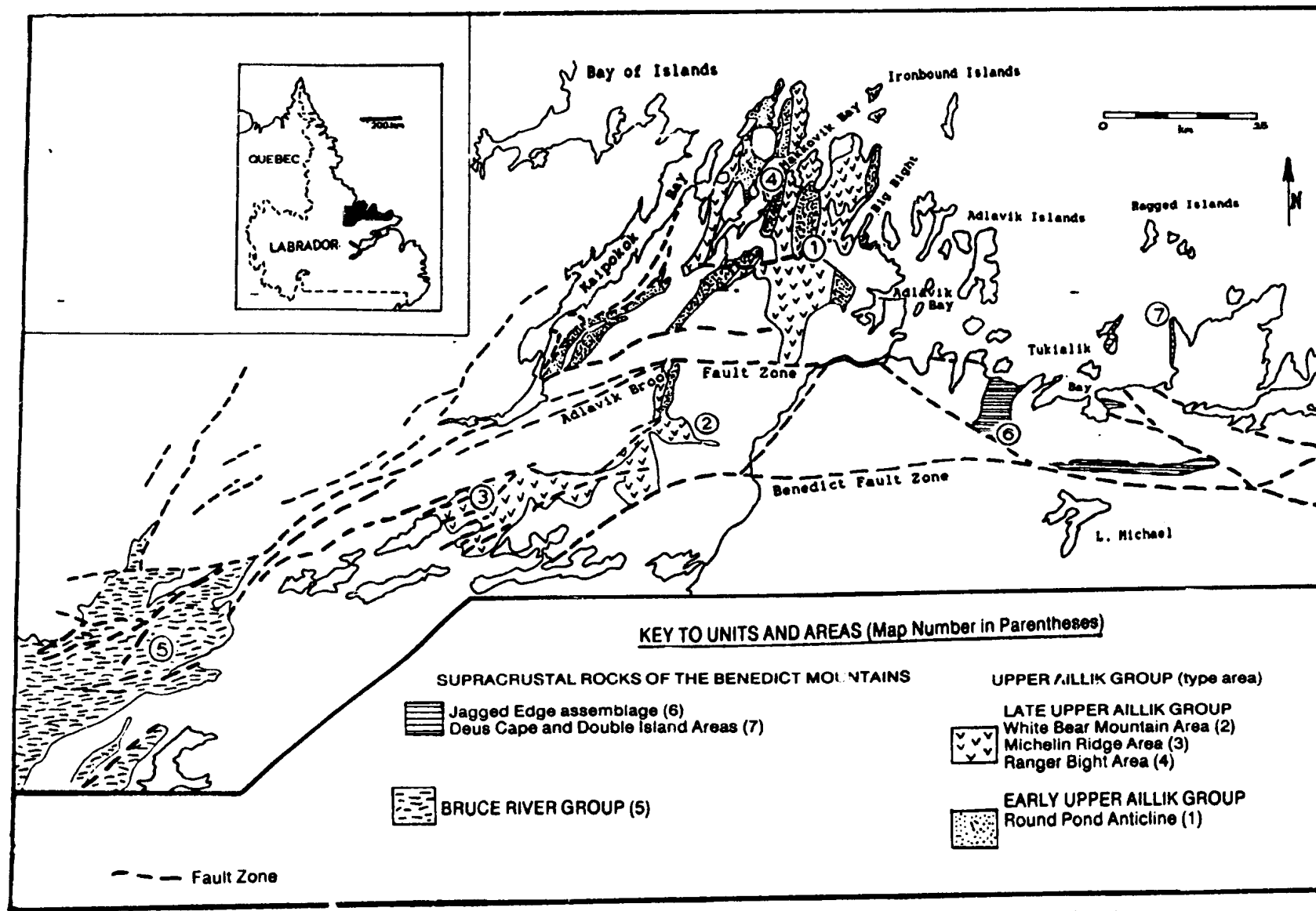


Figure 7.1. Summary map illustrating the distribution and extent of Makkovikian and Labradorian volcanic assemblages.

sequence in eastern Labrador. This reflects rapid lateral facies changes that complicate its stratigraphy, and the variable overprint of greenschist to lower amphibolite facies metamorphism and associated deformation (Gower et al., 1982; Gower and Ryan, 1987). Parts of the sequence are structurally complex and polydeformed (e.g. Clark, 1973), but (paradoxically) some rhyolites and hypabyssal intrusive rocks are massive or only weakly cleaved (e.g. Bailey, 1979). Metamorphic grades range from lower amphibolite near Kaipokok Bay, to sub-greenschist in the east and south of the area (Gower et al., 1982).

The sequence is most extensive in the north of the study area, where it is areally dominant over plutonic units. It also forms a narrow zone extending into the southwest of the area, where it is bounded mostly by faults. This area (termed the Michelin area) has been the focus of most previous studies (e.g. Bailey, 1979; Evans, 1980; White and Martin, 1980).

No systematic mapping of the Upper Aillik Group was conducted during this project, but the sequence was examined in a number of coastal areas, and also during helicopter and ground mapping of adjacent plutonic rocks. Upper Aillik Group country rock types were sampled routinely for geochemistry, but no grid sampling program was undertaken over these units.

### Concepts of Aillik Group Stratigraphy

The term "Aillik Series" was proposed initially by Kranck (1939), and subsequently modified to "Aillik Group" by King (1963). Many of the rocks now grouped in the upper portion were initially described as quartzite, arkose, feldspathic quartzite and banded quartzite - misnomers that

reflect the saccharoidal textures of many recrystallized rocks exposed on the coast. King (1963), Clark (1973) and White (1973) recognized that at least some of these siliceous rocks were of volcanic origin, and this was subsequently confirmed on a regional scale (e.g. Gandhi, 1978; Bailey, 1979; Gower et al., 1982).

The contact between Lower and Upper Aillik Groups is tectonized, and, despite repeated examination (Marten, 1977; Evans, 1980; Wardle, pers. comm., 1985), no consensus has emerged regarding its significance. Marten (1977) suggested that deformed conglomerate at the base of the Upper Aillik Group (which contains clasts typical of the Lower Aillik Group) represents a major unconformity. There is consensus that the Upper Aillik Group has a generally simpler structural style than the Lower Aillik Group, which has undergone isoclinal folding and thrusting (Marten, 1977). There are, however, equally strong contrasts in deformation state within the Upper Aillik Group (Gower et al., 1982; Gower and Ryan, 1987).

These contradictions led to a revised concept of Upper Aillik Group stratigraphy, in which it was divided into an "early" and "late" component (Gower and Ryan, 1987). The late Upper Aillik Group is dominated by felsic volcanic rocks, whereas the early portion comprises a mixed volcanic and clastic sedimentary assemblage. It was suggested that these early and late components could be separated by a mafic metavolcanic marker horizon. Gower and Ryan (1987) further speculated that early and late components correlated with syn-tectonic and post-tectonic plutonic assemblages respectively; the latter were at that time considered to be wholly of ca. 1650 Ma (Labradorian) age. Schärer et al. (1988) subsequently reported U-Pb zircon ages of 1856  $\pm$  2 Ma and 1807  $\pm$  3 Ma from two separate localities assigned

by Gower and Ryan (1987) to the late Upper Aillik Group. A rhyolite flow interbedded with volcanoclastic sediments that are probably part of the early sequence gave a U-Pb zircon age of  $1861 \pm 9/-3$  Ma (Schärer et al., 1988). These ages appear to rule out a relationship between the Upper Aillik Group and Labradorian plutonic rocks.

The two-stage stratigraphic concept is, however, still valid in the light of new Rb-Sr and U-Pb zircon data (this study and Krogh et al., in prep.). Post-tectonic Makkovikian plutonic rocks dated at ca. 1800 Ma are similar in age to the youngest rocks recognized within the Upper Aillik Group, and to some of their syn-tectonic, foliated counterparts. It is suggested here that early and late components of the Upper Aillik Group correspond broadly to syn-tectonic and post-tectonic Makkovikian plutonic associations, and that an unconformity or discontinuity may be present within the sequence. However, contrasts in deformation state amongst the metavolcanic rocks may also be a function of inhomogeneous deformation, as discussed for equivalent plutonic assemblages (Chapter 4). There is, however, no evidence of plutonic rocks of equivalent age to the earliest rocks (ca. 1850 Ma) recognized in the Upper Aillik Group. The oldest age yet obtained from plutonic rocks is ca. 1840 Ma (Deus Cape Granitoid; Krogh et al., in prep.), although Gandhi et al. (1988) report ages of ca. 1800 Ma to the west of the Study area.

This interpretation must be confirmed by systematic mapping of the Upper Aillik Group, and by dating its components with reference to stratigraphy. The central problem is the delineation of early and late components, complicated by the possibility that the mafic volcanic "marker" may not be the same unit everywhere, a conclusion supported by recent geochemical data (MacDougall, 1988).

Undeformed granitoid rocks invariably intrude the Upper Aillik Group. Foliated Makkovikian plutonic rocks also appear to post-date adjacent supracrustal rocks, but in most areas these correspond to the early Upper Aillik Group of Gower and Ryan (1987). However, the inverse relationship (i.e. Upper Aillik Group hypabyssal intrusive lithologies intruding older granitoid rocks) would be indistinguishable from normal outcrop-scale details observed in most granitoid units. Also, many plutons are known to intrude their own ejecta as a consequence of the greater longevity of plutonic systems and cauldron subsidence (e.g. Lipman, 1988).

#### Early Upper Aillik Group

The early Upper Aillik Group, as outlined by Gower and Ryan (1987), forms the core of an anticline at Round Pond, and also three broadly parallel belts that are infolded with the predominant later sequence (Figure 7.1). It also occurs in minor amounts in the southwest of the area. It has not been examined in detail during this study, and descriptions below are summarized from Gower et al. (1982).

The sequence is lithologically varied, but dominated by metasedimentary rocks. These include arkose, banded tuff, laminated arenite, siltstone, pebble conglomerate and breccia with volcanic clasts. Subordinate volcanic rocks include dacite-rhyolite compositions, and lesser mafic flows and tuffs. The top of the sequence is supposedly defined by the "marker" mafic- intermediate tuff horizon, which locally includes pillow lavas and possible subaerial volcanic rocks. The rock types present immediately below this unit are laterally variable; this could indicate rapid lateral facies changes, the presence of an angular unconformity at its base, or both (Gower and Ryan, 1987). Alternatively, as

discussed above, it may indicate the presence of more than one "marker" horizon within the sequence. The early Upper Aillik Group is deformed and metamorphosed in most areas. Deformation is most evident in lithologies such as conglomerate, which show intense flattening, but most other rock types are also completely recrystallized.

#### **General Features of the Late Upper Aillik Group**

The late Upper Aillik Group, as outlined by Gower and Ryan (1987), corresponds essentially to unit 9 of Gower et al. (1982). It is dominated by felsic volcanic and pyroclastic rocks, with lesser tuffaceous arkose and sandstone. It also includes hypabyssal intrusive rocks. All of these were examined during this project, but geochemical sampling is biased towards areas marginal to plutonic bodies. Recrystallization during regional metamorphism, particularly in the northwest, and thermal metamorphism around younger intrusions, have destroyed primary volcanic textures in most areas. In general, recrystallization is more intense in extrusive rock types than in the hypabyssal intrusive rocks. General characteristics of these rocks are illustrated in Plate 7.1.

#### **Volcanic, Pyroclastic and Volcaniclastic Rocks**

**Field Relations and Lithology :** Outcrops are commonly heterogeneous. The best candidate for a "dominant" lithology is a fine to very fine-grained, pink to grey or buff, variably banded metavolcanic rock that has a saccharoidal texture. Volcanic textures are only rarely preserved, and in many cases it is impossible to differentiate between massive rhyolite and crystal tuff. Larger grains of quartz,

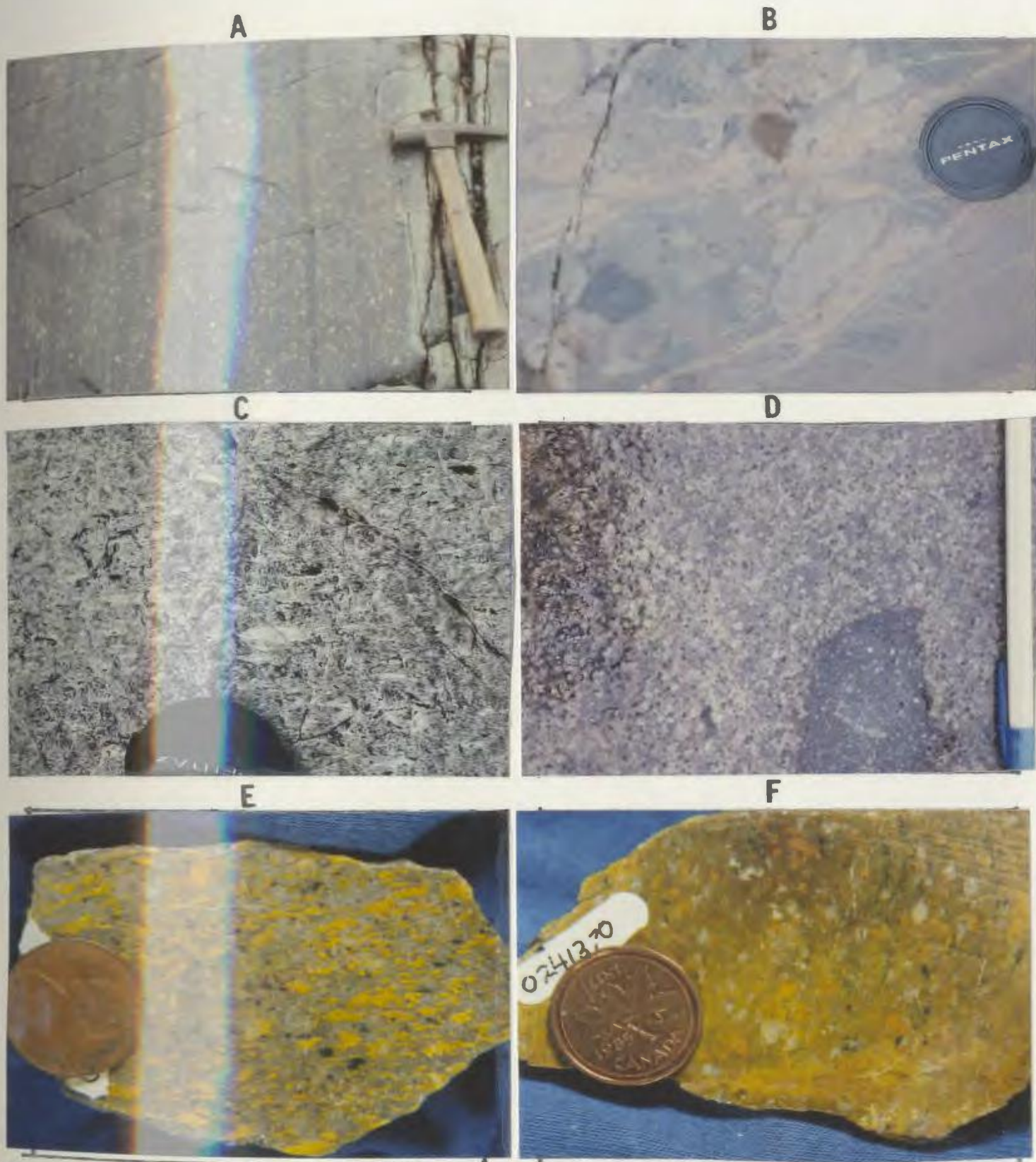


Plate 7.1 Features of the Upper Aillik Group (see also Plate 7.2). (a) Flow-banded, porphyritic rhyolite, Manak Bay area. (b) Rhyolite breccia, with rounded clasts of porphyry and flow-banded rhyolite, Manak Bay area. (c) Recrystallized tuff with deformed lithic fragments, Ranger Bight. (d) Purple feldspar-porphyry, including part of a rhyolite xenolith, Ironbound Islands. (e) and (f) Typical enigmatic Upper Aillik Group lithologies, that could be flows or pyroclastic rocks. Slabs stained for K-feldspar.



K-feldspar and plagioclase are commonly present, and represent either phenocrysts or crystal fragments. Banding is locally recognizable as a primary flow-banding, but relict fragmental textures suggest that it may also result from strong deformation of lithic tuff or agglomerate. Lithic fragments, in many cases recognisable only as blotches or diffuse ellipsoids, occur widely and, unless they represent xenoliths in rhyolitic flows, indicate a fragmental origin for much of the recrystallized material. The few areas where Upper Aillik group volcanic rocks preserve original volcanic textures (e.g. at Ranger Bight in Makkovik Bay, and at Michelin Ridge) also consist dominantly of pyroclastic material that resembles ash-flow tuff, associated with subordinate rhyolite flows.

**Petrography** : Pervasive recrystallization has obliterated most original textures, leaving a groundmass of very fine grained quartz and feldspar. Broken crystals or phenocrysts are preserved as coarser grain aggregates. The most common "phenocryst" phases are K-feldspar and plagioclase; quartz is less abundant. The mafic mineral assemblage in most samples has been degraded to aggregates of iron oxide, sphene, chlorite and epidote. Amphibole (actinolite, more rarely hornblende) and pyroxene are present locally. Blue amphibole of sodic composition, associated with accessory fluorite, is a distinctive component in some areas, particularly adjacent to some small granitoid plutons in the north. It is uncertain whether this is a primary or metasomatic feature, since metasomatic effects involved with mineralization and/or granitoid intrusion have been documented in several areas (White and Martin, 1980; Evans, 1980; Kerr, 1988; see also



sections 3.3 and 7.2). Upper Aillik Group rocks are not commonly fluorite-bearing, except in areas adjacent to plutonic units.

#### **Hypabyssal Intrusive Rocks**

*Field Relations and Lithology* : Massive feldspar and quartz-feldspar porphyry form several mappable bodies, and also occur as dykes and veins on an outcrop scale within the metavolcanic rocks. The largest body, at White Bear Mountain, consists of purple or grey porphyry with large (up to 2 cm) K-feldspar phenocrysts and less abundant, smaller, rounded, blue quartz eyes. Similar (but less spectacular) rock types are present near Round Pond (MacDougall, 1988), south of Cape Strawberry, and on offshore Islands north of Cape Strawberry. Relationships between these and the dominant metavolcanic rocks were not examined in this study. Bailey (1981) suggested that subvolcanic intrusive rocks passed gradationally into felsic volcanic rocks in several areas.

*Petrography* : Samples from White Bear Mountain consist of a recrystallized microcrystalline groundmass assemblage of quartz, microcline and sodic plagioclase, that locally retains a granophyric texture. Euhedral to ovoidal perthitic microcline phenocrysts locally show rims of sodic plagioclase. Quartz phenocrysts are less common; in places they have a bipyramidal habit suggesting that they were originally a high-temperature polymorph (Payette and Martin, 1986). Fine aggregates of biotite and chlorite are present in most samples, blue-green amphibole occurs locally, but the most obvious mafic species are opaque oxides associated

with granular sphene. Other Upper Aillik Group porphyry bodies are similar in mineralogy, and commonly show less evidence of recrystallization than adjacent metavolcanic rocks.

#### 7.1.2 Supracrustal Rocks of The Benedict Mountains (Jagged Edge Assemblage)

##### **General Overview**

The label "Jagged Edge assemblage" is used here for felsic volcanic and volcanoclastic rocks in the east of the study area (Figure 7.1), that are geographically isolated from the type area of the Upper Aillik Group. Gower (1981) correlated these with the type area (7.1.1), but stated that their equivalence was mostly an assumption. The name is introduced mostly to avoid tedious repetition of the phrase "volcanic sequences of the Benedict Mountains area". There is however, no guarantee that all these belts are of the same age or affinity. However, if dextral displacement along the suggested continuation of the Adlavik Brook Fault zone is removed (Figure 7.1), most of them coalesce into a single discontinuous unit. Occurrences on the mainland were examined and sampled during this project; those on Double Island and near Deus Cape were not visited, but are described by Gower (1981). Archibald and Farrar (1979) report an Ar-Ar age of  $1630 \pm 10$  Ma from muscovite in a pegmatite pod within volcanic rocks southeast of Stag Bay, which provides a younger limit on the age of the sequence. Typical features of these rocks are illustrated in Plate 7.2.

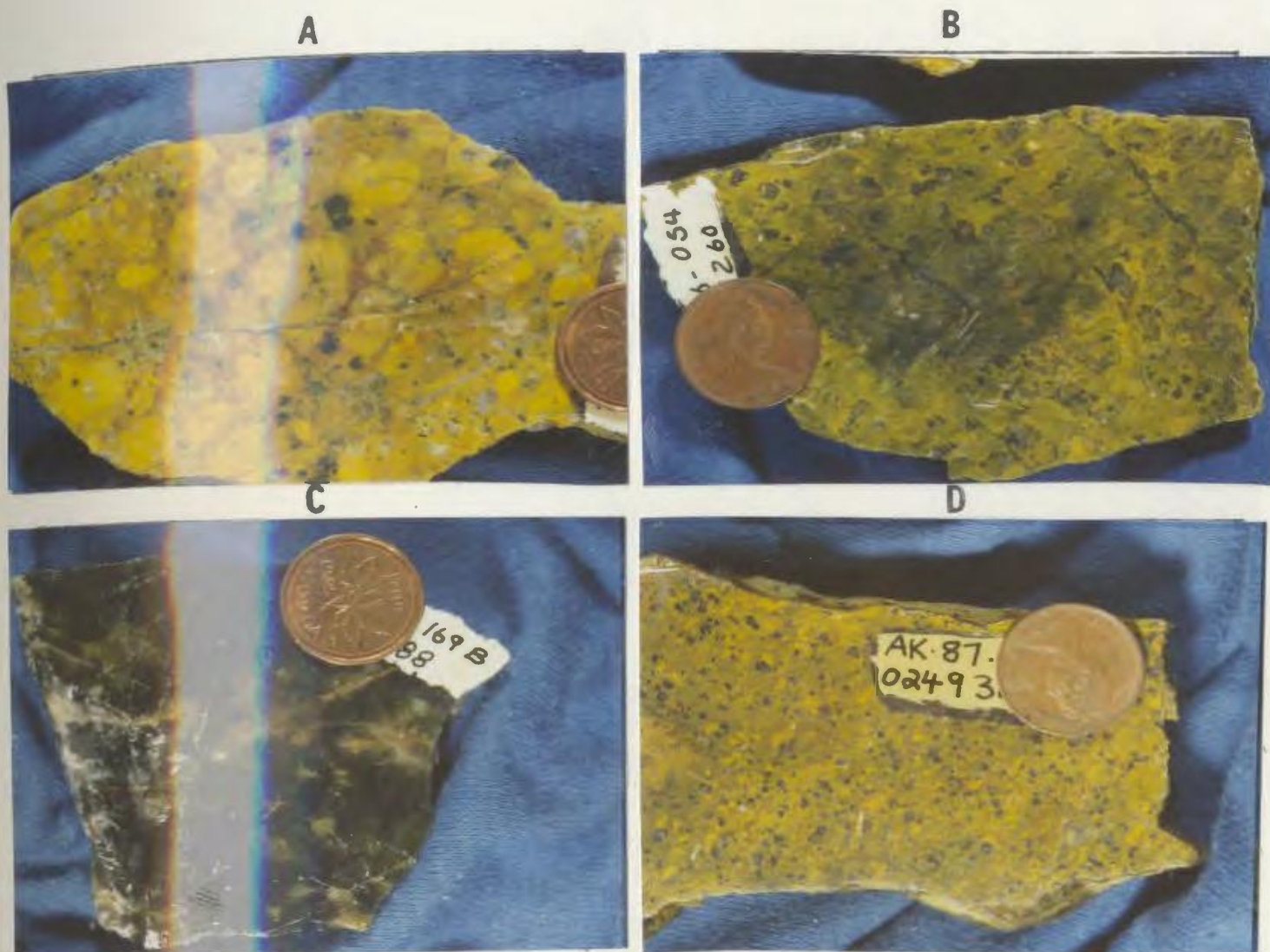


Plate 7.2 Features of the Upper Aillik Group and the Jagged Edge Assemblage. (a) and (b) Quartz-porphyry and quartz-feldspar porphyry from White Bear Mountain area. (c) Glassy, silicified rhyolite with spherulitic appearance, Jagged Edge. (d) Fine-grained, very fresh, quartz-feldspar porphyry, Jagged Edge. Slabs stained for K-feldspar.

## Field Relations and Lithology

The best exposures are in a rugged area east of Stag Bay (Figure 7.1), and comprise a sequence of pink, grey and purple-brown felsic tuffs, agglomerates, flows(?), and hypabyssal intrusive rocks associated with lesser volcaniclastic sedimentary rocks (Gower, 1981). The agglomerates are essentially undeformed, and contain rhyolite fragments up to 30 cm in diameter. A distinctive lithology observed during this project is a grey, extremely hard, highly siliceous tuff that locally retains flattened shard-like fragment shapes and spherulitic textures. Massive, undeformed, grey to purple feldspar-porphyry (and lesser quartz-feldspar porphyry) is also present.

East of Tukialik Bay, a similar assemblage of rock types forms a triangular enclave within the Tukialik Granite. D.Bailey (pers.comm to C.F.Gower, 1979) suggested that these may have a gradational relationship with the surrounding granite, but they are cut locally by granite veins (however, these veins are not obviously similar to the nearby Tukialik Granite). Volcanic rocks are also present in an elongate, east-trending belt immediately north of the Benedict fault zone that, based on its strongly sheared appearance, is interpreted as a fault-bounded sliver. Original characteristics in this area have mostly been destroyed by cataclasis, and it is possible that some banded, rhyolite-like rocks are in fact mylonites. However, quartz-eye and fragmental textures are locally preserved.

Supracrustal rocks also occur on Double Island, and as a narrow coastal strip south of Deus Cape. Gower (1981) reports more intense deformation in these areas, and a higher proportion of metasedimentary material. These descriptions are reminiscent of the early Upper Aillik Group

of Gower and Ryan (1987). It is therefore possible that "Jagged Edge assemblage" also includes more than one sequence; geochemical features discussed here (7.2) apply only to the fresher rocks exposed on the mainland.

### 7.1.3 Bruce River Group

#### **General Overview**

The Bruce River Group (defined initially by Smyth et al., 1978) is a well-preserved volcanosedimentary sequence exposed beyond the western boundary of the study area (Figure 7.1). It has been examined only in scattered localities during this study but, as geochemical data are used below for comparative purposes, a brief review (drawn from Ryan, 1984, and Ryan et al., 1987) is included here.

The Bruce River Group rests unconformably upon the pre-Makkovikian Moran Lake Group, and is affected only by Grenvillian deformation. It has a well-defined stratigraphy consisting of three formations defined by Ryan (1984). The two lower formations are dominated by terrestrial sedimentary rocks, whereas the uppermost and thickest (Sylvia Lake Formation) comprises a bimodal (felsic > mafic) volcanic assemblage.

Previous Rb-Sr geochronological studies (Wanless and Loveridge, 1972; Kontak, in Ryan, 1984) suggested ages of 1530 to 1510 Ma for the volcanic rocks. U-Pb zircon dating (Schärer et al., 1988) yielded 1649 +/- 1 Ma for a rhyolite, indicating that it is of Labradorian age. It is the only known Labradorian volcanic assemblage in eastern Labrador, although parts of the Petskapiskau group in central Labrador have yielded Labradorian ages (Krogh, 1985).

### Field Relations and Lithology

The lowermost (Heggart Lake) formation is a laterally discontinuous package of conglomerate, sandstone, arkose and lesser mafic flows. The overlying Brown Lake Formation consists dominantly of conglomerates and arenites containing significant amounts of volcanic detritus. The uppermost (Sylvia Lake) formation is over 8 km thick, and consists of mafic and felsic (and minor intermediate) volcanic rocks, agglomerates, breccias and (especially in the upper part) welded and non-welded tuff. Ryan et al. (1987) distinguish two large-scale cycles of volcanism, that each commence with mafic and intermediate rocks, and culminate in thick felsic sequences. They estimate the ratio of felsic to mafic/intermediate rocks as approximately 2.2:1; the intermediate compositions are rare. On the basis of outcrop areas, the sequence appears to contain a higher proportion of mafic volcanic rocks than the Upper Aillik Group.

Mafic and intermediate volcanic rocks comprise grey to green, vesicular and/or porphyritic flows containing phenocrysts of plagioclase and clinopyroxene, with lesser orthopyroxene and olivine. Felsic rocks are dominated by grey, red, green or purplish welded ash-flow tuffs with prominent fragments and/or phenocrysts of feldspar. Well-preserved original features include eutaxitic foliations and lithophysae. Coarse fragmental rocks occur locally, as do cross-bedded (aeolian?) sandstones. Detailed petrographic descriptions of the volcanic rocks are presented by Ryan (1984).

## 7.2 DESCRIPTIVE GEOCHEMISTRY

Volcanic and hypabyssal intrusive rocks sampled during this project are represented by a total of 73 analyses. No distinction is made below between regional, follow-up and geological sample populations, as grid sampling systems were not employed. Most of the samples were collected in areas adjacent to intrusive rocks. Data presented here do, however, provide a good indication of the compositional spectrum of the Upper Aillik Group as, unlike most previous studies (see below), they were collected without reference to mineralized areas. Comparative data from the Bruce River Group used below are from Ryan (1984).

### 7.2.1 Previous Studies

Several geochemical studies of the Upper Aillik Group have been conducted in areas of uranium mineralization, particularly in the Michelin area. These rocks have variously been described as calc-alkaline, alkaline or peralkaline in affinity.

Geochemical investigations are hampered by strong compositional (particularly alkali) disturbance, recognized initially by White (1976) and White and Martin (1980). White and Martin (1980) concluded that the rocks of the Michelin area were originally of alkaline composition, but were affected by Na-metasomatism and desilication, and by lower-temperature K-metasomatism, both associated with mobility of U and Zr.

Subsequent studies in the same area by Evans (1980) further emphasized the links between metasomatism and

•

uranium mineralization and suggested that metasomatism took place via cation-exchange and substitution of Na-Al for Si in feldspars. A high-K calc-alkaline affinity was suggested for the sequence as a whole. Similar conclusions were reached by Bailey (1979) and Wardle and Bailey (1981). Gower et al.(1982) did not speculate on such matters, but pointed out that there were geochemical differences between the early and late components of the Upper Aillik Group.

Payette and Martin (1986), working also in the Michelin area, attempted to circumvent metasomatic complications by analyzing "melt inclusions", i.e., tiny glassy pockets that represent globules of magma trapped in growing phenocrysts. However, microprobe analyses revealed strong alkali variation amongst inclusions, implying that even these did not escape compositional disturbance. They suggested that an alkaline magma was most consistent with the observed compositional range of melt inclusions. MacDougall (1988) examined the sequence in the mineralized Round Pond area, and suggested a bimodal compositional spectrum, partly reflecting the presence of one of the few mafic units in the sequence in this area. He documented metasomatic patterns analogous to those of the Michelin area, and suggested that apparent peralkaline compositions were due to alteration.

Ryan (1984), and Ryan et al.(1987) conducted petrochemical studies on the Bruce River Group. This sequence appears to be less disturbed than the Aillik Group; they also suggested that it had affinities to high-K calc-alkaline sequences, at both mafic and felsic ends of its compositional spectrum.



Table 7.1 . Average compositions of Makkovikian and Labradorian volcanic assemblages. Bruce River Group data from Ryan (1984).

UNIT	1.0		1.0 (unaltd)		1.1		1.2		1.2 (unaltd)		1.3		1.4	
n1	13		6		5		16		9		14		21	
n2	3		1		5		15		9		13		6	
(Wt%)	Mean	S.D.	Mean	S.D.	Mean	S.D.	Mean	S.D.	Mean	S.D.	Mean	S.D.	Mean	S.D.
SiO <sub>2</sub>	72.81	3.54	73.12	3.54	75.42	1.56	74.26	3.29	74.53	1.79	71.27	3.99	71.62	4.37
TiO <sub>2</sub>	0.32	0.22	0.35	0.16	0.22	0.08	0.23	0.11	0.20	0.09	0.36	0.11	0.26	0.13
Al <sub>2</sub> O <sub>3</sub>	13.61	1.59	13.25	1.86	11.75	0.24	12.49	1.35	12.39	0.96	13.61	1.80	14.15	2.08
Fe <sub>2</sub> O <sub>3</sub>	1.47	1.10	2.00	0.95	1.86	0.78	1.65	0.56	1.57	0.58	1.82	0.88	1.28	0.55
FeO	0.60	0.62	0.24	0.18	1.20	0.50	0.77	0.67	0.81	0.55	0.79	0.46	0.70	0.51
MnO	0.04	0.02	0.05	0.02	0.05	0.02	0.04	0.02	0.04	0.02	0.06	0.02	0.05	0.02
MgO	0.44	0.40	0.25	0.17	0.07	0.06	0.23	0.52	0.10	0.09	0.28	0.28	0.50	0.55
CaO	1.09	0.93	0.86	0.67	0.52	0.22	0.59	0.59	0.55	0.27	1.19	1.13	1.40	1.13
Na <sub>2</sub> O	4.02	1.90	3.72	1.01	5.62	1.60	4.08	1.62	4.12	0.48	3.90	0.28	3.72	1.10
K <sub>2</sub> O	4.67	2.89	5.08	0.88	2.22	2.17	4.77	2.81	4.71	0.52	5.52	0.45	4.81	1.17
P <sub>2</sub> O <sub>5</sub>	0.07	0.06	0.06	0.04	0.02	0.00	0.03	0.03	0.03	0.02	0.04	0.04	0.06	0.04
LOI	0.69	0.38	0.68	0.37	0.46	0.28	0.44	0.22	0.39	0.13	0.57	0.31	0.95	0.72
TOTAL	99.83		99.64		99.41		99.58		99.44		99.41		99.49	
(ppm) Trace Elements														
Li	16.5	19.0	13.5	12.2	7.4	8.8	11.7	15.4	16.2	19.7	13.1	6.2	19.0	14.7
F	378.5	339.8	384.0	290.1	331.8	346.3	272.0	401.2	419.1	491.5	541.1	347.2	540.7	491.0
Sc	1.7	0.9	0.7	0.0	1.8	1.4	2.2	1.9	1.8	1.3	4.8	1.7	3.4	1.4
V	21.1	9.6	22.0	6.5	11.4	1.7	18.4	22.1	13.0	6.9	13.3	9.9	25.8	14.8
Cr	6.0	10.4	3.3	2.7	7.2	11.8	7.6	8.2	7.8	9.1	5.9	3.7	19.0	55.3
Ni	2.5	3.3	1.5	0.8	5.4	9.8	1.4	1.5	1.0	0.0	2.0	2.8	5.3	14.9
Cu	4.2	3.4	2.0	1.5	14.6	24.3	4.7	3.7	4.4	3.3	6.9	8.8	6.9	5.1
Zn	44.0	34.1	52.0	47.1	66.8	64.9	86.1	81.0	112.2	94.8	77.8	41.7	44.9	22.9
Ga	12.6	4.3	12.3	5.0	24.2	6.7	15.4	6.9	16.7	7.9	11.5	6.7	7.8	1.7
Rb	138.1	105.8	134.8	26.8	56.4	48.2	139.4	86.2	149.4	48.8	168.2	28.8	156.3	58.2
Sr	156.4	144.7	142.3	157.3	48.8	35.1	53.4	46.3	57.2	50.5	140.9	226.4	216.6	187.0
Y	32.0	24.3	33.3	20.3	71.2	22.4	54.7	32.2	69.1	31.0	69.9	17.1	25.2	9.4
Zr	317.3	155.6	407.7	137.2	593.6	354.3	529.8	264.6	550.2	338.7	490.4	129.4	262.5	78.8
Nb	15.5	7.1	18.7	4.5	33.8	19.5	27.8	10.7	30.4	11.0	29.2	7.6	14.2	5.6
Mo	2.9	1.2	2.5	1.0	14.0	22.5	7.4	15.2	4.7	5.9	2.8	1.1	2.6	0.9
Sn	3.0	3.5	1.0	0.0	9.2	9.4	5.2	2.8	6.1	3.1	6.4	2.9	2.3	1.4
Cs	1.0	0.9	0.5	0.0	0.5	0.0	1.0	0.9	1.2	1.1	1.3	0.5	1.3	1.6
Ba	695.3	593.1	965.3	779.0	540.6	643.1	507.8	517.6	423.6	492.9	512.4	189.2	648.6	495.3
La	40.8	32.0	51.2	38.7	43.0	33.0	62.8	42.0	71.9	37.0	86.2	22.8	40.5	14.8
Ce	85.8	63.1	106.2	72.4	122.2	53.0	138.7	74.2	152.6	68.2	180.6	40.3	82.8	30.0
Sm	11.6	10.0	21.4	0.0	12.1	4.1	12.6	7.0	13.5	6.3	13.4	3.5	7.9	4.0
Yb	5.8	2.9	8.0	0.0	8.3	3.8	7.5	4.0	7.9	4.3	7.9	1.6	4.0	1.5
Hf	10.3	5.7	15.0	0.0	17.0	5.2	14.6	6.9	14.6	8.7	13.3	2.6	9.0	2.2
Pb	14.9	8.3	16.2	4.9	9.6	3.7	20.7	12.5	23.4	11.7	24.0	9.1	18.1	10.2
Th	7.2	4.7	5.5	4.6	13.6	4.2	12.2	7.9	13.2	8.3	22.6	6.6	8.6	6.9
U	2.7	1.3	3.0	1.3	4.3	0.6	5.6	3.4	6.1	4.1	7.9	3.5	5.8	1.9
(Wt%) Partial CIPW norms														
Q	25.59	10.28	23.12	13.49	33.48	1.88	31.06	7.58	31.61	4.03	25.18	6.96	28.41	10.34
C	0.45	0.74	0.46	1.02	0.00	0.00	0.05	0.11	0.03	0.07	0.00	0.01	0.72	2.21
Or	27.68	17.87	30.49	5.81	13.23	12.91	28.38	16.68	28.05	3.06	32.96	2.68	28.83	6.97
Ab	35.12	16.65	33.18	8.88	47.18	12.78	34.37	14.19	34.96	4.58	33.38	2.36	31.92	9.40
An	4.45	4.15	3.90	3.54	0.73	0.59	1.79	3.01	1.48	1.78	3.36	4.90	5.87	5.51
Di	0.50	0.68	0.45	0.60	1.07	1.25	0.42	0.48	0.39	0.44	1.69	0.67	0.41	0.89
Hf	1.42	1.41	0.53	0.54	0.51	1.13	0.81	2.07	0.50	0.78	0.47	0.77	1.35	1.85
Ol	0.00	0.00	0.00	0.00	0.00	0.00	0.00	0.00	0.00	0.00	0.00	0.00	0.00	0.00
Mt	0.49	0.86	0.13	0.28	1.92	1.13	1.22	0.97	1.42	1.00	1.24	0.78	1.21	0.64
Il	0.52	0.37	0.55	0.25	0.42	0.15	0.42	0.21	0.39	0.17	0.68	0.22	0.46	0.27

KEY TO UNITS (UAG - Upper Aillik Group JEA - Jagged Edge assemblage)

- 1.0 -- (UAG) Undivided volcanic and volcanoclastic rocks 1.3 -- (UAG) Hypabyssal Intrusive Rocks  
 1.0 (unaltd) -- As above, excluding M/N+K > 0.65 or < 0.3 1.4 -- (JEA) Volcanic and volcanoclastic rock  
 1.1 -- (UAG) Early sequence of Gover and Ryan (1988)  
 1.2 -- (UAG) Late sequence of Gover and Ryan (1988)  
 1.2 (unaltd) -- As above, excluding M/N+K > 0.65 or < 0.3

n1 -- Number of analyses for all elements except those listed below

n2 -- Number of analyses for Sc, Sn, Cs, Sm, Yb and Hf

Table 7.1 (continued)

UNIT	1.5		2.1		2.2		2.3		2.4		2.5		2.6	
n1	4		3		9		6		3		27		22	
n2	1		0		0		0		0		0		0	
(Wt%)	Mean	S.D.	Mean	S.D.	Mean	S.D.	Mean	S.D.	Mean	S.D.	Mean	S.D.	Mean	S.D.
SiO <sub>2</sub>	73.54	3.28	54.43	5.46	60.17	3.83	51.25	5.43	55.20	3.22	71.20	2.99	70.10	8.38
TiO <sub>2</sub>	0.28	0.15	0.69	0.14	0.73	0.10	1.41	0.82	0.71	0.02	0.34	0.11	0.37	0.23
Al <sub>2</sub> O <sub>3</sub>	11.90	2.17	13.38	2.76	15.36	1.16	16.78	1.01	15.77	0.64	14.22	1.12	13.80	1.67
Fe <sub>2</sub> O <sub>3</sub>	2.38	0.67	2.88	0.96	4.72	1.61	5.71	3.44	3.08	0.77	1.73	0.57	1.25	1.15
FeO	0.62	0.48	4.27	1.33	1.07	1.16	3.63	1.61	4.06	0.60	0.40	0.26	1.25	1.47
MnO	0.07	0.06	0.12	0.03	0.08	0.03	0.13	0.04	0.13	0.03	0.04	0.02	0.07	0.07
MgO	0.28	0.29	9.45	6.59	3.06	2.48	4.59	1.72	5.07	1.41	0.37	0.22	1.43	2.42
CaO	1.85	2.00	5.70	1.85	3.08	1.37	5.64	1.33	6.93	1.33	0.81	0.49	1.87	2.37
Na <sub>2</sub> O	2.38	1.29	2.90	1.43	3.75	0.75	3.25	0.83	2.92	0.41	4.20	0.91	3.60	0.66
K <sub>2</sub> O	5.80	0.85	2.92	0.81	4.67	1.53	2.63	0.55	3.31	0.35	5.20	0.90	4.93	1.31
P <sub>2</sub> O <sub>5</sub>	0.07	0.06	0.19	0.07	0.22	0.08	0.30	0.15	0.11	0.07	0.04	0.04	0.08	0.08
LOI	0.56	0.11	3.25	0.61	2.98	0.90	4.39	2.67	2.11	0.53	1.13	0.46	0.88	0.46
TOTAL	99.72		100.18		99.89		99.71		99.40		99.68		99.63	

(ppm)

Li	12.5	10.9												
F	551.3	377.6												
Sc	2.7	0.0												
V	21.8	14.9	141.3	22.6	107.4	37.6	182.8	46.4	182.3	54.7	11.4	6.8	37.2	53.7
Cr	7.0	2.6	682.7	594.5	208.3	273.6	57.3	67.6	114.7	57.5	4.9	0.4	44.2	93.7
Ni	1.0	0.0	274.0	231.0	88.9	97.5	36.3	20.4	46.3	13.5	13.7	5.3	20.9	21.8
Cu	17.3	24.2	58.7	43.8	10.9	19.9	10.5	14.9	4.0	3.5	2.4	1.5	6.0	11.2
Zn	54.3	10.0	54.7	4.2	49.6	20.4	114.8	51.9	66.0	3.5	33.1	12.9	43.2	53.4
Ga	8.8	2.9	12.0	2.7	15.4	2.9	20.0	6.1	16.0	1.0	15.2	2.7	13.9	2.2
Rb	183.5	44.6	74.3	9.5	123.9	45.1	86.8	28.8	92.7	17.8	169.7	40.0	163.7	40.6
Sr	148.8	164.0	407.7	103.9	375.0	150.8	388.7	165.3	499.7	100.0	134.3	96.9	173.9	185.9
Y	56.3	36.4	23.7	5.1	29.9	4.2	29.3	9.7	23.3	2.1	42.9	10.4	31.1	6.0
Zr	509.3	330.4	149.3	79.4	237.1	50.9	177.3	57.2	126.7	51.8	312.7	68.4	178.5	59.7
Nb	21.3	13.6	10.0	2.7	13.4	3.1	10.0	3.3	7.3	3.1	19.7	4.1	18.9	5.4
Mo	2.3	0.5												
Sn	5.0	0.0												
Cs	0.9	0.0												
Ba	721.5	812.0	899.7	328.5	1268.1	189.2	972.8	261.7	1080.3	257.5	983.2	540.1	614.0	551.9
La	54.0	14.7												
Ce	125.5	52.5												
Sm	10.5	0.0												
Yb	6.6	0.0												
Hf	12.0	0.0												
Pb	20.8	4.0	13.3	1.2	13.6	7.1	9.7	4.4	10.3	0.6	20.7	5.8	28.2	15.7
Th	14.3	12.6	4.7	4.7	9.0	5.4	5.5	5.3	1.3	0.6	17.4	6.5	14.0	6.6
U	6.4	3.0	1.0	0.0	2.1	1.8	1.7	1.0	1.0	0.0	3.4	2.0	3.1	2.0

(Wt%)

Q	34.51	5.73	3.73	3.81	10.65	5.81	6.16	5.22	4.65	4.06	24.94	5.59	25.00	13.18
C	0.21	0.33	0.00	0.00	0.26	0.52	0.66	1.04	0.00	0.00	0.36	0.43	0.31	0.41
Or	34.56	5.12	17.75	4.86	28.44	9.19	16.31	3.59	20.12	2.23	31.15	5.34	29.48	7.69
Ab	20.25	10.95	25.22	12.38	32.69	6.49	28.15	6.48	25.39	3.84	36.08	7.84	30.77	5.66
An	4.13	4.49	15.32	4.00	10.94	4.31	22.80	3.21	20.65	4.36	3.67	2.48	6.18	7.19
Di	0.33	0.62	10.17	6.49	2.84	3.42	3.87	3.60	11.45	2.12	0.19	0.36	2.15	4.02
Hx	0.55	0.81	15.15	6.69	7.01	6.51	6.87	6.35	11.34	2.94	0.88	0.61	2.60	4.31
Ol	0.00	0.00	6.38	11.05	0.00	0.00	3.76	5.83	0.15	0.25	0.00	0.00	0.76	2.70
Wt	1.44	1.19	4.29	1.44	0.88	1.42	5.08	2.16	4.59	1.12	0.48	0.58	1.40	1.65
Il	0.53	0.28	1.35	0.27	1.37	0.24	2.79	1.60	1.38	0.03	0.61	0.24	0.69	0.44

KEY TO UNITS : (JEA - Jagged Edge assemblage, BRG - Bruce River Group)

- |   |   |
|---|---|
| 1.5 -- (JEA) Hypabyssal intrusive rocks       | 2.4 -- (BRG) Basalt and andesite (Pearl Lake)         |
| 2.1 -- (BRG) Lowermost basalt and andesite    | 2.5 -- (BRG) Trachyte and Rhyolite (Sylvia Lake Fm)   |
| 2.2 -- (BRG) Andesite and Trachyte            | 2.6 -- (BRG) Undivided (mostly felsic) volcanic rocks |
| 2.3 -- (BRG) Basalt and andesite (Camel Lake) |   |

n1 -- Number of analyses for all elements except those listed below

n2 -- Number of analyses for Sc, Sn, Cs, Sm, Yb and Hf  
(For analytical details of BRG data, see Ryan, 1984)

### 7.2.2 General Geochemistry

#### Summary of Numerical Data

Mean compositions of various volcanic units are listed in Table 7.1. Data for the Bruce River Group are from Ryan (1984), and are subdivided into his six principal units.

The Upper Aillik Group in its type area is subdivided into "early" and "late" components (c.f. Gower and Ryan, 1987), hypabyssal intrusive rocks and unclassified samples (most of these are strongly recrystallized). The Jagged Edge assemblage is similarly subdivided into volcanic or pyroclastic rocks and hypabyssal intrusive rocks.

Major element compositions of all felsic rock types are closely similar. The mean composition of samples from the early Upper Aillik Group (c.f. Gower and Ryan, 1987) is sodic (i.e.  $\text{Na}_2\text{O} > \text{K}_2\text{O}$ ) compared to other subdivisions. However, this average is based on only 5 samples, and is radically different from representative compositions listed by Gower and Ryan (1987). It is, however, similar to the mean for these units in the Round Pond area reported by MacDougall (1988). There are problems in differentiating recrystallized arenites from rhyolites in the early Upper Aillik Group, and these averages are not necessarily "igneous" compositions. Undivided Upper Aillik Group rocks are similar in mean composition to the Late Upper Aillik Group and hypabyssal intrusive rocks. "Unaltered" mean compositions (for samples where  $0.3 < \text{N}/\text{N}+\text{K} < 0.65$ ) are similar to those for all data. This reflects complementary patterns of Na and K-metasomatism, with total alkali contents remaining approximately constant (see below).

Trace element patterns are broadly similar for all felsic units, but the Jagged Edge assemblage and Bruce

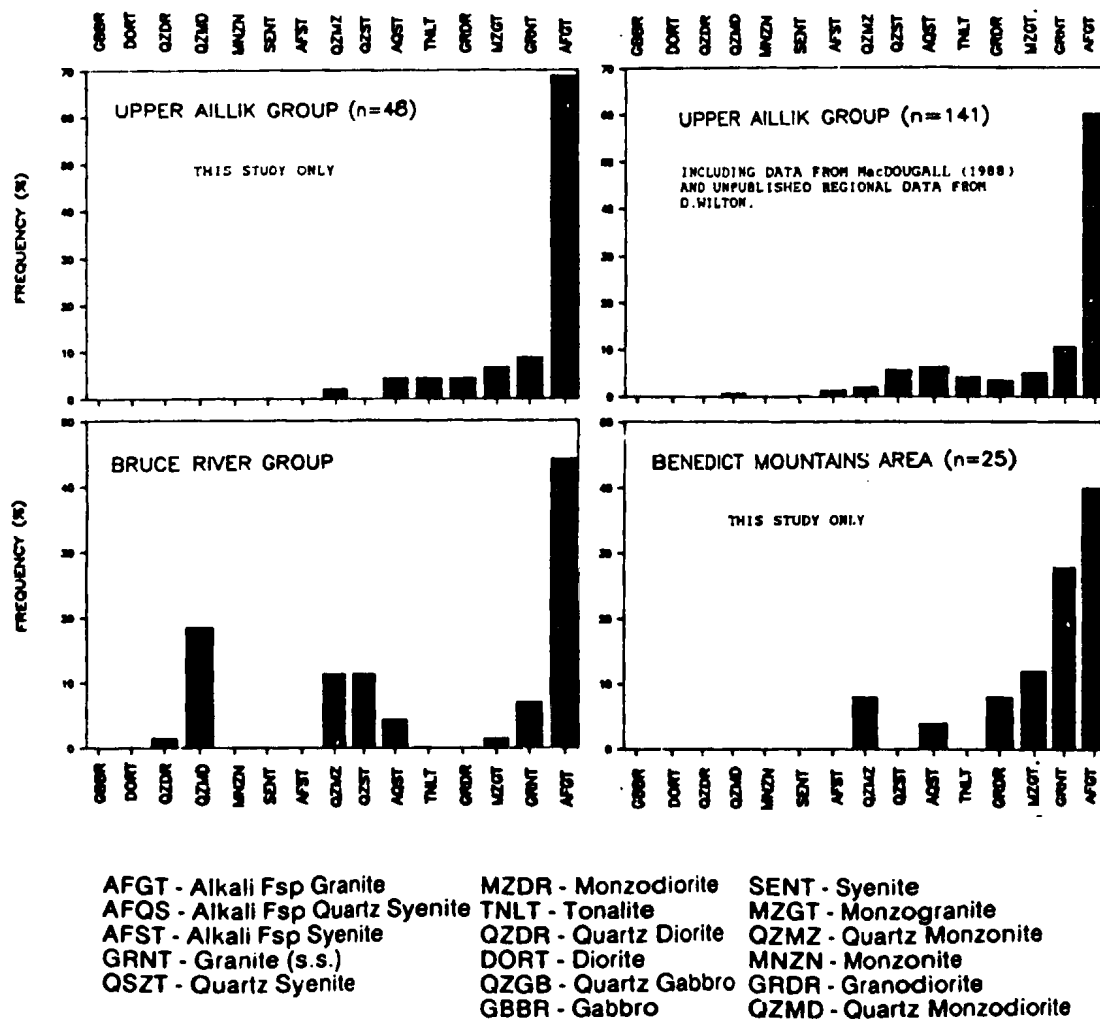


Figure 7.2. Relative abundance of IUGS rock types calculated from normative mineralogy after Streckeisen and LeMaitre (1979). Note that this is based on Barth mesonorms, not the CIPW norms listed in Table 7.2.

River Group display somewhat lower La, Ce, Zr and Y contents than the Upper Aillik Group. All volcanic sequences have relatively low fluorine contents.

#### **Abundance and Distribution of Rock Types**

Relative abundances of IUGS rock types, expressed as equivalent plutonic rocks (Figure 7.2) have been calculated from normative data using the method of Streckeisen and LeMaitre (1979). It is recognized that sampling is unstructured compared to that for plutonic suites, and that these patterns may not be fully representative.

The Upper Aillik Group is dominated by equivalents of alkali-feldspar granite, with only minor equivalents of granite, tonalite, monzogranite and granodiorite. Addition of regional data from D.Wilton (unpublished) and MacDougall (1988) does not change the distribution of rock types significantly. Note that mafic volcanic and tuffaceous rocks were not included in this compilation. The Jagged Edge assemblage includes a higher proportion of granite and monzogranite equivalents. If the data of Ryan (1984) are representative, the Bruce River Group has a strongly bimodal distribution of rock types. Alkali-feldspar granite equivalents are dominant, but there is a lesser population corresponding to quartz monzodiorite, quartz monzonite and quartz syenite. True basaltic compositions (i.e. equivalent to normative gabbro) are absent. Ryan et al. (1987) also note a bimodal  $\text{SiO}_2$  distribution in a larger dataset including unpublished data obtained from W.R.Baragar. The Upper Aillik Group has also been described as bimodal in previous studies (see above) but, on the basis of map areas, is poorer in mafic compositions.

### 7.2.3 Geochemical Trends and Contrasts

Geochemical data are divided into three groups (A, B and C) to avoid clutter in diagrams. The X-axis scales in Harker variation diagrams are expanded for the Bruce River Group to compensate for its greater  $\text{SiO}_2$  range. Y axis scales are constant for all figure groups.

#### **Major Element Patterns**

Major element oxides show expected trends. All except  $\text{Na}_2\text{O}$  and  $\text{K}_2\text{O}$  have strong negative correlations with  $\text{SiO}_2$  (e.g.  $\text{TiO}_2$  and  $\text{FeO}$  total; Figure 7.3).  $\text{K+N/A}$  (Agpaitic Index) values (Figure 7.3) are mostly  $> 0.9$  in the Upper Aillik Group, and several samples are peralkaline. There are no peralkaline rocks in the Jagged Edge assemblage or Bruce River Group, which show lower  $\text{K+N/A}$  at equivalent  $\text{SiO}_2$  contents. The Upper Aillik Group includes a few peraluminous samples (Figure 7.3), but most samples have  $\text{A/C+N+K} < 1.0$ . In contrast, ca. 50% of the Jagged Edge assemblage and Bruce River Group samples are peraluminous above 65%  $\text{SiO}_2$ .

Alkali disturbance in the Upper Aillik Group is indicated by variation of  $\text{N/N+K}$  ratios versus total alkali content (Figure 7.4). As noted previously (Evans, 1980; MacDougall, 1988), many Upper Aillik Group volcanic rocks lie outside the "igneous spectrum" of Hughes (1973). The Jagged Edge assemblage and Bruce River Group show less evidence of alkali disturbance.

AFM projections (Figure 7.5) are totally useless in unit discrimination. CNK projections (Figure 7.5) illustrate the alkali disturbance in the Upper Aillik Group well. Alkali-  $\text{SiO}_2$  plots (Figure 7.5) indicate that all volcanic suites are subalkaline, at least in terms of their present compositions.

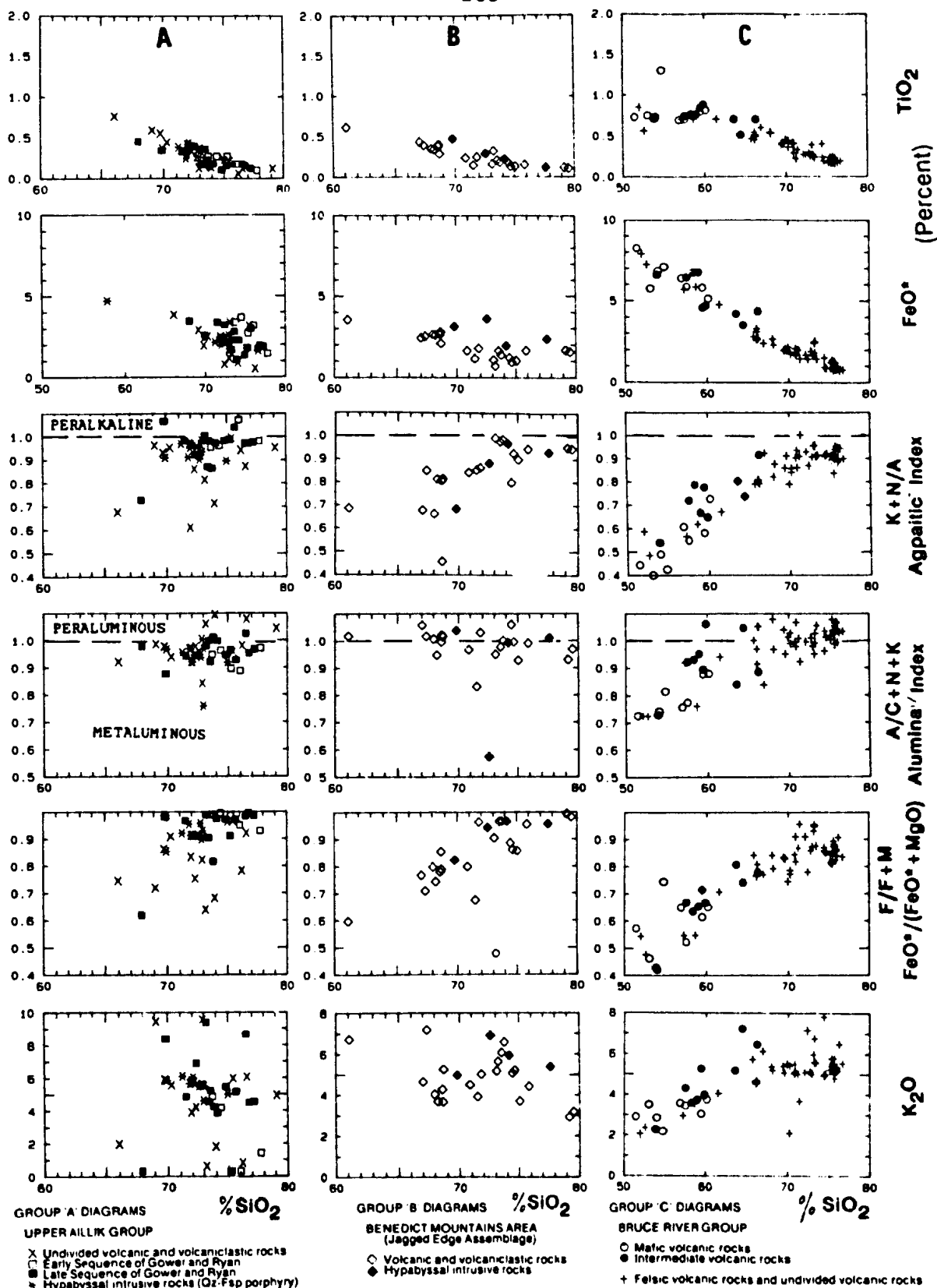


Figure 7.3. Variation of selected major elements and derived parameters in volcanic assemblages. See text for discussion.

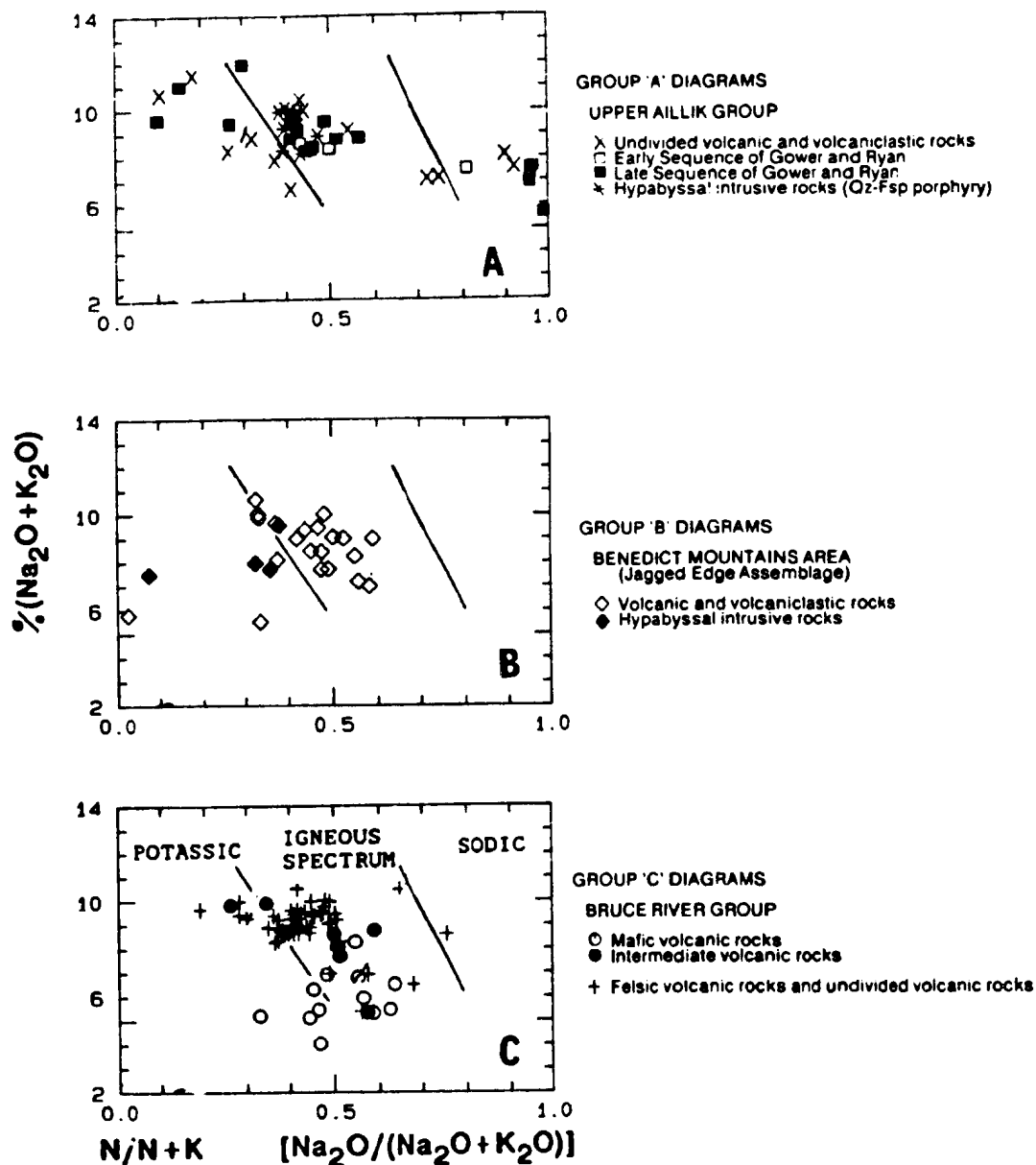


Figure 7.4. Variation in  $\text{N}/\text{N} + \text{K}$  ( $\text{Na}_2\text{O}/(\text{Na}_2\text{O} + \text{K}_2\text{O})$ ) and total alkali content in volcanic assemblages in relation to the igneous spectrum (after Hughes, 1973).



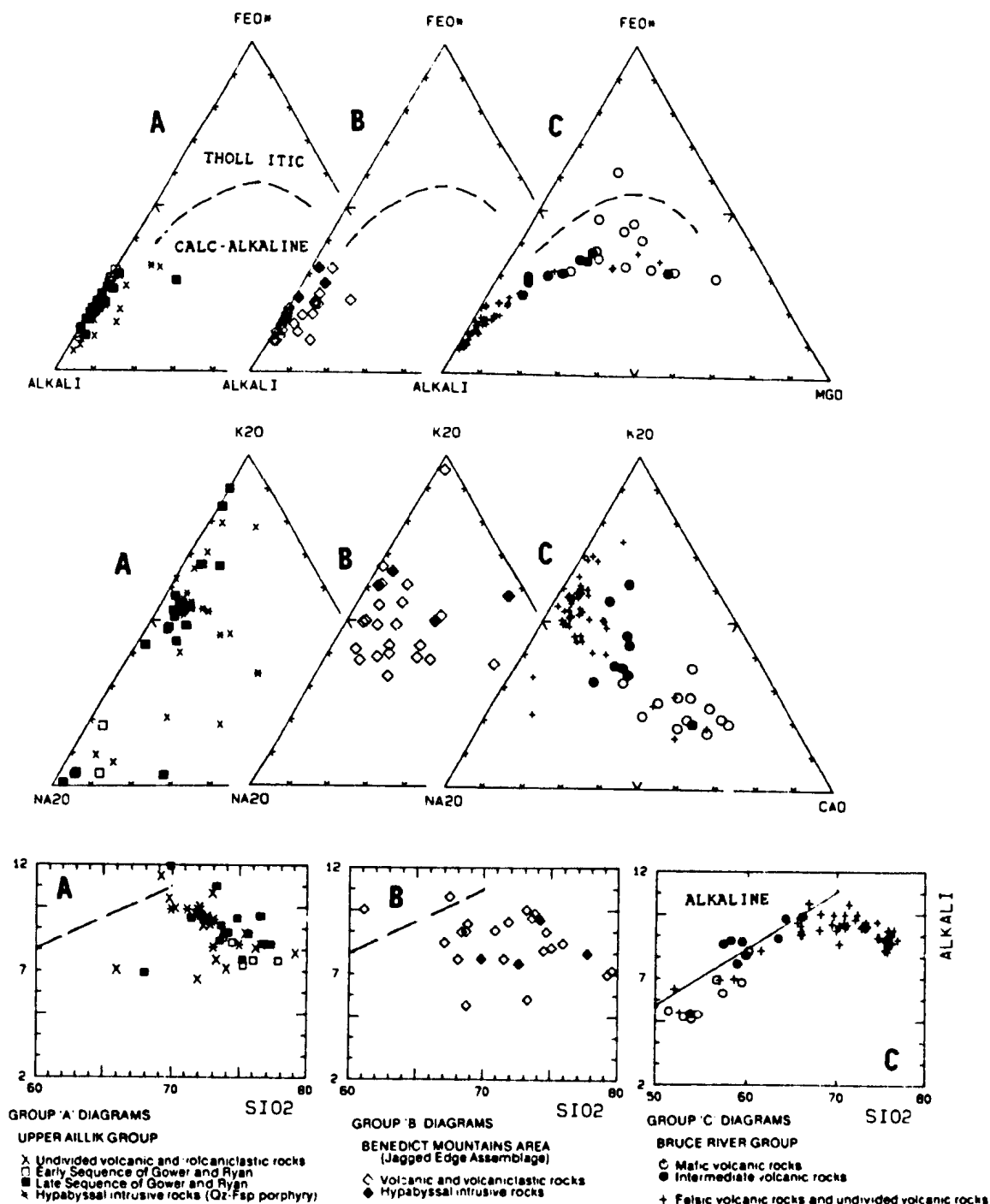


Figure 7.5 Ternary AFM and CNK projections, and binary  $\text{SiO}_2$ -Alkali projections for volcanic assemblages. See text for discussion.

### Normative Compositions

The Upper Aillik Group has a scattered distribution in the Q-Ab-Or-An system (Figure 7.6), due to alkali disturbance. The Bruce River Group has the most coherent distribution, but all volcanic sequences are scattered compared to plutonic suites described in preceding chapters (Figure 3.6, p.81; Figure 4.5, p.136; Figure 5.13, p.208). The felsic volcanic rocks of all sequences occupy the general area of ternary minima in the granite system (James and Hamilton, 1969).

### Trace Element Patterns

**Octahedrally Co-ordinated Cation (OCC) Elements :** Cu, Ni, Sc, Cr and V) have closely similar, negative trends against  $\text{SiO}_2$  and do not discriminate sequences (e.g. V; Figure 7.7). Mafic volcanic rocks of the Bruce River Group show the highest levels of these elements.

**Low-Field Strength (LFS) Trace Elements :** Incompatible LFS elements (e.g. Rb and U; Figure 7.7) have similar average abundances in all sequences (Table 7.1), but exhibit considerable scatter in the Upper Aillik Group, probably in response to alkali metasomatism. Volcanic rocks show much greater scatter than hypabyssal intrusive rocks.

Compatible LFS elements (e.g. Ba and Sr; Figure 7.7) show negative trends against  $\text{SiO}_2$ , but some high- $\text{SiO}_2$  Upper Aillik Group volcanic rocks show suspiciously high Sr and Ba. The convex-upward Ba trend in the Bruce River Group resembles patterns in compositionally expanded plutonic suites such as the Labradorian Mount Benedict Intrusive Suite (Chapter 5), but the felsic compositions do not show strong incompatible element enrichment.

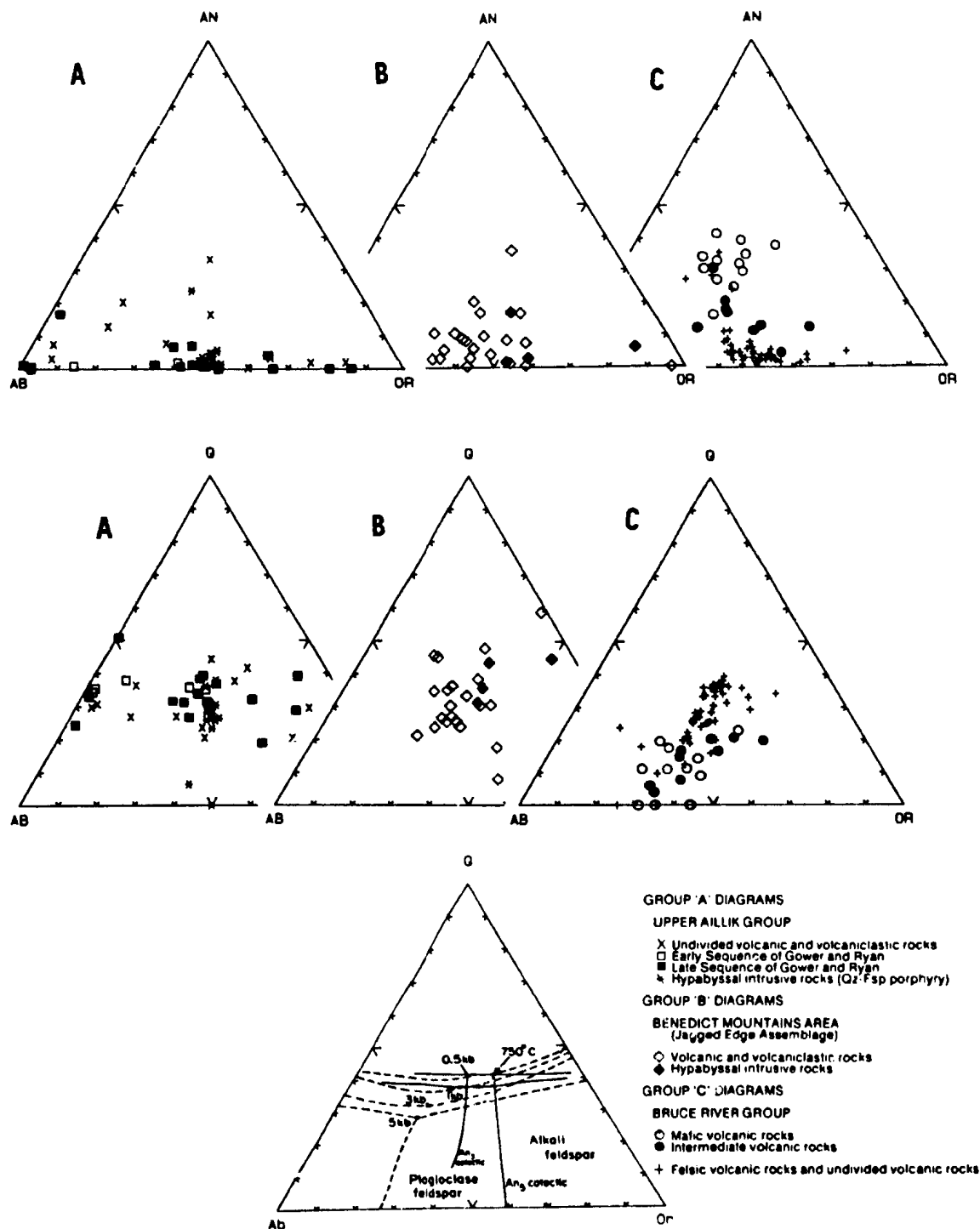


Figure 7.6. Composition of volcanic assemblages in the quartz - albite - anorthite - orthoclase quaternary system. All norms are CIPW. See text for discussion.

**High Field Strength (HFS) Elements** : Zr and Nb (Figure 7.8) are enriched in the Upper Aillik Group relative to the Bruce River Group and Jagged Edge assemblage volcanics. The volcanic rocks of the Upper Aillik Group show greater variation than hypabyssal intrusive rocks. Upper Aillik Group patterns closely resemble those of syn- and post-tectonic Makkovikian granites, in particular the Kennedy Mountain, Strawberry and Lanceground Intrusive Suites, whose distribution is indicated by dashed boxes in Figures 7.7 and 7.8.

**Rare Earth Elements (REE)** : Ce and Y (Figure 7.8) are enriched in the Upper Aillik Group relative to the Jagged Edge assemblage. Their distribution resembles those of HFS elements described above.

**Indeterminate Trace Elements** : Fluorine (Figure 7.7) is generally low ( $< 700$  ppm) in the Upper Aillik Group and Jagged Edge assemblage, but locally ranges up to 1500 ppm. There appears to be a negative trend against  $\text{SiO}_2$  in the latter sequence. Hypabyssal intrusive rocks have higher F contents than volcanic rocks, but not to the levels of some Makkovikian granites. Zn (Figure 7.7) has an inverse trend against  $\text{SiO}_2$  in the Bruce River Group (Figure 7.8), but is scattered in the Upper Aillik Group, where Zn contents are anomalously high above 70%  $\text{SiO}_2$ .

#### **Trace Element Variation in Response to Disturbance of Major Element Compositions**

Strong negative correlations are present between LFS trace elements (e.g. Rb, U, Pb, also Li) and  $\text{N}/\text{N}+\text{K}$  ratios (Figure 7.9), indicating that soda enrichment is

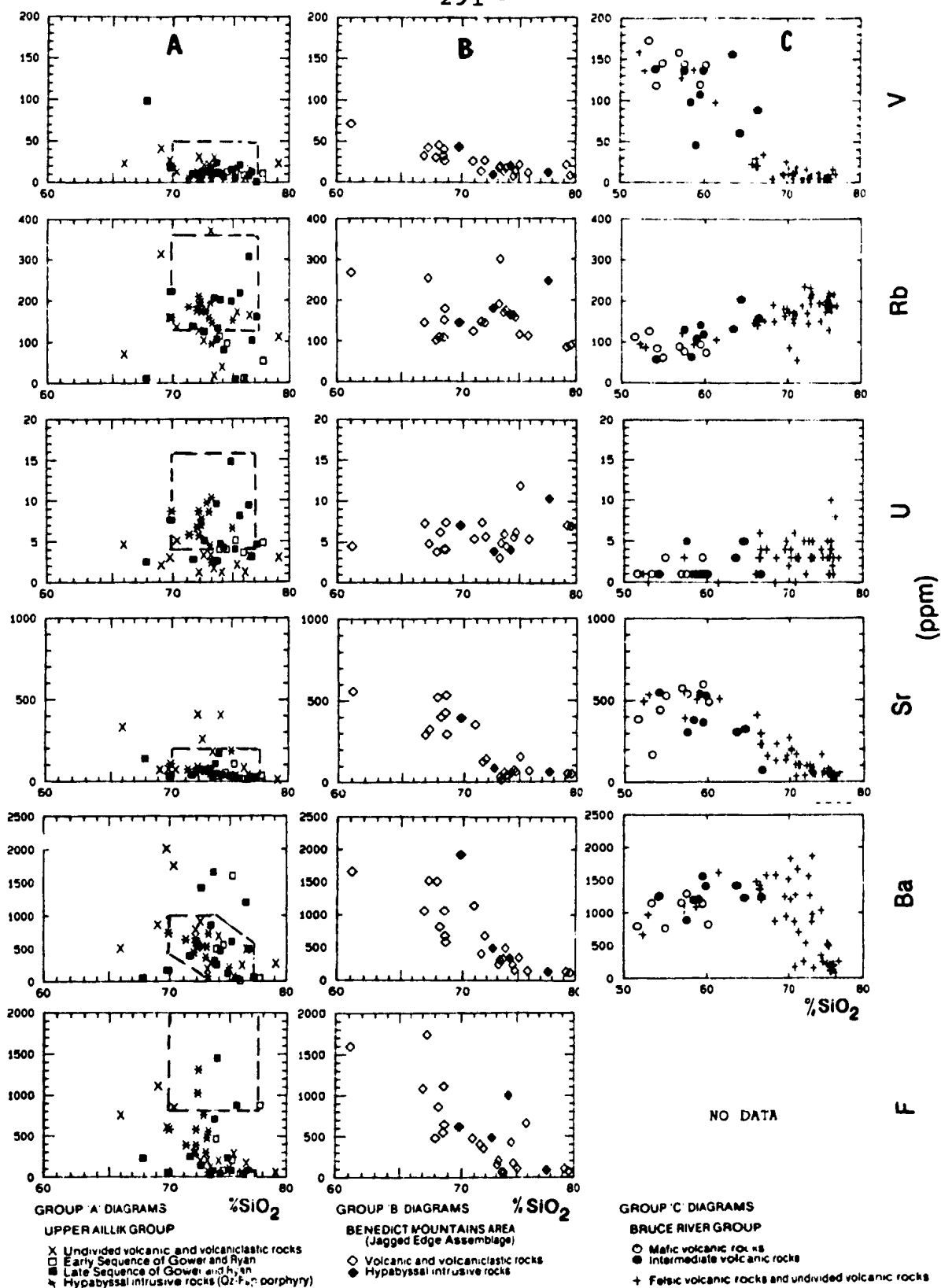


Figure 7.7. V, Rb, U, Sr, Ba and F versus  $\text{SiO}_2$  in volcanic assemblages. See text for discussion.

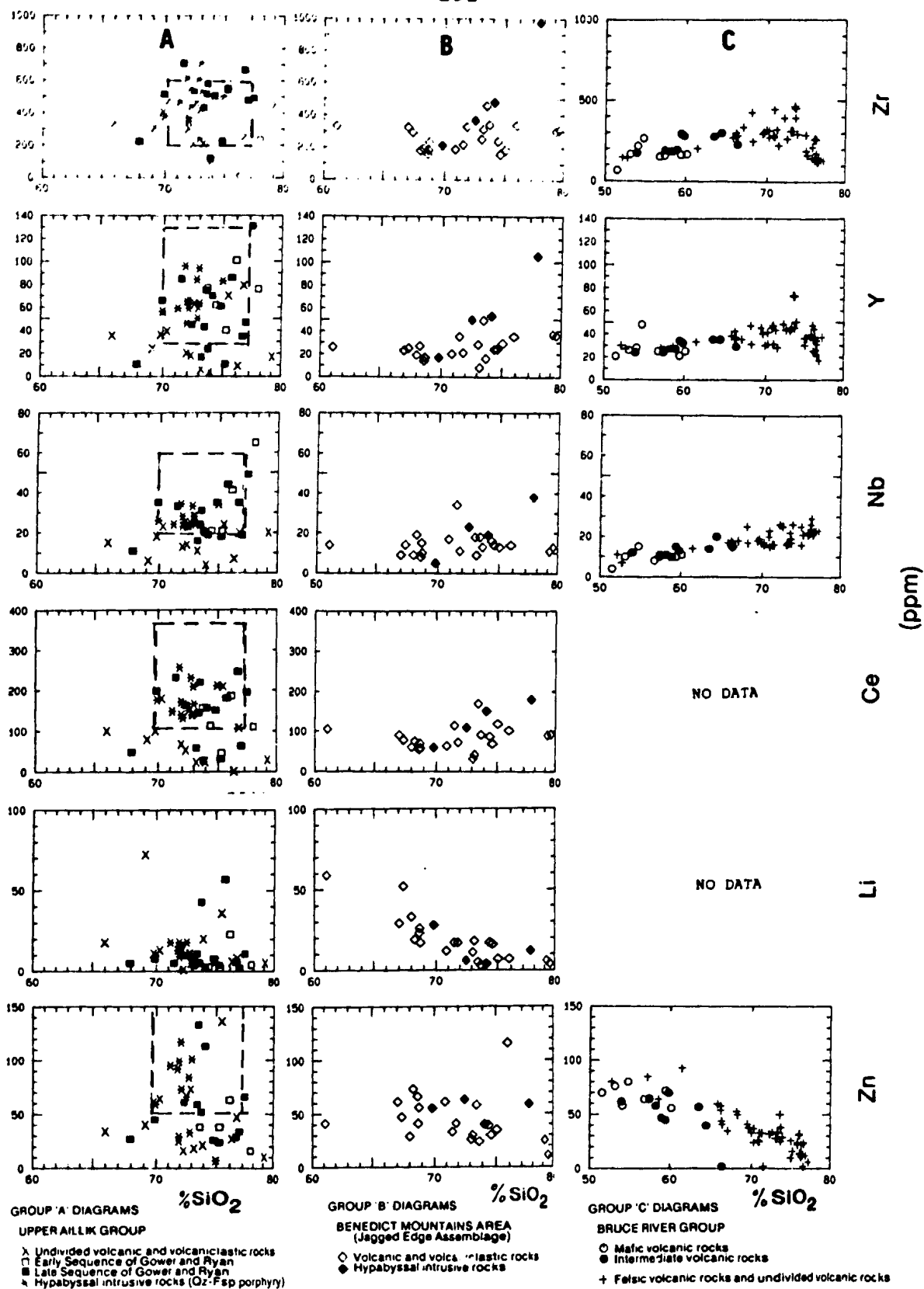


Figure 7.8. Zr, Nb, Y, Ce, Li and Zn versus SiO<sub>2</sub> in volcanic assemblages. See text for discussion.

accompanied by depletion of these elements, and potash enrichment by an increase. Other trace elements (e.g. Zr, Y and Nb) are uncorrelated with  $N/(N+K)$ , and fluorine is depleted in both sodic and potassic variants. This indicates that the higher Zr, Y and Nb in the Upper Aillik Group (compared to other sequences) is a primary feature, and unrelated to metasomatic effects. The patterns of alkali disturbance, and trace element behaviour, are remarkably similar to those documented from the plutonic rocks of the Kennedy Mountain Intrusive Suite (Chapter 3; Figure 3.9, p.86).

#### Trace Element Ratios

K/Rb ratios (Figure 7.10) are constant in all three groups of volcanic rocks at ca. 400 - 500, but the Upper Aillik Group includes a disturbed population with very low K/Rb.

Rb/Sr ratios (Figure 7.10) range from less than 0.1 to greater than 10 in all three suites, and show great variation in the Upper Aillik Group; this variation is almost certainly related to alkali metasomatism. In contrast, the Bruce River Group has a well-defined curvilinear trend, which becomes flat-lying in high-silica rocks.

Ba/Sr ratios (Figure 7.10) are obviously disturbed in the Upper Aillik Group, but show a consistent trend ( $Ba/Sr = 2$  to 4) in the Jagged Edge assemblage. The Bruce River Group has a curvilinear trend.  $La_N/Y_N$  ratios are consistent (ca. 10 to 20) in all groups, but the absolute abundances differ (see Figure 7.8 also)

Bruce River Group trends are consistent with removal of plagioclase ( $\pm$  mafic minerals) from less evolved

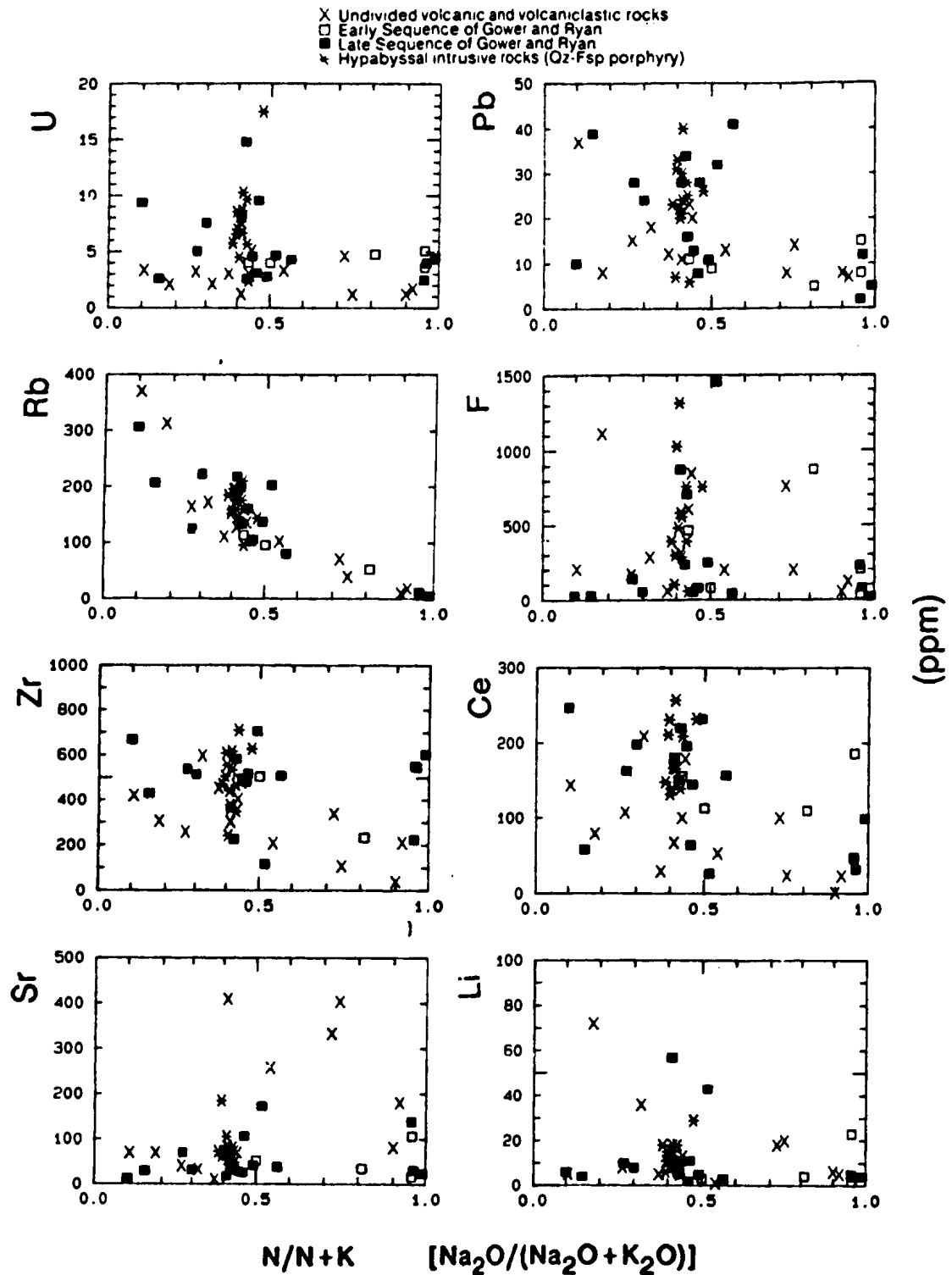


Figure 7.9. Variation of selected trace elements against N/(N+K) ( $Na_2O/(Na_2O+K_2O)$ ) for the Upper Aillik Group.



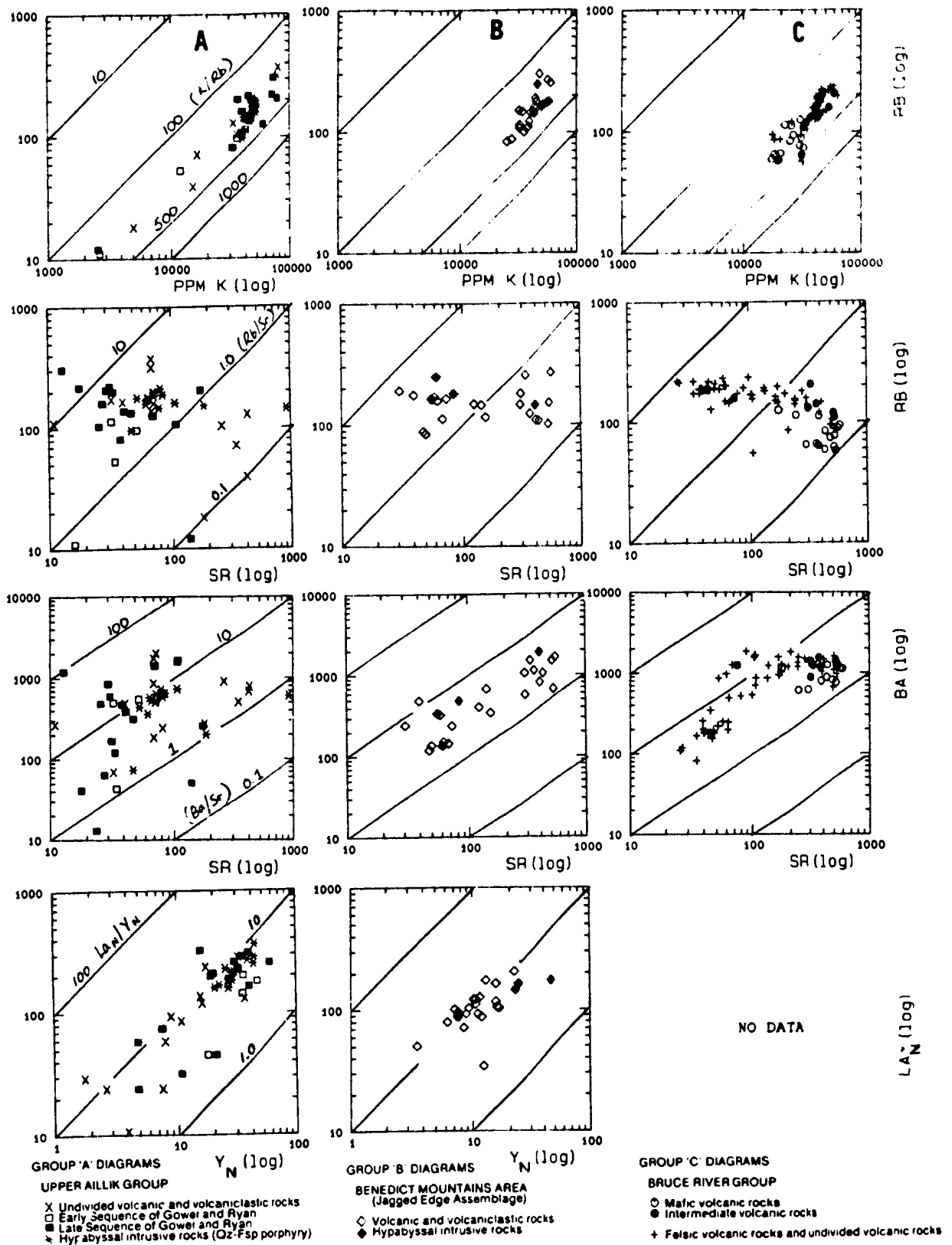


Figure 7.10. Variation in the trace element ratios K/Rb, Rb/Sr, Ba/Sr and  $La_N/Y_N$  in volcanic assemblages. See text for discussion.

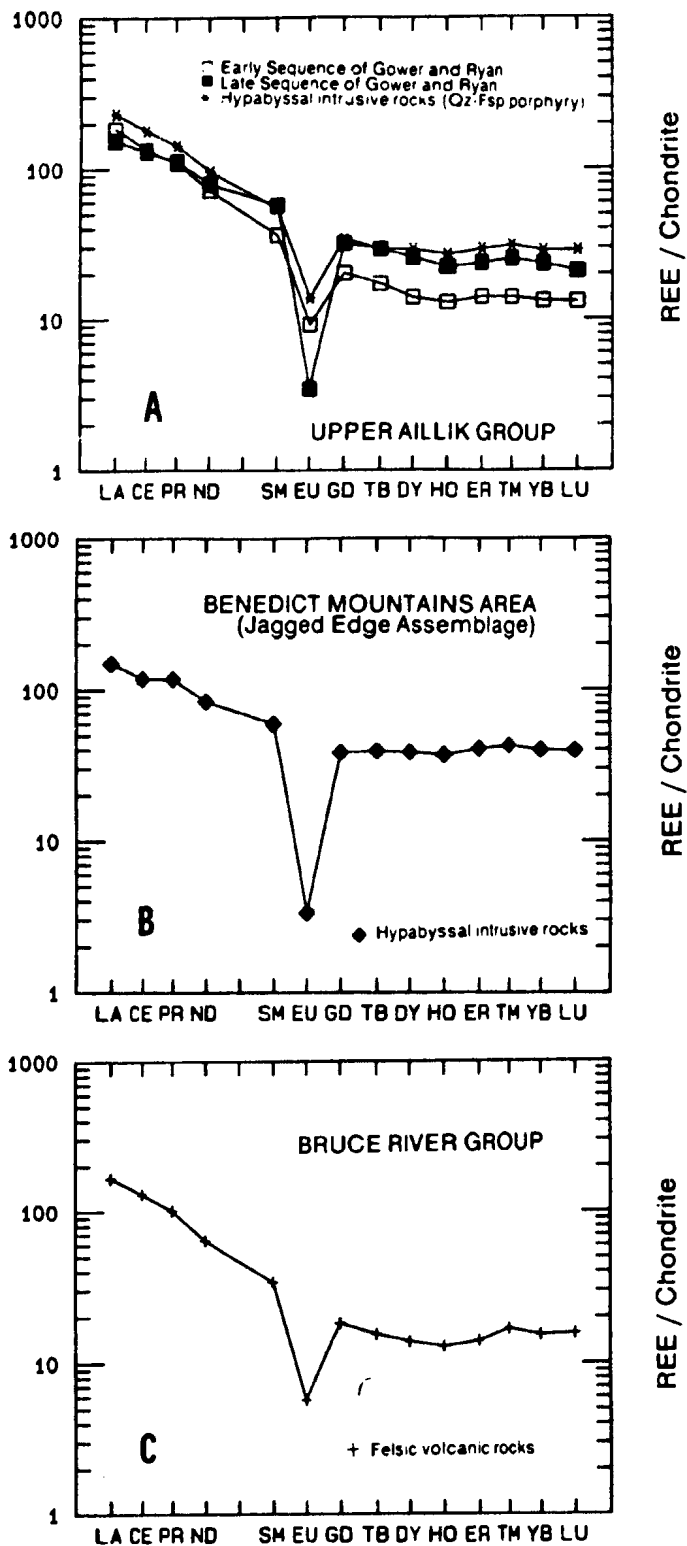


Figure 7.11. Rare Earth element (REE) patterns samples from volcanic assemblages. Values are normalized to chondritic values (listed in Appendix C).

compositions, and increased K-feldspar fractionation in more siliceous magmas. Jagged Edge assemblage trends are also consistent with feldspar fractionation. No conclusion can be drawn from Upper Aillik Group data.

#### **Rare-Earth Element (REE) Patterns**

Five samples were analyzed for the complete REE spectrum (Figure 7.11); samples from the Upper Aillik and Bruce River Group are from fresh, unaltered localities dated by Scharer et al. (1988). All have closely similar patterns, which are similar to those of Makkovikian and some Labradorian granites (Figures 3.11, p.91; 4.9, p.145; 5.17, p.216).

This similarity is not, however, an indication of a direct relationship between the volcanic sequences, as the White Bear Mountain porphyry is 50 Ma younger than other Upper Aillik volcanic rocks and 150 Ma older than the Bruce River Group (Schärer et al., 1988). Patterns are similar to those previously reported by White and Martin (1980), Gower and Ryan (1987) and Ryan et al. (1987) from the Upper Aillik and Bruce River Groups respectively.

### **7.3 SUMMARY and DISCUSSION**

#### **Correspondance of Volcanic and Plutonic Assemblages**

Table 7.2 compares the average compositions of volcanic and hypabyssal rocks of the Upper Aillik Group and Jagged Edge assemblage to granitoid plutonic units that have similar major element compositions.

With the exception of fluorine, trace element patterns for the Upper Aillik Group are very close to those of the Kennedy Mountain, Strawberry and Lanceground Intrusive

Table 7.2. A comparison of average compositions of volcanic assemblages to Makkovikian and Labradorian plutonic units of similar major element composition.

UNIT	1.0		1.1		1.2		1.3		11		23-26		27-29	
n1	13		5		16		14		97		197		82	
n2	3		5		15		13		22		142		66	
(wt%)	Mean	S.D.	Mean	S.D.	Mean	S.D.	Mean	S.D.	Mean	S.D.	Mean	S.D.	Mean	S.D.
SiO <sub>2</sub>	72.81	3.54	75.42	1.56	74.26	3.29	71.27	3.99	73.58	2.98	71.29	4.71	72.12	2.93
TiO <sub>2</sub>	0.32	0.22	0.22	0.08	0.23	0.11	0.36	0.11	0.29	0.19	0.31	0.27	0.32	0.19 <sup>a</sup>
Al <sub>2</sub> O <sub>3</sub>	13.61	1.59	11.75	0.24	12.49	1.35	13.61	1.80	12.67	1.15	13.68	1.55	13.22	1.34
Fe <sub>2</sub> O <sub>3</sub>	1.47	1.10	1.86	0.78	1.65	0.56	1.82	0.88	1.24	0.70	1.05	0.74	1.21	0.57
FeO	0.60	0.62	1.20	0.50	0.77	0.67	0.79	0.46	1.39	1.17	1.68	1.47	1.44	0.87
MnO	0.04	0.02	0.05	0.02	0.04	0.02	0.06	0.02	0.06	0.02	0.06	0.06	0.06	0.04
MgO	0.44	0.40	0.07	0.06	0.23	0.52	0.28	0.28	0.19	0.25	0.36	0.50	0.18	0.17
CaO	1.09	0.93	0.52	0.22	0.59	0.59	1.19	1.13	0.82	0.56	1.14	1.04	0.88	0.47
Na <sub>2</sub> O	4.02	1.90	5.62	1.60	4.08	1.62	3.90	0.28	4.00	0.48	4.09	0.86	3.97	0.61
K <sub>2</sub> O	4.67	2.89	2.22	2.17	4.77	2.81	5.52	0.45	4.85	0.64	5.12	1.10	5.47	0.90
P <sub>2</sub> O <sub>5</sub>	0.07	0.06	0.02	0.00	0.03	0.03	0.04	0.04	0.05	0.05	0.07	0.09	0.04	0.04
LOI	0.69	0.38	0.46	0.28	0.44	0.22	0.57	0.31	0.45	0.22	0.67	0.37	0.53	0.20
TOTAL	99.83		99.41		99.58		99.41		99.57		99.52		99.44	
(ppm) Trace Elements														
Li	16.5	19.0	7.4	8.8	11.7	15.4	13.1	6.2	14.9	11.7	25.0	23.5	13.9	11.7
P	378.5	339.8	331.8	346.3	272.0	401.2	541.1	343.2	1029.9	803.8	1420.0	1141	1244.6	935.7
Sc	1.7	0.9	1.8	1.4	2.2	1.9	4.8	2.7	1.4	0.9	3.1	4.1	3.8	5.3
V	21.1	9.6	11.4	1.7	18.4	22.1	13.3	9.9	15.9	13.4	23.3	29.2	12.8	7.7
Cr	6.0	10.4	7.2	11.8	7.6	8.2	5.9	3.7	4.7	3.8	5.1	6.5	3.7	2.9
Ni	2.5	3.3	5.4	9.8	1.4	1.5	2.0	2.8	1.3	1.2	2.2	3.9	1.5	1.8
Cu	4.2	3.4	14.6	24.3	4.7	3.7	6.9	8.8	3.9	3.9	9.3	38.4	6.0	9.2
Zn	44.0	34.1	66.8	64.9	86.1	81.0	77.8	41.7	77.1	29.9	75.1	69.6	89.6	59.6
Ga	12.6	4.3	24.2	6.7	15.4	6.9	11.5	6.7	16.5	6.8	16.9	8.6	21.4	10.0
Rb	138.1	105.8	56.4	48.2	139.4	86.2	168.2	28.8	153.5	47.1	178.4	65.0	172.5	44.1
Sr	156.4	144.7	48.8	35.1	53.4	46.3	140.9	226.4	60.8	77.5	111.7	130.2	61.2	65.8
Y	32.0	24.3	71.2	22.4	54.7	32.2	69.9	17.1	70.9	28.9	55.4	43.8	74.4	32.8
Zr	317.3	155.6	593.6	354.3	529.8	264.6	490.4	129.4	387.0	151.8	491.5	558.5	675.7	439.3
Nb	15.5	7.1	33.8	19.5	27.8	10.7	29.2	7.6	27.9	14.0	26.0	21.0	29.3	11.1
Mo	2.9	1.2	14.0	22.5	7.4	15.2	2.8	1.1	3.7	1.9	4.3	7.7	4.3	2.3
Sn	3.0	3.5	9.2	9.4	5.2	2.8	6.4	2.9	3.5	2.5	5.8	9.9	4.0	2.6
Cs	1.0	0.9	0.5	0.0	1.0	0.9	1.3	0.5	0.6	0.4	1.2	1.0	1.1	0.7
Ba	695.3	593.1	540.6	643.1	507.8	517.6	512.4	189.2	453.1	411.7	501.9	382.6	329.6	260.1
La	40.8	32.0	43.0	33.0	62.8	42.0	86.2	22.8	76.6	33.3	90.7	111.7	122.8	62.6
Ce	85.8	63.1	122.2	53.0	138.7	74.2	180.6	40.3	158.7	65.7	178.7	197.0	247.2	121.1
Sm	11.6	10.0	12.1	4.1	12.6	7.0	13.4	3.5	12.6	3.5	13.1	10.4	20.8	9.8
Yb	5.8	2.9	8.3	3.8	7.5	4.0	7.9	1.6	7.7	3.2	6.6	4.7	8.8	4.3
Hf	10.3	5.7	17.0	5.2	14.6	6.9	13.3	2.6	12.1	3.1	13.3	13.3	19.1	10.3
Pb	14.9	8.3	9.6	3.7	20.7	12.5	24.0	9.1	20.3	10.4	37.3	205.3	24.5	13.5
Th	7.2	4.7	13.6	4.2	12.2	7.9	22.6	6.6	15.2	9.6	18.3	20.5	18.9	8.0
U	2.7	1.3	4.3	0.6	5.6	3.4	7.9	3.5	4.7	3.0	5.8	7.0	5.5	2.3
(Wt%) Partial CIPW norms														
Q	25.59	10.28	33.48	1.88	31.06	7.58	25.18	6.96	29.80	6.01	24.90	9.23	26.22	7.51
C	0.45	0.74	0.00	0.00	0.05	0.11	0.00	0.01	0.02	0.06	0.12	0.23	0.10	0.70
Or	27.68	17.87	13.23	12.91	28.38	16.68	32.96	2.68	28.89	3.89	30.38	5.96	32.64	5.34
Ab	35.12	16.65	47.18	12.78	34.37	14.19	33.38	2.36	34.11	4.02	34.90	7.35	33.79	5.15
An	4.45	4.15	0.73	0.59	1.79	3.01	3.36	4.90	2.30	2.27	3.66	2.94	1.90	1.64
Di	0.50	0.68	1.07	1.25	0.42	0.48	1.09	0.67	1.08	0.87	1.28	2.82	1.62	1.35
Hy	1.42	1.41	0.51	1.13	0.81	2.07	0.47	0.77	1.22	2.00	2.15	2.26	0.96	1.05
Ol	0.00	0.00	0.00	0.00	0.00	0.00	0.00	0.00	0.00	0.00	0.03	0.26	0.00	0.00
Wt	0.49	0.86	1.92	1.13	1.22	0.97	1.24	0.78	1.58	0.75	1.38	1.00	1.63	0.77
Il	0.52	0.37	0.42	0.15	0.42	0.21	0.68	0.22	0.54	0.36	0.61	0.52	0.62	0.36

KEY TO UNITS (UAG -- Upper Aillik Group)

1.0 -- (UAG) Undivided volcanic and volcanoclastic rocks

1.1 -- (UAG) Early sequence of Gover and Ryan (1988)

1.2 -- (UAG) Late sequence of Gover and Ryan (1988)

1.3 -- (UAG) Hypabyssal intrusive rocks

11 -- Kennedy Mountain Intrusive Suite

23-26 -- Strawberry Intrusive Suite

27-29 -- Lanceground Intrusive Suite

n1 -- Number of analyses for all elements except those listed below

n2 -- Number of analyses for Sc, Sn, Cs, Sm, Yb and Hf

Table 7.2 (continued)

UNIT	29		WBM		1.4		45		46-47		44		48	
n1	41		11		21		70		34		67		49	
n2	31		11		6		57		29		39		11	
(Wt%)	Mean	S.D.	Mean	S.D.	Mean	S.D.	Mean	S.D.	Mean	S.D.	Mean	S.D.	Mean	S.D.
SiO <sub>2</sub>	72.84	2.75	72.28	1.25	71.62	4.37	73.50	4.42	73.24	3.22	70.69	3.31	68.54	4.42
TiO <sub>2</sub>	0.30	0.11	0.35	0.06	0.26	0.13	0.14	0.12	0.15	0.11	0.30	0.18	0.44	0.20
Al <sub>2</sub> O <sub>3</sub>	12.99	1.34	13.32	0.55	14.15	2.08	13.49	1.18	13.98	1.49	14.39	1.06	14.98	1.62
Fe <sub>2</sub> O <sub>3</sub>	1.07	0.39	1.57	0.33	1.28	0.55	1.08	3.23	0.61	0.45	0.97	0.40	1.20	0.61
FeO	1.35	0.68	0.73	0.33	0.70	0.51	0.70	1.56	0.62	0.31	1.09	0.66	1.87	1.01
MnO	0.06	0.03	0.06	0.02	0.05	0.02	0.05	0.04	0.04	0.01	0.05	0.02	0.06	0.03
MgO	0.17	0.15	0.21	0.09	0.50	0.55	0.21	0.24	0.18	0.13	0.38	0.27	0.86	0.54
CaO	0.82	0.42	0.81	0.25	1.40	1.13	0.76	0.44	0.78	0.36	0.97	0.49	2.04	1.02
Na <sub>2</sub> O	3.92	0.66	3.90	0.27	3.72	1.10	4.26	1.07	4.27	1.11	4.28	0.43	3.89	0.55
K <sub>2</sub> O	5.42	0.67	5.67	0.30	4.81	1.17	4.72	1.22	4.98	0.87	5.58	0.51	4.70	0.62
P <sub>2</sub> O <sub>5</sub>	0.04	0.02	0.04	0.02	0.06	0.04	0.03	0.03	0.02	0.03	0.05	0.06	0.15	0.09
LOI	0.50	0.18	0.46	0.09	0.95	0.72	0.58	0.27	0.50	0.13	0.75	0.11	0.77	0.24
TOTAL	99.48		99.48		99.49		99.48		99.37		99.50		99.50	

(ppm)

Li	14.6	15.2	12.5	4.2	19.0	14.7	20.5	13.6	20.7	19.8	25.3	11.0	25.7	12.5
F	1084.7	763.1	588.6	340.5	540.7	491.0	511.7	436.6	177.7	120.6	1240.5	617.4	679.1	257.1
Sc	3.2	1.7	4.5	1.0	3.4	1.4	1.4	1.2	1.9	1.2	2.9	1.7	6.8	2.4
V	13.8	7.4	11.5	6.3	25.8	14.8	17.4	18.1	14.6	6.8	23.1	13.1	44.6	30.2
Cr	3.8	3.3	5.3	3.0	19.0	55.3	4.0	6.4	3.5	3.8	6.5	3.8	6.5	7.0
Ni	1.8	2.4	1.4	1.2	5.3	14.9	1.4	1.3	1.7	2.1	1.9	1.7	2.1	3.0
Cu	4.7	3.5	8.2	9.6	6.9	5.1	9.2	20.2	3.8	3.7	10.1	8.8	9.1	18.7
Zn	82.8	59.0	69.4	34.6	44.9	22.9	34.9	30.5	28.8	10.9	39.9	14.0	46.9	21.4
Ga	16.2	7.3	8.7	1.0	7.8	1.7	12.0	6.6	11.7	5.8	8.6	2.1	12.8	4.1
Rb	167.1	52.5	176.3	20.4	156.3	58.2	181.7	71.7	191.1	68.2	315.3	81.3	140.5	38.7
Sr	60.0	68.8	86.5	34.8	216.6	187.0	134.5	210.4	87.1	75.8	126.8	108.3	277.7	154.8
Y	75.5	29.3	63.1	11.8	25.2	9.4	26.5	23.0	25.3	20.2	27.8	7.6	28.2	10.2
Zr	560.7	280.9	446.5	106.6	262.5	78.8	160.1	99.3	185.6	172.3	345.0	140.0	240.0	83.8
Nb	29.2	10.1	26.8	3.7	14.2	5.6	17.2	8.5	20.8	13.6	29.0	8.6	13.6	4.4
Mo	3.6	1.5	2.6	0.9	2.6	0.9	84.5	578.7	28.1	142.9	4.3	2.7	3.2	1.2
Sn	4.2	2.8	5.7	2.2	2.3	1.4	2.9	2.3	2.4	2.1	7.2	4.2	3.9	3.3
Cs	1.1	0.7	1.5	0.5	1.3	1.6	2.2	2.1	1.9	1.3	9.0	4.3	4.1	1.8
Ba	308.1	244.0	550.1	155.9	648.6	495.3	391.2	360.5	519.0	675.5	381.9	352.6	961.5	542.3
La	104.7	36.4	78.8	17.4	40.5	14.8	22.1	21.4	30.9	22.3	56.3	22.9	50.6	14.8
Ce	211.9	71.6	166.4	30.9	82.8	30.0	45.4	43.8	63.2	45.7	114.0	43.7	100.1	28.5
Sm	18.0	6.6	12.5	2.9	7.9	4.0	4.4	4.0	4.2	1.9	6.9	1.7	9.3	3.0
Yb	8.5	2.9	7.5	1.1	4.0	1.5	3.9	3.6	2.8	0.6	4.5	0.9	2.5	0.0
Hf	16.8	7.0	12.6	2.1	9.0	2.2	5.6	3.0	5.6	1.5	9.9	3.1	12.5	21.1
Pb	24.7	12.0	25.5	8.6	18.1	10.2	22.6	9.2	26.8	11.5	23.4	8.0	16.8	8.1
Th	22.3	7.3	21.5	4.4	8.6	6.9	13.6	8.5	19.1	9.2	37.5	13.8	14.8	7.3
U	6.3	2.4	7.6	1.8	5.8	1.9	6.0	5.1	7.4	5.0	10.4	4.4	4.0	2.4

(Wt%)

Q	27.49	7.01	26.50	3.51	28.41	10.34	28.99	5.57	26.82	9.65	22.13	7.27	22.14	8.29
C	0.01	0.05	0.01	0.02	0.72	2.21	0.25	0.24	0.26	0.21	0.12	0.24	0.26	0.36
Or	32.33	3.97	33.83	1.81	28.83	6.97	27.82	7.14	29.78	5.21	33.36	3.06	28.14	3.71
Ab	33.46	5.51	33.32	2.32	31.92	9.40	36.63	8.56	36.39	9.20	36.65	3.68	33.29	4.70
An	1.84	1.57	2.11	1.03	5.87	5.51	3.22	1.70	3.61	1.64	3.30	1.78	8.95	4.23
Di	1.50	1.17	0.89	0.38	0.41	0.89	0.25	0.72	0.16	0.41	0.79	0.82	0.49	0.74
Hy	0.92	0.89	0.27	0.55	1.35	1.85	0.86	0.99	0.87	0.62	1.41	1.11	3.77	2.10
Ol	0.00	0.00	0.00	0.00	0.00	0.00	0.00	0.00	0.00	0.00	0.00	0.00	0.00	0.00
Nt	1.50	0.57	1.24	0.69	1.21	0.64	1.29	4.96	0.82	0.46	1.36	0.59	1.76	0.90
Il	0.57	0.20	0.67	0.11	0.46	0.27	0.26	0.22	0.30	0.22	0.58	0.34	0.85	0.38

KEY TO UNITS

29 -- (Lanceground Intrusive Suite) Tarun Granite

WBM -- (DAG) White Bear Mountain porphyry body

1.4 -- (JEA) Volcanic and volcanoclastic rocks

45 -- Monkey Hill Intrusive Suite

46-47 -- Witchdoctor and Burnt Lake Granites

44 -- Mount Benedict Intrusive Suite (granitic unit)

48 -- Otter Lake - Walker Lake Granitoid

n1 -- Number of analyses for all elements except those listed below

n2 -- Number of analyses for Sc, Sn, Cs, Sm, Yb and Rf

Suites (see also Figures 7.7 and 7.8). They also resemble patterns from the post-tectonic Makkovikian Big River Granite (not listed). High Zn, Zr, Y and Nb contents are characteristic of all, but the plutonic rocks have higher REE abundances. Hypabyssal intrusive rocks show the closest similarity (including high fluorine); this is particularly so for the White Bear Mountain porphyry and the spatially associated Tarun granite (Table 7.2). Differences in fluorine content between volcanic and plutonic associations are to be expected, as volatile components would be lost in extrusive environments. The HFS element and REE patterns for the Upper Aillik Group are dissimilar to those of most Labradorian plutonic rocks of equivalent major element composition, although Zr contents are similar to parts of the Mount Benedict Intrusive Suite. LFS element patterns of all units are broadly similar; however, the Upper Aillik Group shows great scatter, and generally higher Sr contents than most plutonic rocks.

The close compositional similarity between the Upper Aillik Group and Makkovikian high-silica granites is consistent with, but not definitive of, a genetic link between them. In the case of younger components of the former, geochronological data (Loveridge et al., 1987; Scharer et al., 1988; Gandhi et al., 1988; Krogh et al., in prep.) indicate that they are of essentially the same age. However, the Upper Aillik Group also includes volcanic rocks of ca. 1850-1860 Ma age (Schärer et al., 1988); for which there are, at present, no recognized plutonic equivalents. The oldest syn-tectonic Makkovikian granitoid is of ca. 1840 Ma age (Deus Cape Granitoid, Krogh et al., in prep.). It appears that, although the Upper Aillik Group spans the time-period represented by compositionally

similar plutonic suites, it also includes older episodes of volcanism that show closely similar characteristics. Similarly, the younger (ca. 1760 Ma) post-tectonic plutonic rocks of the Strawberry Suite lie outside the known period of Upper Aillik Group volcanism.

#### Geochemical Disturbance in Upper Aillik Group Volcanic Rocks

Upper Aillik Group data collected in this study show clear evidence of soda and potash metasomatism. As sampling was conducted without reference to mineralization, this suggests that disturbance is a regional feature of the Upper Aillik Group, and not restricted to mineralized areas. However, as data in this study is somewhat biased towards areas near intrusive contacts, it could also be argued that this disturbance is linked to plutonic rocks. Hypabyssal intrusive rocks within the Upper Aillik Group, however, do not have disturbed compositions.

There is a striking similarity between these patterns and those identified in the foliated granites of the Kennedy Mountain Intrusive Suite (Chapter 3). As previously discussed (3.3), if these are indeed manifestations of the same event, it indicates post-volcanic, rather than syn-volcanic metasomatism with respect to extrusion of the Upper Aillik Group. The strong compositional similarity between the Upper Aillik Group and the Kennedy Mountain Suite (Table 7.2; Figures 7.7; 7.8) may indicate that they are in part equivalent. This is, however, difficult to prove without precise dates and evaluation of the proportions of ca. 1850 and 1800 Ma volcanism in the Upper Aillik Group. It should also be noted that there is also

some minor alkali disturbance in the post-tectonic Cape Strawberry Granite and the Labradorian Monkey Hill Intrusive Suite (Chapters 4 and 5). Alkali-metasomatism is probably a general feature of high-silica granitoid suites, but was obviously of greatest intensity in the Upper Aillik Group and Kennedy Mountain Suite.

#### **Contrasts Between Makkovikian and Labradorian Volcanic Sequences**

Geochemical contrasts between Makkovikian and Labradorian plutonic assemblages are subtle (chapters 3,4 and 5), and their compositions overlap. The differences between the Upper Aillik Group and Bruce River Group are, however, analogous to contrasts previously noted between their plutonic equivalents.

Specifically, The Bruce River Group evolves to peraluminous compositions, and shows generally lower levels of HFS elements and REE than the Upper Aillik Group, which evolves instead to "borderline-peralkaline" compositions. The latter characteristic could arguably be imposed via metasomatism, but the HFS element and REE patterns of the latter are also consistent with transitional alkaline or "A-type" character (e.g. Whalen et al., 1987), and are independent of alteration (see Figure 7.9). Previous conflicts over the affinity of Upper Aillik Group volcanism are explicable if, as this study suggests, it shares the characteristics of Makkovikian plutonism, i.e., it is alkali-calcic to slightly peralkaline in composition, rather than calc-alkaline in the original sense of the word.



The Jagged Edge assemblage is, broadly speaking, closer in composition to the Bruce River Group than the Upper Aillik Group. It also lacks alkali disturbance seen in the Aillik Group and (as noted previously), is extremely fresh. Such characteristics suggest a possible equivalence to the Labradorian plutonic assemblage, but there is no geochronological proof of this as yet. The only unequivocal Labradorian suite in the general area is the Mount Benedict Intrusive Suite, but the incompatible element enrichment and lower  $\text{SiO}_2$  content of these rocks does not correspond to the features of the Jagged Edge assemblage (Table 7.2). A further complication is provided by Nd isotope data, which give a distinctive mantle-like signature shared only by certain plutons of the Strawberry Intrusive Suite (Chapter 8). U-Pb zircon dating, preferably of a volcanic sample, is required to resolve these contradictions, and is planned. It is conceivable that these rocks are equivalents of the younger post-tectonic plutons such as the Strawberry Suite, but their geochemistry appears at variance with this interpretation.

It should be noted also that the data presented here do not cover all supracrustal rocks in the Benedict Mountains area, as Gower (1981) describes N or NE-trending foliations suggesting a Makkovikian age for localities on Double Island and Deus Cape.

## CHAPTER EIGHT ISOTOPE GEOCHEMISTRY

---

### Chapter Abstract

Variable disturbance of the Rb-Sr isotopic system in the study area limits geochronological applications of the method, particularly in high-silica, Rb-enriched, granitoid rocks. Nevertheless, Makkovikian emplacement ages were obtained for the Big River Granite ( $1798 \pm 28$  Ma) and Freshsteak Granitoid ( $1798 \pm 48$  Ma). Both units have low initial Sr isotope ratios ( $< 0.703$ ). An ambiguous age of  $1714 \pm 44$  Ma was obtained from the Stag Bay Granitoid. Data from the Lanceground Intrusive Suite yield an apparent age of 1695-1670 Ma, but evidence for loss of radiogenic Sr suggests that this is an underestimate. A composite isochron from the Strawberry Intrusive Suite yields a similar age, and an unreasonably low initial Sr isotope ratio ( $< 0.698$ ). This age is not in agreement with U-Pb ages of ca. 1760 Ma. High-silica granites of the Kennedy Mountain Intrusive Suite yield no useful Rb-Sr data, probably due to alkali disturbance and metasomatism.

Initial Sr isotope ratios from isochron studies of TLGB granitoid rocks in all areas generally lie within or slightly above the spectrum of mantle isotopic evolution. Few useful initial Sr isotope ratios can be obtained from single-sample Rb-Sr data, due to age uncertainties and generally high Rb-Sr ratios in granites. Also, the probable existence of depleted, granulite facies lower crust under the Archean Craton block limits the ability of Sr isotope data to distinguish mantle and crustal sources in this area. In contrast, Nd isotope geochemistry is much less sensitive to age and analytical uncertainty and, due to relatively constant Sm/Nd in crustal rocks, is a powerful indicator of source materials and their crustal residence periods.

Makkovikian plutonic and volcanic rocks display striking geographic variations in initial Nd isotopic composition. In the west of the area, Makkovikian units have  $\epsilon_{Nd}^{CHUR}$  of -3 to -14; these negative values indicate significant amounts of older (pre-1800 Ma) crust in their source materials. One unit (Brumwater Granite,  $\epsilon_{Nd}^{CHUR} = -14$ ) was derived entirely by anatexis of Archean crust, but most have  $\epsilon_{Nd}^{CHUR}$  values above those predicted for Archean crust at ca. 1800 Ma. It is suggested that they represent variable mixtures of juvenile, mantle-derived magma and older sialic crust. Simplified mixing calculations indicate from 25% to 40% Archean component in these magmas, using reasonable assumptions about the juvenile end-member.

In the east of the area, units with equivalent bulk elemental geochemistry have  $\epsilon_{Nd}^{CHUR}$  from +1 to +6 ; these positive values

preclude significant contributions from Archean material, and the higher values are similar to those postulated for a depleted mantle reservoir at ca. 1800 Ma. Older crustal components, if present, must have had short crustal residence times.

The sharp boundary between these contrasting domains is interpreted as the eastern limit of Archean lower crust in the study area. Granites of the Strawberry Intrusive Suite show an east-west shift in  $\epsilon_{\text{Nd}}^{\text{CHUR}}$  from +6 to -6 across this line. The geochemical continuity of the suite suggests that the eastern plutons must include crustal contributions of similar magnitude to those indicated by negative  $\epsilon_{\text{Nd}}^{\text{CHUR}}$  in the west. It is therefore suggested that the eastern domain is floored by Proterozoic sialic crust generated during pre-Makkovikian or Makkovikian orogenic events. The Cape Harrison Metamorphic Suite may represent part of this basement, but it does not fulfill all isotopic requirements for the Strawberry Suite.

The Nd isotopic compositions of Makkovikian magmas were clearly influenced by the nature of local sialic crust. This suggests that crust-mantle interaction took place via direct melting, assimilation and homogenization of lower crust by mantle-derived, presumably mafic, juvenile magmas.

Labradorian plutonic and volcanic rocks show significantly less variation in  $\epsilon_{\text{Nd}}^{\text{CHUR}}$ , and compositions from gabbro to alaskitic granite have consistent  $\epsilon_{\text{Nd}}^{\text{CHUR}}$  values -1 to +1, i.e. they approximate bulk-earth compositions of 0. Geographic variations are subdued compared to those amongst Makkovikian units. There is evidence for crustal contamination in suites that had mafic parental magmas (Adlavik and Mount Benedict Suites), but the covariance of isotopic and major element compositions suggests that this was a high-level process that accompanied fractionation. Even mafic rocks of the Adlavik Suite have modest  $\epsilon_{\text{Nd}}^{\text{CHUR}}$  values of ca. +1, significantly lower than depleted mantle at 1650 Ma.

Derivation of these magmas from an undepleted mantle reservoir is unlikely in view of above evidence for depleted sources at 1800 Ma, and suites with mafic parental magmas cannot be derived by anatexis of older crustal material. It is concluded that Labradorian magmas are also mixtures of crustal and depleted mantle materials, but that the proportions of each are relatively constant and largely independent of the nature of the local lower crust. The proportion of older crust, assuming it approximates the Archean terrane, is probably no more than 10-15%. Similar "bulk-earth" characteristics in Proterozoic granitoids of other shield areas have been attributed to efficient subcrustal mixing and homogenization, possibly via the subduction of continent-derived sediment, as documented by studies of modern arc systems. This is a plausible and attractive explanation for some Labradorian magmas, but direct derivation by anatexis of Makkovikian crust remains possible for some granitoid units that lack associated mafic compositions.

## Introduction

This chapter is concerned mostly with the use of Sr and (particularly) Nd isotopic systematics to constrain petrogenetic models. Rb-Sr geochronology is also employed in an attempt to determine the emplacement ages of several units. Although this method is inherently less precise than U-Pb zircon geochronology, it provides some constraints (probably minimum ages) that may be used to assign units to Labradorian or Makkovikian associations. Nd isotopic variations provide the best petrogenetic information, as Sr isotopic compositions are variably disturbed. Preliminary Nd isotope data from this project are reported by Kerr and Fryer (in press); this thesis provides data from a greater number of samples, and more detailed discussion of results.

## Analytical Methods

All Sr and Nd isotope ratios were measured via thermal ionization mass-spectrometry at Memorial University, following separation of Sr and Nd by standard ion-exchange methods.  $^{87}\text{Rb}/^{86}\text{Sr}$  ratios were determined by repeated high-precision Atomic Absorption (AA) Rb and Sr measurements at the Department of Mines Laboratory, and  $^{147}\text{Sm}/^{144}\text{Nd}$  ratios were measured directly by high-precision Inductively-Coupled Plasma (ICP) mass spectrometry at Memorial University. Concentrations of Rb and Sr were measured by AA (Dept. of Mines), and Sm and Nd concentrations were measured by ICP-MS (MUN). Details of isotope analysis procedures are given in appendix A. Precision for concentration data is estimated at  $\pm 5\%$ .

## 8.1 STRONTIUM ISOTOPE GEOCHEMISTRY

### 8.1.1 Rb-Sr Geochronology

#### Data and Methodology

Rb and Sr concentration and isotopic data employed in geochronology are listed in Table 8.1. All errors are within-run statistics quoted at the 95% confidence level ( $2\sigma$ ).

Isochron regressions were performed with a regression spreadsheet program written by H. Longerich of Memorial University, corresponding essentially to the method of York (1969). A decay constant for  $^{87}\text{Rb}$  of  $1.42 \times 10^{-11} \text{ yrs}^{-1}$  (Steiger and Jager, 1977) was used in all isochron regressions.

The Mean Square of Weighted Deviates (MSWD) is used to assess the presence of scatter not accounted for by analytical error (Brooks et al., 1972); regressions with a MSWD value above 2.5 are termed errorchrons, and their uncertainty in age is amplified by the square root of the MSWD ( $\sqrt{\text{MSWD}}$ ). Analytical uncertainties used as input for regression are the  $2\sigma$  within-run values listed in Table 8.1; these represent a good approximation to  $1\sigma$  errors based on duplicate analyses (Appendix A), and are a conservative estimate of analytical uncertainty.

#### Constraints From Previous Rb-Sr Investigations

Previous Rb-Sr geochronological studies in the study area indicate that the Rb-Sr isotopic system is commonly disturbed and that results must be interpreted with caution.

Table 8.1. Rb-Sr concentration and isotopic data used for age determinations. Some of the Sr data is also listed in Table 8.3. Note that  $^{87}\text{Rb}/^{86}\text{Sr}$  ratios are corrected for measured Sr isotopic compositions. See Appendix A for analytical techniques.

Sample Number	Unit or Comment	CONCENTRATIONS (ppm)		ISOTOPE RATIOS			
		Rb	Sr	87Rb/86Sr +/-	2 $\sigma$	87Sr/86Sr +/-	2 $\sigma$
BIG RIVER GRANITE							
0241137		193	79	7.209 +/-	71	0.887087 +/-	180
0241138		162	122	3.242 +/-	57	0.787668 +/-	110
0241158		150	117	3.070 +/-	31	0.781498 +/-	134
0241167		105	469	0.655 +/-	14	0.719634 +/-	52
0241538		132	126	3.081 +/-	74	0.779743 +/-	518
0241560		111	32	10.993 +/-	370	0.995702 +/-	1143
0241562		98	216	1.325 +/-	27	0.736004 +/-	104
FRESHSTEAK GRANITOID							
0241286		97	408	0.694 +/-	14	0.721194 +/-	106
0241290		85	85	2.983 +/-	38	0.779526 +/-	120
0241305		81	413	0.569 +/-	7	0.718135 +/-	35
0241307		106	69	4.472 +/-	93	0.816171 +/-	60
0241308		130	65	5.968 +/-	127	0.860213 +/-	62
0241325		126	354	1.029 +/-	17	0.727454 +/-	62
0241342		64	443	0.416 +/-	7	0.713432 +/-	76
STAG BAY GRANITOID							
0241164		134	116	3.347 +/-	60	0.783465 +/-	122
0241166		195	117	4.896 +/-	49	0.826132 +/-	72
0241253		65	801	0.236 +/-	5	0.709118 +/-	89
0249060		67	631	0.316 +/-	8	0.711426 +/-	69
AKZ-6		163	102	4.680 +/-	57	0.817134 +/-	60
LANCEGROUND HILLS GRANITE							
0241152		130	69	5.529 +/-	87	0.834173 +/-	440
0241154		178	19	28.729 +/-	381	1.368654 +/-	628
0241332	Pistol Lk Granite	155	24	19.828 +/-	295	1.192142 +/-	1050
0248125		168	28	18.313 +/-	189	1.140939 +/-	668
0248126		169	35	14.613 +/-	143	1.052059 +/-	874
0249038		178	17	32.973 +/-	301	1.503070 +/-	1574
STRAWBERRY INTRUSIVE SUITE							
0241391	Bayhead Granite	198	45	12.542 +/-	198	1.012539 +/-	296
AKZ-14	C.Strawberry Grnt	160	77	6.257 +/-	95	0.847986 +/-	82
AKZ-4	Dog Islands Grnt	153	76	5.984 +/-	111	0.842791 +/-	56
GSZ-1	Tukialik Granite	195	105	5.452 +/-	66	0.831219 +/-	230
GSZ-2	Tukialik Granite	164	19	27.009 +/-	283	1.349971 +/-	480
KENNEDY MOUNTAIN INTRUSIVE SUITE							
0241020	Kennedy Mtn Grnt	135	19	22.424 +/-	230	1.333317 +/-	462
0241043	Narrows Granite	196	96	6.001 +/-	41	0.849300 +/-	1080
0241044	Narrows Granite	198	95	6.148 +/-	38	0.853896 +/-	240
0241068	Narrows Granite	170	77	6.523 +/-	73	0.862445 +/-	99
AKZ-13	Narrows Granite	103	78	3.864 +/-	63	0.801955 +/-	390
0241041	Long Is. Qz-monzite	113	348	0.945 +/-	10	0.724362 +/-	62

NOTE: Errors in  $^{87}\text{Rb}/^{86}\text{Sr}$  are  $\times 10^{-3}$ , Errors in  $^{87}\text{Sr}/^{86}\text{Sr}$  are  $\times 10^{-6}$

In the west of the study area, several Rb-Sr ages (White, 1976; Kontak, in Ryan, 1984; Brooks, 1982) are 50 to 150 Ma younger than subsequent U-Pb zircon age determinations from the same units (Brooks, 1983; Schärer et al., 1988). Most units in the west have undergone at least minor Grenvillian tectonism, and isotopic disturbance may be a function of these effects (MacKenzie and Wilton, 1988), or of post-crystallization magmatic-hydrothermal activity (e.g. Walraven et al., 1986). Resetting of Rb-Sr ages is not, however, restricted to areas near the Grenville Front Zone, as the Round Pond Granite near Makkovik yields a suspiciously young Rb-Sr age of less than 1500 Ma (D.Wilton and C.MacDougall, pers. comm., 1988).

In the eastern part of the TLGB, ages ranging from  $1787 \pm 35$  to  $1677 \pm 77$  Ma from granitoid rocks in the Smokey area (Owen et al., 1988) are broadly in agreement with the ca. 1800 Ma U-Pb zircon ages subsequently obtained from undeformed TLGB granitoid rocks in the study area (Krogh et al., in prep.). Similarly, the  $1625 \pm 50$  Ma Rb-Sr age from the Mount Benedict Intrusive Suite (Brooks, 1982) agrees generally with its U-Pb zircon age of  $1650 \pm 10$  Ma (Krogh et al., in prep.).

In summary, there are indications that Rb-Sr geochronology can resolve Makkovikian and Labradorian associations in the east of the study area at least. Disturbance acts generally to lower apparent age, via partial homogenization (Faure, 1978) or hydrothermal loss of radiogenic Sr (e.g. Walraven et al., 1986). Rb-Sr ages are therefore regarded conservatively as minimum estimates of actual emplacement age.

### Big River Granite

Seven samples were analyzed (Table 8.1; Figure 8.1a). These are regional geochemical samples collected from a relatively small ( $< 20 \text{ km}^2$ ) area in the north-central part of the body. All but one have the characteristic pseudorapakivi texture of the unit; the exception (0241560) is a coarse-grained, equigranular granite.

The data define an isochron ( $\text{MSWD} = 0.83$ ), indicating an age of  $1798 \pm 28 \text{ Ma}$  ( $2 \sigma$ ), and an initial  $^{87}\text{Sr}/^{86}\text{Sr}$  ratio of  $0.70173 \pm 88$  ( $2 \sigma$ ). Sample 0241560 has a large error in  $^{87}\text{Rb}/^{86}\text{Sr}$ , but exclusion of this point does not affect the age significantly. The initial  $^{87}\text{Sr}/^{86}\text{Sr}$  ratio is consistent with mantle compositions at ca. 1800 Ma (Faure and Powell, 1972), and the age is geologically reasonable\*. It is therefore interpreted to date crystallization, and indicates that the Big River Granite is a post-tectonic Makkovikian Intrusion.

### Freshsteak Granitoid

Seven samples were analyzed (Table 8.1; Figure 8.1c,d). These are regional samples clustered in the centre of the body; all are typical medium-grained melanocratic granitoid rocks, and show variable, but slight, recrystallization.

The data define an errorchron ( $\text{MSWD} = 4.67$ ), indicating an age of  $1776 \pm 80 \text{ Ma}$  ( $2 \sigma$ ), and an initial  $^{87}\text{Sr}/^{86}\text{Sr}$  ratio of  $0.70288 \pm 94$  ( $2 \sigma$ ). If the age error is amplified

---

\* NOTE : Just prior to submission of this thesis, a U-Pb zircon age (concordant) of  $1802 \pm 2 \text{ Ma}$  was obtained from this unit (Krogh et al., in prep.). This confirms (with greater precision) the Rb-Sr age obtained here.



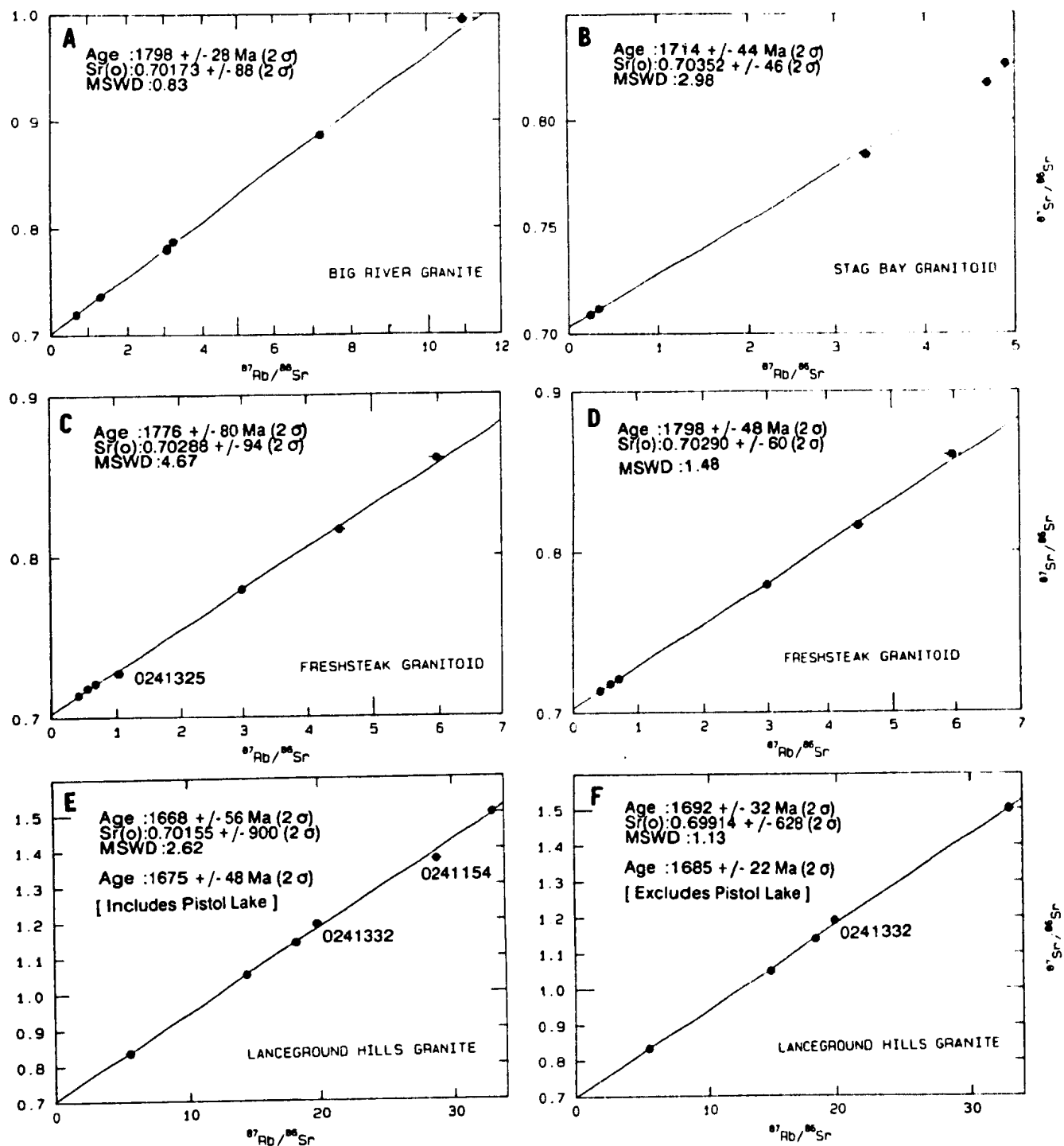


Figure 8.1. Rb-Sr isochron diagrams. (a) Big River Granite. (b) Stag Bay Granitoid. (c,d) Freshsteak Granitoid. (e,f) Lanceground Hills Granite (e,f). See text for discussion.

by  $\sqrt{\text{MSWD}}$ , this becomes an inconclusive  $1776 \pm 173 \text{ Ma}$  ( $2 \sigma$ ). The high MSWD is a largely due to sample 0241325. If this is excluded, the data define an isochron ( $\text{MSWD} = 1.49$ ) indicating an age of  $1798 \pm 48 \text{ Ma}$  ( $2 \sigma$ ) and an initial  $^{87}\text{Sr}/^{86}\text{Sr}$  ratio of  $0.70290 \pm 60$  ( $2 \sigma$ ). Sample 0241325 is saussuritized and epidotized relative to the other samples, and contains chlorite. Its position to the right of the isochron is consistent with a loss of radiogenic Sr, and the second result is thus preferred. Both age and initial ratio are geologically reasonable, and indicate that the Freshsteak Granitoid is a Makkovikian intrusion, of generally similar age to the Big River Granite.

#### Stag Bay Granitoid

Five samples from this unit were analyzed (Table 8.1; Figure 8.1b). These are regional geochemical samples distributed around Stag Bay, plus a geochronology sample (AKZ-6). The data define an errorchron ( $\text{MSWD} = 2.98$ ), indicating an age of  $1714 \pm 44 \text{ Ma}$  ( $2 \sigma$ ), and an initial  $^{87}\text{Sr}/^{86}\text{Sr}$  ratio of  $0.70352 \pm 46$  ( $2 \sigma$ ). In view of the small number of samples, this is regarded here as an isochron. (c.f. Brooks et al., 1972; Fryer and Taylor, 1985).

The initial ratio is reasonable, but the age is between Makkovikian and Labradorian episodes, yet similar to Rb-Sr ages reported from granites in the Smokey area (Owen et al., 1988). As a minimum, it suggests a Makkovikian age \*, but the error suggests a younger limit of 1670 Ma.

---

\* NOTE : Discordant U-Pb zircon data (Krogh et al., in prep., see note on p.243) indicate that this Rb-Sr age is too young, and the unit is 1790 - 1805 Ma old, i.e. of similar age to the Big River and Freshsteak units.

### Lanceground Intrusive Suite

Five samples from the Lanceground Hills Granite (within an 8 km<sup>2</sup> area), and one from the adjacent Pistol Lake Granite, were analyzed (Table 8.1; Figure 8.1e,f). All have high Rb/Sr ratios and are thus susceptible to loss of radiogenic Sr (c.f. Faure, 1978; Walraven et al., 1986).

Data for the Lanceground Hills Granite alone almost define an isochron (MSWD = 2.62) indicating an age of 1668 ± 46 Ma (2  $\sigma$ ), and an initial <sup>87</sup>Sr/<sup>86</sup>Sr ratio of 0.70155 ± 900 (2  $\sigma$ ). Sample 0241332 lies very close to this line, suggesting a similar age; regression of all data gives 1675 ± 48 Ma (2  $\sigma$ ). The large uncertainty in initial <sup>87</sup>Sr/<sup>86</sup>Sr ratio reflects the very high <sup>87</sup>Rb/<sup>86</sup>Sr (5 - 33) of all samples.

One sample (0241154) lies below the regression line. It is probable that this sample has lost radiogenic Sr, and the same may also be true of others. If it is excluded the fit is much better (MSWD = 1.13), and the age becomes 1692 ± 32 Ma (2  $\sigma$ ) or 1685 ± 22 Ma without the Pistol Lake Granite sample. Both produce unreasonably low (< 0.70) initial <sup>87</sup>Sr/<sup>86</sup>Sr ratios, but with large uncertainties.

It is suggested that post-crystallization hydrothermal effects have reduced the apparent age with partial retention of isochron behaviour, similar to effects described by Walraven et al (1986). The age is thus interpreted as an underestimate, and the Lanceground Suite is regarded as a Makkovikian association, consistent with its distinctive trace element geochemistry (see 4.2).

### Strawberry Intrusive Suite

Several samples analyzed from this suite as part of regional isotope geochemistry (see below) can be used to

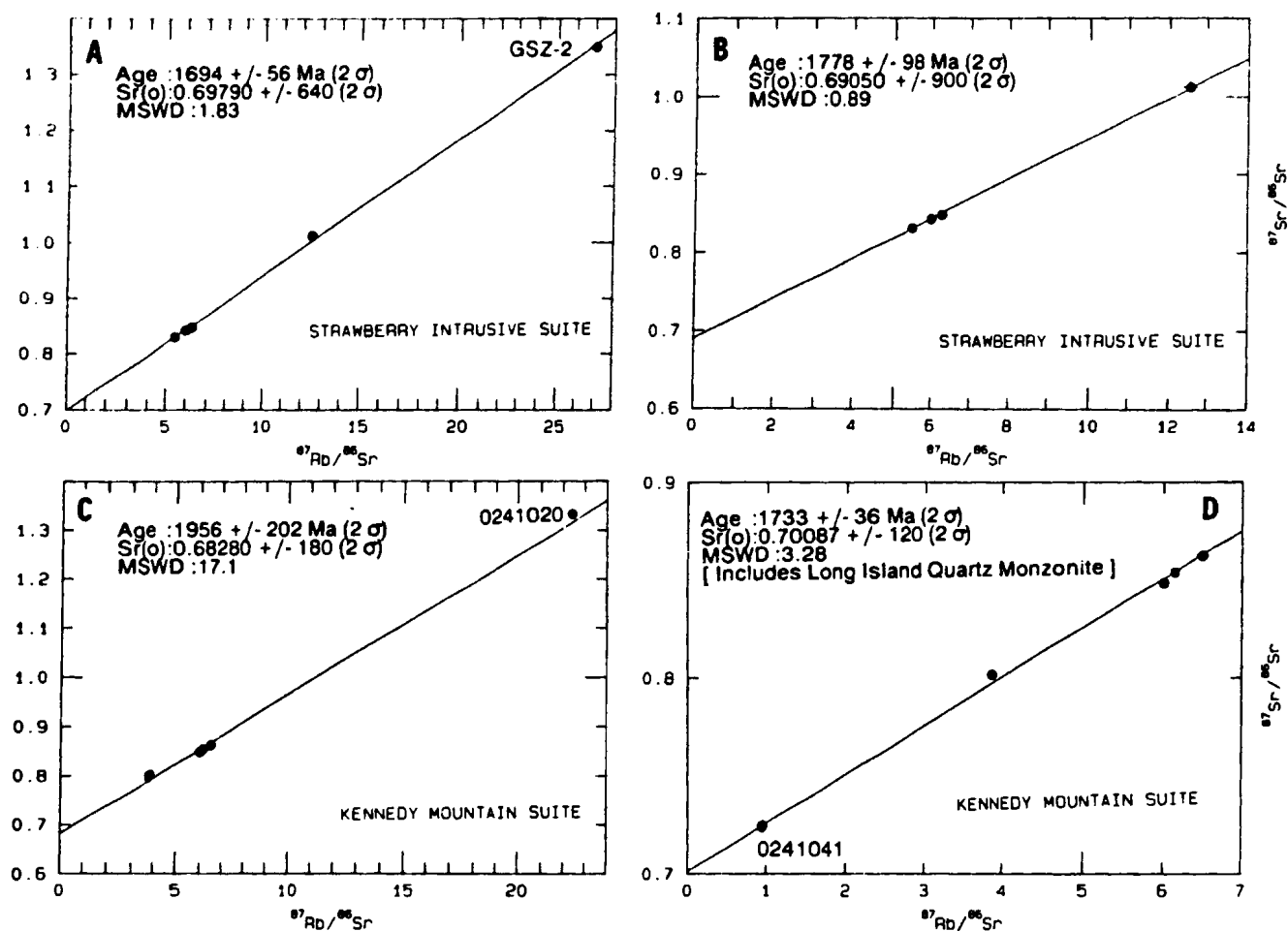


Figure 8.2. Composite Rb-Sr isochron diagrams. (a,b) Strawberry Intrusive Suite. (c,d) Kennedy Mountain Intrusive Suite. See text for discussion.

construct a composite isochron, but this is vulnerable to differences in initial  $^{87}\text{Sr}/^{86}\text{Sr}$  between plutons. Five samples from the suite (Table 8.1; Figure 8.2a) define a surprisingly good line (MSWD = 1.83) yielding an age of  $1694 \pm 56$  Ma ( $2\sigma$ ), and an initial  $^{87}\text{Sr}/^{86}\text{Sr}$  ratio of  $0.69790 \pm 640$  ( $2\sigma$ ). The large uncertainty in the initial ratio is due to the high  $^{87}\text{Rb}/^{86}\text{Sr}$  of all samples.

The slope of this line is controlled by the most Rb-rich samples, in which isotopic disturbance is likely. If GSZ-2 is excluded (Figure 8.2b), the age becomes  $1778 \pm 98$  Ma ( $2\sigma$ ), but the initial  $^{87}\text{Sr}/^{86}\text{Sr}$  ratio is unreasonably low ( $0.69050 \pm 900$ ). Results are similar to those from the Lanceground Hills Granite (see above), but younger than the ca. 1760 Ma age indicated by U-Pb zircon data (Krogh et al., in prep.) for the Cape Strawberry Granite. The apparent Rb-Sr age is probably not significant in view of source differences between plutons indicated by Nd isotope data (see 8.2.2) and the high probability of disturbance in these rocks.

#### Kennedy Mountain Intrusive Suite

As discussed previously (3.2, 3.3), there is strong evidence for alkali-metasomatism in some members of this suite, and thus no reason to expect coherent isotopic behaviour. Four samples (mostly from the Narrows Granite; Table 8.1; Figure 8.2c) define an errorchron (MSWD = 17) indicating an age of  $1956 \pm 202$  ( $2\sigma$ ), and an impossible initial  $^{87}\text{Sr}/^{86}\text{Sr}$  ratio of  $0.68280 \pm 180$ . If amplified by  $\sqrt{\text{MSWD}}$ , the age error is huge ( $> 800$  Ma). The slope is controlled by sample 0241020, which has a very high  $^{87}\text{Rb}/^{86}\text{Sr}$  ratio, and is probably disturbed.

As the unit intrudes the Upper Aillik Group, it cannot be older than 1860 Ma, and this "age" is meaningless. A more reasonable errorchron (MSWD = 3.28) age of  $1733 \pm 36$  ( $2 \sigma$ ) with an initial ratio of  $0.70087 \pm 120$  ( $2 \sigma$ ) is obtained if 0241020 is excluded (Figure 8.2d), and a sample from the possibly related Long Island Quartz Monzonite added. The rationale for doing this is, to say the least, tenuous, and no conclusions are drawn from these data.

### 8.1.2 Regional Variations In Sr Isotope Geochemistry

#### **Sr<sub>i</sub> Variation : Isochron Studies**

Table 8.2 lists Sr<sub>i</sub> values from the isochrons discussed above (preferred solutions), and published and unpublished data compiled from other Rb-Sr studies of TLGB granitoid rocks (sources listed in table). It should be noted that some of these ages are known, or suspected, to be disturbed, and their Sr<sub>i</sub> values are similarly suspect. In most isochrons, however, Sr<sub>i</sub> is fixed by the sample with lowest Rb/Sr and is hence less subject to disturbance than is the age.

Sr<sub>i</sub> values from isochrons in all parts of the TLGB fall dominantly within the field of  $^{87}\text{Sr}/^{86}\text{Sr}$  ratios for the mantle in the interval from 2000 to 1400 Ma (Figure 8.3a; Faure and Powell, 1972). Isochrons with Sr<sub>i</sub> below mantle evolution are mostly known to be disturbed. Several Sr<sub>i</sub> values lie above the mantle spectrum; these include the Makkovikian Island Harbour Bay Intrusive Suite (data of Grant et al., 1983), and possibly disturbed isochrons from the Labradorian Witchdoctor, Burnt Lake and Otter Lake - Walker Lake units. There is no apparent systematic variation in Sr<sub>i</sub> values between different portions of the TLGB.

Table 8.2. Initial Sr isotopic compositions calculated from Rb-Sr isochrons throughout the Trans-Labrador Granitoid Belt (this and previous studies).

Unit or Suite	Age	+/- 2 $\sigma$	Sr(o)	+/- 2 $\sigma$	Source
WESTERN TLGB SEGMENT (West of L.Michikamau)					
Monzonite, Churchill Falls	1720	+/- 55	0.70253	+/- 28	Brooks, 1982
Granite, Michikamau Lake	1715	+/- 100	0.70260	+/- 22	Brooks, 1982
North Pole Brook Int. Suite	1669	+/- 36	0.70250	+/- 40	Fryer, 1984
North Pole Brook Int. Suite	1637	+/- 12	0.70290	+/- 20	Fryer, 1984
North Pole Brook Int. Suite	1709	+/- 188	0.70240	+/- 100	Fryer, 1984
North Pole Brook Int. Suite *	1513	+/- 100	0.70450	+/- 120	Fryer, 1984
Blueberry Lake Group *	1540	+/- 40	0.70370	+/- 80	Brooks, 1979
CENTRAL TLGB SEGMENT (L.Michikamau to Michelin area)					
Island Harbour Bay Int. Suite	1794	+/- 71	0.70440	+/- 30	Grant et al., 1983
Island Harbour Bay Int. Suite	1805	+/- 42	0.70200	+/- 150	Grant et al., 1983
Island Harbour Bay Int. Suite	1843	+/- 90	0.70440	+/- 30	Grant et al., 1983
Foliated Granitoid, Anna Lake*	1795	+/- 50	0.70500	+/- 80	Brooks, 1979
Witchdoctor Granite	1595	+/- 34	0.70380	+/- 30	Brooks, 1979
Burnt Lake Granite	1548	+/- 90	0.70673	+/- 356	MacKenzie and Wilton, 1988
Otter Lk - Walker Lk Granite	1548	+/- 73	0.70718	+/- 85	Kontak, in Ryan, 1984
Otter Lk - Walker Lk Granite *	1498	+/- 46	0.70517	+/- 98	Kontak, in Ryan, 1984
Bruce River Group Volcanics *	1506	+/- 40	0.70109	+/- 56	Kontak, in Ryan, 1984
Bruce River Group Volcanics *	1530	+/- 35	0.70717	+/- 56	Kontak, in Ryan, 1984
Bruce River Group Volcanics *	1526	+/- 42	0.70380	+/- 150	Wanless and Loveridge, 1972
Upper Aillik Group *	1786	+/- 38	0.69589	+/- 124	Kontak, in Ryan, 1984
EASTERN TLGB SEGMENT (Michelin area to Smokey Islands)					
Cape Harrison Met. Suite	1740	+/- 85	0.70340	+/- 60	Brooks, 1982
Mount Benedict Intr. Suite	1625	+/- 50	0.70160	+/- 240	Brooks, 1982
"Late" Syenite, Benedict Mtns	1725	+/- 135	0.70240	+/- 410	Brooks, 1982
Granodiorite, Smokey Area	1787	+/- 35	0.70233	+/- 20	Owen et al., 1988
Monzodiorite, Smokey Area	1697	+/- 41	0.70400	+/- 50	Owen et al., 1988
Granite, Smokey Area	1725	+/- 31	0.70320	+/- 60	Owen et al., 1988
Big River Granite	1798	+/- 28	0.70173	+/- 88	This study
Freshsteak Granitoid	1798	+/- 48	0.70290	+/- 60	This study
Stag Bay Granitoid	1714	+/- 44	0.70352	+/- 46	This study
Lanceground Hills Granite *	1692	+/- 32	0.69914	+/- 628	This study
Strawberry Int. Suite (comp) *	1694	+/- 56	0.69790	+/- 640	This study
Round Pond Granite Stock *	1483	+/- 40	0.70584	+/- 213	Wilton and MacDougall (unpublished)

NOTE : All errors in initial  $^{87}\text{Sr}/^{86}\text{Sr}$  ratios are  $\times 10^{-5}$

\* This age has been shown to be, or is suspected to be, disturbed.

Table 8.3. Initial Sr isotopic compositions calculated from single sample measurements conducted via this study, using ages based on U-Pb and Rb-Sr determinations. Note that samples with high Rb/Sr ratios generally give unreasonable values.

Sample Number	Unit and Comments	Assumed Age	87Rb/86Sr Mean +/- 2 $\sigma$	87Sr/86Sr Mean +/- 2 $\sigma$	87Sr/86Sr(1) Mean +/- 2 $\sigma$
Syn-tectonic Makkovikian Intrusive / Extrusive Rocks					
AKZ-15*	Upper Aillik Gr., Ranger Bight	1850	16.701 +/- 534	1.092711 +/- 136	0.64815 +/- 1434
W84138*	Upper Aillik Gr., Michelin	1850	9.656 +/- 149	0.914201 +/- 67	0.65718 +/- 403
AKZ-2	Manak Island Granitoid	1800	0.313 +/- 5	0.710627 +/- 281	0.70233 +/- 42
0241041*	Long Island Quartz Monzonite	1800	0.945 +/- 10	0.724362 +/- 62	0.69990 +/- 31
[ Kennedy Mountain Intrusive Suite ]					
0241020	Kennedy Mountain Granite	1800	22.424 +/- 230	1.333317 +/- 462	0.75276 +/- 642
AKZ-13	Narrows Granite	1800	3.864 +/- 63	0.801955 +/- 390	0.70191 +/- 202
AKZ-11	Melody Granite	1800	7.379 +/- 130	0.887209 +/- 186	0.69616 +/- 356
Post-tectonic Makkovikian Intrusive Rocks					
[ Numok Intrusive Suite ]					
AKZ-3	Monzonite to Quartz Monzonite	1800	3.322 +/- 63	0.780105 +/- 130	0.69410 +/- 175
AKZ-5*	Syenite to Quartz Syenite	1800	1.368 +/- 33	0.734527 +/- 64	0.69911 +/- 92
[ Strawberry Intrusive Suite ]					
0241391	Bayhead Granite	1760	12.542 +/- 198	1.012539 +/- 296	0.69514 +/- 542
AKZ-14	Cape Strawberry Granite	1760	6.257 +/- 95	0.847986 +/- 82	0.68965 +/- 253
AKZ-4	Dog Islands Granite	1760	5.984 +/- 111	0.842791 +/- 56	0.69137 +/- 292
GSZ-1	Tukialik Granite	1760	5.452 +/- 66	0.831219 +/- 230	0.69324 +/- 194
GSZ-2	Tukialik Granite	1760	27.009 +/- 283	1.349971 +/- 480	0.66645 +/- 780
[ Lanceground Intrusive Suite ]					
0241154	Lanceground Hills Granite	1800	28.729 +/- 381	1.368654 +/- 628	0.62488 +/- 1048
0241332	Pistol Lake Granite	1800	19.828 +/- 295	1.192142 +/- 1050	0.67881 +/- 868
0241538	Big River Granite	1800	3.081 +/- 74	0.779743 +/- 518	0.69998 +/- 243
0241286	Freshsteak Granitoid	1800	0.694 +/- 14	0.721194 +/- 106	0.70323 +/- 47
Labradorian Intrusive and Extrusive Rocks					
0241173	Adlavik Intr. Suite Gabbro	1650	0.032 +/- 5	0.703137 +/- 133	0.70239 +/- 24
0249030*	Adlavik Intr. Suite Diorite	1650	0.314 +/- 9	0.711421 +/- 108	0.70399 +/- 32
GSZ-4	M.Benedict Intr. Suite Syenite	1650	11.535 +/- 198	0.945953 +/- 496	0.67250 +/- 520
AKZ-12	Monkey Hill Granite	1650	3.489 +/- 50	0.782133 +/- 440	0.69943 +/- 162
AKZ-7	Witchdoctor Granite	1630	22.602 +/- 439	1.224032 +/- 498	0.69479 +/- 1077
AKZ-8	Otter Lk - Walker Lk Granitoid	1650	1.358 +/- 20	0.736971 +/- 106	0.70477 +/- 58
AKZ-9	Otter Lk - Walker Lk Granitoid	1650	1.203 +/- 21	0.730720 +/- 106	0.70219 +/- 61
BR84187*	Bruce River Group Volcanic	1650	18.580 +/- 354	1.142885 +/- 149	0.70242 +/- 855
Other					
AKZ-6	Stag Bay Granitoid	1725	4.680 +/- 57	0.817134 +/- 60	0.70107 +/- 146

\* Age constrained by Precise U-Pb determination

NOTE : Errors in 87Rb/86Sr are x 10<sup>3</sup>, errors in initial 87Sr/86Sr are x 10<sup>5</sup>



At face value, these  $Sr_i$  values indicate derivation largely from the mantle, with variable admixtures of older continental crust enriched in radiogenic Sr. However, studies of high-grade gneisses indicate that granulite-facies rocks commonly have very low Rb/Sr ratios that differ only minimally from postulated upper mantle compositions (e.g. Faure, 1978). Lower crustal rocks of this type are known to exist in the Archean Nain Province (Collerson and Bridgwater, 1979), and cannot be precluded as sources on the basis of Sr isotope data alone. They may, however, be identified via Nd geochemistry (see 8.2).

#### **$Sr_i$ Variation : Single Sample Data**

If the age of a rock is known,  $Sr_i$  may be calculated from the systematics of a single sample. This method has been used widely in Phanerozoic and recent rocks (e.g. Thirlwall, 1982; Pankhurst et al., 1988; Hildreth and Moorbath, 1988), and has even been applied to Archean amphibolites (Wooden and Mueller, 1988). Table 8.3 lists Sr isotope data and calculated  $Sr_i$  for a subset of the 48 samples analyzed for Nd compositions, using ages based on U-Pb zircon or whole-rock Rb-Sr dates. Information on these samples is listed subsequently (Table 8.5). Calculated  $Sr_i$  values vary wildly, and many fall well below mantle evolution (Figure 8.3b; Faure and Powell, 1972). In general, only samples with low  $^{87}\text{Rb}/^{86}\text{Sr}$  ( $< 3.0$ ) have calculated  $Sr_i$  values that are geologically reasonable (Table 8.3).

#### **Problems In Calculating $Sr_i$**

TLGB granitoid rocks present significant problems for single-sample  $Sr_i$  studies. Firstly, their age allows

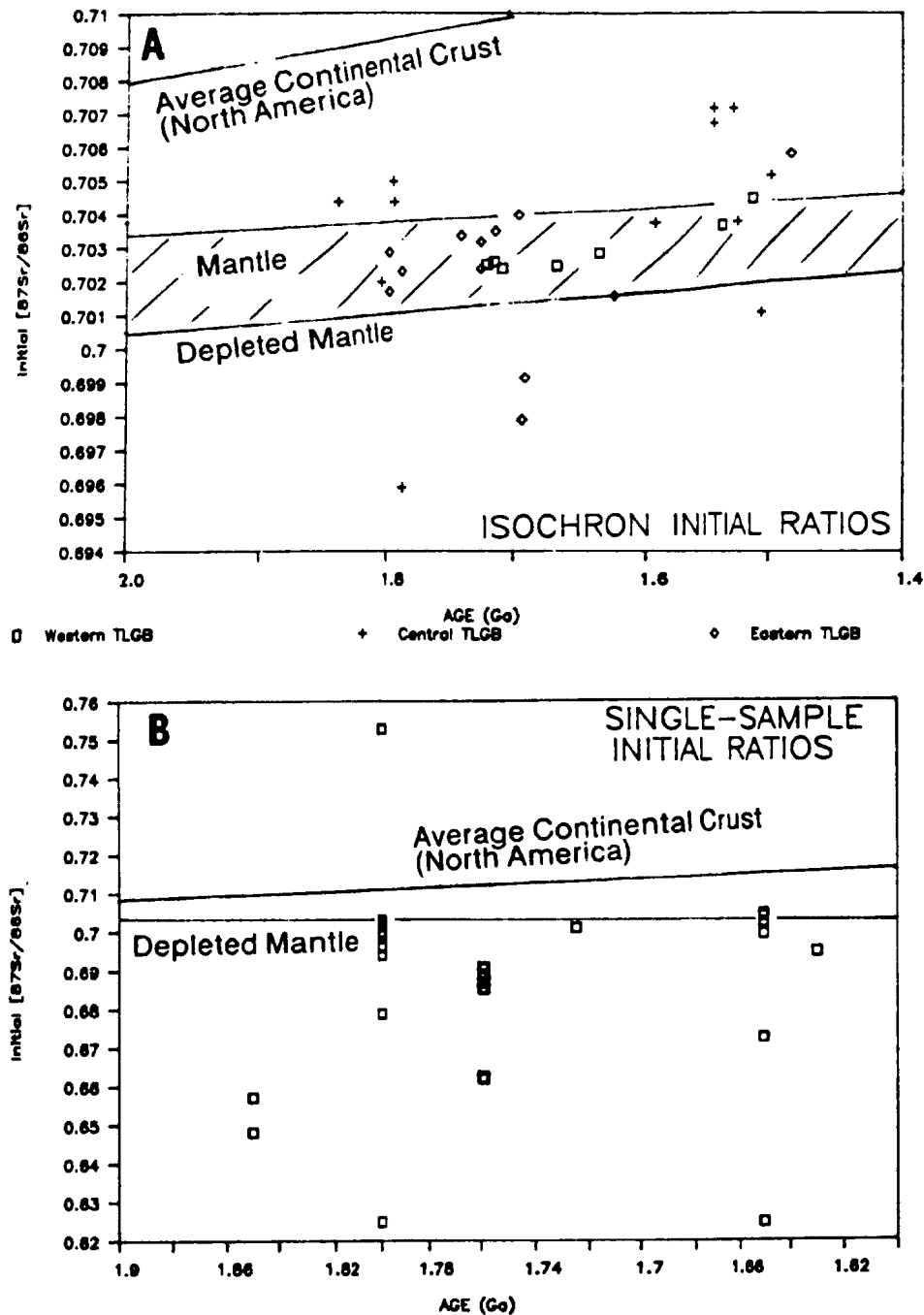


Figure 8.3. Initial Sr isotopic compositions with reference to postulated mantle evolution. (a) initial ratios calculated from isochrons. (b) initial ratios calculated by extrapolation from single-sample data. Sources for isochron data are listed in Table 8.2. Mantle growth band after Faure and Powell (1972).

ample time for Sr isotope evolution, increasing the magnitude of corrections required for isotopic growth. Secondly, large uncertainties in  $^{87}\text{Rb}/^{86}\text{Sr}$  resulting from generally high Rb/Sr ratios propagate during extrapolation to 0 to obtain  $\text{Sr}_i$ , and generate very large errors (e.g. Table 8.3). Thirdly, even slight loss of radiogenic Sr from high Rb/Sr samples displaces their calculated  $\text{Sr}_i$  to unreasonably low values. A consequence of these problems is that calculated  $\text{Sr}_i$  is extremely sensitive to small variations in assumed age. Note that the  $2\sigma$  uncertainties listed in Table 8.3 do not include possible age uncertainty (see 8.2.2 for details of error calculation methods).

These problems are illustrated by three samples (Table 8.4), dated by precise U-Pb zircon methods (Schärer et al., 1988; Krogh et al., in prep.). Sample 0249030, which has a low  $^{87}\text{Rb}/^{86}\text{Sr}$  ratio, produces a reasonable  $\text{Sr}_i$  value that changes only minimally if its assumed age is altered by up to 100 Ma. In contrast, BR-84-187 ( $^{87}\text{Rb}/^{86}\text{Sr} = 18.6$ ), which provides a reasonable result using its U-Pb zircon age of 1650 Ma, has a range of calculated  $\text{Sr}_i$  (for a 100 Ma range) that covers the full range from basaltic achondrites to evolved continental crust ! Sample W-84-138, dated precisely at ca. 1850 Ma, shows similarly extreme behaviour, and impossibly low  $\text{Sr}_i$  at all assumed ages, presumably resulting from loss of radiogenic Sr. In contrast, all three show only small changes in calculated initial Nd isotopic composition (expressed as  $\epsilon_{\text{Nd}}^{\text{CHUR}}$ ; see 8.2.2) as a result of age uncertainty.

No further attempt is made here to use calculated whole-rock  $\text{Sr}_i$  values. The only solution is to separate and analyze minerals with low Rb/Sr ratios, such as plagioclase or (ideally) apatite or sphene, in which measured  $^{87}\text{Sr}/^{86}\text{Sr}$  deviates only minimally from  $\text{Sr}_i$ .

Table 8.4. An illustration of the great sensitivity of rocks with high Rb/Sr ratios to age uncertainties in the calculation of initial Sr isotopic compositions from a single sample. Note that Initial Nd isotopic compositions, expressed as  $\epsilon_{Nd}^{CHUR}$ , are much less sensitive to variations in assumed age.

Assumed Age	Calculated $[87Sr/86Sr]_0$	+/- Estimated 2 $\sigma$ Error	Calculated $\epsilon_{(Nd)CHUR}$	+/- Estimated 2 $\sigma$ Error
-------------	----------------------------	--------------------------------	----------------------------------	--------------------------------

SAMPLE 0249030 (Adlavik Intrusive Suite Diorite)  
 $87Rb/86Sr = 0.31$ ,  $147Sm/144Nd = 0.1099$

1700	0.70376		0.30	
1675	0.70387		0.02	
* 1650	0.70398	+/- 32	- 0.26	+/- 0.82
1625	0.70410		- 0.54	
1600	0.70421		- 0.83	

SAMPLE W-84-138 (Upper Aillik Group Rhyolite)  
 $87Rb/86Sr = 9.66$ ,  $147Sm/144Nd = 0.0978$

1900	0.65014		- 4.83	
1875	0.65336		- 5.15	
* 1850	0.65718	+/- 403	- 5.47	+/- 1.0
1825	0.66070		- 5.79	
1800	0.66421		- 6.11	

SAMPLE BR-84-187 (Bruce River Group Felsic Volcanic)  
 $87Rb/86Sr = 18.6$ ,  $147Sm/144Nd = 0.1014$

1700	0.68890		0.09	
1675	0.69566		- 0.22	
* 1650	0.70241	+/- 854	- 0.53	+/- 0.68
1625	0.70917		- 0.84	
1600	0.71591		- 1.14	

\* Indicates age given by precise U-Pb zircon determination

## 8.2 NEODYMIUM ISOTOPE GEOCHEMISTRY

### Neodymium as a Petrogenetic Tool

Neodymium has inherent advantages over strontium in isotopic studies of Precambrian granitoid rocks.

Sm/Nd ratios vary minimally in crustal rocks (their mean  $^{147}\text{Sm}/^{144}\text{Nd}$  is estimated at ca.  $0.115 \pm 0.01$ ; Goldstein et al., 1984), and this ratio is largely independent of magmatic differentiation. Age corrections to obtain initial Nd isotopic compositions are small compared to those required for Sr (due to the long half-life of  $^{147}\text{Sm}$ ), and are almost constant for all rock types (e.g. Table 8.4). The uncertainty in correcting single-sample data is thus much smaller than for Sr.

The coherent behaviour of Sm and Nd reflects the supposed inability of crustal processes to strongly fractionate two closely similar rare-earth elements. There are, however, significant differences in Sm/Nd between the crust and values inferred for the mantle on the basis of meteorite studies (e.g. DePaolo and Wasserburg, 1976). The initial Nd isotopic composition of crustal rocks thus constrains the time elapsed since their precursor(s) separated from the mantle, regardless of the number of times this material was "reprocessed" in the crust. In this regard, Sm and Nd differ radically from Rb and Sr, which



are strongly fractionated by magmatic processes in the crust, and commonly undergo multi-stage evolution in crustal reservoirs (e.g. Faure and Powell, 1972).

Finally, Nd and Sm reside primarily in accessory and mafic phases (as opposed to feldspars), and are generally less subject to disturbance by hydrothermal activity or alteration, although the REE may be mobile under certain conditions (e.g. Taylor and Fryer, 1982; Windrim et al., 1984).

Such flawless behaviour is, of course, subject to exceptions! McCulloch and Black (1984), and Windrim et al. (1984), have discussed the effects of granulite facies metamorphism and hydrothermal processes on Sm and Nd behaviour, and the unusual isotopic characteristics of the Pitre Lake Granite determined in this study (see 8.3.1) imply local strong fractionation of Sm from Nd during anatexis. The geochronological applications of Sm and Nd indicate that there must be slight fractionation of Sm and Nd during igneous processes (O'Nions et al., 1979), but it is minimal compared to that observed for Rb and Sr.

#### **Overview of Neodymium Isotope Geochemistry Database**

Nd isotopic data are reported here for 48 samples; about half of these were also analyzed for Sr isotopic composition (see 8.1.2; Sr results listed in Table 8.3).

The samples are representative examples of major geological units, and (wherever possible) are from localities for which U-Pb zircon dates are available or planned. All samples are listed and described in Table 8.5, and located in Figure 8.4. In addition to the plutonic and volcanic rocks, two orthogneisses from the Cape Harrison Metamorphic Suite (Gower, 1981) were analyzed to

Table 8.5. Listing of samples analyzed for Nd isotopic compositions, with descriptive comments and age information. Sample locations are shown in Figure 8.4. Note that some of these were also analyzed for Sr (see table 8.3 for results)

SAMPLE	Unit	Age	Description and Comments
SYN-TECTONIC MAKKOVIKIAN PLUTONIC ROCKS			
0241041	Long Island Quartz Monzonite	1802 $\pm$ 13/-10 Ma [U-Pb Zr]	Hb-Bi Quartz Monzonite, close to location dated by (Gandhi et al.(1988).
KENNEDY MOUNTAIN INTRUSIVE SUITE			
0241020	Kennedy Mountain Granite	Not Yet Dated	Fluorite-bearing biotite granite.
AKZ-13	Narrows Granite		Biotite-Hornblende Monzogranite.
0231058	Cross Lake Granite		Biotite granite with fluorite, allanite.
0241060	Cross Lake Granite		Porphyritic Bi-Hb leucogranite.
ISLAND HARBOUR BAY INTRUSIVE SUITE (Samples provided by Bruce Ryan)			
0140067	Homogeneous granite unit	1805 $\pm$ - 5 Ma [U-Pb Zr]	Porphyritic biotite granite, part of unit dated by Loveridge et al.(1987).
0140037	Tonalite-granodiorite unit		Melanocratic Bi-Hb granodiorite.
OTHER SYN-TECTONIC MAKKOVIKIAN GRANITOIDS			
AKZ-11	Melody Granite	Not Yet Dated	Porphyritic biotite granite, hematized.
0249213	Brumwater Granite		biotite monzogranite, faintly layered.
0249195	Pitme Lake Granite		biotite-muscovite granite.
AKZ-2	Manak Island Granitoid		leucocratic, slightly porphyritic, granodiorite.
0249015	Deus Cape Granitoid	1837 $\pm$ 6/-4 Ma [U-Pb Zr]	Porphyritic, leucocratic granite. Dated by Krogh et al., in prep.)
POST-TECTONIC MAKKOVIKIAN PLUTONIC ROCKS			
NIMOK INTRUSIVE SUITE			
AKZ-5	Syenite (Northern Zone)	1801 $\pm$ - 2 Ma [U-Pb Zr]	Coarse grained Cpx-fayalite syenite dated by Krogh et al.(in prep.)
AKZ-3	Quartz Monzonite (Northern Zone) (Adjacent to agmatitic border)	1801 $\pm$ - 2 Ma [U-Pb Zr]	Coarse grained Hb-Bi (Px) quartz monzonite ca. 2 km from dated locality.
0241338	Quartz Syenite (Southern Zone)	Not Dated	Slightly deformed porphyritic quartz syenite.
STRAWBERRY INTRUSIVE SUITE			
AKZ-14	Cape Strawberry Granite	1800-1760 Ma [U-Pb Zr]	Coarse grained, porphyritic biotite granite, with accessory fluorite. Dated by Krogh et al.(in prep.)
0241391	Rayhead Granite	Not Yet Dated	Coarse grained, porphyritic, biotite granites similar to AKZ-14.
0241181	October Harbour Granite		
AKZ-4	Dog Islands Granite		
GSZ-1	Tukialik Granite		
GSZ-2	Tukialik Granite		
LANCEGROUND INTRUSIVE SUITE			
0241154	Lanceground Hills Granite	1692 $\pm$ - 32 Ma [Rb-Sr WR]	Coarse-grained Bi-Hb alkali-fsp granite; age is probably disturbed.
0241332	Pistol Lake Granite	Not Yet Dated	Porphyritic alkali-fsp quartz syenite.
0248101	Tarun Granite		Coarse grained granite, slightly deformed.
OTHER POST-TECTONIC MAKKOVIKIAN GRANITOIDS			
0241538	Big River Granite	1798 $\pm$ - 28 Ma [Rb-Sr WR]	Coarse-grained Hb-Bi granite with pseudorapakivi texture.
0241286	Freshsteak Granitoid	1798 $\pm$ - 48 Ma [Rb-Sr WR]	Medium-grained melanocratic Hb-Bi quartz monzonite.
0241356	Noarse Lake Granitoid	Not Dated	Similar to above.



Table 8.5

SAMPLE	Unit	Age	Description and Comments
LABRADORIAN PLUTONIC ROCKS			
ADLAVIK INTRUSIVE SUITE			
0241173	Gabbro Unit (Main Body)	Not	Olivine gabbro
0249062	Gabbro Unit (Pamiulik Point)	Yet	Melanocratic olivine gabbro
0241441	Gabbro Unit (East MicMac Lake)	Dated	Hornblende gabbro, minor interstitial K-fsp
0249030	Diorite Unit (Main Body)	1649 +/- 1 Ma [U-Pb Zr]	Potassic monzodiorite to syenodiorite dated by Krogh et al. (in prep.)
MOUNT BENEDICT INTRUSIVE SUITE			
0242136	Diorite Unit		Plag-porphyratic (cumulate?) Cpx-diorite.
0242144	Monzonite to Syenite Unit	1650 +/- 10 Ma [U-Pb Zr]	Syenite with relict Plag-porphyratic texture. Dated by Krogh et al. (in prep.)
CSZ-4	Quartz Syenite	1625 +/- 50 Ma [Rb-Sr WR]	Similar to above, but richer in quartz. Dated by Brooks (1982), probably disturbed.
MONKEY HILL INTRUSIVE SUITE			
AKZ-12	Monkey Hill Granite	1640 +/- 10 Ma	Fine-grained biotite monzogranites.
0248191	Little Monkey Hill Granite	[U-Pb Zr]	Monkey Hill Granite dated by Krogh et al. (in prep.)
OTHER LABRADORIAN GRANITOIDS			
AKZ-7	Witchdoctor Granite	1628 +/- 9 [U-Pb Zr]	Recrystallized Bi (Ms) leucogranite with accessory garnet. Site dated by Brooks (1983).
0249074	Burnt Lake Granite		Fine grained, leucocratic Bi (Ms) granite.
AKZ-8	Otter Lake - Walker Lake Gran	1548 +/- 73 Ma [Rb-Sr WR]	Quartz Monzonite to Monzogranite with phenocrysts of both feldspars. Same area dated by Kontak (in Ryan, 1984).
UNCLASSIFIED PLUTONIC ROCKS			
AKZ-6	Stag Bay Granitoid	1714 +/- 44 Ma [Rb-Sr WR]	K-feldspar porphyritic Mb-Bi granodiorite to monzogranite.
0242030	Thunder Mountain Syenite	Not Dated	Coarse grained Cpx-Hb quartz syenite.
VOLCANIC ROCKS			
UPPER AILLIK GROUP			
AKZ-15	Early Upper Aillik Group ?	1861 +/- 3 Ma [U-Pb Zr]	Thin rhyolite flow or sill in metasediments. Sample dated by Scharer et al. (1988).
W84138	Late Upper Aillik Group ? (provided by R.J. Wardle)	1856 +/- 2 Ma [U-Pb Zr]	Weakly deformed rhyolitic ash-flow tuff. Sample dated by Scharer et al. (1988).
0248237	Hypabyssal Intrusive Rocks	1807 +/- 2 Ma [U-Pb Zr]	Quartz-feldspar porphyry. Same locality as sample dated by Scharer et al. (1988).
0249324	Jagged Edge Assemblage	Not Dated	Fresh feldspar-porphyry.
BRUCE RIVER GROUP			
BR84187	Sylvia Lake Formation (Provided by B. Ryan)	1649 +/- 1 Ma [U-Pb Zr]	Weakly deformed rhyolitic ash-flow tuff. Same locality as sample dated by Scharer et al. (1988).
CAPE HARRISON METAMORPHIC SUITE			
AKZ-20	Tonalitic gneiss unit	Not Yet Dated	Grey, foliated, locally banded tonalitic to granodioritic gneiss.
AKZ-21	Foliated Granodiorite		Homogeneous, leucocratic, foliated granodiorite or monzogranite.

represent possible "basement" in the east of the area. No samples from the Archean basement rocks in the west of the area were analyzed; however, data for these are provided by Brooks (1983). Note that the Freshsteak and Noarse Lake granitoids are here grouped as Makkovikian intrusions, based on Rb-Sr data (8.1.1).

#### 8.2.1 Sm-Nd "Geochronology"

Sm and Nd are of limited value as geochronometers in post-Archean rocks (e.g. O'Nions et al., 1979; Cox et al., 1979). However, isochron diagrams may define quasi-linear trends that may be significant in terms of other processes such as mixing and variation in initial  $^{143}\text{Nd}/^{144}\text{Nd}$  ratios amongst units. "Ages" were obtained by least-squares regression as outlined previously (8.1.1), but no attempt is made to assess them statistically; they are quoted mostly as an indication of the slope of correlations relative to those expected for isochron behaviour. Sm and Nd concentration and isotopic data are listed subsequently (Tables 8.6; 8.7). A  $^{147}\text{Sm}$  decay constant of  $6.54 \times 10^{-12} \text{ yr}^{-1}$  (Steiger and Jager, 1977) was used in calculation of age, and subsequent calculation of  $\epsilon_{\text{Nd}}$  (see 8.2.2 for details of the latter).

#### **Syn-Tectonic Makkovikian Plutonic Rocks**

Units in the west of the study area mostly define a  $1553 \pm 330 \text{ Ma}$  ( $2 \sigma$ ) pseudoisochron (Figure 8.5a), except for AKZ-11 and 0249213, which are below this line. Units from the east (Manak Island and Deus Cape; AKZ-2, 0249015) lie well above this line and, with AKZ-13 and two samples from the Cape Harrison Metamorphic Suite, define a  $2046 \pm$

694 Ma (2  $\sigma$ ) pseudoisochron. Sample 0249195 (Pitre Lake Granite) has an anomalous  $^{147}\text{Sm}/^{144}\text{Nd}$  ratio (ca. 0.23) and lies well to the right of the diagram; it is discussed separately (8.3.1).

#### Post-Tectonic Makkovikian Plutonic Rocks

No obvious pattern exists amongst these samples (Figure 8.5b); possible "ages" range from 2741 Ma to 3364 Ma, depending upon which samples are included in the regression. Assuming that groupings based on petrology and elemental geochemistry (Chapter 4) are valid, this points to differences in their initial Nd isotopic composition. This is shown well by six samples from the Strawberry Intrusive Suite (Figure 8.5c), which are highly variable; their apparent age of  $4516 \pm 680$  Ma (1  $\sigma$ ), is meaningless, and AKZ-14 and AKZ-4 both lie well away from this "line". Note that 5 of these samples (including the two most deviant) define a reasonably well-fitted composite 1695 Ma Rb-Sr isochron (8.1.1). In view of their strong petrological and geochemical affinity (Chapter 4), this variation indicates significant differences in initial Nd isotopic composition, that are apparently not present for Sr. Note that the highest  $^{143}\text{Nd}/^{144}\text{Nd}$  values are from plutons in the east (Tukialik and Dog Islands Granites; GSZ-1, GSZ-2, AKZ-4). Plutons in the west lie close to the lower pseudoisochron described above from syn-tectonic Makkovikian units and, if regressed with 3 samples from the Kennedy Mountain Suite and one from Long Island, yield a reasonable  $1902 \pm 142$  Ma (2  $\sigma$ ) pseudoisochron (Figure 8.5c).

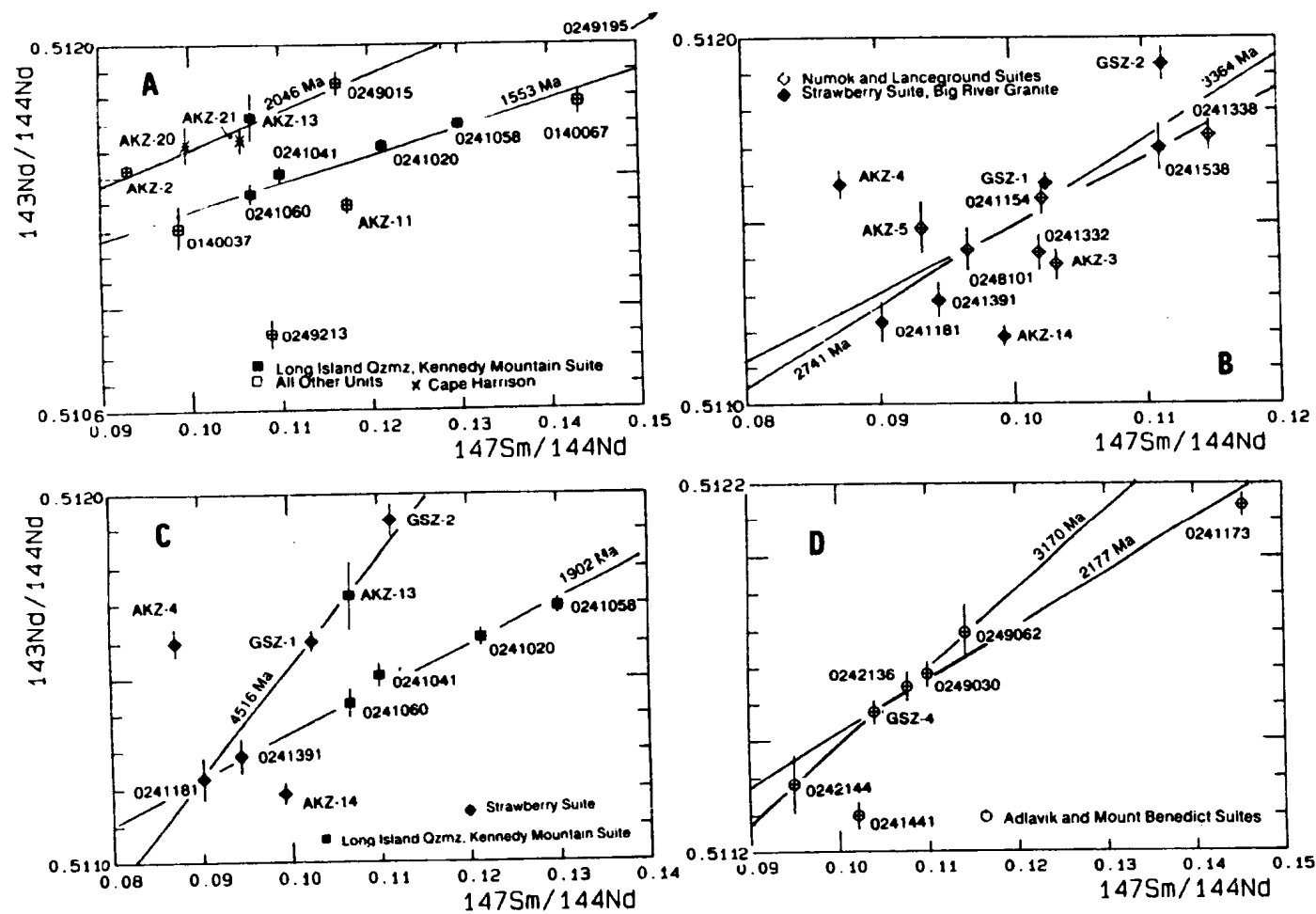


Figure 8.5. Sm-Nd isochron diagrams. (a) Syn-tectonic Makkovikian units. (b) Post-tectonic Makkovikian units. (c) Detail of Strawberry and Kennedy Mountain Suites. (d) Adlavik and Mount Benedict Suites. See text for discussion.

## Labradorian Plutonic Rocks

The ca. 1650 Ma old Adlavik and Mount Benedict Intrusive Suites (excluding 0241441; a gabbro from East MicMac Lake) define a  $2177 \pm 410$  Ma ( $2 \sigma$ ) pseudoisochron (Figure 8.5d). The slope is strongly influenced by sample 0241173; if this is excluded, the remaining samples define a  $3170 \pm 217$  Ma ( $2 \sigma$ ) pseudoisochron. A similar age is defined by three samples from the Mount Benedict Suite alone. This "age" is obviously untenable. This pseudoisochron could be interpreted as an argument against a genetic relationship but the presence of a linear array would be a remarkable coincidence under such conditions. Also, there is independent geochemical evidence for a genetic link (Chapter 5). An alternative explanation is that the more differentiated rocks are variably contaminated by material with low  $^{147}\text{Sm}/^{144}\text{Nd}$  and  $^{143}\text{Nd}/^{144}\text{Nd}$ , i.e. this is a steepened isochron. Binary mixing of this type would produce a linear array. A similar proposal was advanced by Ashwal et al. (1986) to explain anomalously old (3300 Ma) Sm-Nd isochron ages from the ca. 1300 Ma old Harp dykes of central Labrador.

Labradorian granitoid plutonic rocks (not figured) define no obvious trends in isochron diagrams, and, in general, show much less variation in present-day  $^{143}\text{Nd}/^{144}\text{Nd}$  than their Makkovikian counterparts. Similar comments apply to unclassified units from Stag Bay and Thunder Mountain.

### 8.2.2 Regional Variations In Nd Isotope Geochemistry

Sm and Nd concentration and isotopic data are listed in Tables 8.6 and 8.7, with the calculated parameters  $\epsilon_{\text{Nd}}^{\text{CHUR}}$ ,  $\epsilon_{\text{Nd}}^{\text{DM}}$  and  $T_{\text{DM}}$ . (DePaolo and Wasserburg,

1976; DePaolo, 1979). All errors are within-run statistics quoted at the  $2\sigma$  level; errors for  $^{147}\text{Sm}/^{144}\text{Nd}$  are calculated as  $\pm 0.5\%$ , based on duplicate analyses (see Appendix A).

### Data Notation and Representation

**Epsilon ( $\epsilon_{\text{Nd}}$ ) Notation** : The initial  $^{143}\text{Nd}/^{144}\text{Nd}$  ratio of a sample at time T is readily calculated from the radioactive decay equation, assuming that  $^{147}\text{Sm}/^{144}\text{Nd}$  and T are known. It is conventional to represent initial Nd compositions as  $\epsilon_{\text{Nd}}$  units (DePaolo, 1979). These indicate deviations (in parts per  $10^4$ ) from the calculated  $^{143}\text{Nd}/^{144}\text{Nd}$  of a reference material that evolved with a known  $^{147}\text{Sm}/^{144}\text{Nd}$  ratio. Unless an age is specifically stated,  $\epsilon_{\text{Nd}}$ , as used below, refers to Nd isotopic compositions at the time of formation, i.e. time of crystallization.

$\epsilon_{\text{Nd}}$  is commonly expressed relative to a chondritic uniform reservoir (CHUR), for which accepted present-day values (employed here) are  $^{143}\text{Nd}/^{144}\text{Nd} = 0.512638$  and  $^{147}\text{Sm}/^{144}\text{Nd} = 0.196593$  (Jacobsen and Wasserburg, 1980; normalized to a  $^{146}\text{Nd}/^{144}\text{Nd}$  ratio of 0.7219). The parameter  $\epsilon_{\text{Nd}}$  at time T is given by the expression:

$$\epsilon_{\text{Nd}}^{\text{CHUR}} = 10^4 \times \left[ \frac{^{143}\text{Nd}/^{144}\text{Nd}_{(\text{sample})} \text{ at T}}{^{143}\text{Nd}/^{144}\text{Nd}_{\text{CHUR}} \text{ at T}} - 1 \right]$$

Negative  $\epsilon_{\text{Nd}}^{\text{CHUR}}$  values indicate initial  $^{143}\text{Nd}/^{144}\text{Nd}$  ratios below chondritic evolution (typical of crustal material, with a lower Sm/Nd ratio than the

mantle) and positive values indicate derivation from material that has a higher Sm/Nd than CHUR. Positive  $\epsilon_{\text{Nd}}^{\text{CHUR}}$  values are common in modern and ancient mafic extrusive rocks (e.g. Nelson and DePaolo, 1984; White and Patchett, 1984). They indicate that substantial portions of the earth's mantle were depleted in Nd relative to Sm at an early stage; this is inferred to result from the extraction of the continental crust.

As post-Archean crust formation probably tapped this depleted mantle reservoir, the notation  $\epsilon_{\text{Nd}}^{\text{DM}}$  is also widely employed, indicating initial  $^{143}\text{Nd}/^{144}\text{Nd}$  relative to postulated depleted mantle evolution. However, there is no firm consensus regarding the isotopic evolution of the mantle, and  $\epsilon_{\text{Nd}}^{\text{CHUR}}$  values are preferable for comparison of data from different sources.  $\epsilon_{\text{Nd}}^{\text{DM}}$  values quoted below are with reference to evolution from  $\epsilon_{\text{Nd}}^{\text{CHUR}}$  of ca +2 at ca. 2800 Ma to ca + 5 at ca. 1800 Ma ago (c.f. Patchett and Bridgwater, 1984; Chauvel et al., 1987). This is consistent with observed  $\epsilon_{\text{Nd}}^{\text{CHUR}}$  values for ca. 1700 Ma old mafic volcanics of up to + 6 (Nelson and DePaolo, 1984). For the sake of simplicity, mantle evolution over this time interval is assumed here to be linear.

**Model Ages and Crustal Residence Ages** : A Nd Model age is the time at which the  $^{143}\text{Nd}/^{144}\text{Nd}$  ratio of a sample and a reference material (model) have the same value. In the  $\epsilon_{\text{Nd}}$  notation used here,  $T_{\text{CHUR}}$  is the time at which  $\epsilon_{\text{Nd}}^{\text{CHUR}} = 0$ , and  $T_{\text{DM}}$  the time at which  $\epsilon_{\text{Nd}}^{\text{DM}} = 0$ . In each case there is a unique solution, which can be calculated by iteration or equations presented by DePaolo (1979,1981b). The key assumption is that, if a sample is the end product of a multi-stage crustal process, its Sm/Nd ratio has not changed significantly since its initial

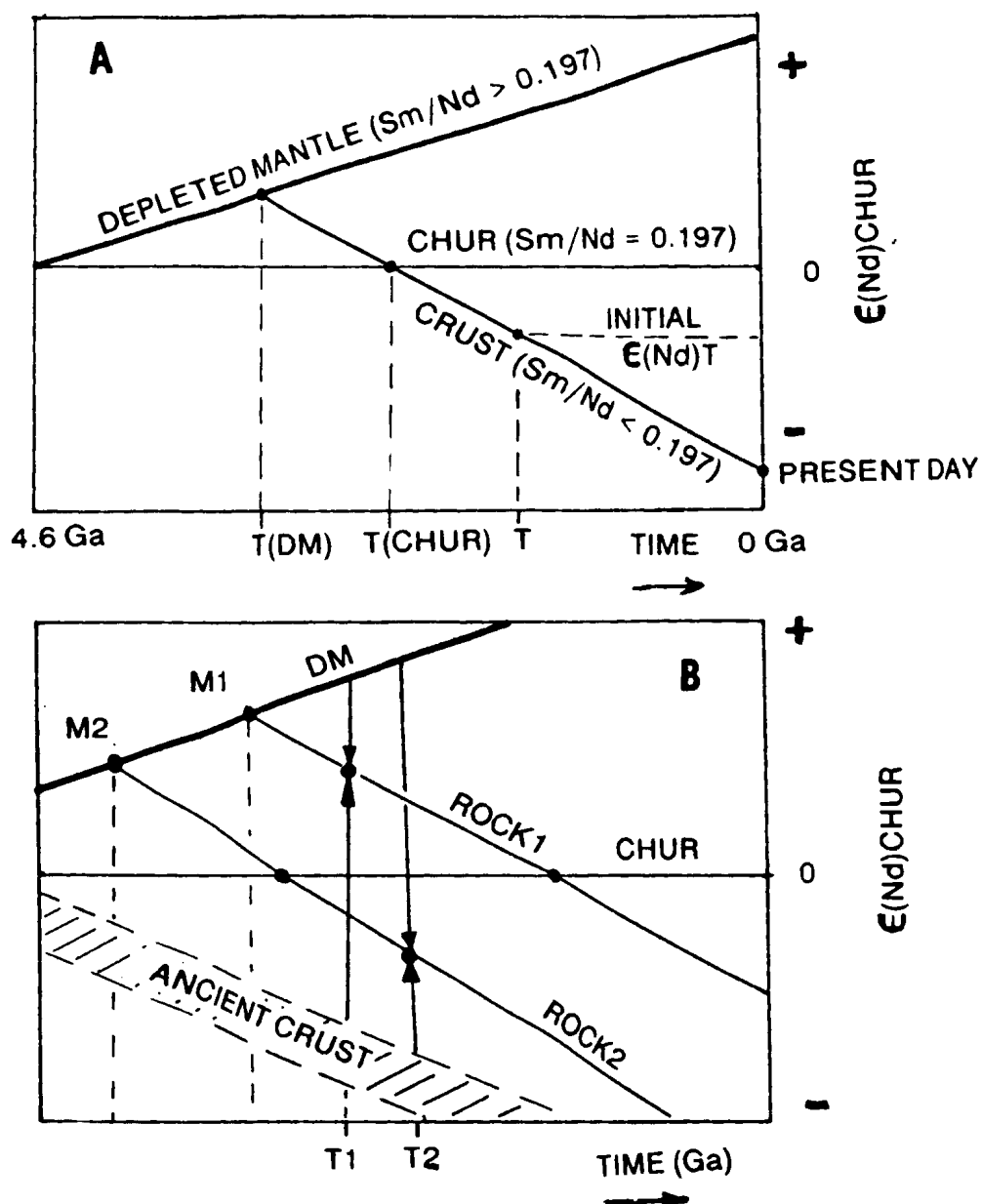


Figure 8.6. Schematic illustrations of the principles of Nd isotope geochemistry. (a) Contrasting variation of crustal material and depleted mantle relative to CHUR, and geometric representation of model ages  $T_{\text{DM}}$  and  $T_{\text{CHUR}}$ . (b) Complications due to mixed sources; model ages M1 and M2 for two rocks result from different mixtures of mantle- and crustal-derived magmas, and have no true geochronological meaning. Adapted partly from Arndt and Goldstein (1987).



derivation from the mantle. Extrapolation of its Nd isotopic growth line back to CHUR or DM evolution lines thus provides the earliest time at which it or its precursor(s) could have been generated from such a source (Figure 8.6a).

It is important to note that the above is true only if the sample was derived from a single source material with a simple history. If a rock is derived from two or more sources themselves derived from the mantle at different times (e.g. a juvenile magma assimilating much older crust; Figure 8.6b), any Nd model age is a function of the relative proportions and Nd contents of these end members and has no direct geochronological significance (e.g. Patchett and Bridgwater, 1984; Arndt and Goldstein, 1987). Nevertheless, there may be situations in which model ages reflect the actual time at which the precursor separated from the mantle, particularly when model ages correspond with orogenic events documented via geochronology.

**Estimation of Uncertainty** : Analytical uncertainty in  $\epsilon_{Nd}$  and  $T_{DM}$  was calculated using a "worst-case" scenario where  $^{143}Nd/^{144}Nd$  and  $^{147}Sm/^{144}Nd$  both deviate by  $2\sigma$  in opposite directions. As it is highly unlikely that perfect anticorrelation of errors would occur, an arbitrary value corresponding to 66% of this worst-case error is used below to indicate  $2\sigma$  uncertainty. In most cases (Tables 8.6; 8.7) this is  $\pm 0.7 \epsilon_{Nd}$  units or less. Errors due to age uncertainties are more difficult to assess; however, variations of  $\pm 50$  Ma in assumed age (e.g. Table 8.4) cause only small changes in  $\epsilon_{Nd}$ , that are within analytical errors, and have a negligible impact on model age calculations.

**Age Assumptions** : Ages assumed in calculations are listed in Tables 8.6 and 8.7; in most cases these are based on U-Pb or Rb-Sr geochronology, rounded to the nearest 10 Ma. For some units of uncertain age, values were calculated for both 1800 and 1650 Ma, or for an intermediate value of 1725 Ma.  $\epsilon_{Nd}$  Values for Archean gneisses (Brooks, 1983) are calculated for 2600 Ma (Sm/Nd isochron age, probably metamorphic; Brooks, 1983), 1800 Ma and 1650 Ma; the latter values indicate their characteristics during Makkovikian and Labradorian magmatism respectively. An age of 1850 Ma has been assumed for the Cape Harrison Metamorphic Suite, by reasoning that it predates the Deus Cape Granitoid (ca. 1840 Ma; Krogh et al., in prep.), and its  $\epsilon_{Nd}$  at ca. 1650 Ma is also listed.

#### **Syn-Tectonic Makkovikian Plutonic Rocks**

$\epsilon_{Nd}^{CHUR}$  values for these units range from -13.8 to +3.6 (Table 8.6). Units in the west of the area mostly have negative  $\epsilon_{Nd}^{CHUR}$  (generally  $< -2.0$ ), whereas those in the east have  $\epsilon_{Nd}^{CHUR}$  of ca. +3.0. The Narrows Granite of the Kennedy Mountain Suite (sample AKZ-13; ca. + 3.0) is an exception to this pattern. Positive values in the east are similar to those of the Cape Harrison Metamorphic Suite at an assumed 1850 Ma age. This confirms pseudoisochron behaviour noted above (8.2.1).

In the east,  $T_{DM}$  model ages are ca. 2000 - 1950 Ma for the Manak Island and Deus Cape Granitoids, and also for the Cape Harrison Suite. As the latter is undated, its model age may correspond to its time of formation. These values indicate that the precursor(s) to units in the east had a short crustal residence period, probably less than 200 Ma (subject to qualifications previously outlined with

Table 8.6

GENERAL INFORMATION				CONCENTRATIONS			ISOTOPIC RATIOS			INITIAL Nd CHARACTERISTICS		
Sample Number	Unit or Comments	Age (Ma)	Sr (ppm)	Nd (ppm)	<sup>147</sup> Sm/ <sup>144</sup> Nd	Mean $\pm$ 2 $\sigma$	<sup>143</sup> Nd/ <sup>144</sup> Nd	Mean $\pm$ 2 $\sigma$	$\epsilon$ (Nd)CHUR	Mean $\pm$ 2 $\sigma$	$\epsilon$ (Nd)DM	Mean $\pm$ 2 $\sigma$
SYN-TECTONIC MAKROVIRIAN PLUTONIC ROCKS												
0241061	Long Island Gneiss	1800	6.9	38.1	0.1100 $\pm$	55	0.511511 $\pm$	33	-2.0 $\pm$	0.5	-7.0	2290 $\pm$ 47
KENNEDY MOUNTAIN INTRUSIVE SUITE												
0241070	Kennedy Mtn Granite	1800	12.2	59.4	0.1214 $\pm$	61	0.511615 $\pm$	25	-2.6 $\pm$	0.4	-7.6	2390 $\pm$ 44
AKZ-13	Narrows Granite	1800	10.6	59.0	0.1068 $\pm$	53	0.511725 $\pm$	90	3.0 $\pm$	1.3	-2.0	1940 $\pm$ 110
0241078	Cross Lake Granite	1800	13.9	63.2	0.1299 $\pm$	65	0.511695 $\pm$	20	-3.0 $\pm$	0.4	8.0	2485 $\pm$ 42
0241060	Cross Lake Granite	1800	13.6	75.5	0.1106 $\pm$	53	0.511433 $\pm$	39	-2.8 $\pm$	0.6	-7.7	2325 $\pm$ 51
ISLAND HARBOUR BAY INTRUSIVE SUITE												
0160061	Granite Unit	1800	4.6	18.8	0.1434 $\pm$	72	0.511776 $\pm$	48	-4.5 $\pm$	0.7	-9.5	2760 $\pm$ 108
0160047	Tonalite-Granodiorite	1800	5.5	32.6	0.0987 $\pm$	49	0.511310 $\pm$	81	-3.3 $\pm$	1.1	-8.3	2325 $\pm$ 91
OTHER UNITS												
AF-11	McLarty Granite	1800	7.8	42.4	0.1175 $\pm$	59	0.511388 $\pm$	29	-6.1 $\pm$	0.5	-11.1	2632 $\pm$ 46
0259213	Brunswick Granite	1800	2.6	13.9	0.1088 $\pm$	54	0.510894 $\pm$	55	-13.8 $\pm$	0.8	-18.8	3100 $\pm$ 72
0259195	Pitt Lake Granite	1800	7.5	19.6	0.2262 $\pm$	113	0.512892 $\pm$	35	-1.9 $\pm$	0.6	-6.9	n/a
AKZ-2	Manak Is. Granitoid	1800	2.4	15.5	0.0930 $\pm$	47	0.511529 $\pm$	26	2.3 $\pm$	0.4	-2.7	1960 $\pm$ 31
0269015	Deas Cape Granitoid	1840	8.6	43.0	0.1165 $\pm$	58	0.511851 $\pm$	47	3.6 $\pm$	0.7	-1.3	1940 $\pm$ 69
POST-TECTONIC MAKROVIRIAN PLUTONIC ROCKS												
NEOK INTRUSIVE SUITE												
AKZ-3	Horizontal (N Zone)	1800	16.7	94.4	0.1030 $\pm$	51	0.511326 $\pm$	26	-4.0 $\pm$	0.4	-9.0	2390 $\pm$ 35
AKZ-5	Syncline (N Zone)	1800	7.9	50.8	0.0933 $\pm$	47	0.511485 $\pm$	69	1.4 $\pm$	1.0	-3.6	2020 $\pm$ 74
0251345	Qtz. Syenite (S Zone)	1800	12.0	69.4	0.1149 $\pm$	57	0.511734 $\pm$	41	1.3 $\pm$	0.6	-3.7	2080 $\pm$ 60
STRABERRY INTRUSIVE SUITE												
0251491	Bayhead Granite	1760	9.0	57.7	0.0944 $\pm$	47	0.511288 $\pm$	47	-3.3 $\pm$	0.7	-8.4	2275 $\pm$ 53
AKZ-16	Cape Strawberry Gneiss	1760	9.9	63.1	0.0993 $\pm$	50	0.511188 $\pm$	29	-6.3 $\pm$	0.5	-11.4	2490 $\pm$ 37
0251181	October Hr. Granite	1760	10.6	71.3	0.0902 $\pm$	45	0.511228 $\pm$	56	-3.5 $\pm$	0.8	-8.6	2275 $\pm$ 59
AKZ-4	Bay Islands Granite	1760	10.5	72.0	0.0872 $\pm$	44	0.511606 $\pm$	50	4.6 $\pm$	0.7	-0.5	1790 $\pm$ 51
GSZ-1	Tukialik Granite	1760	6.7	39.3	0.1076 $\pm$	51	0.511605 $\pm$	28	1.1 $\pm$	0.4	-4.0	2075 $\pm$ 37
GSZ-2	Tukialik Granite	1760	13.9	73.0	0.1114 $\pm$	56	0.511927 $\pm$	46	5.4 $\pm$	0.7	0.3	1740 $\pm$ 63
LANCEGROUND INTRUSIVE SUITE												
0251194	Lanceground Granite	1800	26.8	156.2	0.1023 $\pm$	51	0.511563 $\pm$	43	0.8 $\pm$	0.6	-4.2	2075 $\pm$ 55
0241347	First of LK Granite	1800	22.9	133.9	0.1020 $\pm$	51	0.511418 $\pm$	50	-1.9 $\pm$	0.7	-6.9	2250 $\pm$ 60
0248103	Laram Granite	1800	11.9	73.6	0.0966 $\pm$	48	0.511426 $\pm$	60	-0.6 $\pm$	0.9	-5.5	2150 $\pm$ 67
OTHER UNITS												
0251508	Kuk River Granite	1800	9.8	54.8	0.1111 $\pm$	56	0.511701 $\pm$	61	1.5 $\pm$	0.9	-3.5	2050 $\pm$ 81
0241286	Freshwater Granitoid	1800	8.1	42.9	0.1099 $\pm$	55	0.511575 $\pm$	81	-0.7 $\pm$	1.1	-5.7	2200 $\pm$ 105
0241356	Seaside LK Granitoid	1800	8.1	41.7	0.1127 $\pm$	56	0.511576 $\pm$	40	-1.3 $\pm$	0.6	-6.3	2250 $\pm$ 57

GENERAL INFORMATION			CONCENTRATIONS		ISOTOPIC RATIOS		INITIAL Nd CHARACTERISTICS						
Sample Number	Unit or Comments	Age (Ma)	Sm (ppm)	Nd (ppm)	$^{147}\text{Sm}/^{144}\text{Nd}$ Mean +/- 2 $\sigma$		$^{143}\text{Nd}/^{144}\text{Nd}$ Mean +/- 2 $\sigma$		$\epsilon(\text{Nd})_{\text{CHUR}}$ Mean +/- 2 $\sigma$		$\epsilon(\text{Nd})_{\text{DM}}$ Mean	$T(\text{DM})$ Mean +/- 2 $\sigma$	
MAKOVIKIAN VOLCANIC ROCKS													
284138	U Aillik, Michelin	1850	8.4	51.3	0.0978 +/-	49	0.511156 +/-	50	-5.5 +/-	0.7	-10.3	2500 +/-	58
AKZ-15	U Aillik, Ranger B.	1850	11.2	56.4	0.1395 +/-	70	0.511956 +/-	39	0.2 +/-	0.6	-4.6	2290 +/-	85
0248237	White Bear Mtn. Qzfp	1810	12.6	68.6	0.1100 +/-	55	0.511657 +/-	36	1.0 +/-	0.6	-4.0	2090 +/-	50
0249324	Jagged Edge Area	1810	13.7	59.7	0.1371 +/-	69	0.512157 +/-	28	4.5 +/-	0.5	-0.5	1860 +/-	62
"BASEMENT" ROCKS (Archean Gneiss Data from Brooks, 1983)													
ARCHEAN BASEMENT													
M1-AV	Lavaed Gneiss (n=3)	2600	3.9	26.0	0.0995 +/-	50	0.510697 +/-	35	-5.4 +/-	0.6	-8.0	3110 +/-	46
M2-AV	Lavaed Gneiss (n=2)	2600	4.1	23.6	0.1105 +/-	55	0.510910 +/-	21	-5.0 +/-	0.4	-7.5	3130 +/-	36
M1-AV	Lavaed Gneiss (n=3)	1800			Calculations For The Same Samples				-15.5 +/-	0.5	-20.5	3110 +/-	43
M2-AV	Lavaed Gneiss (n=2)	1800			At T = 1800 Ma				-13.9 +/-	0.4	-18.9	3130 +/-	33
CAPE HARRISON METAMORPHIC SUITE													
AKZ-20	Tonalitic Gneiss	1850	5.8	35.4	0.0996 +/-	50	0.511623 +/-	70	3.2 +/-	1.0	-1.6	1950 +/-	80
AKZ-21	Granodiorite Gneiss	1850	3.2	18.1	0.1057 +/-	53	0.511639 +/-	48	2.1 +/-	0.7	-2.7	2035 +/-	61

NOTES: Initial Neodymium Compositions are calculated assuming CHUR values of  $^{147}\text{Sm}/^{144}\text{Nd} = 0.196593$  and  $^{143}\text{Nd}/^{144}\text{Nd} = 0.512638$  (Present Day)  
 DM values are with respect to  $\epsilon(\text{Nd})_{\text{CHUR}}(2800) = +2$  and  $\epsilon(\text{Nd})_{\text{CHUR}}(1800) = +5$  (Linear Evolution)  
 Errors in  $^{147}\text{Sm}/^{144}\text{Nd}$  are  $\times 10^{-4}$ , Errors in  $^{143}\text{Nd}/^{144}\text{Nd}$  are  $\times 10^{-6}$

Table 8.6. Sm and Nd concentration and isotopic data for Makkovikian plutonic and volcanic rocks, and basement rocks in the east and west at ca. 1800 Ma.

respect to model ages). It also indicates unequivocally that the Cape Harrison Metamorphic Suite is of Proterozoic, and not Archean, age.

$T_{DM}$  model ages in the west vary from 3100 Ma to 1940 Ma, but are mostly older than 2300 Ma. The ca. 3100 Ma model age for the Brumwater Granite is close to the probable formation age of the Archean gneisses (Loveridge et al., 1987), and, with its very low  $\epsilon_{Nd}^{CHUR}$  value, indicates that this unit was derived from Archean crustal material. This result is consistent with the gradational relationship with surrounding migmatites described by Marten (1977).

Most other units in the west have  $\epsilon_{Nd}^{CHUR}$  values higher than the Archean gneisses, and model ages that are younger than 3000 Ma. They cannot therefore be derived entirely from Archean crust formed prior to 3000 Ma, although they may incorporate some of this material.

Similar values of -2.0 to -3.0 for the Long Island unit and two granites of the Kennedy Mountain Intrusive Suite support the suggestion that they are related (Chapter 3), and had similar source(s); however, the value for the Narrows Granite (+3.0) is inconsistent. Note, however, that this is imprecise compared to the other samples, and should carry less weight .

The Pitre Lake Granite, which appears to be a product of anatexis, has surprisingly high  $\epsilon_{Nd}^{CHUR}$  (-1.9), considering its sedimentary protolith, and a very high  $^{147}Sm/^{144}Nd$  ratio (see 8.3.1 for further discussion).

#### Post-Tectonic Makkovikian Plutonic Rocks

$\epsilon_{Nd}^{CHUR}$  values for these rocks vary widely (Table 8.6).

In the Numok Intrusive Suite, syenites from northern and southern zones both have  $\epsilon_{\text{Nd}}^{\text{CHUR}}$  of ca. +1.4. However, quartz monzonite from near to the agmatitic western border of the suite in the northern zone has an anomalous low value of -4.0, and a high Nd content (94 ppm).

Granites from the Strawberry Intrusive Suite display remarkable variation. Three plutons in the west (Bayhead, Cape Strawberry and October Harbour Granites) have  $\epsilon_{\text{Nd}}^{\text{CHUR}}$  of -6.0 to -3.0, whereas those in the east (Dog Islands and Tukialik Granites) have  $\epsilon_{\text{Nd}}^{\text{CHUR}}$  of up to +5.0. There are obviously profound differences in the sources of these rocks from east to west. The Lanceground Hills and Tarun Granites have identical  $\epsilon_{\text{Nd}}^{\text{CHUR}}$  (within error) of ca. 0; the Pistol Lake Granite is slightly, but significantly, lower (-1.9).

To summarize, post-tectonic Makkovikian units show negative  $\epsilon_{\text{Nd}}^{\text{CHUR}}$  in the west, and positive  $\epsilon_{\text{Nd}}^{\text{CHUR}}$  in the east -- a pattern very similar to that of their syn-tectonic counterparts (see above).

Most units have negative  $\epsilon_{\text{Nd}}^{\text{DM}}$ , indicating some component of older crustal material, except for the eastern plutons of the Strawberry Intrusive Suite, which are very close to depleted mantle evolution (i.e.  $\epsilon_{\text{Nd}}^{\text{DM}} = 0$ ). If these granites have a crustal component, it has a crustal residence time below isotopic resolution. Several units in the east have consistent  $T_{\text{DM}}$  model ages of ca. 2000 Ma, similar to those noted above for the syn-tectonic units.

#### **Makkovikian Volcanic Rocks**

The Upper Aillik Group at Ranger Bight has an approximate bulk-earth value ( $\epsilon_{\text{Nd}}^{\text{CHUR}} = 0$ ) for 1850 Ma whereas the Michelin Ridge locality has a low value (-5.5).

The White Bear Mountain porphyry has a moderate (+1.0) value. This is just within error of the adjacent Tarun Granite, which may be a plutonic equivalent of the porphyry. If the Jagged Edge assemblage porphyry is Makkovikian, it would have  $\epsilon_{\text{Nd}}^{\text{CHUR}}$  of +4.5. Amongst plutonic rocks, only the eastern plutons of the Strawberry Intrusive Suite show such characteristics.

On the basis of 4 samples, it is an act of faith to discuss geographic variation; however, the eastward change from -5.5 to +4.5 is consistent with patterns in Makkovikian plutonic rocks described above.

#### Labradorian Plutonic and Volcanic Rocks

In general, Labradorian rocks show less variation in  $\epsilon_{\text{Nd}}^{\text{CHUR}}$  than their Makkovikian counterparts (Table 8.7; also Figure 8.7). Most samples are clustered around bulk-earth  $\epsilon_{\text{Nd}}^{\text{CHUR}}$  values of ca. 0.

In the Adlavik Intrusive Suite, units from the main body and Pamiulik Point areas have similar  $\epsilon_{\text{Nd}}^{\text{CHUR}}$  of ca. +1.0 to -0.5. However, a gabbro from the westernmost intrusion at East MicMac Lake has significantly lower  $\epsilon_{\text{Nd}}^{\text{CHUR}}$  of -6.1, indicating a crustal input. Three samples from the Mount Benedict Intrusive Suite have variable, slightly negative  $\epsilon_{\text{Nd}}^{\text{CHUR}}$ . The lowest value (-2.9, but with a large error) is shown by quartz syenite (0242144) from the most evolved unit. As a group, the Adlavik and Mount Benedict Suites (excluding 0241441) show a smooth progression from values of ca. +1.0 in mafic rocks to ca. -2.0 in syenite and granite, consistent with their Sm-Nd pseudoisochron behaviour (8.2.1).

GENERAL INFORMATION			CONCENTRATIONS		ISOTOPIC RATIOS		INITIAL Nd CHARACTERISTICS			
Sample Number	Unit or Comments	Age (Ma)	Sm (ppm)	Nd (ppm)	$^{147}\text{Sm}/^{144}\text{Nd}$ Mean $\pm$ 2 $\sigma$	$^{143}\text{Nd}/^{144}\text{Nd}$ Mean $\pm$ 2 $\sigma$	$\epsilon(\text{Nd})_{\text{CHUR}}$ Mean $\pm$ 2 $\sigma$	$\epsilon(\text{Nd})_{\text{DM}}$ Mean	$T(\text{DM})$ Mean $\pm$ 2 $\sigma$	
LABRADORIAN PLUTONIC ROCKS										
ADLAVIK INTRUSIVE SUITE										
0241173	Gabbro, Main Body	1650	2.5	10.6	0.1455 $\pm$ 73	0.512141 $\pm$ 33	1.1 $\pm$ 0.5	-4.3	2100 $\pm$ 82	
0241641	Gabbro, East Micmac	1650	4.5	25.4	0.1021 $\pm$ 51	0.511299 $\pm$ 38	-6.1 $\pm$ 0.6	-11.6	2410 $\pm$ 47	
0249062	Gabbro, Pamiulik Pt.	1650	2.2	11.2	0.1142 $\pm$ 57	0.511797 $\pm$ 72	1.0 $\pm$ 1.0	-4.4	1975 $\pm$ 97	
0249039	Diorite, Main Body	1650	5.0	26.9	0.1099 $\pm$ 55	0.511684 $\pm$ 36	-0.3 $\pm$ 0.5	-5.7	2050 $\pm$ 49	
MOUNT BENEDICT INTRUSIVE SUITE										
0242136	Diorite	1650	7.5	40.1	0.1076 $\pm$ 54	0.511649 $\pm$ 40	-0.5 $\pm$ 0.6	-5.9	2050 $\pm$ 53	
0242144	Syenite	1650	9.1	57.1	0.0949 $\pm$ 47	0.511385 $\pm$ 78	-2.9 $\pm$ 1.1	-8.4	2170 $\pm$ 84	
GSZ 6	Quartz Syenite	1650	11.3	63.6	0.1039 $\pm$ 52	0.511579 $\pm$ 32	-1.0 $\pm$ 0.5	-6.5	2080 $\pm$ 41	
MONKEY HILL INTRUSIVE SUITE										
AKZ 12	Monkey Hill Granite	1650	3.8	22.8	0.1063 $\pm$ 53	0.511640 $\pm$ 47	-0.4 $\pm$ 0.7	-5.8	2050 $\pm$ 60	
0248191	Little Monkey Hill	1650	2.0	11.3	0.1093 $\pm$ 55	0.511621 $\pm$ 41	-1.4 $\pm$ 0.6	-6.8	2125 $\pm$ 55	
OTHER UNITS										
AKZ 7	Witchdoctor Granite	1630	1.7	10.9	0.0933 $\pm$ 47	0.511316 $\pm$ 47	-4.2 $\pm$ 0.7	-9.7	2225 $\pm$ 51	
0249076	Burnt Lake Granite	1630	3.1	17.4	0.1105 $\pm$ 55	0.511537 $\pm$ 33	-3.5 $\pm$ 0.5	-9.0	2260 $\pm$ 46	
AKZ 8	Other Lk.-Walker Lk.	1650	7.0	41.2	0.1021 $\pm$ 51	0.511607 $\pm$ 36	-0.1 $\pm$ 0.5	-5.6	2010 $\pm$ 45	
UNCLASSIFIED, POSSIBLY LABRADORIAN PLUTONIC ROCKS										
AKZ 6	Stag Bay Granitoid	1725	12.2	70.3	0.1025 $\pm$ 51	0.511604 $\pm$ 61	0.7 $\pm$ 0.9	-4.6	2025 $\pm$ 72	
0242030	Thunder Mtn Syenite	1725	12.1	66.1	0.1077 $\pm$ 54	0.511633 $\pm$ 66	0.1 $\pm$ 0.9	-5.1	2077 $\pm$ 83	
LABRADORIAN VOLCANIC ROCKS										
0249324	Lagged Edge Area	1650	13.7	59.7	0.1371 $\pm$ 69	0.512157 $\pm$ 28	3.2 $\pm$ 0.5	-2.2	1860 $\pm$ 62	
BRB4187	Bruce River Group	1650	7.9	45.8	0.1014 $\pm$ 51	0.511578 $\pm$ 29	-0.5 $\pm$ 0.4	-6.0	2040 $\pm$ 37	
"BASEMENT ROCKS" (Archean data from Brooks, 1983)										
ARCHEAN BASEMENT										
M1-AV	Layered Gneiss (n=3)	1650	3.9	26.0	0.0995 $\pm$ 50	0.510697 $\pm$ 55	-17.4 $\pm$ 0.6	-22.8	3110 $\pm$ 46	
M2-AV	Layered Gneiss (n=2)	1650	4.1	23.6	0.1105 $\pm$ 55	0.510910 $\pm$ 21	-15.6 $\pm$ 0.4	-21.0	3130 $\pm$ 36	
CAPE HARRISON METAMORPHIC SUITE										
AKZ-20	Tonalitic Gneiss	1850	5.8	35.4	0.0996 $\pm$ 50	0.511623 $\pm$ 70	0.7 $\pm$ 1.0	-4.7	1950 $\pm$ 80	
AKZ-21	Granodiorite Gneiss	1850	3.2	18.1	0.1057 $\pm$ 53	0.511639 $\pm$ 48	-0.3 $\pm$ 0.7	-5.7	2035 $\pm$ 61	

Table 8.7. Sm and Nd concentration and isotopic data for Labradorian plutonic and volcanic rocks, and basement rocks in the east and west at ca. 1650 Ma.

Details of initial Nd and model age calculations as for Table 8.6.



Two samples from the Monkey Hill Intrusive Suite have identical (within error)  $\epsilon_{\text{Nd}}^{\text{CHUR}}$  of 0 to -1.0, a surprisingly high value for siliceous leucogranites. The Witchdoctor and Burnt Lake Granites, despite lithological similarity to the above, have significantly lower  $\epsilon_{\text{Nd}}^{\text{CHUR}}$  of ca. -4.0. The Otter Lake - Walker Lake Granite has an approximate bulk-earth value. Kerr and Fryer (in press) report similarly neutral  $\epsilon_{\text{Nd}}^{\text{CHUR}}$  from two samples (including a biotite-muscovite leucogranite) correlated with this unit in the Nipishish Lake area, 100 km west of the study area.

The Bruce River Group sample has  $\epsilon_{\text{Nd}}^{\text{CHUR}}$  of ca. -0.5, also surprisingly high for a siliceous rhyolite. The Jagged Edge assemblage, if assumed to be of ca. 1650 Ma age, would have  $\epsilon_{\text{Nd}}^{\text{CHUR}}$  of +3.2. This is lower than its  $\epsilon_{\text{Nd}}^{\text{CHUR}}$  at 1810 Ma (see above), but is still higher than any Labradorian plutonic unit, including gabbros of the Adlavik Suite.

All Labradorian samples have negative  $\epsilon_{\text{Nd}}^{\text{DM}}$ , and  $T_{\text{DM}}$  model ages are remarkably consistent at 2100 - 2000 Ma. Spatial variation in  $\epsilon_{\text{Nd}}^{\text{CHUR}}$  and  $T_{\text{DM}}$  is muted compared to that shown by Makkovikian units. The Monkey Hill Suite lies within the same area as older granitoid rocks with negative  $\epsilon_{\text{Nd}}^{\text{CHUR}}$ , but clearly does not share their isotopic characteristics. In general, widely different Labradorian rock types show consistent initial Nd compositions -- a pattern that contrasts with the wide  $\epsilon_{\text{Nd}}$  variations shown by Makkovikian intrusions with relatively constant compositional features.

#### Unclassified Plutonic Rocks

The Stag Bay Granitoid and Thunder Mountain Syenite have  $\epsilon_{\text{Nd}}^{\text{CHUR}}$  within 1  $\epsilon_{\text{Nd}}$  unit of bulk-earth values (0)

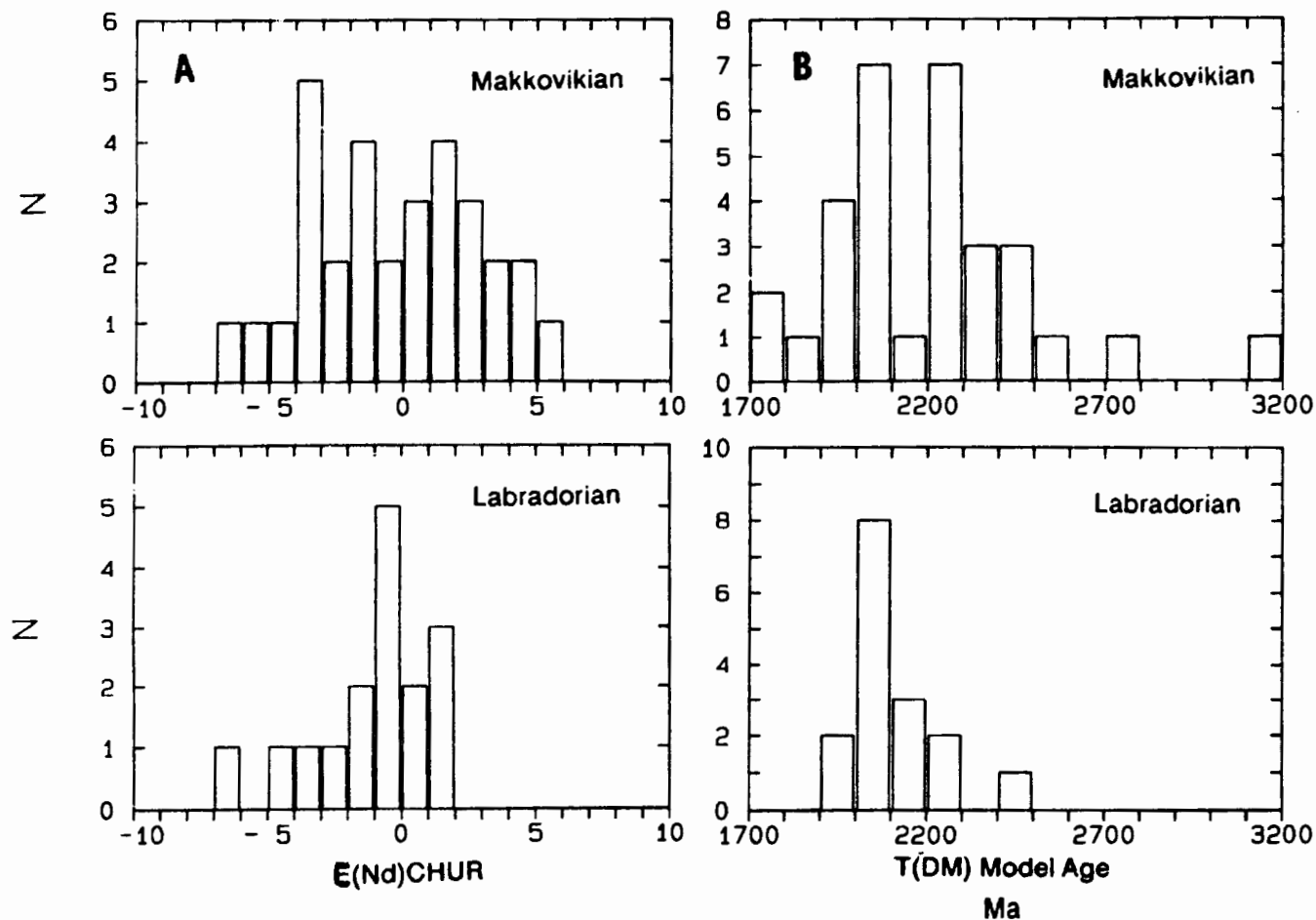


Figure 8.7. Histograms of  $\epsilon_{Nd}^{CHUR}$  and  $T_{DM}$  values for Makkovikian and Labradorian magmatic associations. Units of uncertain age are omitted from compilation.

for  $T = 1725$  Ma. Changing their age to 1800 or 1650 Ma does not affect  $\epsilon_{Nd}$  beyond the limits of analytical uncertainty. Values of this general magnitude are typical of some Makkovikian and most Labradorian plutonic rocks in the east of the area. In subsequent discussions, these unclassified units are arbitrarily grouped with the latter; in practice, their assignation has no impact on interpretation of results.

#### Spatial Variation in $\epsilon_{Nd}^{CHUR}$ and $T_{DM}$

Geographic variation of  $\epsilon_{Nd}^{CHUR}$  and  $T_{DM}$  is illustrated in Figures 8.8 and 8.9. The western and eastern parts of the area are characterized by negative and positive  $\epsilon_{Nd}^{CHUR}$  respectively. The variation is shown most clearly by Makkovikian units. North of the Adlavik Brook fault zone, the generalized boundary between domains is in the vicinity of the Adlavik Islands, where there is a mixture of positive and negative values. South of the Adlavik Brook fault zone, the boundary must be further to the west, as Makkovikian Granitoids west of Big River have positive  $\epsilon_{Nd}^{CHUR}$ . This dextral displacement of ca. 20-30 km is broadly equivalent to that indicated by outcrop patterns of granitoid and supracrustal units north and south of the Adlavik Brook fault zone (Chapter 2; Gower et al., 1982).

The simplest explanation of this variation is that the inversion line indicates the eastern limit of Archean crust in the Makkovik Province. The nature of the crust east of this line is debatable (see later discussion), but it is, without doubt, significantly younger than Archean. A very similar variation pattern is indicated by the distribution of  $T_{DM}$  model ages (Figure 8.9). In both cases the inversion line is a sharp boundary, not a gradational one.

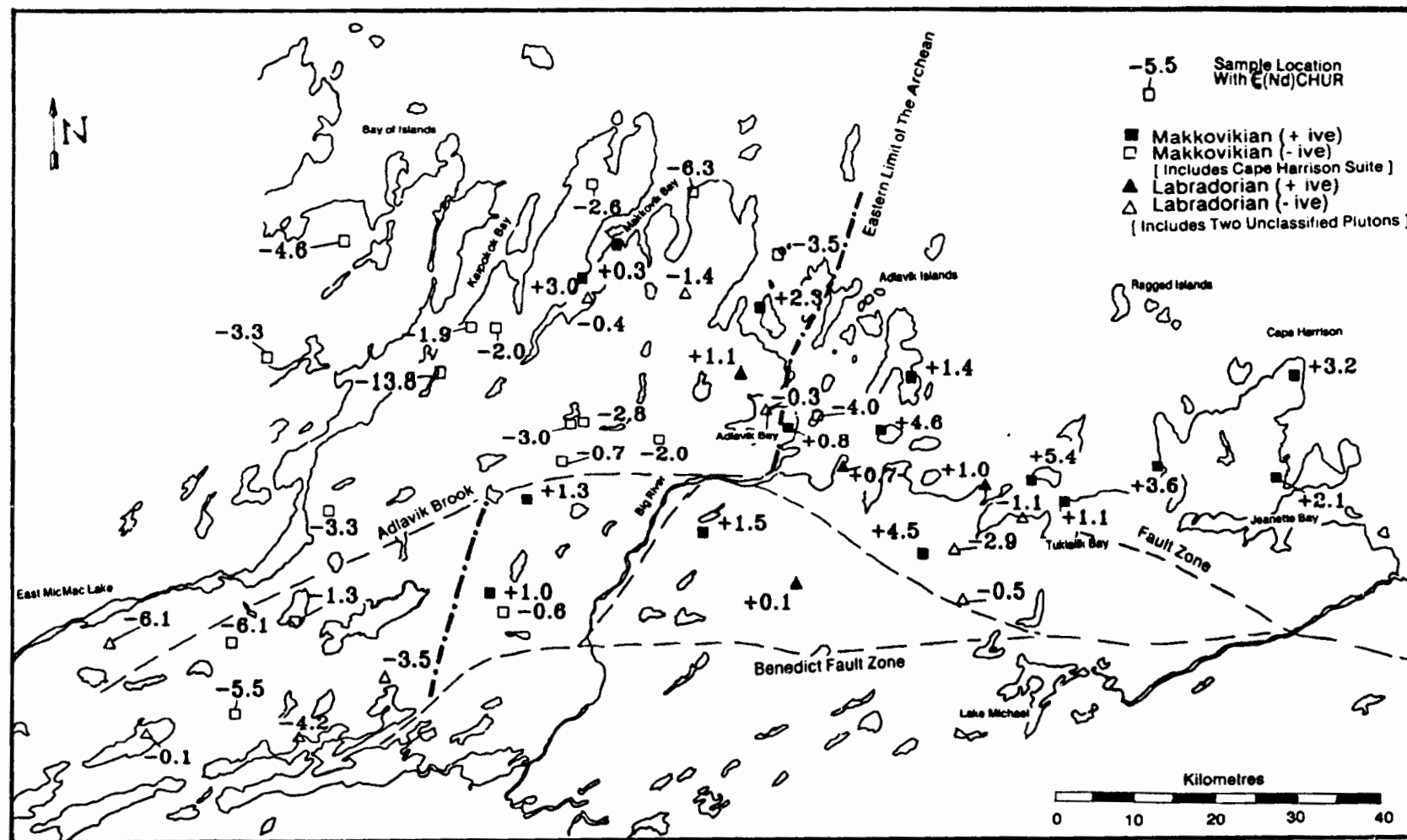


Figure 8.8. Spatial variation of  $\epsilon_{Nd}^{CHUR}$  in Makkovikian and Labradorian magmatic associations, showing the proposed eastern limit of Archean crust. Sample numbers are shown in Figure 8.4.

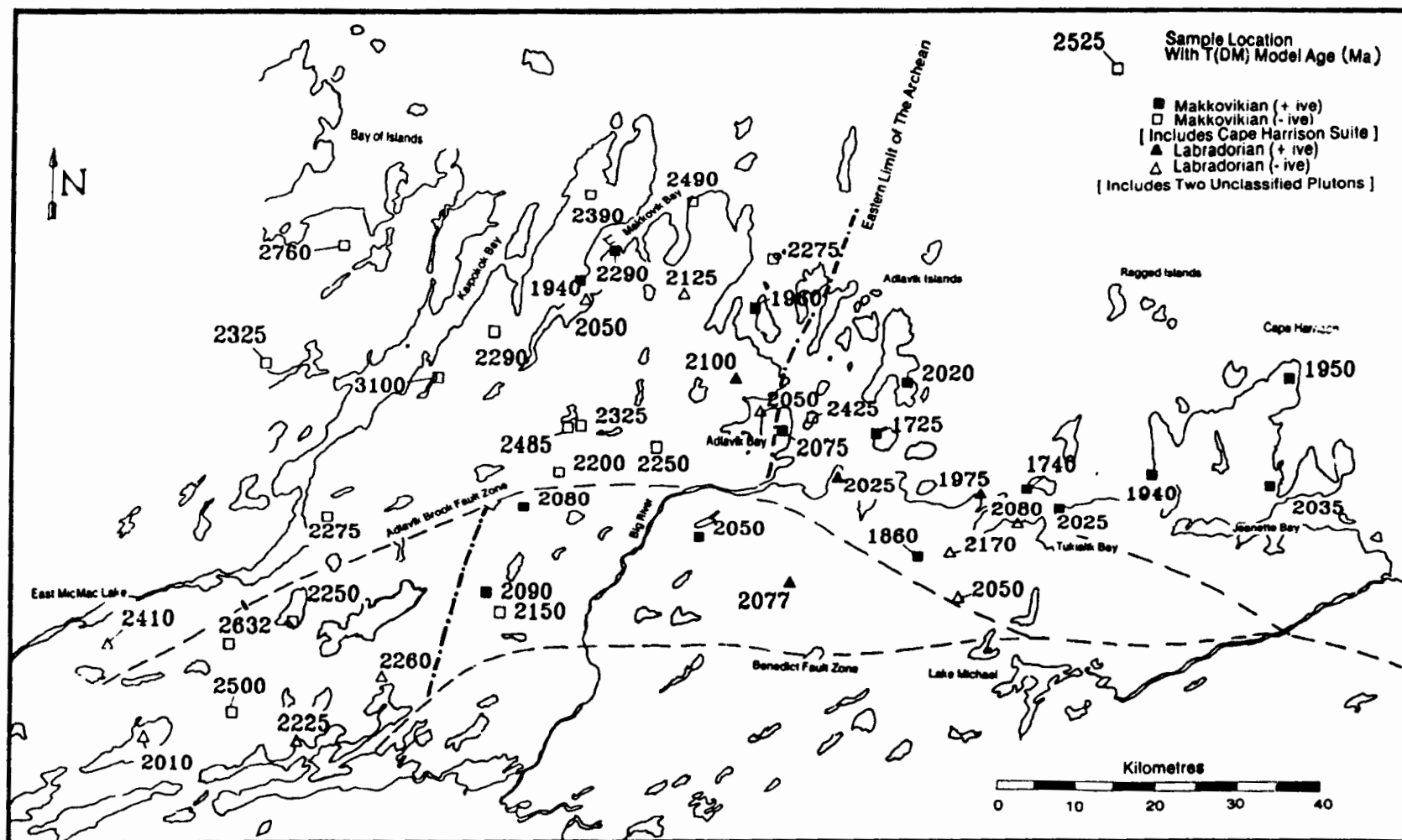


Figure 8.9. Spatial variation of  $T_{DM}$  in Makkovikian and Labradorian magmatic associations, showing the proposed eastern limit of Archean crust. Sample numbers are shown in Figure 8.4.

### 8.2.3 Nd Isotopic Trends and Contrasts

Trace element data discussed below are ICP-MS data (MUN) determined on the sample splits used for Nd analysis (see Appendix B; precision and accuracy estimates in Appendix A). The Jagged Edge porphyry has been grouped tentatively as Makkovikian (on the basis of high  $\epsilon_{Nd}$ ), and Stag Bay and Thunder Mountain are included with Labradorian units.

#### Major Element Patterns

$\epsilon_{Nd}$  is poorly correlated with major element composition (Figure 8.10). The initial isotopic composition of Labradorian units appears independent of major element variation, except for a tendency towards slightly negative  $\epsilon_{Nd}^{CHUR}$  at high  $SiO_2$ .

However, Makkovikian rocks show great variation in  $\epsilon_{Nd}^{CHUR}$  at high  $SiO_2$  contents. In the western domain  $\epsilon_{Nd}^{CHUR}$  decreases with increasing  $SiO_2$ ; this is a common pattern in igneous suites, where siliceous compositions usually contain a greater crustal component. However, the increasing  $\epsilon_{Nd}^{CHUR}$  seen at high  $SiO_2$  contents in the east is very unusual. It should be noted, however, that this trend is imparted largely by samples from the eastern Strawberry Suite and Jagged Edge assemblage, and may not be typical of all units. Similar antithetic behaviour of  $\epsilon_{Nd}^{CHUR}$  in Makkovikian rocks is shown by correlations against FeO,  $Na_2O$  and N/N+K ratios, but no correlation is present against  $Al_2O_3$  and  $K_2O$  (Figure 8.10).

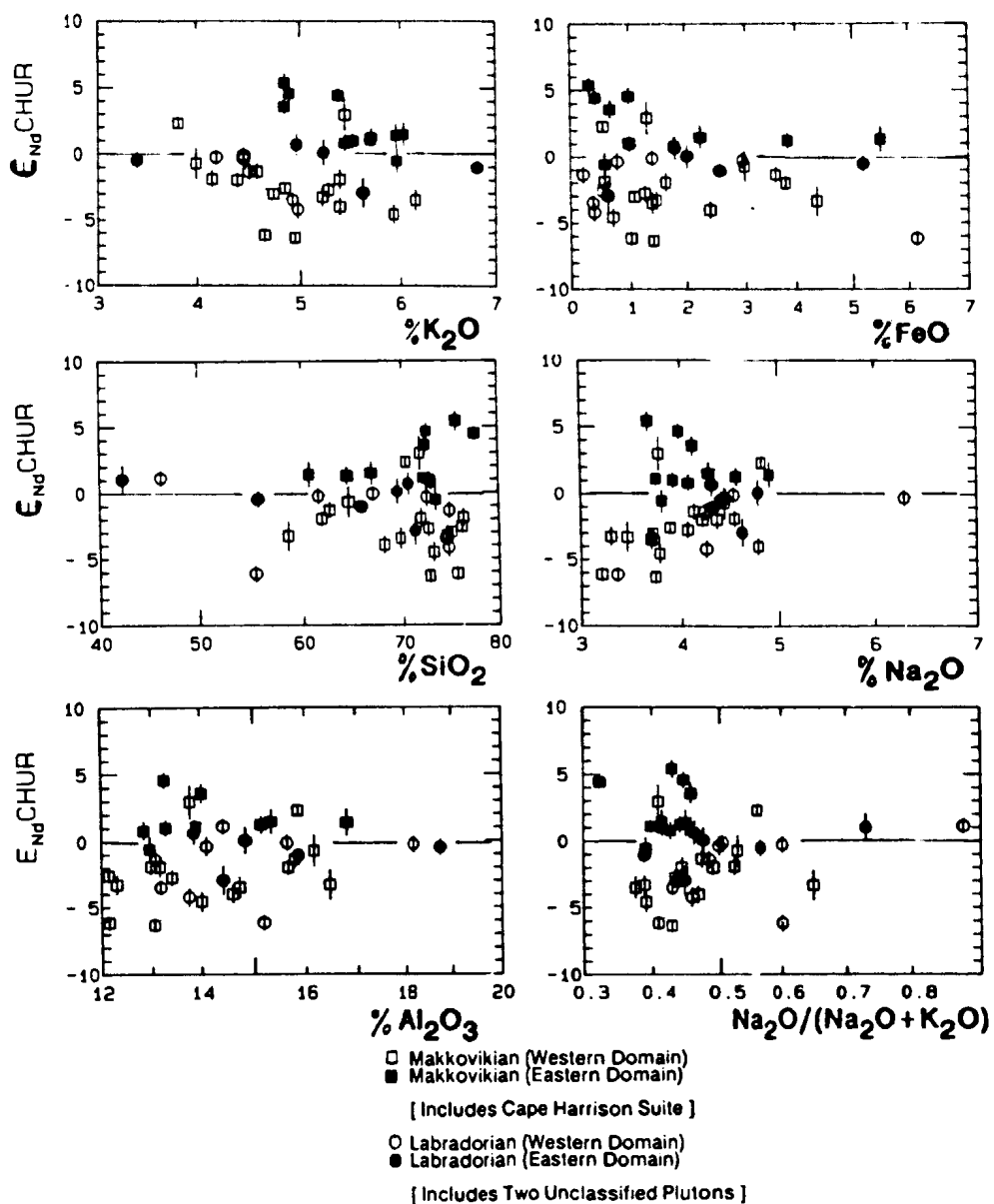


Figure 8.10. Correlations between initial Nd isotopic composition ( $\epsilon_{Nd}^{CHUR}$ ) and major element compositional variations.

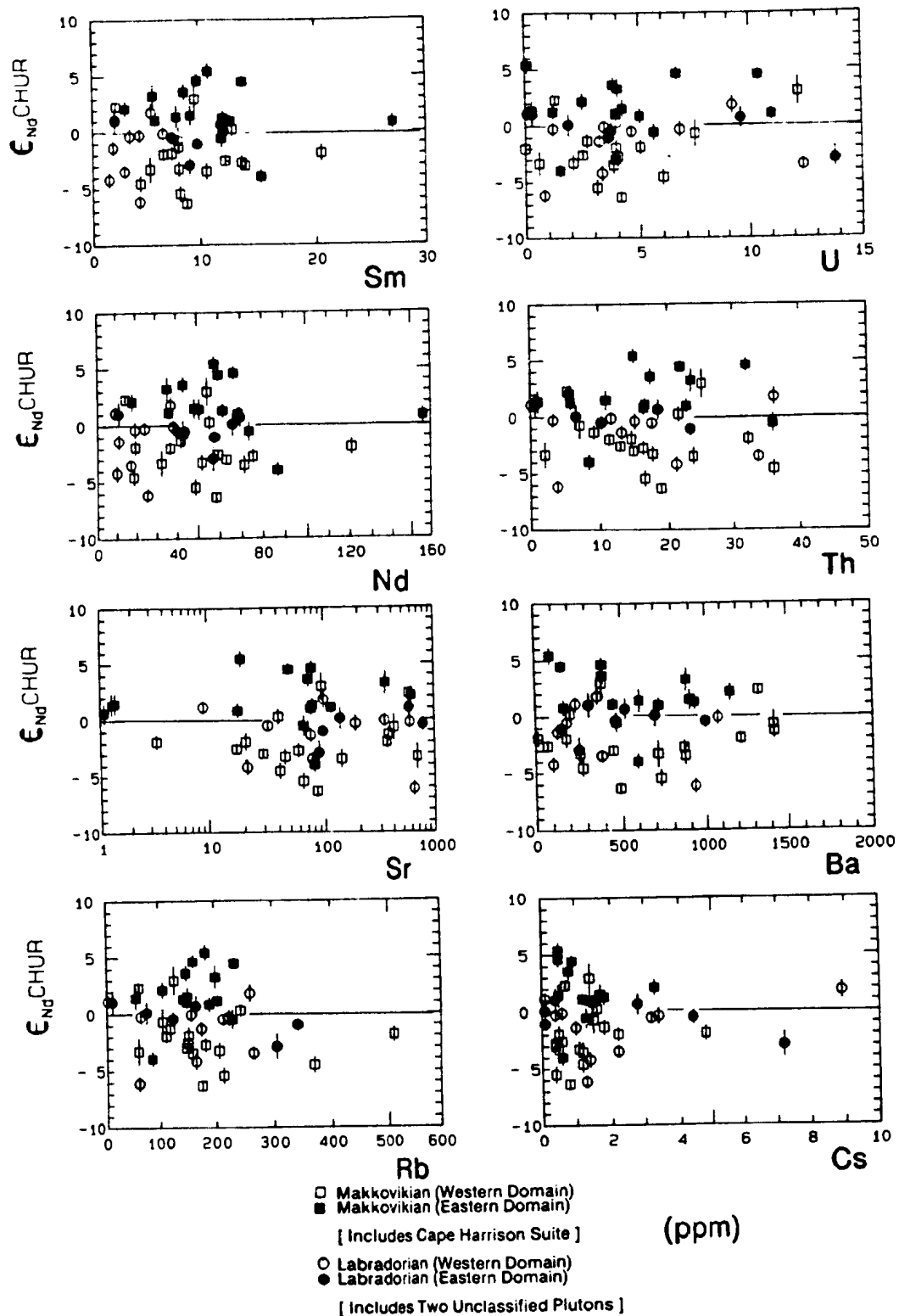


Figure 8.11. Correlations between initial Nd isotopic composition ( $\epsilon_{NdCHUR}$ ) and trace element compositional variations.



### Trace Element Patterns

There is no correlation between  $\epsilon_{\text{Nd}}$  and either Nd or Sm (Figure 8.11). Trace elements which measure differentiation (e.g. Rb and Th; Figure 8.11) illustrate the same divergent behaviour as analogous major element parameters (e.g.  $\text{SiO}_2$ ). In the east,  $\epsilon_{\text{Nd}}^{\text{CHUR}}$  increases with differentiation, whereas it decreases with differentiation in the west. In the western domain, there is a good inverse linear relationship between  $\epsilon_{\text{Nd}}^{\text{CHUR}}$  and Th, defined by the Long Island unit, Kennedy Mountain Intrusive Suite and western plutons of the Strawberry Suite. There are no obvious correlations between  $\epsilon_{\text{Nd}}^{\text{CHUR}}$  and these trace elements amongst Labradorian or unclassified rocks. Ba, Sr and Cs (Figure 8.11) show no clear patterns for either group.

### Initial Ratio Trends

Initial Sr and Nd isotopic compositions are commonly inversely correlated in crustal rocks (e.g. DePaolo, 1981b; McCulloch and Chappell, 1982; Farmer and DePaolo, 1983; Wilson et al., 1985), and are commonly assessed via  $\epsilon_{\text{Nd}} - \epsilon_{\text{Sr}}$  diagrams, where hyperbolic trends are characteristic of mixing processes (e.g. Gray, 1984). This method cannot be used in this study due to the unreliability of whole-rock Sr data. However, "initial ratio isochron" diagrams where initial Nd compositions are plotted against  $^{147}\text{Sm}/^{144}\text{Nd}$  ratios (Figure 8.12) should define linear trends in situations dominated by simple mixing, although such trends may be complicated by subsequent fractionation (Gray, 1984).

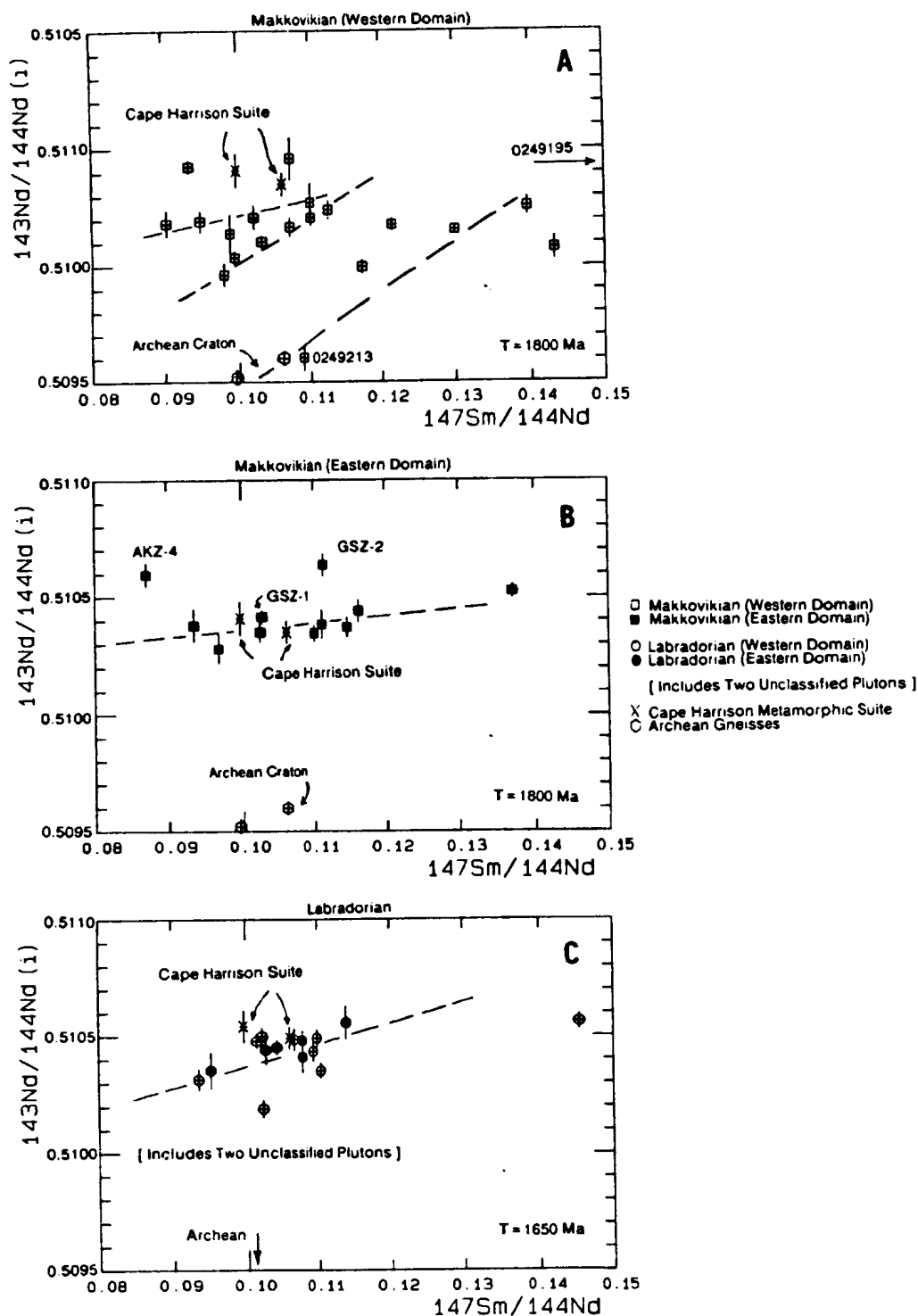


Figure 8.12. "Initial Ratio Isochron Diagrams" (after Gray, 1984), showing initial  $^{143}\text{Nd}/^{144}\text{Nd}$  versus  $^{147}\text{Sm}/^{144}\text{Nd}$ . (a) Makkovikian (eastern domain). (b) Makkovikian (western domain) (c) Labradorian and unclassified units (both domains). Lines a visual estimates of linear (mixing?) trends.

Makkovikian units in the eastern domain define a gently inclined to flat-lying array (Figure 8.12). Two samples from the Strawberry Intrusive Suite (AKZ-4; GSZ-2) lie well above this trend.

Makkovikian units in the western domain are scattered, but define linear subtrends (Figure 8.12); however, these trends do not correspond to petrological associations or suites. They are steeply inclined, and the Archean gneisses of Brooks (1983) plot close to the lower end of one feature.

Labradorian units mostly lie on a positive linear array (Figure 8.12); this has an orientation intermediate between those defined by Makkovikian units from eastern and western domains.

Linear trends of this type are consistent with (but not diagnostic of) two-component mixing relationships (e.g. Gray, 1984). If they have such a cause, the flat-lying trend of Makkovikian units in the east indicates similar  $^{143}\text{Nd}/^{144}\text{Nd}$  for both end members, whereas the steep trends in the west indicate significant differences in their Nd isotopic composition. The disorganized pattern amongst Makkovikian units in the west suggests a complex mixing system with a variety of end-member compositions.

Note that the Cape Harrison Metamorphic Suite lies in the centre of the data array for Makkovikian (east) units, and cannot therefore strictly represent an end-member of a two-component system. However, any fractionation of Sm and Nd would move points along the trend to lower  $^{147}\text{Sm}/^{144}\text{Nd}$ , so this is not an absolute constraint. The Cape Harrison Suite lies above the Labradorian array at  $T = 1650$  Ma.

### 8.3 SUMMARY and DISCUSSION

This section is concerned mostly with the implications of Nd isotopic data, and also attempts to model the sources of Makkovikian and Labradorian magmas quantitatively.

#### 8.3.1 The Unusual Case of The Pitre Lake Granite

**Isotopic Evolution** : The Pitre Lake Granite has  $^{147}\text{Sm}/^{144}\text{Nd}$  (0.226) that is higher than accepted present-day values for CHUR (ca. 0.1966). It is evolving in the opposite direction (relative to CHUR) from most crustal rocks, i.e. its  $\epsilon_{\text{Nd}}^{\text{CHUR}}$  is increasing with time. Isotopic evolution of this granite is subparallel to postulated depleted mantle evolution, and its  $T_{\text{DM}}$  model age is infinite (Figure 8.13). These unusual features are demonstrated by its contrast with the anatectic Brumwater Granite, which evolves "normally" within the spectrum of its Archean precursors (Figure 8.13).

**Fractionation of Sm and Nd** : The high  $^{147}\text{Sm}/^{144}\text{Nd}$  ratio indicates strong parent/daughter element fractionation during its generation. Such anomalous values have rarely been reported from crustal rocks.

Stevenson and Patchett (1988) attributed a similar value in an Archean leucogranite to garnet fractionation, but do not specify whether the anomalous granite is itself garnetiferous. Windrim et al. (1984) interpreted huge variations of  $^{147}\text{Sm}/^{144}\text{Nd}$  and  $\epsilon_{\text{Nd}}$  in sapphirine granulites in terms of pre-metamorphic hydrothermal

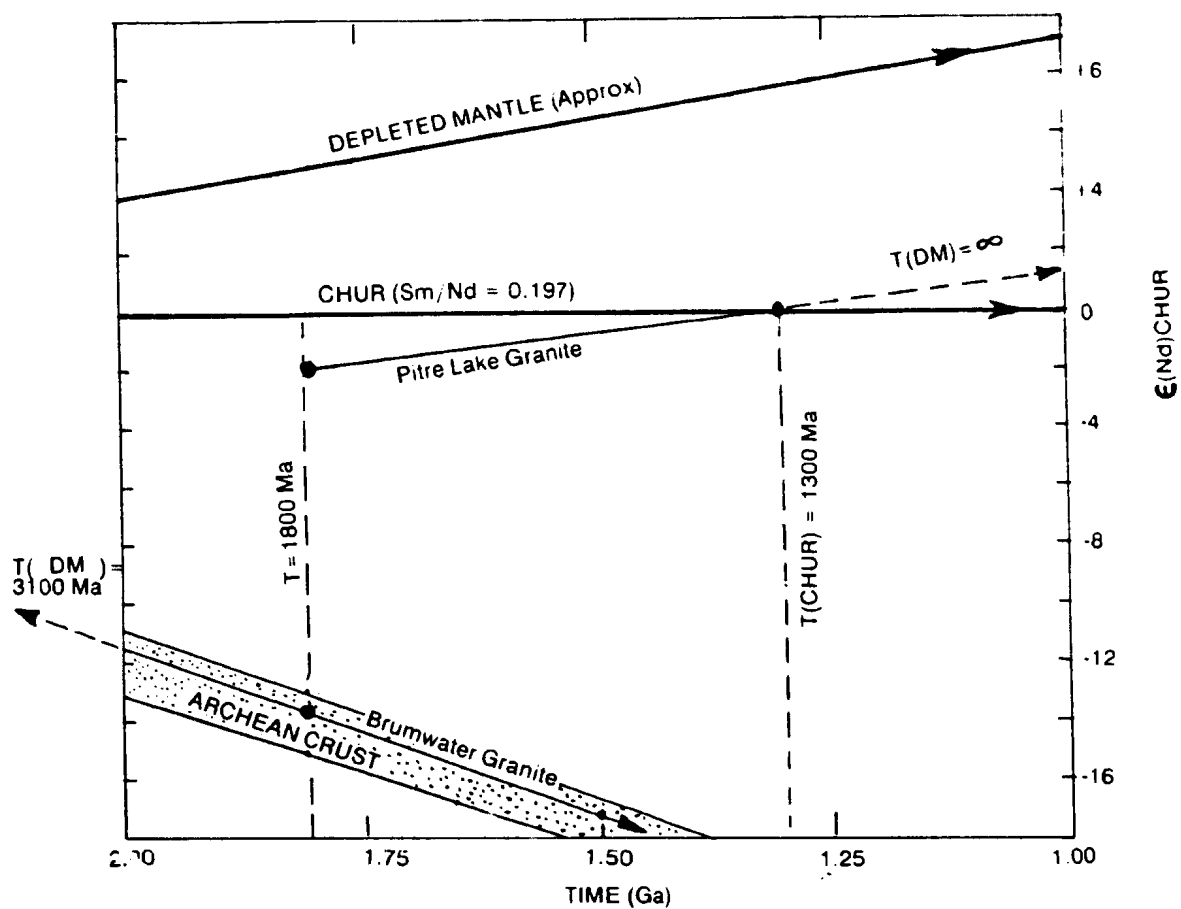


Figure 8.13. The unusual characteristics of the Pitre Lake Granite, compared to the relatively "normal" behaviour of the Brumwater Granite. Note that the Pitre Lake Granite evolves in the opposite direction (relative to CHUR) from most crustal rocks (compare to Figure 8.6).

processes. Unusual LREE-depleted geochemical patterns in Himalayan leucogranites have similarly been attributed to fluid activity (Vidal et al., 1982; Searle and Fryer, 1988)

The Pitre Lake Granite is not garnetiferous, and any residual garnet during anatexis would decrease Sm/Nd in an anatectic melt, based on distribution coefficients. Garnet fractionation could also not generate the unusual REE pattern of the granite (Figure 3.11, p.91). The normal behaviour of the adjacent Brumwater Granite, also of anatectic origin, argues against regional hydrothermal or metamorphic effects.

It is tentatively suggested that a residual accessory phase may have retained Nd during anatexis. Allanite and/or monazite are possible culprits, as both could strongly deplete partial melts in Nd (Miller and Mittlefehdt, 1982; Michael, 1983). As no samples were collected from the metasedimentary rocks, this cannot be tested directly at present.

**Source Characteristics :** Regardless of subsequent evolution, the high  $\epsilon_{Nd}^{CHUR}$  of -1.9 indicates the characteristics of the source to the granite at 1800 Ma. This indicates a dearth of ancient Archean material in precursor metasediments, a surprising result in view of previous suggestions that they were deposited on local Archean Crust (Sutton, 1972). It may indicate that metasedimentary rocks of the Lower Aillik Group represent detritus from juvenile Proterozoic material, and/or a highly allochthonous setting for the sequence, which is everywhere separated from Archean basement by ductile slides (Marten, 1977).

**Implications** : Any discussion must remain speculative until the mineralogy and geochemistry of the metasedimentary precursors of the granite are better known. A detailed examination of Nd behaviour during anatexis of different components of the Kaipokok Bay fold belt is an interesting avenue for further work. Rocks such as the Pitre Lake Granite represent low melting-point components of the crust, and their importance as potential contaminants to other magmas (given time for isotopic evolution) outweighs their actual abundance. This example shows that crustal rocks do not invariably contrast strongly with the mantle in terms of Nd isotopic composition. It would also be interesting to test the equivalence of Moran Lake and Lower Aillik Group supracrustal sequences via their Nd isotopic compositions, which would record the proportion of Archean versus Proterozoic detritus in each.

### 8.3.2 Possible Sources of Makkovikian Magmas

#### **Nature of Basement In The Makkovik Province**

Variations in initial Nd isotopic composition indicate that Makkovikian rocks had different source material(s) in east and west (Figures 8.8; 8.9). Negative  $\epsilon_{\text{Nd}}^{\text{CHUR}}$  in the western domain indicates a contribution from older material, probably Archean continental crust. Generally positive  $\epsilon_{\text{Nd}}^{\text{CHUR}}$  in the eastern domain precludes a significant contribution from such material. Possible "basement" in the east (Cape Harrison Metamorphic Suite) is unlikely to be older than 2100 Ma, based on  $T_{\text{DM}}$  model ages (Table 8.6).

This striking geographic variation suggests that the isotopic features of Makkovikian magmas were influenced by the nature of local basement rocks, and implies that they were in part derived from such materials.

Continuity of elemental geochemical patterns from east to west, particularly amongst post-tectonic units, indicates that magmas in both domains had similar sources (and proportions thereof) in bulk compositional terms. For example, five plutons of the Strawberry Intrusive Suite have almost identical petrological and geochemical features, yet have a westward shift in  $\epsilon_{\text{Nd}}^{\text{CHUR}}$  from +5.0 to -6.0. If the western plutons contain a component derived from sialic crust, it follows that the eastern plutons also contain such material.

It is therefore concluded that the eastern Makkovik Province is underlain by sialic continental crust of Proterozoic age generated during pre-Makkovikian and/or Makkovikian episodes. The Cape Harrison Metamorphic Suite may represent some of this material; however, as discussed below, it does not fulfill all isotopic requirements.

The inferred edge of the Archean Craton is offset dextrally by the Adlavik Brook fault zone (Figures 8.8, 8.9). Taken at face value, this indicates a major structure that extends through the continental crust. However, as the fault zone was active during the Grenvillian orogeny, the apparent displacement may only be in the upper levels of the crust -- i.e., intrusions may no longer be above their original source regions.

#### Sources of Makkovikian Magmas

**Western Domain** : Low  $\epsilon_{\text{Nd}}^{\text{CHUR}}$  and high  $T_{\text{DM}}$  in the west indicate contributions from older crust. The most extreme example is the Brumwater Granite, which is



isotopically indistinguishable from the Archean (Table 8.6; Figure 8.13), and was probably derived entirely by anatexis of this material. Most other units in the west, however, have higher  $\epsilon_{\text{Nd}}^{\text{CHUR}}$  than the Archean gneisses would have at 1800 Ma.

It is suggested here that they are mixtures of juvenile mantle-derived material and older continental crust. An alternative explanation is that they were derived by anatexis of continental crust generated at a variety of times between 2600 and 2000 Ma ago (c.f. McCulloch and Chappell, 1982). This is considered unlikely, as there is no evidence of orogenic activity during this period in Labrador, or on a worldwide scale (Patchett and Arndt, 1986). Mantle-crust interaction during granitoid magmatism was suggested by DePaolo (1981b) in the western U.S.A, and by Halliday (1984) in the British Caledonides. However, the initial ratio isochron diagram for the western domain (Figure 8.12) suggests that there is no simple two-component mixing system in this area.

In view of the lithological and structural complexity of the Archean Nain Province, this is not unexpected. The  $\epsilon_{\text{Nd}}^{\text{CHUR}}$  of the Brumwater Granite (ca. -14.0) indicates that, at least locally, values calculated from the data of Brooks (1983) are representative, but anatexis commonly samples the lowest melting-point compositions within its precursor. The Archean of the Hopedale area also includes extensive tonalitic and trondhjemitic granitoid rocks of ca. 2800 Ma age (Loveridge et al., 1987), and a range of Archean supracrustal rocks. These would all have different Sm/Nd ratios and  $\epsilon_{\text{Nd}}^{\text{CHUR}}$  values at 1800 Ma, and cannot therefore be represented as a point-source in a mixing diagram.

**Eastern Domain** : Units in the eastern domain define a linear initial ratio trend that is almost flat-lying (Figure 8.12). This is consistent with simple mixing of two components with similar  $^{143}\text{Nd}/^{144}\text{Nd}$ , but different  $^{147}\text{Sm}/^{144}\text{Nd}$ . It is suggested here that these magmas were mixtures between a "juvenile" component and slightly older Proterozoic sialic crust perhaps represented by material such as the Cape Harrison Metamorphic Suite. The well-defined linear trend suggests a simpler system, possibly with only two end-members. Two samples from eastern plutons of the Strawberry Suite (e.g. AKZ-4, GSZ-2) lie above this trend, but a third (GSZ-1) lies within it. These units may therefore have had somewhat different sources.

#### Crust-Mantle Mixing Models

**Methodology** : The proportion of continental crust (X) added to one part of a more juvenile magma to form new crust is given by the simplified expression :

$$X = \frac{C_{\text{Nd}}(\text{JV}) [\epsilon_{\text{Nd}}(\text{NC}) - \epsilon_{\text{Nd}}(\text{JV})]}{C_{\text{Nd}}(\text{CC}) [\epsilon_{\text{Nd}}(\text{CC}) - \epsilon_{\text{Nd}}(\text{NC})]}$$

where JV = juvenile component, NC = new crust, CC = crustal component, and  $C_{\text{Nd}}$  = Nd concentration (Pushkar et al., 1972; Patchett and Bridgwater, 1984; Chauvel et al., 1987). The percentage of crustal component is given simply by  $100X / (1 + X)$ . Results depend heavily on Nd concentrations in the end-members; in the case of the juvenile component, these are difficult to constrain. An upper limit to its  $\epsilon_{\text{Nd}}^{\text{CHUR}}$  is provided by depleted mantle at ca. 1800 Ma

(+5.0; Nelson and DePaolo, 1984; Patchett and Bridgwater, 1984). However, modern island-arc magmas commonly have slightly lower  $\epsilon_{\text{Nd}}$  than inferred depleted mantle compositions (e.g. White and Patchett, 1984). The Nd content of a mantle-derived basalt to andesite magma could range from 5 to 20 ppm, based on modern island arcs (White and Patchett, 1984). A Nd content of 25 ppm is assumed for the crustal component, based on data from Brooks (1983). This is slightly lower than estimated mean values for sialic crust based on composite samples (e.g. Patchett and Bridgwater, 1984).

**Results :** Due to the difficulty in constraining end-members, model results are given as matrices (Table 8.8), which give the percentages of crustal material required to generate a specific final  $\epsilon_{\text{Nd}}^{\text{CHUR}}$  value. The parameters of crustal end-members are based on the Archean gneisses and Cape Harrison Suite in west and east respectively; the average  $\epsilon_{\text{Nd}}^{\text{CHUR}}$  of the former is increased to -12.0, to account for younger (2800 Ma) material within it. . It is assumed that the juvenile magma had  $\epsilon_{\text{Nd}}^{\text{CHUR}}$  of +5.0. All are conservative estimates which, if anything, will overestimate the proportion of crustal material required.

For a value of 10 ppm Nd in the juvenile component (c.f. Patchett and Bridgwater, 1984), a typical Makkovikian magma in the west must include from 26% (final  $\epsilon_{\text{Nd}}^{\text{CHUR}} = -3.0$ ) to 42% (final  $\epsilon_{\text{Nd}}^{\text{CHUR}} = -6.0$ ) Archean crust (Table 8.8a). The proportion of Archean material required varies in sympathy with the Nd concentration in the juvenile component. In the eastern domain, equivalent amounts of mixing using Cape Harrison material as "crust" would reduce  $\epsilon_{\text{Nd}}^{\text{CHUR}}$  by less than two  $\epsilon_{\text{Nd}}$  units (Table 8.8b).

A

WESTERN DOMAIN (Archean Continental Crust)

$\epsilon(\text{Nd})_{\text{CHUR}}$  of Crustal Component = -12.0 (Conservative)  
 $\epsilon(\text{Nd})_{\text{CHUR}}$  of Juvenile Component = +5.0 (Depleted Mantle)  
 Concentration of Nd in Crustal Component = 25 ppm

Final $\epsilon(\text{Nd})_{\text{CHUR}}$ Value	Concentration of Nd in Juvenile Component						Percentage Of Crustal Component Required
	5 ppm	7.5 ppm	10 ppm	15 ppm	20 ppm	25 ppm	
+5	0	0	0	0	0	0	
+4	1	2	2	4	5	6	
+3	3	4	5	7	10	12	
+2	4	6	8	11	15	18	
+1	6	8	11	16	20	24	
0	8	11	14	20	25	29	
-1	10	14	18	25	30	35	
-2	12	17	22	30	36	41	
-3	15	21	26	35	42	47	
-4	18	25	31	40	47	53	
-5	22	30	36	46	53	59	
-6	27	35	42	52	59	65	
-7	32	42	49	59	66	71	
-8	39	49	57	66	72	76	
-9	48	58	65	74	79	82	
-10	60	69	75	82	86	88	
-11	76	83	86	91	93	94	
-12	100	100	100	100	100	100	

B

EASTERN DOMAIN (Juvenile Proterozoic Continental Crust)						
$\epsilon(\text{Nd})_{\text{CHUR}}$ of Crustal Component = +2.0 (Cape Harrison Suite)						
$\epsilon(\text{Nd})_{\text{CHUR}}$ of Juvenile Component = +5.0 (Depleted Mantle)						
Concentration of Nd in Crustal Component = 25 ppm						
	Concentration of Nd in Juvenile Component					
Final	5 ppm	7.5 ppm	10 ppm	15 ppm	20 ppm	25 ppm
$\epsilon(\text{Nd})_{\text{CHUR}}$ Value						
+5.0	0	0	0	0	0	0
+4.5	4	6	7	11	14	17
+4.0	9	13	17	23	29	33
+3.5	17	23	29	38	44	50
+3.0	29	38	44	55	62	67
+2.5	50	60	67	75	80	83
+2.0	100	100	100	100	100	100

Percentage Of  
Crustal Component  
Required

Table 8.8. Two-component mixing matrices for Makkovikian magmas, showing percentages of crustal component required to generate a specific final  $\epsilon_{\text{Nd}}^{\text{CHUR}}$  value. (a) Western domain (Archean Crust). (b) Eastern Domain (Proterozoic Crust).

These are model-dependant results, and no unique solution is possible. However, the amounts of mixing required in the west are reasonable for combined assimilation - fractional crystallization (DePaolo, 1981a), and it is clear that equivalent interaction in the east would be very difficult to recognize isotopically, particularly if the Nd content of the juvenile component was lower, or its  $\epsilon_{\text{Nd}}^{\text{CHUR}}$  higher than postulated.

However, eastern plutons of the Strawberry Intrusive Suite have higher  $\epsilon_{\text{Nd}}^{\text{CHUR}}$  than permitted if they incorporate significant amounts even of Cape Harrison-type materials. Any crustal component in these rocks must have a minimal crustal prehistory. Three samples in the east also have  $\epsilon_{\text{Nd}}^{\text{CHUR}}$  values that are equivalent to or slightly below those for the Cape Harrison Metamorphic Suite at 1800 Ma, but within analytical error of these rocks. If this difference is real, it may indicate that material with lower  $\epsilon_{\text{Nd}}^{\text{CHUR}}$  than the Cape Harrison Suite also contributed some material to the magmas.

### 8.3.3 Possible Sources Of Labradorian Magmas

#### **Continuity of Isotopic Compositions**

Labradorian suites show less variation in  $\epsilon_{\text{Nd}}^{\text{CHUR}}$  (Table 8.7), and show no strong geographic variation (Figure 8.8). With the exception of three samples in the west, most have values close to those of CHUR (0), regardless of their composition or location. There are, however, some slightly negative  $\epsilon_{\text{Nd}}^{\text{CHUR}}$  values in the Benedict Mountains area (see below).

Similar observations were made by Patchett and Bridgwater (1984) and Patchett and Kouvo (1986), who found

that a wide range of Proterozoic igneous rocks in Greenland and Finland also clustered around approximate bulk-earth  $\epsilon_{\text{Nd}}^{\text{CHUR}}$  values (ca. 0).

#### Sources Of Labradorian Magmas

Processes which could account for  $\epsilon_{\text{Nd}}^{\text{CHUR}}$  values of ca. 0 include derivation from an undepleted mantle reservoir or melting of slightly older continental crust. In terms of the study area, the first appears unlikely in view of direct evidence for depleted source materials in Makkovikian granitoid rocks. The second cannot be ruled out for granites (s.s), as the Cape Harrison Metamorphic Suite and some Makkovikian rocks in the east would have  $\epsilon_{\text{Nd}}^{\text{CHUR}}$  of ca. 0 at 1650 Ma, and some have similar  $T_{\text{DM}}$  to the Labradorian samples. However, it is difficult to visualize a partial melting process that could generate mafic and intermediate magmas of the Adlavik and Mount Benedict Intrusive suites from such materials; these must surely be derived from mantle materials. Also, the  $\epsilon_{\text{Nd}}^{\text{CHUR}}$  of Makkovikian rocks in the western domain indicates that some Makkovikian crust in this part of the area would have had  $\epsilon_{\text{Nd}}^{\text{CHUR}}$  of -4.0 to -8.0 at 1650 Ma.

A third alternative is that Labradorian magmas are mixtures of juvenile material and older crust -- but in relatively constant proportions. Patchett and Bridgwater (1984) and Patchett and Kouvo (1986) preferred this alternative in their studies, and suggested that mixing and homogenization of end-members was achieved by subduction of continent-derived sediment into zones of mantle melting. Observed compositional variation was then produced by fractionation and remelting of this material in the crust.

In general terms, this model appears to be applicable to Labradorian plutonic rocks, but it should be noted that

the role of subducted sediment in arc magmatism has been questioned (e.g. Pankhurst et al., 1988; Hildreth and Moorbath, 1988; see chapter 9). Distal (subcrustal?) mixing is also consistent with the lack of evidence for direct contributions from local Archean basement rocks, and with the constancy of  $\epsilon_{\text{Nd}}^{\text{CHUR}}$  across the Labradorian compositional spectrum.

The Witchdoctor and Burnt Lake Granites, however, contain greater amounts of an older component. These could incorporate local Archean basement material or, alternatively, could be anatectic melts derived from Makkovikian granitoid rocks. However, they lie on a well-defined initial ratio isochron with other Labradorian samples (Figure 8.12), suggesting that they may simply be part of the same mixing spectrum.

### Mixing and Contamination Models

Mixing calculations for Labradorian magmas are summarized in Table 8.9a. Using  $\epsilon_{\text{Nd}}^{\text{CHUR}} = +5.5$  and 10 ppm Nd for juvenile mantle-derived material, and -12.0 and 25 ppm respectively for the crustal component (c.f. Patchett and Bridgwater, 1984; 8.3.2), a Labradorian magma with final  $\epsilon_{\text{Nd}}^{\text{CHUR}}$  of 0 must contain ca. 15% crustal material. This is geologically reasonable, and similar to estimates of the sedimentary component in some modern arc magmas (White and Patchett, 1984). It is also a reasonable proportion for direct assimilation but, as discussed above, such an explanation requires that gabbro and leucocratic granites both contain the same proportions of assimilated crust, which is unlikely.

Variation of  $\epsilon_{\text{Nd}}^{\text{CHUR}}$  in the Adlavik and Mount Benedict Suites is treated in the same manner to assess contamination by crustal material (Table 8.9b). The

A

Labradorian Plutonic Rocks (General)

$\epsilon(\text{Nd})_{\text{CHUR}}$  of Crustal Component = -12.0 (Conservative)  
 $\epsilon(\text{Nd})_{\text{CHUR}}$  of Juvenile Component = +5.5 (Depleted Mantle)  
Concentration of Nd in Crustal Component = 25 ppm

Final $\epsilon(\text{Nd})_{\text{CHUR}}$ Value	Concentration of Nd in Juvenile Component					
	5 ppm	7.5 ppm	10 ppm	15 ppm	20 ppm	25 ppm
+5	0	1	1	2	2	3
+4	1	3	4	5	7	9
+3	2	5	6	9	12	14
+2	2	7	9	13	17	20
+1	3	9	12	17	22	26
0	4	12	15	22	27	31
-1	6	15	19	26	32	37
-2	7	18	23	31	38	43
-3	9	22	27	36	43	49
-4	11	26	32	42	49	54
-5	13	31	38	47	55	60
-6	16	37	43	53	61	66
-7	20	43	50	60	67	71
-8	25	50	57	67	73	77
-9	33	59	66	74	79	83
-10	44	70	76	82	86	89
-11	62	93	87	91	93	94
-12	100	100	100	100	100	100

Percentage Of  
Crustal Component  
Required

Contamination Of Adlavik and Mount Benedict Intrusive Suites

**B**

$\epsilon(\text{Nd})_{\text{CHUR}}$  of Crustal Component = -12.0

$\epsilon(\text{Nd})_{\text{CHUR}}$  of Parental Magma = +1.0 (Adlavik Gabbro)

Concentration of Nd in Crustal Component = 25 ppm

	Concentration of Nd in Parental Magma						
Final $\epsilon(\text{Nd})_{\text{CHUR}}$ Value	5 ppm	7.5 ppm	10 ppm	15 ppm	20 ppm	25 ppm	
+1.0	0	0	0	0	0	0	Percentage Of Crustal Component Required
+0.5	1	1	2	2	3	4	
0.0	2	2	3	5	6	8	
-0.5	3	4	5	7	9	12	
-1.0	4	5	7	10	13	15	
-1.5	5	7	9	13	16	19	
-2.0	6	8	11	15	19	23	
-2.5	7	10	13	18	23	27	
-3.0	8	12	15	21	26	31	
-3.5	10	14	17	24	30	35	
-4.0	11	16	20	27	33	38	
-4.5	13	18	23	31	37	42	
-5.0	15	20	26	34	41	46	

Table 8.9. Two-component mixing matrices for Labradorian magmas, showing percentages of crustal component required to generate a specific final  $\epsilon_{\text{Nd}}$  CHUR value. (a) General crust-mantle mixtures. (b) Contamination of Adlavik or Mount Benedict Suite mafic magma by Archean crust.



$\epsilon_{\text{Nd}}^{\text{CHUR}}$  of the parental magma is taken to be +1.0 (based on Adlavik Suite gabbro), considered to be a signature acquired prior to emplacement. If it had 10 ppm Nd, such a magma must assimilate a further 10-15% of crustal material ( $\epsilon_{\text{Nd}}^{\text{CHUR}} = -12.0$ ) to obtain a final value of -2.0 to -3.0 in the most differentiated material. This proportion is substantially reduced (< 7.5%) if the Nd content of the parent magma was below 10 ppm, or if the contaminant actually had  $\epsilon_{\text{Nd}}^{\text{CHUR}}$  of ca. -17.0, which is the calculated value for Archean gneiss (Brooks, 1983) at 1650 Ma (Table 8.7). Contamination effects also explain the negative (ca. -6)  $\epsilon_{\text{Nd}}^{\text{CHUR}}$  of the gabbro at East Micmac Lake in the western domain, which also has a higher  $\text{SiO}_2$  than gabbro in the west. The amount of Archean material required to generate this value, however, is over 30%, assuming 10 ppm Nd for the juvenile magma (Table 8.9). This unreasonable figure is reduced significantly if the conditions discussed above applied here also.

Only Archean crustal material is a viable contaminant for Adlavik and Mount Benedict Suite magmas; however, the latter lies well east of the edge of the Archean craton as inferred from Makkovikian data (Figures 8.8; 8.9). It is, however, unlikely that this crustal boundary is a simple vertical interface. The signatures of Makkovikian granitoid rocks probably reflect their partial lower crustal sources, whereas contamination of the Mount Benedict Suite probably took place in the upper crust, which may have contained some Archean or Archean-derived material. The presence of some upper crustal Archean material would also explain the mixture of positive and negative  $\epsilon_{\text{Nd}}^{\text{CHUR}}$  values along the proposed boundary (Figure 8.8), and anomalously low  $\epsilon_{\text{Nd}}^{\text{CHUR}}$  at the border of the Numok Intrusive Suite, close to the proposed boundary (Sample AKZ-3; Table 8.6).

## CHAPTER NINE

# A COMPARATIVE ANALYSIS

---

### Chapter Abstract

In order to evaluate the affinities and possible tectonic settings of the TLGB Makkovikian and Labradorian plutonic assemblages, a quantitative comparative analysis was attempted. This employs published and unpublished data from several granitoid batholiths taken to represent specific tectonic environments.

Volcanic-arc batholiths are represented by data from Mesozoic to Cenozoic, circum-Pacific batholiths of Peru, Chile and southern California. All are associated with active or recently active zones where oceanic crust is subducted beneath a continental margin. Collisional environments representing later stages of orogenesis are represented by Cenozoic granitoid rocks from the Himalayan belt of Afghanistan, and by the late- to post-orogenic Paleozoic granites of the Newfoundland Appalachians. The latter assemblage probably represents the most complete sampling of the later magmatic products of orogeny. Within-plate granitoid batholiths are represented by Middle Proterozoic granitoid rocks from northern Labrador, which are closely similar in petrology to Phanerozoic anorogenic suites. Large amounts of generally representative data are available from most of these areas. This allows the use of extensive parameters such as frequency spectra, abundance of rock types and evolutionary trends as comparative tools, in addition to conventional intensive methods such as discrimination diagrams.

The Makkovikian assemblage contrasts very strongly with volcanic arc batholiths. Specifically, it is characterized by enrichment in  $\text{SiO}_2$ ,  $\text{K}_2\text{O}$ ,  $\text{Na}_2\text{O}$ ,  $\text{K+N/A}$ ,  $\text{F/F+M}$ , and depletion of  $\text{MgO}$ ,  $\text{CaO}$  and  $\text{N/N+K}$ . It is compositionally restricted in comparison to the broad, expanded spectrum of arc compositions. Although most major element frequency spectra resemble the Newfoundland assemblage, Makkovikian granites are significantly more aluminous and Fe-enriched at all  $\text{SiO}_2$  contents. Such features suggest that they are transitional towards within-plate assemblages such as Flowers River, which has similar, but more extreme, tendencies in these directions. Compositional evolution in the Makkovikian assemblage follows a "quartz-poor" trend via monzonite and syenite, that is distinct from the "quartz-rich" (via granodiorite and monzogranite) trend of the Newfoundland granites. Trace element data indicate enrichment in Zr, Y, F and REE relative to Newfoundland, but not to levels typical of Flowers River. The Makkovikian assemblage falls in within-plate granite or A-type granite fields in trace element discrimination plots.

It is suggested that a post-orogenic, possibly post-collisional, affinity is more consistent with the geological setting of the Makkovikian assemblage than an anorogenic environment. It is clear, however, that the Makkovikian assemblage has many features that are akin to granites generated in such settings. These differences require explanation in any tectonic model incorporating a post-collisional setting for these granitoid magmas (see Chapter 10).

The Labradorian assemblage is difficult to classify via geochemical comparisons, partly because it is only the northern fringe of a much wider belt, and may not represent its full compositional anatomy. It includes a range of compositions similar to those of volcanic-arc batholiths, but has a bimodal compositional spectrum, and is generally more siliceous and potassic. Labradorian granitic rocks have some tendencies towards Fe-enrichment and high K+N/A, but not to the same degree as the Makkovikian assemblage. They do not show the distinctive trace element signatures of Makkovikian granites, and could belong to either arc or collisional assemblages. The Labradorian assemblage falls mostly in the volcanic-arc or I-type granite fields on trace element discrimination plots. Labradorian mafic and intermediate rocks, as discussed in Chapter 5, have affinities to high-K calc-alkaline or shoshonitic associations, and fall dominantly in the calc-alkaline basalt field in trace element discrimination plots.

A distal portion of a magmatic arc (i.e. well removed from the locus of subduction) is one possible setting for Labradorian magmatism. This is consistent with its siliceous and potassic character relative to proximal volcanic-arc batholiths, and the lack of a recognisable Labradorian "orogeny" in the study area could be then attributed to great distance from the main orogenic belt. However, similar assemblages also occur in post-orogenic, post-collisional settings, where granite compositions overlap partly with those of mature or distal arcs. At the present time, it is difficult to select between these alternatives. However, the Nd isotopic signatures of Labradorian mafic rocks favour an arc environment, and there are obvious contrasts between Labradorian granites and the categorically post-orogenic Makkovikian assemblage.

## Introduction

This chapter assesses TLGB magmatic assemblages with reference to Proterozoic and Phanerozoic assemblages that represent diverse environments of granitoid magmatism.

This comparative analysis is presented partly in terms of their compositional spectra and evolutionary trends, combined with traditional methods based on intensive parameters such as major and trace element abundances. Kerr (in press) presents a preliminary analysis of this nature, for the TLGB, which was completed prior to the recognition of discrete post-tectonic Makkovikian and Labradorian assemblages. The following discussion employs a wider selection of comparative data, and revises some earlier conclusions in the light of this improved geochronological framework.

Genetic and/or tectonic classifications of granitoid rocks are a veritable "growth industry" in petrology. Current mainstream viewpoints concerning environments and classification of granitoid magmatism are reviewed in Chapter 1.

## Spectral Analysis of Granitoid Batholiths

Phanerozoic granitoid magmatism forms a compositional continuum, and unique rock types characteristic of specific environments do not exist. Furthermore, diverse tectonic environments are likely to be spatially and/or temporally superimposed in ancient orogenic belts. This reality poses formidable problems in classification, particularly when conclusions are based on small numbers of data that represent restricted areas or time-slices in the history of a belt, as is normally the case.

Modern geochemistry emphasizes intensive parameters such as element abundances or REE patterns as classification tools (e.g. Pearce et al., 1984). An alternative approach is to use extensive parameters such as frequency spectra, proportions of rock types and geochemical changes with space, time and differentiation. "Spectral analysis" of this type is not a new concept (e.g. Martin and Piwinski, 1972; Petro et al., 1979), but it has not been widely applied.

Spectral analysis methods require large, statistically representative, geochemical databases, such as the information presented here for the TLGB. Such information is increasingly available (e.g. the ARTEMISE data bank, maintained by CNRS in France; Leterrier et al., 1983) and, coupled with unpublished data available to the author, allows an analysis of this type to be attempted here. There are, naturally, difficulties in assessing the degree to which such data represents specific environments, and some potential problems in comparing trace element data of variable quality from different sources. However, these problems are also inherent in trace element discrimination schemes based on intensive parameters.

### 9.1 OVERVIEW OF COMPARATIVE GEOCHEMICAL DATA

Seven comparative geochemical databases were assembled (Table 9.1). A brief description of each is presented below, and any problems in interpretation or use of these data are noted. Wherever possible, tectonic environments have been duplicated, to allow a parallel assessment of variations in the character of a single setting. Note that the TLGB data used in comparisons comprise the regional (grid-based) sample population only, and that unclassified plutonic rocks and all volcanic rocks are excluded.

Area and Source(s)	Age and Setting	Area [sq. km]	Number Analyses	Density	Trace Element Analysis Suite	Comments
Trans-Labrador Granitoid Belt [This Study]	Makkovikian Assemblage	8,500	511	1/10 km <sup>2</sup>	F Be Li V Cr Co Ni Cu Zn Ga Rb Sr Y Zr Nb Mo Sn Ba La Ce W Pb Th U	Samples from regional grid population only, excluding all unclassified and volcanic rocks.
	Labradorian Assemblage		332	1/10 km <sup>2</sup>		
Coastal Batholith Of Peru [Pitcher et al., 1985]	Mesozoic Magmatic Arc Batholith	80,000	217	n/a	Sc V Cr Co Ni Cu Zn Ga Rb Sr Y Zr Nb Cs Ba La Ce Hf Pb Th U	Traverse-based sampling. Trace element coverage is heterogeneous.
Mesozoic Batholiths Of North-Central Chile [Brown, pers. comm.]	Mesozoic Magmatic Arc Batholith	12,000	280	1/40 km <sup>2</sup>	V Cr Co Ni Cu Zn Ga Rb Sr Y Zr Nb Ba La Ce Pb Th U	Setting is analogous to Peru. Generally representative of all rock types areally. Homogeneous trace element data.
Batholithic Rocks Of Southern California [Baird and Miesch, 1984]	Mesozoic Magmatic Arc Batholith	20,000	482	1/40 km <sup>2</sup>	major elements only	Grid-based sampling used in multivariate statistical model. Numerous other studies of batholith are published.
Alpine-Himalayan Plutonic Belts Of Afghanistan [Debon et al., 1987a,b]	Mesozoic To Cenozoic Collisional Orogen	> 100,000 [ estimates very approximate ]	670	1/100 km <sup>2</sup>	V Cr Co Ni Cu Rb Sr Ba	Size of study precludes estimation of sampling density. Poor detection limits for Cr, Co, Ni.
	Cenozoic Only [Collisional]		334	-	-	Peraluminous biotite-muscovite leucogranites and coeval metaluminous granitoid rocks.
	Mesozoic Only [Magmatic Arcs?]		336	-	-	Polyphase tonalite-granodiorite-granite batholiths
Post Taconic Granitoid Rocks Of The Newfoundland Appalachians [Strong et al., 1974; Dept. of Mines, Unpublished Data]	Middle Paleozoic Syn- and Post-Collisional Batholiths [Excludes Ordovician Arc Granitoids]	ca. 30,000	1202	1/25 km <sup>2</sup>	F Be Li V Cr Co Ni Cu Zn Ga Rb Sr Y Zr Nb Mo Sn Ba La Ce W Pb Th U	Most recent data used wherever possible. Aggregate database is thought to be geographically and lithologically representative. Early (1974) data has a limited trace suite comprising F Cu Zn Rb Sr Zr Ba U.
Anorogenic Granites Of Northern Labrador [McConnell, Unpublished data]	Middle Proterozoic [ca. 1270 Ma] "anorogenic" Batholith	2,500	367	1/7 km <sup>2</sup>	F Be Li V Cr Co Ni Cu Zn Ga Rb Sr Y Zr Nb Mo Sn Ba La Ce W Pb Th U	Grid Sampling Program similar to TLGB project. Database mostly represents peralkaline granites. Associated Granitoid rocks are under-represented.

Table 9.1. Summary of databases (including TLGB data) employed in comparative geochemical studies.

## Coastal Batholith Of Peru

The Mesozoic-Cenozoic Coastal Batholith of Peru (Pitcher, 1977; Atherton, 1984; Pitcher et al., 1985) is the type example of a "cordilleran" or "volcanic-arc" batholith. It is situated 200 km east of the trench of an active subduction zone, stretches for over 2000 km, and has an average width of ca. 70 km (Figure 9.1). The following summary is taken from the above sources.

**Geological Setting** : The batholith is composite, and is divided into segments (longitudinal sectors), and "super-units" (Cobbing et al., 1977). The latter are mafic to felsic intrusive sequences. Diorite, quartz-diorite and tonalite, associated with lesser mafic rocks, are their dominant components; granitic (s.s) plutons commonly form ring-complexes that are the youngest intrusive phases. High, probably subvolcanic, emplacement levels were attained by many plutons. Subaerial basalt, dacite and rhyolite (Calipuy Group), are younger than most of the plutonic rocks, and may not be directly related to the exposed plutons. The dominant host rocks are Mesozoic turbidites and mafic volcanic rocks. However, much of the batholith is probably underlain by Phanerozoic or Precambrian basement at depth.

**Geochemical Database** : Pitcher et al. (1985) list 217 XRF and INAA analyses, including volcanic rocks. These represent "traverses" across the batholith, and are not geographically representative of any specific area. Trace element data are heterogeneous, due to collection by different workers over a 20 year period. It is not clear if they are truly representative of the Coastal Batholith.

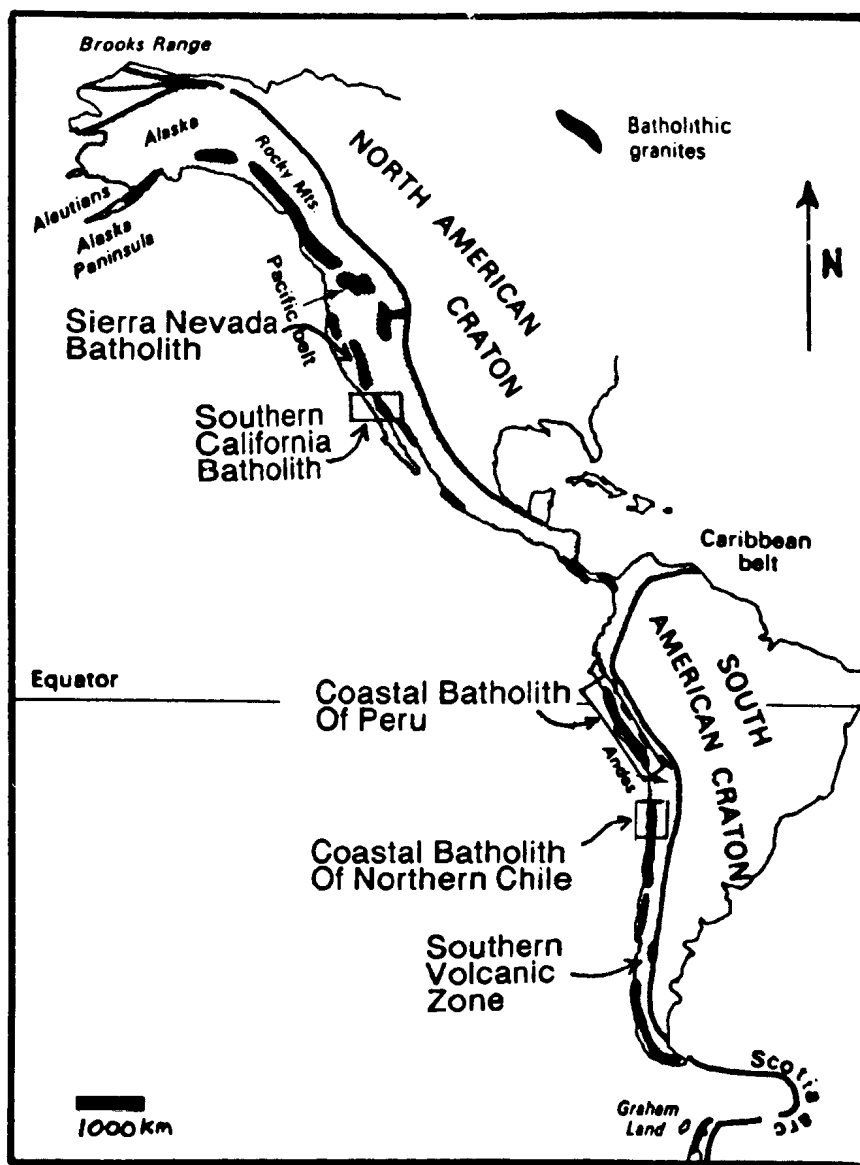


Figure 9.1. Distribution of major volcanic-arc batholiths in the Andean - Cordilleran orogenic belt, showing areas discussed in this study. Adapted from Read and Watson (1975).



### **Mesozoic Batholith Of North-Central Chile**

The coastal cordillera of northern Chile (Figure 9.1) are formed by a Mesozoic batholith that is continuous with the Peruvian example and has a similar setting (Coira et al., 1982; Naranjo et al., 1986; Brown, 1987; 1988). The following summary is taken from the above sources.

**Geological Setting** : Plutonic rocks in this area are Triassic to Jurassic (220-160 Ma) and Cretaceous (130-100 Ma) in age. The locus of magmatism migrated eastward from the trench axis with time. Country rocks include Paleozoic metasediments containing leucogranite intrusions, overlain by Mesozoic basinal sedimentary rocks. The Paleozoic rocks are unrelated to Andean orogenesis. Most of the batholith is considered to be underlain at depth by basement of at least Paleozoic age. It is dominated by diorite, tonalite and granodiorite, with subordinate gabbro and granite (Brown, 1987; 1988). Volcanic cover rocks are not widespread, but Cenozoic volcanic rocks are widespread inland, reflecting continued eastward migration of the active volcanic front.

**Geochemical Database** : M. Brown (pers. comm., 1988) provided 280 unpublished analyses from this batholith. Sample collection was not rigidly structured, but the data are geographically and lithologically representative, and are far more homogeneous than those of Pitcher et al. (1985). Major and trace elements were analyzed by XRF at the British Geological Survey, and appear reliable, at least in terms of their detection limits.

## **Mesozoic Batholith Of Southern California**

This is also a classic area of "cordilleran" magmatism, and has been intensely studied (Baird et al., 1974; DePaolo, 1981b; Baird and Miesch, 1984; Silver and Chappell, 1988). This area includes part of the Peninsular Ranges Batholith (Silver and Chappell, 1988), and also the Transverse Ranges, where the batholith is transitional to the Sierra Nevada Batholith (Figures 9.1 and 9.2). The following description is taken from the above sources.

**Geological Setting** : The batholith is largely of Cretaceous (140-80 Ma) age. The oldest rocks are in the west, suggesting that magmatism migrated away from the trench, as in Chile. The area in Figure 9.2 has well-developed transverse petrographic, geochemical and isotopic trends, suggesting progressively more evolved compositions to the east. Major shifts in composition coincide with faults of the San Andreas system, and it is possible that transverse trends may have been telescoped (see Baird and Miesch, 1984, for a review of discussion).

The country rocks are mostly Mesozoic metasediments in the Peninsular Ranges, but include possible Proterozoic basement material east of the San Andreas fault and in adjacent Mexico.

**Geochemical Database** : Baird and Miesch (1984) list 482 major element analyses from a grid-based, representative sample population analogous to the TLGB database, but with a lower sample density. Data are subdivided by geographic block (Figure 9.2). Gabbroic rocks (mostly in the west) were excluded by Baird and Miesch (1984) as they were considered to have a separate origins from the granitoid rocks. Data were acquired by XRF.

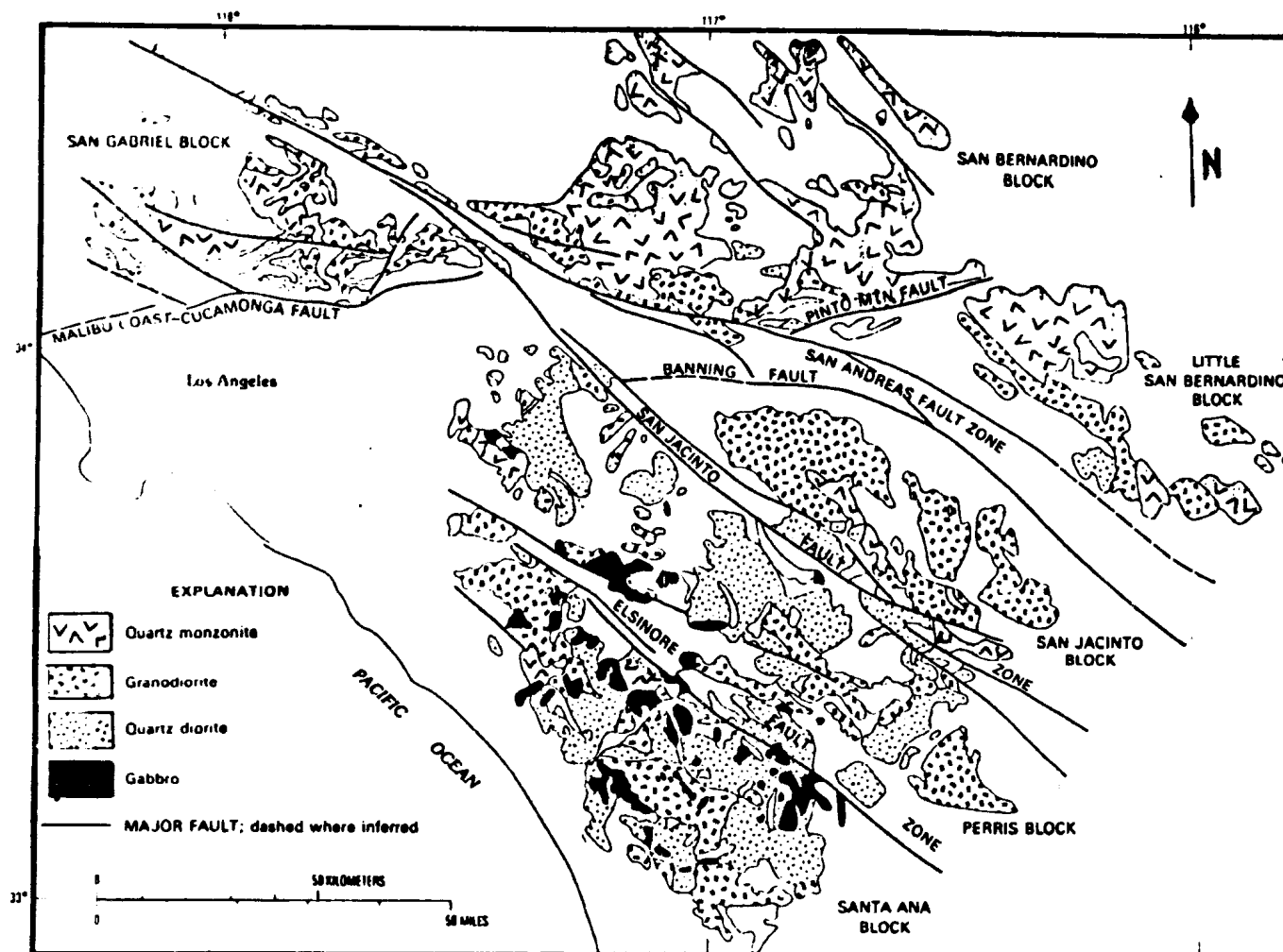


Figure 9.2. Simplified geology of the Southern California Batholith, including part of the northern Peninsular Ranges Batholith. From Baird and Miesch (1984).

## Plutonic Belts of Afghanistan

The Alpine-Himalayan Belt is the type area for collisional orogenesis. The following account is summarized from studies by the CNRS of France (Debon et al., 1986; 1987a,b,c) in Afghanistan, Pakistan, Nepal and Tibet. Geochemical data from Afghanistan (Debon et al., 1987b) were utilized.

**Geological Setting** : Major plutonic belts in Afghanistan (Figure 9.3) comprise a tectonic collage of pre-, syn- and post-collisional magmatic provinces that belong to both Eurasian and Gondwanaland portions of the Himalayas. The oldest granitoid rocks are Lower Paleozoic (ca. 500 Ma) leucogranites, associated with earlier (unrelated) Gondwanaland events. These were followed by Triassic (210-160 Ma) and Cretaceous (100-70 Ma) polyphase granitoid batholiths that are considered to record subduction of Tethys under the Eurasian and Gondwanaland margins respectively. All of these rocks were formed prior to collision between India and Eurasia ca. 54 Ma ago.

Syn- and post-collisional magmatism occurred in Cenozoic (Eocene to Miocene) times. Rocks of this age comprise two-mica peraluminous (S-type) leucogranites of classical "Himalayan" affinity (e.g. Lanord and LeFort, 1988), and also metaluminous (I-type) granitoid rocks. Both associations transgress the tectonic boundaries between older plutonic belts, and they appear to be partly coeval. The dominant country rocks are poorly-known Mesozoic metasediments, but metavolcanic sequences, and Paleozoic (possibly also Proterozoic) metamorphic rocks occur locally.

**ALPINE-HIMALAYAN BELT OF AFGHANISTAN  
PLUTONIC BELTS AND DOMINANT AGE OF INTRUSIVES  
(Excluding Paleozoic Intrusions)**

Feroz Koh -- Cenozoic  
Band-e-Bayan -- Cenozoic  
Northwest Farah Rod -- Cenozoic  
Spin Boldak -- Cenozoic  
Western Nuristan -- Cenozoic

Eastern Nuristan -- Cretaceous-Cenozoic  
Helmand -- Cretaceous  
Arghandab -- Cretaceous  
Safed Khers -- Cretaceous (?)  
Wakhan -- Cretaceous

Western Hindu Kush -- Triassic  
Western Badakhshan -- Triassic

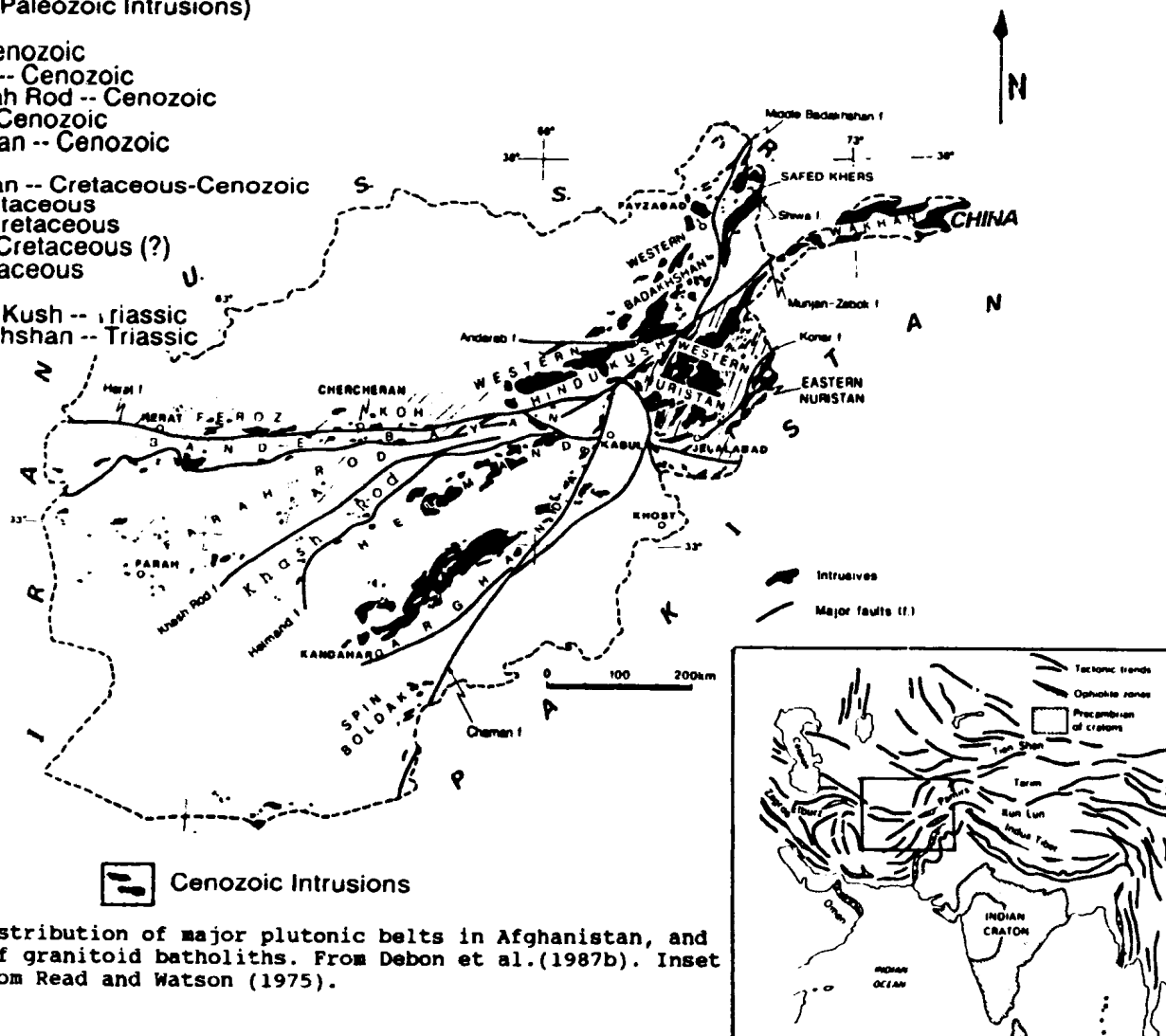


Figure 9.3. Distribution of major plutonic belts in Afghanistan, and location of granitoid batholiths. From Debon et al. (1987b). Inset adapted from Read and Watson (1975).

**Geochemical Database** : F. Debon (pers. comm., 1988) provided 723 analyses from the ARTEMISE data bank. The data are subdivided according to age and plutonic belt; this study is concerned with 334 Cenozoic granitoid rocks and 336 samples from Mesozoic batholiths; analyses from Paleozoic granites were excluded. Mesozoic batholiths are of interest mostly in terms of their correspondence to assemblages that retain a spatial relationship to subduction (e.g. Peru, Chile). The area covered by the Afghan data is immense, and sample locations were governed largely by access; however, Debon et al. (1987b) consider the database to be representative on a broad scale. All data are XRF; the trace element suite is very limited, and useful data are present only for V, Rb, Ba and Sr.

#### **Late- and Post-Orogenic Granitoid Rocks Of Newfoundland**

Appalachian-Caledonian granites define an important subtype in the classification of Pitcher (1983). The Newfoundland Appalachians are a two-stage collisional orogen that have been compared directly to the Alpine-Himalayan belt (Colman-Sadd, 1982). Voluminous granitoid rocks in the central portion of the orogen (Figure 9.4) mostly post-date closure of Iapetus (locally) during the Taconic Orogeny. Although it is simplistic to burden these suites with a single label such as "collisional", they provide a good representation of the character of magmatism in later stages of Phanerozoic orogenic cycles. The following summary is drawn largely from Hayes et al. (1987), Dickson et al. (1988), and Williams et al. (1989).

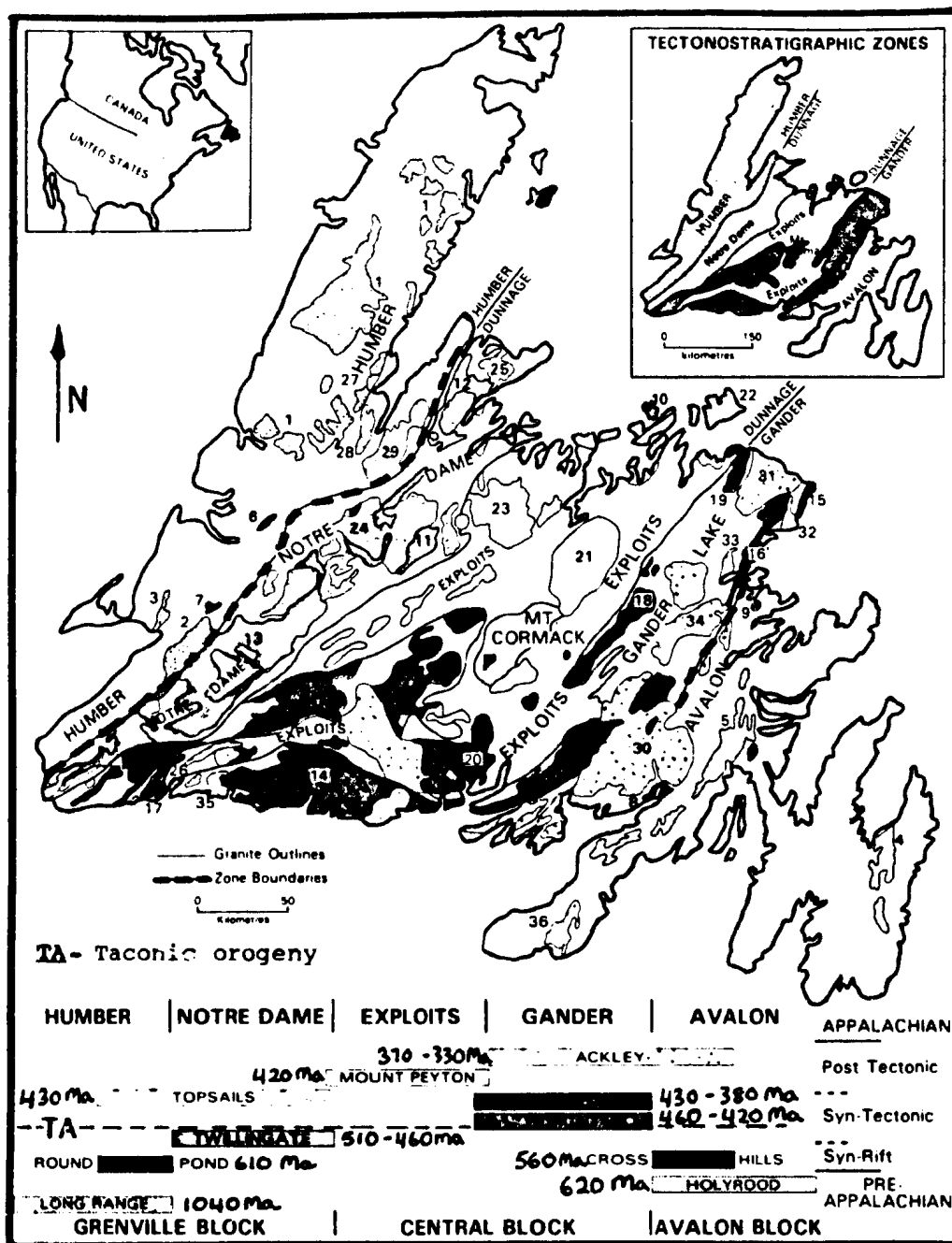


Figure 9.4. Distribution and setting of granitoid intrusive rocks in the Newfoundland Appalachians. From Williams et al. (1989).

**Geological Setting** : Granitoid rocks in Newfoundland are divisible into several groups, which are assigned names from type localities (Figure 9.4). Ordovician suites are considered to represent volcanic-arc environments that predate the Taconic orogeny. Post-Taconic, (largely Siluro-Devonian) magmatism continued for up to 100 Ma, and transcends the Devonian Acadian orogeny. The country rocks vary from ocean-floor and island-arc volcanic assemblages in the Dunnage Zone to high-grade metamorphic rocks in the Gander Zone and Precambrian volcanosedimentary sequences in the Avalon Zone.

Variably foliated, metaluminous to peraluminous ("S-type") granites (Burgeo and Middle Ridge type) in the metasedimentary Gander Zone are considered to have been generated during accretionary or collisional events (Williams et al., 1989). Undeformed Siluro-Devonian (predominantly I-type) plutons of the Topsails, Ackley and Mount Peyton associations (Figure 9.4) transgress the major zones of the orogen, and are probably post-collisional. Some (e.g. Topsails) are peralkaline; a number of others are described as "A-type" granites (Hayes et al., 1987). No attempt is made here to subdivide these diverse rocks according to age or zone; they are treated as a single assemblage. There appear to be systematic differences in geochemistry and isotopic character between the various tectonic zones (Dickson et al., 1988; B.Fryer, pers.comm., 1988), that probably record the influence of contrasting lower crustal blocks.

**Geochemical Database** : Geochemical studies include early work (Strong et al., 1974), and several recent investigations (e.g. Dickson, 1983; Dickson et al., 1989). Since 1982, grid-based sampling programs akin to the TLGB study have been employed. Data for the Topsails Igneous Suite were provided by Whalen et al. (1987b).



There are great variations in sample density amongst these studies. An optimum sampling density (ca. 1 sample per 25 km<sup>2</sup>) was therefore established, and intensely sampled plutons were reduced to this level by random selection of a sample subset. It is felt that the aggregate database of 1202 analyses is approximately representative. Individual plutons are not equally represented, but associations defined by Williams et al. (1989) are included in rough proportion to their areal extent.

Wherever possible, the most recent data have been employed; analytical methods and precision for these are equivalent to this study (Appendix A). Other sources are primarily XRF data, and of reasonable to good quality (Strong et al., 1974; Whalen et al., 1987b).

#### **Proterozoic Anorogenic Granites Of Northern Labrador**

Anorogenic, within-plate suites of Phanerozoic age (e.g. Kinnaird and Bowden, 1987) are very poorly represented by public-domain geochemical data.

However, published and unpublished data are available from the ca. 1270 Ma old Flowers River Igneous Suite (Figure 9.5) in northern Labrador (Hill, 1982; Collerson, 1982; Hill and Thomas, 1983). This is similar to classic anorogenic granitoid complexes such as the younger granites of Nigeria, and has an anorogenic setting (Collerson, 1982; Hill, 1982).

**Geological Setting** : The complex is part of a major belt of Middle Proterozoic plutons extending from Labrador to the midcontinent United States (Emslie, 1978; Anderson, 1983). The Flowers River Suite is spatially associated with granitoid rocks of the Nain Igneous Complex, and is similar

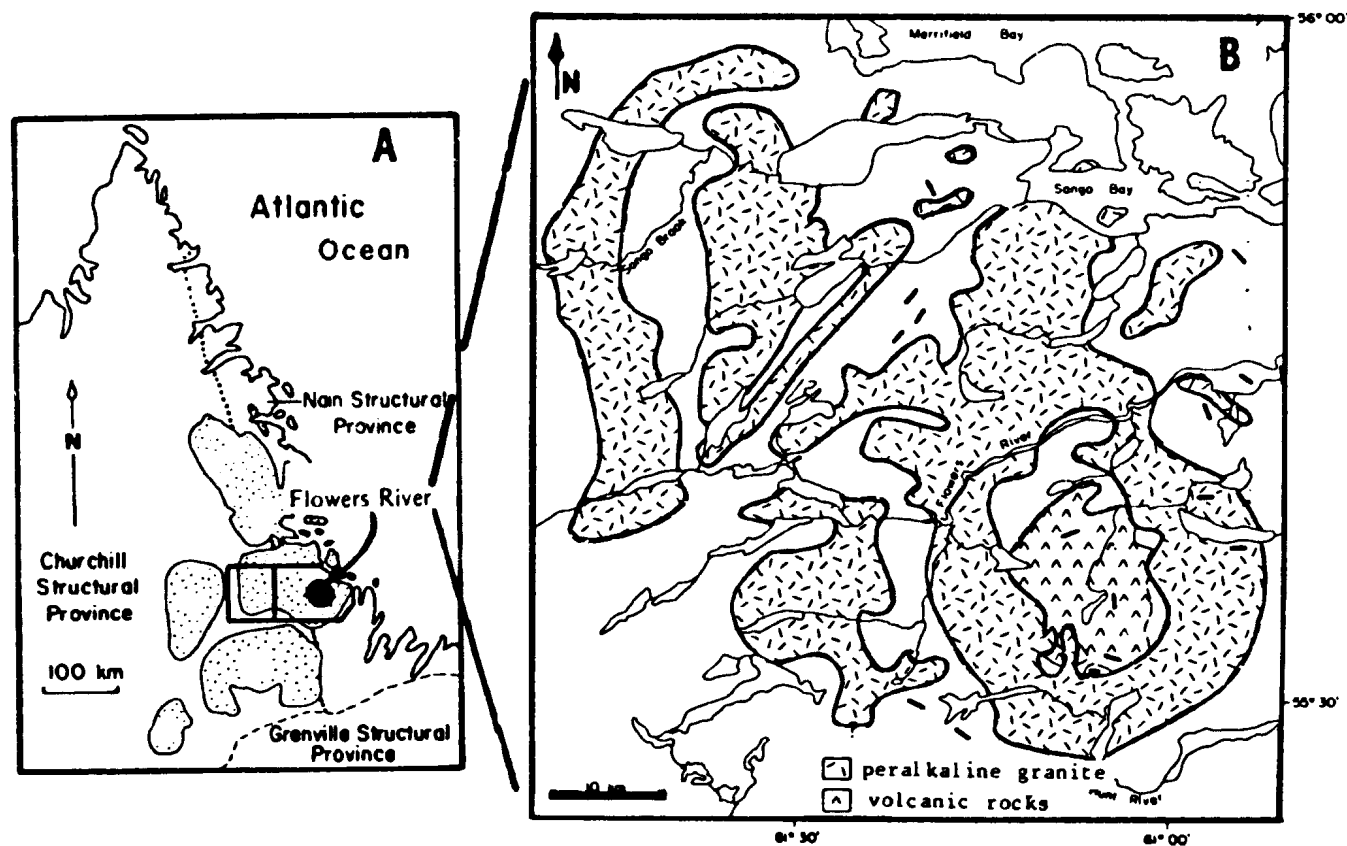


Figure 9.5. Location and distribution of peralkaline, anorogenic granitoid rocks of the Flowers River Igneous Suite in Northern Labrador. Stippled areas in (A) are the anorthosite-granitoid plutons (e.g. Nain Igneous Complex) with which these rocks are spatially associated. From Hill (1982).

in age to some of them (Collerson, 1982). It is dominated by subsolvus and hypersolvus metaluminous to peralkaline granites and associated volcanic rocks. The Nain Igneous Complex includes anorthosite, monzonite, fayalite-bearing syenite and granite. Anorthositic rocks are probably not directly related to the granites, but are an integral part of most Proterozoic anorogenic complexes (Emslie, 1978). The country rocks are high-grade Archean and Proterozoic gneisses of the Nain and Churchill Provinces. The peralkaline granites were emplaced as high-level ring complexes (Hill, 1982; 1988). The granitoid rocks of the Nain Complex probably form sheath-like units around and above the anorthosites (B.Ryan, pers.comm., 1988)

**Geochemical Data** : McConnell (1986) sampled the complex using a 2 x 2 km random grid system, and provided 367 unpublished analyses. Most represent peralkaline and associated metaluminous granites, but there is a subordinate population from the Nain Complex. These are augmented by data from Collerson (1982) and Hill (1982) representing granitoid rocks of the Nain Complex, and a few anorthosites. The database is representative of the area around the Flowers River Suite but, compared to other within-plate associations, is probably somewhat biased towards peralkaline compositions. Trace element analysis suites and data quality are equivalent to TLGB and Newfoundland databases.

#### **A-type Granites of The Lachlan Fold Belt**

The Paleozoic Lachlan Fold Belt of southeastern Australia was used by Collins et al.(1982) to define the characteristics of "A-type" granites. 45 analyses from

these rocks (Whalen et al., 1987b) are used here. These are post-orogenic, metaluminous, variably hypersolvus granites (s.s.) that have enhanced levels of LFS and HFS trace elements (Collins et al., 1982). The database is too small for analysis of compositional spectra, but it has been used to assess differentiation trends for "A-type" granites relative to the other assemblages. This is required because there is some disagreement about the diagnostic features of so-called "A-type" suites (e.g. Tuach et al., 1986; Whalen et al., 1987) versus highly fractionated granites assigned to I- or S-type associations.

## 9.2 COMPARATIVE MAJOR ELEMENT GEOCHEMISTRY

### 9.2.1 Comparative Frequency Spectra

To facilitate comparisons between assemblages, all histograms for each variable are scaled equally, using 20 frequency intervals (Figure 9.6). This procedure requires exclusion of small amounts (<1%) of outlying data. Vertical (percentage frequency) scales may differ between assemblages.

#### **Major Element Frequency Spectra**

**SiO<sub>2</sub> (Figure 9.6a)** : Magmatic arc assemblages (e.g. Peru, Chile) have broad, approximately normal, frequency distributions with maxima at 57 to 65 % SiO<sub>2</sub>; those from California and Afghanistan (Figure 9.7) are displaced to slightly higher SiO<sub>2</sub>. All arc assemblages have expanded SiO<sub>2</sub> frequency distributions. In contrast, Newfoundland and Afghanistan (Cenozoic), and Flowers River, have asymmetric, negatively-skewed distributions with maxima at 71-77% SiO<sub>2</sub>.

Both TLGB assemblages have bimodal SiO<sub>2</sub> histograms; in Labradorian rocks, the lesser peak is at gabbro-diorite composition, compared to monzonite-syenite in the Makkovikian rocks. In general terms, Makkovikian rocks resemble collisional or within-plate assemblages, and are totally distinct from volcanic arc assemblages.

**MgO (Figure 9.6b)** : MgO frequency spectra are superficially similar for all assemblages. However, collisional and within-plate assemblages are strongly depleted in MgO relative to volcanic arcs. Makkovikian

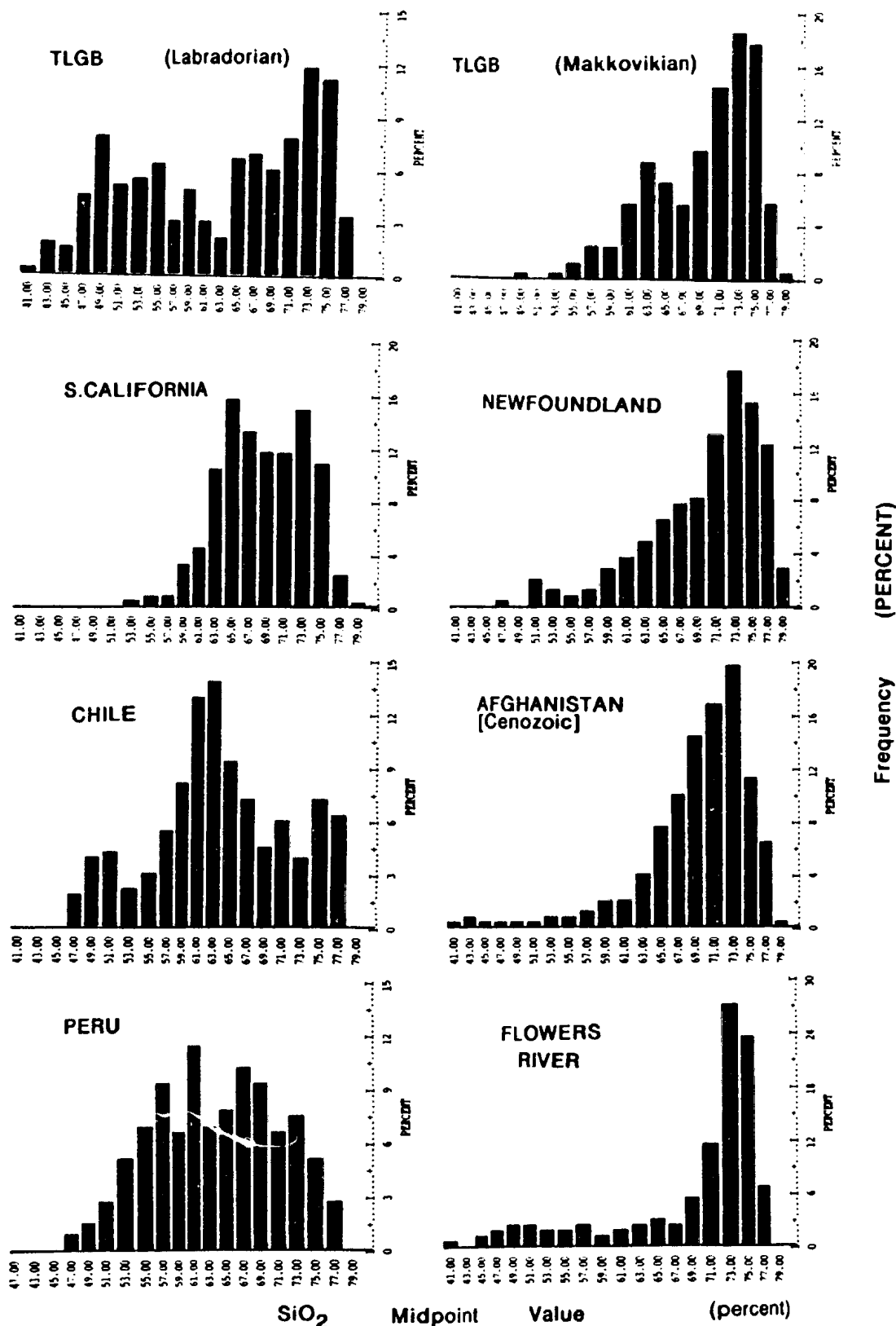


Figure 9.6a. Comparative  $\text{SiO}_2$  frequency spectra.

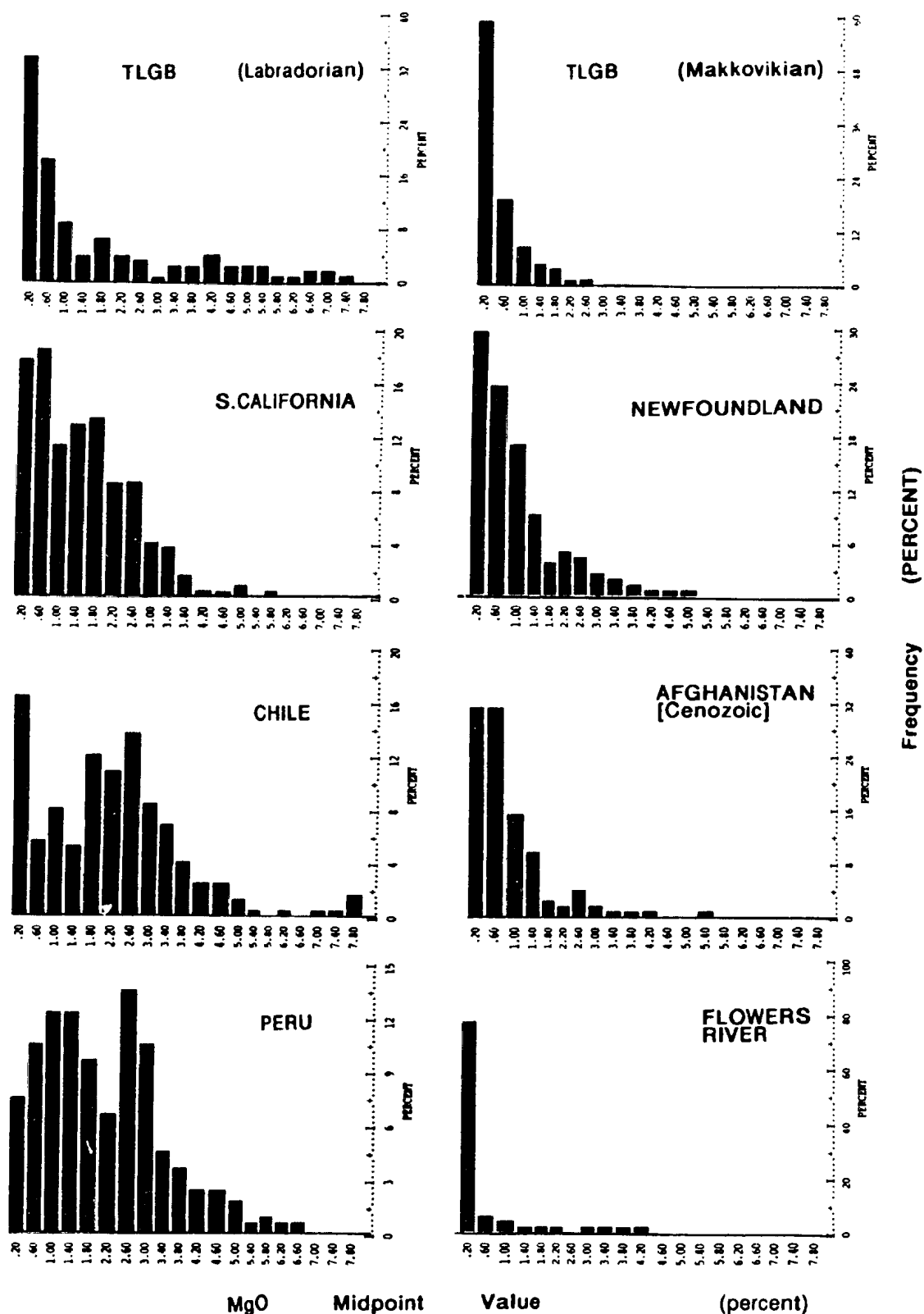


Figure 9.6b. Comparative MgO frequency spectra.

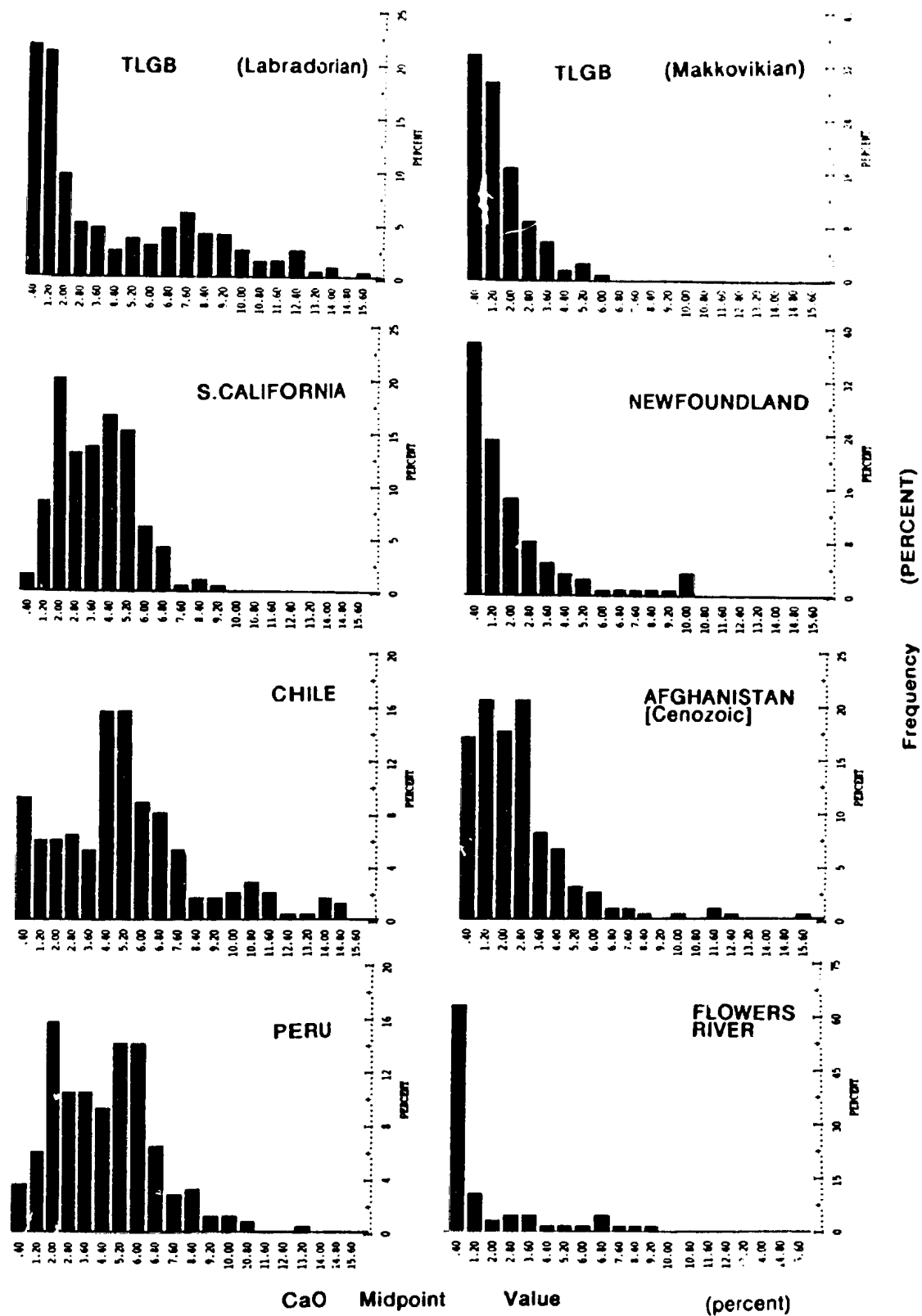


Figure 9.6c. Comparative CaO frequency spectra.



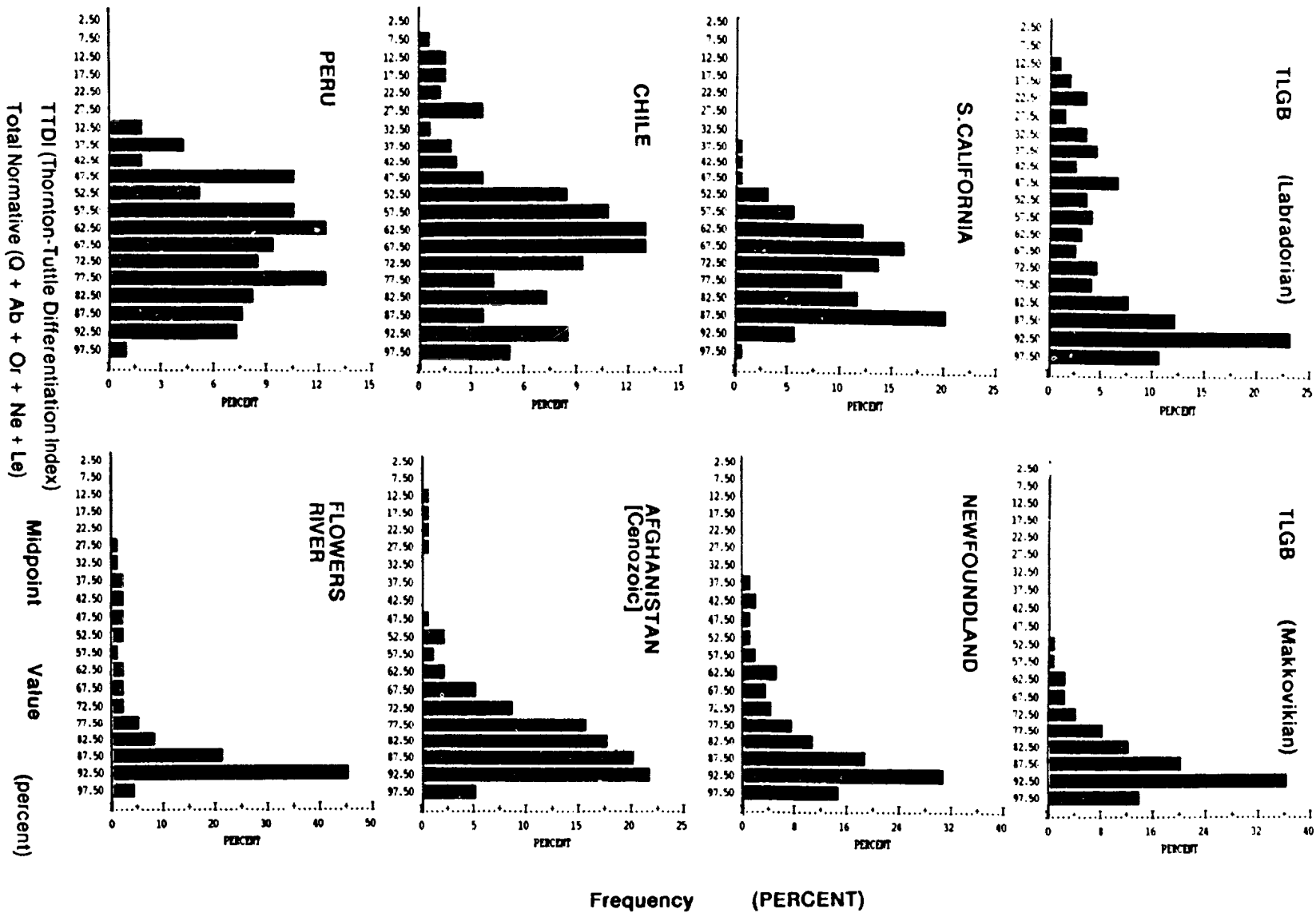


Figure 9.6d. Comparative Differentiation Index (TTDI) frequency spectra.

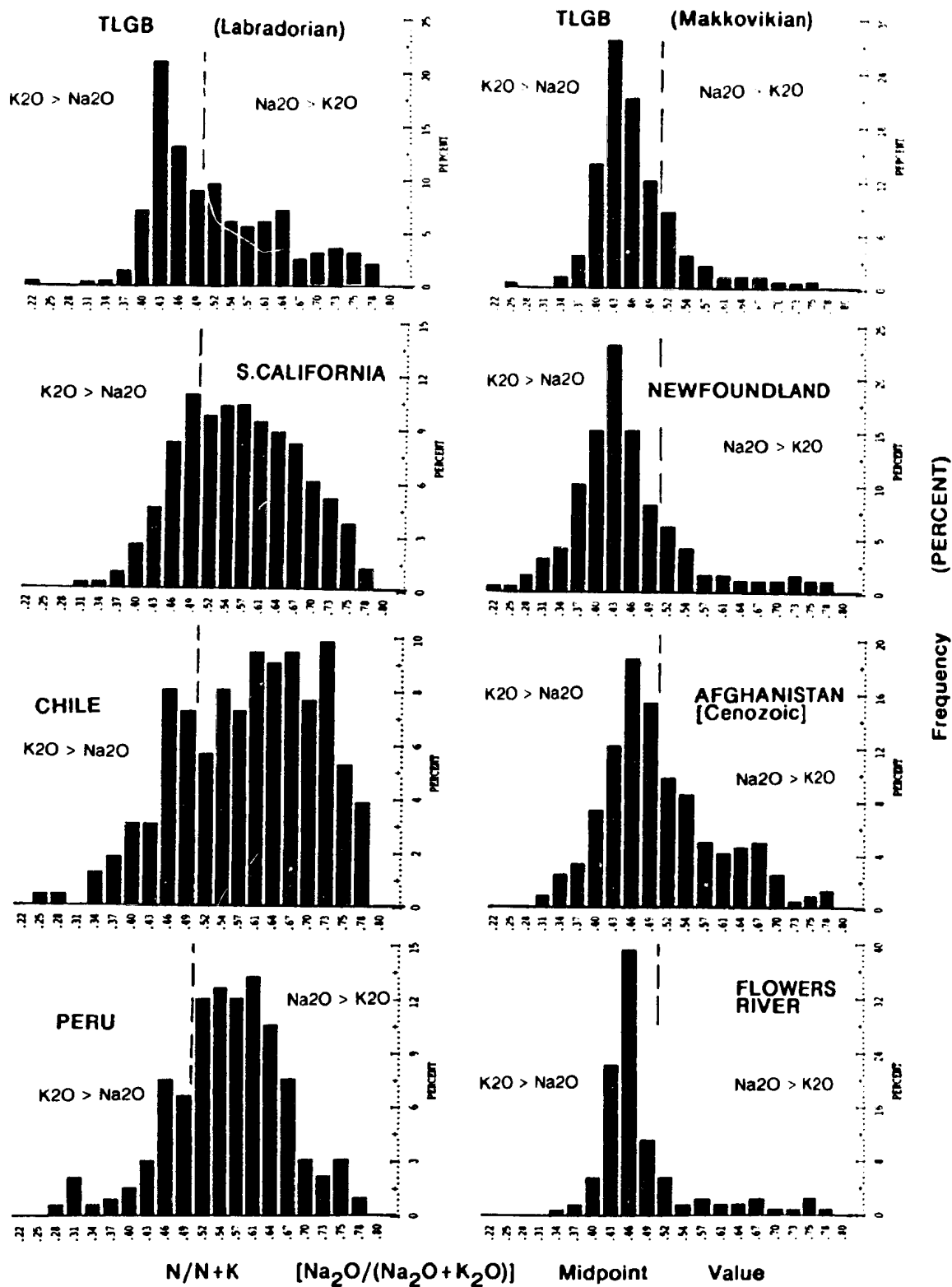


Figure 9.6e. Comparative  $N/N+K$  frequency spectra.

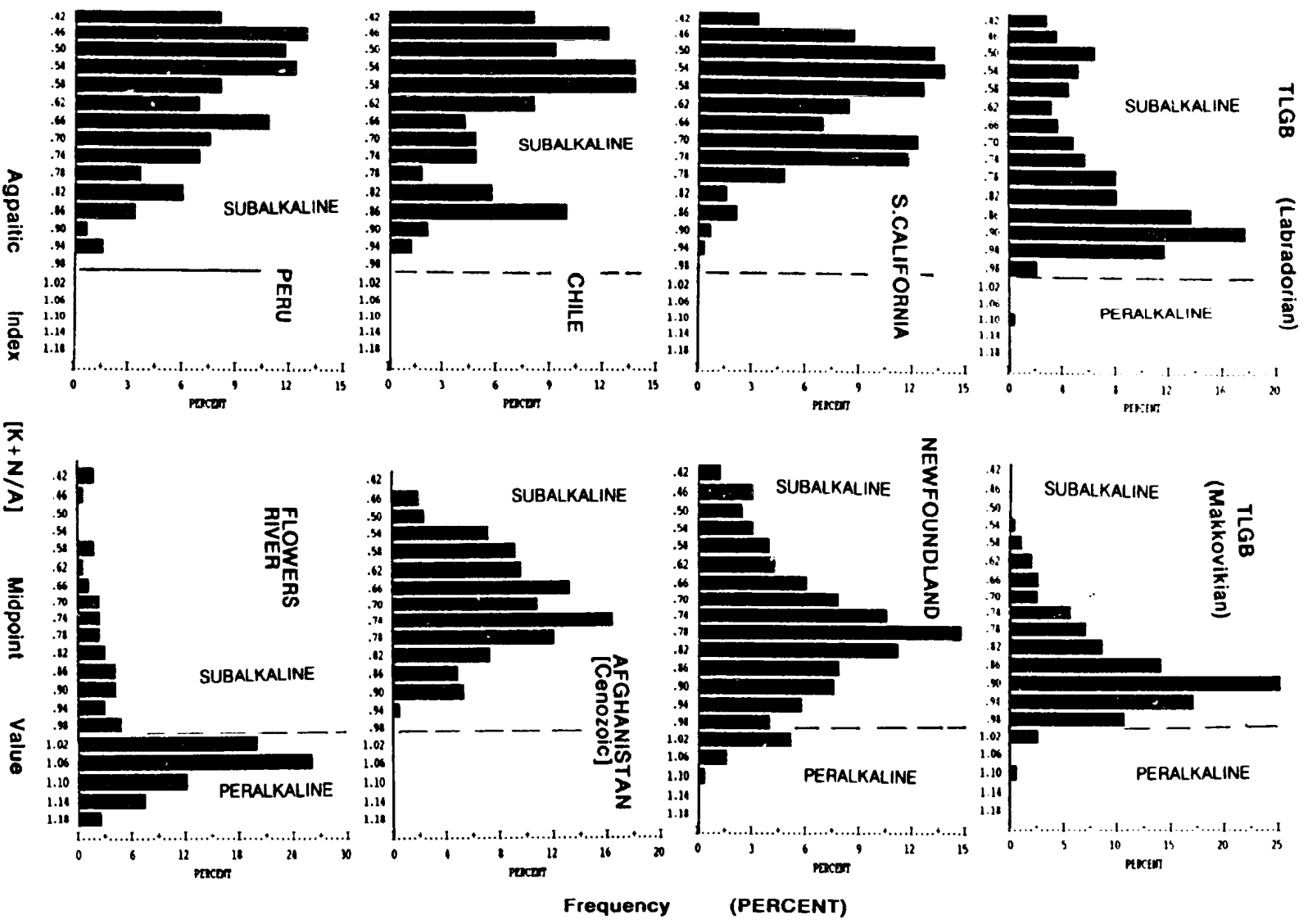


Figure 9.6f. Comparative Apatitic Index frequency spectra.

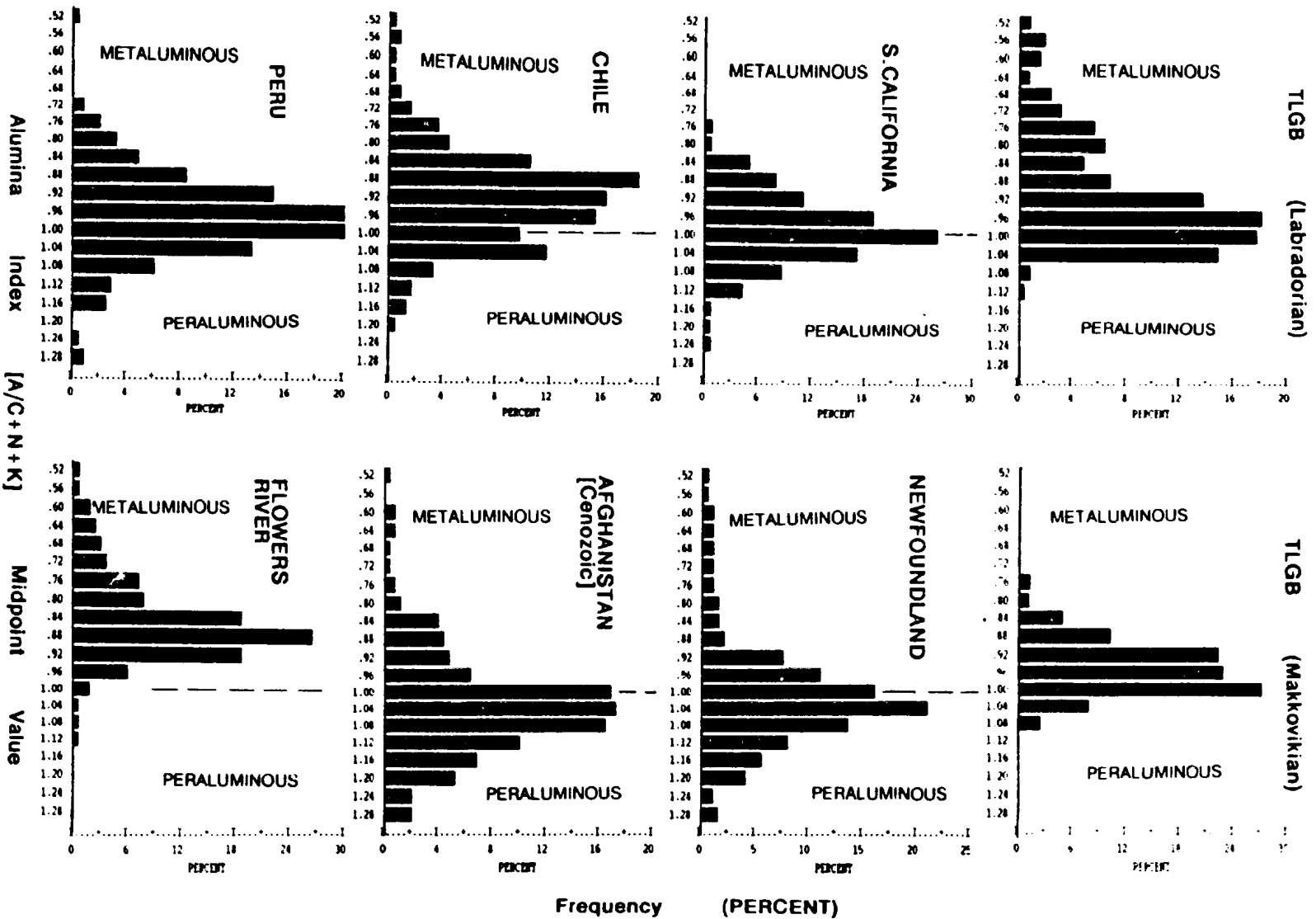


Figure 9.6g. Comparative Alumina Index Frequency spectra.

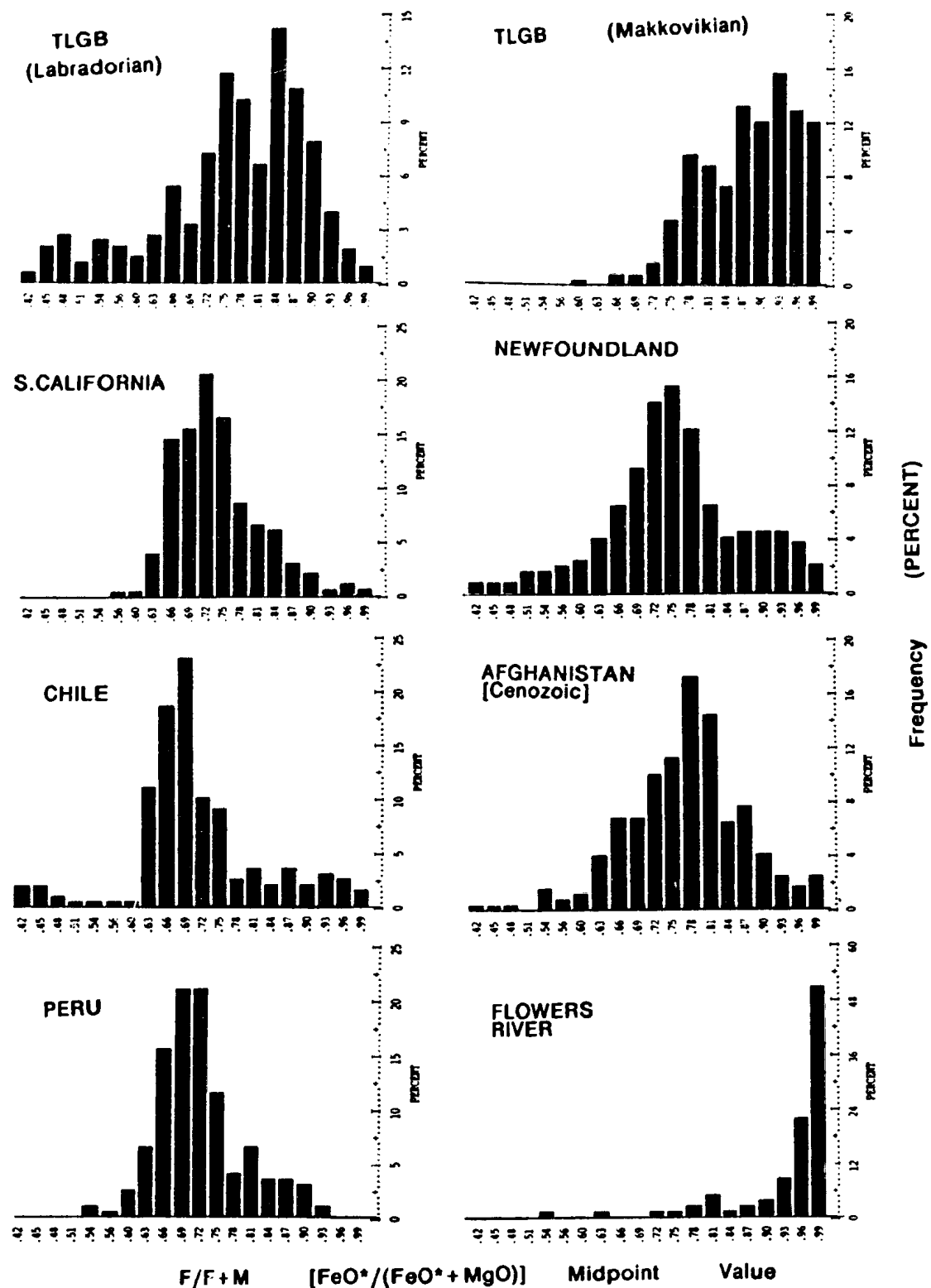


Figure 9.6h. Comparative  $F/F+M$  frequency spectra.

suites resemble both collisional and within-plate assemblages, but more closely resemble the latter. Labradorian suites show a wide range of MgO (mostly reflecting the mafic rocks of the Adlavik and Mount Benedict Suites), but are also dominated by MgO-poor compositions compared to arc assemblages.

**CaO (Figure 9.6c)** : CaO spectra resemble MgO spectra, and distinguish arc and collisional assemblages in a similar manner. The Makkovikian suites have a closer affinity to collisional assemblages than to within-plate assemblages. The Labradorian assemblage is distinctly bimodal.

#### Major Element Ratio and Function Frequency Spectra

**TTDI (Differentiation Index) (Figure 9.6d)** : The Thornton-Tuttle Differentiation Index (TTDI; sum of normative Q + Ab + Or + feldspathoids) is superior to  $\text{SiO}_2$  as an indicator of igneous differentiation, as it is less dependent upon silica-saturation.

TTDI spectra discriminate arc and collisional assemblages in a similar manner to  $\text{SiO}_2$ . The bimodal  $\text{SiO}_2$  frequency distributions of TLGB assemblages are, however, less obvious in their TTDI spectra. This contrast reflects the presence of evolved intermediate felsic rocks (e.g. monzonite and syenite) in both TLGB assemblages; these have moderate  $\text{SiO}_2$  contents, but high TTDI values.

**N/N+K (Figure 9.6e)** : Arc assemblages are predominantly sodic ( $\text{Na}_2\text{O} > \text{K}_2\text{O}$ ), and have broad, normal to negatively skewed, frequency spectra. They contrast

AFGHANISTAN  
[Mesozoic]

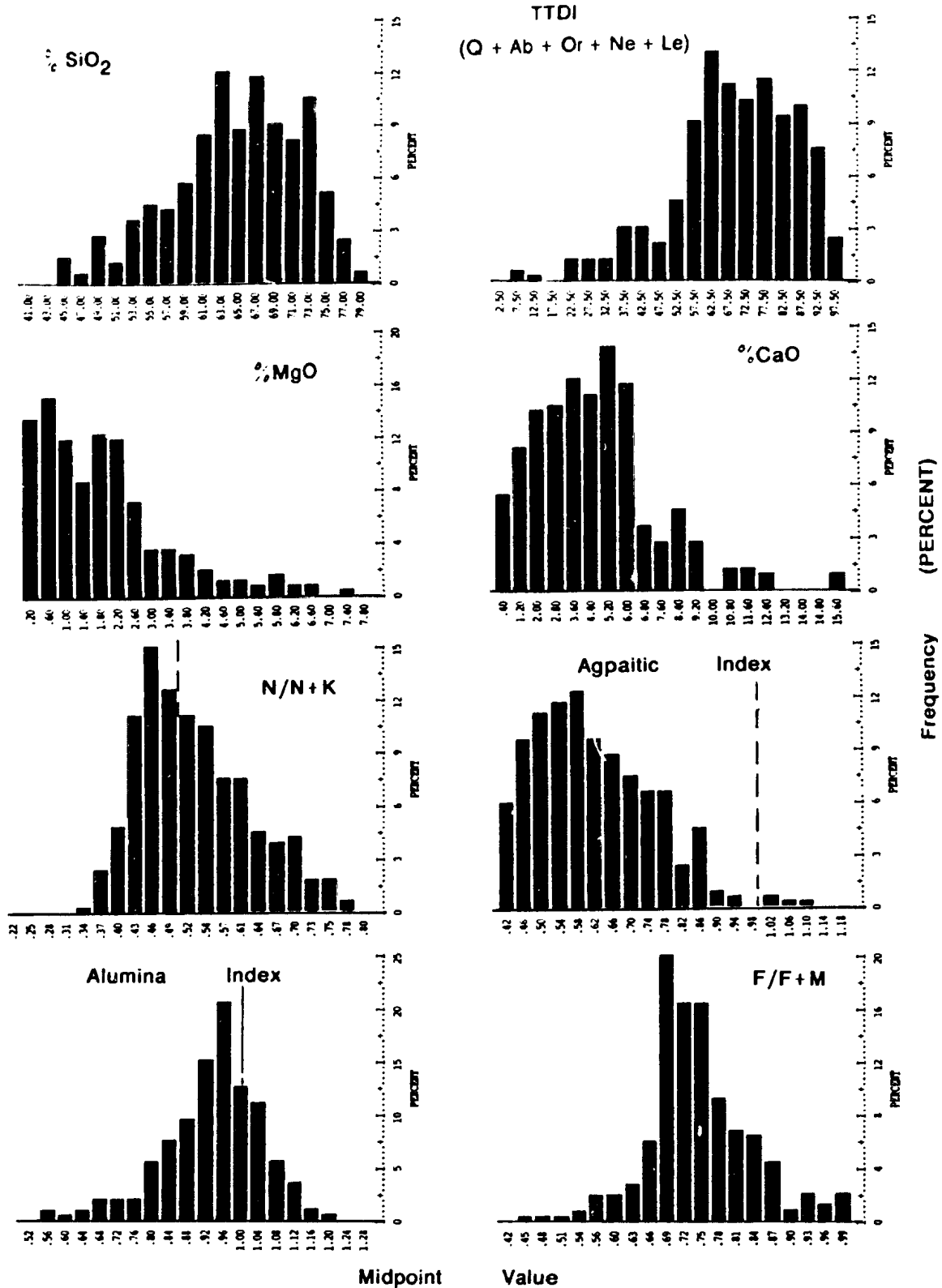


Figure 9.7. Frequency spectra for major elements and derived parameters in Mesozoic batholiths from Afghanistan. Compare with arc assemblages (PERU, CHILE, S.CALIFORNIA) in Figure 9.6.

strongly with the narrow, positively skewed, potassic ( $K_2O > Na_2O$ ) frequency distributions of collisional and within-plate assemblages.

The Makkovikian assemblage is closely similar to Newfoundland and Afghanistan (Cenozoic) assemblages, but also resembles Flowers River. The Labradorian spectrum is unique, but is clearly potassic relative to the arc assemblages.

***K+N/A -- Aqpaitic Index (Figure 9.6f) : Arc***  
assemblages have positively skewed, commonly bimodal, patterns with maxima at ca. 0.5 and ca. 0.7; they do not include peralkaline rocks. Collisional assemblages have a more restricted range (maxima ca. 0.8), and Newfoundland includes ca. 7 % peralkaline compositions.

The Makkovikian assemblage is similar to the Newfoundland assemblage, but has distinctly higher K+N/A at 0.9 to 1.0. The Labradorian assemblage is bimodal, but includes some rocks with similarly high K+N/A values. Neither TLGB assemblage is as extreme in composition as Flowers River, where ca. 60% of compositions are peralkaline.

***A/C+N+K -- Alumina Index (Figure 9.6g) : All suites***  
except Chile and Flowers River have similar frequency spectra with peaks at ca. 1.0. Collisional assemblages include by far the largest proportion (> 50%) of peraluminous rocks, whereas the Flowers River assemblage is devoid of such material. Both Makkovikian and Labradorian assemblages contain fewer peraluminous rocks than collisional or arc assemblages, and rarely include rocks with  $A/C+N+K > 1.1$  (lower limit for S-type granites; Chappell and White, 1974).



**F/F+M (Figure 9.6h)** : Arc and collisional assemblages both have peaks at ca. 0.7 - 0.8. Granitoid rocks from Flowers River are distinguished by very high F/F+M (>0.95).

The Makkovikian assemblage has a negatively skewed distribution (maximum at 0.9 to 0.96) that has some affinity to the Flowers River Spectrum, but is not as extreme or restricted. Labradorian suites are bimodal and compositionally expanded, but also include Fe-enriched compositions.

### **9.2.2 Abundance and Distribution Of Rock Types**

Contrasts in compositional spectra may also be assessed via proportions of IUGS rock types (Figure 9.8) calculated from normative mineralogy (after Streckeisen and LeMaitre, 1979).

Arc assemblages are dominated by normative tonalite, granodiorite and monzogranite, with significant quartz diorite and quartz monzodiorite. Collisional assemblages from Newfoundland are more evolved than those of Afghanistan, but both are dominated by monzogranite to alkali-feldspar granite, and lack significant quartz-diorite or tonalite. The Flowers River assemblage is dominated by alkali-feldspar granite. TLGB assemblages are obviously bimodal, and both contain monzonite-syenite components that are essentially absent from all other assemblages. In general, the Makkovikian assemblage most closely resembles the Newfoundland assemblage. The Labradorian assemblage has no obvious analogue.

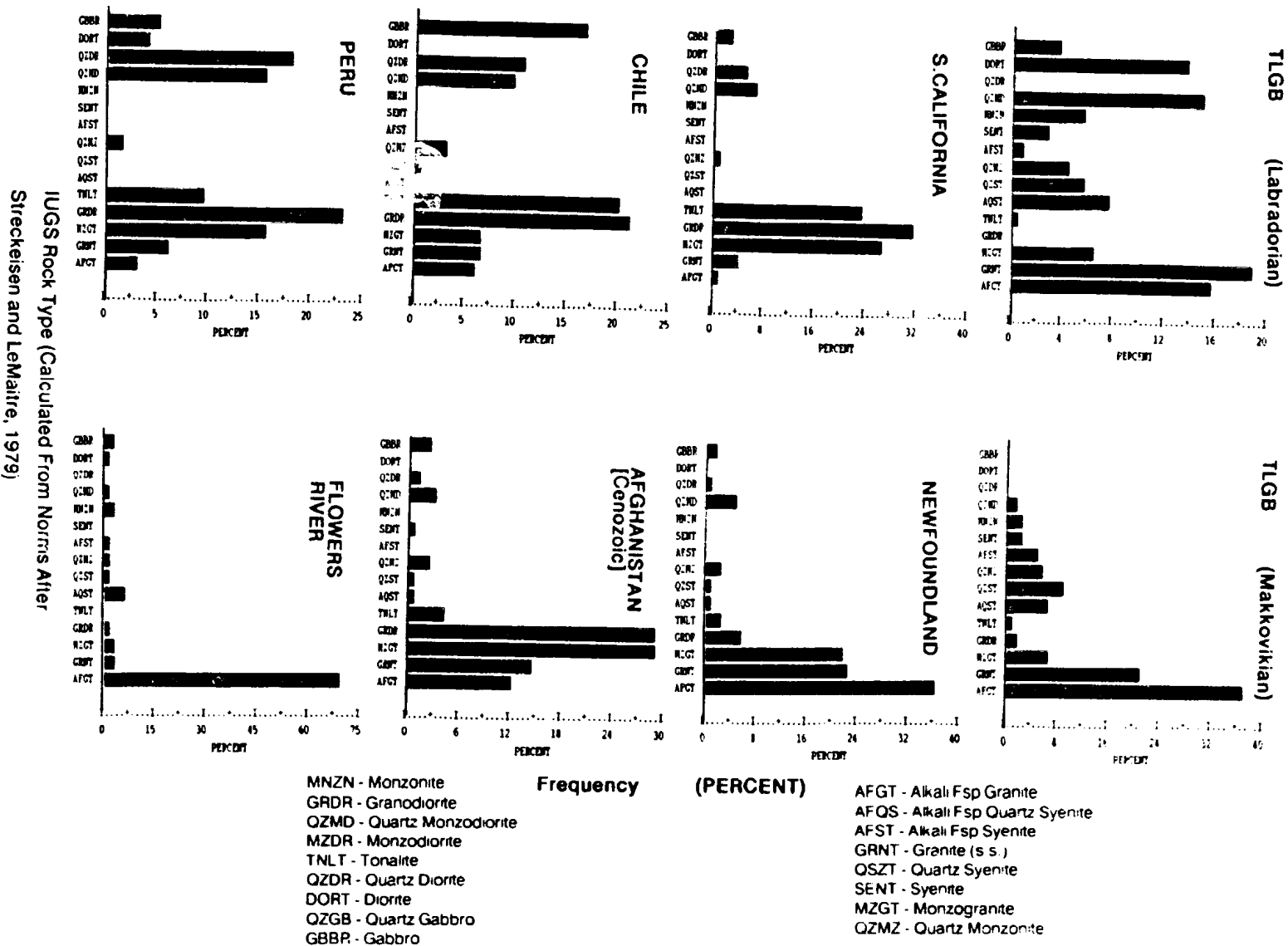


Figure 9.8. Proportions of IUGS rock types in the TLGB assemblages and comparative assemblages (calculated from normative data after Streckeisen and LeMaitre, 1979).

### 9.2.3 Evolutionary Trends

#### **Quartz-Poor Versus Quartz-Rich Trends**

Contrasts of compositional anatomy described above are placed in an evolutionary context in the Q'-ANOR diagram (Figure 9.9) of Streckeisen and LeMaitre (1979). Arc assemblages have quasi-linear trends extending from gabbro to granite (s.s.), but cluster primarily in the quartz and anorthite-rich tonalite and granodiorite fields. Collisional assemblages are shifted to more evolved compositions (monzogranite to granite), but lie essentially on the same "quartz-rich" evolutionary trend.

Both TLGB assemblages have arcuate, "quartz-poor" trends that proceed from gabbro to alkali-feldspar granite via monzonite and syenite (Figure 9.9). The Flowers River assemblage, although restricted in compositional range, has a similar quartz-poor evolutionary trend, but is virtually anorthite-free at silicic compositions. These trends are analogous to those defined by Bowden et al. (1984) using the ternary Quartz - Plagioclase - Alkali-feldspar modal diagram, where "within-plate" assemblages such as the Nigerian younger granites have similar quartz-poor evolutionary trends.

These quartz-rich and quartz-poor trends are visible also in the Q-Ab-Or system (Figure 9.10), where the TLGB and Flowers River assemblages have well-defined trends from the Ab-Or join at Or<sub>40</sub> to the ternary minimum area. These correspond to the general location of the plagioclase - alkali-feldspar cotectic at low pressures and An contents (James and Hamilton, 1969).

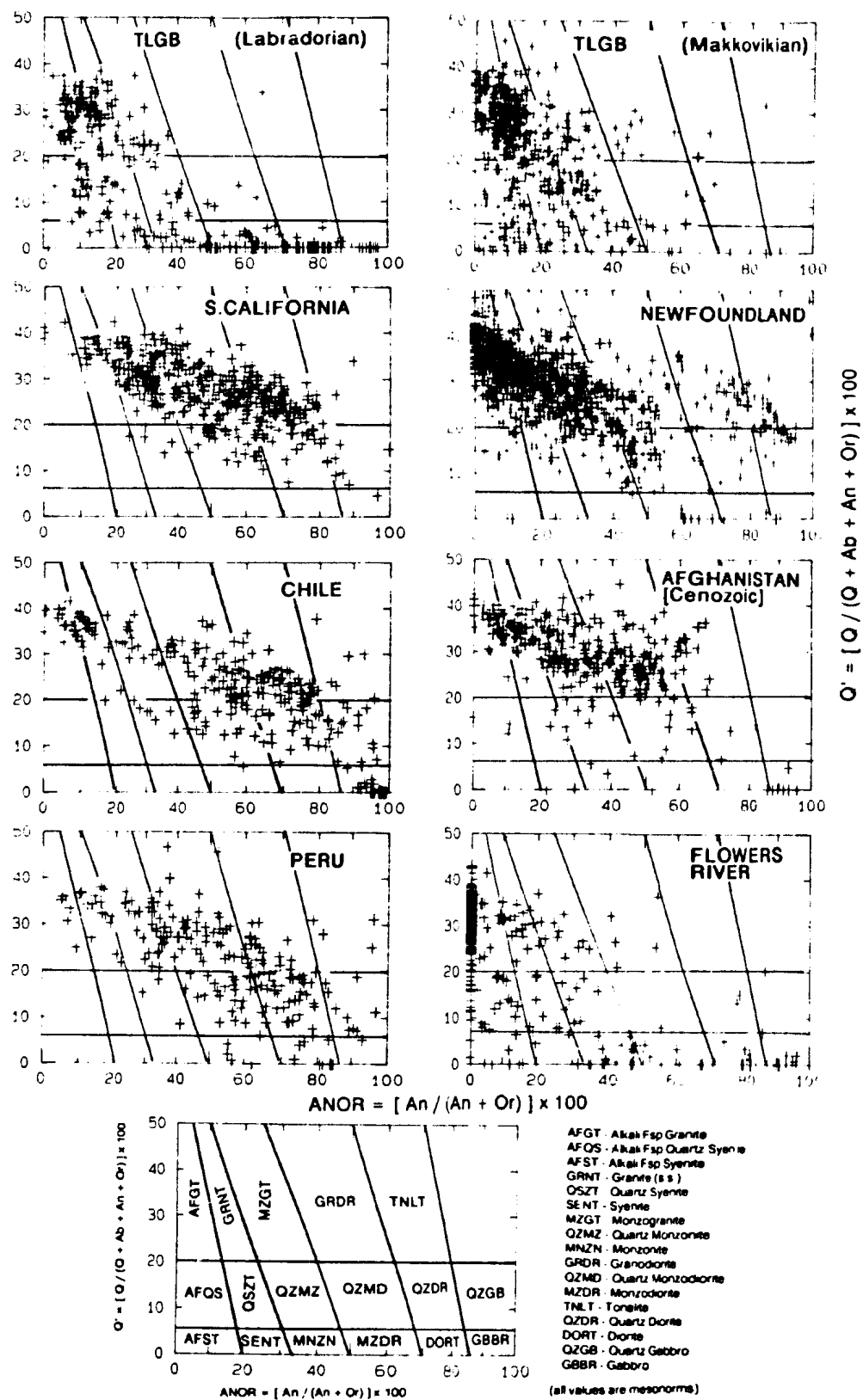


Figure 9.9. Distribution of the TLGB and comparative assemblages in the  $Q'$  - ANOR diagram of Streckeisen and LeMaitre (1979).

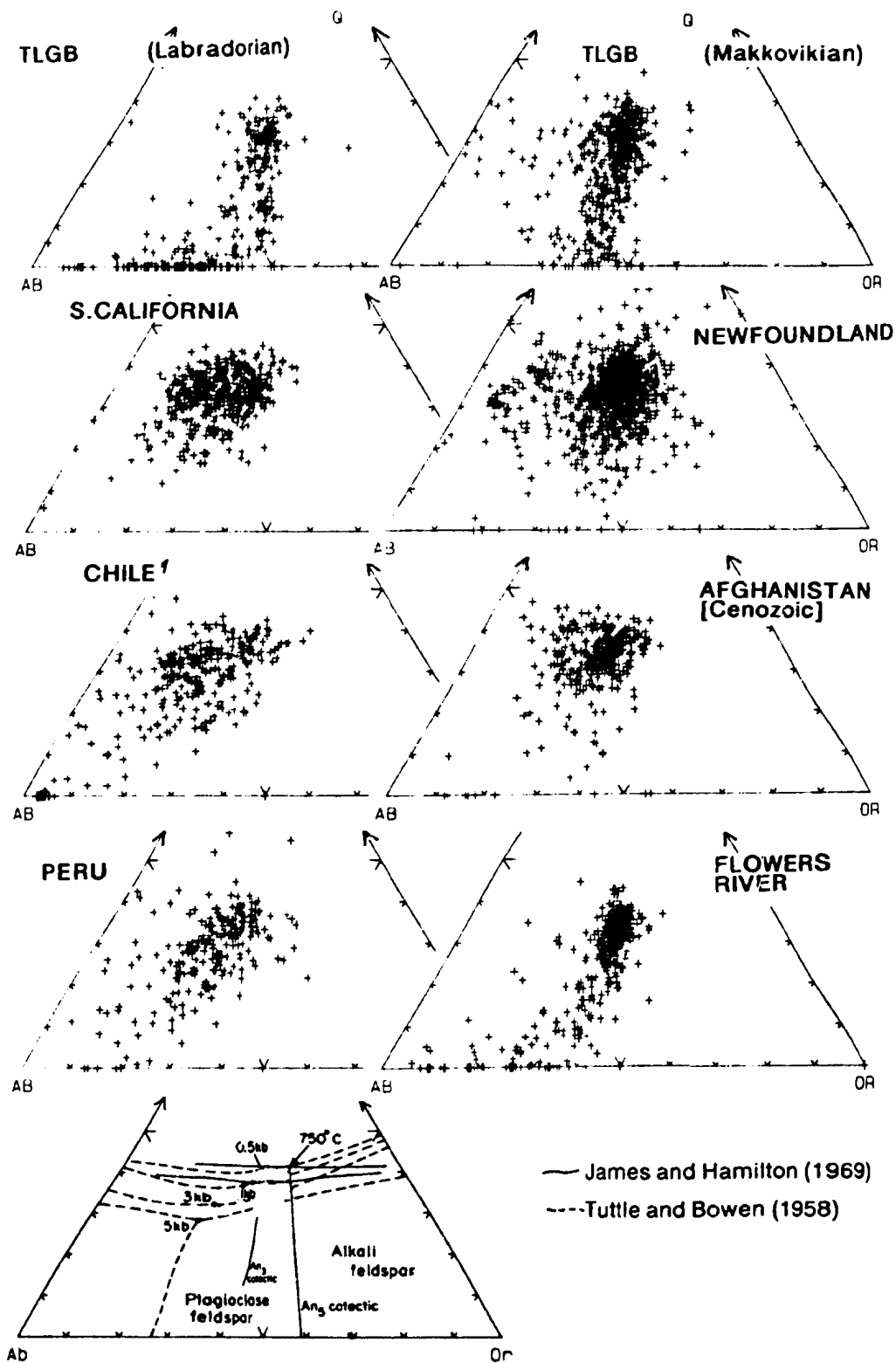


Figure 9.10. Distribution of the TLGB and comparative assemblages in the quartz - albite - orthoclase ternary system.

## Major Element Differentiation Trends

Differentiation trends were summarized by aggregating data into  $\text{SiO}_2$  intervals of 5% width, and calculating univariate statistics for each interval. Minor numbers of data (< 1%) with  $\text{SiO}_2$  < 37.5% or  $\text{SiO}_2$  > 82.5% were excluded in this procedure. "A-type" granites of the Lachlan Fold Belt (Collins et al., 1982; Whalen et al., 1987b) are also included in this compilation. No direct association via liquid line-of-descent is implied by this largely descriptive aggregation procedure.

**AFM and CNK trends** : These methods, despite wide application, are of little or no value in discrimination (see also Debon and Lefort, 1982; Bowden et al., 1984). Summary trends (Figure 9.11) are almost identical for all assemblages. The Flowers River assemblage lies closest to the Alkali-FeOt join, reflecting its Fe-enrichment. Petro et al. (1979) and Brown (1981) suggest this as a discrimination method for extensional or anorogenic suites, but there is no separation at the alkali-rich end of the trends.

**Harker Variation Trends** : Summary major element trends are closely similar for  $\text{TiO}_2$ ,  $\text{Al}_2\text{O}_3$ ,  $\text{CaO}$ ,  $\text{P}_2\text{O}_5$ ,  $\text{MnO}$ , and  $\text{MgO}$  (not figured) in all assemblages. TLGB assemblages show enrichment in  $\text{K}_2\text{O}$  and  $\text{Na}_2\text{O}$  (Figure 9.12) at all  $\text{SiO}_2$  contents, and their high- $\text{SiO}_2$  trends partly coincide with Flowers River.  $\text{K+N/A}$ ,  $\text{A/C+N+K}$  and  $\text{F/F+M}$  trends for TLGB assemblages lie between those of collisional assemblages and Flowers River, as indicated also by frequency spectra (Figure 9.6).

"A-type" granites from the Lachlan Fold belt lie closest to the Newfoundland trend, and are significantly less agpaitic than Flowers River or TLGB assemblages.

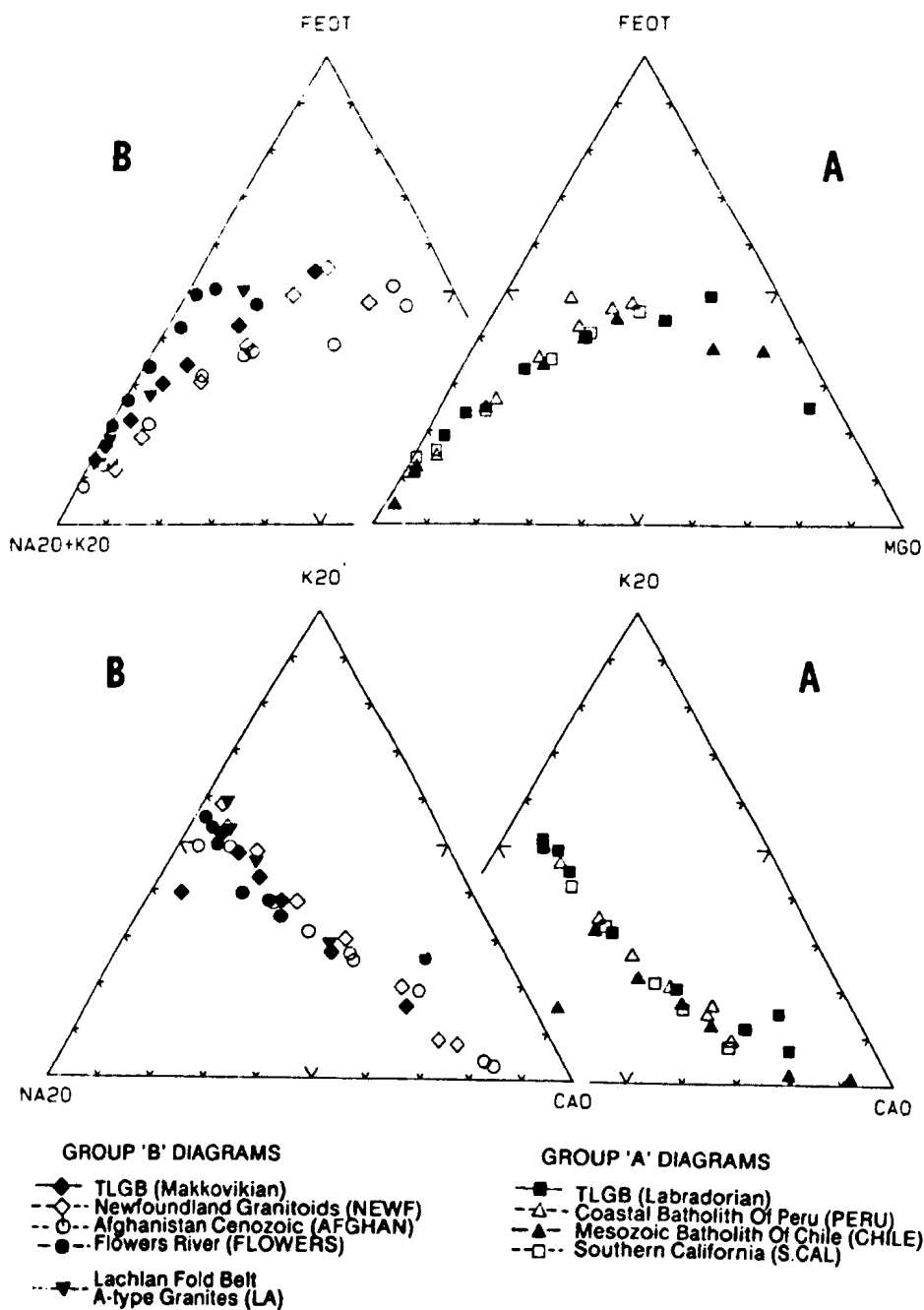
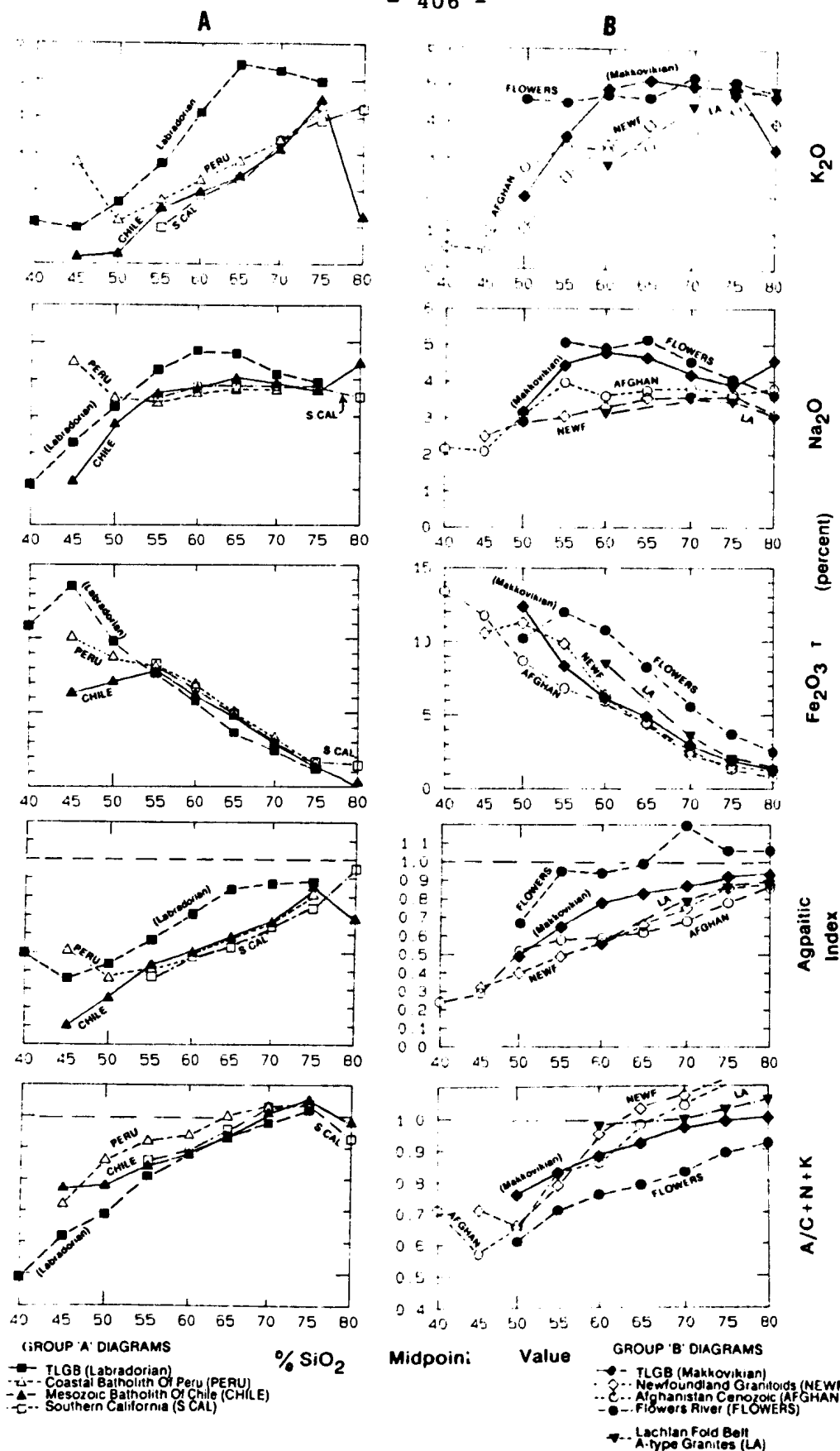


Figure 9.11. AFM and CNK trends for the TLGB and comparative assemblages. Note the lack of obvious contrasts.





### 9.3 COMPARATIVE TRACE ELEMENT GEOCHEMISTRY

Trace element data from comparative assemblages vary in completeness and quality. The Chile, Newfoundland and Flowers River databases include a trace element suite comparable to that available for the TLGB (Table 9.1), and can be compared fully. Other databases contain incomplete and/or restricted trace element suites. Mesozoic batholiths from Afghanistan are regarded here as an arc assemblage, based on their major element spectra (9.3.1; Figure 9.7) and other arguments presented by Debon et al. (1987a,b)

#### 9.3.1 Comparative Frequency Spectra

Trace element frequency spectra were standardized in the same manner as for major elements. The number of valid cases indicated for each element (Figure 9.13) provides an indication of the completeness of data in each assemblage.

##### **Trace Element Spectra**

**Vanadium (Figure 9.13a)** : Vanadium spectra are broad and flat in arc assemblages, whereas collisional assemblages have log-normal, positively skewed distributions similar to MgO. There is a clear affinity between Makkovikian and collisional assemblages; the Labradorian assemblage has a wide V range similar to some arc suites, but contains a higher proportion of low-V compositions.

**Rubidium (Figure 9.13b)** : Rb spectra show only subtle variation. Collisional and within-plate assemblages have higher median Rb contents than arcs, and tend towards

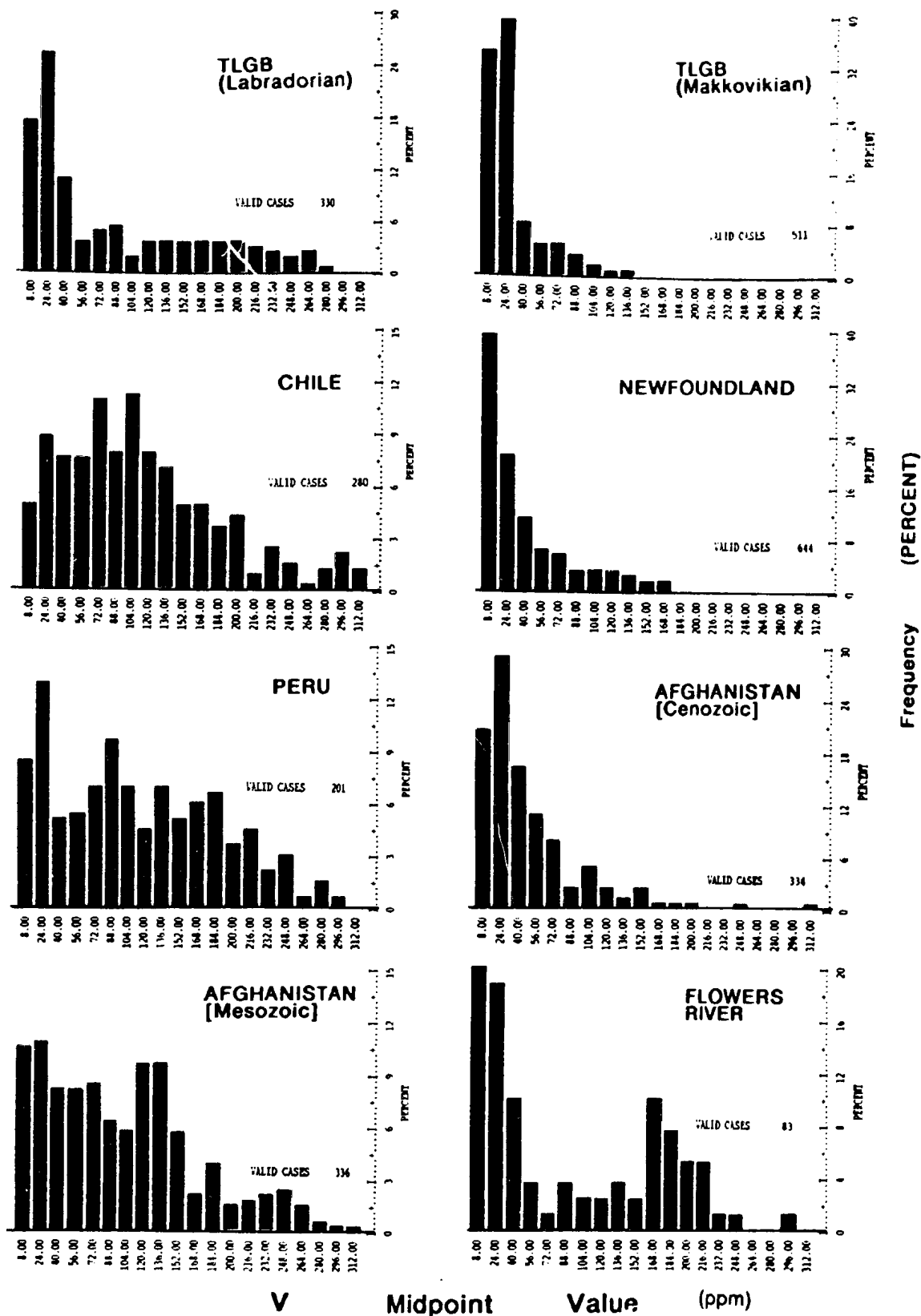


Figure 9.13a. Comparative vanadium (V) frequency spectra.

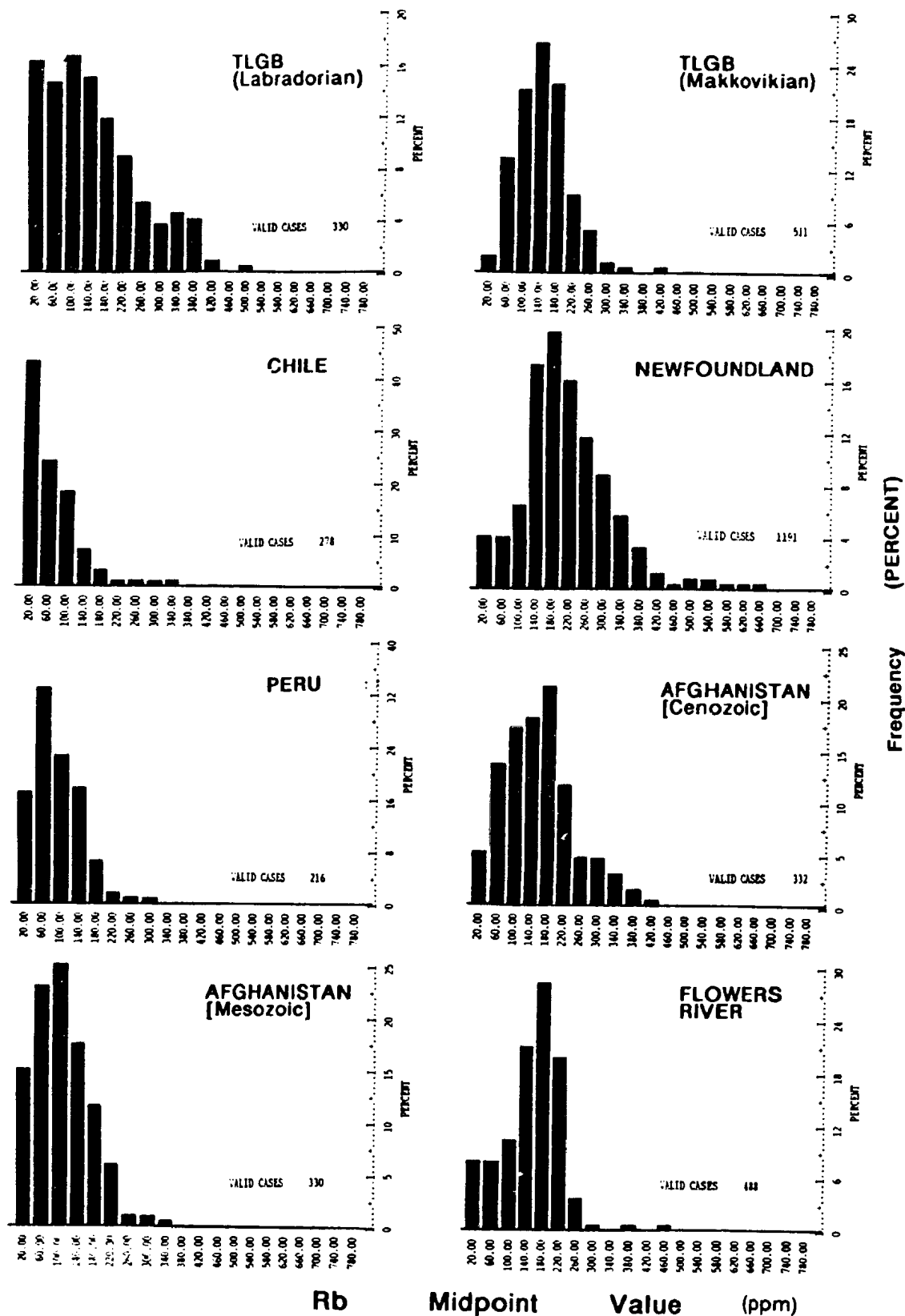


Figure 9.13b. Comparative rubidium (Rb) frequency spectra.

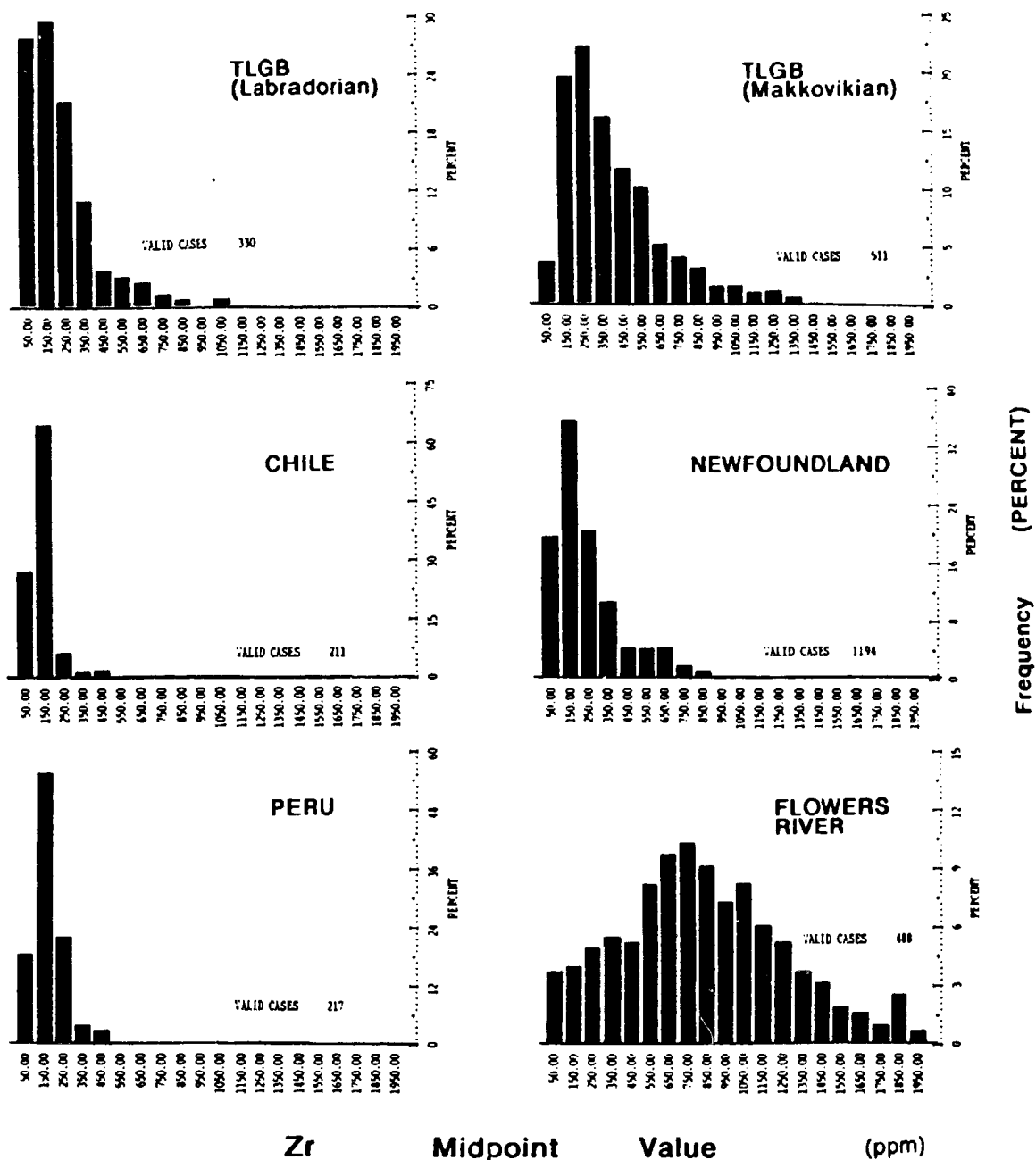
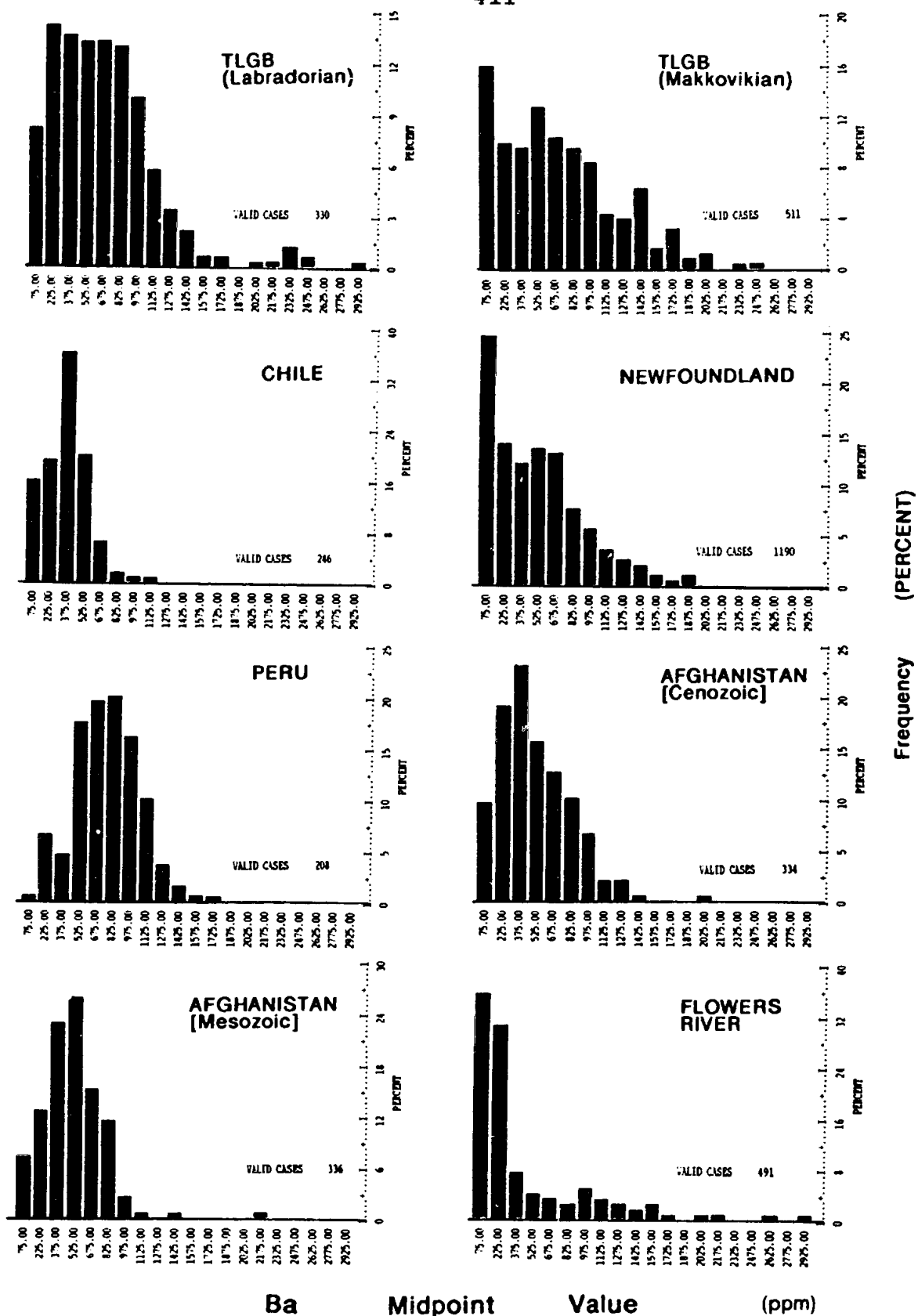


Figure 9.13c. Comparative zirconium (Zr) frequency spectra.



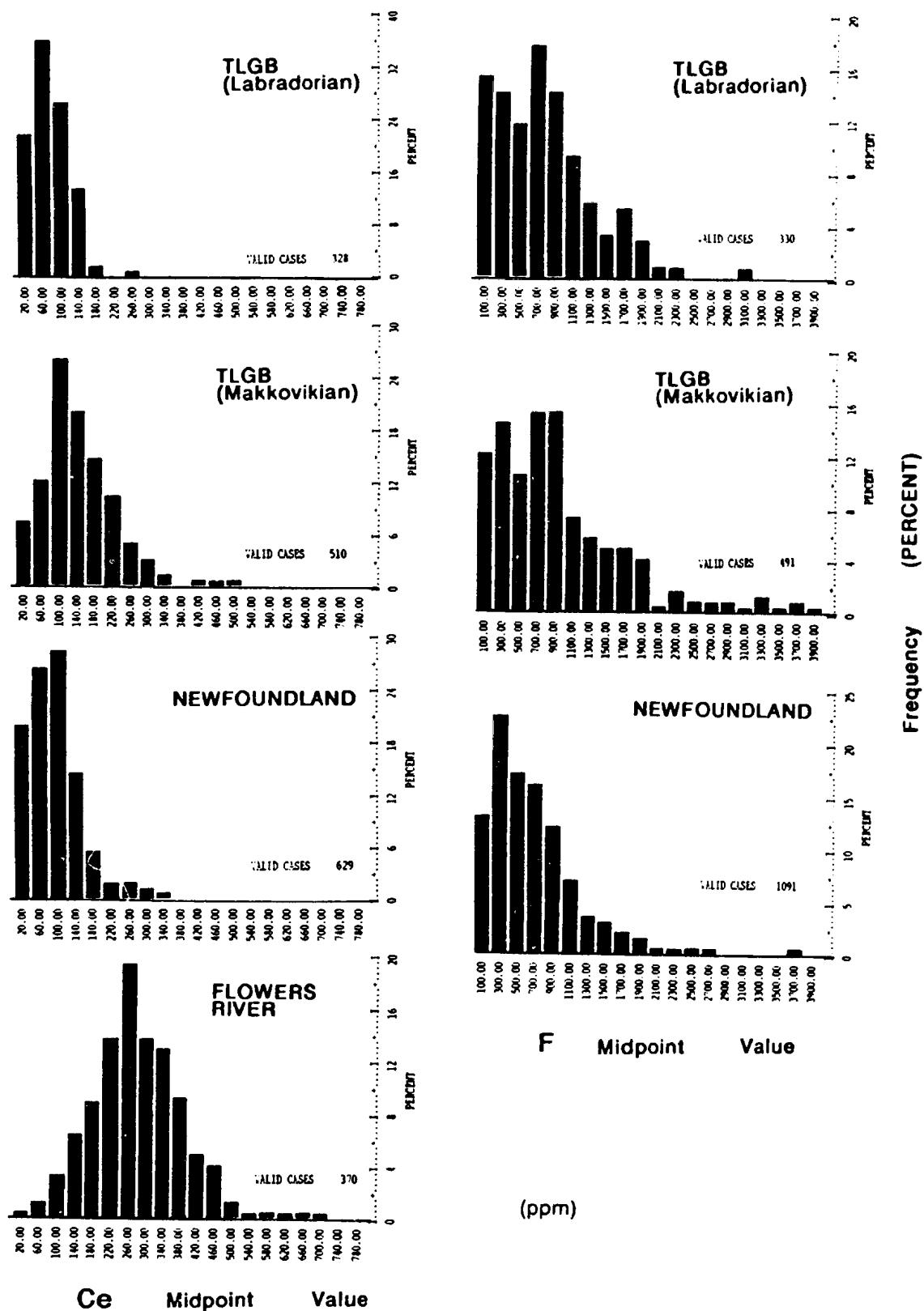


Figure 9.13e. Comparative cerium (Ce) and fluorine (F) frequency spectra.

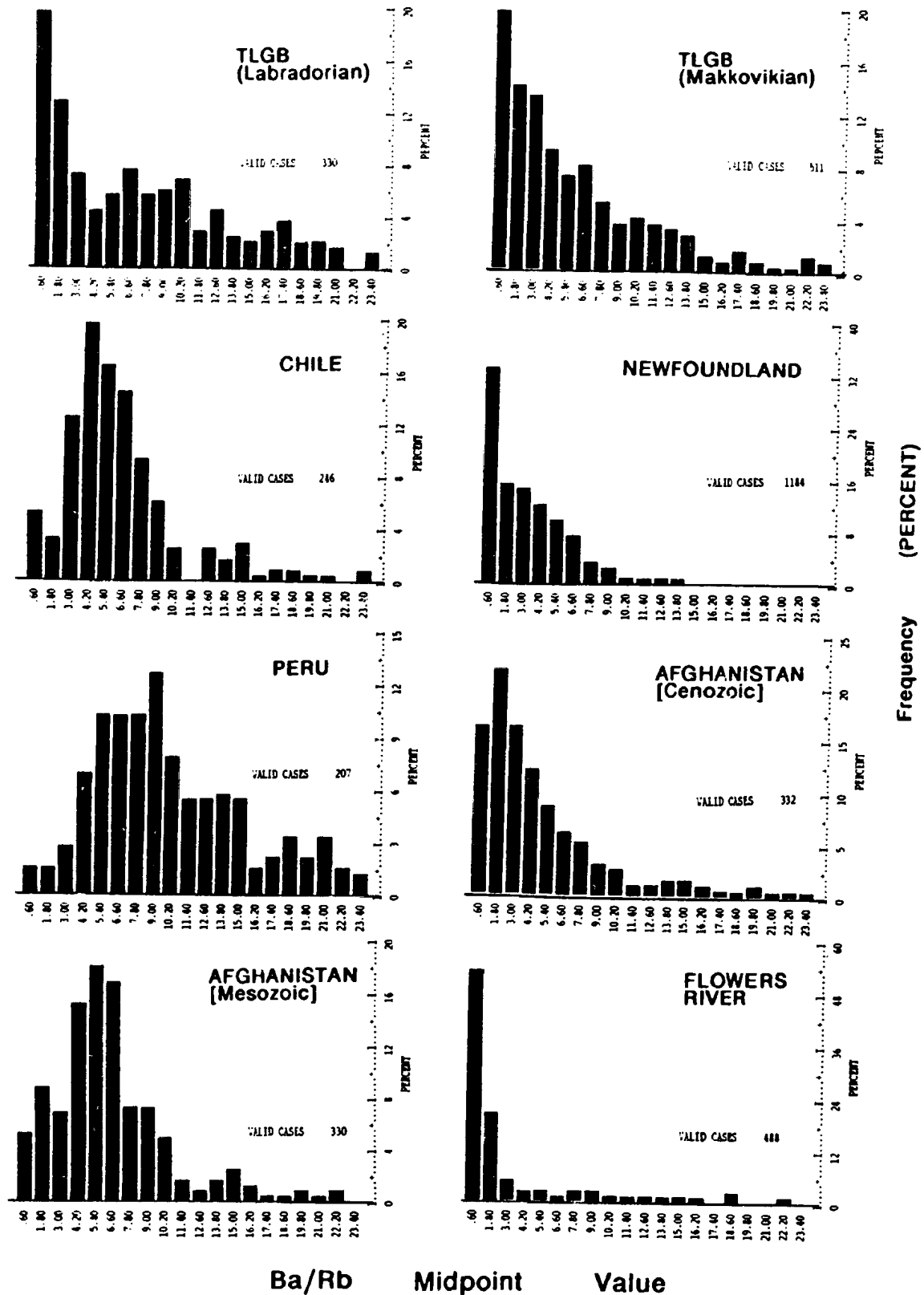


Figure 9.13f. Comparative Ba/Rb frequency spectra.

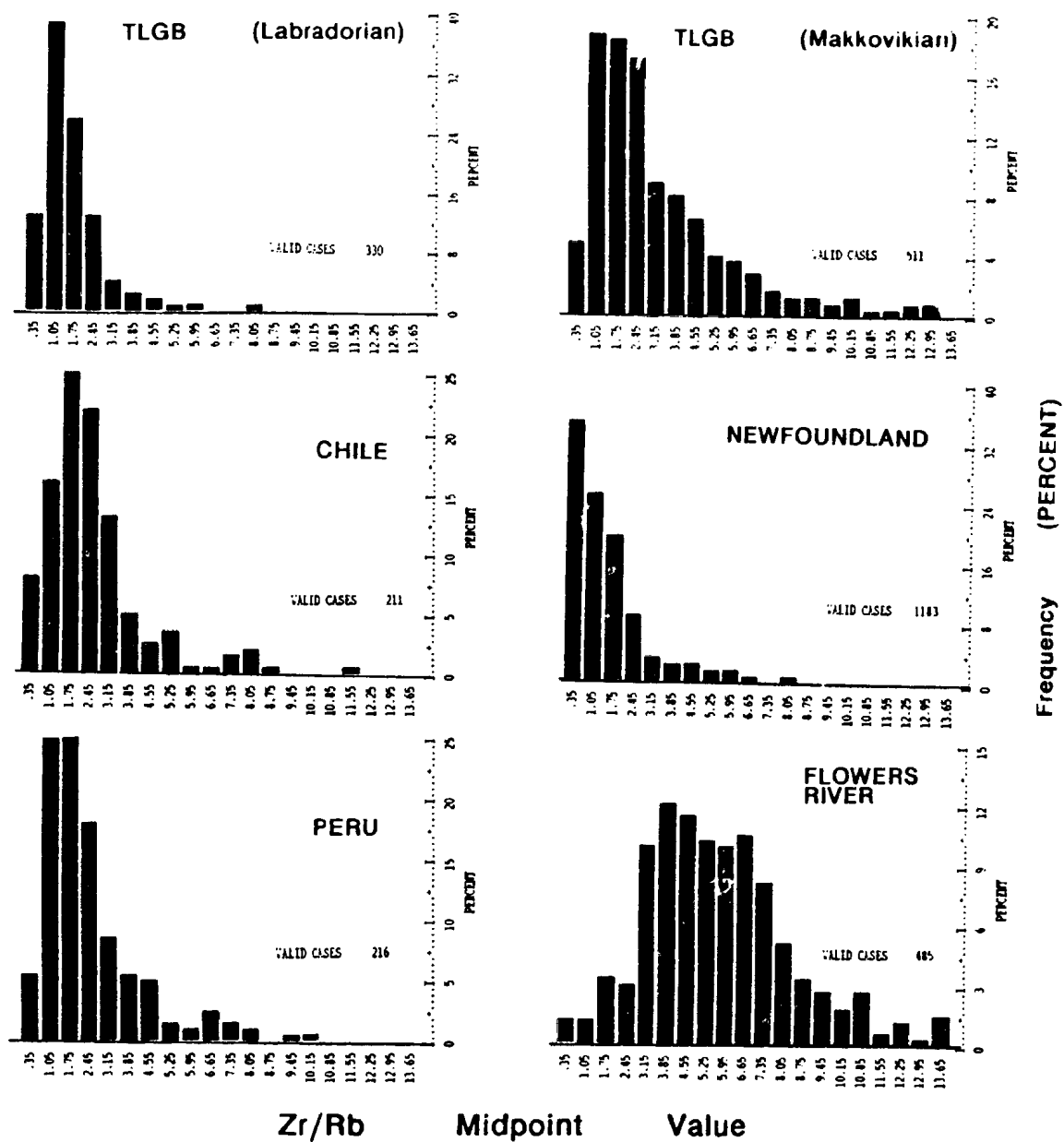


Figure 9.13g. Comparative Zr/Rb frequency spectra.



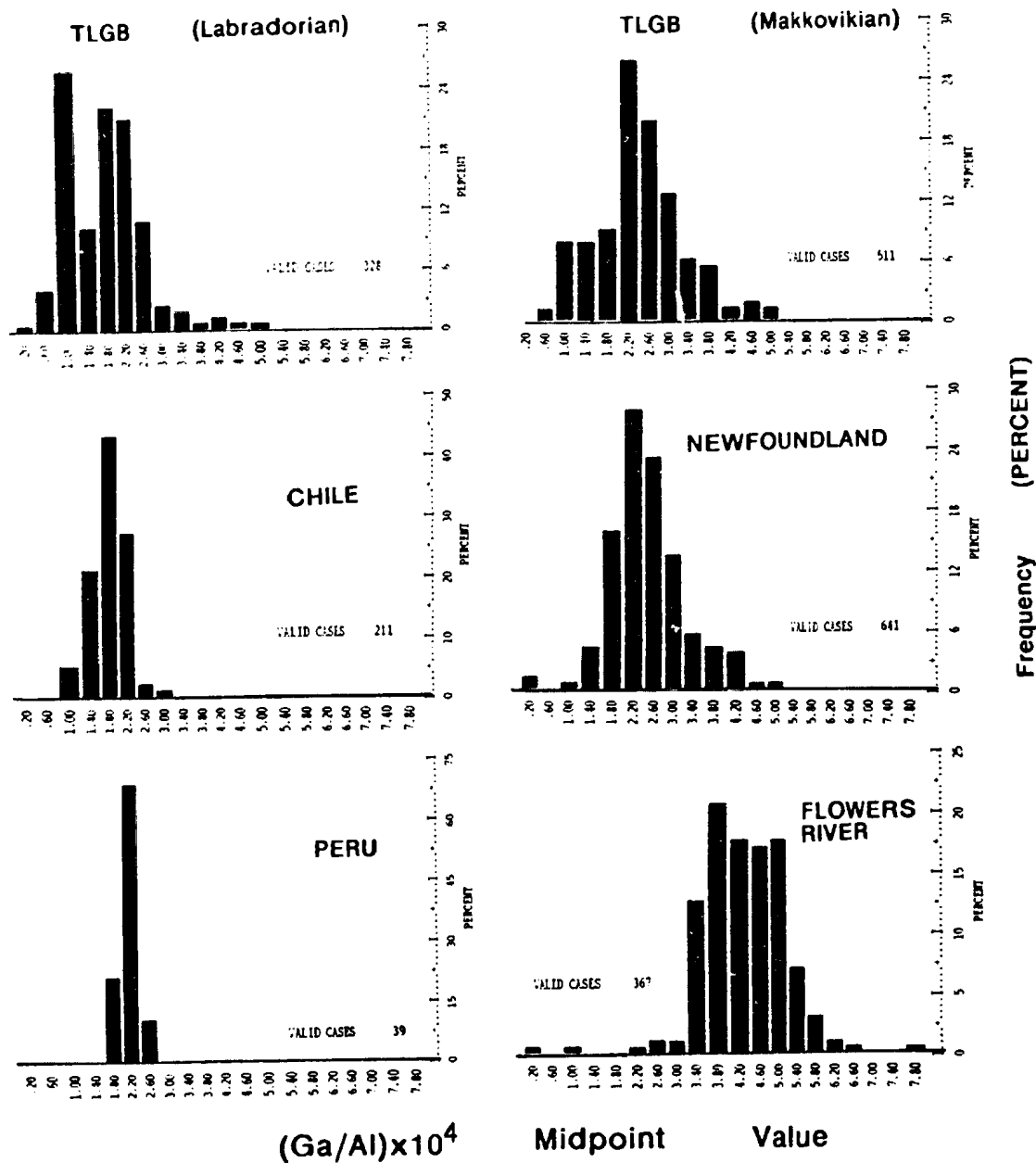


Figure 9.13h. Comparative  $Ga/Al \times 10^4$  frequency spectra.

normal or negatively-skewed patterns. Makkovikian and collisional assemblages show general similarity, but the former have slightly lower median Rb contents. The Labradorian spectrum resembles those of arc assemblages, but includes more Rb-rich compositions.

**Zirconium (Figure 9.13c)** : Zr characterizes the Flowers River assemblage very clearly. The Makkovikian spectrum includes a greater proportion of high-Zr rocks than the Newfoundland or Labradorian assemblages, but is similar in shape to both. Zr does not discriminate arc and collisional assemblages effectively. Zn and Y spectra (not figured) are closely similar to Zr.

**Barium (Figure 9.13d)** : Ba provides poor distinction of arc and collisional environments. Both Makkovikian and Labradorian assemblages contain a higher proportion of high-Ba compositions than either arc or collisional assemblages. The former resembles the Newfoundland spectrum in general shape.

**Cerium and Fluorine (Figure 9.13e)** : Data are incomplete for these elements. Ce characterizes the Flowers River assemblage, and partly discriminates the Makkovikian and Newfoundland assemblages. Both TLGB assemblages have higher median F contents than the Newfoundland assemblage. The similarity in the Labradorian and Makkovikian patterns is deceptive, as their F evolution trends are distinct. (Figure 9.18; see below).

### Trace Element Ratio Frequency Spectra

*Ba/Rb ratios (Figure 9.13f)* : These elements behave in contrasting fashions in arc and collisional assemblages (see also Figure 9.17). Collisional and anorogenic assemblages (characterized by Ba compatibility) have positively-skewed log-normal spectra, and lower median values than arc assemblages. The Makkovikian spectrum is similar to collisional assemblages, but richer in high-Ba compositions (see also Ba spectra).

*Zr/Rb ratios (Figure 9.13g)* : Zr/Rb offers little distinction between Newfoundland and arc assemblages, but characterizes Flowers River well. Zr/Rb spectra also illustrate the Zr-enriched and slightly Rb-depleted nature of much of the Makkovikian assemblage compared to Newfoundland.

*Ga/Al ratios (Figure 9.13h)* : This parameter has been proposed as a fingerprint of "A-type" granites (Collins et al., 1982; Whalen et al., 1987), and characterizes the Flowers River assemblage well. The Makkovikian and Newfoundland assemblages are closely similar.

### 9.3.2 Trace Element Discrimination Diagrams

#### Tectonic Setting Discrimination Diagrams

The Rb - (Y + Nb) diagram (Figure 9.14a) of Pearce et al. (1984) demonstrates a marked contrast between Makkovikian and Labradorian assemblages, which plot mostly in WPG (within-plate granite) and VAG (volcanic arc granite) fields respectively. There is some overlap in the

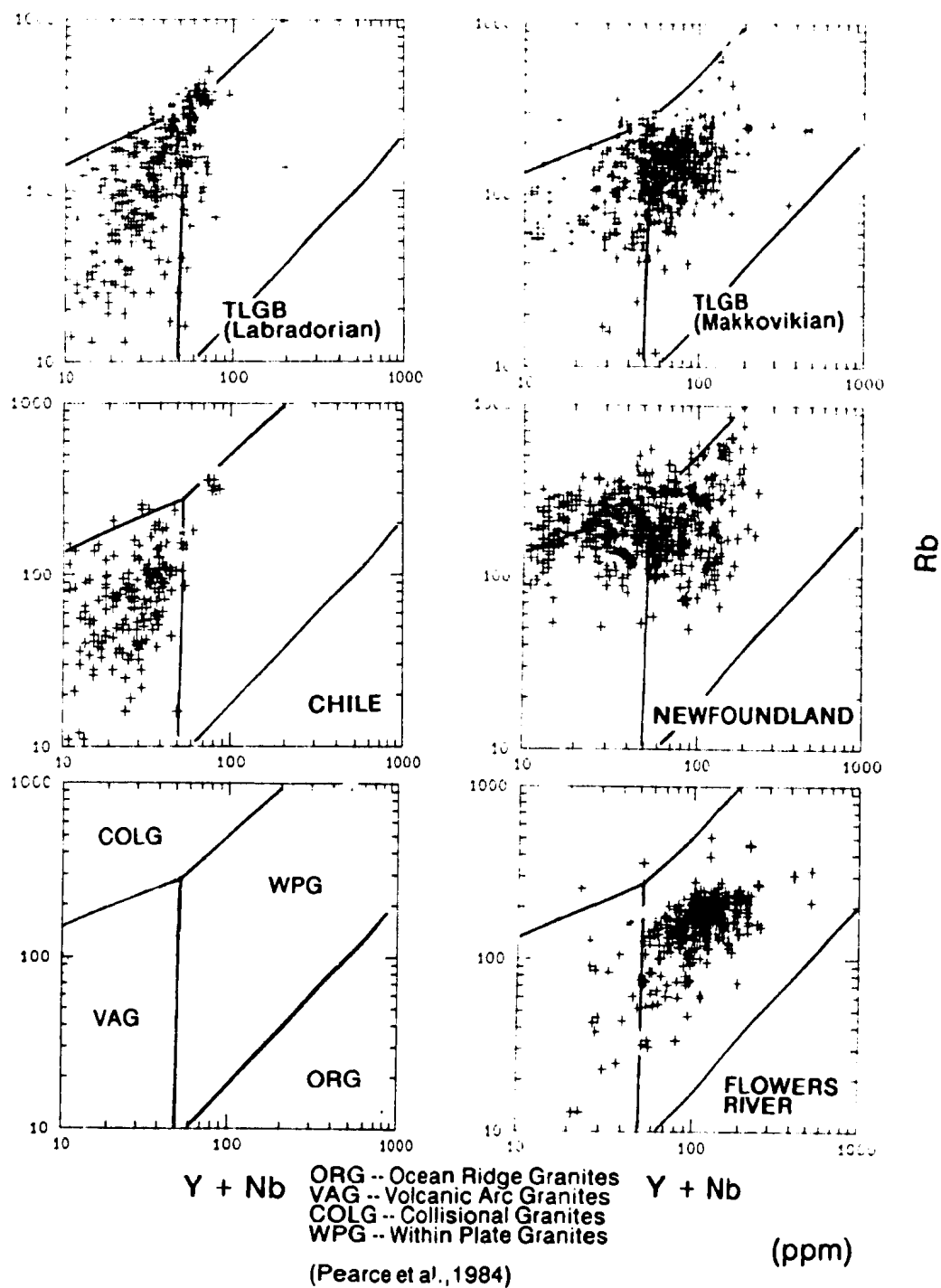
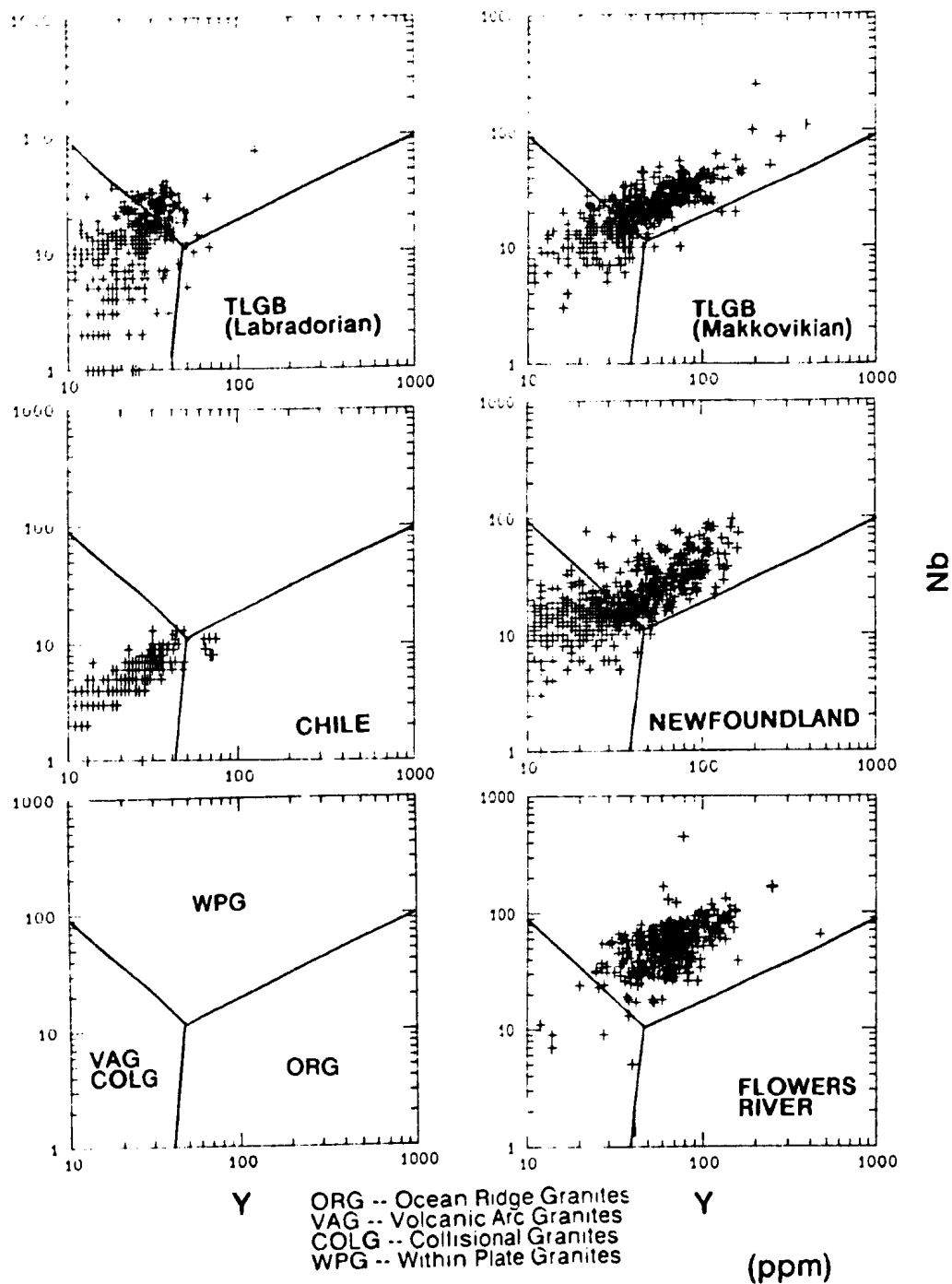


Figure 9.14a. Rb - (Y + Nb) discrimination diagrams (after Pearce et al., 1984) for TLGB and comparative assemblages.



(Pearce et al., 1984)

Figure 9.14b. Nb - Y discrimination diagrams (after Pearce et al., 1984) for TLGB and comparative assemblages.

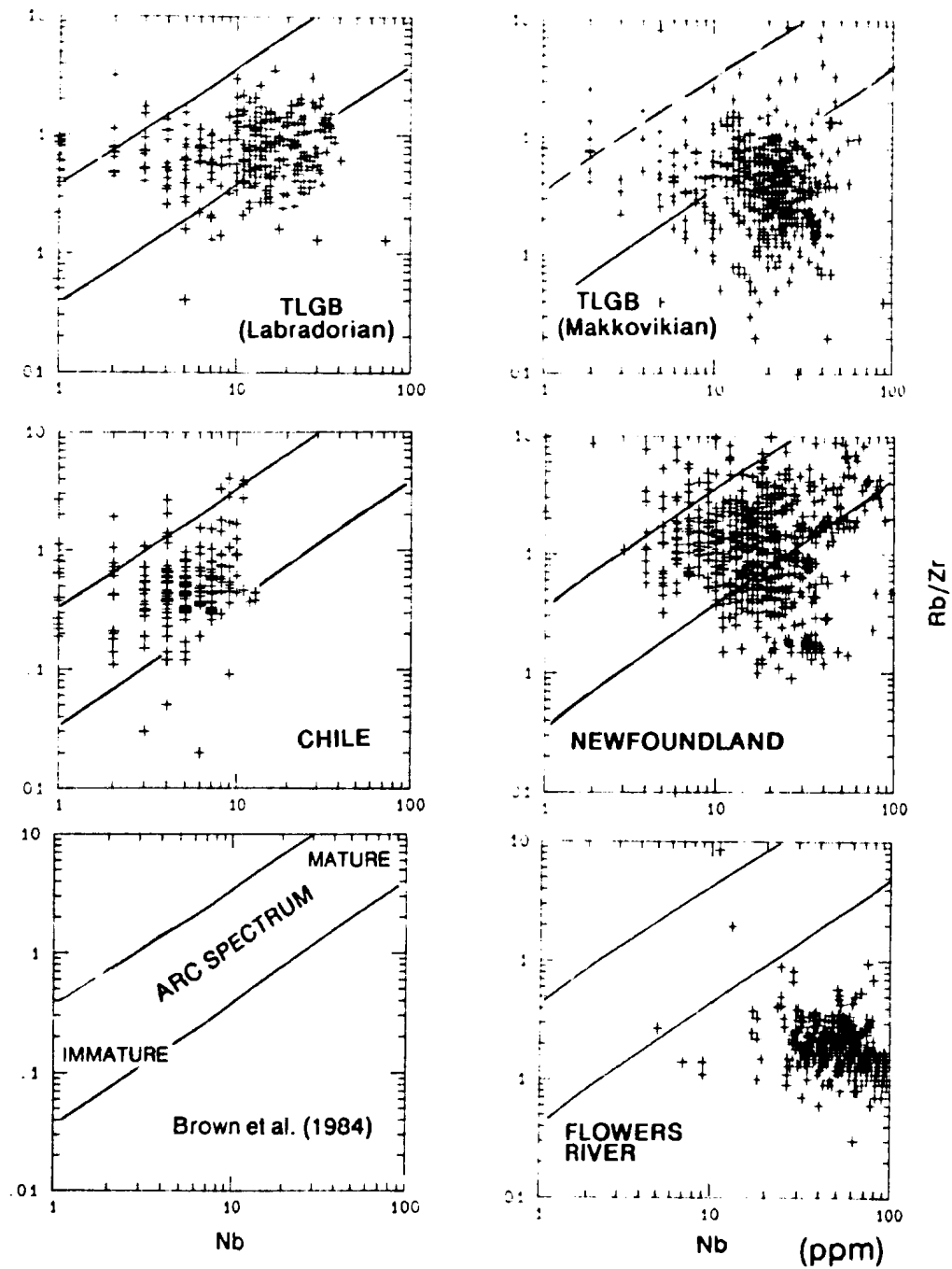


Figure 9.15. Rb/Zr - Nb discrimination diagrams (after Brown et al., 1984) for TLGB and comparative assemblages.

VAG field, and at the "triple point", but the TLGB (as a whole) lacks significant data within the COLG (collisional granite) field. However, the latter is primarily defined using syn-collisional suites; post-collisional suites (Harris et al., 1984) cannot be classified effectively in this system. This is shown well by Newfoundland data, which are smeared across all three fields. The Chile and Flowers River assemblages are correctly classified as VAG and WPG respectively. The Nb - Y diagram (Pearce et al., 1984) provides essentially the same divisions (Figure 9.14b), but shows greater overlap between TLGB assemblages.

In the Rb/Zr - Nb diagram (Figure 9.15) of Brown et al. (1984), the Labradorian assemblage lies partly within the mature portion of the arc spectrum, and corresponds to the most evolved Chilean data. The Makkovikian assemblage lies mostly below the arc spectrum, reflecting its Zr enrichment; a similar, but much more extreme, distribution is shown by Flowers River. The Newfoundland assemblage is widely scattered, but more strongly biased towards the mature arc area than Makkovikian granitoids.

#### **Discrimination Diagrams for Identification of A-type Granites**

Whalen et al. (1987) propose methods for separation of "A-type" granites from other evolved granitoid rocks. Their Zr - Ga/Al diagram (Figure 9.16a) discriminates Makkovikian and Labradorian assemblages, which fall predominantly in "A-type" and "Other" fields respectively. The Flowers River assemblage, however, has significantly higher Ga/Al and Zr than either Makkovikian or Newfoundland assemblages (see also Figure 9.13). The  $(K_2O + Na_2O / CaO) - (Zr + Y + Nb + Ce)$  diagram (Figure 9.16b) provides less effective

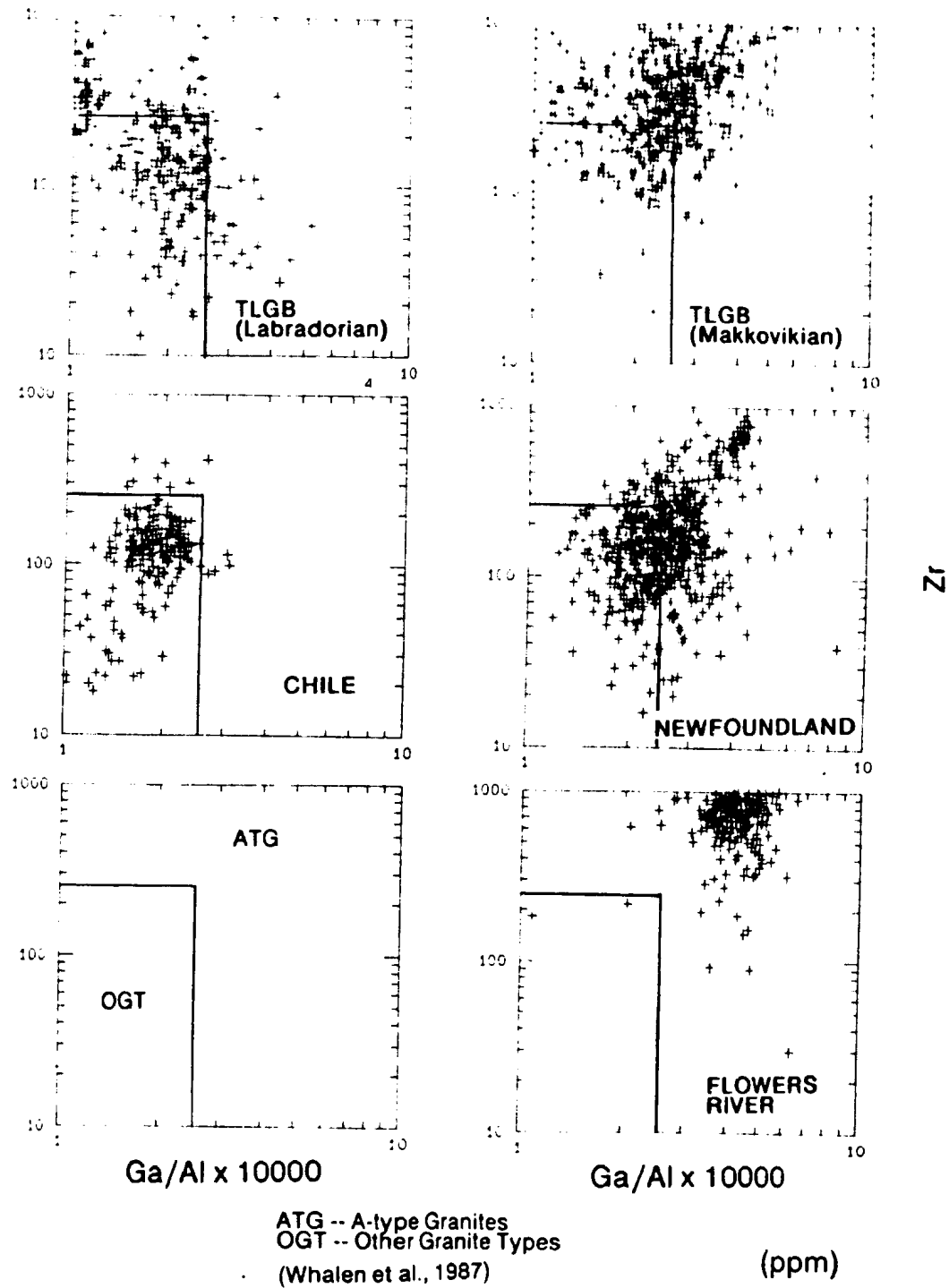


Figure 9.16a. Zr - Ga/Al discrimination diagrams (after Whalen et al, 1987) for TLGB and comparative assemblages.



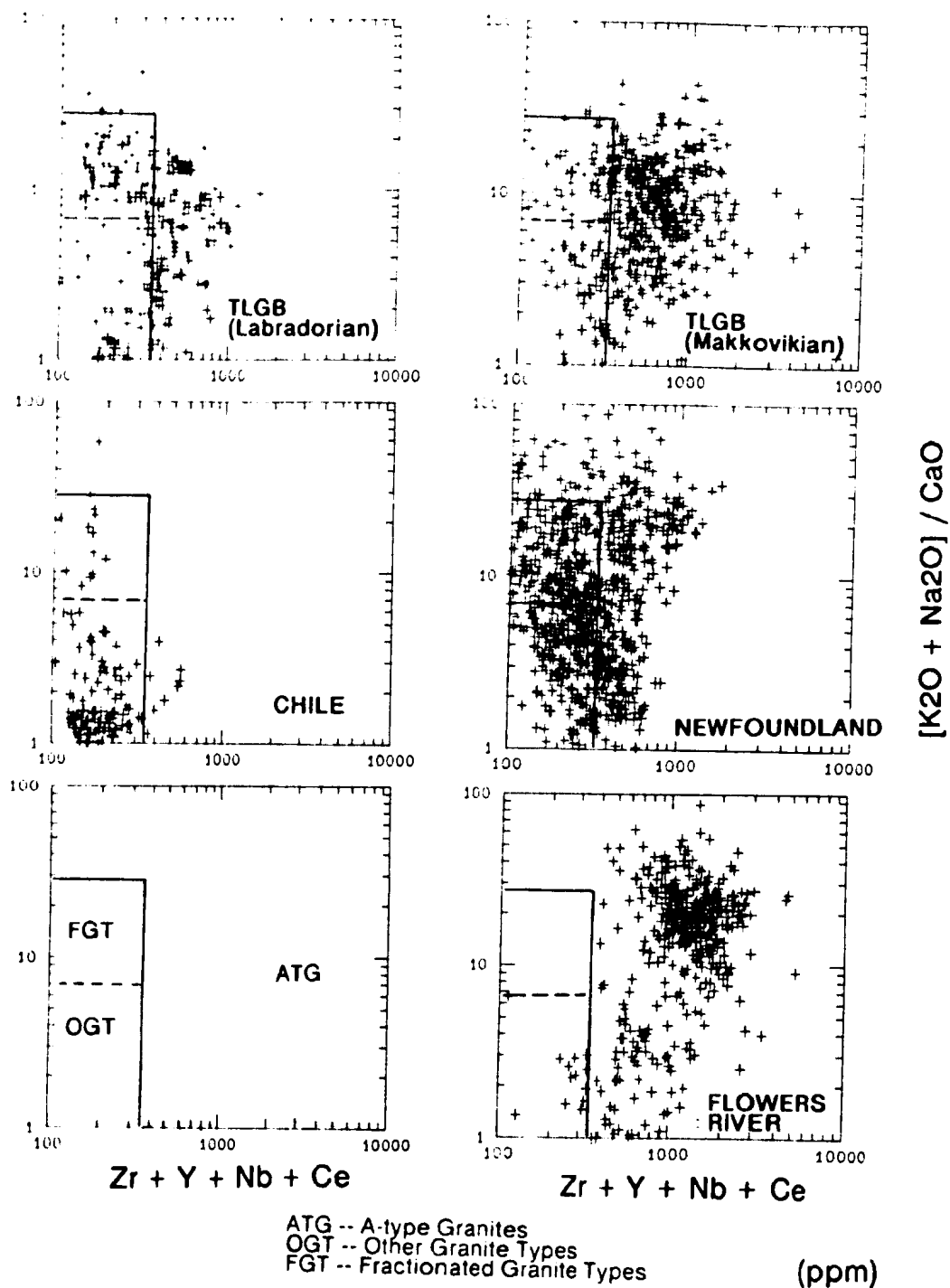


Figure 9.16b.  $[(K_2O + Na_2O) / CaO] - [Zr + Y + Nb + Ce]$  discrimination diagrams (after Whalen et al., 1987) for TLGB and comparative assemblages.

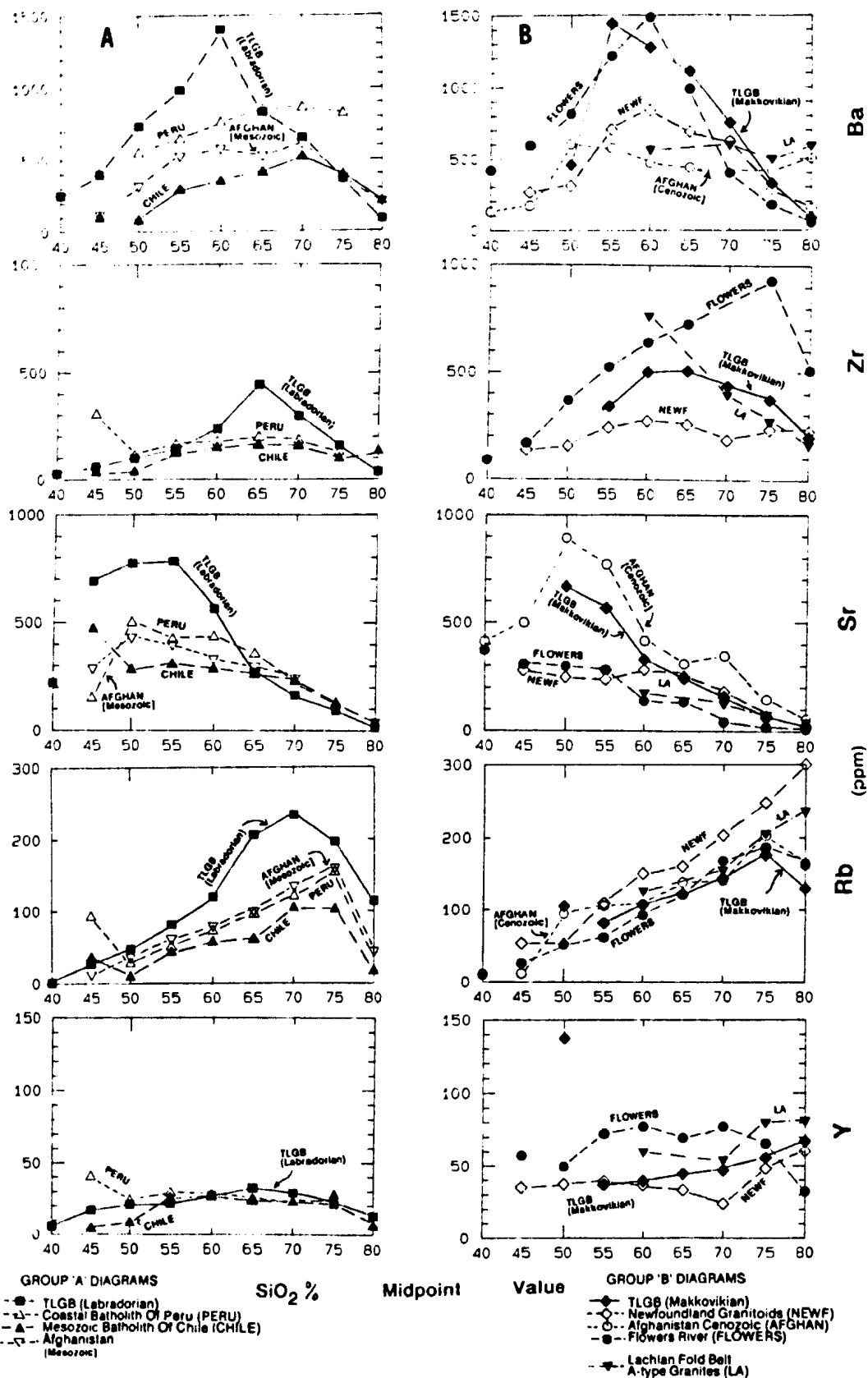
discrimination, but classifies Makkovikian and Flowers River assemblages as A-type granites. The definition and significance of so-called "A-type" granites is a subject of discussion (e.g. Whalen et al., 1987), but there is no doubt that many Makkovikian granitoid rocks belong to this category on the basis of these parameters.

### 9.3.3 Evolutionary Trends

Trace element evolution trends were assessed by aggregating data into 5%  $\text{SiO}_2$  intervals (Figure 9.17), as described above for major elements. Problems caused by outlying data at extreme  $\text{SiO}_2$  contents are more acute for trace elements; this applies particularly to the Makkovikian assemblage at 50%  $\text{SiO}_2$ , which is biased by two cumulate rocks with very high Zr, Y and REE reflecting concentration of accessory minerals. These aberrant points have been ignored in constructing trends.

Ba evolution varies widely. Both Labradorian and Makkovikian assemblages have convex-upward trends reaching peak Ba contents of 1000-1500 ppm Ba at 55-60%  $\text{SiO}_2$ . Arc assemblages have largely incompatible Ba behaviour up to 70-75%  $\text{SiO}_2$ , but variable Ba content at a given  $\text{SiO}_2$  value. Newfoundland and Flowers River assemblages both show inversion of Ba behaviour at ca. 60%  $\text{SiO}_2$ , similar to the TLGB trends. This contrast reflects the "early" fractionation of K-feldspar in these potassic suites compared to the relatively sodic arc assemblages.

Sr trends in arc assemblages are remarkably similar. Both TLGB assemblages are enriched in Sr below 60%  $\text{SiO}_2$  compared to all other areas, except Afghanistan Cenozoic granites. Both Ba and Sr are sensitive to changes in feldspar stability, which depend on a variety of factors,



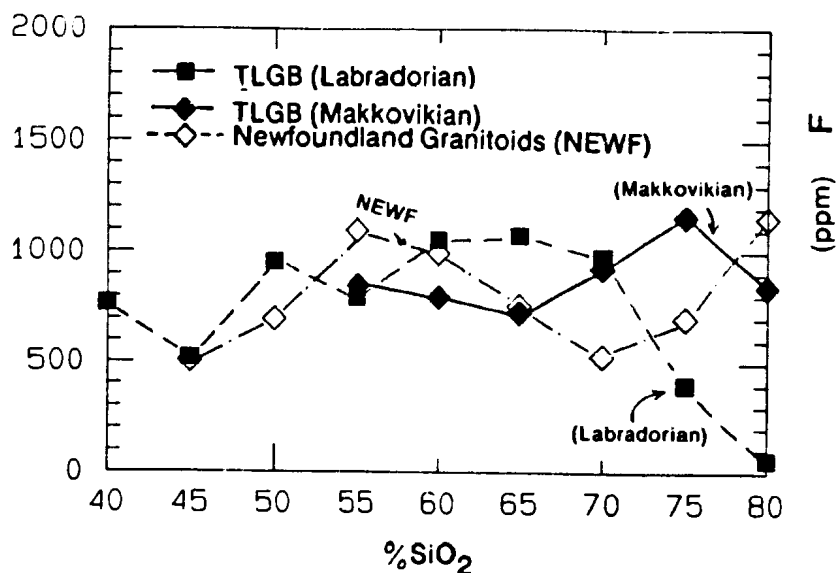


Figure 9.17 (continued) . Fluorine (F) evolution trends for TLGB and Newfoundland assemblages

including pressure and H<sub>2</sub>O content. Although absolute values vary widely, the contrasting trends appear to be viable discrimination methods. Despite its use in discrimination plots (e.g. Figure 9.14), Rb shows little systematic variation between assemblages.

Zr and Y trends amplify contrasts noted in frequency spectra and discrimination diagrams (see above). Flowers River is strongly enriched at all SiO<sub>2</sub> contents; lesser enrichment is shown by the Makkovikian assemblage. Similar patterns are shown by Zn and REE (not figured). The Labradorian trend is similar to arc assemblages, except for a Zr peak at 65% SiO<sub>2</sub> that represents part of the Mount Benedict Intrusive Suite. Note the similarity between A-type granites of the Lachlan fold belt and parts of the Makkovikian assemblage.

The Makkovikian assemblage shows strong F enrichment above 70% SiO<sub>2</sub> compared to the Labradorian and Newfoundland assemblages (Figure 9.17). Depletion of F is evident amongst Labradorian high-SiO<sub>2</sub> granites compared to their Makkovikian counterparts.

## 9.4 SUMMARY and DISCUSSION

### 9.4.1 Evaluation of Geochemical Discrimination Methods

Frequency spectra for major element parameters such as  $\text{SiO}_2$ , TTDI, F/F+M, N/N+K, Agpaitic Index and A/C+N+K, discriminate volcanic-arc, collision-zone and within-plate settings effectively (Figures 9.6; 9.7). Martin and Piwinski (1972) and Petro et al. (1979) previously suggested that "compressional" and "extensional" environments could be discriminated via  $\text{SiO}_2$  or TTDI spectra. It is suggested here that different types of "compressional" environment may also be resolved effectively by use of a wider range of parameters.

Frequency spectra for trace elements are less effective in dividing the compressional assemblages into arc and collisional environments. However, several elements, in particular Zr, Y and Zn, and the ratios Zr/Rb and Ga/Al, characterize within-plate granites of the Flowers River assemblage very clearly (Figure 9.13). The contrasting behaviour of Ba with differentiation appears to be the most consistent trace element parameter for distinction of arc and collisional assemblages.

Trace element discrimination diagrams suggested by Pearce et al. (1984) also distinguish arc and within-plate assemblages well, but encounter problems with the Newfoundland assemblage. They also simplify relationships, e.g. by suggesting a much closer affinity between the Makkovikian and Flowers River assemblage than indicated by spectral comparisons (see below). They are certainly useful, but are best used in combination with other types of data that emphasize extensive parameters.

A criticism that may be levelled at all empirical comparisons is that reference databases may not be truly representative of a specific environment. This is most acute for within-plate assemblages, represented here by only one database of Proterozoic, rather than Phanerozoic age. However, where environments are duplicated, as in arc assemblages, frequency spectra are internally consistent (Figures 9.6; 9.7; 9.13).

A second problem exists with respect to space - time - composition trends in arc environments (Brown, 1981; Brown et al., 1984), which migrate to siliceous, potassic compositions with age (maturity) and distance from the locus of subduction, and possibly in response to changes in subduction angle (e.g. Pankhurst et al., 1988). The Andean-Cordilleran arc assemblages used in this study are located close to subduction zones, and probably do not represent the full range of arc compositions. The generally more evolved composition of the Afghanistan (Mesozoic) assemblage relative to Peru and Chile (Figures 9.6; 9.7) may reflect preservation of both proximal and distal arc granitoids in Afghanistan, where these batholiths have been deformed and presumably telescoped. Such considerations are particularly important in interpretation of the Labradorian assemblage (see below).

Variations in the fourth dimension may be equally significant in assessing collisional zone magmatism. In the Appalachians, magmatism continued for up to 100 Ma after the Taconic orogeny (Colmann-Sadd, 1982; Williams et al., 1989; Figure 9.4). In the Himalayas, collision occurred a mere 50 Ma ago, and it is probable that some post-collisional suites are not yet generated or emplaced or exposed. There are also significant differences in erosion level between recent and ancient collisional belts, which complicate direct comparisons between them.

#### 9.4.2 Geochemical Affinity of the Makkovikian Assemblage

##### Major Element Characteristics

The Makkovikian assemblage shows a number of distinct features. The most important of these are generally high  $\text{SiO}_2$  and (particularly) TTDI values, indicating evolved compositions, depletion in CaO and MgO, high K+N/A and F/F+M indices at all  $\text{SiO}_2$  contents, and a notable absence of peraluminous compositions. Comparative frequency spectra (Figures 9.6; 9.7) illustrate these characteristics well, and set the Makkovikian assemblage apart from comparative assemblages, with which there is no exact correspondance.

It is clear, however, that there are fundamental contrasts between these rocks and volcanic arc assemblages, as represented by data from California, Chile and Peru. The latter are dominated by intermediate  $\text{SiO}_2$  contents, show much higher CaO and MgO and, most importantly, have low N/N+K and K+N/A indices that emphasize their relatively sodic and alkali-depleted compositions.

There is a much closer affinity between the Makkovikian assemblage and post-orogenic, broadly "collisional" assemblages from Afghanistan and (particularly) Newfoundland. Frequency spectra for  $\text{SiO}_2$ , MgO, CaO, TTDI and N/N+K are similar for all three assemblages. There are, however, contrasts in K+N/A, A/C+N+K and F/F+M frequency spectra and trends. The Makkovikian assemblage has higher K+N/A and F/F+M at all  $\text{SiO}_2$  contents, indicating a tendency towards agpaitic and Fe-enriched behaviour during evolution. It also has very few peraluminous compositions compared to Newfoundland and (particularly) Afghanistan assemblages, and shows a quartz-poor evolution trend characterized by the presence of monzonite and syenite.

Within-plate assemblages (represented here by Flowers River) show extremely agpaitic and Fe-enriched tendencies, and are of much more restricted composition than the Makkovikian assemblage. Nevertheless, the Makkovikian assemblage has some affinity to them.

In summary, the Makkovikian assemblage most closely resembles the Newfoundland assemblage, but is transitional towards the agpaitic and alkalic granitoid rocks of Flowers River. This is shown well by evolution trends (Figures 9.10; 9.11) where the Makkovikian trend lies between the Newfoundland and Flowers River trends for most parameters.

#### Trace Element Characteristics

V, Rb and Ba frequency spectra, and Ba evolutionary trends, suggest contrasts between the Makkovikian and volcanic arc assemblages, but show greater overlap than major element parameters. Zr, Ce, Zr/Rb and Ga/Al frequency spectra illustrate the distinctive character of the Flowers River assemblage, which is enriched in all these parameters. In general, there is a very good correspondence between the Makkovikian and Newfoundland assemblages. However, the former shows some relative enrichment in Zr, Ce and Y, but falls well short of the strongly enriched Flowers River assemblage. Such characteristics are in agreement with the transitional major element characteristics noted above.

Trace element discrimination diagrams demonstrate clear contrasts with volcanic-arc assemblages, and suggest a general affinity to within-plate granitoid suites. The similarity to the Newfoundland assemblage is maintained, but Makkovikian granites are more strongly biased towards the within-plate field. The Makkovikian assemblage also



corresponds in part to "A-type" granite suites, as defined by Collins et al.(1982) and Whalen et al.(1987), although it does not show the strong HFS element, REE and Ga enrichment of Flowers River, also clearly of A-type affinity. Evolutionary trends resemble those of A-type granites from the Lachlan fold belt in Australia.

### Conclusions

The Makkovikian assemblage is best described as transitional between collisional and within-plate assemblages, as represented here by Newfoundland and Flowers River respectively. Some discrimination diagrams indicate a strong affinity to the latter, but this is misleading, as its extreme trace element compositions are rarely observed in Makkovikian granites. Major and trace element frequency spectra closely resemble Newfoundland, with the exception of F/F+M, A/C+N+K and K+N/A (see below).

The temporal setting of the Makkovikian assemblage is also consistent with the syn- to post-orogenic environment of the Newfoundland assemblage. Post-tectonic Makkovikian granites were emplaced within a 50-80 Ma\* period following final deformational events, a period of time that is similar to the 100 Ma (Silurian to Carboniferous) duration of post-Taconic Appalachian plutonism.

The systematic differences between the Makkovikian assemblage and this possible Phanerozoic analogue must, however, be explained in any model of their development.

---

\* NOTE : The ca. 1720 Ma U-Pb age for the Cape Strawberry Granite obtained just prior to submission (Krogh et al., in prep.) indicates that Makkovikian plutonism continued for at least 80 Ma after final deformation.

Agpaitic and Fe-enriched tendencies may indicate different source materials and/or different conditions in their environment of generation. Granites of "supracrustal" or S-type affinity, widely viewed as derivatives of sedimentary rocks, are noticeably absent from the Makkovikian assemblage. Such absence may indicate an absence of such sources, which has obvious implications for plate tectonic models involving destruction of oceanic basins and attendant sedimentary basins. These problems, and possible models, are discussed in Chapter 10.

#### 9.4.3 Geochemical Affinity Of The Labradorian Assemblage

##### **Major Element Characteristics**

The Labradorian assemblage has expanded  $\text{SiO}_2$ , TTDI and major element spectra that resemble (in terms of range) arc assemblages from Peru and Chile. The Labradorian assemblage, however, is bimodal, and includes few rocks in the 55% to 67%  $\text{SiO}_2$  range typical of these volcanic arcs. Most major element frequency spectra indicate a relative bias towards silicic, potassic compositions. The Labradorian assemblage also has a quartz-poor differentiation trend, and relatively high F/F+M and agpaitic index values (at high  $\text{SiO}_2$ ); such features partly resemble the Makkovikian assemblage.

##### **Trace Element Characteristics**

Bimodal major element compositional spectra have widely been proposed as hallmarks of anorogenic or within-plate magmatism (e.g. Martin and Piwinski, 1972; Petro et al., 1979). However, trace element frequency spectra suggest no

affinity between Labradorian granites and those from Flowers River. Most resemble spectra from volcanic-arc suites such as Peru or Chile, although some also resemble Newfoundland. Granitoid rocks with enhanced levels of Zr, Y and REE (typical of the Flowers River and, to a lesser extent, Makkovikian assemblages) are not abundant.

An affinity to some arc assemblages is also suggested by discrimination diagrams, where the Labradorian assemblage lies mostly within the VAG (volcanic-arc granite) field of Pearce et al. (1984). In the terminology of Brown et al. (1984), the Labradorian assemblage lies at the "mature" end of the arc compositional spectrum. Relatively few Labradorian granites qualify as within-plate or A-type granites.

#### **Affinity Of Labradorian Mafic and Intermediate Rocks**

Labradorian granitic (s.s.) rocks could belong to any of the comparative assemblages (except Flowers River), and plot essentially at the triple point in trace element discrimination diagrams of Pearce et al. (1984). Mafic and intermediate rocks, however, generally have simpler differentiation histories than felsic intrusive rocks, and are thus more likely to preserve original geochemical contrasts (e.g. Pearce and Cann, 1973; Brown et al., 1984). Labradorian mafic-intermediate rocks are here defined simply as those with  $< 60\% \text{ SiO}_2$ .

Alkali-silica relationships (Figure 9.18a,b) and mean compositions (Table 5.5, p.231-232) indicate that these rocks correspond broadly to "shoshonites", and are enriched in  $\text{K}_2\text{O}$  relative to "normal" calc-alkaline compositions of similar  $\text{SiO}_2$  content. A few fall within the field of alkaline volcanic rocks (Irvine and Baragar, 1971).

SHO - Shoshonites (Morrison, 1980)  
ALK - Alkaline Basalts (Irvine and Baragar, 1971)

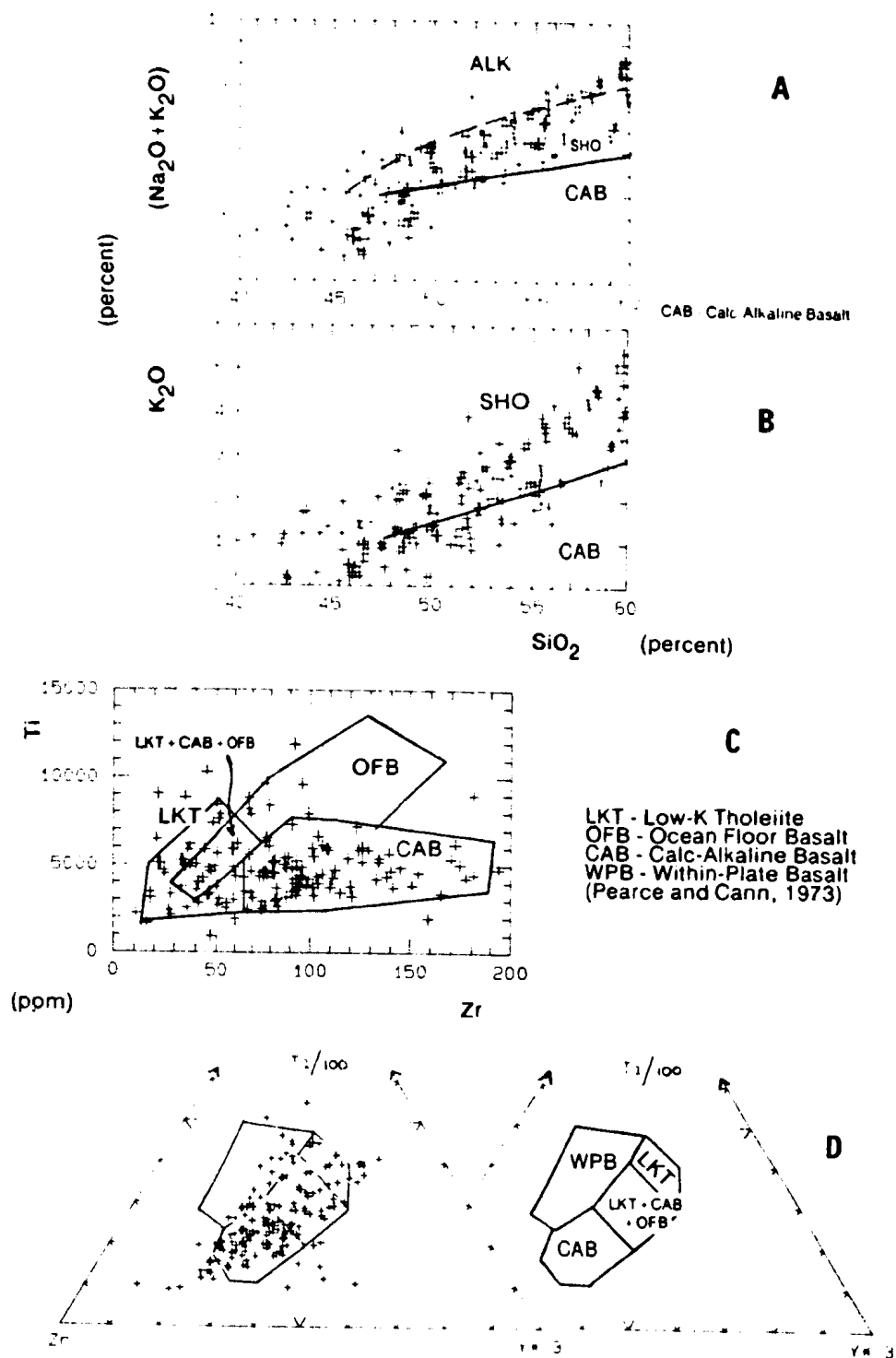


Figure 9.18. Characteristics of Labradorian mafic and intermediate intrusive rocks. (a)  $(\text{Na}_2\text{O} + \text{K}_2\text{O})$  -  $\text{SiO}_2$  diagram. (b)  $\text{K}_2\text{O}$  -  $\text{SiO}_2$  diagram. Field boundaries from Irvine and Baragar (1971) and Morrison (1980). (c) Ti-Zr diagram. (d)  $\text{Ti}/100$  -  $\text{Y} \times 3$  diagram. Field boundaries from Pearce and Cann (1973).

Trace element discrimination diagrams (Figure 9.18c,d) place Labradorian mafic rocks within LKT (Low-K tholeiite, typical of island arcs) and CAB (calc-alkaline basalt) fields (Pearce and Cann, 1973). A few are transitional to the WPB (within-plate basalt) field.

### Discussion and Conclusions

Previous studies of Labradorian volcanic rocks (Ryan, 1984; Ryan et al., 1987) did not reach any firm conclusions regarding tectonic setting. Problems in classification remain partly unresolved, and the following discussion echoes some of their suggestions and viewpoints.

An anorogenic, within-plate setting is partially supported by bimodal  $\text{SiO}_2$  and TTDI frequency spectra, and relatively high  $\text{F}/\text{F}+\text{M}$  and  $\text{K}+\text{N}/\text{A}$  in some granitic rocks (e.g. Martin and Piwinski, 1972; Petro et al., 1979). However, distinctive trace element patterns typical of granites in such settings (Anderson, 1983; Pearce et al., 1984) are absent. Also, although there is no evidence of orogeny in the study area, Labradorian deformation and metamorphism was widespread to the south (Wardle et al., 1986), and may be directly or indirectly connected to magmatism.

A second possibility is a distal ("mature") arc setting analogous to bimodal basalt-trachyte volcanism east of the main Andean volcanic arc or Cenozoic volcanism in the western U.S.A. Calc-alkaline to shoshonitic mafic rocks are important components of such mature arc assemblages (Morrison, 1980; Brown et al., 1984; Munoz and Stern, 1989). Labradorian granitoid rocks have more evolved compositions than proximal arc assemblages (e.g. Peru, Chile), which is consistent with a distal location. The

absence of regional Labradorian deformation in the study area may thus be a consequence of its position relative to active subduction.

A post-collisional setting is also possible, as potassic magmatism in such settings overlaps geochemically with the magmas of mature arcs (e.g. Pearce et al., 1984; Brown et al., 1984). The 150 Ma interval between the Makkovikian orogeny and Labradorian magmatism argues against a post-orogenic relationship to this event, but the ca. 1650 Ma deformation and high-grade metamorphism south of the Grenville Front Zone (Wardle et al., 1986) may record a collisional event outside the study area.

It is difficult to choose between the latter two alternatives. Labradorian igneous rocks in the study area are at the northern fringe of a much wider magmatic province, probably do not record the full range of compositions in this belt. This difficulty may be resolvable via scrutiny of Labradorian granitoid rocks within the high-grade terranes, particularly in terms of their transverse compositional variations. The presence of unidirectional compositional and isotopic trends, as described by Brown (1981) and Brown et al. (1984) would support a "mature-arc" tectonic setting.

This uncertainty does not, however, dissuade the author from speculation in Chapter 10.

## CHAPTER TEN

# MAGMATISM AND CRUSTAL EVOLUTION IN THE MAKKOVIK PROVINCE

---

### Chapter Abstract

It is suggested that most Makkovikian magmas were generated as part of a complex syn- to post-orogenic process involving the emplacement of anhydrous, mantle-derived, mafic magmas into intermediate rocks of Archean and slightly older Proterozoic sialic crust. This interaction took place via coupled assimilation-fractional crystallization, and generation of and mixing with crustal anatexic melts. Anatexis took place under conditions where zircon and accessory phases were unstable. This is not compatible with the prevalent model for generation of other similar "A-type" granites, which invokes anatexis of previously dehydrated and melted lower crustal rocks. However, material of this type may have contributed to magma genesis.

As a consequence of greater heat production in the Early Proterozoic Earth, mantle-derived magmas may have been high-temperature, high-Mg liquids of komatiitic affinity, which have enormous capacity for direct assimilation and thermal transfer. The transitional "anorogenic" affinity of the Makkovikian assemblage (and other Proterozoic granitoid suites) may thus be a consequence of the volume and characteristics of this subcrustal magma flux, rather than any one specific crustal source. In younger environments, such conditions only occur in zones of exceptionally high heat flow, such as rift zones related to thermal plumes in the mantle.

Labradorian magmatism is more difficult to model. A generally similar mantle-crust interaction model is proposed, but it is suggested that cooler, wetter, mantle-derived mafic magmas were generated by hydrous melting of peridotite, and thus had significantly less capacity for assimilation and thermal transfer. It is suggested that such magmas were generated by addition of volatiles (and recycled crustal material) to the mantle wedge overlying a subduction zone. Labradorian granites (s.s.) were probably generated by melting of Makkovikian lower crust with varied Nd isotopic characteristics under less extreme conditions, where zircon and refractory phases remained stable.

The presence of mantle-derived material in virtually all Makkovikia, and some Labradorian magmas supports the importance of Early Proterozoic crustal growth, as documented by other studies of the Northern Hemisphere American Precambrian. In this

case, however, at least some of this growth occurred in a post-orogenic setting with many characteristics of "anorogenic" magmatism. In addition to adding to the crust, these events contributed to the gross compositional stratification that appears to discriminate Proterozoic domains from undisturbed Archean cratons.

A model is proposed where juvenile terranes generated in ensimatic arc environments were accreted to the margin of the North Atlantic Craton. The insulating effects of newly accreted crust induced melting of the subjacent mantle, and underplating of the crust by mantle-derived mafic magmas. This model resembles several recent proposals for Precambrian and Phanerozoic magmas of similar affinity. This protracted Makkovikian magmatism was followed by the establishment of a new northward-dipping subduction zone, of which Labradorian magmatism was a distal manifestation. A possible younger analogue to these events took place on the South American margin of Gondwanaland, where Andean arc magmatism is partly superimposed on Late Paleozoic to Early Mesozoic post-orogenic to "anorogenic" plutonism. The latter was the final stage in the assembly of Gondwanaland, an event that resembles the Proterozoic assembly of proto-Laurentia recently proposed by Paul Hoffman.

On a broader scale, this model is consistent with recent speculation concerning cyclic patterns in orogenic history, that propose aggregation of continental plates over mantle downwellings, followed by insulation of subjacent mantle, thermal upwelling (leading to anorogenic magmatism) and (eventually) rifting. In a hotter, Proterozoic Earth, the time-lag between continental aggregation and mantle upwelling would be reduced, and conditions analogous to those of "anorogenic" magmatism would prevail in post-orogenic settings. Distinctions between "post-orogenic" and "anorogenic" granitoid magmatism should become increasingly blurred in Early Precambrian orogenic belts, a prediction that is consistent with the transitional affinity of the Makkovikian assemblage, and Early Proterozoic batholiths from other shield areas. Also, growth and vertical reorganization of the continental crust by post-orogenic magmatism may have been proportionally more important in a hotter Earth, particularly during and following periods of continental aggregation. This may (in part) explain the apparently high rates of crustal growth calculated by some workers for this period in Earth history.



## Introduction

It is difficult to concisely summarize and synthesize the varied information discussed in this thesis. The characteristics of specific magmatic assemblages are discussed in the concluding sections of previous chapters and reviewed in individual chapter abstracts. This final chapter is concerned with wider models for Lower Proterozoic magmatism and crustal evolution in the Makkovik Province.

The first two sections examine the petrogenesis of Makkovikian and Labradorian magmatic assemblages. Source materials, source regions and generative mechanisms are evaluated and coordinated into petrogenetic models for each. Some possible younger analogues for the Makkovikian assemblage (in addition to those assessed in Chapter 9) are discussed. The third section presents a model for crustal evolution of the Makkovik Province, that integrates these petrogenetic models and other information in a plate-tectonic framework. Following this model, some speculative discussion concerning the role of Proterozoic magmatism in Earth evolution is presented, drawing upon recent work concerned with long-term cyclic or secular behaviour in tectonic processes.

The final section briefly reviews some avenues of further investigation that could fill gaps remaining in this study, or form future projects in their own right. This is by no means an exhaustive list !

## 10.1 PETROGENESIS OF MAKKOVIKIAN MAGMAS

### Summary of Important Characteristics

The syn- to post-tectonic Makkovikian assemblage is dominated by metaluminous to slightly peralkaline, siliceous, potassic, K-feldspar porphyritic, granite and alkali-feldspar granite, and volcanic equivalents (Chapters 3, 4 and 7). A subordinate (syn-tectonic) association consists of peraluminous granitoid rocks that appear, in some cases, to have been derived by anatexis of local country rocks. Both associations have evolved major element compositions, and the most "mafic" Makkovikian rocks are monzonite and syenite.

The dominant plutonic association shows variably agpaitic behaviour ( $K+N/A = 0.9$  to  $1.05$ ) and Fe-enrichment ( $F/F+M > 0.85$ ). Distinctive trace element features include enrichment in fluorine, HFS elements and REE (3.2, 3.3). These granitoid rocks qualify as "within-plate" or "A-type" granites in popular classifications (Chapter 9), but generally lack the extremely agpaitic compositions associated with peralkaline or undersaturated suites. A comparative analysis indicates that they are transitional in character between the post-orogenic, post-collisional granitoid suites of the Newfoundland Appalachians, and true "anorogenic" suites such as Middle Proterozoic granites in northern Labrador (Chapter 9). They are distinct in all respects from volcanic arc suites such as Andean or Cordilleran batholiths.

Subordinate peraluminous granites have generally low  $\gamma$ , HFS element and REE contents that indicate different sources and/or conditions of generation from the dominant association (3.2, 3.3). These are not strongly aluminous "S-type" granites ( $A/C+N+K > 1.1$ ) in the sense of Chappell

and White (1974), and their peraluminosity is not necessarily indicative of metasedimentary sources, except in the case of the Pitre Lake Granite. As noted in Chapter 9, the Makkovikian assemblage is notably deficient in strongly peraluminous compositions.

### Source Materials and Source Regions

*Isotopic Arguments* : In the west of the area, negative  $\epsilon_{\text{Nd}}^{\text{CHUR}}$  (-3 to -14) unequivocally indicates older crustal material in Makkovikian magmas (8.2.2). However, excluding one anatectic granite, their  $\epsilon_{\text{Nd}}^{\text{CHUR}}$  is too high to permit derivation entirely by melting of 3100 - 2800 Ma old Archean crust, which would have  $\epsilon_{\text{Nd}}^{\text{CHUR}}$  of -12 to -15 at 1800 Ma. Derivation by melting of assorted 2600-2200 Ma old crust is unlikely, as there is little evidence of activity during this period in Labrador. It is therefore concluded that Makkovikian magmas in the west are variable mixtures of juvenile (mantle-derived) material and polycyclic Archean crust (8.3.2).

In the east, positive  $\epsilon_{\text{Nd}}^{\text{CHUR}}$  (+2 to +5), indicates predominantly juvenile sources. Possible "basement" in the east (Cape Harrison Metamorphic Suite) has  $\epsilon_{\text{Nd}}^{\text{CHUR}}$  of +2 to +3, and is thus unlikely to be older than ca. 2100 Ma. The eastern plutons of the Strawberry Intrusive Suite were isotopically identical to postulated depleted mantle at the time of their emplacement. By analogy with compositionally similar granites in the western domain, it is suggested that these eastern domain magmas were also mixtures of mantle and "sialic" crust (8.3.2). However, the sialic crust in the east consists of Proterozoic material, probably no older than 2100 Ma. The Cape Harrison Metamorphic Suite is the best candidate for this older pre-Makkovikian crustal component with a short crustal

residence period. The relative contributions of end-members are difficult to assess in the east, as there is little contrast in their Nd isotopic compositions (8.3.2).

There is clear isotopic evidence of an Archean crustal component in western plutons of the Strawberry Intrusive Suite. The mantle-like  $\epsilon_{\text{Nd}}^{\text{CHUR}}$  of the eastern plutons, however, indicates that any crustal component in them was extremely juvenile, and even the Cape Harrison Suite is unsuitable. A possible solution is that the "crustal" component in these magmas is the "juvenile" component derived from the mantle during slightly earlier Makkovikian magmatism. This is consistent with geochronological data indicating that the Strawberry Intrusive Suite is younger than other Makkovikian granites. (Krogh et al., in prep.)

*Elemental Arguments* : Several elemental geochemical arguments also suggest that Makkovikian magmas contained a mantle-derived component. Monzonite, quartz monzonite and syenite of the Long Island unit and (particularly) the Numok Intrusive Suite are impossible to derive by melting a crustal source of intermediate composition (Wyllie, 1984). These relatively low-SiO<sub>2</sub> rocks have higher Sr and Ba contents than any comparative assemblage (9.3.1, 9.3.3). Such features are inconsistent with partial melting of a feldspar-bearing source, and suggest contributions from mafic magmas derived from the mantle, where partial melting and subsequent fractionation would act to enrich both Ba and Sr.

As a counter argument, many Makkovikian granites are close to ternary minimum compositions in the granite system (Figure 3.6, p.81; Figure 4.5, p.136) and could be derived by crustal anatexis. Their evolutionary trends, however, lie close to the plagioclase - K-feldspar cotectic surface, indicating that at least some evolved to eutectic

compositions via fractional crystallization. Trace element trends in most units are consistent with evolution by plagioclase and K-feldspar ( $\pm$  mafic mineral) fractionation, which also suggests a non-eutectic parental magma composition, possibly monzonitic to syenitic. Such features argue against wholly crustal sources for Makkovikian granites, although they may have partly originated in the crust.

HFS element and REE enrichment in Makkovikian magmas (3.2; 4.2) indicate that zircon, sphene and other accessory minerals were not present as residual material in their sources. This is consistent with a significant mantle-derived component and/or breakdown of these phases during crustal anatexis. The latter probably requires high temperatures, in excess of 850°C (e.g. Whitney, 1988; Clemens et al., 1986), but may also be facilitated by fluorine, which encourages complexing of HFS elements and REE (Harris and Marriner, 1980; Collins et al., 1982; Whalen et al., 1987). Halogens may be introduced as a volatile flux associated with a mantle-derived component (e.g. Harris and Marriner, 1980), or released by hornblende breakdown, which also requires high temperatures (Wyllie, 1984; Whitney, 1988). The presence of fluorine during subsequent high-level fractional crystallization would also inhibit accessory mineral crystallization, leading to HFS element and REE enrichment.

#### **Petrogenetic Model -- General Features**

It is proposed that most Makkovikian magmas were generated by thermal and chemical interaction between anhydrous, mantle-derived, mafic magmas and lower crustal rocks of generally intermediate composition (Figure 10.1). Similar models have been proposed elsewhere (Barker et al., 1975; Hildreth, 1981; Fyfe, 1988; Hildreth and Moorbath,

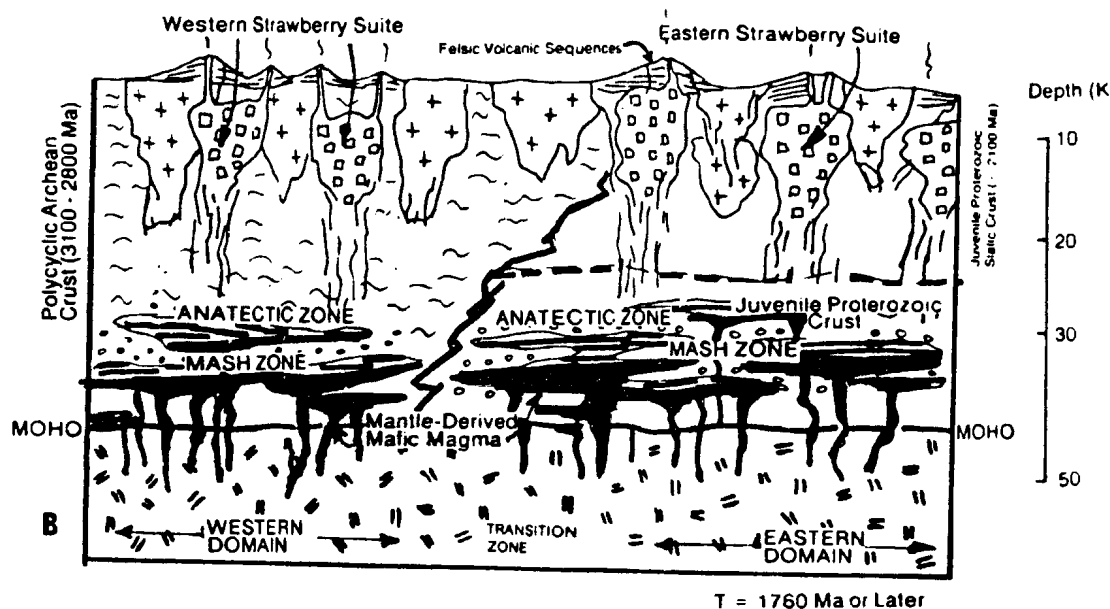
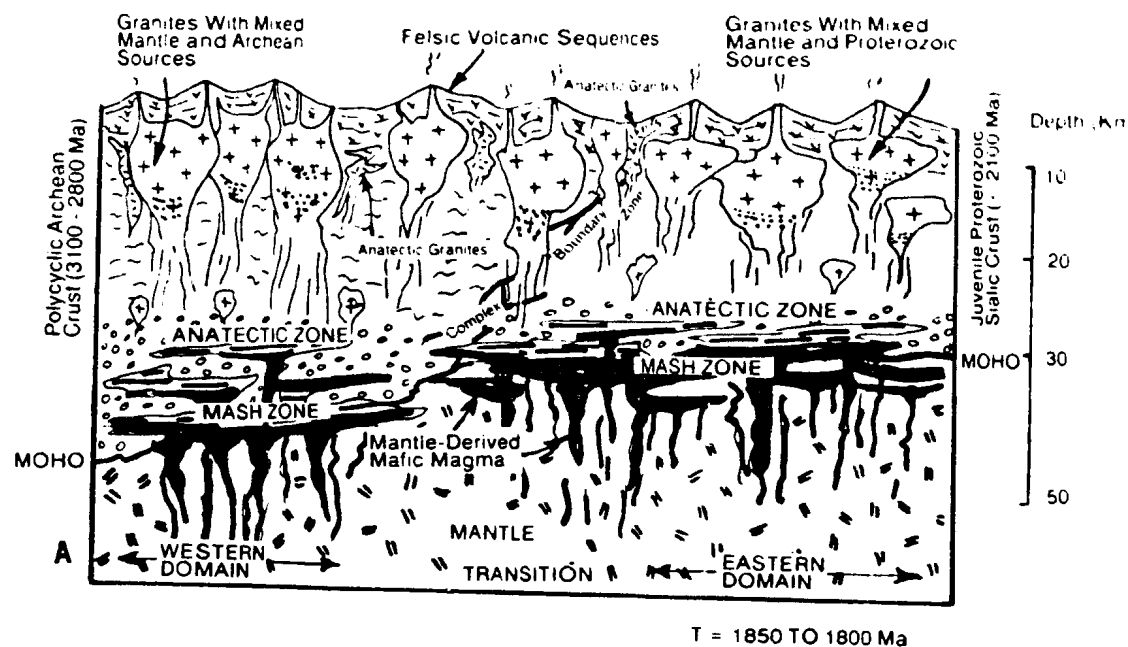


Figure 10.1. A generalized, schematic model for the petrogenesis of Makovikian magmas. (a) relatively early stages, in which juvenile crust of the eastern zone is extensively thickened. (b) later stages, corresponding to emplacement of the Strawberry Intrusive Suite. Not that depth scales are entirely hypothetical, and approximate. See text for discussion of details.

1988; Whitney, 1988), and are increasingly viewed as a general mechanism for granite generation in all continental environments.

The model presented here is influenced by Hildreth and Moorbath (1988), who suggest that mantle-derived mafic liquids solidify at or near the crust-mantle boundary, where their crystallization releases energy. These dense magmas are "stalled" in the lower crust, where they assimilate crustal rocks and mix with melts derived from such sources. The continental crust acts as a density filter (c.f. Fyfe, 1988), that impedes further ascent of magmas until compositions evolve to suitably low densities. Increased ductility and plasticity of partially molten lower crust also provides a physical barrier to the ascent of the mafic magmas.

Hildreth and Moorbath (1988) coin the acronym MASH zone (Melting, Assimilation, Storage and Homogenization zone) to describe this process. "Base-level" geochemical and isotopic signatures are established in the MASH zone as a function of the rate and characteristics of subcrustal magma flux, and composition and thickness of overlying crust. Magmas that ascend from the MASH zone undergo further modification by combined assimilation - fractional crystallization (DePaolo, 1981a) at intermediate and upper crustal levels.

The east-west contrast of initial Nd isotopic compositions observed in Makkovikian rocks illustrates the influence of the local lower crust on base-level Nd isotopic signatures developed in the MASH zone. The base-level elemental signature, however, appears constant in both domains, indicating that other factors (e.g. bulk compositions, rate of transfer) were generally similar.

In the eastern domain, the Nd isotopic characteristics of crustal contributors changed with time. Initially, the

MASH zone was established in slightly older Proterozoic crust, such as the Cape Harrison Metamorphic Suite. During emplacement of the Strawberry Intrusive Suite at ca. 1760 Ma or later, the MASH zone was situated at levels of the crust occupied by juvenile rocks emplaced during previous magmatic episodes, and "crustal" contributions came instead from this material (Figure 10.1b).

This implies thickening of the eastern domain crust via underplating of juvenile material. The greater preservation of volcanic sequences in the western domain, and isotopic evidence for Archean material in western Strawberry Suite magmas, suggests that the western domain was not thickened and uplifted to the same degree, and that its MASH zone remained fixed in Archean lower crust throughout.

Minor syn-tectonic peraluminous granites of the Makkovikian assemblage are interpreted as products of localized anatexis in specific units (e.g. Pitre Lake Granite; Brumwater Granite) or crustal melts that escaped from the upper part of the MASH zone without encountering juvenile material (Figure 10.1a). The Manak Island Granitoid (3.1.6), which is closely similar in composition to the Brumwater Granite, is a possible example of an anatectic granite derived entirely from the juvenile Proterozoic crust of the eastern domain.

#### **Petrogenetic Model -- Some Special Features**

It is relevant to consider some consequences of a significantly hotter Earth in early Proterozoic times. Komatiites (ultramafic lava) and komatiitic basalts of Archean and Early Proterozoic terranes (e.g. Bickle, 1982; Hynes and Francis, 1982) probably reflect extensive mantle melting due to higher thermal gradients, and have high (up to 1600°C) liquidus temperatures. High-Mg magmas of this



general affinity have important implications for the ultimate products of the MASH process. Sparks (1986) concludes that they have enormous capacities for thermal transfer and energy release, as a consequence of high liquidus temperatures and the large heat of fusion of olivine, and have great capacities for assimilation and melting of crustal rocks. Such magmas will evolve initially via olivine fractionation, which could produce the Fe-enrichment trends typical of Makkovikian (and other Proterozoic) granitoid suites.

It is therefore suggested, after Sparks (1986), that Makkovikian parental magmas were potassic, alkali-rich, iron-enriched, intermediate magmas generated by interaction and mixing of (fractionated) high-Mg mafic magma and lower crustal material. The energy released by olivine crystallization provided the high temperatures required to break down hornblende and refractory accessory minerals in the lower crust. Source materials were probably complex in detail, as high-Mg mafic magmas can also assimilate or partially melt mafic compositions, including their own differentiates (Sparks, 1986). "Zone refining" (e.g. O'Hara, 1977) processes may thus also contribute to incompatible element enrichment.

#### **Implications For The Origin Of "A-type" Granites**

The Kennedy Mountain, Strawberry and Lanceground Intrusive Suites are "A-type" or "within-plate" granites according to most criteria (Chapter 2). A popular model for generation of such magmas involves melting of felsic, granulite-facies, gneisses ("restite") from which anatectic melts have previously been extracted (Collins et al., 1982; Whalen et al., 1987). This premise has rarely been investigated using Nd isotopes.

The "restite" model is incompatible with isotopic data from these rocks, which indicate mixing of mantle and crustal materials, particularly in the western domain (8.2.2). The negligible residence period of any crustal component in the eastern Strawberry Suite also argues against a complex polymetamorphic history. Data from these eastern plutons suggest that some A-type granites are derived entirely from mantle-like sources, although this is probably not a single-stage process (see above).

Nd isotopic data reported here are consistent with an earlier model (Barker et al., 1975), that invoked interaction of mafic magmas and lower crustal rocks. The requirement for prior anatexis in the sources for A-type granites has also been questioned elsewhere (e.g. Anderson, 1983; Kay et al., 1989; Sylvester, 1989). As outlined above, the distinctive characteristics of these rocks may be controlled by the nature of the subcrustal magma flux, rather than by specific sources within the crust.

#### **Two Younger Analogues of The Makkovikian Assemblage**

Chapter 9 documents similarities between Makkovikian and Newfoundland granitoid assemblages, but also points out important differences. This section refers briefly to two other possible analogues that have influenced tectonic models presented below. Rapela and Kay (1988) and Kay et al. (1989) draw parallels between Permian to Jurassic felsic magmatism in southern South America and anorogenic magmatism in North America described by Anderson (1983). The South American provinces are dominated by fluorine-rich, "A-type" granites and rhyolites, that appear compositionally similar (on the basis of limited geochemical data) to the Makkovikian assemblage. They formed over a 100 to 150 Ma period of magmatism that

followed accretion of juvenile terranes of island-arc or microcontinental affinity to the margin of Gondwanaland. Kay et al.(1989) propose that juvenile Paleozoic crust was underplated and melted by mantle-derived mafic magmas, in a similar manner to the above model. This area is also particularly interesting in view of spatial and temporal relationships to younger Andean magmatism, and assembly of the Gondwanaland supercontinent (see below).

A Late Proterozoic to Early Paleozoic analogue of the Makkovik Province may exist in the "Pan-African" mobile belt of the Arabian Shield (Duyverman et al., 1982; Jackson et al., 1984; Stoesser, 1986). This is regarded as the prime example of a Late Proterozoic Wilson cycle, and includes ophiolitic belts (Pallister et al., 1987). Voluminous, post-orogenic, granitoid rocks, many of which have "A-type" affinities, were emplaced over 100 - 150 Ma following postulated accretion of juvenile volcanoplutonic terranes interpreted as fossil island arcs (Stoesser and Camp, 1985). The youngest rocks are fluorine-enriched, variably peralkaline, mineralized, high-level, granite ring-complexes of classic "anorogenic" type.

Jackson et al.(1984) and Jackson (1986) proposed that these suites were generated by fusion of newly accreted crust, in response to thermal input from the mantle. Although mantle sources are not specified, it is difficult to envisage thermal transfer that is unaccompanied by mass transfer, and consequent geochemical interaction.

## **10.2 PETROGENESIS OF LABRADORIAN MAGMAS**

### **Summary of Important Characteristics**

The Labradorian assemblage comprises a bimodal association of gabbro-diorite-monzonite-syenite suites

(derived by fractionation of mafic magmas), and assorted siliceous, generally leucocratic granitoid rocks (Chapter 5). These magmas were emplaced, at least in the study area, under passive tectonic conditions. The mafic rocks are of high-potassium, calc-alkaline to shoshonitic affinity; their felsic differentiates have strong incompatible LFS element enrichment as a consequence of protracted fractionation (5.3).

Labradorian granitoid rocks without mafic parental suites have weakly peraluminous compositions, and generally low levels of fluorine, HFS elements and REE, compared to most Makkovikian granitoid rocks. However, they resemble some of the minor, peraluminous, syn-tectonic units of the Makkovikian assemblage.

A comparative analysis of the Labradorian assemblage (Chapter 9) is difficult, probably because these rocks are a small portion of a much wider belt, and may not be fully representative of it. Possible analogues include bimodal, potassic volcanism in distal arc settings (e.g. Brown et al., 1984; Munoz and Stern, 1989) or post-collisional environments (e.g. Sloman, 1989). The former alternative is preferred, mostly on isotopic grounds (8.3.3).

#### Source Materials and Source Regions

Nd data provide no evidence for depleted mantle sources. Melanocratic, olivine-bearing mafic rocks have  $\epsilon_{Nd}^{CHUR}$  of ca. +1, well below postulated values (ca. +5 to +6) for a depleted mantle reservoir at 1650 Ma (8.2.2).

Most other Labradorian rocks have similarly neutral isotopic signatures. Excluding the Witchdoctor and Burnt Lake Granites, and a (probably contaminated) gabbro in the extreme west, all have  $\epsilon_{Nd}^{CHUR}$  of +1 to -2, regardless of composition or geographic location. It is concluded that,

although some Labradorian granites (s.s) could be derived by anatexis of Makkovikian crust, Labradorian mafic magmas are mixtures of mantle and crustal materials (8.3.3). It is suggested that mixing took place in a subcrustal environment, and not via assimilation and melting of local lower crust, although some contamination effects are seen in the Mount Benedict Suite.

By analogy with modern arc magmas (White and Patchett, 1984) and Nd studies of other Proterozoic calc-alkaline granitoid assemblages (Patchett and Bridgwater, 1984; Patchett and Kouvo, 1986), it is concluded that crustal material may have been introduced to the mantle by subduction of continent-derived sediment (see 8.3.3). The H<sub>2</sub>O-rich nature of the Adlavik Intrusive Suite is also consistent with this mechanism. Parental magmas to the mafic-parent suites possibly originated via hydrous melting of the mantle wedge overlying a subduction zone, initiated by volatiles and silicic magma derived from the subducted slab and sediments (Wyllie, 1984; Tatsumi, 1989).

Labradorian granitoid rocks without mafic parental magmas present a more difficult problem. Their elemental geochemical features are consistent with derivation by melting of crustal material under moderate (650-750°C) conditions, probably as a consequence of biotite breakdown (c.f. Whitney, 1988). Low HFS and REE contents indicate stable zircon and/or sphene in their source regions, which is also consistent with relatively low temperatures. The central problem is the identity of a crustal source, especially in the western domain, where most crustal rocks probably had negative  $\epsilon_{Nd}^{CHUR}$  at 1650 Ma, based on the observed features of Makkovikian suites. The Witchdoctor and Burnt Lake Granites could be derived from such a source, but other Labradorian granitoids require a more juvenile source, possibly material underplated to the western domain during Makkovikian magmatism.

### Petrogenetic Models

A model for Labradorian magma genesis (Figure 10.2) is, in general terms, a MASH hypothesis (after Hildreth and Moorbath, 1988). The subcrustal magma flux, however, is derived by hydrous melting, has a lower liquidus temperature, lower MgO, and significantly lower  $\epsilon_{\text{Nd}}^{\text{CHUR}}$  of ca. +1, compared to the mantle-derived magmas that were involved in Makkovikian magmatism.

The negative displacement of 4 to 5  $\epsilon_{\text{Nd}}$  units relative to concurrent depleted mantle is identical (in time-adjusted terms) to the shift observed in primitive mafic arc magmas in northern Chile and the Antarctic Peninsula (Pankhurst et al., 1988).

Thermal input from these magmas is limited (compared to the Makkovikian input), crustal melting was less extensive, and took place at lower temperatures. The ability of the MASH process to homogenize and mix mantle and crustal components is also reduced, and there are fewer obstacles to the ascent of variably modified mafic magmas, which fractionate and become contaminated at higher levels. The Mount Benedict Intrusive Suite ascended within the complex boundary zone between eastern and western Makkovikian domains, where it must have encountered some Archean crust at higher levels.

The bimodal Labradorian assemblage is a consequence of suppressed interaction of mantle and crust. In Figure 10.2, Labradorian granites (s.s) are depicted as derivatives of Makkovikian "mixed" granites at intermediate levels, and/or juvenile Makkovikian material that had solidified in the lower crust. It is logical to expect that Archean lower crust of the western domain was extensively diluted by Makkovikian magmatism. In this model the similarity of Nd signatures between Labradorian gabbros and granites (s.s) is coincidental, as they have discrete sources.

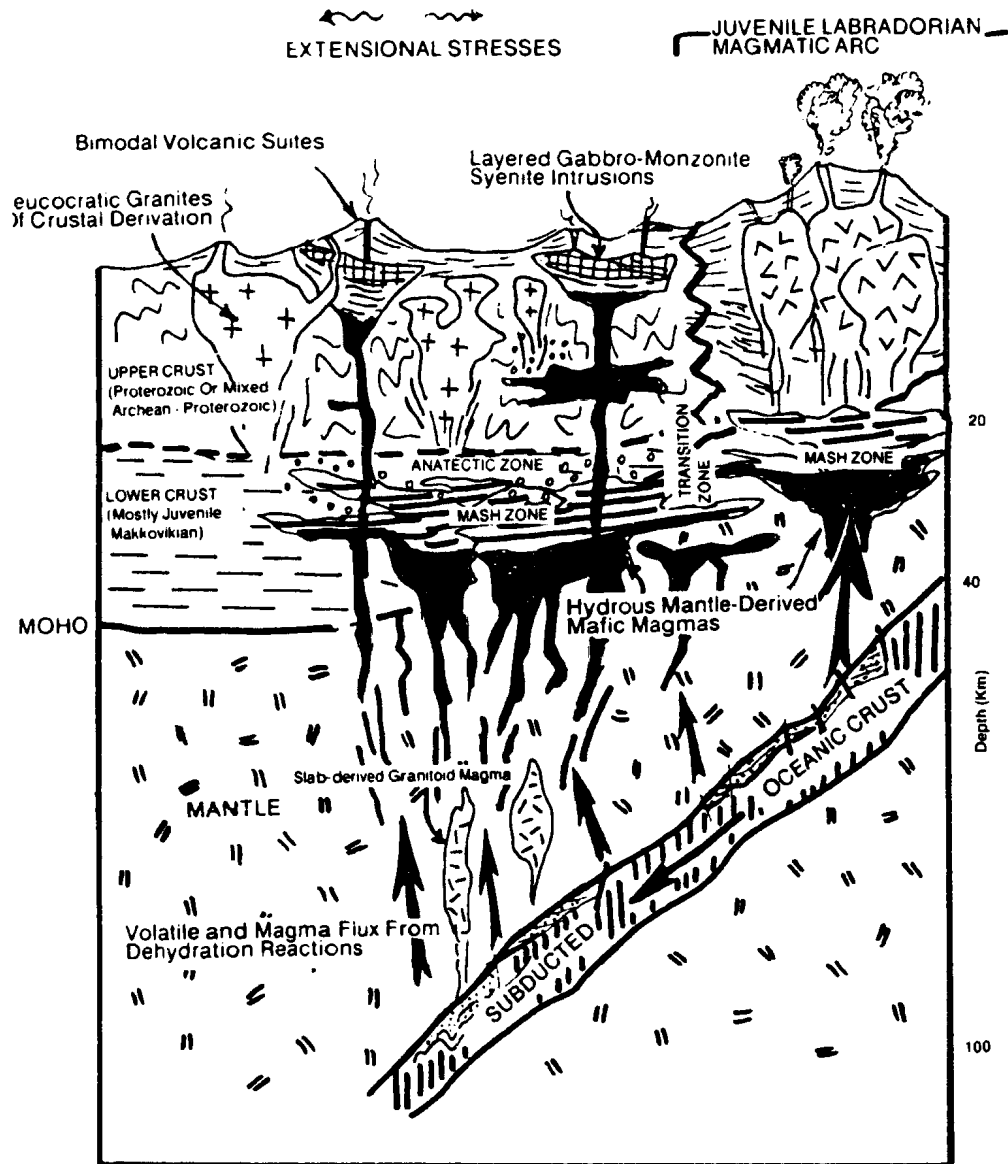


Figure 10.2. A generalized, schematic model for the petrogenesis of Labradorian magmas above a north-dipping subduction zone at ca. 1650 Ma. Note that the main locus of Labradorian activity is inferred to lie south of the study area. Depth scale is approximate.

### 10.3 PROTEROZOIC CRUSTAL EVOLUTION IN THE MAKKOVIK PROVINCE

#### **Implications For Crustal Growth Models**

**Makkovikian Events** : The period from 2000 to 1700 Ma ago involved widespread orogenic activity and magmatism in the northern hemisphere (e.g. Windley, 1977), and is also important in the southern hemisphere (e.g. Page, 1988; Cordani et al., 1988). Isotopic studies (particularly using Nd) demonstrate that most 2000-1700 Ma crust in North America and Eurasia consists of ca. 80% newly generated, mantle-derived material (Patchett and Arndt, 1986).

The study area is part of this extensive Early Proterozoic tract (e.g. Figure 2.2, p.30), and Nd isotopic data (8.2, 8.3) are broadly consistent with these conclusions, particularly in the eastern domain, where crust formed no earlier than 2100 Ma ago. In the western domain, Archean crust contributed to Proterozoic magmas, but rocks produced entirely from such sources are rare; most contain 50% or more juvenile material, based on conservative mixing calculations (8.3.2). The Makkovik Province was therefore an area of new crust generation in both domains. However, Makkovikian plutonic rocks retain local lower crustal isotopic signatures much more clearly than the Greenlandic and Scandinavian rocks of similar age described by Patchett and Arndt (1986).

**Labradorian Events** : Nd isotopic data indicate that Labradorian events in the Makkovik Province also added new material to the crust. The isotopic characteristics of these rocks resemble those of the older Scandinavian and



Greenlandic suites examined by Patchett and Bridgwater (1984) and Patchett and Kouvo (1986) in that they consistently contain a small (< 20%) crustal component. However, in the case of Labradorian granites (s.s.), recycling of slightly older, juvenile, Makkovikian crust by anatexis cannot be ruled out. Schärer (1988) found that most Labradorian igneous rocks within the high-grade terranes had neutral or positive  $\epsilon_{Nd}^{CHUR}$ , and therefore also represent crust generated at or slightly before 1650 Ma.

*Stages In Crust Formation* : Bickford (1988) reviewed continental crust formation as a three-stage process that occurs sequentially at mid-ocean ridges, above subduction zones, and within accretion-collision zones. In subsequent discussion, these are referred to as Stage 1, Stage 2 and Stage 3 crustal growth. Bickford (1988) interprets Stage 3 as mostly post-orogenic anatectic melting of material formed in stage 2. However, data presented here indicate that post-orogenic magmatism in the Makkovik Province contributed significantly to new crust generation.

Stage 3 crustal growth is thus visualized here as a consequence of post-orogenic or anorogenic magmatism (the distinction may be semantic at this early stage in Earth history; see later discussion), that results in a vertical reorganization of the crust (after Anderson, 1987; Hoffman, 1989). The mechanism is addition of mantle-derived mafic material at lower levels ("underplating"), coupled with migration of potassic melts or hybrid magmas to form a geochemically evolved upper crust.

Seismic studies indicate that Proterozoic crust is commonly horizontally layered, has a high-velocity lower domain of probable mafic composition (e.g. Drummond and

Collins, 1986), and may have prominent horizontal reflectors in the Middle and Lower Crust (e.g. Pratt et al., 1988). Such features are absent from undisturbed Archean cratons, and are progressively diminished in younger crustal domains. These features are probably a consequence of Stage 3 crustal growth, as described above, which may not have operated widely during the Archean. It is predicted that a proposed seismic transect in the Labrador Sea (Keen et al., 1988) will detect this layered crustal structure under the Makkovik Province (particularly under the eastern domain) but not under the Archean Nain Province.

Labradorian magmatism in the study area is viewed as a distal manifestation of Stage 2 crustal growth processes, occurring via melting of the mantle promoted by dehydration of wet stage 1 crust (ocean floor), with variable addition of continent-derived sediment (White and Patchett, 1984; Bickford, 1988).

**Summary** : Data from this project support the importance of Early Proterozoic crust formation, as deduced by Patchett and Arndt (1988). It has been suggested that this implies very high rates or large domains of arc magmatism at this time, possibly as much as six times present global arc magma production (Reymer and Schubert, 1986). It may, however, be misleading to assume that all crust is generated by this Stage 2 process, as new crust generation may also take place in post-orogenic environments, and this Stage 3 crust production may have been of greater importance in a hotter Proterozoic Earth (see later discussions).

## **A Wilson-Cycle Model For The Evolution Of The Makkovik Province**

A speculative plate-tectonic model for the evolution of the Makkovik Province is presented below (Figure 10.3). All models of this type are derivative, and this proposal has inherited some features from previous reconstructions by Ryan (1984), who presented alternative collisional and ensialic models. Gower (1985) proposed a tectonic model for Labradorian to Grenvillian events, which covers the period following the final (1650 Ma) step of this proposal. In a general sense, it is also influenced by other models presented for both Precambrian and Phanerozoic orogenic belts (e.g., Stoeser and Camp, 1985; Hoffman, 1988).

The cases for and against Proterozoic lithospheric plate motions have been discussed in counterpoint for many years (e.g. papers in Kroner, 1981, and Medaris et al., 1983), and are beyond the scope of this discussion. The strongest argument in favour of plate tectonics is that it is an observable process resulting from mantle convection and heat loss, facilitated and lubricated by the hydrosphere (Dickinson, 1981; Fyfe, 1988). As Precambrian heat flow cannot have been less than that of today, and the hydrosphere has existed since at least 3800 Ma, it is difficult to imagine an Earth on which processes of this general type did not take place.

### **Early Stages -- Rifting, sedimentation and Stage 1 Crust Generation**

Archean crust of the Nain Province was stabilized by ca. 2800 Ma, and remained stable for a long interval. Mafic dyke swarms were emplaced at ca. 2200 Ma (Grant et al., 1983; Gower and Ryan, 1986). This is ascribed to rifting

and distension of the Archean crust, preceding development of an oceanic basin to the south-east (Figure 10.3a,b). There is no direct evidence of this basin, but isotopic data from the eastern domain indicate a lack of Archean crust beneath this area.

Supracrustal rocks of the Moran Lake and Lowermost Aillik Group were subsequently deposited on the margins of the Archean block; Gower and Ryan (1986) suggested formation at or before 1900 Ma. There is no direct evidence that the Lower Aillik Group was deposited on Archean basement, and it may be part of an oceanic domain, later thrust over the Archean craton. Mafic volcanic rocks in the upper part of the Moran Lake Group resemble mid-ocean ridge basalt (MORB), based on trace element geochemistry (J.North, pers.comm., 1988).

#### **Ensimatic Stages -- Subduction and Stage 2 Crust Generation**

Crustal evolution in the oceanic domain eventually changed from Stage 1 (ocean-ridge) to Stage 2 (subduction-zone) crust generation (Figure 10.3c). Mafic volcanic rocks in the upper portion of the Moran Lake and (possibly) Lower Aillik Groups may record a back-arc setting, which is not inconsistent with a MORB-like geochemistry. Nd isotopic data from the Pitre Lake Granite indicate (albeit indirectly) that pelitic metasediments of the Lower Aillik Group had a relatively juvenile source (8.3.1), which could have been an arc edifice within the area now occupied by the eastern domain. It is envisaged that one or more arc systems provided sites for generation of juvenile sialic crust over subduction zones.

There is evidence of such primitive calc-alkaline magmatism in other Lower Proterozoic domains. The

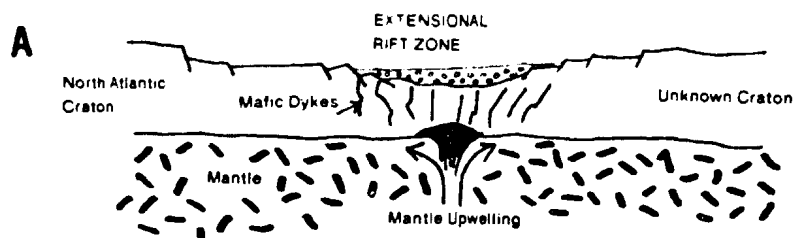
Svecokarelian belt of Finland includes 1930 - 1860 Ma old gabbro, tonalite and trondhjemite suites that resemble younger ensimatic and continental arc assemblages (Nurmi and Haapala, 1986). In Sweden, volcanic belts of 1900 - 1850 Ma age are both geochemically and metallogenically similar to modern island arcs, and were intruded by tonalitic granitoid rocks (Wilson et al., 1985; Lagerblad et al., 1987). Nd Isotopic studies suggest that these areas all represent juvenile, Proterozoic crust (Wilson et al., 1985; Patchett and Kouvo, 1986). The southern part of the Ketilidian Belt (migmatite zones of Allaart, 1976) may also represent such material (see later discussions).

Direct evidence of oceanic crust has always been a central problem in the interpretation of Proterozoic mobile belts. Scott et al. (1989) have, however, described a convincing 2000 Ma old ophiolitic assemblage from the Cape Smith Fold Belt of northern Quebec. To date, however, no such assemblages have been reported from the Ketilidian or Svecokarelian belts.

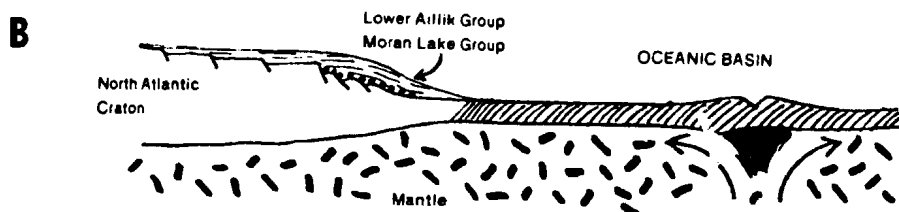
#### **Early Ensialic Stages -- Accretion Of Juvenile Terranes and Initiation of Stage 3 Crust Generation**

Subduction of oceanic crust leads inexorably to accretion of exotic terranes to the active margin, as postulated for modern orogenic systems (e.g. Coney et al., 1980). This accretion probably took place ca. 1850 Ma or earlier (Figure 10.3d), and is recorded by subhorizontal deformation and high-grade metamorphism of the Lower Aillik Group, and generation of minor anatectic granites from both juvenile and Archean crustal blocks. The Cape Harrison Metamorphic Suite is the largest preserved fragment of an accreted, pre-Makkovikian, juvenile terrane. Gneissic rocks

EARLY STAGES (ca. 2200 Ma)



STAGE TWO (ca. 2100 - 2000 Ma)



STAGE 3: ENSIMATIC STAGES (ca. 2000 - 1900 Ma)

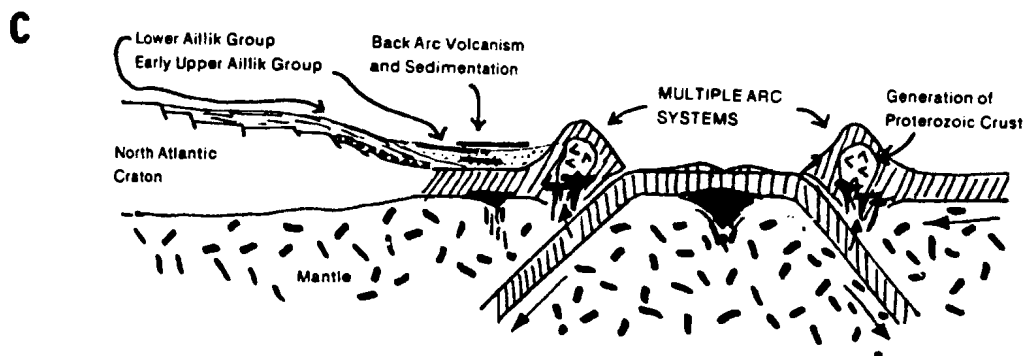
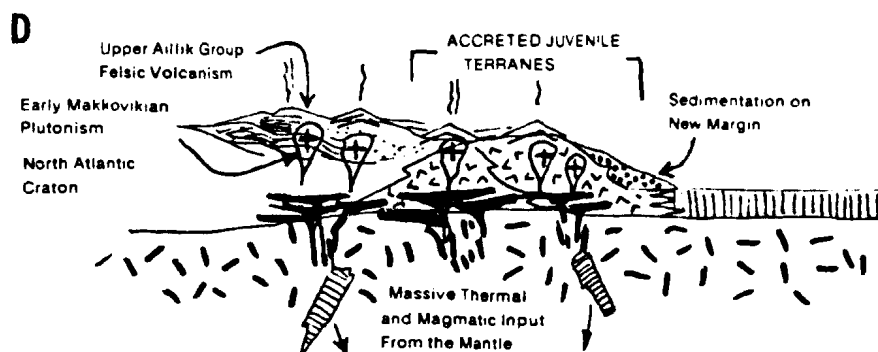
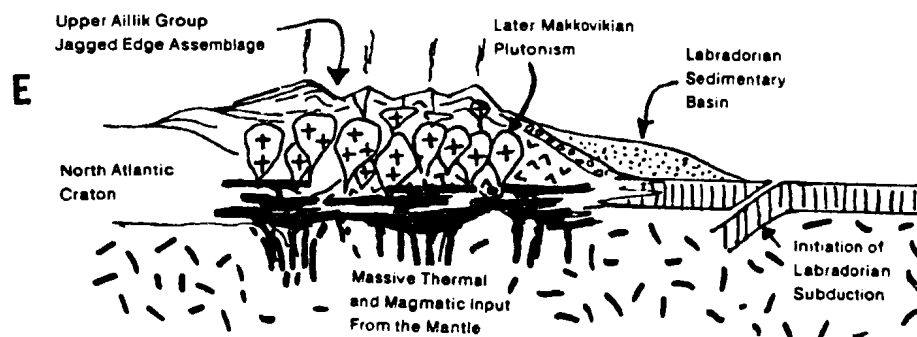


Figure 10.3. A proposed plate-tectonic framework for Makkovikian and Labradorian events in the study area. For a continuation of possible events after 1650 Ma, see Gower (1985). See text for discussion of subfigures (a) to (f).

STAGE 4 : EARLY ENSIALIC STAGE (ca. 1850 Ma)



STAGE 5 : LATE ENSIALIC STAGE (ca. 1800 - 1700 Ma)



STAGE 6 : LABRADORIAN CYCLE (ca. 1650 - 1600 Ma)

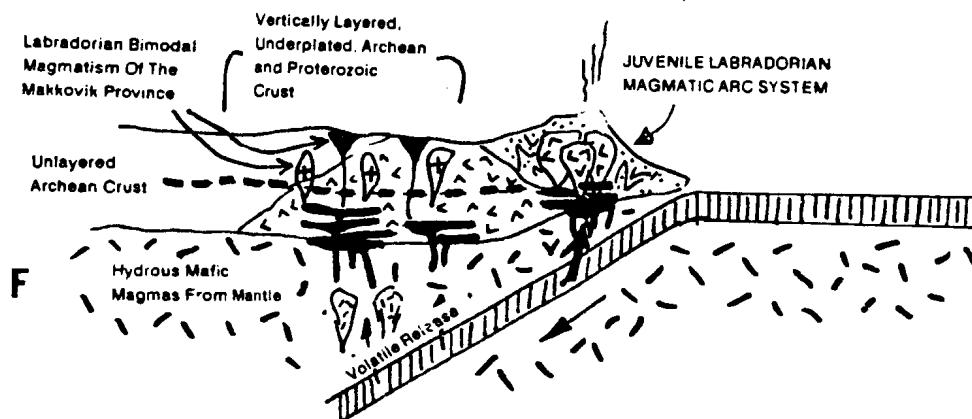


Figure 10.3 (continued). The heavy dashed line in (f) indicates the vertical layering of crust affected by Proterozoic events, as opposed to undisturbed Archean cratonic areas.

east of the study area in Labrador (Owen et al., 1986) are also possible candidates. Tonalitic and trondhjemitic rocks of the Island Harbour Bay Intrusive Suite (which are highly atypical of Makkovikian magmatism) may record a brief period of subduction beneath the Archean continental margin.

During accretion, crust generated by Stage 2 processes was tectonically thickened. An insulating blanket was formed over hot mantle, and the build-up of heat induced mantle melting. Early Stage 3 crust generation commenced shortly after accretion, via emplacement of mafic magmas into the base of both Archean and juvenile domains. The consequences of this activity are discussed above (10.1). Final tectonic movements were partly contemporaneous with this early Makkovikian magmatism, and some intrusions are deformed by virtue of their age and/or location. Initiation of Upper Aillik Group felsic volcanism dates from this period; the mixed assemblage of the earliest Upper Aillik Group may record part of the back-arc setting indicated in Figure 10.3c.

#### **Late Ensialic Stages -- Episodic Post-Tectonic Magmatism and Stage 3 Crust Formation**

This stage corresponds to the main Makkovikian plutonic assemblage of ca. 1800 - 1760 Ma (and possibly younger) age. This activity continued vertical reorganization of the crust, as discussed previously (10.1). Thickening via underplating was greatest in the thinner eastern domain crust, which was also probably hotter, and richer in volatiles than granulitic Archean lower crust in the west (Figure 10.3e).

By the time the Strawberry Intrusive Suite was emplaced, both domains had similar thicknesses and



elemental compositions, accounting for the geochemical coherence of these plutons across the margin of the Archean craton. Volcanic rocks of the Jagged Edge assemblage may record volcanism associated with the Strawberry Suite, as they have a similarly primitive initial Nd composition. However, they could also be of Labradorian age (see 7.3, 8.3 for discussions).

Extensive reprocessing of the juvenile, recently-accreted crust is implicit in the stage 3 crust formation envisaged during this period. Scattered, enigmatic outcrops of layered or banded material encountered during mapping of plutonic units may be enclaves or screens of older juvenile crust, in addition to the larger remnant at Cape Harrison.

#### **Labradorian Stages -- Initiation of a New Active Margin South Of The Makkovik Province**

The waning stages of the Makkovikian episode were followed by, or were contemporaneous with, the initiation of Labradorian events. It is suggested that northward-directed subduction began under this margin after cessation of Makkovikian plutonism, and was well underway by 1650 Ma. The study area was by now distal to the active zone, and magmatic and deformational effects were minor. Bimodal Labradorian magmatism, corresponding to the model presented above (10.2), was the result.

Gower (1985) proposed that a long-lived convergent plate boundary developed during the Labradorian event, and offers some interesting speculations on the nature of the subsequent Grenvillian Orogeny, a subject deliberately avoided here.

These suggestions do not imply that all igneous rocks in the Labrador Orogen are related to this northward-directed subduction, as it is likely that Stage 3 crust formation subsequently took place in this area also.

### Relationship of Makkovikian and Labradorian Magmatic Provinces Within The TLGB

Makkovikian and Labradorian events are viewed as phases in long-term crustal evolution along the margin of a developing supercontinent. Makkovikian magmatism was associated with the accretion of Proterozoic terranes to an Archean nucleus, and (in a broader sense) to the assembly of this supercontinent (Hoffman, 1988). Labradorian magmatism reflects subsequent subduction along its southern boundary. The TLGB in the Makkovik Province is thus a composite belt, but dominated by Makkovikian rocks.

A possible reconstruction of the situation at ca. 1650 Ma is illustrated in Figure 10.4a. Makkovikian and Labradorian magmatic belts diverge, and continue into southern Greenland and southern Labrador respectively. The Granitoid Zone of the Ketilidian Mobile Belt (Allaart, 1976) contains a similar assemblage of intrusive rocks, but may contain more remnants of Stage 2 crust. The folded and flat-lying migmatite zones in the south of the Ketilidian belt (Allaart, 1976) may represent the accreted juvenile block (*Ketilidia*?). To the west, the Makkovikian belt may join with the ca. 1800 Ma old Ungava or DePas batholith (Wardle et al., in press) in the Churchill Province. Alternatively, it may be continuous with the Penokean belt of the midcontinent region, as implied by Thomas et al. (1985).

Either alternative implies that central and western portions of the TLGB are also composite Makkovikian-Labradorian magmatic provinces. Makkovikian U-Pb ages have not yet been reported from this area (Thomas et al., 1986), but Makkovikian rocks would be very hard to recognize using field criteria. Unless these areas are underlain by Archean material, Makkovikian and Labradorian components of the TLGB would probably also have similar  $\epsilon_{Nd}$  signatures.

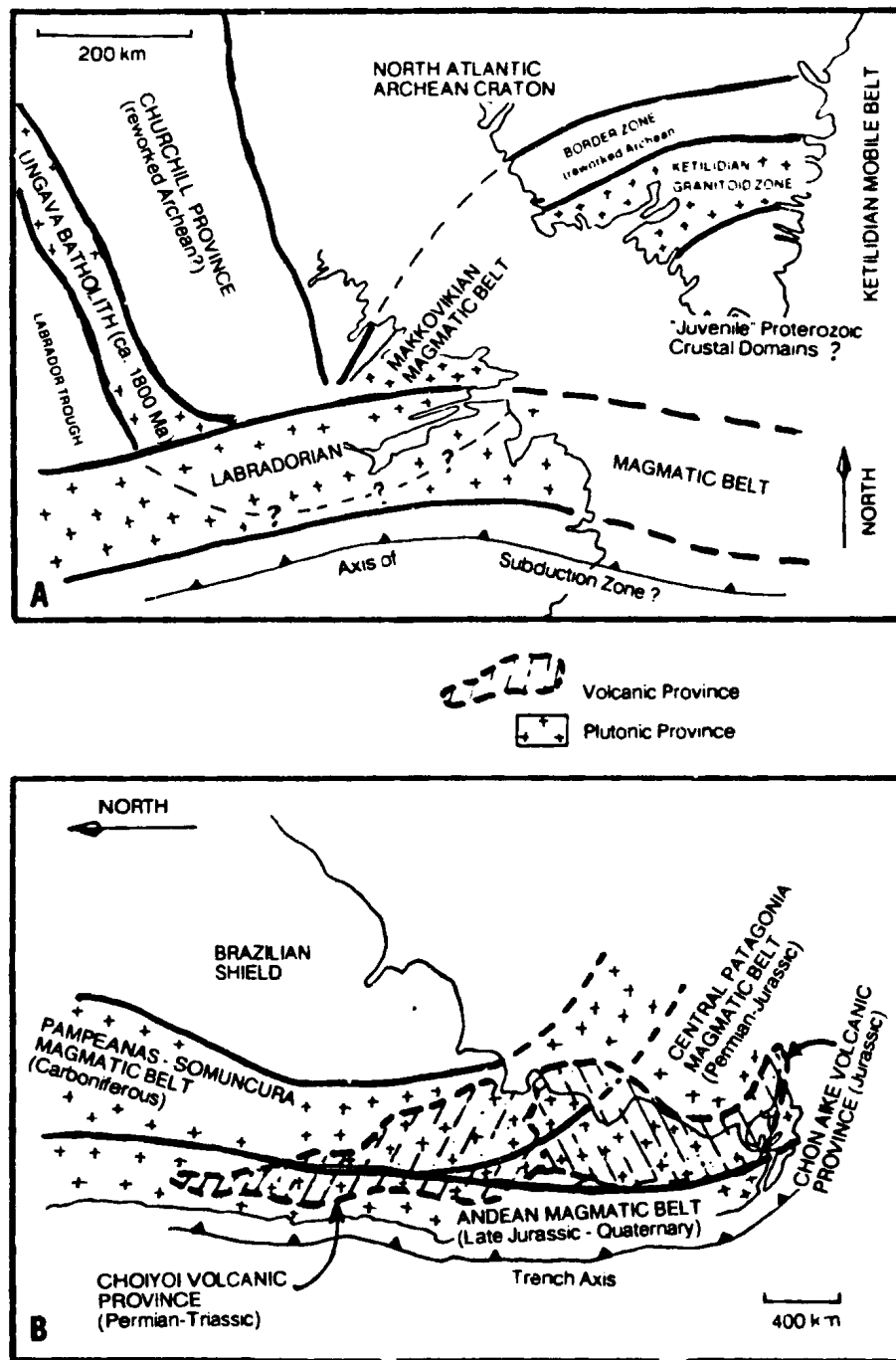


Figure 10.4. (a) A possible paleogeographic configuration of Makkovikian, Ketilidian and Labradorian magmatic provinces at ca. 1650 Ma. (b) Paleozoic, Mesozoic and Cenozoic magmatic belts developed at the margin of Gondwanaland in southern South America (after Ramos, 1988; Rapela and Kay, 1988). This area is proposed as a possible analogue to sequential events in the study area. Note that there is a large difference in scale between (a) and (b).

### **A Younger Analogue -- The Margin of Gondwanaland in Southern South America**

The southern South American margin of Gondwanaland (Ramos et al., 1986; Ramos, 1988; Rapela and Kay, 1988; Kay et al., 1989) may provide a general analogue to the above model. A simplified map of its major tectonic elements is shown in Figure 10.4b. There is a very large difference in scale between Figures 10.4a and 10.4b, and no exact geographic correspondences are implied. The comparison simply illustrates similarly protracted magmatic evolution on the margin of a developing supercontinent.

The earliest rocks in this area consist of Middle to Late Paleozoic supracrustal rocks and syntectonic granitoid rocks. Ramos et al. (1986) view these as continental margin and oceanic terranes that were assembled into Gondwanaland at the end of the Devonian, recording final stages in assembly of the supercontinent. Their accretion was followed by emplacement of the Pampeanas - Somuncura (Carboniferous to Permian) and Central Patagonia (Triassic-Jurassic) granitoid batholiths (Rapela and Kay, 1988). Both are siliceous and potassic granitoid belts, rather than expanded calc-alkaline suites. In Patagonia, their trends diverge from the younger Andean belt. However, in the north, they are parallel to it, and rocks of similar affinity occur within the Andean magmatic belt. The Gondwanaland batholiths are associated with the aforementioned Choyoi (Permian) and Chon Aike (Early Jurassic) silicic volcanic provinces, for which petrogenetic models (Kay et al., 1989) are similar to those presented above for the Makkovikian assemblage (10.1).

These final Gondwanaland events were soon followed by initiation of a new active margin, represented by the Late Jurassic to Quaternary magmatism of the Andes, built on a

Paleozoic substrate in the north and upon juvenile "arc" crust in the south (Hildreth and Moorbath, 1988). Where Gondwanaland and Andean magmatic provinces are superimposed, magmatism was episodic from Devonian to Cenozoic, a 250 - 300 Ma period that easily encompasses Makkovikian and Labradorian events in Labrador. It is suggested here, partly after Kay et al.(1989), that assembly of Gondwanaland is analogous to the creation of Proto- Laurentia and establishment of a mobile zone along its southern margin, as described by Hoffman (1988).

In this context, it is interesting to speculate on eventual destruction of the Pacific Ocean. When this event finally transpires, will the resultant collisional orogeny bear the same temporal relationship to Gondwanaland and Andean cycles as the Grenvillian orogeny bears to Makkovikian and Labradorian events ?

#### **The Makkovik Province as Part of a Chelogenic Cycle**

Sutton (1963) proposed the term "chelogenic cycle" to explain the episodic nature of global orogenies in terms of the aggregation and dispersal of large continents. A recent revival of such ideas is exemplified by two brief papers from the contrasting disciplines of theoretical geophysics and regional geology (Gurnis, 1988; Hoffman, 1989).

Gurnis (1988) modelled "feedback" between lithospheric plate motions and mantle convection patterns. He suggested that continents will inevitably aggregate over downwellings (cool areas) in the mantle. Once aggregated, they become stationary or slow-moving, and insulate large areas of the mantle. Rising temperatures in the mantle create a thermal upwelling (i.e., a series of plumes) that eventually rifts the continent and disperses the fragments towards colder mantle areas (downwellings).

Hoffman (1989) applied these (and other) model results in an elegant discussion of the North American Precambrian Shield, couched in an interesting four-movement musical analogy (referred to by the editors of *Geology* as a "Superswell Symphony"). The model proposes that a Proterozoic supercontinent (c.f. Piper, 1983) aggregated over a mantle downwelling between 1900 and 1700 Ma ago, and that its assembly is defined by worldwide orogeny and crust generation at this time, followed by further crust generation along its margins. These events correspond to Makkovikian and Labradorian stages described above.

Insulation of the mantle by Archean cratons and large tracts of juvenile crust induced the long-lived "anorogenic" magmatism of the Middle Proterozoic via episodic thermal and magmatic input from the mantle. A similar model for anorogenic magmatism was previously advocated by Anderson (1987).

The model proposed here fits into these events well, and with the proposals of Kay et al. (1989), who also applied the models of Gurnis (1988) to the final assembly of Gondwanaland. Significantly, the Pan-African belt of Arabia, referred to above as another possible analogue to Makkovikian events, is also part of a period of continental assembly (e.g. Bowden and Kinnaid, 1987).

Hoffman (1989) suggested qualitatively that the first supercontinental assembly would experience the most intense "anorogenic" magmatism as a consequence of greater mantle heat flow during the Early Proterozoic. A hotter mantle also has implications for the relationships between "post-orogenic" and "anorogenic" magmatism, and for crustal growth mechanisms.

### Proterozoic Magmatism and Crustal Evolution : Reprise

If, as suggested by this study, Stage 3 (post-orogenic) crustal growth is an important process, it must have played a greater role in a hotter Earth, where the build-up of heat in subcontinental mantle would be greater and more rapid. Gurnis (1988) proposed a ca. 300 Ma interval between assembly and rifting of supercontinents, based on present-day Earth parameters. A hotter mantle, and greater radiogenic heat production, would shorten this interval. In such a situation, Stage 2 crust accreted to a aggregating continent would encounter the effects of overheated mantle very soon after its arrival. Stage 3 crustal growth would occur widely in post-orogenic settings, and would be more intense and widespread than in younger belts. It may therefore have contributed to the apparent high growth rates of some Early Proterozoic crustal provinces noted by Reymer and Schubert (1986). These authors also proposed unusually rapid growth for the Pan-African of Arabia, which may also record a period of supercontinent assembly.

Diminishing importance of Stage 3 crustal growth through geological time also accounts for differences between Proterozoic and Phanerozoic crustal structure noted by Drummond and Collins (1986).

A corollary of this proposal is that the distinction between "post-orogenic" and "anorogenic" magmatism becomes progressively blurred as we reach back in geological time. In Phanerozoic and modern environments, "anorogenic" magmatism is seen as a separate, discrete environment because the time lag between continental assembly and mantle upwelling is long ( $\geq 300$  Ma). In the Early Proterozoic, post-orogenic and anorogenic magmatism probably formed a continuum, linked by a common process,

i.e. a large thermal and magmatic input from the mantle. In a younger, cooler Earth, this is present only in more restricted environments such as hot-spots, and requires a longer preceding period of insulation to develop.

If the relative importance of Stage 2 (subduction zone) and Stage 3 (post-orogenic to anorogenic) crustal growth has changed through time, preservation of juvenile calc-alkaline material should be less common in older terranes, as a consequence of greater reprocessing, and of greater uplift and erosion caused by underplating. Testing such a prediction is very difficult, but a scarcity of such material is the most common objection cited against plate tectonic models (e.g. Kroner, 1983; Glikson, 1983). This scarcity may be a real feature, but does not imply absence of Stage 2 crustal growth processes, but rather greater intensity of Stage 3 processes, particularly during periods of continental aggregation.

It should be stressed also that preservation of juvenile volcanic-arc like assemblages is rare in orogenic belts of all ages, excluding incomplete cycles such as those of the circum-Pacific region. In the Appalachians, for example, pre-Taconic tonalitic and trondhjemitic granitoid rocks of probable arc affinity represent only a few percent of exposed granitoid rocks, most of which are post-orogenic (Hayes et al., 1987; Williams et al., 1989). The dominant granitoid intrusive rocks in orogenic belts of all ages are invariably the post-orogenic products of Stage 3 crustal growth processes.

This study has shown that Lower Proterozoic magmatism in the Makkovik Province is indeed geochemically distinct from younger analogues (Chapter 9). However, it is felt that such differences do not necessarily require unique, non-uniformitarian models, but are explicable via plate tectonics, with some modifications to account for declining heat flow through geological time.



#### 10.4 FUTURE PATHS

Regional projects such as this inevitably pose more questions than they are able to resolve. Some areas of further investigation and possible subprojects are listed in point form here.

*Isotope Geochemistry* : Multiple isotopic systems are required in an ideal study of crust generation. Sr data from mineral separates, and Pb isotope data, could both constrain mantle and crustal contributions more precisely, by requiring a more unique mixing solution. Oxygen isotope studies could discriminate upper, lower and supra-crustal sources.

The Kaipokok Bay fold belt offers a chance to examine the behaviour of isotopic systems during anatexis of different protoliths. The very unusual Nd signature of the Pitre Lake granite suggests that results could have important implications.

*Geochronology* : Geochronological problems are as numerous as units. Recent revision of the age of the Strawberry Intrusive Suite to ca. 1720 Ma (Krogh et al., in prep, see footnote on p.113) has extended the duration of post-tectonic Makkovikian plutonism. The extent of this younger Makkovikian magmatism requires evaluation. Units that require dating include the Kennedy Mountain Suite (which may delimit Makkovikian deformation), the Lanceground Intrusive Suite (is this the same age as the Numok Suite, or is it similar in age to the Strawberry Suite ?), and the volcanic rocks of the Jagged Edge assemblage (are these equivalent to the Strawberry Suite, or Labradorian ?). Dating of the Cape Harrison Metamorphic Suite is also crucial.

**Petrological and Geochemical Studies** : The Adlavik and Mount Benedict Intrusive Suites are fascinating intrusions that record the protracted fractionation of potassic, possibly shoshonitic mafic magmas. Trace element models presented here (5.3) are only a first approximation to the problem and require constraining by major element mass-balance solutions, and further exploration of coupled assimilation-fractional crystallization models (DePaolo, 1981a). The greatest problem with the mafic intrusions is their horrific complexity; they require devoted and time-consuming detailed mapping to delineate their many individual magma batches. The scale of this study has precluded such rigorous mapping. Amongst granitoid suites, the Strawberry Intrusive Suite and similar A-type suites are of most interest to the author, particularly in terms of their implications for the petrogenesis of such rocks. The Cape Harrison Metamorphic Suite requires further work, as it has an important role in models. Description as tonalitic to granodiorite is presently based mostly on field and petrographic data (Gower, 1981), .

**Mineral Chemistry Studies** : This aspect is largely untouched here (a few imprecise probe analyses were carried out purely for identification purposes). Recent studies by Ague and Brimhall (1988a,b) use mafic and accessory mineral geochemistry to study source characteristics and conditions of emplacement in the Sierra Nevada Batholith. These have potential for application in the TLGB, particularly in combination with isotopic data, and with reference to contrasts between eastern and western domains.

*Spectral Analysis Of Granitoid Batholiths* : The largely univariate treatment of Chapter 9 can be expanded with multivariate techniques, and some work of this type has already been done using factor analysis (e.g. Kerr, 1988). It is increasingly apparent that discriminant diagrams do not provide adequate characterization of tectonic environments, and it is important that emphasis also be placed on extensive parameters, and compositional structure and evolution. This can only be addressed via structured sampling programs of the type employed here, and by greater international availability of representative data. It is felt that this general approach has potential, and it is hoped that these TLGB data, although far from fully understood, will eventually contribute to better characterization of granitoid magmatism via geochemistry. Data will be made available via the ARTEMISE data bank and via the Newfoundland Department of Mines. Much effort is addressed in granite petrology towards categorization of unique magma types, as exemplified by the ever-popular I-, S-, A- and M- type terminology. In the words of Hildreth (1987), *".....such cryptonyms encourage pigeonholing rather than the thoughtful consideration needed to understand multicomponent compositional spectra...."*. I hope, as does Fyfe (1988), that the origins of granites will no longer be subjects of debate in 2089 (see quotations after title page), but I wonder if such statements might be overly optimistic in view of the inherent complexity of the topic !

## REFERENCES CITED

- ABBEY, S. , 1979.  
Studies in "standard samples" for use in the general analysis of silicate rocks and minerals. Part 6 : 1979 edition of "usable" values. Geological Survey of Canada, Paper 80-14, 30 pp.
- ABBEY, S. , 1983.  
Studies in "standard samples" of silicate rocks and minerals. Geological Survey of Canada, Paper 83-14, 114 pp.
- AGUE, J.J. and BRIMHALL, G.H. , 1988a.  
Regional variations in bulk chemistry, mineralogy, and the compositions of mafic and accessory minerals in the batholiths of California. Bulletin of the Geological Society of America, v.100, p.891-911.
- AGUE, J.J. and BRIMHALL, G.H. , 1988b.  
Magmatic arc asymmetry and distribution of anomalous plutonic belts in the batholiths of California: Effects of assimilation, crustal thickness, and depth of crystallization. Bulletin of the Geological Society of America, v.100, p.912-917.
- ALLAART, J.H. , 1976.  
Ketilidian mobile belt of West Greenland. In: Escher, A. and Watt, W.S., (eds.). Geology of Greenland. Gronlands Geologiske Undersogelse, Copenhagen, p.120-152
- ANDERSON, J.L. , 1983.  
Proterozoic anorogenic granite plutonism of North America. In: Medaris, L.G., et al. (eds.). Proterozoic Geology. Geological Society of America, Memoir 161, p.133-154.
- ANDERSON, J.L. , 1987.  
The nature and origin of the A-type magmatism in the Proterozoic IGCP Project 217 (Proterozoic Geochemistry), Lund, Sweden, June 1987. Program with abstracts, p.1.
- ARCHIBALD, D. and FARRAR, E. , 1979.  
40Ar/39Ar mineral ages from the Walker - Benedict granodiorite, Central Mineral Belt, Labrador. Newfoundland Dept. Mines and Energy, Mineral Development Division, unpublished report, 12 pp.
- ARNDT, N.T. and GOLDSTEIN, S.L. , 1987.  
Use and abuse of crust-formation ages. Geology, v.15, p.893-895.
- ARTH, J.G. , 1976.  
Behaviour of trace elements during magmatic processes - A summary of theoretical models and their applications. Journal of Research of the U.S. Geological Survey, v.4, p.41-47.
- ASHWAL, L.D., WOODEN, J.L. and EMSLIE, R.F. , 1986.  
Sr, Nd and Pb isotopes in Proterozoic intrusives astride the Grenville Front in Labrador: Implications for crustal contamination and basement mapping. Geochimica et Cosmochimica Acta, v.50, p.2571-2585.
- ATHERTON, M.P. , 1984.  
The coastal batholith of Peru. In : Harmon, R.S. and Barriero, B.A. (eds.) Andean Magmatism. Shiva Publishing, Nantwich, U.K., p.168-180.
- BAILEY, D.G. , 1979.  
Geology of the Walker Lake-Maclean Lake area, Central Mineral Belt, Labrador. Newfoundland Dept. Mines and Energy, Mineral Development Division, Report 79-3. 36 pp.

- BAILEY, D.G., FLANAGAN, M.J. and LALONDE, A. , 1979.  
Geology of the eastern Central Mineral Belt, Labrador. Newfoundland  
Dept. Mines and Energy, Mineral Development Division, Report 79-1,  
p. 103-108.
- BAILEY, J.C. , 1977.  
Fluorine in granitic rocks and melts: A review. Chemical Geology,  
v.19, p.1-42.
- BAIRD, A.K. and MIESCH, A.T. , 1984.  
Batholithic rocks of southern California - A model for the  
petrochemical nature of their source materials. United States  
Geological Survey, Professional Paper 1284, 42 pp.
- BAIRD, A.K., BAIRD, K.W. and WELDAY, E.E. , 1974.  
Chemical trends across Cretaceous batholithic rocks of southern  
California. Geology, v.2, p.493-496.
- BARKER, F., WONES, D.R., SHARP, W.N. and DESBOROUGH, G.A. , 1975.  
The Pikes Peak Batholith, Colorado Front Range, and a model for the  
origin of the gabbro-anorthosite-syenite-potassic granite suite.  
Precambrian Research, v.2, p.97-160.
- BARTH, T. , 1955.  
Presentation of rock analyses. Journal of Geology, v.63, p.348-363.
- BARUA, M.C. , 1969.  
Geology of uranium-molybdenum bearing rocks of the Aillik-Makkovik  
Bay areas, Labrador. Unpublished M.Sc Thesis, Queen's University,  
Kingston, Ontario, 76 pp.
- BATEMAN, P.C. , 1988.  
Stratigraphic classification and nomenclature of igneous and  
metamorphic rock bodies - Discussion. Bulletin of the Geological  
Society of America, v.100, p.995-997.
- BEAVAN, A.P. , 1958.  
The Labrador uranium area. Proceedings of the Geological Association  
of Canada, v.10, p.137-145.
- BICKFORD, M.E. , 1988.  
The formation of continental crust: Part 1. A review of some  
principles; Part 2. An application to the Proterozoic evolution of  
southern North America. Bulletin of the Geological Society of  
America, v.100, p.1375-1391.
- BICKLE, M.J. , 1982.  
The magnesium contents of komatiitic liquids. In: Arndt, N.T. and  
Nisbet, E.G.(eds.). Komatiites, p.479-494. Allen and Unwin.
- BOWDEN, P. and KINNAIRD, J. , 1987.  
Proterozoic orogenies, magmatism and related metallogeny. Geological  
Journal, v.22, p.81-85. (thematic issue on African geology).
- BOWDEN, P., BATCHELOR, R.A., CHAPPEL, B.W., DIDIER, J. and I MEYRE, J.,  
1984.  
Petrological, geochemical and source criteria for the classification  
of granitic rocks: A discussion. Physics of Earth and Planetary  
Interiors, v.35, p.1-11.
- BRIDGWATER, D., ESCHER, A., JACKSON, G.D., TAYLOR, F.C., and  
WINDLEY, B.F. , 1973.  
Development of the Precambrian shield in West Greenland, Labrador  
and Baffin Island. In: Arctic Geology. American Association of  
Petroleum Geologists, Memoir 19, p.99-116.

- BROOKS, C. , 1979.**  
Report on the geochronology of Labrador (Subproject 1.09).  
Newfoundland Dept. Mines and Energy, Mineral Development Division,  
unpublished report.
- BROOKS, C. , 1982.**  
Third report on the geochronology of Labrador. Newfoundland Dept.  
Mines and Energy, Mineral Development Division, unpublished report.
- BROOKS, C. , 1983.**  
Fourth report on the geochronology of Labrador. Newfoundland Dept.  
Mines and Energy, Mineral Development Division, unpublished report.
- BROOKS, C., HART, S.R. and WENDT, I. , 1972.**  
Realistic use of two-error regression treatments as applied to Rb-Sr  
data. Reviews of Geophysics and Space Physics, v.10, p.551-577.
- BROWN, G.C. , 1981.**  
Time and space in granitoid plutonism. Philosophical Transactions of  
the Royal Society of London, v.A301, p.321-336.
- BROWN, G.C., THORPE, R.S., and WEBB, P.C. , 1984.**  
The geochemical characteristics of granitoids in contrasting arcs,  
and comments on magma sources. Journal of the Geological Society of  
London, v.141, p.413-426.
- BROWN, M. , 1987.**  
The granites of the coastal cordillera, northern Atacama region,  
Chile. Terra Cognita, v.7, p.277.
- BROWN, M. , 1988.**  
Geochemistry of the granitic complexes, 26-27 degrees south,  
northern Chile. Actas de Congreso Geologico Chileno, v.5, Tomo 3,  
p.153-166. Departamento de Geologia y Geofisica, Universidad de  
Chile.
- CHAPPELL, B.W. and WHITE, A.J.R , 1974.**  
Two contrasting granite types. Pacific Geology, v.8, p.173-174.
- CHAPPELL, B.W and STEPHENS, W.E. , 1988.**  
Origin of infracrustal (I-type) granite magmas. Transactions of the  
Royal Society of Edinburgh, Earth Sciences, v.79, p.71-86.
- CHAPPELL, B.W., WHITE, A.J.R, and HINE, R. , 1988.**  
Granite provinces and basement terranes in the Lachlan Fold Belt,  
southeastern Australia. Australian Journal of Earth Sciences, v.35,  
p.505-521.
- CHAUVEL, C., ARNDT, N.T., KIELINZCUK, S. and THOM, A. , 1987.**  
Formation of Canadian 1.9 Ga old continental crust. 1: Nd isotopic  
data. Canadian Journal of Earth Sciences, v.24, p.396-406.
- CHRISTIE A.M. , ROSCOE, S.M. and F'YRIG, W.F. , 1953.**  
Central Labrador Coast, Newfoundland. (Descriptive Notes).  
Geological Survey of Canada, Paper 53-14, 3 pp.
- CLARK, A.M.S. , 1970.**  
A structural re-interpretation of the Aillik Series, Labrador.  
Unpublished M.Sc. thesis, Memorial University, St.John's,  
Newfoundland, 76 pp.
- CLARK, A.M.S. , 1973.**  
A re-interpretation of the stratigraphy and structure of the Aillik  
Group, Makkovik, Labrador. Unpublished Ph.D. thesis, Memorial  
University, St. John's, Newfoundland, 346 pp.

- CLARK, A.M.S. , 1979.  
Proterozoic deformation and igneous intrusion in part of the Makkovik subprovince. *Precambrian Research*, v.10, p. 95-114.
- CLEMENS, J.D., HOLLOWAY, J.R. and WHITE, A.J.R. , 1986.  
Origin of an A-type granite: experimental constraints. *American Mineralogist*, v.71, p.317-324.
- COBBING, E.J., PITCHER, W.S. and TAYLOR, W.P. , 1977.  
Segments and superunits in the Coastal Batholith of Peru. *Journal of Geology*, v.85, p.625-631.
- COIRA, B., DAVIDSON, J., MPOZODIS, C. and RAMOS, V.A. , 1982.  
Tectonic and magmatic evolution of the Andes of northern Argentina and Chile. *Earth Science Reviews*, v.18, p.303-333.
- COLLERSON, K.D. , 1982.  
Geochemistry and Rb-Sr geochronology of associated Proterozoic peralkaline and subalkaline granites from Labrador. *Contributions to Mineralogy and Petrology*, v.81, p.126-147.
- COLLERSON, K.D. and BRIDGWATER, D. , 1979.  
Metamorphic development of Early Archean tonalitic and trondhjemitic gneisses, Saglek area, Labrador. In Barker, F. (ed.). *Trondhjemitic, Dacites and Related Rocks*. Elsevier, Amsterdam, p.205-273.
- COLLINS, W.J., BEAMS, S.D., and WHITE, A.J.R , 1982.  
Nature and origin of A-type granites with particular reference to Southeastern Australia. *Contributions to Mineralogy and Petrology*, v.80, p.189-200.
- COLMAN-SADD, S.P. , 1982.  
Two-stage continental collision and plate driving forces. *Tectonophysics*, v.90, p.263-282.
- CONDIE, K.C. , 1981a.  
Precambrian rocks of southwestern United States and adjacent areas of Mexico. Scale 1:1,000,000. New Mexico Bureau of Mines and Mineral Resources, Map 13.
- CONDIE, K.C. , 1981b.  
Archean Greenstone Belts. Elsevier, Amsterdam, 434 pp.
- CONDIE, K.C. , 1982.  
Plate tectonics model for Proterozoic continental accretion in the Southwestern United States. *Geology*, v.10, p.37-42.
- CONEY, P.J., JONES, D.L., MONGER, J.W.H. , 1980.  
Cordilleran suspect terranes. *Nature*, v.288, p.329-333.
- CORDANI, U.G., TEIXEIRA, W., TASSINARI, C.G., KAWASHITA, K and SATO, K. , 1988.  
The growth of the Brazilian Shield. *Episodes*, v.11, p.163-167.
- COX, K.G., BELL, J.D. and PANKHURST, R.J. , 1979.  
The Interpretation of Igneous Rocks. Allen & Unwin, London, 450 pp.
- DALY, R.A. , 1902.  
The geology of the northeast coast of Labrador. *Bulletin of the Museum of Comparative Zoology, Harvard University*, v.38, p.205-269.
- DEBON, F. and LEFORT, P. , 1982.  
A chemical mineralogical classification of common plutonic rocks and associations. *Transactions of the Royal Society of Edinburgh, Earth Science*, v.73, p.135-149.

- DEBON, F., LEFORT, P., SHEPPARD, S.M. and SONET, J. , 1986.  
The four plutonic belts of the Transhimalaya-Himalaya: A chemical, mineralogical, isotopic and chronological synthesis along a Tibet-Nepal section. *Journal of Petrology*, v.27, p.219-250.
- DEBON, F., APZALI, H., LEFORT, P. and SONET, J. , 1987a.  
Major intrusive stages in Afghanistan: Typology, age and geodynamic setting. *Geologische Rundschau*, v.76, p.245-264.
- DEBON, F., APZALI, H., LEFORT, P., SONET, J. and ZIMMERMAN, J.L. , 1987b.  
Plutonic rocks and associations in Afghanistan: Typology, age and geodynamic setting. CNRS-CRPG, Nancy, France. *Memoires Sciences de la Terre*, Numero 49, 132 pp.
- DEBON, F., LEFORT, P., DAUTEL, D., SONET, J and ZIMMERMAN, J.L. , 1987c.  
Granites of western Karakorum and northern Kohistan (Pakistan): A composite Mid-Cretaceous to Upper Cenozoic Magmatism. *Lithos*, v.20, p.13-40.
- DePAOLO, D.J. , 1979.  
Implications of correlated Nd and Sr isotopic variations for the chemical evolution of the crust and mantle. *Earth and Planetary Science Letters*, v.43, p.201-211.
- DePAOLO, D.J. , 1981a.  
Trace element and isotopic effects of combined wall-rock assimilation and fractional crystallization. *Earth and Planetary Science Letters*, v.53, p.189-202 .
- DePAOLO, D.J. , 1981b.  
A Nd and Sr isotopic study of the Mesozoic calc-alkaline granitic batholiths of the Sierra Nevada and Peninsular Ranges, California. *Journal of Geophysical Research*, v.B86, p.10470-10488.
- DePAOLO, D.J. and WASSERBURG, G.J. , 1976.  
Nd isotopic variations and petrogenetic models. *Geophysical Research Letters*, v.3, p.249-252.
- DICKINSON, W.R. , 1981.  
Plate tectonics through geological time. *Philosophical Transactions of the Royal Society of London*, v.A301, p.207-215.
- DICKSON, W.L. , 1983.  
Geology, geochemistry and mineral potential of the Ackley granite and parts of the Northwest Brook and Eastern Meelpaeg Complexes southeast Newfoundland. Newfoundland Dept. Mines and Energy, Mineral Development Division, Report 83-6, 129 pp.
- DICKSON, W.L., WILLIAMS, H., HAYES, J.P and TUACH, J. , 1988.  
Plutonic expression of Appalachian tectonostratigraphic zones in Newfoundland. Unpublished manuscript.
- DICKSON, W.L., O'BRIEN, S.J. and HAYES, J.P. , 1989.  
Aspects of the mid-Paleozoic magmatic history of the south-central Hermitage flexure area, Newfoundland. Newfoundland Dept. Mines and Energy, Mineral Development Division, Report 89-1, p.81-95.
- DIDIER, J., DUTHOU, J.L., and LAMEYRE, P. , 1982.  
Mantle and crustal granites: genetic classification of orogenic granites and their enclaves. *Journal of Volcanology and Geothermal Research*, v.14, p.125-132.



- DINGWELL, D.B. , 1968.  
The structures and properties of fluorine-rich magmas : A review of experimental studies. In: Taylor, R.P and Strong, D.F (eds.): Recent Advances in the Study of Granite-Related Mineral Deposits. Canadian Institute of Mining and Metallurgy, p.1-12.
- DOHERTY, R.A. , 1980.  
Geology of the Adlavi Islands. Newfoundland Dept. Mines and Energy, Mineral Development Division, Report 80-1, p. 161-165.
- DOUGLAS, G.V. , 1953.  
Notes on localities visited on the Labrador coast in 1946 and 1947. Geological Survey of Canada, Paper 53-1, 67 pp.
- DRUMMOND, B.J. and COLLINS, C.D.N. , 1986.  
Seismic evidence for underplating of the lower continental crust of Australia. Earth and Planetary Science Letters, v.79, p.361-372.
- DUYVERMAN, H.J., HARRIS, N.B.W. and HAWKESWORTH, C.J. , 1982.  
Crustal accretion in the Pan-African : Nd and Sr isotope evidence from the Arabian Shield. Earth and Planetary Science Letters, v.59, p.315-326.
- EMSLIE, R.F. , 1978.  
Anorthosite massifs, rapakivi granites and Late Proterozoic rifting of North America. Precambrian Research, v.7, p.61-98.
- ERMANOVICS, I.P., KORSTGARD, J. and BRIDGEWATER, D. , 1982.  
Structural and lithological chronology of the Archean Hopedale block and adjacent Makkovik Subprovince, Labrador. Geological Survey of Canada, Paper 82-1B, p. 153-165.
- ETHERIDGE, M.A., RUTLAND, R.W. and WYBORN, L.A. , 1987.  
Orogenesis and tectonic process in the Early to Middle Proterozoic of northern Australia. In: Kroner, A.(ed.). Proterozoic Lithospheric Evolution. American Geophysical Union, Geodynamic Series, v.17, p.115-130.
- EVANS, D. , 1980.  
Geology and petrochemistry of the Kitts and Michelin Uranium deposits and related prospects, Central Mineral Belt, Labrador. Unpublished Ph.D. thesis, Queen's University, Kingston, Ontario, 311 pp.
- FARMER, G.L. and DePAOLO, D.J. , 1983.  
Origin of Mesozoic and Tertiary granite in the western United States and implications for pre-Mesozoic crustal structure. 1. Nd and Sr isotopic studies in the northern Great Basin. Journal of Geophysical Research, v.88, p.3379-3401.
- FAURE, G. , 1978.  
Principles of Isotope Geology. Wiley, New York.
- FAUR, G. and POWELL, J.L. , 1972.  
Strontium Isotope Geology. Springer-Verlag, Berlin, 188 pp.
- FOWLER, M.B. , 1988.  
Ach'uaie hybrid appinite pipes: Evidence for mantle-derived shoshonitic parent magmas in Caledonian granite genesis. Geology, v.16, p.1026-1030.
- FRYER, B.J. , 1984.  
Report on Geochronology for the Labrador Mapping Section. Newfoundland Dept. Mines and Energy, Mineral Development Division unpublished report, 34 pp.

- FRYER, B.J. and TAYLOR, R.P. , 1985.  
Sm-Nd direct dating of the Collins Bay hydrothermal uranium deposit, Saskatchewan. Reply to comments by K.R.Ludwig. *Geology*, v.13, p.748.
- FUMERTON, S.L., STAUFFER, M.R. and LEWRY J.F. , 1984.  
The Wathaman Batholith: largest known Precambrian pluton. *Canadian Journal of Earth Sciences*, v.21, p.1082-1097.
- FYFE, W.S. , 1988.  
Granites and a wet convecting ultramafic planet. *Transactions of the Royal Society of Edinburgh, Earth Sciences*, v.79, p.339-346.
- GANDHI, S.S. , 1978.  
Geological Setting and genetic aspects of uranium occurrences in the Kaipokok Bay - Big River area, Labrador. *Economic Geology*, v.73, p.1492-1523.
- GANDHI, S.S, GRASTY, R.L. and GRIEVE, R.A.F. , 1969.  
The geology and geochronology of the Makkovik Bay area, Labrador. *Canadian Journal of Earth Sciences*, v.6, p.1019-1034.
- GANDHI, S.S, KROGH, T.E. and CORFU, F. , 1988.  
U-Pb zircon and titanite dates on two granitic intrusions of the Makkovik Orogen and a peralkaline granite of the Redwine Complex, central Labrador. *Geological Association of Canada. Annual Meeting, St.John's, 1988. Program with abstracts*, p. A42.
- GARRETT, R.G. , 1983.  
Sampling methodology. In : Howarth, R.J. (ed): *Statistics and Data Analysis in Geochemical Prospecting*, Elsevier, Amsterdam, p.84-110.
- GILL, F.D. , 1966.  
Petrography of molybdenite-bearing gneisses, Makkovik Area, Labrador (abstract). *Canadian Mining Journal*, v.89, p.100-101.
- GLIKSON, A.Y. , 1983.  
Geochemical, isotopic, and paleomagnetic tests of early sial-sima patterns: The Precambrian crustal enigma revisited. In: Medaris, L.G. et al.(eds.): *Proterozoic Geology*. Geological Society of America, Memoir 161, p.95-118.
- GOLDSTEIN, S.L., O'NIONS, R.K. and HAMILTON, P.J. , 1984.  
A Sm-Nd study of atmospheric dusts and particulates from major river systems. *Earth and Planetary Science Letters*, v.70, p.221-236.
- GOWER, C.F. , 1981.  
The geology of the Benedict Mountains, Labrador. Newfoundland Dept. Mines and Energy, Mineral Development Division, Report 81-3, 26 pp.
- GOWER, C.F. , 1985.  
Correlations between the Grenville Province and Sveconorwegian orogenic belt - Implications for Proterozoic Evolution of the southern margins of the Canadian and Baltic Shields. In: Tobl, A.C. and Touret, J. (eds.). *The Deep Proterozoic Crust in the North Atlantic Provinces*. NATL ASI Series, v.158, p.246-259.
- GOWER, C.F. , 1986.  
Geology of the Double Mer White Hills and surrounding region, Grenville Province, Eastern Labrador. Geological Survey of Canada, Paper 86-15, 50 pp.
- GOWER, C.F and OWEN, J.V. , 1984.  
Pre-Grenvillian and Grenvillian lithotectonic domains in Eastern Labrador -- Correlations with the Sveconorwegian Orogenic belt in Sweden. *Canadian Journal of Earth Sciences*, v.21, p.678-693.

- GOWER, C.F. and RYAN, A.B. , 1986.  
Proterozoic Evolution of the Grenville Province and adjacent Makkovik Province in east-central Labrador. In: Moore et al., 1986 (eds.). The Grenville Province. Geological Association of Canada, Special Paper 31, p.281-295.
- GOWER, C.F. and RYAN, A.B. , 1987.  
Two stage felsic volcanism in the Lower Proterozoic Upper Aillik Group, Labrador, Canada: Its relationship to syn- and post-kinematic plutonism. In: Pharoah et al. (eds). Geochemistry and mineralization of Proterozoic Volcanic Suites. Geological Society Special Publication 33, p.201-210.
- GOWER, C.F., RYAN, A.B. , BAILEY, D.G. and THOMAS, A. , 1980.  
The position of the Grenville Front in eastern and central Labrador. Canadian Journal of Earth Sciences, v.17, p.784-788.
- GOWER, C.F., FLANAGAN, M.J., KERR, A. and BAILEY, D.G. , 1982.  
Geology of the Kaipokok Bay-Big River Area, Central Mineral Belt, Labrador. Newfoundland Dept. Mines and Energy, Mineral Development Division, Report 82-7. 77 pp.
- GOWER, C.F., NEULAND, S., NEWMAN, M. and SMYTH, J. , 1987.  
Geology of the Port Hope Simpson map region, Grenville Province, eastern Labrador. Newfoundland Dept. Mines and Energy. Mineral Development Division, Report 87-1, p.183-189.
- GOWER, C.F., Van NOSTRAND, T., and SMYTH, J. , 1988.  
Geology of the St.Lewis River map region, Grenville Province, eastern Labrador. Newfoundland Dept. Mines and Energy. Mineral Development Division, Report 88-1, p.59-73.
- GRANT, N.K., VONER, F.R., MARZANO, M.C., HICKMAN, M.H. and ERMANOVICS, I, 1983.  
A summary of Rb-Sr isotope studies in the Archean Hopedale block and the adjacent Makkovik Subprovince, Labrador. Geological Survey of Canada, Current Research, Paper 83-1B, p.127-134.
- GRAY, C.M. , 1984.  
An isotopic mixing model for the origin of granitic rocks in southeastern Australia. Earth and Planetary Science Letters, v.70, p.47-60.
- GREENE, B.A. , 1974.  
An outline of the geology of Labrador. Newfoundland Dept. Mines and Energy, Mineral Development Division, Information circular 15, 64 pp.
- GROMET, L.P. and SILVER, L.T. , 1983.  
Rare earth element distributions among minerals in a granodiorite and their petrogenetic implications. Geochimica et Cosmochimica Acta, v.47, p.925-939.
- GURNIS, M. , 1988.  
Large-scale mantle convection and the aggregation and dispersal of supercontinents. Nature, v.332, p.695-699.
- HALDEN, N.M., CLARK, G.S., LENTON, P.G., CORKERY, N.T and SCHLEDWITZ, D. , 1987.  
Geochemical and isotopic constraints on the tectonic significance of the Chipewyan batholith, and Proterozoic magma genesis. Geological Association of Canada, Annual Meeting, Saskatoon, 1987, Program with abstracts, p.A51.
- HALLIDAY, A.W. , 1984.  
Coupled Sm-Nd and U-Pb systematics in late Caledonian granites and the basement under northern Britain. Nature, v.307, p.229-233.

- HANSON, G.W. , 1978.  
The application of trace elements to the petrogenesis of igneous rocks of granitic composition. *Earth and Planetary Science Letters*, v.38, p.26-43.
- HARRIS, N.B.W. and MARRINER, G.P. , 1980.  
Geochemistry and petrogenesis of a peralkaline granite complex from the Midian Mountains, Saudi Arabia. *Lithos*, v.13, p.325-337.
- HARRIS, N.B.W., PEARCE, J.A. and TINDLE, A.G. , 1984.  
Geochemical characteristics of collision-zone magmatism. In: Coward, M.P., and Reis, A.C.(eds.). *Collision Tectonics*. Geological Society Special Publication 19, p.67-81.
- HAWKESWORTH, C.J., MENZIES, M.A. and van CALSTEREN, P. , 1986.  
Geochemical and tectonic evolution of the Damara Belt, Namibia. In: Coward, M.P. and Reis, A.C. (eds.). *Collision Tectonics*. Geological Society Special Publication 19, p.305-319.
- HAYES, J.P., DICKSON, W.L. and TUACH, J. , 1987.  
Newfoundland granitoid rocks: Map with marginal notes. Newfoundland Dept. Mines and Energy, Mineral Development Division, Open File 87-85.
- HILDRETH, E.W. , 1979.  
The Bishop Tuff: Evidence for the origin of compositional zonation in silicic magma chambers. *Geological Society of America, Special Paper* 180, p.43-76.
- HILDRETH, E.W. , 1981.  
Gradients in silicic magma chambers: Implications for lithospheric magmatism. *Journal of Geophysical Research*, v.B86, p.10153-10192.
- HILDRETH, E.W. , 1987.  
Essay Review: Magmatism at a plate edge. *Tectonophysics*, v.140, p.335-339.
- HILDRETH, E.W and MOORBATH, S. , 1988.  
Crustal contributions to arc magmatism in the Andes of central Chile. *Contributions to Mineralogy and Petrology*, v.98, p.455-489.
- HILL, J.D. , 1982.  
Geology of the Flowers River - Notokwanon River area, Labrador Newfoundland Dept. Mines and Energy, Mineral Development Division Report 82-6, 137 pp.
- HILL, J.D. , 1988.  
Ring-complex features in the Neohelikian Flowers River Igneous Suite, southeastern Main Complex, Labrador. *Geological Association of Canada. Annual Meeting, St.John's, Nfld, 1988. Program with abstracts*, p.A56.
- HILL, J.D. and THOMAS, A. , 1983.  
Correlation of two Helikian peralkaline granite-volcanic centres in central Labrador. *Canadian Journal of Earth Sciences*, v.20, p.753-763.
- HOFFMAN, P.F. , 1973.  
Evolution of an Early Proterozoic continental margin: The Coronation Geosyncline and associated aulacogens of the northwest Canadian Shield. *Philosophical Transactions of the Royal Society of London*, v.A273, p.547-581.

- HOFFMAN, P.F. , 1980.  
The Wopmay Orogen: A Wilson cycle of early Proterozoic age in the north west of the Canadian Shield. In: Strangway, D.W (ed.). The Continental Crust and its Mineral Deposits. Geological Association of Canada, Special Paper 20, p.523-553.
- HOFFMAN, P.F. , 1988.  
United plates of America, the birth of a craton: Early Proterozoic assembly and growth of Proto-Laurentia. Annual Reviews of Earth and Planetary Sciences, v.16, p.543-603.
- HOFFMAN, P.F. , 1989.  
Speculations on Laurentia's first gigayear (2.0 to 1.0 Ga). Geology, v.17, p.135-138.
- HUGHES, C.J. , 1973.  
Spilites, keratophyres and the igneous spectrum. Geological Magazine, v.109, p.513-527.
- HYNES, A. , 1982.  
Stability of the oceanic tectosphere - A model for early Proterozoic intercratonic orogeny. Earth and Planetary Science Letters, v.61, p.333-345.
- HYNES, A. and FRANCIS, D. , 1982.  
Komatiitic basalts of the Cape Smith Fold Belt, New Quebec, Canada. In: Arndt, N.T. and Nisbet, E.G.(eds.). Komatiites. Allen and Unwin, p.159-170.
- IRVINE, T.N. and BARAGAR, W.R. , 1971.  
A guide to the chemical classification of the common volcanic rocks. Canadian Journal of Earth Sciences, v.8, p.523-548.
- JACKSON, N.J. , 1986.  
Petrogenesis and evolution of Arabian felsic plutonic rocks. Journal of African Earth Sciences, v.4, p.47-59.
- JACKSON, N.J., WALSH, J.N. and PEGRAM, E. , 1984.  
Geology, geochemistry and petrogenesis of late Precambrian granitoids in the Central Hijaz region of the Arabian Shield. Contributions to Mineralogy and Petrology, v.87, p.205-219.
- JACOBSEN, S.B. and WASSERBURG, G.J. , 1980.  
Sm-Nd isotopic evolution of chondrites. Earth and Planetary Science Letters, v.50, p.139-155.
- JAKES, P. and WHITE, A.J.R. , 1972.  
Major and trace element abundance in volcanic rocks of orogenic areas. Bulletin of the Geological Society of America, v.83, p.29-39.
- JAMES, R.S. and HAMILTON, D.L. , 1969.  
Phase relations in the system albite-orthoclase-anorthite-quartz at 1 Kilobar water vapour pressure. Contributions to Mineralogy and Petrology, v.21, p.111-141.
- JARL, L.G. and JOHANSSON, A. , 1988.  
U-Pb zircon ages of granitoids from the Smaland-Varmland granite porphyry belt, southern and central Sweden. Geologiska Foreningens i Stockholm Forhandlingar, v.110, p.21-28.
- JENNER, G.A. , 1984.  
Partition coefficients used in trace element modelling. Course notes for Earth Science 6510, Memorial University, St.John's, Newfoundland. Unpublished compilation of data.

- JOHANNSEN, A. , 1920.  
A quantitative mineralogical classification of igneous rocks.  
Journal of Geology, v.28, p.38-60.
- KAY, S.M., RAMOS, V.A., MPOZODIS, C. and SRUOGA, P. , 1989.  
Late Paleozoic to Jurassic silicic magmatism at the Gondwana margin:  
Analogy to the Middle Proterozoic in North America ? Geology, v.17,  
p.324-328.
- KEEN, C.E., WARDLE, R.J., GOWER, C.F., WOODSIDE, J., HALL, J.,  
SRIVASTAVA, S.P. and LOUDEN, K., 1988.  
The Eastern Canadian Shield Offshore Transect (ECSOT). Unpublished  
project proposal to Lithoprobe East, 46 pp.
- KERR, A. , 1986.  
Plutonic rocks of the eastern Central Mineral Belt, Labrador:  
General geology and description of regional granitoid units.  
Newfoundland Dept. Mines and Energy, Mineral Development Division,  
Report 86-1, p.89-100.
- KERR, A. , 1987a.  
Plutonic rocks of the eastern Central Mineral Belt, Labrador:  
Lithogeochemical patterns and the identification of potential  
specialized granitoids. Newfoundland Dept. Mines and Energy, Mineral  
Development Division, Report 87-1, p.15-36.
- KERR, A. , 1987b.  
Geochemistry and mineral potential of evolved granitoid rocks and  
layered mafic intrusions within the Trans-Labrador Batholith,  
eastern Labrador. Newfoundland Dept. Mines and Energy, Mineral  
Development Division, Report of Activities for 1987, p.42-48.
- KERR, A. , 1988.  
Geochemical characteristics and mineral potential of specialized  
granitoid plutons in the Trans-Labrador batholith, eastern Labrador.  
Newfoundland Dept. Mines and Energy, Mineral Development Division,  
Report 88-1, p.15-36.
- KERR, A. , in press.  
Geochemistry of the Trans-Labrador Granitoid Belt, Canada: A  
quantitative comparative study of a Proterozoic batholith and  
possible Phanerozoic counterparts. Precambrian Research, special  
volume from a Proterozoic Geochemistry symposium in Lund, Sweden,  
1987.
- KERR, A. and FRYER, B.J., in press.  
Sources of Early Proterozoic magmas in the Makkovik Province of  
eastern Labrador: Evidence from Nd isotope data. Geological  
Association Of Canada, Special Paper on the Middle Proterozoic  
Evolution of the Laurentian and Baltic Shields.
- KING, A.F. , 1963.  
Geology of the Cape Makkovik peninsula, Aillik, Labrador.  
Unpublished M.Sc. thesis, Memorial University, St.John's,  
Newfoundland, 114 pp.
- KINNAIRD, J and BOWDEN, P. , 1987.  
African anorogenic alkaline magmatism and mineralization: A  
discussion with reference to the Niger-Nigerian province. Geological  
Journal, v.22, p.297-341.
- KORSTGARD, J. and ERMANOVICS, I. , 1985.  
Tectonic evolution of the Hopedale Block and the adjacent Makkovik  
Subprovince, Labrador, Newfoundland. In: Ayres et al.(eds).  
Evolution of Archean Supracrustal Sequences. Geological Association  
of Canada, Special Paper 28, p.223-239.

- KRANCK, E.N. , 1939.  
Bedrock geology of the seaboard region of Newfoundland and Labrador. Geological Survey of Newfoundland, Bulletin 19, 44pp.
- KRANCK, E.N. , 1953.  
Bedrock geology of the seaboard of Labrador between Domino Run and Hopedale, Newfoundland. Geological Survey of Canada, Bulletin 26, 41pp.
- KROGH, T.E. , 1985.  
Determination of U-Pb zircon and sphene ages. Newfoundland Dept. Mines and Energy, Mineral Development Division, Open File LAB (506).
- KROGH, T.E., SCHARER, U., KWOK, Y.Y and KERR, A. , in preparation.  
U-Pb zircon geochronology of Early and Middle Proterozoic plutonic rocks in the Makkovik Province, Labrador, Canada.
- KRONER, A.J.(Editor) , 1981.  
Precambrian plate tectonics. Elsevier, Amsterdam. 782 pp.
- KRONER, A. , 1983.  
Proterozoic mobile belts compatible with the plate tectonic process. In: Medaris, L.G. et al.(eds). Proterozoic Geology. Geological Society Of America, Memoir 161, p.59-75.
- LA ROCHE, H., LETERRIER, J., GRANDCLAUDE, P., and MARCHAL, M. , 1980.  
A classification of volcanic and plutonic rocks using R1-R2 diagrams and major element analyses. Chemical Geology, v.29, p.183-210.
- LAGERBLAD, B., TRAGARDH, J., RIPA, M. and GORBATSCHEV, R. , 1987.  
Bergslagen field excursion guide. IGCP Project 217 (Proterozoic Geochemistry). Lund, Sweden, June 1987. Field trip guide and summary of geology. 68 pp.
- LANORD, C.F. and LeFORT, P. , 1988.  
Crustal melting and granite genesis during the Himalayan collision orogenesis. Transactions of the Royal Society of Edinburgh, Earth Sciences, v.79, p.183-195.
- LeMAITRE, R.W. , 1976.  
The chemical variability of some common igneous rocks. Journal of Petrology, v.17, p.589-637.
- LETERRIER, J., MARCHAL, M., DUBUIT, M. and DREUX, G. , 1983.  
La banque de donnees geochemiques ARTEMISE (analyses roches totales, mineraux, sols et eaux) exemples de valorisation scientifique. Bulletin Societe Geologique de France, v.25, p.697-704.
- LEWRY, J.F. , 1981.  
Lower Proterozoic arc-microcontinent collisional tectonics in the Western Churchill Province. Nature, v.294, p.69-72.
- LEWRY, J.F.; STAUFFER, M.R. and FUMERTON, S. , 1981.  
A Cordilleran-type batholithic belt in the Churchill Province in Northern Saskatchewan. Precambrian Research, v.14, p. 277-313
- LIEBER, O.M. , 1860.  
Notes on the geology of the coast of Labrador. Report of the United States Coastal Survey for 1860, p.402-408.
- LINDH, A. , 1987.  
Westward growth of the Baltic Shield. Precambrian Research, v.35, p.53-70.
- LINTHOUT, K. , 1984.  
Alkali-zirconosilicates in peralkaline rocks. Contributions to Mineralogy and Petrology, v.86, p.155-158.

- LIPMAN, P.W. , 1988.  
Evolution of silicic magma in the upper crust: The mid-Tertiary Latir volcanic field and its cogenetic granitic batholith, northern New Mexico, U.S.A. Transactions of the Royal Society of Edinburgh, Earth Sciences, v.79, p.265-288.
- LOISELLE, M.C., and WONES, D.R. , 1979.  
Characteristics and origin of anorogenic granites. Geological Society of America, programs with abstracts, v.11, p.468.
- LONGERICH, H.L., JACKSON, S.E., JENNER, G.A. and FRYER, B.J.,  
in preparation.  
Inductively coupled plasma mass spectrometric analysis of rocks. Part 1 : Determination of 33 trace elements, including the rare earths, using a standard addition procedure, standardless calibration, and naturally occurring internal standards.
- LOVERIDGE, W.D., ERMANOVICS, I.F., and SULLIVAN, R.W. , 1987.  
U-Pb ages on zircon from the Maggo Gneiss, the Kanairiktok Plutonic Suite and the Island Harbour Plutonic Suite, coast of Labrador, Newfoundland. In: Radiogenic Age and Isotopic Studies; Report 1, Geological Survey of Canada, Paper 87-2, p.59-65.
- LYELL, Charles, Sir , 1885.  
The Student's Elements Of Geology. Fourth Edition, revised. John Murray, London, 621 pp.
- MacDONALD, R. and SMITH, R.L. , 1988.  
Relationships between silicic plutonism and volcanism: geochemical evidence. Transactions of the Royal Society of Edinburgh, Earth Sciences, v.79, p.257-265.
- MACDOUGALL, C.S. , 1988.  
A metallogenic study of polymetallic, granophile mineralization within the Early Proterozoic Upper Aillik Group, Round Pond area, Central Mineral Belt, Labrador. Unpublished M.Sc. Thesis, Memorial University, St.John's, Newfoundland, 187 pp.
- MacDOUGALL, C.S., and WILTON, D.H. , 1987.  
Middle Proterozoic granite-related mineralization in the Round Pond area, Labrador. Geological Survey of Canada, Current Research, Report 87-1A, p.457-466.
- MacDOUGALL, C.S., and WILTON, D.H. , 1988.  
Geology of radioactive zones in the Round Pond area, Labrador. Geological Survey of Canada, Current Research, Report 88-1C, p.271-275.
- MacKENZIE, L.M. , 1988.  
Geology and mineralization of the Burnt Lake area, Central Mineral Belt, Labrador. Unpublished M.Sc. thesis, Memorial University, St.Johns, Newfoundland.
- MacKENZIE, L.M. and WILTON, D.H. , 1987.  
Uranium, molybdenum and base-metal sulphide mineralization in the Burnt Lake area, central Labrador: three different styles of ore formation. Geological Survey of Canada, Current Research, Report 87-1A, p.467-476.
- MacKENZIE, L.M., and WILTON, D.H. , 1988.  
The Grenville Province boundary in the Burnt Lake area, Central Mineral Belt of Labrador. Geological Survey of Canada, Current Research, Report 88-1C, p.233-237.
- MARSH, B.D. , 1988.  
Crystal capture, sorting, and retention in convecting magmas. Bulletin of the Geological Society of America, v.100, p.1720-1737.



- MARTEN, B.E. , 1977.  
The relationship between the Aillik Group and the Hopedale Gneiss Kaipokok Bay, Labrador. Unpublished Ph.D. thesis, Memorial University, St.John's, Newfoundland, 389 pp.
- MARTIN, R.F. and PIWINSKI, A.J. , 1972.  
Magmatism and tectonic settings. Journal of Geophysical Research, v.B77, p.4966-4975.
- MCCARTHY, T.S. and HASTY, R.A. , 1976.  
Trace element distribution patterns and their relationship to the crystallization of granitic melts. Geochimica et Cosmochimica Acta, v.40, p. 1351-1358.
- MCCONNELL, J. , 1986.  
Exploration geochemical studies of Labrador granitoids. Newfoundland Dept. Mines and Energy. Mineral Development Division, Report 86-1, p.219-220.
- MCCULLOCH, M.T., and CHAPPELL, B.W. , 1982.  
Nd isotopic characteristics of S- and I- type granites. Earth and Planetary Science Letters, v.58, p.51-64.
- MCCULLOCH, M.T. and BLACK, L.P. , 1984.  
Sm-Nd systematics of Enderby Land granulites and evidence for the redistribution of Sm and Nd during metamorphism. Earth and Planetary Science Letters, v.71, p.46-58.
- MEDARIS, L.G., BYERS, C.W., MICKELSON, D.M. and SHANKS, W.C. (Editors), 1983.  
Proterozoic Geology: Selected papers from an international Proterozoic symposium. Geological Society Of America, Memoir 161.
- MICHAEL, P.J. , 1983.  
Chemical differentiation of the Bishop Tuff and other high-silica magmas through crystallization processes. Geology, v.11, p.31-34.
- MILLER, C.F. and MITTFELDLT, D.W. , 1982.  
Depletion of light rare-earth elements in felsic magmas. Geology, v.10, p.129-133.
- MITTFELDLT, D.W. and MILLER, C.F. , 1983.  
Geochemistry of the Sweetwater Wash pluton, California : Implications for "anomalous" trace element behaviour during differentiation of felsic magmas. Geochimica et Cosmochimica Acta, v.47, p.109-124.
- MORRISON, G.W. , 1980.  
Characteristics and setting of the shoshonite rock association. Lithos, v.13, p.97-108.
- MULLAN, H.S. and BUSSELL, M.A. , 1977.  
The basic rock series in batholithic associations. Geological Magazine, v.114, p.265-280.
- MUNOZ, J.B. and STERN, C.R. , 1989.  
Alkaline magmatism within the segment 38-39 S of the Plio-Quaternary volcanic belt of the southern South American continental margin. Journal of Geophysical Research, v.B94, p.4545-4560.
- NARANJO, J.A., PUIG, A. and SUAREZ, M. , 1986.  
A note on lower Jurassic magmatism in the coastal cordillera of Atacama, Chile. Geological Magazine, v.123, p.699-702.

- NELSON, B.K. and DePAOLO, D.J. , 1984.  
1700 Myr greenstone volcanic successions in southwestern North America and isotopic evolution of the Proterozoic mantle. *Nature*, v.312, p.143-146.
- NUNN, G.A.G., THOMAS, A. and KROGH, T.E. , 1985.  
The Labradorian Orogeny : Geochronological database. Newfoundland Dept. Mines and Energy, Mineral Development Division, Report 85-1, p.43-54.
- NUNN, G.A. and STAFF, Labrador Section. In preparation.  
1:1,500,000 scale interim geological map of Labrador. Newfoundland Dept. Mines and Energy. Geological Survey Branch. Scheduled for release in 1989 or 1990.
- NURMI, P.A. and HAAVALA, I. , 1986.  
The Proterozoic granitoids of Finland : Granite types, metallogeny and relation to crustal evolution. *Bulletin of the Geological Society of Finland*, v.58, p.203-233.
- NYSTROM, J.O. , 1982.  
Post-Svecokarelian andinotype evolution in Central Sweden. *Geologisches Rundschau*, v.71, p.141-157.
- O'HARA, M.J. , 1977.  
Geochemical evolution during fractional crystallization of a periodically refilled magma chamber. *Nature*, v.266, p.503-507.
- O'NIONS, R.K., CARTER, S.R., EVENSON, N.M. and HAMILTON, P.J. , 1979.  
Geochemical and cosmochemical applications of Nd isotope analysis. *Annual Reviews of Earth and Planetary Science*, v.7, p.11-38.
- OWEN, J.V., RIVERS, T. and GOWER, C.F. , 1986.  
The Grenville Front on the Labrador coast. In: Moore et al., 1986 (eds). *The Grenville Province*. Geological Association of Canada, Special Paper 31, p.95-107.
- OWEN, J.V., DALLMEYER, R.D., GOWER, C.F., and RIVERS, T. , 1988.  
Metamorphic conditions and  $^{40}\text{Ar}/^{39}\text{Ar}$  geochronologic contrasts across the Grenville Front Zone, coastal Labrador, Canada. *Lithos*, v.21, p.13-35.
- PACKARD, A.S. , 1891.  
*The Labrador Coast*. Hodges, New York, 513pp.
- PAGE, R.W. , 1988.  
Geochronology of Early to Middle Proterozoic fold belts in northern Australia: A review. *Precambrian Research*, v.41, p.1-19.
- PALLISTER, J.S., STACEY, J.S., FISCHER, L.B. and PREMOS, W.R. , 1987.  
Arabian Shield ophiolites and Late Proterozoic microplate accretion. *Geology*, v.15, p.320-323.
- PANKHURST, R.J., HOLE, M.J. and BROOK, M. , 1988.  
Isotopic evidence for the origin of Andean granites. *Transactions of the Royal Society of Edinburgh, Earth Sciences*, v.79, p.123-133.
- PATCHETT, P.J. and BRIDGWATER, D. , 1984.  
Origin of continental crust of 1.9-1.7 Ga age defined by Nd isotopes in the Ketilidian terrain of South Greenland. *Contributions to Mineralogy and Petrology*, v.87, p.311-318.
- PATCHETT, P.J. and ARNDT, N.T. , 1986.  
Nd isotopes and tectonics of 1.9-1.7 Ga crustal genesis. *Earth and Planetary Science Letters*, v.78, p.329-338.

- PATCHETT, P.J. and KOUVO, O. , 1986.  
Origin of continental crust of 1.9-1.7 Ga age: Nd isotopes and U-Pb zircon ages in the Svecokarelian terrain of South Finland. Contributions to Mineralogy and Petrology, v.92, p.1-12.
- PATERSON, S.R. and TOBISCH, O.T , 1988.  
Using pluton ages to date regional deformations: Problems with commonly used criteria. Geology, v.16, p.1108-1111.
- PAYETTE, C. and MARTIN, R.F. , 1986.  
The glass inclusions and mineralogy of rhyolites, Upper Aillik Group, Labrador. Unpublished report to the Geological Survey of Canada, 98 pp.
- PEACOCK, M.A. , 1931.  
Classification of igneous rock series. Journal of Geology, v.39, p.54-67.
- PEARCE, J.A. and CANN, J.R. , 1973.  
Tectonic setting of basic volcanic rocks investigated using trace element analyses. Earth and Planetary Science Letters, v.19, p.290-300.
- PEARCE, J.A., HARRIS, N.B.W. and TINDLE, A.G. , 1984.  
Trace element discrimination diagrams for the tectonic interpretation of granitic rocks. Journal of Petrology, v.25, p.956-974.
- PETRO, W.L., VOGEL, T.A. and WILBRAND, J.T. , 1979.  
Major element chemistry of plutonic rock suites from compressional and extensional plate boundaries. Chemical Geology, v.26, p.217-235.
- PHAROAH, T.C., BECKINSALE, R.D. and RICKARD, D. (editors) , 1987.  
Geochemistry and Mineralization of Proterozoic Volcanic Suites. Geological Society Special Publication 33, 560 pp.
- PIPER, J.D.A. , 1983.  
Dynamics of the continental crust in Proterozoic times. In: Medaris et al.(Eds.). Proterozoic Geology. Geological Society of America, Memoir 161, p.11-35.
- PITCHER, W.S. , 1977.  
The anatomy of a batholith. Journal of the Geological Society of London, v.135, p.157-182.
- PITCHER, W.S , 1983.  
Granite type and tectonic environment. In: Hsu, K.(ed), Mountain Building Processes, Academic Press, London, p.19-44.
- PITCHER, W.S. and BERGER, A.R. , 1972.  
The geology of Donegal: A study of granite emplacement and unroofing. Wiley, New York, 435 pp.
- PITCHER, W.S., ATHERTON, M.P., COBBING, E.J. and BECKINSALE, R.D. , 1985.  
Magmatism at a Plate Edge: The Peruvian Andes. Wiley, New York. 330 pp.
- PRATT, T. and Numerous Others , 1988.  
COCORP profiling of the midcontinent of North America: Overview and Proterozoic layered rocks. EOS (American Geophysical Union Transactions), v.69, p.496.

- PUSHKAR, P., McBIRNEY, A.R. and KUDO, A.M. , 1972.  
The isotopic composition of Sr in Central American ignimbrites.  
Bulletin Volcanologique, v.35, p.265-294.
- RAMOS, V.A. , 1988.  
~~late Proterozoic~~ Early Paleozoic of South America - A collisional
- RAMOS, V.A., JORDAN, T.E., ALLMENDINGER, R.W., MPOZODIS, C., KAY, S.M.,  
CORTES, J.M. and PALMA, M., 1986.  
Paleozoic terranes of the central Argentine-Chilean Andes.  
Tectonics, v.5, p.855-880.
- RAPELA, C.W. and KAY, S.M. , 1988.  
Late Paleozoic to recent magmatic evolution of northern Patagonia.  
Episodes, v.11, p.175-181.
- READ, H.H. and WATSON, J., 1975.  
Later Stages in Earth History. MacMillan Press, London, 371 pp.
- REYMER, A. and SCHUBERT, G. , 1986.  
Rapid growth of some major segments of continental crust. Geology,  
v.14, p.299-302.
- RICE, A. , 1981.  
Convective fractionation: A mechanism to provide cryptic zoning  
(macrosegregation), layering, crescumulates, banded tuffs and  
explosive volcanism in igneous processes. Journal of Geophysical  
Research, v.B86, p.405-417.
- RYAN, A.B. , 1984.  
Regional geology of the central part of the Central Mineral belt,  
Labrador. Newfoundland Dept. Mines and Energy, Mineral Development  
Division, Memoir 3, 185 pp.
- RYAN, A.B. and HARRIS, A. , 1978.  
Geology of the Otter-Nipishish-Stipec Lakes area, Labrador.  
Newfoundland Dept. Mines and Energy, Mineral Development Division,  
Report 78-1, p. 63-70.
- RYAN, A.B. and KAY, A. , 1982.  
Basement-cover relationships and plutonic rocks in the Makkovik  
subprovince, north of Postville, coastal Labrador. Newfoundland  
Dept. Mines and Energy, Mineral Development Division, Report 82-1,  
p. 109-121.
- RYAN, A.B., KAY, A. and ERMANOVICS, I. , 1983.  
The geology of the Makkovik Subprovince between Kaipokok Bay and Bay  
of Islands, Labrador. Newfoundland Dept. Mines and Energy, Mineral  
Development Division, Maps 83-38 and 83-41 (notes), 21 pp.
- RYAN, A.B., BARAGAR, W.R.A., and KONTAK, D.J. , 1987.  
Geochemistry, tectonic setting and mineralization of high-potassium  
middle Proterozoic rocks in central Labrador, Canada. In: Pharoah et  
al.(eds.). Geochemistry and Mineralization of Proterozoic Volcanic  
Suites. Geological Society Special Publication 33, p.241-254.
- SALVADOR, A., (Chairman) , 1987.  
Stratigraphic classification and nomenclature of igneous and  
metamorphic rock bodies. Bulletin of the Geological Society of  
America, v.99, p.440-442.
- SAUNDERS, A.D, TARNEY, J., MARSH, N.G. and WOOD, D.A. , 1979.  
Ophiolites as ocean crust or marginal basin crust : A geochemical  
approach. Proceedings of an International Ophiolite Symposium.  
Geological Survey of Cyprus. p. 193-205.

- SCHÄRER, U. , 1988.  
Origin and evolution of Proterozoic crust in eastern Labrador.  
Geological Association of Canada. Annual Meeting, St. John's.  
Program with abstracts, v.13, p.A109.
- SCHÄRER, U., and GOWER, C.F., 1988.  
Crustal evolution in eastern Labrador: constraints from precise U-Pb  
ages. Precambrian Research, v.38, p.405-421.
- SCHÄRER, U., KROGH, T.E. and GOWER, C.F. , 1986.  
Age and Evolution of the Grenville Province in eastern Labrador from  
U-Pb systematics in accessory minerals. Contributions to Mineralogy  
and Petrology, v.94, p.428-451.
- SCHÄRER, U., KROGH, T.Z., WARDLE, R.J., RYAN, A.B. and GANDHI, S.S. ,  
1988.  
U-Pb ages of Early and Middle Proterozoic volcanism and metamorphism  
in the Makkovik Orogen, Labrador. Canadian Journal of Earth  
Sciences, v.25, p.1098-1107.
- SCOTT, D.J., ST-ONGE, M.R., LUCAS, S.B. and HAELMSTEDT, H. , 1989.  
The 2.00 Ga Purtiniq ophiolite: imbricated and metamorphosed oceanic  
crust in the Cape Smith thrust-fold belt, New Quebec. Geological  
Association of Canada, Annual Meeting, Montreal, 1989. Programs with  
abstracts, v.14, p.A57.
- SEARLE, M.P. and FRYER, B.J. , 1988.  
Garnet, tourmaline and muscovite-bearing leucogranites, gneisses  
and migmatites of the higher Himalayas from Zaskar, Kulu, Lahoul  
and Kashmir. In; Coward, M.P. and Reis, A.C. (Eds.). Collision  
Tectonics. Geological Society Special Publication 19, p.185-201.
- SHAND, S.J. , 1927.  
Eruptive Rocks. Thomas Murby and Co., London, 360 pp.
- SILVER, L.T. and CHAPPELL, B.W. , 1988.  
The Peninsular Ranges Batholith : an insight into the evolution of  
the Cordilleran batholiths of southwestern North America.  
Transactions of the Royal Society of Edinburgh, Earth Sciences,  
v.79, p.105-121.
- SIMS, P.K., KISVARSAANYI, E.B. and MOREY, G.B. , 1987.  
Geology and metallogeny of Archean and Proterozoic basement terranes  
in the northern midcontinent U.S.A.: An overview. United States  
Geological Survey, Bulletin 1815, 51 pp.
- SLOMAN, L.E. , 1989.  
Triassic shoshonites from the Dolomites, northern Italy: Alkaline  
arc rocks in a strike-slip setting. Journal of Geophysical Research,  
v.B94, p.4655-4666.
- SMYTH, W.R., MARTEN, B.E. and RYAN, A.B. , 1978.  
A major Aphebian - Helikian unconformity within the Central Mineral  
Belt of Labrador: Definition of new groups and metallogenic  
implications. Canadian Journal of Earth Sciences, v.15, p.1954-1966.
- SPARKS, R.S.J. , 1986.  
The role of crustal contamination in magma evolution through  
geological time. Earth and Planetary Science Letters, v.78,  
p.211-223.
- STEIGER, R.H. and JAGER, E. , 1977.  
Subcommission on geochronology: convention on the use of decay  
constants in geochronology and cosmochronology. Earth and Planetary  
Science Letters, v.36, p.359-362.

- STEINHAEUER, H. , 1814.  
Notes on the geology of the Labrador coast. Transactions of the Geological Society, v.2, p.486-491.
- STEVENSON, I.M. , 1970.  
Rigolet and Groswater Bay areas, Newfoundland (Labrador). Geological Survey of Canada, Paper 69-49, 24 pp.
- STEVENSON, R.K. and PATCHETT, P.J. , 1988.  
Nd isotopic data for Archean granitoids in the Portman Lake area, Northwest Territories, Canada. Geological Association of Canada, Annual Meeting, St. John's, 1988. Program with abstracts, p. A118.
- STEWART, D.B. , 1959.  
Rapakivi granite from eastern Penobscot Bay, Maine. Proceedings of the 20th International Geological Congress, Mexico City. Petrology and Geochemistry, p.293-320.
- STOCKWELL, C.H. , 1972.  
Revised Precambrian time scale for the Canadian Shield. Geological Survey of Canada, Paper 72-52, 4 pp.
- STOESER, D.B. , 1986.  
Distribution and tectonic setting of plutonic rocks of the Arabian Shield. Journal of African Earth Sciences, v.4, p.21-46.
- STOESER, D.B. and CAMP, V.E. , 1985.  
Pan-African microplate accretion of the Arabian Shield. Bulletin of the Geological Society of America, v.96, p.817-826.
- STRECKEISEN, A.L. , 1976.  
To each plutonic rock its proper name. Earth Science Reviews, v.12, p.1-33.
- STRECKEISEN, A.L. and LEMAITRE, R.W. , 1979.  
Chemical approximation to modal QAPF classification of the igneous rocks. Neues Jahrbuch Mineral Abn, v.136, p. 169-206.
- STRONG, D.F. , 1980.  
Granitoid rocks and associated mineral deposits of eastern Canada and western Europe. In: Strangway, D.W.(Ed.). The Continental Crust and its Mineral Deposits. Geological Association of Canada, Special Paper 20, p.741-771.
- STRONG, D.F. , 1981.  
Ore deposit models : A model for granophile mineral deposits. Geoscience Canada, v.8, p.154-161.
- STRONG, D.F., DICKSON, W.L., O'DRISCOLL, C.F. and KEAN, B.F. , 1974.  
Geochemistry of eastern Newfoundland granitoid rocks. Newfoundland Dept. Mines and Energy, Mineral Development Division, Report 74-3, 140 pp.
- SUTTON, J. , 1963.  
Long-term cycles in the evolution of continents. Nature, v.198, p.731-735.
- SUTTON, J.S. , 1972.  
The Precambrian gneisses and supracrustal rocks of the western shore of Kaipokok Bay, Labrador. Canadian Journal of Earth Sciences, v.9, p.1677-1692.
- SYLVESTER, P.J. , 1989.  
Post-collisional alkaline granites. Journal of Geology, v.97, p.261-280.

- TATSUMI, Y. , 1989.  
Migration of fluid phases and genesis of basalt magmas in subduction zones. *Journal of Geophysical Research*, v.B94, p.4697-4707.
- TAYLOR, F.C. , 1975.  
Geology, Makkovik area. Geological Survey of Canada, Map 1444A.
- TAYLOR, R.P and FRYER, B.J. , 1982.  
Rare Earth Element geochemistry as an aid to interpreting hydrothermal ore deposits. In: Evans, A.M. (ed.). *Metallization Associated With Acid Magmatism*. Wiley, London. p.357-365.
- TAYLOR, S.R. and MCCLENNAN, S.M. , 1985.  
The Continental Crust: its Composition and Evolution. An Examination of the Geochemical Record Preserved in Sedimentary Rocks. Blackwell Scientific Publications. 312 pp.
- THIRLWALL, M.F. , 1982.  
Systematic variation in chemistry and Nd-Sr isotopes across a Caledonian calc-alkaline volcanic arc: implications for source materials. *Earth and Planetary Science Letters*, v.58, p.27-50.
- THOMAS, A. , NUNN, G. and WARDLE, R.J. , 1985.  
A 1650 Ma orogenic belt within the Grenville Province of north-eastern Canada. In: Tobi, A. and Touret, L.(eds): *The deep Proterozoic crust in the north Atlantic provinces*. NATO ASI series, v.158, p.151-161.
- THOMAS, A. , NUNN, G.A.G., and KROGH, T.E. , 1986.  
The Labradorian Orogeny: Evidence for a newly identified 1600 to 1700 Ma orogenic event in Grenville Province crystalline rocks from Central Labrador. In: Moore et al., 1986 (eds). *The Grenville Province*. Geological Association of Canada, Special Paper 31, p.175-189.
- TUACH, J., DAVENPORT, P.H., DICKSON, W.L. and STRONG, D.F. , 1986.  
Geochemical trends in the Ackley Granite, southeast Newfoundland: Their relevance to magmatic metallogenic processes in high-silica granitoid systems. *Canadian Journal of Earth Sciences*, v.23, p.747-765.
- TUTTLE, O.F. and BOWEN, N.L. , 1958.  
Origin of granite in the light of experimental studies in the system  $\text{NaAlSi}_3\text{O}_8\text{-KAlSi}_3\text{O}_8\text{-SiO}_2\text{-H}_2\text{O}$ . Geological Society of America, Memoir 74, 153 pp.
- VAN SCHMUS, W.R. and BICKFORD, M.E. , 1981.  
Proterozoic chronology and evolution of the midcontinent region of North America. In: Kroner, A. (ed). *Precambrian Plate Tectonics*, p.261-296. Elsevier, Amsterdam.
- VIDAL, P., COCHERIE, A. and LeFORT, P. , 1982.  
Geochemical investigations of the origin of the Manaslu leucogranite (Himalaya, Nepal). *Geochimica et Cosmochimica Acta*, v.64, p.2274-2292.
- VILLEMANT, B., JAFFREZIC, H., JORON, J-L., and TREUIL, M. , 1981.  
Distribution coefficients of major and trace elements, fractional crystallization in the alkali-basalt series of Chaîne des Puys, Massif Central, France. *Geochimica et Cosmochimica Acta*, v.45, p.1997-2016.
- VORMA, A. , 1976.  
The petrology of rapakivi granites with special reference to the Laitila massif, southwest Finland. Geological Survey of Finland, Bulletin 285, 98 pp.

- WAGENBAUER, H.A. , 1988.  
Report of the geochemical laboratory for 1988. Newfoundland Dept. Mines and Energy, Mineral Development Division, Report of Activities for 1988, p.123-124.
- WAGENBAUER, H.A., RILEY, C.A., and DAWE, G. , 1983.  
Geochemical laboratory report. Newfoundland Dept. Mines and Energy, Mineral Development Division, Report 83-1, p.133-137.
- WALL, W.J., CLEMENS, J.D. and CLARKE, D.B. , 1987.  
Models for granitoid evolution and source compositions. Journal of Geology, v.95, p.731-749.
- WALRAVEN, F. KLEEMAN, G.J. and ALLSOPP, H.L. , 1986.  
Disturbance of trace element and isotopic systems and its bearing on mineralization in acid rocks of the Bushveld Complex, South Africa. In: High Heat Production Granites. Institute of Mining and Metallurgy, Conference Proceedings, St.Austell, U.K., September, 1985, p.393-408.
- WANLESS, R.K. and LOVERIDGE, W.D. , 1972.  
Rubidium-strontium isotopic studies, report 1. Geological Survey of Canada, Paper 72-23, p.57-59.
- WANLESS, R.K., STEVENS, R.D., LACHANCE, G.R. and DELABIO, R.N. , 1970.  
Age determinations and geological studies, K-Ar isotopic ages, Report 9. Geological Survey of Canada, Paper 69-2A, p.73-74.
- WARDLE, R.J. , 1984.  
Geological fieldwork in the lower Proterozoic Aillik Group, eastern Labrador. Newfoundland Dept. Mines and Energy, Mineral Development Division, Report of activities for 1984, p.14-18.
- WARDLE, R.J. and BAILEY, D.G. , 1981.  
Early Proterozoic sequences in Labrador. In: Campbell, F.H.A. (ed.): Proterozoic Basins of Canada. Geological Survey of Canada, Special Paper 81-10, p.331-359.
- WARDLE, R.J. AND Staff, Labrador Section. , 1982.  
The Trans-Labrador batholith: A major pre-Grenvillian feature of the eastern Grenville Province. Ottawa-Carleton Centre for Geoscience Studies. Grenville Workshop, 1982, Program with abstracts. p.11.
- WARDLE, R.J. and WILTON, D.H.C. , 1984.  
Reconnaissance sampling for precious metals in the Kaipokok Bay - Big River area, Labrador. Newfoundland Dept. Mines and Energy, Mineral Development Division, Open File Report LAB(1679), 17 pp.
- WARDLE, R.J., RIVERS, T., GOWER, C.F., NUNN, G.A.G. and THOMAS, A. , 1986.  
The northeastern Grenville Province : New insights. In: Moore et al., 1986 (Eds). The Grenville Province. Geological Association of Canada, Special Paper 31, p.13-29.
- WARDLE, R.J., RYAN, B., NUNN, G.A. and MENGEL, F. in press.  
Labrador segment of the Trans-Hudson Orogen: Crustal development through oblique convergence and collision. Geological Association of Canada. Special paper on the evolution of the Trans-Hudson Orogen.
- WATSON, E.B. , 1982.  
Zircon saturation in felsic liquids: Experimental results and applications to trace element geochemistry. Contributions to Mineralogy and Petrology, v.70, p. 407-419.



- WHALEN, J.B., CURRIE, K.L. and CHAPPELL, B.W. , 1987.  
A-type granites : geochemical characteristics, discrimination and petrogenesis. Contributions to Mineralogy and Petrology, v.95, p.407-419.
- WHALEN, J.B., CURRIE, K.L. and CHAPPELL, B.W. , 1987b.  
A-type granites: descriptive and geochemical data. Geological Survey of Canada, Open File Report 1411, 33 pp.
- WHITE, A.J. and CHAPPELL, B.W. , 1977.  
Ultrametamorphism and granitoid genesis. Tectonophysics, v.43, 7-22.
- WHITE, A.J. and CHAPPELL, B.W. , 1983.  
Granitoid types and their distribution in the Lachlan Fold Belt, southeastern Australia. In: Roddick, J.A.(ed.). Circum-Pacific Plutonic Terranes. Geological Society of America, memoir 159, p.21-34.
- WHITE, M.V.W. , 1976.  
A petrological study of acid volcanic rocks of the Aillik series, Labrador. Unpublished M.Sc. Thesis, McGill University, Montreal, 92 pp.
- WHITE, M.V. and MARTIN, R.F. , 1980.  
The metasomatic changes that accompany mineralization in the non-orogenic rhyolites of the upper Aillik Group, Labrador. Canadian Mineralogist, v.18, p.459-479.
- WHITE, W.M., and PATCHETT, P.J. , 1984.  
Hf-Nd-Sr isotopes and incompatible element abundances in island arcs: implications for magma origins and crust-mantle evolution. Earth and Planetary Science Letters, v.67, p. 167-185.
- WHITNEY, J.A. , 1988.  
The origin of granite : The role and source of water in the evolution of granitic magmas. Bulletin of the Geological Society of America, v.100, p.1886-1897.
- WILLIAMS, H., DICKSON, W.L., CURRIE, K.L., HAYES, J.P. and TUACH, J. , 1989.  
Preliminary report on classification of Newfoundland granitic rocks and their relations to tectonostratigraphic zones and lower crustal blocks. Geological Survey of Canada, Current Research, Paper 89-1B, p.47-53.
- WILSON, M.R., HAMILTON, P.J., FALLICK, A., APTALION, M. and MICHARD, A. , 1985.  
Granites and Early Proterozoic crustal evolution in Sweden: Evidence from Sm-Nd, U-Pb and O isotope systematics. Earth and Planetary Science Letters, v.72, p.376-388.
- WILTON, D.H. and WARDLE, R.J. , 1987.  
Two contrasting granophile and non-granophile metallogenic styles in the Early Proterozoic Upper Aillik Group, Central Mineral Belt, Labrador. Mineralium Deposita, v.22, p. 198-206.
- WILTON, D.H.C., MACDOUGALL, C.M. and MACKENZIE, L.M. , 1986.  
Final report on 1985 field work in the Central Mineral Belt of Labrador. Geological Survey of Canada, unpublished internal report, 98 pp.
- WILTON, D.H.C. , MACDOUGALL, C.S., MACKENZIE, L.M. and NORTH, J.W. , 1987.  
Final report on 1986 field work in the Central Mineral Belt of Labrador. Geological Survey of Canada, unpublished internal report, 121 pp.

WINDLEY, B.F. , 1977.

The Evolving Continents. Wiley, London. 385 pp.

WINDLEY, B.F. , 1983.

A tectonic review of the Proterozoic. In: Medaris, L.G. et al. (eds). Proterozoic Geology. Geological Society Of America, Memoir 161, p.1-11.

WINDRIM, D.P., MCCULLOCH, M.T., CHAPPELL, B.W. and CAMERON, W.E. , 1984.

Nd and Sr isotopes and REE in central Australian sapphirine granulites: a case study of rare earth element mobility. Earth and Planetary Science Letters, v.70, p.27-41.

WOODEN, J.L. and MUELLER, P.A. , 1988.

Pb, Sr and Nd isotopic compositions of a suite of Late Archean igneous rocks, eastern Beartooth Mountains. Implications for crust-mantle evolution. Earth and Planetary Science Letters, v.87, p.59-72.

WRIGHT, A.E. and BOWES, D.R. , 1979.

Geochemistry of the appinite suite. In: Harris, A.L. et al. (eds.). The Caledonides of the British Isles - Reviewed. Geological Society Special Publication 8, p.699-704.

WYBORN, L.A. , 1988.

Petrology, geochemistry and origin of a major Australian 1880 - 1840 Ma felsic volcano-plutonic suite: A model for intracontinental felsic magma generation. Precambrian Research, v.41, p.37-60.

WYBORN, L.A., PAGE, R.W., and PARKER, A.J. , 1987.

Geochemical and geochronological signatures in Australian Proterozoic igneous rocks. In: Pharoah et al., (Eds.): Geochemistry and Mineralization Of Proterozoic Volcanic Suites. Geological Society Special Publication 33, p.377-394.

WYLLIE, P.J. , 1964.

Sources of granitoid magmas at convergent plate boundaries. Physics of the Earth and Planetary Interiors, v.35, p.12-18.

YORK, D. , 1969.

Least squares fitting of a straight line with correlated errors. Canadian Journal of Earth Sciences, v.5, p.320-324.

## APPENDICES

### APPENDIX A : METHODS AND PROCEDURES

#### A1. SAMPLE COLLECTION AND PREPARATION

**Site Selection** : The regional sampling program used preselected sample sites (after Dickson, 1983), based on a 2 x 2 km grid cell network constructed from the Universal Transverse Mercator (UTM) grid superimposed on National Topographic System (NTS) 1:50,000 scale maps. Each cell was subdivided into 16 sub-cells, one of which was selected on a random basis for the sample site. Where a 2 x 2 km grid cell straddled a geological contact indicated on existing maps, sites were selected on both sides of the contact. Follow-up sampling employed a similar method, but used 1 x 1 km primary cells.

Samples were collected as close as possible to the preselected site, subject to outcrop availability and topography. If outcrops contained more than one rock type, both were noted and sampled. Sites for "geological" samples collected during mapping were chosen on the basis of lithology or field relationships, as is normal in mapping.

**Field Procedures** : Weathered material was removed and discarded on outcrop, and 2 to 5 kg of fresh material was reduced to fragments small enough for direct input to the jaw crusher (< 5 cm maximum dimension). Material for hand samples and thin sections was set aside. About half

the samples were thin-sectioned, and most were slabbed, etched with HF, and stained for K-feldspar with a saturated sodium dichromate solution. This turns K-feldspar yellow, and alters plagioclase to a white colour. Quartz is unaffected. All hand samples depicted in plates have been processed in this manner.

**Sample Processing** : All samples were processed at the Department of Mines laboratory in St. John's. Each was reduced to a fine gravel using a jaw crusher, which was cleaned between samples. About 20-30 grams of this material was reduced to powder using a ceramic disk and ring grinder (to minimize contamination by tungsten) and stored in a clean medicine vial. The ceramic grinder was cleaned between runs with pure  $\text{SiO}_2$  sand, distilled water and acetone.

## A2. MAJOR AND TRACE ELEMENT ANALYSIS PROCEDURES

### A2.1 Assessment of Geochemical Analysis Program

**Precision** : Precision of analysis was assessed using blind duplicates. At the Department of Mines laboratory, 1 analysis in 20 was a duplicate, split prior to grinding. "Precision" is defined as :

$$\text{PRECISION } (\pm \%) = 100 \times \frac{\text{absolute value } (V_1 - V_2)}{\text{mean value of } (V_1, V_2)}$$

( $V_1$  and  $V_2$  are duplicate determinations of a sample).

At low abundance levels, precision is worse (i.e.,  $\pm$  a higher percentage) than at high values. Mean precision is thus strongly influenced by outlying values at or near detection limits, and the median (50th percentile) value is preferred here as an assessment of "average" precision in analysis.

**Detection Limit** : Detection limits quoted for the Department of Mines laboratory are concentration values at which precision is approximately  $\pm$  100%. These are based on blind duplicates measured over several years from all rock types (Wagenbauer et al., 1983; Wagenbauer, 1988).

**Accuracy** : At the Department of Mines laboratory, 1 sample in 20 is either an internal or international standard. Repeated determinations conducted during this project were compared with recommended values quoted by Abbey (1979, 1983). Recommended values for internal standards are based on measurements over several years by different methods.

## **A2.2 Department of Mines Analysis Program**

### **Laboratory Procedures**

Laboratory procedures at the Department of Mines laboratory are described in detail by Wagenbauer et al. (1983). About 0.1 g of sample was fused with lithium metaborate and taken into solution via HCl-HF digestion for major element and Zr analysis.

About 1 g of sample was taken into solution via a HF-HCl-HClO<sub>4</sub> digestion for trace element analysis

Variable	Lab.	Analytical Method	Detection Limit	Mean Value	Range	Number of Analyses*	Number of Duplicates	PRECISION (+/- %)	
								Mean	Median
Oxide (wt%)									
SiO2	N.D.M	AAS	0.07	67.42	39.25 - 88.45	1489	73	0.57%	0.38%
TiO2	N.D.M	AAS	0.01	0.48	0.01 - 2.77	1489	73	8.37%	4.35%
Al2O3	N.D.M	AAS	0.01	14.53	4.60 - 25.40	1489	73	1.06%	0.87%
Fe2O3	N.D.M	AAS	0.01	1.45	0.00 - 27.39	1489	73	10.39%	6.54%
FeO	N.D.M	Titration	0.01	2.32	0.01 - 14.04	1481	73	9.16%	3.96%
MnO	N.D.M	AAS	0.01	0.08	0.01 - 0.45	1489	73	5.92%	0.00%
MgO	N.D.M	AAS	0.01	1.35	0.01 - 28.02	1489	73	9.69%	2.30%
CaO	N.D.M	AAS	0.01	2.44	0.01 - 16.20	1489	73	4.17%	1.46%
Na2O	N.D.M	AAS	0.01	4.10	0.15 - 10.90	1489	73	1.45%	0.79%
K2O	N.D.M	AAS	0.01	4.52	0.06 - 12.06	1489	73	4.22%	1.01%
P2O5	N.D.M	AAS	0.01	0.13	0.01 - 2.26	1489	73	12.86%	4.65%
LOI	N.D.M	Oven Drying	n/a	0.71	0.02 - 6.02	1485	73	13.70%	7.02%
Element (ppm)									
Li	N.D.M	AAS	5	21.0	1 - 286	1491	73	13.29%	8.22%
F	N.D.M	ISE	30	866.5	11 - 9968	1487	52	15.51%	9.38%
Sc	Becquerel	INAA	0.1	4.5	0.2 - 75.0	529	23	22.14%	9.52%
V	N.D.M	AAS	20	49.7	1 - 705	1494	73	25.52%	15.40%
Cr	N.D.M	AAS	1	34.3	1 - 1840	1491	73	20.39%	5.70%
Ni	N.D.M	AAS	1	10.3	1 - 823	1491	73	18.86%	0.00%
Cu	N.D.M	AAS	1	15.1	1 - 809	1491	73	7.41%	0.00%
Zn	N.D.M	AAS	1	70.0	1 - 527	1491	73	3.69%	2.53%
Ga	N.D.M	ICP-ES	1	15.9	1 - 71	1490	74	5.26%	4.44%
Rb	N.D.M	AAS	5	144.5	1 - 1250	1491	73	6.69%	2.84%
Sr	N.D.M	AAS	2	250.8	2 - 1930	1490	73	5.76%	1.90%
Y	N.D.M	ICP-ES	1	40.9	2 - 381	1490	74	3.90%	3.45%
Zr	N.D.M	ICP-ES	1	229.4	11 - 2880	1490	74	6.24%	4.44%
Nb	N.D.M	ICP-ES	1	19.0	1 - 249	1490	74	7.00%	3.64%
Mo	N.D.M	AAS	2	8.3	1 - 4752	1491	73	19.60%	0.00%
Sn	B-C	XRF-ES	1	4.4	1 - 116	529	23	73.29%	66.67%
Cs	Becquerel	NAA	0.5	2.42	0.5 - 32.0	529	23	26.41%	5.97%
Ba	N.D.M	AAS	30	690.8	6 - 5140	1491	73	9.14%	3.13%
La	N.D.M	ICP-ES	1	59.3	1 - 1312	1490	74	5.26%	4.65%
Ce	N.D.M	ICP-ES	2	119.7	1 - 2226	1490	74	5.46%	4.06%
Sm	Becquerel	NAA	0.1	11.3	0.1 - 113.0	529	23	7.44%	4.26%
Yb	Becquerel	NAA	0.5	5.6	3.0 - 36.0	529	23	14.85%	4.00%
Hf	Becquerel	NAA	1.0	11.5	1.0 - 150.0	529	23	24.76%	12.24%
Pb	N.D.M	AAS	2	20.1	1 - 2900	1491	73	6.19%	5.13%
Th	N.D.M	ICP-ES	1	13.3	1 - 163	1490	74	27.85%	13.33%
U	N.A.S	NAA	0.2	4.5	0.1 - 74.7	1491	52	9.20%	6.45%
ANALYSTS :						ANALYTICAL METHODS :			
N.D.M --- Newfoundland Department of Mines, St. John's.						AAS --- Atomic Absorption Spectrophotometry			
N.A.S --- Nuclear Activation Services, Hamilton.						ICP-ES --- Inductively-Coupled Plasma Emission Spectrometry			
Becquerel --- Becquerel Laboratories, Mississauga						INAA --- Instrumental Neutron Activation Analysis			
B-C --- Bondar-Clegg and Co. Ltd., Ottawa.						ISE --- Ion-Selective Electrode			
						XRF-ES --- X-Ray Fluorescence Emission Spectrometry			

Table A.1. Abundance levels, detection limits and estimates of precision for major and trace elements determined at, or via, the Department of Mines laboratory.

(excluding Zr and F). About 0.25 g of sample was fused with  $\text{Na}_2\text{CO}_3$  -  $\text{KNO}_3$  flux, and taken into solution with citric acid for fluorine analysis. Loss on ignition (LOI) was determined after heating a portion of the sample powder to  $1000^\circ\text{C}$  in a muffle furnace. Separate aliquots of sample powder were weighed and sent out for external analysis of selected trace elements (see below).

### **Analytical Methods**

**Major Elements** : These were determined by atomic absorption spectrophotometry (AAS), using standard solutions supplied by CANLAB Ltd. Ferrous iron was determined by addition of vanadium, followed by titration using standard potassium dichromate solutions. Details are supplied by Wagenbauer et al.(1983)

**Li, V, Cr, Ni, Cu, Zn, Rb, Sr, Ba and Pb** : These elements were determined by AAS, as described above. Details of procedures are supplied by Wagenbauer et al.(1983).

**Ga, Y, Zr, Nb, La, Ce and Th** : These elements were determined by inductively-coupled plasma emission spectroscopy (ICP-ES) using an ARL 3520 sequential spectrometer, and standard solutions supplied by SPEX Industries Ltd. Note that Zr was analyzed on solutions from the major element fusion.

**Fluorine** : This element was determined via ion-selective electrode (ISE) analysis using a digital ion-analyzer, and standard solutions supplied by CANLAB Ltd.

**Uranium** : This element was determined externally by Nuclear Activation Services Ltd, via neutron activation analysis (NAA). About 2 g of each sample was irradiated.

**Sc, Cs, Sm, Yb and Hf** : These elements were determined externally in selected samples by Becquerel Laboratories, using standard NAA methods. This forms part of the "gold+33" commercial package. About 10 g of each sample was irradiated. A range of other elements determined via this method are not reported here because of low and imprecise abundances, or because they duplicate data obtained by other methods.

**Tin** : This element was determined in selected samples by Bondar-Clegg Incorporated, via wavelength-dispersive X-Ray fluorescence (XRF) analysis, on a pellet containing about 5 g of sample.

#### **Precision and Detection Limits**

Table A.1 lists relevant information for all elements determined at or via the Department of Mines laboratory. Detection limits for Sn (1 ppm) are those quoted by the analyst; all others are based on multiple determinations over several years (see above). Detection limits for Sc, Cs, Sm, Yb and Hf are based on a survey by Davenport (pers. comm., 1988) using lake sediment samples, and are generally higher than limits quoted by the analyst.

The median (50th percentile) value is the preferred estimate of analytical precision. For elements with generally low abundances (e.g. V), poor mean precision results from many determinations at or near detection



Table A.2. Mean analyses of the international standards MRG-1, SY-2 and GSP-1 by the Department of Mines laboratory, compared to recommended values of Abbey (1979, 1983).

STD:	SY-2			MRG-1			GSP-1		
MAJOR ELEMENTS (wt% Oxide)									
	Mean n=3	S.D.	R.V.	Mean n=3	S.D.	R.V.	Mean n=6	S.D.	R.V.
SiO2	60.02	0.72	60.10	39.02	0.25	39.32	66.83	0.56	67.32
TiO2	0.14	0.01	0.14	3.89	0.05	3.69	0.66	0.02	0.66
Al2O3	12.20	0.13	12.20	8.54	0.04	8.50	14.97	0.13	15.28
Fe2O3t	6.36	0.07	6.28	17.81	0.30	17.82	4.27	0.06	4.3
MnO	0.32	0.01	0.32	0.18	0.00	0.17	0.05	0	0.04
MgO	2.72	0.02	2.70	13.89	0.12	13.49	0.97	0.01	0.97
CaO	8.04	0.04	7.98	14.75	0.04	14.77	1.98	0.04	2.03
Na2O	4.29	0.05	4.34	0.71	0.00	0.71	2.79	0.03	2.81
K2O	4.47	0.06	4.48	0.17	0.00	0.18	5.58	0.11	5.51
P2O5	0.43	0.03	0.43	0.06	0.00	0.06	0.27	0.03	0.28
TRACE ELEMENTS BY AAS (ppm)									
	n=18			n=18					
N	90.2	7.6	93.0	10.4	3.9	4			
Li	61.4	10.6	52.0	539.9	19.5	520			
V	7.2	1.4	10.0	327.3	21.2	420			
Cr	4.6	0.9	10.0	145.3	5.5	200			
Ni	5.2	0.6	5.0	109.1	4	136			
Cu	264.3	50.3	250.0	193.4	7	185			
Zn	210.0	21.3	220.0	12.7	4	8			
Rb	274.5	8.9	275.0	260.5	14.6	260			
Sr	3.3	0.4	3.0	4.7	1.2	5.0			
Mo	460.4	31.3	460.0	83.5	16	50			
Ba	76.6	2.7	86.0	10	0	10			
Pb									
TRACE ELEMENTS BY ICP-ES (ppm)									
	n=18			n=18					
Ga	23.9	1.4	28.0	24.5	1.2	18.0			
Y	129.7	4.6	130.0	10.5	0.8	16.0			
Zr	313.8	18.9	280.0	121.3	17.3	105.0			
Nb	25.6	1.0	23.0	13.5	0.8	20.0			
La	69.4	3.0	88.0	17.5	5.7	10.0			
Ce	164.8	5.7	210.0	38.7	3.0	25.0			
Th	383.4	27.0	380.0	1.0	0.2	1.0			
TRACE ELEMENTS BY NAA (ppm)									
	n=12			n=9					
Sc	6.0	0.5	7.0	53.8	4.1	48.0			
Cs	2.7	0.3	2.3	0.8	0.2	0.6			
Sm	8.6	2.1	15.0	4.9	0.3	5.0			
Yb	20.4	4.0	17.0	2.2	2.0	1.0			
Hf	8.3	0.8	8.0	3.8	0.5	3.0			
OTHER TRACE ELEMENTS (ppm)									
Sn	4.6	2.2	4.0	1	0	3.2			

R.V. = Recommended Value (Abbey, 1979; 1983) S.D. = Standard Deviation

limit; note the large differences between mean and median precision for Cr, Ni and Mo. In the case of Sn, data are capable only of resolving anomalous samples. Apparent poor precision for Th is mostly induced by mafic rocks containing only 1-2 ppm Th; if these are excluded, precision is closer to  $\pm 6\%$ .

### **Accuracy**

Table A.2 lists mean analyses and standard deviations for the international standards MRG-1, SY-2 and GSP-1, compared to the recommended values listed by Abbey (1979,1983),. There is good agreement for most elements. Notable exceptions include Ni and Ce, which are somewhat lower than recommended values for MRG-1 and SY-2 respectively. However, in the case of Ce, ICP-ES data for SY-2 are in close agreement with the ICP-MS data from MUN (Table A.3).

Accuracy for U and F was monitored only by internal Department of Mines standards. Data for these are in good agreement with compilations of previous results (Wagenbauer, pers.comm., 1989), and are within their respective precision envelopes.

### **A2.3 Memorial University Analysis Program**

Selected samples were analyzed for REE and a range of other trace elements at Memorial University. About 0.5 g of sample was digested in HF-HNO<sub>3</sub> in sealed teflon bombs to ensure dissolution of zircon. A subset of the samples were also processed using NaOH fusion methods followed by HNO<sub>3</sub> digestion. This method is now standard for REE analysis at MUN; however, in the case of TLGB samples, there was little difference between results from the two methods.

Table A.3. Mean trace element analysis of SY-2 by ICP-MS analysis at Memorial University, compared to recommended values of Abbey (1979, 1983).

Element	SY-2			SY-2 Recommended Value	Quoted Detection Limit
	N	Mean	S.D.		
(ppm)					
Li	5	90.1	5.1	93.0	0.3
Be	2	23.0	1.4	23.0	0.4
Sc	2	6.7	0.0	7.0	1.2
Rb	5	219.8	7.0	220.0	0.1
Sr	5	268.8	12.2	275.0	0.2
Y	6	111.7	5.1	130.0	0.1
Zr	6	251.3	11.4	280.0	0.2
Nb	3	25.1	1.6	23.0	0.1
Mo	2	0.8	0.1	3.0	0.1
Cs	5	2.7	0.0	2.3	0.1
Ba	7	444.4	18.5	460.0	0.1
La	7	67.6	1.5	88.0	0.1
Ce	7	154.0	3.2	210.0	0.1
Pr	7	18.9	0.6	21.0	0.1
Nd	7	70.9	1.8	75.0	0.7
Sm	7	15.1	0.6	15.0	0.2
Eu	7	2.3	0.1	2.7	0.1
Gd	7	14.8	1.1	17.0	0.1
Tb	7	2.8	0.1	2.5	0.1
Dy	7	19.1	0.7	20.5	0.1
Ho	7	4.3	0.2	5.0	0.1
Er	7	14.5	0.9	14.0	0.1
Tm	7	2.3	0.2	2.3	0.1
Yb	7	16.6	1.3	17.0	0.1
Lu	7	2.8	0.3	3.0	0.1
Hf	6	8.5	0.5	8.0	0.1
Ta	3	0.6	0.4	1.2	0.1
Tl	5	1.5	0.1	1.4	0.2
Pb	5	68.1	12.4	86.0	0.1
Bi	5	0.1	0.0	0.1	0.1
Th	7	365.0	56.5	380.0	0.1
U	5	292.3	21.7	290.0	0.1

Recommended values after Abbey (1979,1983), or accepted  
MUN values in the case of Tl, Ta and Bi.

Analysis was conducted on a SCIEX inductively-coupled plasma mass spectrometer (ICP-MS). Details of analytical techniques and instrument specifications are provided by Longerich et al. (in prep.). Precision is estimated at  $\pm 6\%$  or better for most elements (based on duplicate analyses over several years), with the exception of Be, Sc, Ta and Li, for which it may be as poor as  $\pm 10\%$ , particularly at low levels (Longerich et al., in prep.).

The results of repeated ICP-MS analyses of SY-2 are listed in Table A.3. For most elements, there is good agreement with the Department of Mines laboratory, even where measured values are somewhat lower than recommended for (e.g. Ce). Detection limits quoted in Table A.3 are based on mean background +  $3\sigma$ , and are probably underestimates of true limits of analytical precision.

### A3. STRONTIUM ISOTOPIC ANALYSIS PROCEDURES

#### A3.1 Laboratory Procedures

Samples were prepared for measurement of Rb/Sr ratios at the Department of Mines laboratory, as described above for trace elements. For Sr isotopic composition analysis, 0.1 to 0.2 g of sample was taken into solution via HF-HNO<sub>3</sub> digestion, and converted to chloride. Sr was separated by standard ion-exchange procedures using amberlite resin and chloride solutions. Each sample was passed through ion-exchange columns twice to ensure removal of all Rb. Sr separates were stored as chloride solutions. Sr separations were performed by Pamela King at Memorial University.

### A3.2 Determination of $^{87}\text{Rb}/^{86}\text{Sr}$

$^{87}\text{Rb}/^{86}\text{Sr}$  ratios were determined at the Department of Mines laboratory by repeated AAS analysis of each sample for Rb and Sr. Precision was assessed by calculating the mean and standard error for each sample, based on 10 - 20 repeated determinations, and by running several samples twice (Table A.4). Calculated  $^{87}\text{Rb}/^{86}\text{Sr}$  ratios are corrected for  $^{87}\text{Sr}/^{86}\text{Sr}$  ratios measured by mass spectrometry. The precision is poorest at low Rb contents, but 2  $\sigma$  within-run uncertainties are  $\pm 2\%$  or better for most samples. Duplicate determinations suggest that 2  $\sigma$  within-run uncertainties approximate or underestimate true 1  $\sigma$  analytical uncertainty, and 2  $\sigma$  within-run values were therefore used in isochron regression (Chapter 8).

Table A.4. Duplicate determinations of  $^{87}\text{Rb}/^{86}\text{Sr}$  ratios by repeated AAS analyses at the Department of Mines laboratory. Errors are 2  $\sigma$ .

Sample Number	Determination 1		Determination 2	
0241041	0.945 +/-	10	0.895 +/-	15
0249030	0.314 +/-	9	0.351 +/-	4
0241391	12.542 +/-	198	11.660 +/-	166
0241173	0.032 +/-	5	0.021 +/-	5
0241538	3.081 +/-	73	3.232 +/-	80

NOTE: All errors are  $\times 10^3$

### A3.3 Determination of $^{87}\text{Sr}/^{86}\text{Sr}$

#### Mass Spectrometry

$^{87}\text{Sr}/^{86}\text{Sr}$  ratios were determined by thermal ionization mass spectrometry, using the venerable Vacuum

Generators Micromass 30B single-collector instrument known (affectionately ?) as "Miss Piggy". Most samples were run by the author; a few were run in early stages of the project by Pamela King. Samples were loaded as chloride on single W filaments, and coated with tantalum fluoride. During runs, all measured ratios were normalized to a  $^{86}\text{Sr}/^{88}\text{Sr}$  ratio of 0.1194.

Samples were run under automatic control for periods ranging from 4 to 24 hours, corresponding to 40 to 250 cycles of data acquisition, organized into blocks of 20 or 30 cycles. Samples with low Sr contents are difficult to run, as they do not generally last long enough to produce high-precision data. Accordingly, samples with  $^{87}\text{Sr}/^{86}\text{Sr} > 1.0$  were run using a gain of x10 on the Faraday cup detector, and an ion beam intensity measurement of 2 - 3 volts. All other samples were run using a gain of x1, and an ion beam intensity of 0.8 - 1.0 volts.

The control program automatically rejects observations that fail a Q-test, and blocks of data exhibiting poor internal precision were not included in final calculations. Data were windsorized a maximum of five times to exclude outlying observations that were retained by the program.

### Precision and Accuracy

Three samples were repeated to check between-run precision (Table A.5). Results suggest that  $2\sigma$  within-run errors are a good approximation to true  $1\sigma$  uncertainties, and these values were thus employed in isochron regression (Chapter 8).

Accuracy was assessed by running the Sr-carbonate standard NBS-987, at an average frequency of 1 standard for every six samples. Results for NBS-987 obtained during this project are shown in Table A.6. The mean value is slightly

higher than the recommended value of  $0.710260 \pm 20$ . Data have not been normalized to this value because the uncertainty associated with most TLGB samples (particularly those with high Rb/Sr) is equal to or greater than the discrepancy in standard determinations.

Table A.5. Duplicate determinations of  $^{87}\text{Sr}/^{86}\text{Sr}$  ratios by thermal ionization mass spectrometry at Memorial University. Errors are  $2\sigma$ .

Sample Number	Determination 1	Determination 2
0241538	0.779743 +/- 518	0.780360 +/- 64
0249030	0.711421 +/- 108	0.711398 +/- 106
0241391	1.012539 +/- 296	1.012098 +/- 349
NOTE: All errors are $\times 10^6$		

Table A.6. Determinations and mean value of the Sr-carbonate isotopic standard NBS-987 during the course of this project.

Date	Value +/-	$2\sigma$
ACCEPTED VALUE	0.710260 +/-	20
September 1987	0.710421 +/-	56
October 1987	0.710344 +/-	66
January 1988 *	0.710581 +/-	88
January 1988	0.710350 +/-	78
January 1989	0.710336 +/-	54
February 1989	0.710300 +/-	39
March 1989	0.710376 +/-	55
March 1989	0.710389 +/-	66
Mean Value	0.710387 +/-	57
Mean Value Excluding *	0.710359 +/-	23

NOTE: All errors are  $\times 10^6$

NOTE : Quoted errors on mean values are standard errors of the mean, i.e. 2 standard deviations divided by square root of number of observations.

#### A4. NEODYMIUM ISOTOPE ANALYSIS PROCEDURES

##### A4.1 Laboratory Procedures

Samples for determination of  $^{147}\text{Sm}/^{144}\text{Nd}$  by ICP-MS were processed using the NaOH fusion method described above for trace element (MUN) determinations.

For Nd isotopic analysis, 0.1 to 0.2 g of sample was taken into solution via HF-HNO<sub>3</sub> digestion in teflon bombs for 1 week under clean-lab conditions. After dissolution, a 1 ml aliquot of each sample was spiked with 20 microlitres of a mixed  $^{150}\text{Nd}$  -  $^{147}\text{Sm}$  solution (MUN spike #1). This isotope dilution (ID) split, and the unspiked isotopic composition (IC) split, were then processed via a three stage ion-exchange procedure to isolate Nd and Sm.

Stage 1 employs amberlite resin and chloride solutions, and separates the REE and Ba from all other elements. Stage 2 employs amberlite resin and nitrate solutions, and separates the REE from Ba. Stage 3 employs teflon beads coated with di-2-ethylhexyl orthophosphoric acid, and chloride solutions, and separates Nd (IC split) and Nd and Sm (ID split) from other REE. Samples were stored as chloride or nitrate solutions. All ion-exchange chemistry was conducted under clean-lab conditions in a positive pressure hood. Twenty samples were processed initially by Patricia Horan, and the remainder of the laboratory work was conducted by the author.

Nd and Sm ID separates were prepared fully for about one-third of the samples to assess the accuracy of high-precision ICP-MS  $^{147}\text{Sm}/^{144}\text{Nd}$  determinations used in this study (see below).



#### A4.2 Determination of $^{147}\text{Sm}/^{144}\text{Nd}$

$^{147}\text{Sm}/^{144}\text{Nd}$  values were mostly determined by high-precision ICP-MS. This employs a longer counting period (180 seconds) for each element compared to the ICP-MS multi-element analysis (10 seconds), and is therefore more precise (S.Jackson, pers.comm., 1989). Each sample was run twice, and results averaged. Standards used in calibration were prepared from pure Nd and Sm metals provided by AMES Ltd. Replicate determinations suggest that the average 2  $\sigma$  precision for  $^{147}\text{Sm}/^{144}\text{Nd}$  at Sm and Nd concentrations typical of TLGB granitoid rocks is  $\pm 0.5\%$  or better (H.Longerich, pers.comm., 1988). This value has been used to estimate errors in calculation of  $\epsilon_{\text{Nd}}$  and  $T_{\text{CHUR}}$  (Chapter 8).

A comparison of ICP-MS data with more precise ID data obtained by thermal ionization mass spectrometry (see below) shows a generally close correspondence. All except three ID measurements lie within the  $\pm 0.5\%$  2  $\sigma$  error envelope of the ICP-MS measurements, and several have identical mean  $^{147}\text{Sm}/^{144}\text{Nd}$  by both methods (Table A.7).

Table A.7. Comparison of  $^{147}\text{Sm}/^{144}\text{Nd}$  ratios measured by high-precision ICP-MS methods and by Isotope Dilution (ID) techniques, using thermal ionization mass spectrometry.

Sample Number	$^{147}\text{Sm}/^{144}\text{Nd}$ [ Isotope Dilution ]		$^{147}\text{Sm}/^{144}\text{Nd}$ [ ICP - MS ]	
AKZ-2	0.0922 +/-	21	0.0930 +/-	47
AKZ-3	0.1033 +/-	3	0.1030 +/-	51
AKZ-4	0.0876 +/-	2	0.0872 +/-	44
AKZ-5	0.0924 +/-	46	0.0933 +/-	47
AKZ-6	0.1018 +/-	3	0.1025 +/-	51
AKZ-7	0.1005 +/-	2	0.0933 +/-	47
AKZ-8	0.1039 +/-	2	0.1021 +/-	51
AKZ-11	0.1100 +/-	5	0.1175 +/-	59
AKZ-12	0.1105 +/-	9	0.1063 +/-	53
AKZ-13	0.1070 +/-	2	0.1068 +/-	53
AKZ-14	0.0910 +/-	4	0.0993 +/-	50
AKZ-15	0.1378 +/-	5	0.1395 +/-	70
GSZ-2	0.1116 +/-	9	0.1114 +/-	56

NOTE: All errors are  $\times 10^{-4}$

#### A4.3 Determination of $^{143}\text{Nd}/^{144}\text{Nd}$

##### **Mass Spectrometry**

Samples were run on the same Micromass 30B instrument used for Sr isotopic analysis. Most were run by the author, except for six samples run by Dr.B.J.Fryer in early stages of the project. Samples were loaded as chloride or nitrate on Re side-filaments in a triple-filament assembly, and oxidized after coating with phosphoric acid. All measured ratios were normalized to a  $^{146}\text{Nd}/^{144}\text{Nd}$  ratio of 0.7219. Samples were run under automatic control for periods ranging from 8 to 48 hours, corresponding to 90 to 550 cycles of data acquisition, organized into blocks of 30 cycles. Most were analyzed with a gain of x1 on the Faraday cup, and an ion beam intensity measurement of 0.8 to 1.1 volts. A few (Nd-poor) leucogranite samples were analyzed at a gain of x10 and an ion beam intensity of 2-3 volts, in order to extend their running times. Data reduction methods were identical to those used for Sr isotopic data. The limits for acceptance of a 30-cycle block of data were set at a  $1\sigma$  within-block uncertainty of 0.000100 or less. Using a more stringent limit (e.g. 0.000050) would improve the apparent precision of  $^{143}\text{Nd}/^{144}\text{Nd}$  ratios considerably, but would almost certainly underestimate the true uncertainty of determinations.

Isotope dilution (ID) analysis employed similar procedures to measure  $^{150}\text{Nd}/^{144}\text{Nd}$  (Nd ID) and  $^{147}\text{Sm}/^{149}\text{Sm}$  (Sm ID) respectively. Molar concentrations of  $^{147}\text{Sm}$  and  $^{144}\text{Nd}$  were derived using a spreadsheet written by H.Longerich.

## Precision and Accuracy

Between-run precision was assessed by repeating several sample determinations (Table A.8). Results for each duplicate pair compare well, and are identical within the respective  $2\sigma$  error envelopes. The  $2\sigma$  within-run uncertainties are thus regarded as a good approximation to true  $2\sigma$  analytical errors. Duplicate digestions were not performed.

Table A.8. Duplicate determinations of  $^{143}\text{Nd}/^{144}\text{Nd}$  ratios by thermal ionization mass spectrometry at Memorial University. Errors are  $2\sigma$ .

Sample Number	Determination 1		Determination 2	
AKZ-6	0.511604 +/-	61	0.511515 +/-	85
AKZ-14	0.511188 +/-	29	0.511184 +/-	35
AKZ-3	0.511326 +/-	25	0.511296 +/-	40
AKZ-4	0.511606 +/-	51	0.510665 +/-	54
AKZ-20	0.511623 +/-	70	0.511648 +/-	63
AKZ-12	0.511640 +/-	47	0.511536 +/-	95

NOTE: All errors are  $\times 10^6$

Accuracy was assessed by replicate determinations of the LaJolla Nd isotope standard, at an average frequency of one standard for every six samples. Determinations over the course of this project are listed in Table A.9. The mean values are slightly higher than the recommended value of 0.511850, but compare well to the average MUN value.  $\epsilon_{\text{Nd}}$  values would be reduced by ca. 0.8  $\epsilon$  units if all  $^{143}\text{Nd}/^{144}\text{Nd}$  ratios were normalized to 0.511850, but contrasts among samples would remain unchanged.

Table A.9. Determinations and average value of the LaJolla Nd isotopic standard during the course of this project.

Date	Value +/-	2 $\sigma$
ACCEPTED VALUE	0.511850	
MUN Average	0.511892 +/-	20
October 1987	0.511953 +/-	56
October 1987	0.511890 +/-	24
November 1987	0.511919 +/-	24
November 1987	0.511905 +/-	28
November 1987	0.511896 +/-	60
March 1988	0.511887 +/-	78
May 1988	0.511948 +/-	44
May 1988	0.511977 +/-	34
August 1988 *	0.512003 +/-	58
September 1988	0.511962 +/-	74
November 1988	0.511936 +/-	31
March 1989	0.511940 +/-	26
Mean Value	0.511935 +/-	20
Mean Value (Excluding *)	0.511928 +/-	17

NOTE : Quoted errors on mean values are standard errors of the mean, i.e. 2 standard deviations divided by the square root of number of observations.

NOTE: All errors are  $\times 10^6$

## **APPENDIX B: GEOCHEMICAL DATA LISTINGS**

### **Major and Trace Element Data**

Geochemical data employed in this thesis are presented in microfiche format. Data are organized into the five groupings represented by Chapters 3, 4, 5, 6 and 7, and into separate listings for major and trace element analyses. Within each category, data are sorted by map unit and sample number; a key to the variable MAP UNIT is provided on the first page of the microfiche listing. Note that regional, follow-up and geological sample populations are designated by sample numbering sequences, as follows :

- 0241000 - 0242999 Regional Samples (2 km grid),
- 0248000 - 0248999 Follow-Up Samples (1 km grid),
- 0249000 - 0249999 Geological Samples (no grid).

Locational information included with major element data includes National Topographic System (NTS) map sheet (variable NTS MAP) and Universal Transverse Mercator (UTM) grid coordinates in metres (variables EAST UTM and NORTH UTM). The lithology (variable ROCK TYPE) listed is the normative IUGS plutonic classification according to the method of Streckeisen and LeMaitre (1979).

### **ICP-MS Trace Element Data**

ICP-MS trace element data are also listed in microfiche format. For locations of all these samples, see Figure 8.4. Coordinates for all 024.... series samples are also listed in the main data listing. Major element data for the AKZ- and GSZ- series samples were determined at the Department of Mines Laboratory, as described above.

UNABLE TO FILM MATERIAL ACCOMPANYING THIS THESIS ( I.E.  
DISKETTE(S), SLIDES, MICROFICHE, ETC... ).

PLEASE CONTACT THE UNIVERSITY LIBRARY.

INCAPABLE DE MICROFILMER LE MATERIEL QUI ACCOMPAGNE CETTE THESE  
(EX. DISQUETTES, DIAPOSITIVES, MICROFICHE (S), ETC... ).

VEUILLEZ CONTACTER LA BIBLIOTHEQUE DE L'UNIVERSITE.

NATIONAL LIBRARY OF CANADA  
CANADIAN THESES SERVICE

BIBLIOTHEQUE NATIONALE DU CANADA  
LE SERVICE DES THESES CANADIENNES

## APPENDIX C : MISCELLANEOUS INFORMATION

### Partition Coefficients

Table C.1 lists mineral/melt partition coefficients employed in modelling evolution of the Adlavik and Mount Benedict Intrusive Suites. Values for orthopyroxene (Opx) and amphibole (Hb) are from a compilation of basalt-related studies (Jenner, 1984), as are values for Y and V in all minerals. All others are from Villemant et al.(1981).

### Chondrite Normalization Values

Values (Table C.2) are from Taylor and MacClennan (1985)

### Note on Normative Calculations

Calculations were performed using computer programs developed by K.Parsons of the Department of Mines. CIPW norm calculations recalculate all data on an anhydrous basis, normalized to a 100% total. Calculation steps follow standard procedures, as described in igneous petrology texts. Mesonorm calculations are conducted according to the method of Barth (1955).  $H_2O$  contents are assumed to be given by loss-on-ignition (LOI) measurements, on the basis that hygroscopic water contents are negligible. Assumptions regarding mineral formulae correspond to those of Barth (1955). Iron is recalculated as  $FeO$ , and any excess  $Al_2O_3$  is expressed as normative corundum.

It should be noted that, although Streckeisen and LeMaitre (1979) recommend mesonorms for their classification scheme, other studies (e.g., Bowden et al., 1984), and the author's own comparisons, indicate that results obtained from CIPW and mesonorm data differ only very slightly, except where rocks contain large amounts of biotite or muscovite.

Table C.1. Mineral-Melt partition coefficients employed in trace element modelling. see text for sources.

Mineral:	Plag.	K-fsp	Hb	Cpx	Opx	Ol	Bi	Fe-Ox
Element:								
U	0.04	0.1	0.54	0.05	0.005	0.04	0.13	0.14
Th	0.05	0.09	0.54	0.04	0.005	0.03	0.12	0.11
La	0.2	0.24	0.16	0.12	0.005	0.03	0.7	0.1
Y	0.03	0.015	1	0.5	0.2	0.01	1.06	0.001
Rb	0.13	0.3	0.25	0.04	0.02	0.04	1.9	0.001
Zr	0.13	0.27	0.5	0.27	0.03	0.06	2.5	0.001
Ba	0.56	3.6	0.31	0.04	0.013	0.03	10	0.001
Sr	2.7	10	0.57	0.16	0.016	0.02	0.7	0.001
V	0.08	0.5	4	1.5	0.3	0.09	23	30
Cr	0.08	0.6	3	5.3	10	2.8	5.4	5.3
Ni	0.04	0.5	7	2.5	4	34	1.3	5.5
Ti	0.05	0.05	1.5	1.07	0.1	0.005	13	12

Table C.2. Chondrite normalization values currently in use at Memorial University. Only values for Y and REE were employed here.

Li	2.4	La	0.376	Hf	0.179
Be	0.04	Ce	0.957	Ta	0.026
Sc	8.64	Pr	0.137	W	0.089
Rb	3.45	Nd	0.711	Tl	0.215
Sr	11.9	Sm	0.231	Pb	3.65
Y	2.25	Eu	0.087	Bi	0.167
Zr	5.54	Gd	0.306	Th	0.043
Nb	0.375	Tb	0.058	U	0.012
Mo	1.38	Dy	0.381		
Cs	0.279	Ho	0.085		
Ba	3.41	Er	0.249		
		Tm	0.036		
		Yb	0.248		
		Lu	0.038		



## APPENDIX D : SUMMARY OF U-PB ZIRCON GEOCHRONOLOGICAL DATA

### **General Statement**

This appendix briefly summarizes recent (unpublished) U-Pb zircon ages that are crucial in dividing the TLGB into Makkovikian and Labradorian assemblages.

This work was carried out by Drs. Tom Krogh and Urs Schärer (and their associates), at the Royal Ontario Museum (ROM) geochronology laboratory in Toronto, partly under contract to the Newfoundland Department of Mines, and partly from their personal interests in this project. These U-Pb zircon data are being prepared for full publication elsewhere (Krogh et al., in prep.). Note that any reference to these unpublished ages should be to Krogh et al. (in prep.), and not to this thesis. Note also that some mineral fractions (notably sphenes) have yet to be analyzed, and that ages and error estimates may be subject to minor revisions. Data from the Big River and Stag Bay units, and final data from the Cape Strawberry Granite, were received too late for inclusion in the main body of the text, except as footnotes.

No attempt is made here to review the rigorous processing, grain selection, abrasion and mass spectrometry procedures routinely employed at ROM. These have most recently been described by Schärer et al. (1986).

### **Adlavik Intrusive Suite**

A potassic, monzonitic variant of the dioritic unit of the Adlavik Intrusive Suite was sampled at the entrance to Adlavik Bay, from the 0249030 sample locality (Figure 8.4).

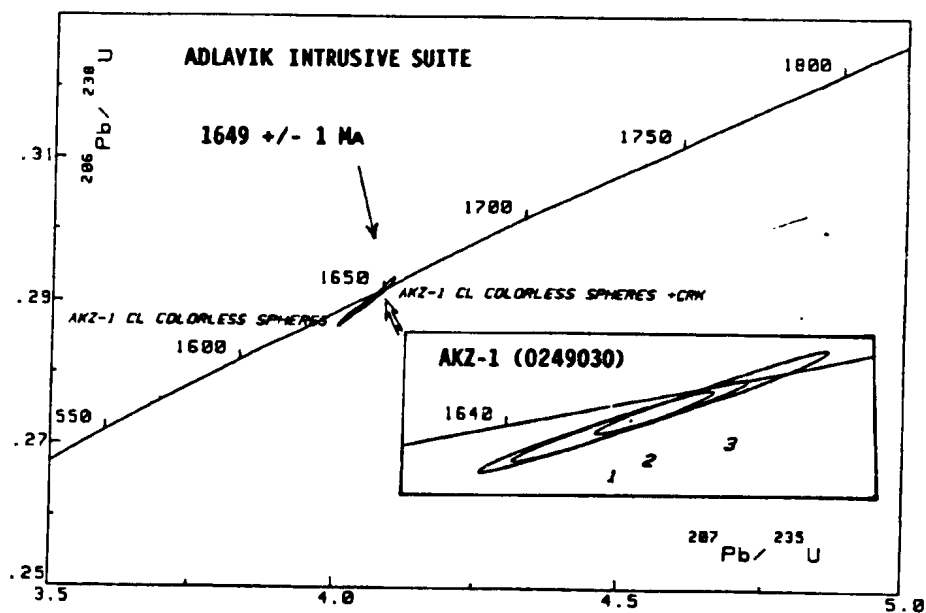


Figure D.1.  $^{206}\text{Pb}/^{238}\text{U}$  -  $^{207}\text{Pb}/^{235}\text{U}$  concordia diagram for the diorite unit of the Adlavi Intrusive Suite.

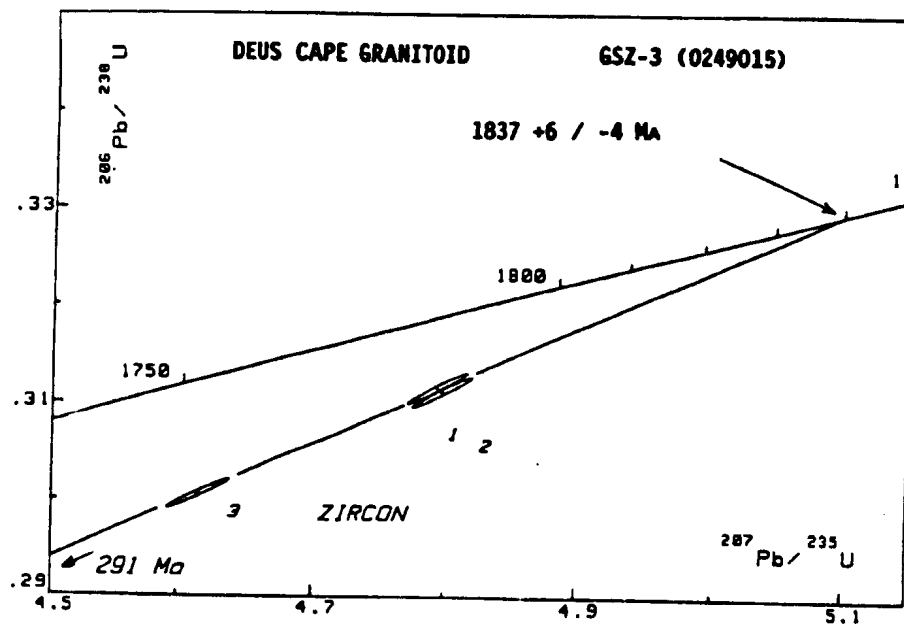


Figure D.2.  $^{206}\text{Pb}/^{238}\text{U}$  -  $^{207}\text{Pb}/^{235}\text{U}$  concordia diagram for the Deus Cape Granitoid.

Three abraded zircon fractions were analyzed in 1987; two are concordant, and a third is about 1% discordant. Two additional fractions analyzed in 1988 gave slightly discordant results. A precise crystallization age of  $1649 \pm 1$  Ma is indicated (Figure D.1), and the zircon population appears simple.

#### **Deus Cape Granitoid**

A foliated, leucocratic granite was sampled south of Deus Cape, from the 0249015 sample locality (Figure 8.4). Three abraded fractions are from 5% to 8% discordant, and define an age of  $1837 +6 / -4$  Ma (Figure D.2). A single sphene analysis suggested a minimum age of ca. 1782 Ma (not figured).

#### **Numok Intrusive Suite**

Two samples were collected. AKZ-5 (located in Figure 8.4) is a fayalite-bearing syenite from Kikkertavak (Numok) Island. HSZ-1 is a foliated quartz monzonite that forms the neosome to the western contact zone agmatite at Adlavik Bay; this was sampled with the intention of providing a maximum age for localized deformation here. HSZ-1 is located about 1 km east of the 0249030 sample locality (Figure 8.4).

AKZ-5 yielded colourless, euhedral, gem-quality zircons that plot on concordia at  $1801 \pm 2$  Ma (Figure D.3). The zircon population appears to be simple. HSZ-1 yielded two fractions that are 4% and 6% discordant along a line from 1800 Ma (concordia) to 1000 Ma (lower intercept). They indicate a closely similar crystallization age to AKZ-5 (Figure D.3)

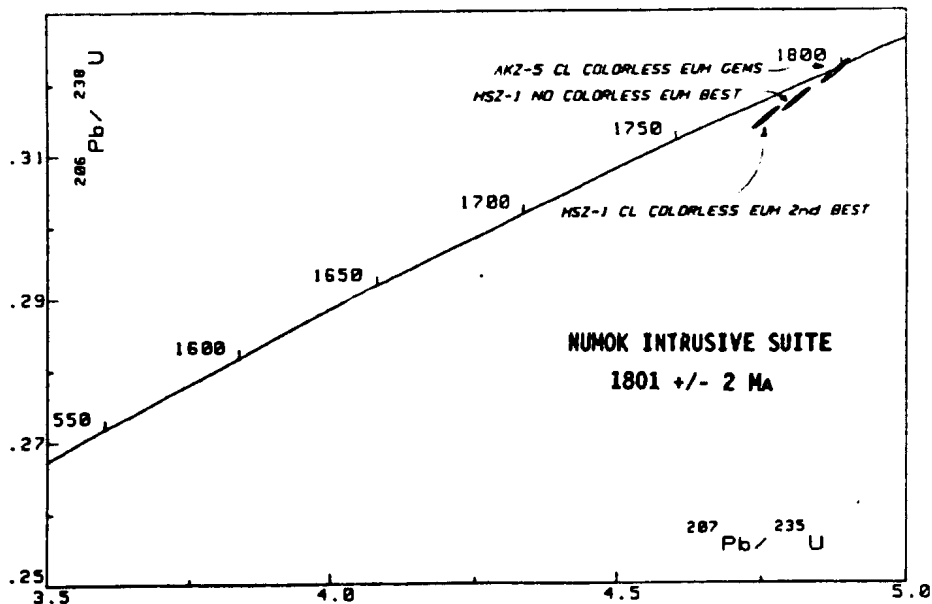


Figure D.3.  $^{206}\text{Pb}/^{238}\text{U}$  -  $^{207}\text{Pb}/^{235}\text{U}$  concordia diagram for units of the Numok Intrusive Suite.

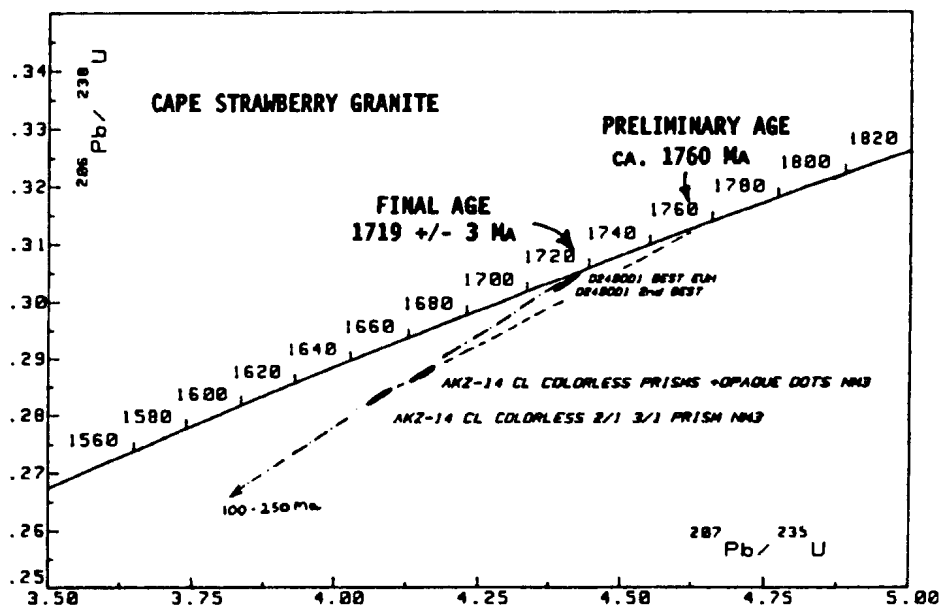


Figure D.4.  $^{206}\text{Pb}/^{238}\text{U}$  -  $^{207}\text{Pb}/^{235}\text{U}$  concordia diagram for The Cape Strawberry Granite, incorporating preliminary data and new data obtained in the spring of 1989.

### Cape Strawberry Granite -- Preliminary Data

Sample AKZ-14 (located in Figure 8.4) is a coarse-grained fluorite-bearing granite. It yielded two discordant zircon fractions that are well removed from concordia and lie (generally) along a line from 1800 Ma (concordia) to ca. 1000 Ma (lower intercept). Interpretation of these data is difficult. Drawing a line through the two points indicates an age of ca. 1760 Ma, but this is not a rigorous regression procedure. Assuming a 1000 Ma lower intercept suggests an age close to 1800 Ma (Figure D.4). It is evident, however, that a Labradorian (ca. 1650 Ma) age is highly unlikely, unless the zircons have a very unusual history of Pb loss. The 1760 Ma estimate was preferred during preparation of this thesis, as it is consistent with field evidence suggesting that the related Dog Islands Granite is younger than the Numok Intrusive Suite (Chapter 4).

### Cape Strawberry Granite -- Spring 1989 Update

T.Krogh (pers.comm., 1988), suggested that the evolved geochemistry of AKZ-14 was responsible for problems with Pb loss, and proposed that another (preferably more "mafic") sample should be examined. Sample 0249001 is from a biotite-rich "cumulate" band exposed several hundred metres south of AKZ-14, which is gradational with identical coarse-grained granite. A small sample contained abundant, euhedral, "cumulus" zircon prisms, with no sign of inheritance. Two fractions are less than 1% discordant, and indicate a precise age of  $1719 \pm 3$  Ma (Figure D.4), some 40 Ma younger than the preliminary estimate of 1760 Ma. These data are not fully colinear with AKZ-14, but if regressed

with these preliminary data, give a lower intercept of 100 - 250 Ma. This revised 1719 Ma age significantly extends the duration of post-tectonic Makkovikian plutonism in the study area.

#### **Mount Benedict Intrusive Suite**

Sample 0242144 (located in Figure 8.4) is a syenite from near Mount Benedict. It contained stubby, euhedral zircon prisms. Two unabraded fractions are discordant, and plot in essentially the same location. However, a Makkovikian age is highly improbable, and the  $^{207}\text{Pb}/^{206}\text{Pb}$  age of ca. 1642 Ma suggests a Labradorian affinity. A second sample of less potassic material (0242125), from a locality some 2 km north-east of 0242144, provided a similar euhedral zircon population. Two fractions are very slightly discordant, and indicate an age of ca. 1650 Ma. Combination of the data yields an age of  $1650 \pm 10$  Ma (conservative error estimate), with a possible maximum age of 1668 Ma if a 1000 Ma lower intercept is assumed.

#### **Otter Lake - Walker Lake Granitoid**

Sample AKZ-8 (located in Figure 8.4) is a seriate to porphyritic two-feldspar quartz monzonite to monzogranite. It yielded cracked, euhedral zircons. Two abraded fractions were concordant and 1.2% discordant respectively, and indicate a precise age of  $1647 \pm 2$  Ma (Figure D.6). This is within error of the Bruce River Group (as determined by Scharer et al., 1988), which was proposed by Ryan (1984) as a volcanic equivalent of the Otter Lake - Walker Lake unit.

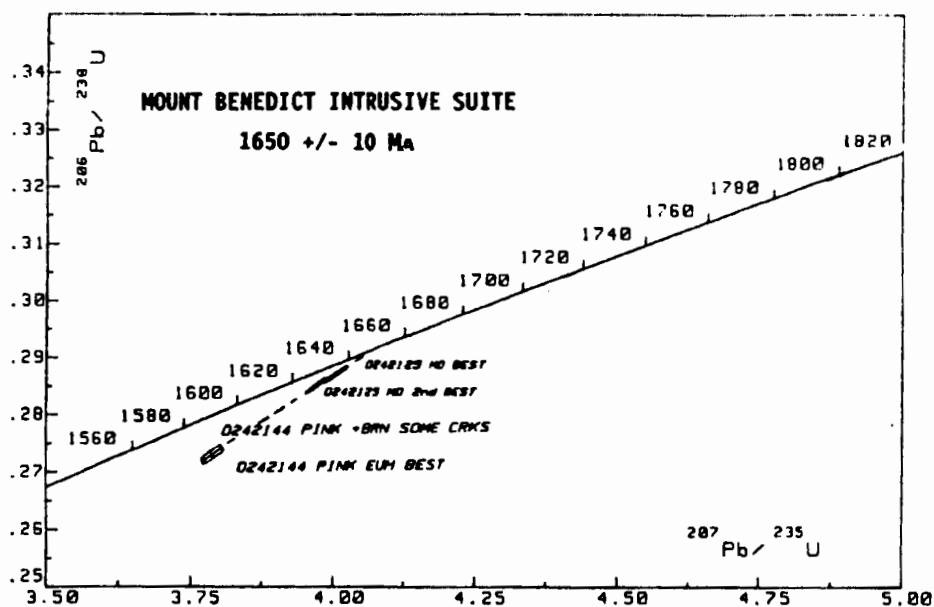


Figure D.5.  $^{206}\text{Pb}/^{238}\text{U}$  -  $^{207}\text{Pb}/^{235}\text{U}$  concordia diagram for Syenite of the Mount Benedict Intrusive Suite.

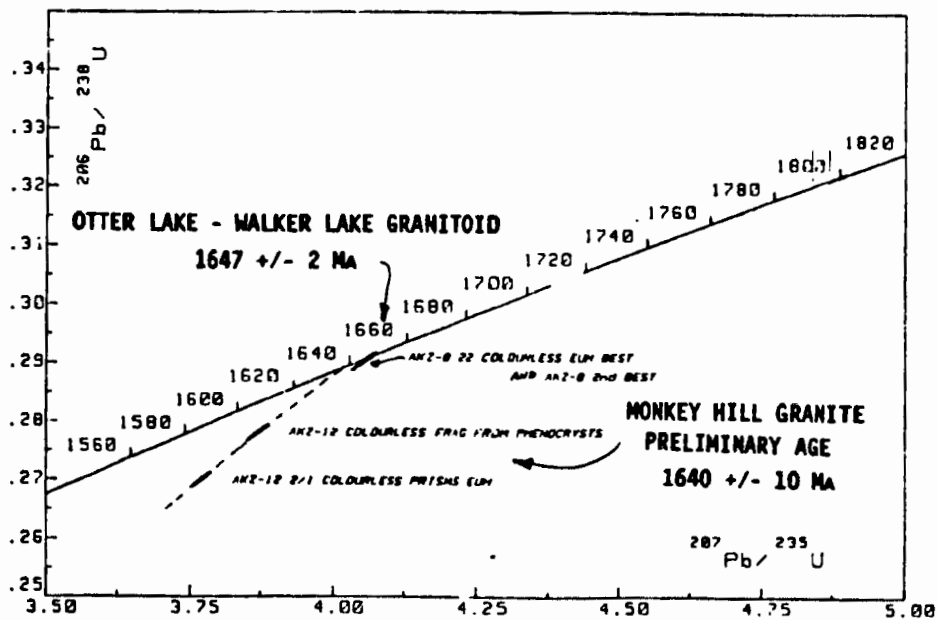


Figure D.6.  $^{206}\text{Pb}/^{238}\text{U}$  -  $^{207}\text{Pb}/^{235}\text{U}$  concordia diagram for the Otter Lake - Walker Lake Granitoid and the Monkey Hill Granite.

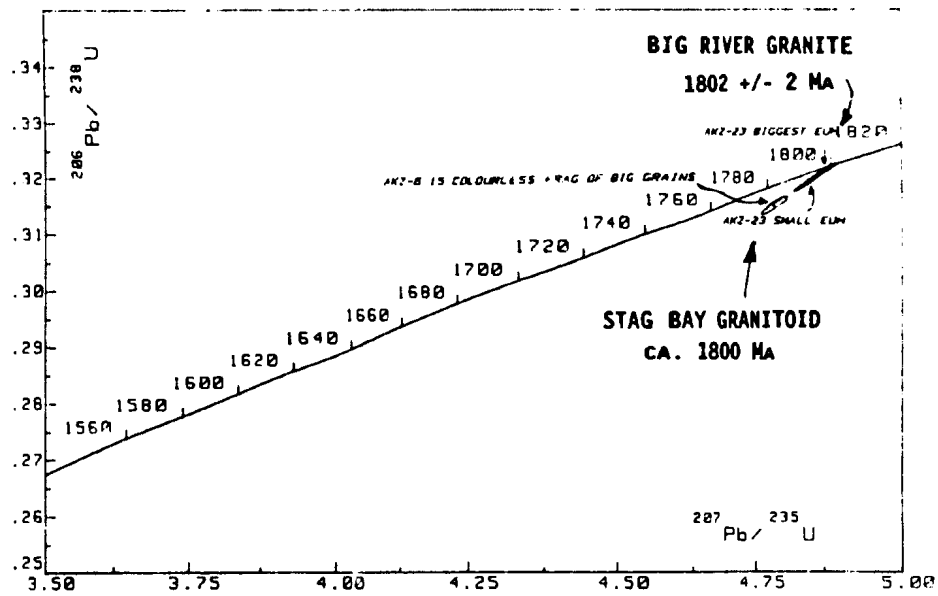


Figure D.7.  $^{206}\text{Pb}/^{238}\text{U}$  -  $^{207}\text{Pb}/^{235}\text{U}$  concordia diagram for the Big River Granite and Stag Bay Granitoid, for which data were obtained in the spring of 1989.



### **Monkey Hill Intrusive Suite**

Sample AKZ-12 (located in Figure 8.4) is a medium-grained equigranular granite from the main Monkey Hill Granite pluton. It contained only a small amount of zircon, consistent with the generally Zr-poor nature of these rocks (Chapter 5). Two abraded fractions are 4% and 7% discordant (Figure D.6). Placing a line through the two points suggests an age of 1640 Ma or less, whereas a regression incorporating AKZ-8 indicates an age of  $1648 \pm 3 / -2$  Ma. To cover all possibilities, a preliminary age of  $1640 \pm 10$  Ma is suggested here. There is no doubt that the unit is of Labradorian age. This preliminary age brackets the  $1632 \pm 9$  Ma age (Brooks, 1983) from the compositionally similar Witchdoctor Granite.

### **Big River Granite**

Sample AKZ-23 is located several kilometres southeast of 0241538 (located in Figure 8.4), and is a typical coarse-grained pseudorapakivi granite. Two fractions of crack-free grains are 0.4% and 1.1% discordant, and indicate a precise age of  $1802 \pm 2$  Ma (Figure D.7), that agrees well with the  $1798 \pm 28$  Ma Rb-Sr age (Chapter 8).

### **Stag Bay Granitoid**

Sample AKZ-6 (located in Figure 8.4) is a K-feldspar porphyritic granite. Two fractions of broken zircon were separated, but one was lost during mass spectrometry. The remaining fraction is 2.6% discordant, but indicates a Makkovikian age of ca. 1800 Ma. This shows that the  $1714 \pm 44$  Ma Rb-Sr isochron obtained during this project (Chapter 8) is erroneously young.

## **APPENDIX E : GEOLOGICAL AND TOPOGRAPHIC MAPS**

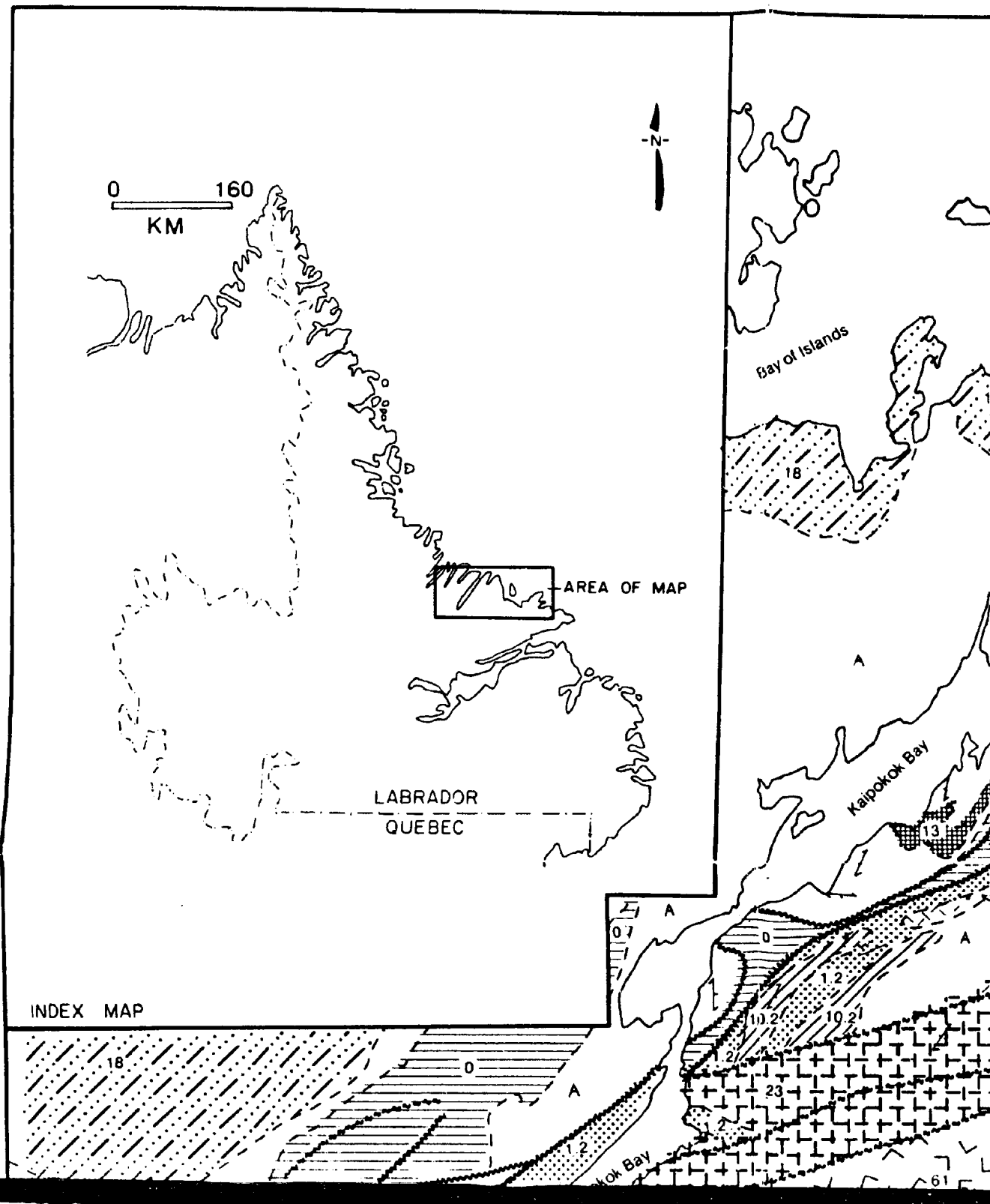
Three enclosures are provided. Enclosure 1 is a 1:250,000 summary map of plutonic rocks in the study area, with a companion legend (Enclosure 2). Note that this is intended as a summary map to illustrate the distribution of units, and the geology has been simplified to accomodate the relatively small scale. Quaternary deposits are not shown, and it should be noted that large areas south of the Benedict Fault, around Big River, and north of MacLean Lake are largely or completely obscured.

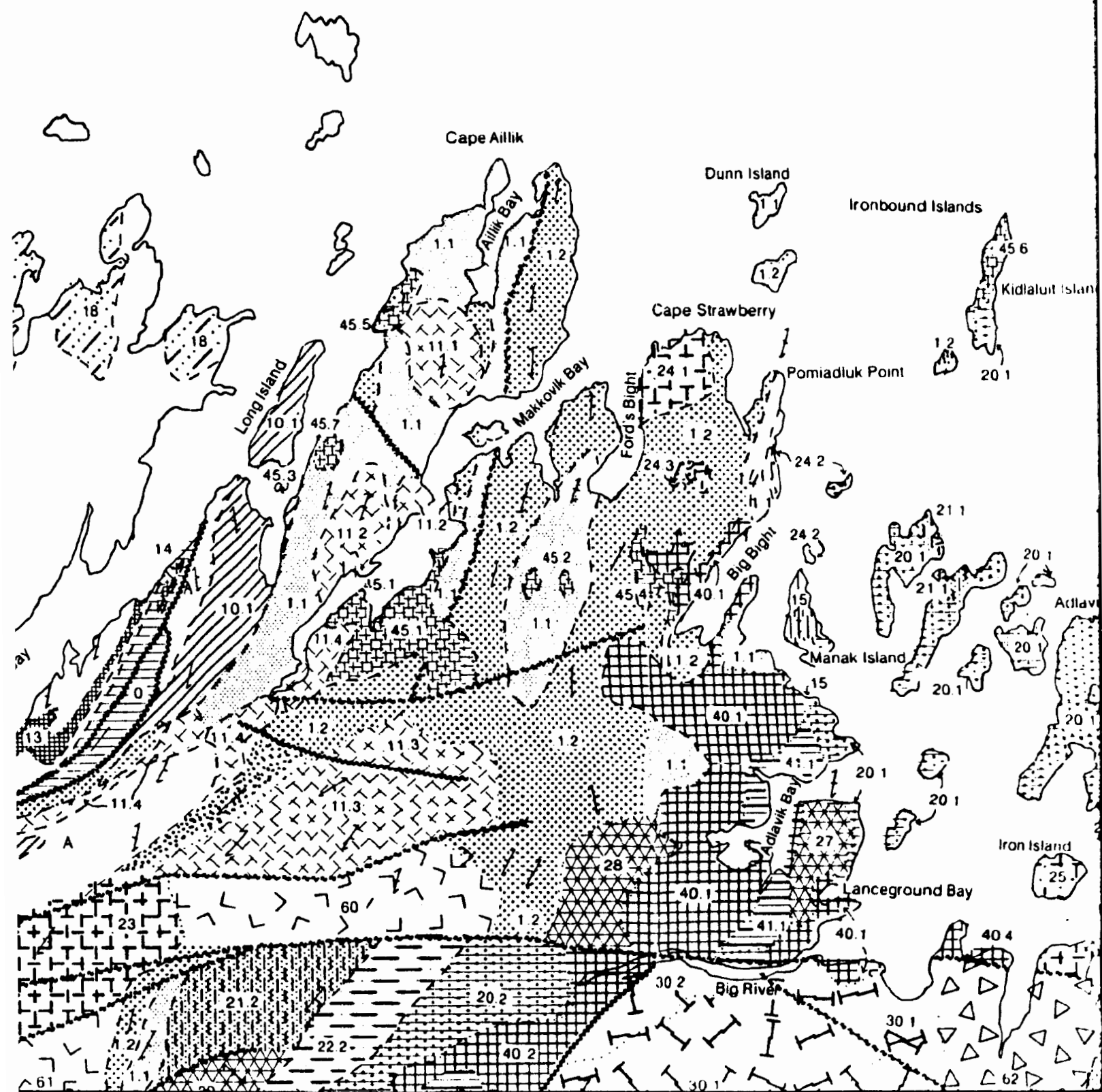
This map is a combination of mapping conducted during this project, and previous work compiled from Gower (1981), Gower et al. (1982) and Ryan (1984). All details of supracrustal rocks have been compiled from these sources, as have some external contacts of plutonic units.

The map and legend were prepared using the GSDRAW and GSMAP cartography computer programs developed by the United States Geological Survey, and modified by Larry Nolan of the Newfoundland Department of Mines. Ken Byrne and the staff of the Department of Mines Cartography and Drafting Section prepared the final composite negatives.

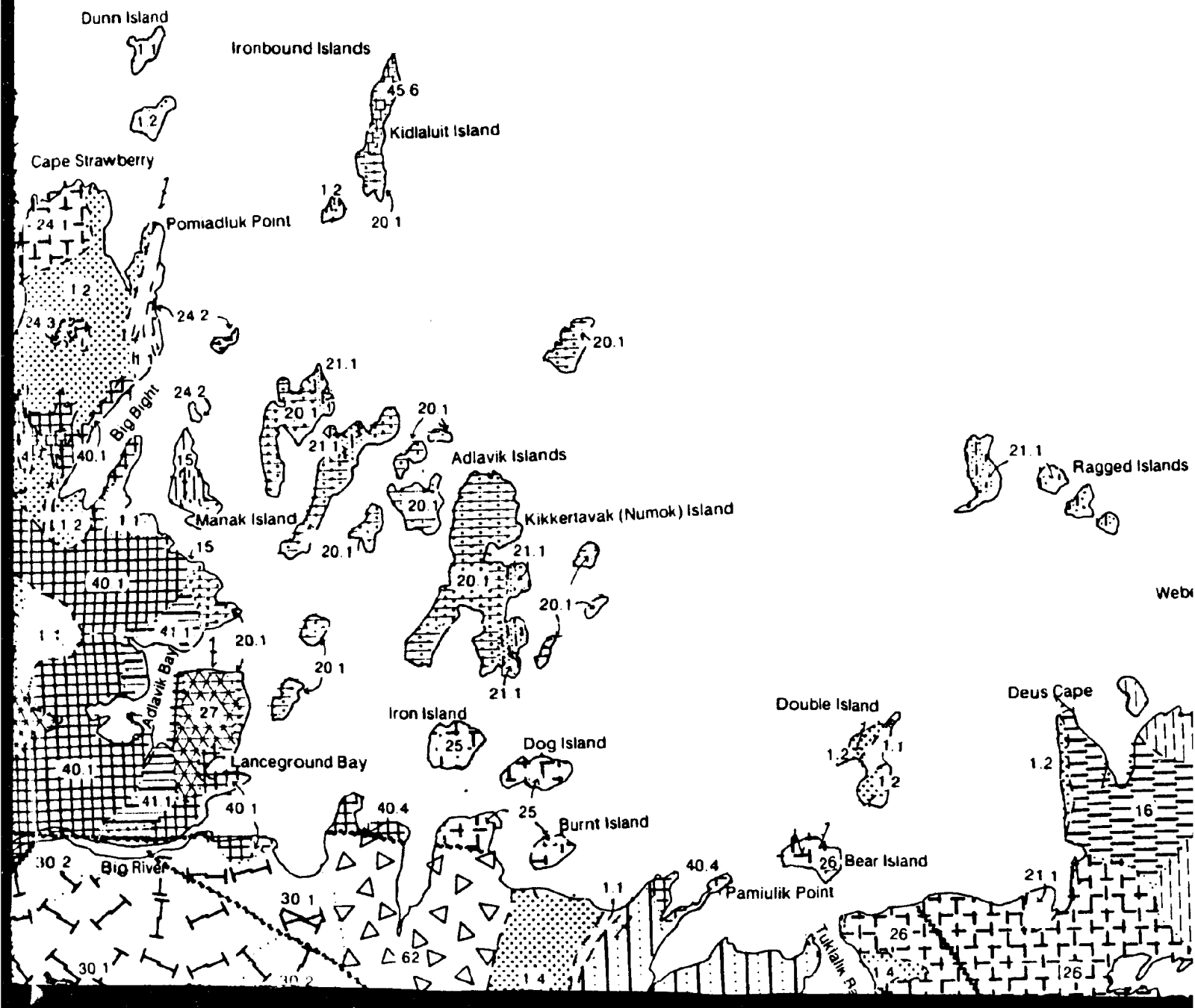
A 1:250,000 scale topographic map is included to allow reference to localities not labelled on Enclosure 1. This is derived from NTS 1:250,000 sheets 13K (Snegamook Lake), 13J (Rigolet), 130 (Makkovik) and 13I (Groswater Bay).

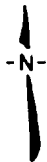
# ENCLOSURE I





Kilometres

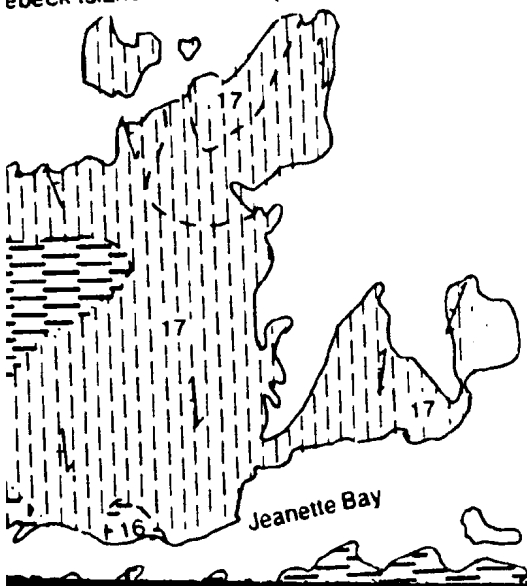




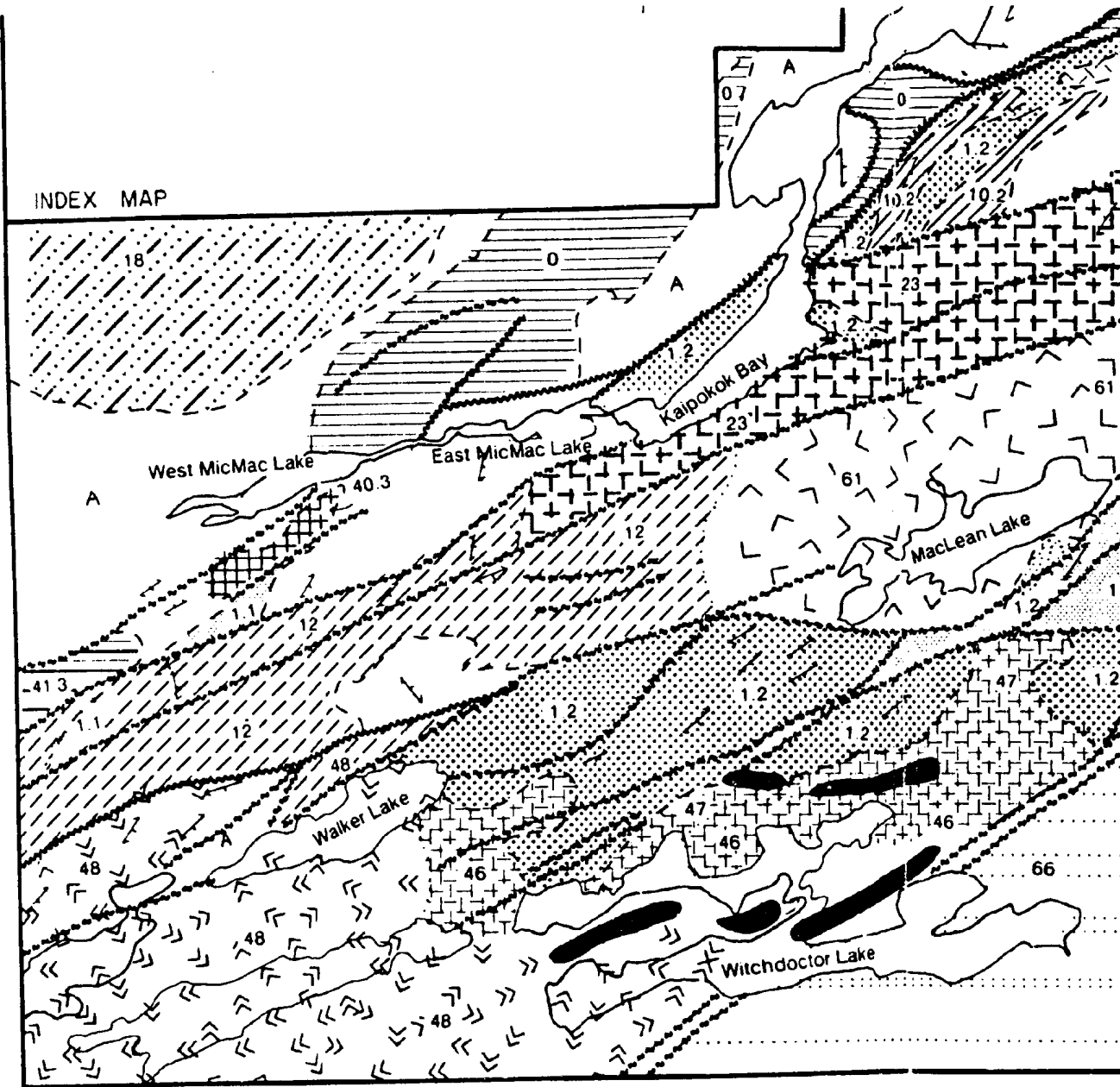
20

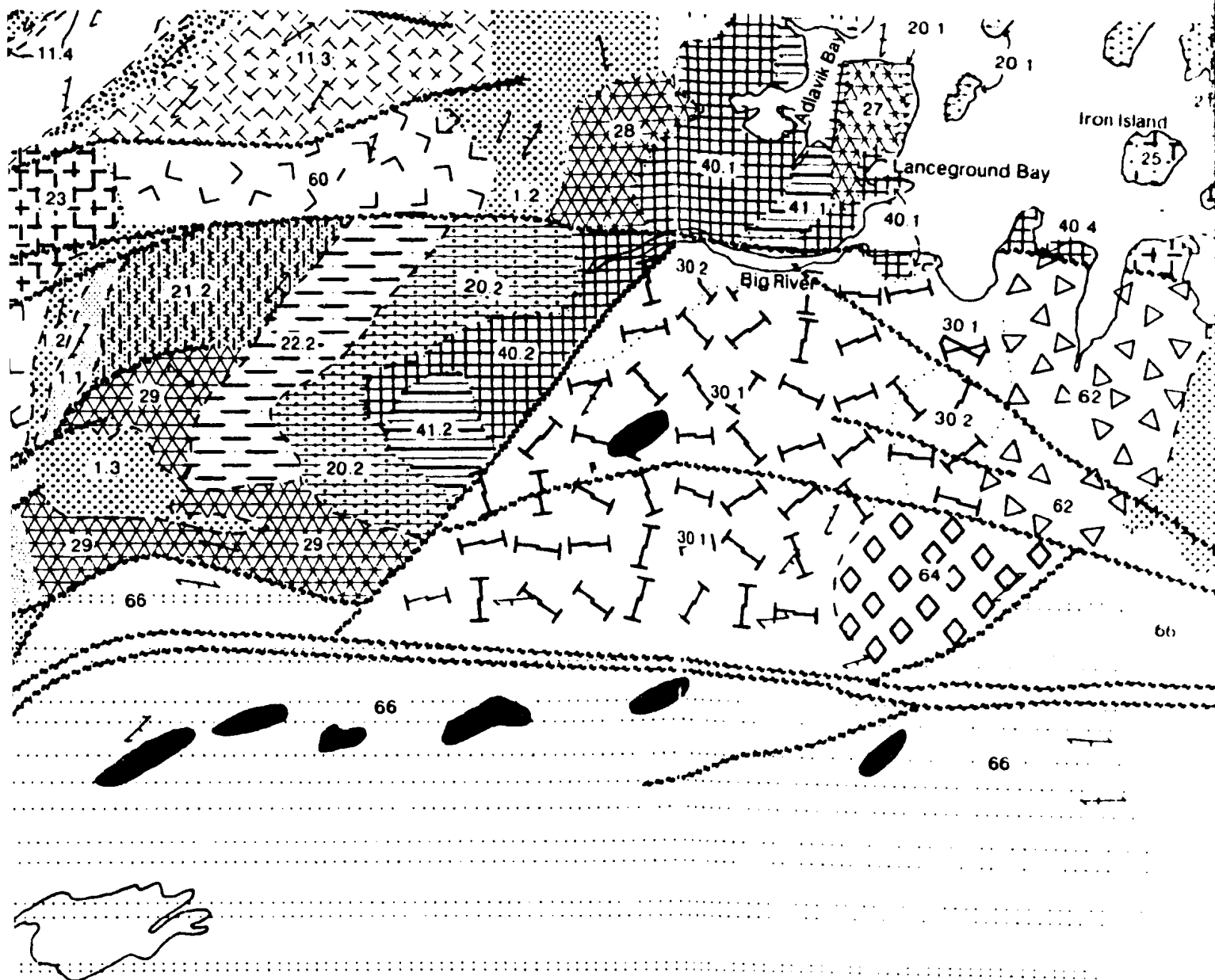
ds  
ebeck Island

Cape Harrison

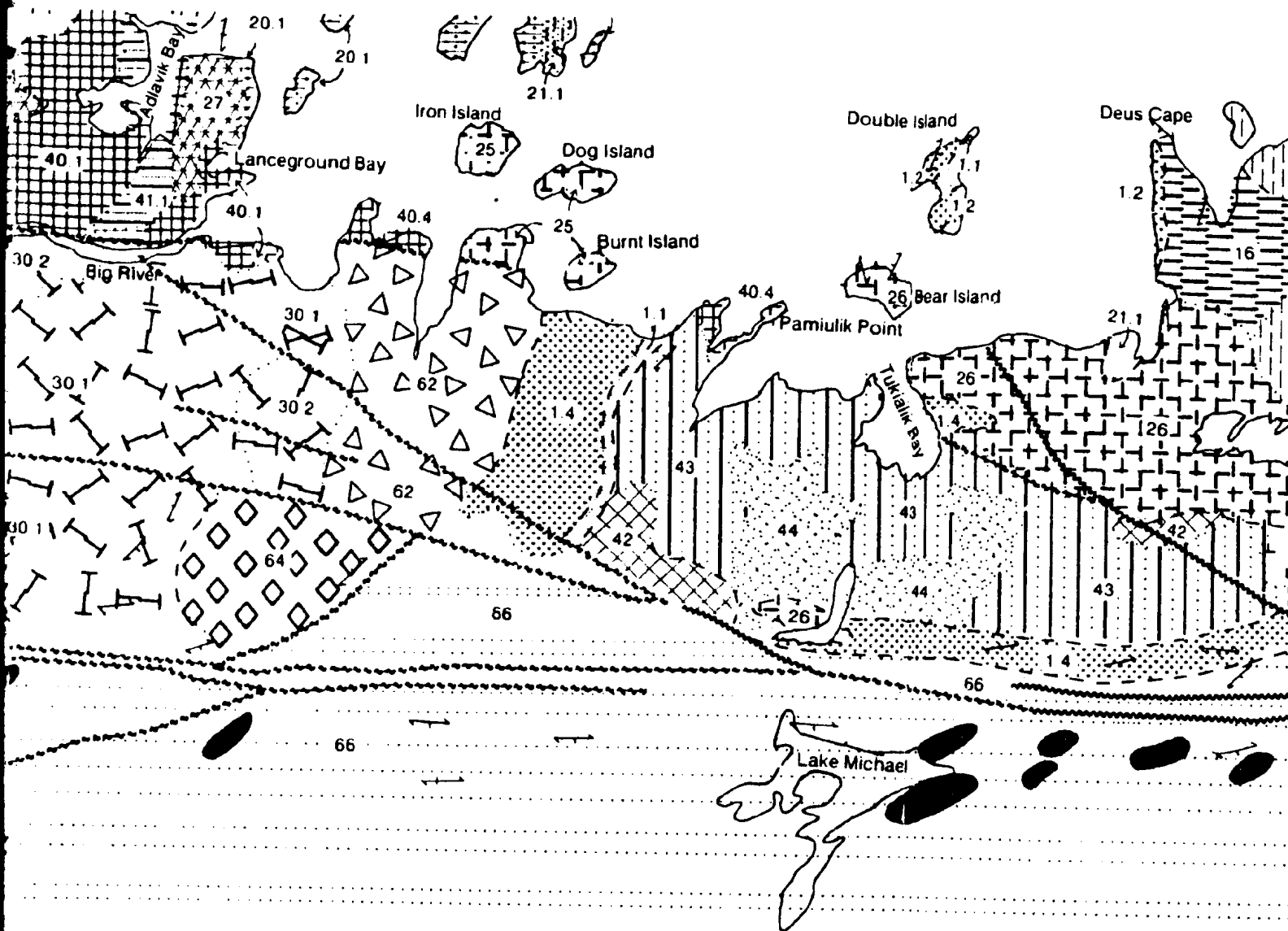


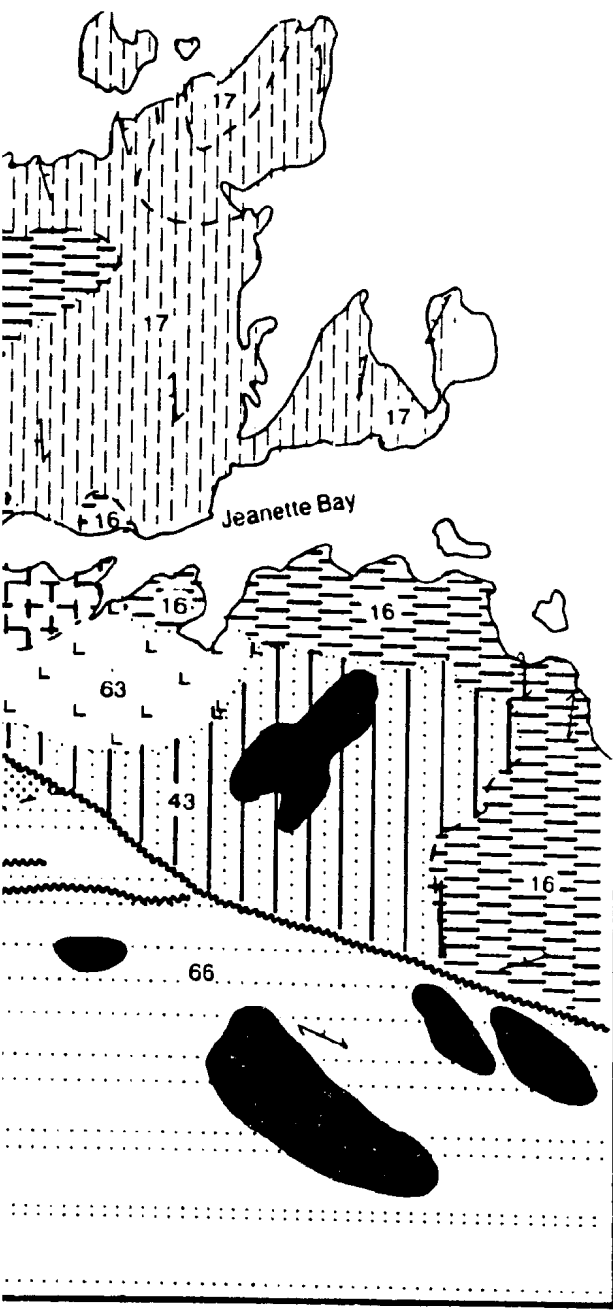
INDEX MAP











## ENCLOSURE 2

# Plutonic Rocks of The Makkovik Province

Unclassified and

- 63 JEANETTE BAY QUARTZ SYENITE : Grey to pink, medium to coarse-grained, K-feldspar porphyritic, biotite-hornblende quartz syenite.
- 62 STAG BAY GRANITOID : Grey to buff, coarse-grained, seriate to porphyritic biotite-hornblende granodiorite to granite. Phenocrysts of both feldspars.
- 1798 +/- 48 60,61 FRESHSTEAK AND NOARSE LAKE GRANITOIDS : Grey to brown, medium-grained, variat plagioclase-porphyritic biotite-hornblende quartz monzonite to monzogranite.

Labradorian f

### MONKEY HILL INTRUSIVE SUITE

- 1640 +/- 10 45 Grey to pink, fine to medium-grained, leucocratic, biotite-chlorite monzo-granite and granite, commonly slightly plagioclase-porphyritic.
- 45.1 - Monkey Hill Granite. 45.2 - Round Pond Granite. 45.3 - Duck Is. Granite. 45.4 - Little Monkey Hill Granite. 45.5 - Bent's Cove Granite 45.6 - Kidlakut Granite. 45.7 - Other Units.

### MOUNT BENEDICT INTRUSIVE SUITE

- 1650 +/- 10 44 Pink to buff, fine to medium-grained, equigranular to K-feldspar (+/- relict plagioclase porphyritic, biotite syenite to alkali-feldspar granite.
- 43 Grey to buff or pink, medium to coarse-grained, biotite - hornblende (+/- pyroxene monzonite, quartz monzonite and syenite. Relict (mantled) plagioclase phenocrysts impart a distinctive "speckled eggshell" texture.
- 42 Grey to black-and-white, plagioclase-porphyritic, leucogabbro and diorite of probable cumulate origin. Resembles parts of Adlavik Intrusive Suite.

Post-Tectonic (generally mass

### LANCEGROUND INTRUSIVE SUITE




- 29 TARUN GRANITE : Variably foliated, buff to pink, medium to coarse-grained, biotite-hornblende quartz syenite, granite and alkali-feldspar granite.
- 28 PISTOL LAKE GRANITE : Pink to buff, medium to coarse-grained, biotite-hornblende quartz syenite to alkali-feldspar granite, locally hypersolus in texture.
- 27 LANCEGROUND HILLS GRANITE : Pink to buff, medium to coarse-grained, biotite-hornblende quartz syenite to alkali-feldspar granite, locally hypersolus.

### NUMOK INTRUSIVE SUITE

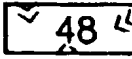


- 22 Grey to dark brown, coarse grained, plagioclase-porphyritic pyroxene-hornblende monzodiorite and monzonite. Present only in the southern zone.
- 1801 +/- 2 21 Pink to brown, coarse grained, K-feldspar porphyritic, pyroxene-syenite and quartz syenite, locally with favailltic olivine. Locally hypersolus.

## LEGEND



### Other Plutonic Rocks

- 1426  MICHAEL GABBRO SUITE :  
Grey to black, medium to coarse-grained, olivine gabbro and diabase, with minor leucogabbro and diorite.
-  GRANITOID GNEISSES OF THE GRENVILLE STRUCTURAL PROVINCE  
Foliated granitoid rocks and granitoid gneisses, variably K-feldspar porphyritic and/or augen textured. Locally cataclastic or mylonitic.
-  THUNDER MOUNTAIN SYENITE : Pink to brown, coarse-grained, K-feldspar porphyritic hornblende (+/- pyroxene) syenite and quartz syenite, with blue quartz.

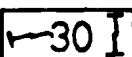
### Plutonic Rocks

- 1647 +/- 2  OTTER LAKE - WALKER LAKE GRANITOID : Grey to pink, medium to coarse-grained, seriate to porphyritic, biotite-hornblende quartz monzonite to monzogranite. Generally fresh, massive and little-deformed; locally foliated.
-  BURNT LAKE GRANITE : Grey, white or pink, fine to medium-grained, leucocratic biotite (+/- muscovite) monzogranite and granite. Locally contains minor garnet.
- 1632 +/- 9  WITCHDOCTOR GRANITE : White to pink, medium to coarse-grained, leucocratic, biotite-muscovite granite, containing accessory garnet. Variably foliated.

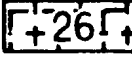
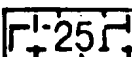

### ADLAVIK INTRUSIVE SUITE

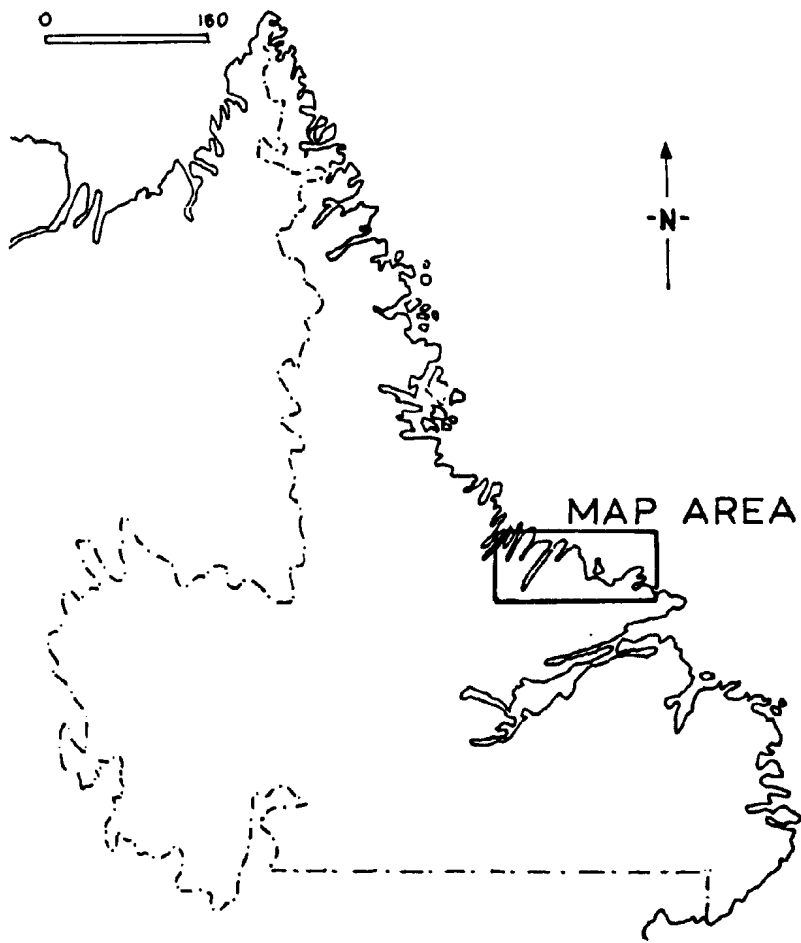
- 1649 +/- 1  Grey to yellow-brown, coarse-grained, pyroxene-hornblende diorite and monzodiorite. Locally displays cumulate texture or layering. Subdivisions as for Unit 40 (below). Locally syenitic in appearance.
-  Grey to green or brown, coarse-grained gabbro, gabbro-norite and leucogabbro. Includes ultramafic and mafic cumulates, massive and composite diabase, and hornblende-plagioclase "pegmatite". 40.1 - Main Body (Adlavik Bay). 40.2 - Big 40.3 - East MicMac Lake. 40.4 - Eastern bodies, including Pamulik Point.

### sive) Makkovikian Plutonic Rocks

- 1798 +/- 28  BIG RIVER GRANITE : 30.1 - pink to red, coarse grained, K-feldspar porphyritic, biotite-hornblende granite with pseudopagvik texture. 30.2 - equigranular to locally quartz-porphyritic phase of generally similar composition.

### STRAWBERRY INTRUSIVE SUITE

-  TUKIALIK GRANITE : Pink to red, coarse-grained, K-feldspar porphyritic, biotite granite and alkali-feldspar granite, containing accessory fluorite.
-  DOG ISLANDS GRANITE : Pink, coarse-grained, K-feldspar (+/- quartz) porphyritic biotite-granite, alkali-feldspar granite and quartz-feldspar porphyry, commonly with abundant accessory fluorite.
- CAPE STRAWBERRY GRANITE AND ASSOCIATED ROCKS
- 1760 +/- 10 ?  White, pink or red, generally coarse grained, texturally varied, K-feldspar

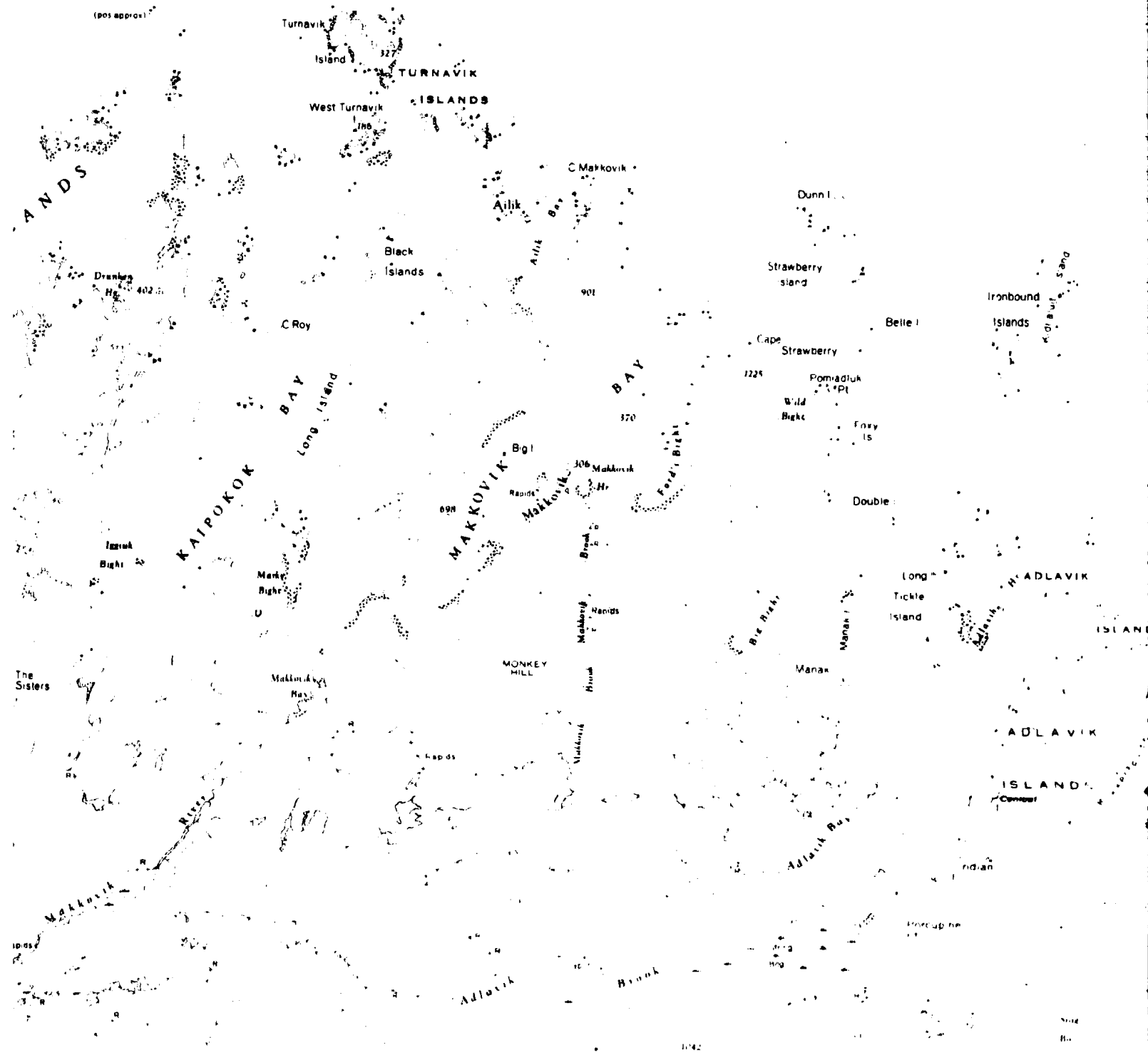


# TOPOGRAPHIC MAP

LANDS

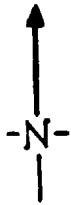
**~ Striped**

(pos approx)



## 182

**:250,000**



Morrison  
Wedell  
Michael Har  
Lape Harrison  
UIVALUR  
PK  
Bett  
Sloop  
etc  
False - SDP

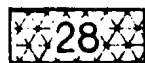


## Post-Tectonic (generally massive)

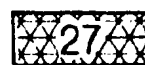
### LANCEGROUND INTRUSIVE SUITE



TARUN GRANITE : Variably foliated, buff to pink, medium to coarse-grained, biotite-hornblende quartz syenite, granite and alkali-feldspar granite.

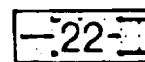


PISTOL LAKE GRANITE : Pink to buff, medium to coarse-grained, biotite-hornblende quartz syenite to alkali-feldspar granite, locally hypersolvus in texture.



LANCEGROUND HILLS GRANITE : Pink to buff, medium to coarse-grained, biotite-hornblende quartz syenite to alkali-feldspar granite, locally hypersolvus.

### NUMOK INTRUSIVE SUITE



Grey to dark brown, coarse grained, plagioclase-porphyritic pyroxene-hornblende monzodiorite and monzonite. Present only in the southern zone.

1801 +/- 2

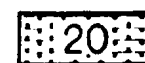


Pink to brown, coarse grained, K-feldspar porphyritic, pyroxene-syenite and quartz syenite, locally with fayalitic olivine. Locally hypersolvus.  
21.1 - Northern Zone (Adlavi Islands) 21.2 Southern Zone (Big River).

17

17

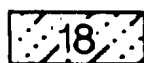
1801 +/- 2



White to pink, medium to coarse-grained, variably plagioclase and K-feldspar porphyritic, hornblende-biotite monzonite, quartz monzonite and syenite.  
20.1 - Northern Zone (Adlavi Islands). 20.2 - Southern Zone (Big River).

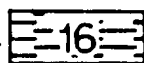
## Syn-Tectonic (generally foliated) Makkovikian Plutonic Rocks

1805 +/- 5



ISLAND HARBOUR BAY INTRUSIVE SUITE : Compositionally and texturally variable diorite, tonalite, quartz monzonite, granodiorite and granite.

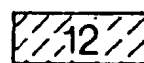
1837 +/- 4



DEUS CAPE GRANITOID : Pink to grey, coarse grained, seriate to K-feldspar megacrystic, foliated biotite-hornblende granodiorite to granite.



PITRE LAKE GRANITE : White to pale pink, medium-grained, equigranular biotite-muscovite leucogranite with "ghost layering" and metasedimentary xenoliths.



MELODY GRANITE : Pink to brick-red, coarse grained, variably K-feldspar porphyritic, strongly foliated, biotite granite, generally leucocratic.

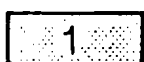
1802 +/- 7



LONG ISLAND QUARTZ MONZONITE : Grey-brown, fine to medium grained, melanocratic plagioclase-porphyritic biotite-hornblende-quartz monzonite to monzogranite  
10.1 - Main Body (Long Is - Mark's Blight) 10.2 - Other units.

## MAKKOVIKIAN OR PRE-MAKKOV

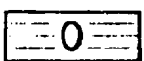
1861 +/- 3



EARLY UPPER AILLIK GROUP : Arkose, bedded tuff, sandstone, siltstone, conglomerate, agglomerated, and minor mafic to felsic metavolcanic rocks.

11

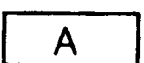
1



LOWER AILLIK GROUP : Amphibolites, pelitic to psammitic metasedimentary rocks, mafic metavolcanic rocks and silicate-oxide iron formation.

## ARCHEAN OR PRE-MAKKOV

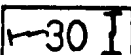
> 2800



ARCHEAN BASEMENT ROCKS (Western Domain Only) : Strongly layered and foliated orthogneisses of tonalite-granodiorite composition, intercalated with amphibolites, and cut by massive to foliated granitoid rocks.

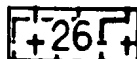
2100

## Massive) Makkovikian Plutonic Rocks

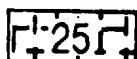
1798 +/- 28 

BIG RIVER GRANITE : 30.1 - pink to red, coarse grained, K-feldspar porphyritic, biotite-hornblende granite with pseudopagvik texture. 30.2 - equigranular to locally quartz-porphyritic phase of generally similar composition.


### STRAWBERRY INTRUSIVE SUITE



TUKIALIK GRANITE : Pink to red, coarse-grained, K-feldspar porphyritic, biotite granite and alkali-feldspar granite, containing accessory fluorite.



DOG ISLANDS GRANITE : Pink, coarse-grained, K-feldspar (+/- quartz) porphyritic biotite-granite, alkali-feldspar granite and quartz-feldspar porphyry, commonly with abundant accessory fluorite.

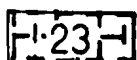
1760 +/- 10 ?  
1719 +/- 3 

#### CAPE STRAWBERRY GRANITE AND ASSOCIATED ROCKS

White, pink or red, generally coarse grained, texturally varied, K-feldspar porphyritic, biotite granite to alkali-feldspar granite with fluorite.

24.1 - Cape Strawberry Granite. 24.2 - October Harbour Granite.

24.3 - Poodle Pond Granite Sills. 24.4 - Other Minor Intrusions.



BAYHEAD GRANITE : White to pink, medium-coarse grained, K-feldspar porphyritic biotite granite, monzogranite and alkali-feldspar granite with fluorite.

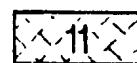
NOTE : SYN-TECTONIC MAKKOVIKIAN PLUTONIC ROCKS ARE CONSIDERED TO BE 1800 Ma OR OLDER, BUT PROBABLY OVERLAP IN TIME WITH POST-TECTONIC MAKKOVIKIAN PLUTONIC ROCKS.



MANAK ISLAND GRANITOID : White to pale grey, medium to coarse-grained, leucocratic, foliated biotite-hornblende granodiorite to monzogranite.



BRUMWATER GRANITE : Grey to pink, medium-grained, equigranular, foliated, biotite-granite and monzogranite, with gneissic xenoliths.




#### KENNEDY MOUNTAIN INTRUSIVE SUITE

Dominantly pink to white or buff, medium-coarse grained, leucocratic, variably K-feldspar porphyritic, foliated biotite monzogranite and granite containing accessory fluorite. Locally alaskitic. 11.1 - Kennedy Mountain Granite 11.2 - Narrows Granite. 11.3 - Cross Lake Granite. 11.4 - Other units.

ritic

## VIKIAN SUPRACRUSTAL ROCKS

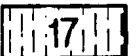
1856 +/- 2  
1807 +/- 3 

#### LATE UPPER ALLIK GROUP AND POSSIBLE CORRELATIVES

1.0 - Undifferentiated. 1.2 - Felsic tuffs and pyroclastic rocks, massive rhyolites and minor tuffaceous metasedimentary rocks. 1.3 - Massive subvolcanic quartz-porphyry and quartz-feldspar porphyry. 1.4 - Jagged Edge Assemblage volcanic rocks. 1.5 - Jagged Edge Assemblage subvolcanic intrusive rocks.

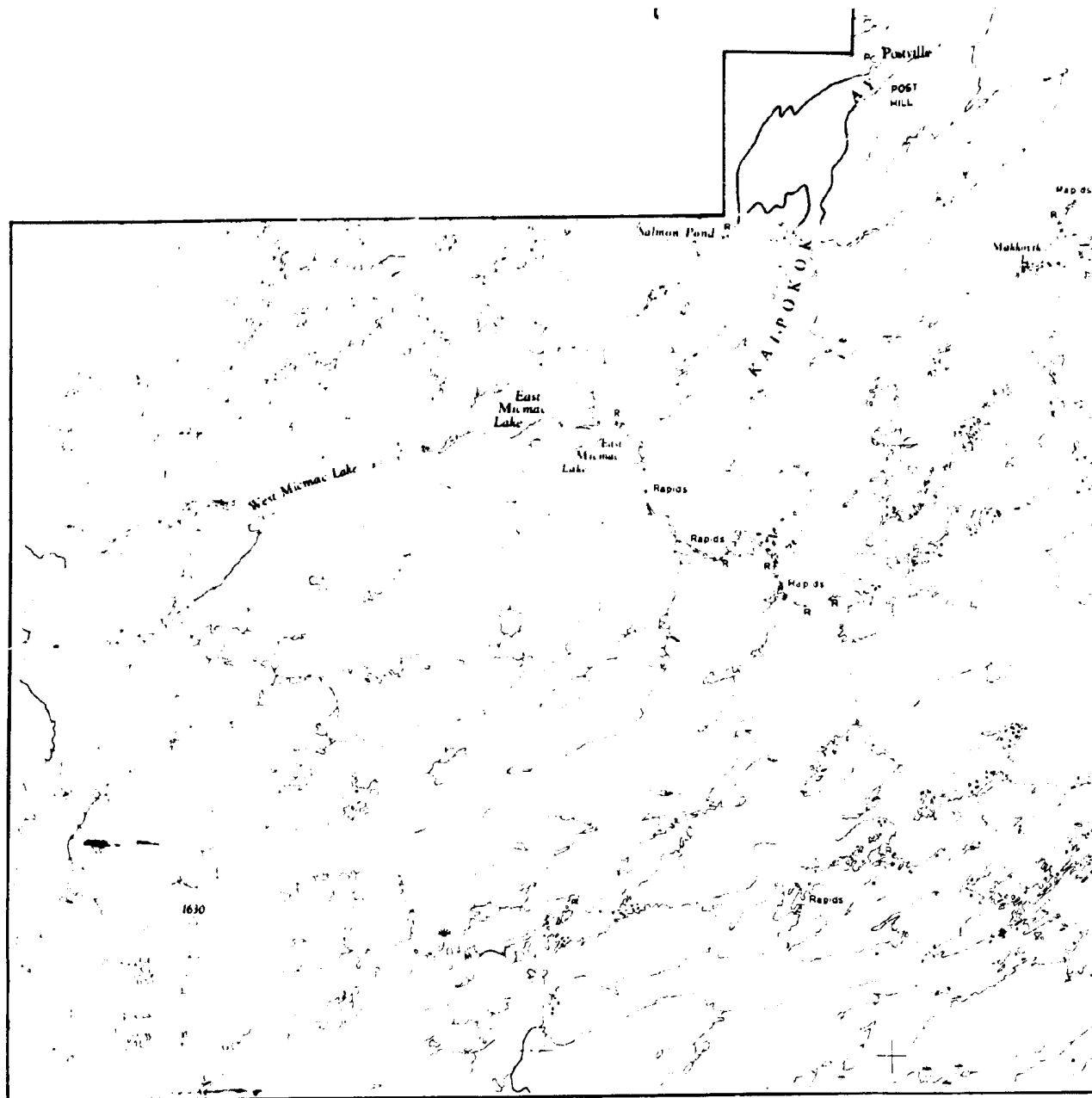
NOTE : Jagged Edge Assemblage may be younger than Upper Allik Group.

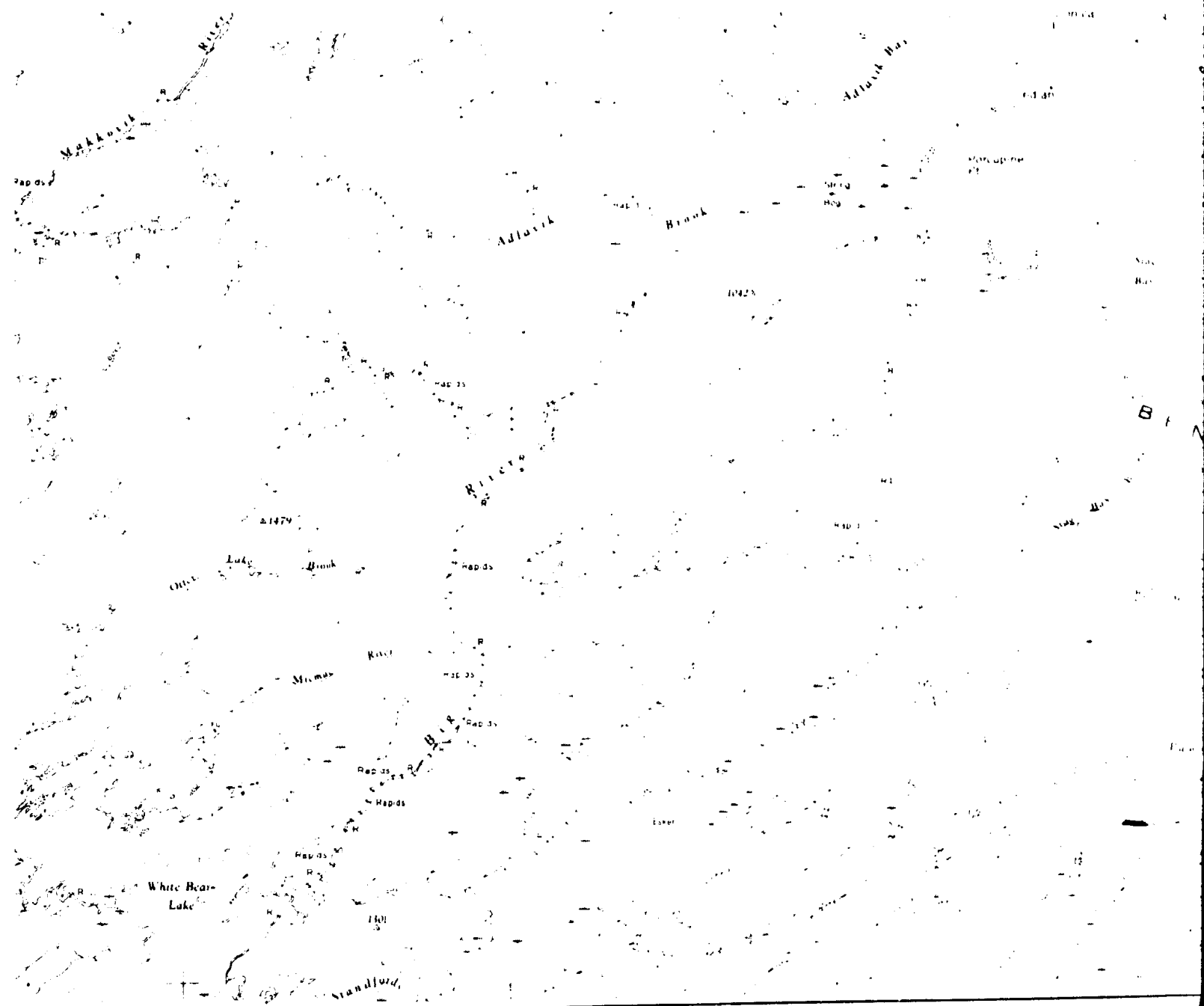
## VIKIAN (?) BASEMENT ROCKS

100 - 1900 ? 

CAPE HARRISON METAMORPHIC SUITE : Strongly layered, banded and foliated orthogneisses of diorite to granodiorite composition, associated with foliated granitoid rocks, and remnants of supracrustal material.

Similar to Archean rocks in field appearance, but probably Proterozoic.





LABRADOR

SEA

Deus  
Cape

Jiggo

Dog  
Islands  
Dog

417 Double  
Island

BENEDICT

MOUNT  
BENEDICT

MOUNTAINS

Rapids Rapids

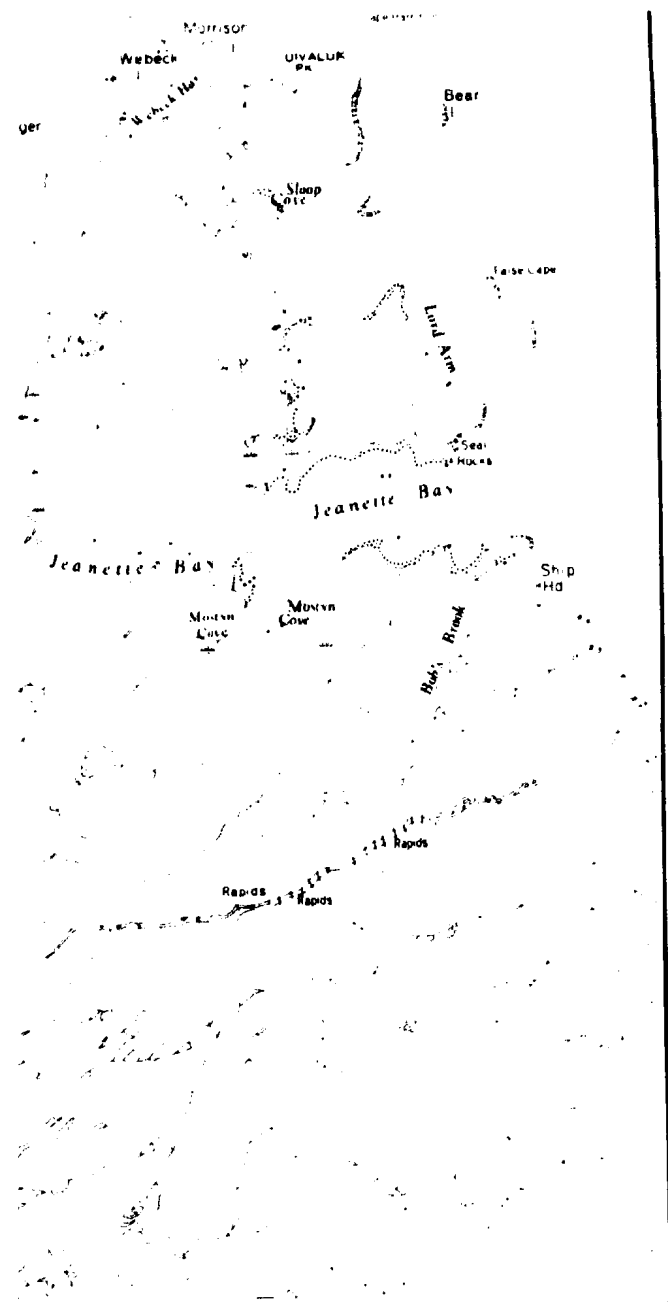
Rapids

Pamiulik  
R

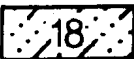
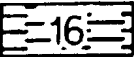


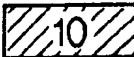
Rapids

Lake

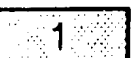

Michael



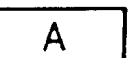
## Syn-Tectonic (generally foliated) Makkovikian Plutonic Rocks

- 1805 +/- 5  ISLAND HARBOUR BAY INTRUSIVE SUITE : Compositionally and texturally variable diorite, tonalite, quartz monzonite, granodiorite and granite.
- 1837 +/- 4  DEUS CAPE GRANITOID : Pink to grey, coarse grained, seriate to K-feldspar megacrystic, foliated biotite-hornblende granodiorite to granite.
-  PITRE LAKE GRANITE : White to pale pink, medium-grained, equigranular biotite-muscovite leucogranite with "ghost layering" and metasedimentary xenoliths.
-  MELODY GRANITE : Pink to brick-red, coarse grained, variably K-feldspar porphyritic, strongly foliated, biotite granite, generally leucocratic.
- 1802 +/- 13/-7  LONG ISLAND QUARTZ MONZONITE : Grey-brown, fine to medium grained, melanocratic plagioclase-porphyritic biotite-hornblende-quartz monzonite to monzogranite  
10.1 - Main Body (Long Is - Mark's Bight) 10.2 - Other units.

## MAKKOVIKIAN OR PRE-MAKKOVIAN

- 1861 +/- 9/-3  EARLY UPPER AILLIK GROUP : Arkose, bedded tuff, sandstone, siltstone, conglomerate, agglomerated, and minor mafic to felsic metavolcanic rocks.
-  LOWER AILLIK GROUP : Amphibolites, pelitic to psammitic metasedimentary rocks, mafic metavolcanic rocks and silicate-oxide iron formation.

## ARCHEAN OR PRE-MAKKOVIAN

- > 2800  ARCHEAN BASEMENT ROCKS (Western Domain Only) : Strongly layered and foliated orthogneisses of tonalite-granodiorite composition, intercalated with amphibolites, and cut by massive to foliated granitoid rocks.

210

## GEOLOGICAL SYMBOLS

- Geological contact (defined, approximate)
- ..... Geological contact (inferred, position uncertain)
- ~~~~~ Fault (defined, approximate)
- ~~~~~ Fault (inferred, position uncertain)
- ↗ Foliation and/or layering (tick indicates dip direction)

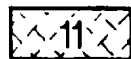
NOTE : SYN-TECTONIC MAKKOVIKIAN PLUTONIC ROCKS ARE CONSIDERED TO BE 1800 Ma OR OLDER, BUT PROBABLY OVERLAP IN TIME WITH POST-TECTONIC MAKKOVIKIAN PLUTONIC ROCKS.



**MANAK ISLAND GRANITOID** : White to pale grey, medium to coarse-grained, leucocratic, foliated biotite-hornblende granodiorite to monzogranite.



**BRUMWATER GRANITE** : Grey to pink, medium-grained, equigranular, foliated, biotite-granite and monzogranite, with gneissic xenoliths.



**KENNEDY MOUNTAIN INTRUSIVE SUITE**

Dominantly pink to white or buff, medium-coarse grained, leucocratic, variably K-feldspar porphyritic, foliated biotite monzogranite and granite containing accessory fluorite. Locally alaskitic. 11.1 - Kennedy Mountain Granite 11.2 - Narrows Granite. 11.3 - Cross Lake Granite. 11.4 - Other units.

ratio

---

## OVIKIAN SUPRACRUSTAL ROCKS

1856 +/- 2  
1807 +/- 3



**LATE UPPER AILLIK GROUP AND POSSIBLE CORRELATIVES**

1.0 - Undifferentiated. 1.2 - Felsic tuffs and pyroclastic rocks, massive rhyolites and minor tuffaceous metasedimentary rocks. 1.3 - Massive subvolcanic quartz-porphyry and quartz-feldspar porphyry. 1.4 - Jagged Edge Assemblage volcanic rocks. 1.5 - Jagged Edge Assemblage subvolcanic intrusive rocks.

NOTE : Jagged Edge Assemblage may be younger than Upper Aillik Group.

---

## OVIKIAN (?) BASEMENT ROCKS

2100 - 1900 ?



**CAPE HARRISON METAMORPHIC SUITE** : Strongly layered, banded and foliated orthogneisses of diorite to granodiorite composition, associated with foliated granitoid rocks, and remnants of supracrustal material. Similar to Archean rocks in field appearance, but probably Proterozoic.

---

## NOTES AND REFERENCES

This 1:250,000 scale map is intended as a summary only. It represents a combination of previous mapping by Department of Mines personnel, and also mapping carried out under this project. Differences between this and previous maps listed below lie in the distribution and grouping of intrusive rocks, particularly in inland areas. The distribution and grouping of other rock types is largely unaltered, although some simplification has been attempted. Sources used in compilation are as follows :

Gower, C.F. 1981. Geology of the Benedict Mountains, Labrador. MDD Report 81-3.

Gower, C.F., Flanagan, M.J., Kerr, A. and Bailey, D.G. 1982. Geology of the Kaipokok Bay-Big River Area, Labrador. MDD Report 82-7.

Ryan, A.B. 1985. Regional geology of the central part of the Central Mineral Belt, Labrador. M.D.D. Memoir 3.

---



EARLY PROTEROZOIC GRANITOID MAGMATISM AND  
CRUSTAL EVOLUTION IN THE MAKKOVIK PROVINCE  
OF LABRADOR: A GEOCHEMICAL AND ISOTOPIC STUDY

CENTRE FOR NEWFOUNDLAND STUDIES

TOTAL OF 10 PAGES ONLY  
MAY BE XEROXED

(Without Author's Permission)

ANDREW KERR, B.Sc., M.Sc.



